Quaternary Geology and Landslide Dam Hazard Assessment of the Shotover Gorge, Otago

A thesis submitted in partial fulfilment

of the requirements for the degree of

Master of Science

in Disaster, Risk and Resilience

at the

University of Canterbury

Timothy Hugh van Woerden

December 2018

Abstract

Formation and failures of landslide dams cause significant immediate and longer-term geomorphic impacts in mountain catchments. In the Shotover River of Otago, New Zealand, these impacts would affect not only the gorge and lower reaches of the Shotover River, but could increase flood risk to Lake Wakatipu and Queenstown (population 15,000) near the Shotover Delta. This thesis addresses unknown or poorly understood factors of landslide dam hazard in the Shotover River, developing and modelling geologically-founded scenarios for future landslide dam events, dambreak flooding and the long-term sediment aggradation.

Geological and geomorphic investigations include mapping of Quaternary geological deposits and geomorphic features, surveying of terrace and fan surfaces, and optically stimulated luminescence (OSL) dating of sedimentary units. Quaternary deposits and landforms of the Shotover Gorge are dominated by events of the last glacial maximum and the postglacial period. Glaciolacustrine sediments in the upper Shotover Gorge show an early Last Glacial Maximum (29.4 ± 3.4 ka; late MIS3/early MIS2) Shotover Glacier advance, followed by formation of an extensive proglacial lake during glacial retreat. Alluvial terraces in the Shotover Gorge and Moonlight Creek are interpreted as remnants of an aggradation surface formed during the LGM, in response to advance of the Wakatipu Glacier into the Wakatipu Basin and the lower Shotover Gorge. Formation of the modern Shotover Gorge has occurred in the postglacial period, incising in response to tectonic uplift. There was no evidence identified for large (1M m3) landslide dam formation in the Shotover Gorge, although smaller events have been noted historically.

From the discovery of alluvial gold in the 1860s, extensive hydraulic sluicing of alluvial terrace gravels took place in the Shotover Valley, with this sediment influx causing a sediment pulse with widespread aggradation in the Shotover River. This sediment pulse had a volume of at least 20-40M m^3 and caused significant geomorphic changes, including aggradation of several metres in the lower Shotover River. The degradation phase of this sediment pulse is ongoing, with channel incision and a narrowing of the active riverbed.

Extensive evidence of landslide activity on the steep slopes in the Shotover Gorge indicates the potential for future landslide occurrence, and the narrow gorge can be easily blocked by landslide debris to form a dam. Any future landslide dam formed in the Shotover Gorge is expected to be short-lived and to fail catastrophically, largely due to the erosive power of river flows from the large, high-rainfall catchment area.

Modelling of peak dambreak flows and routing of dambreak flood waves demonstrates that dambreak floods resulting from sudden failure of a Shotover Gorge landslide dam could be very large (>15,000 m^3/s). These are potentially greater than an order of magnitude larger than the largest known meteorological flood events (1,500 m^3/s), and capable of generating flood waves that would impact on the residential area at the Shotover Delta. Estimations of post-dambreak aggradation indicate geomorphic impacts at the Shotover Delta are limited by sediment buffering at the lower Shotover beach sections. However, any large magnitude sediment inputs are expected to increase the flood risk for the Shotover Delta residential area.

The largest existing landslide scarps in the Shotover Gorge are estimated as being an order of magnitude greater in volume than those used in developing dambreak flood and aggradation assessments. While these larger events are less frequent, a landslide of this size can occur at any time and would have major geomorphic impacts, posing a substantial threat to downstream locations. The landslide dam hazard component of this thesis provides an example of an assessment of the future threats from a landslide-induced hazard events cascade, including the longer-term and further afield geomorphic impacts.

Acknowledgements

During my Masters study I was supported by a University of Canterbury Masters Scholarship and EQC funding. Field and analytical expenses were covered with financial assistance by the Otago Regional Council and a Mason Trust Grant.

Firstly, I must thank Tim Davies for suggesting this as a possible project when I first enquired about returning to study on a natural hazards research project. The Shotover Valley was a great field area to work in, with spectacular views and fascinating geology and history. The broad project scope gave opportunity for exposure to a number of diverse fields; including interpretation of the valley's LGM and postglacial history, evaluation of 1800s alluvial mining activity and recent fluvial geomorphology, to investigating a cascade of possible future hazard events

My supervisors, Tim Davies and Tim Stahl, have been a source of guidance and encouragement throughout, and have immensely improve the quality of this thesis through their advice and thorough reviews of my writing.

Tim Davies, Tim Stahl, Ben Mackey and Sam McColl accompanied me on an initial reconnaissance trip into the valley during the planning stage of this research, and those discussions helped to guide the direction of the project.

Tim Stahl and Ellyse van Woerden assisted with field work; helping with stratigraphic logging and OSL sampling, and useful discussions in the field helped to clarify mapping and interpretations.

Sacha Baldwin and Matt Cockcroft were always helpful when organising field equipment, and John Southward helped resolve IT issues.

Ben Mackey and Ellyse van Woerden at the Otago Regional Council provided various reports, Lidar data, and river gauging data.

Access to field locations was provided by James and Georgie Murray at Branches Station, John and Ginny Foster at Ben Lomond Station, and Bruce Douglas at Mount Creighton Station.

Finally, and most importantly, thanks to my wife Ellyse for your love and encouragement. I couldn't have done this project without your support.

Table of Contents

List of Figures

Chapter One

Chapter Two

Chapter Three

Chapter Four

Chapter Five

Chapter Six

Chapter Seven

Chapter Eight

Chapter Nine

Chapter Ten

List of Tables

Chapter Ten

Chapter One: Introduction and Literature Review

1.1 Project Background

The Shotover River, known in Māori as Kimi Ākau ('searching for the coast') (KTCO Ltd. 2017), is located in the Queenstown Lakes District in central Otago and has a catchment area of 1100 km^2. The Shotover Gorge extends from 12 to 40 kilometres upstream of its confluence with the Kawarau River, and is enclosed by steep slopes up to several hundred meters high. This gorge section shows extensive evidence of landslide activity, ranging from smaller rockfalls to large landslides and schist dip-slope creep slides, with many showing evidence for recent activity (Figures 2.29, 6.11).

Large landslide dams have formed in many locations in New Zealand geologically and geomorphically similar to the Shotover Gorge, for example the Poerua (Hancox et al. 2005) and North Young Rivers (Bryant 2010), where landslide dams formed in schist gorges. The Shotover area has many factors that are favourable for landslide dam formation, with high relief in a schist-dominated, high-rainfall environment, and proximity to several known active faults.

Formation and failure of a landslide dam in the Shotover Gorge has the potential to cause significant immediate and longer-term geomorphic impacts. These impacts would affect not only the riverbed and adjacent areas in the gorge, but could increase flooding risk to Lake Wakatipu and Queenstown via changes to the Shotover Delta.

Sudden failure of a large landslide dam would release impounded water, causing a flood wave which may be many times larger than any recorded meteorological flooding event, and could potentially threaten residential development on low terraces adjacent to the Shotover Delta. With further residential development under consideration in these areas, the magnitude and extent of such flooding needs to be further evaluated.

A large landslide(s) into the river and major dambreak event will input large amounts of sediment into the river in addition to its already high sediment load (Hicks et al. 2000). This sediment will move downriver as a sediment pulse over a period of years or decades, with transported sediment exiting the gorge and potentially causing significant aggradation on wider sections such as Tucker Beach, Big Beach, and the Shotover Delta (Figure 1.10). The geomorphic consequences of dambreak floods are well documented in New Zealand through study of similar events, such as the 1999 Poerua River (Hancox et al. 2005, Davies et al. 2005), and 1981 Ram Creek (Harrison et al. 2015) landslide dam failures.

Extensive sediment deposition elevating bed levels along this portion of the river may also result in increasing flood hazard as meteorological flooding events are superimposed on a higher riverbed level. Of greatest concern are the potential impacts resulting from aggradation of the Shotover Delta toe. High Shotover River flows or delta toe growth can restrict Kawarau River outflows, occasionally to the extent that the Shotover backflows into Lake Wakatipu during flood events (Webby and Waugh 2006).

Queenstown is located on the shores of Lake Wakatipu, with the town centre located on low land adjacent to the lake, and has experienced flooding on many occasions since settlement. The largest flood on record, in November 1999, caused extensive damage and resulted in costs of greater than $50 million (ORC and QLDC 2006). Any change to the Shotover Delta leading to increased flooding impacts in Queenstown could be catastrophic to a town already vulnerable to flooding. Considerable effort has been put into management of the delta in attempts to reduce impacts on the Kawarau River and Lake Wakatipu; this has included gravel extraction, removal of willow islands, and construction of a 'training wall' guiding river flow to the eastern side of the delta and providing for sediment storage.

Several previous studies have considered the potential hazard of Shotover Gorge landslide dam formation (Thompson 1996, Bryant 2011 2017, Davies 2017). However, there is considerable uncertainty in these assessments, and little

consensus in estimations of the threat posed by these events. As concluded by Bryant's (2011, p6) study, "There are too many unknowns regarding location, valley profile, magnitude of failure and height of dam to allow a determination of reservoir size, longevity, breach potential and flood routing characteristics."

1.2 Thesis Objectives and Structure

This thesis aims to address unknown or poorly understood factors of landslide dam hazard in the Shotover River, and is organised in two parts:

1. Chapters Two-Four: An investigation of the Shotover Gorge's geomorphology and Quaternary geology, and a summary of the Shotover River's geomorphic changes within the historic period.
2. Chapters Five-Ten: A landslide dam hazard assessment which develops plausible landslide dam scenarios and estimates of dambreak flood magnitudes and longer-term geomorphic impacts of landslide dam failure.

This introduction chapter outlines the justification for this study, and summarises the study objectives and thesis structure. The basic geomorphic and geological setting of the Shotover Valley is described, and relevant previous investigations in the area are reviewed, including studies focusing on landslides, sediment sources and transport, hydrology and flooding, and landslide dam hazards.

Chapter Two provides the results of geological and geomorphic field mapping, supplemented by GIS analysis and surveys of geomorphic features. The main geomorphic features and Quaternary geological units of the Shotover Gorge and lower Branches Flat are described, including terrace and fan gravels, and glaciolacustrine sediments.

Chapter Three provides interpretations of the formation of the main geomorphic features and Quaternary geological units of the Shotover Gorge. The resulting event chronology is based on the field investigations described in Chapter Two and ages obtained via Optically Stimulated Luminescence (OSL) dating. These new data are used to revise the recent geological history of the gorge, from a previously undocumented last glacial maximum (LGM) glacial advance to events in the postglacial period.

Chapter Four summarises the Shotover River's historic geomorphic changes, compiled from mining-era (1860s-1930s) reports and images, and more recent investigations and monitoring. Additional sediment inputs from hydraulic sluicing of alluvial terrace gravels resulted in significant aggradation and formation of a sediment pulse downstream. This was followed by an ongoing degradation phase as this excess sediment moves through the river system. This example of the Shotover River's response to a major sediment input is a useful analogue for the geomorphic changes resulting from a landslide dam failure.

Chapter Five provides a review of landslide dam literature, summarising the processes of dam formation, failure, and dambreak flooding. This provides a theoretical background required for landslide dam assessments and modelling in the following chapters. The assessment methods in several other landslide dam hazard assessments are reviewed as a basis for the present analysis.

Chapter Six investigates the formation of future dam-forming landslides in the Shotover Gorge. This includes identification of zones where landslide dam formation is considered most likely, and development of possible landslide scenarios within those zones. Existing landslide scarps in the Shotover Gorge are mapped and used to develop a landslide magnitude-frequency relationship which can be used to approximate the likelihood of future landslide events. Landslide dams elsewhere in the Shotover catchment have been summarised, based on dams reported in literature and dams identified from a search of aerial imagery.

Chapter Seven summarises modelling of landslide dams in the Shotover Gorge. The resulting landslide dam characteristics are used to develop landslide dam scenarios, based on the landslide scenarios from Chapter Five. The

modelled landslide dam parameters are used in assessment of dam stability using empirical indices and for estimation of the time to fill the landslide-dammed reservoirs.

Chapter Eight investigates the magnitude of dambreak flooding resulting from failure of Shotover Gorge landslide dams. Based on the landslide dam scenarios developed in Chapters Six and Seven, maximum dambreak discharges and breach characteristics are estimated using empirical, dimensionless and parametric methods. A 1D hydraulic model is used to simulate progression of the dambreak flood wave through the Shotover River, estimating the magnitude of flow attenuation for locations at the Shotover Delta.

Chapter Nine summarises the landslide and dambreak scenarios of Chapters Five-Seven with the creation of landslide dambreak scenarios based on estimations and modelling in the previous chapters. This outlines two possible events sequences for formation of a large (80-100 m height) landslide dam in the Shotover Gorge, and the resulting dam failure and dambreak flood.

Chapter Ten reviews sediment pulse literature and summarises the geomorphic changes expected to result from failure of a large Shotover Gorge landslide dam. The distribution and thickness of dambreak sediment deposits and longer-term aggradation are estimated for Shotover Gorge landslide dam failures. A morphodynamics model is used to simulate the sedimentary impacts of an increase in sediment supply rate.

Chapter Eleven summarises the key findings of this thesis, and discusses limitations of this study and recommendations for further work.

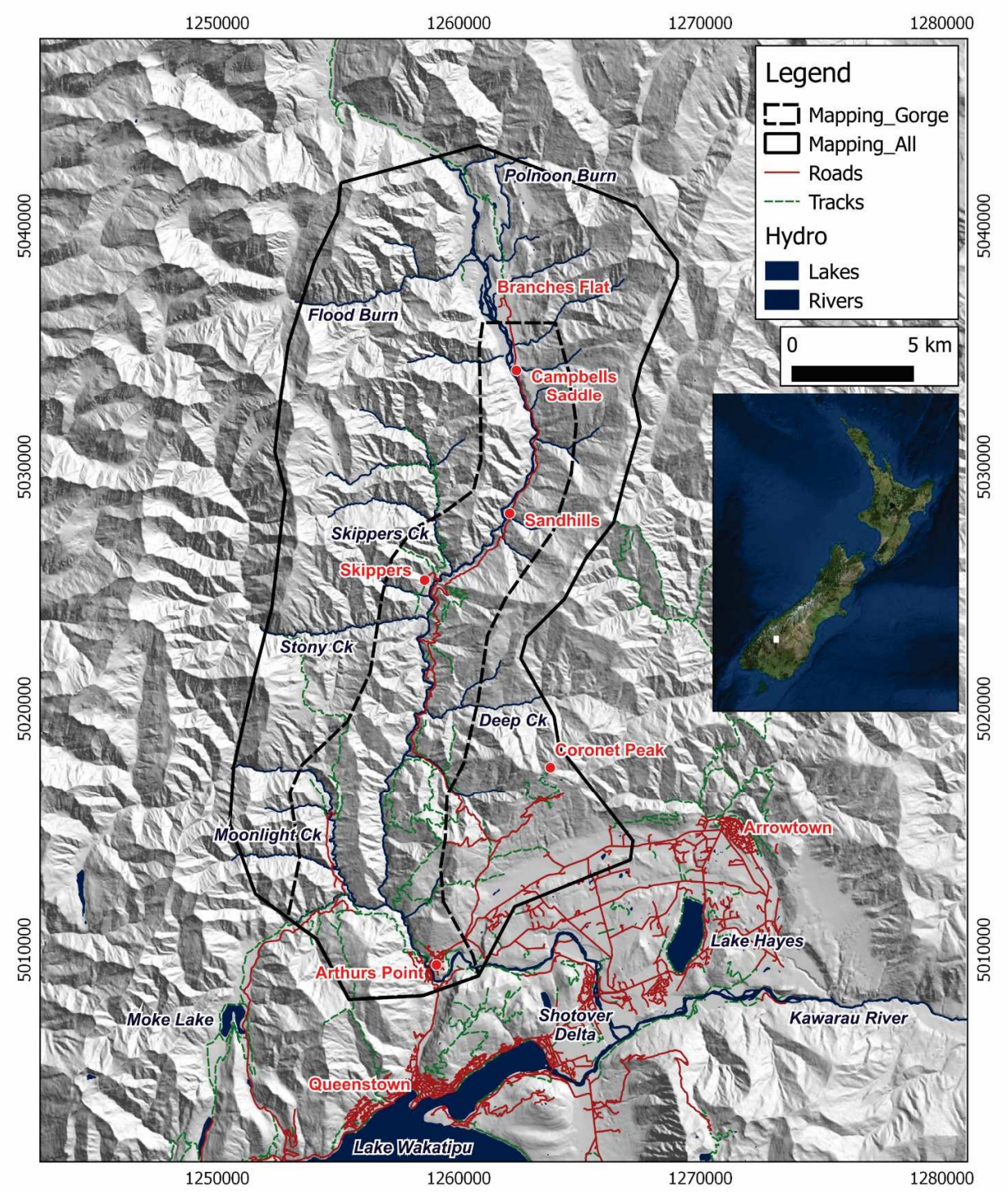

Figure 1.1: *Study area overview and location, showing the Shotover River and major tributaries, access roads and tracks, and the main Wakatipu area settlements. The Shotover Gorge area of interest (dashed outline) shows extent of geological and geomorphic mapping, and the larger area (solid outline) shows the extent of mapping of creeping schist landslides. The inset map shows the location (white box) of the study area within New Zealand.*

1.3 Shotover Catchment Overview

Land-use, Climate, Hydrology and Sedimentation

The Shotover catchment ranges in elevation from ~300 m at its confluence with the Kawarau River, to alpine environments of >1500 m in the upper catchment, with a maximum of 2518 m at Centaur Peak. Most of the catchment is open tussock country with small areas of beech forest, although the spread of wilding conifers have been an increasing issue in some locations. The highest alpine parts contain areas of bare rock, screes and some permanent ice.

Rainfall varies strongly throughout the catchment. At higher altitudes near the main divide, orographic effects increase rainfall intensity, frequency and duration, and mean annual precipitation totals exceed 5,000 mm (Poyck et al. 2011, Strong and Davies 2010)(Figure 1.2). At these higher altitudes precipitation falls partly as snow and does not immediately contribute to river flows until released as melt. Rainfall decreases with elevation in the remainder of the catchment, and below 400 m in the Wakatipu Basin total precipitation averages only 500 mm/year (Jones 2017).

Measurable changes in climate data have occurred over the period of record, with increases in several metrics including annual rainfall totals, number of rain days, daily rainfall intensity (Mojzisek 2006) and maximum lake levels (ORC 2006). These trends are expected to continue, with modelling by Poyck et al. (2011), Jones (2017) and Jobst et al. (2018) predicting future increases in annual precipitation and streamflow volumes, and a decrease in total snowmelt. Shotover catchment winter and spring precipitation and runoff are expected to increase by 20-40% by the year 2090, with relatively unchanged or decreased summer and autumn values (Poyck et al. 2011).

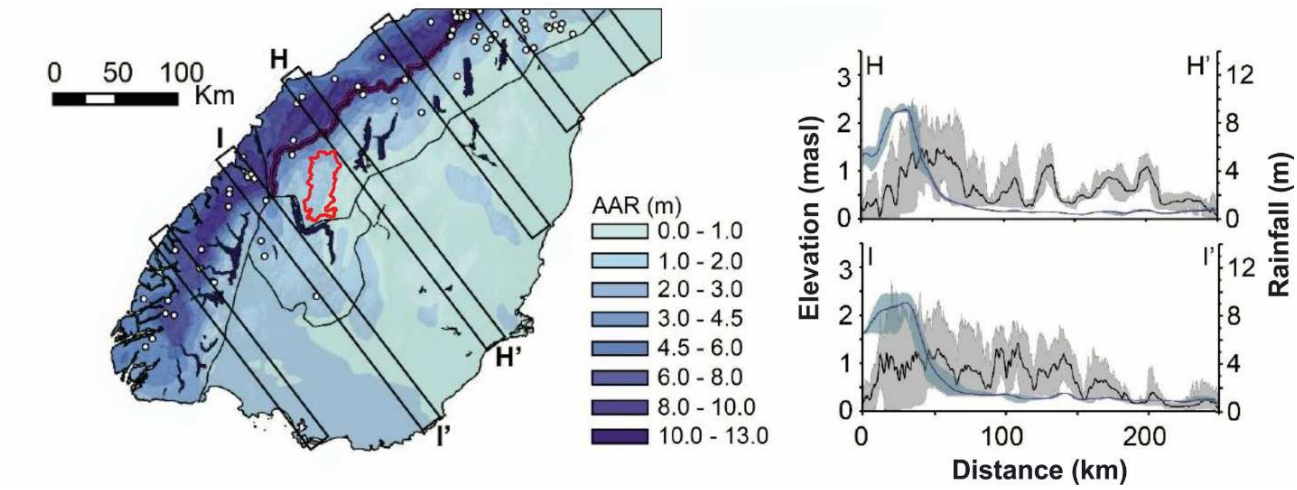

Figure 1. 2: *Rainfall distribution over the southern South Island. Plots show elevation (black) and annual rainfall (blue) within the marked swaths. The Shotover catchment is outlined in red. Modified from Bainbridge (2017).*

Shotover River Hydrology

The Shotover River runs for ~75 km roughly north-south, extending to within 10 km of the main divide. The largest tributaries of the Shotover, from south to north, are; Moonlight Creek, Stony Creek, Skippers Creek, Flood Burn, and Polnoon Burn (Figure 1.1). The longest continuous Shotover River flow record is from the Bowen's Peak water level recorder in the lower Shotover River between Big Beach and Tucker Beach (Figure 1.3). This has a catchment area of 1088 km^2 and was established in 1967 (MWD 1975). The flow rating at this recorder varies due to sediment movements changing the bed level and must be regularly adjusted (ORC 2002a); in 2013 the recorder was relocated

to a more stable downstream site (Damwatch 2017). Over the period 1967-2017, 25 flows have exceeded 450 m^3/s at Bowens Peak, with the three largest flood peaks of 918 m^3/s (1978), 1400-1500 m^3/s (1999), and ~880 m^3/s (2002a) (Damwatch 2017). The November 1999 event was the largest and most damaging recorded flood in Lake Wakatipu. During this flood, the Shotover River's discharge was not directly measured due to scour at the Bowens Peak recorder, but has been inferred from records at other flow gauging stations to be as high as 1400-1500 m^3/s (Brown 2017, Hamilton 2017).

The 50 and 100-year flood flows have been estimated by Hamilton and Associates (2010) using DSIR flood estimation techniques (McKerchar and Pearson 1989), calculated as 1,046 m^3/s (Q_{50}) and 1,176 m^3/s (Q_{100}), but these values were revised upwards by Hamilton (2017) following a reinterpretation of the November 1999 flood peak to ~1,500 m^3/s (Table 1.1).

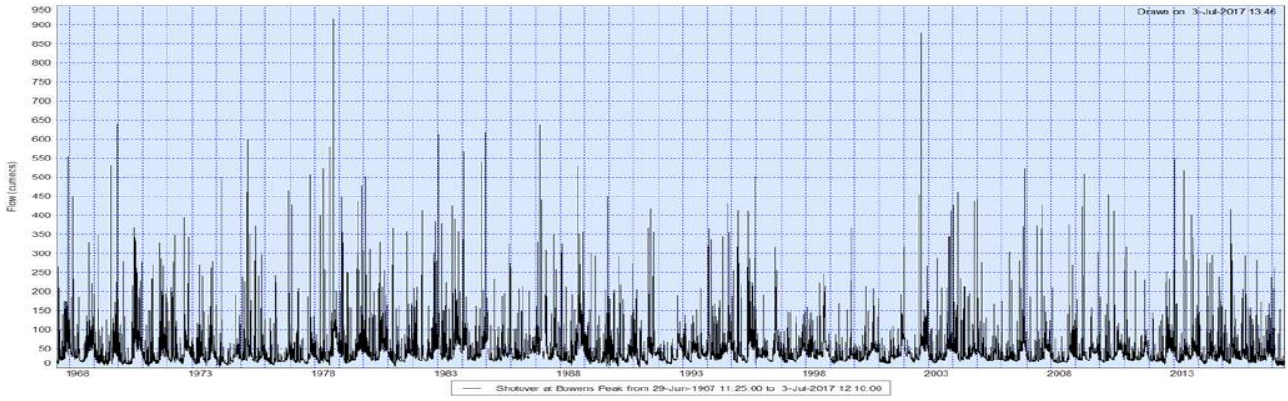

Figure 1.3: *Shotover River flow record at Bowens Peak (1967-2017), showing range from mean flows at <40 m^3/s, to larger flood events at >500 m^3/s. Note the 1999 flood event is not shown to its true peak flow of >1400 m^3/s as it was not accurately gauged (figure provided by ORC).*

Table 1.1: *Estimated magnitudes of Shotover River flood events.*

Event	Flow (m^3/s)	Reference
Mean flow	41	ORC 2007, Hamilton and Associates 2010
Mean annual flood (Q_m)	420	Hamilton and Associates 2010
50-year flood (Q_{50})	1,320	Hamilton 2017
100-year flood (Q_{100})	1,500	Hamilton 2017

Sediment Throughput

The Shotover River is by far the largest sediment contributor to the Clutha River system (Figure 1.4). Hicks et al. (2000) estimated that in the absence of any hydropower dams, the Shotover catchment would supply 72% of the Clutha River sediment at Cromwell, and 61% at Balclutha. Annual total sediment throughputs for the Shotover have been estimated as 2.0M (MWD 1975) and 1.6M m^3 per annum (Hicks et al. 2000). The bedload content has been estimated by Hicks et al. (2000) as ~17% of the total sediment yield, for a bedload supply of 263,000 t/year. Previous modelling studies at the Shotover Delta have used estimated bedload supply rates of 120,000-140,000 m^3/year (ORC 1997, Davies 2007).

Two hydroelectric power stations have been constructed on the Clutha River downstream of the Kawarau confluence; the Roxburgh Dam, filled in 1956 to form Lake Roxburgh, and the Clyde Dam, filled September 1993 to form Lake Dunstan. The Roxburgh dam trapped sediment, rapidly infilling to the extent that by 1992 sedimentation had reduced the lake volume by 44% (Hicks et al. 2000). Concerns regarding this siltation prompted several studies to investigate Shotover catchment sediment sources and possible options for erosion control (MWD 1975, McSaveney 1978). Similar infilling occurred in the Kawarau Arm of Lake Dunstan following completion of the Clyde Dam in 1992 (Hicks et al. 2000).

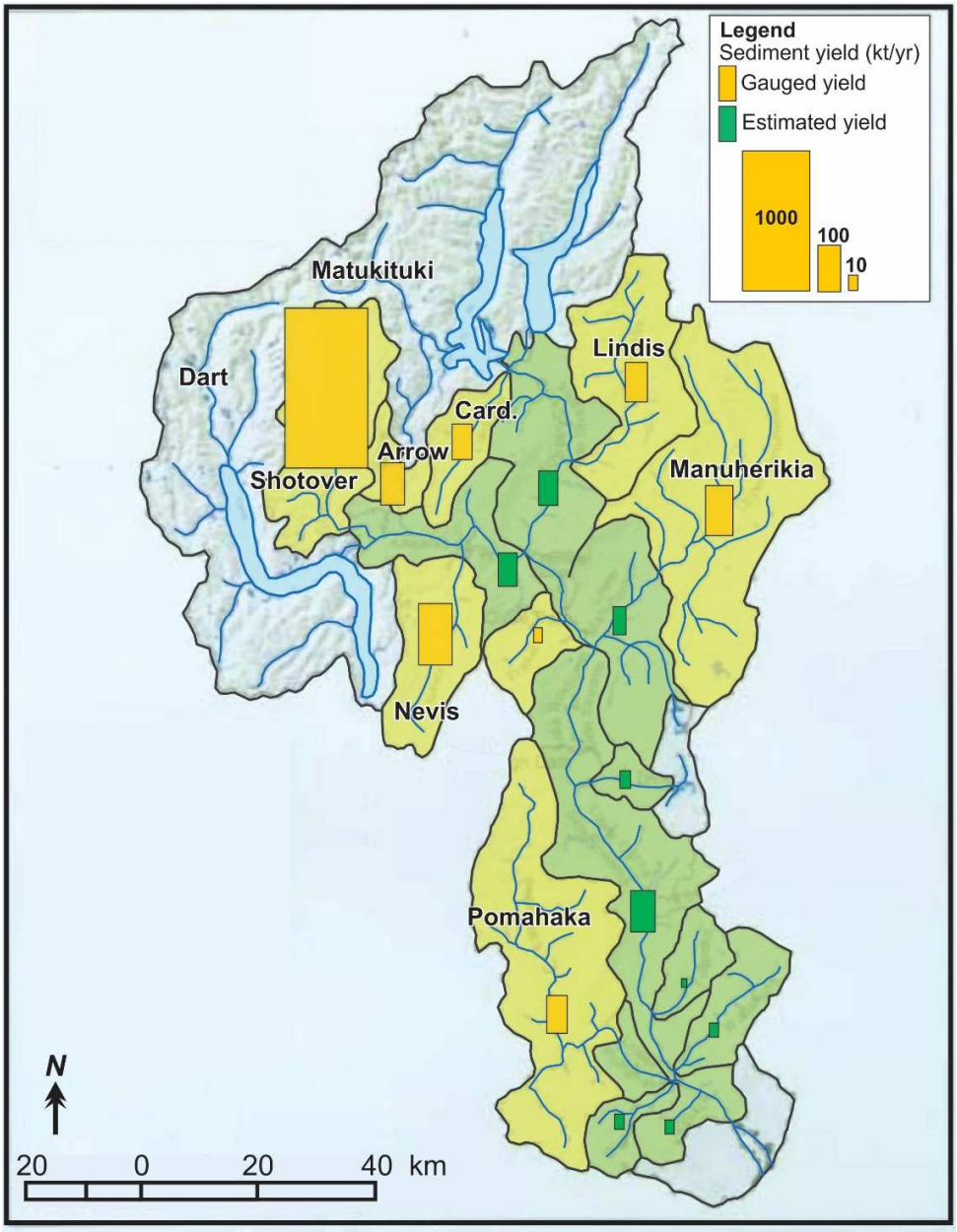

Figure 1.4: *Mean annual suspended sediment yields from tributaries of the Clutha River, showing the Shotover River to be the dominant contributor with >1000 kt annually (modified from Hicks et al. 2000).*

Shotover Delta–Kawarau River Interactions and Lake Wakatipu Flooding

The morphology of the Shotover Delta and its influence on Lake Wakatipu and the Queenstown flood hazard have been the subject of a number of studies. Reports by ORC (1997, 2002a) and Barnett and MacMurray (2017) investigate and summarise relationships between flooding, river flows, delta aggradation trends and gravel extraction. ORC (2002b) developed an empirical sediment transport model used to investigate possible management changes such as modification of Kawarau channel width, and removal of gravel and willow islands on the delta.

A project involving Barnett and MacMurray Ltd, Canterprise Ltd, Hunziker, Zarn and Partner AG and Lincoln University investigated the Shotover-Kawarau interaction and considered options for reducing the Lake Wakatipu flood hazard. Work undertaken included a physical model, and hydraulic and morphological modelling (Barnett and MacMurray et al. 2006). Microscale modelling by Davies (2007) investigated effects of possible delta management options such as removal of willow islands or construction of a training wall to direct delta flows.

Strong and Davies (2010) proposed a strategy of targeted gravel extraction and construction of a training wall in order to increase the delta sediment buffering capacity, and minimise the damming effects of the Shotover flood flows on the Kawarau River. The training wall was subsequently constructed (2012) and has forced the Shotover River to exit into the Kawarau at the far downstream margin of the delta. Barnett and MacMurray have proposed a target delta riverbed profile and discuss a gravel extraction strategy designed to reduce further riverbed degradation at the State Highway Bridge, while also increasing the delta's sediment buffering capacity (Barnett and MacMurray 2017, Damwatch 2017).

Although the Shotover River does not flow directly into Lake Wakatipu, entering the Kawarau River ~4 km downstream from the lake outlet (Figure 1.1), it has a strong influence on the duration and magnitude of flooding events in the lake. Transport of water and sediment by the Shotover River restricts Kawarau River outflow capacity and therefore reduces the ability of Lake Wakatipu to drain. This occurs in two ways (ORC 2002b, Strong and Davies 2010):

1. High flows from the Shotover River have a damming effect as they enter the Kawarau River at right angles, forming a hydraulic barrier;
2. Bedload sediment is deposited on the delta toe, where it raises the bed level and reduces cross-sectional area of the Kawarau River channel. This reduces the channel's carrying capacity, and impedes outflows from lake. The channel remains constricted until sediment is eroded and removed, which may take weeks or months.

On occasion, the combination of these two factors leads to the complete blockage of outflows from Lake Wakatipu and a reverse flow occurs from the Shotover River into the lake. Webby and Waugh (2006) revised and analysed outflow records, showing that this occurred on 26 occasions in the period 1963-2004. The longest and largest backflow recorded was during a 2002 flood, when Kawarau River flows were blocked for 30 hours and the maximum 3-hour average backflow was 225 m^3/s.

Three other factors influence the impact the Shotover River has on Lake Wakatipu flooding levels:

1. The negligible fall of the Kawarau River between the Lake Wakatipu outlet and the Shotover Delta. This gradient is calculated at ~0.1% under normal flow conditions, but reduces significantly during flood events (ORC 2002b). Strong and Davies (2010) show that the difference in levels between Lake Wakatipu and the Kawarau River below the Kawarau Falls weir has been steadily reducing from ~700 mm in the 1970s, to ~300 mm in 2009;

2. The relative timing of peak outflows. When the peak Shotover River flow occurs prior to any significant rise in Lake Wakatipu outflows, the Shotover has a greater damming effect on the comparatively lower Kawarau River;

3. When the main Shotover channel is located on the eastern side of the delta it enters the Kawarau River at the furthest downstream point possible, reducing damming effects. Modelling has shown that the November 1999 flood would have been even more severe if the main channel had been located further towards the western side of the delta at this time (Barnett and MacMurray et al. 2006).

These factors result in a large imbalance between the magnitude of inflows into Lake Wakatipu and its capacity to drain via the Kawarau River. For example, peak inflows to the lake during the November 1999 flood were ~4,000 m^3/s, while the corresponding lake outflow was only ~800 m^3/s (ORC 2006). A single heavy rain event will not usually cause flooding of Lake Wakatipu, it requires a succession of heavy rain events leading to a cumulative increase in lake level (ORC 2006). Therefore the timing between rainfall events, the relative timing of Rees-Dart and Shotover catchment rainfalls, antecedent lake levels and snow accumulations all have an influence on flood occurrence. Since 1926 the Lake Wakatipu outflow has been controlled by a gated weir, constructed in an unsuccessful attempt to dam the lake outlet for gold mining purposes. The gates are now only occasionally operated for short periods (1-2 days), so as to maintain lake levels during times of low inflows (Webby and Waugh 2006).

Queenstown, Glenorchy and Kingston townships are located on low lying land at the Lake Wakatipu lakeside and are vulnerable to flooding. The lake has an average annual level of ~310 m, but when it reaches a level of 311.3 m water enters the storm water system and begins to flood waterfront streets in Queenstown. This has occurred on 20 occasions since 1878, including five times since 1994 (ORC 2006). At a level of 311.6 m water reaches the Steamer Wharf deck at Queenstown, reaching a maximum recorded level of 312.78 m in November 1999. Once flooded, the lake can remain high for days to weeks. For example in April 2010 the lake remained above 311.3 m for five days, and in November 1999 was above this level for two weeks (ORC 2006, 2015).

1.4 Geology and Geomorphology

Regional Geology

The South Island straddles the zone of oblique convergence between the Pacific and Australian tectonic plates, with relative plate movement of ~40 mm/year (Walcott 1998). The majority of this motion is accommodated by the dextral reverse Alpine Fault, with the remainder taken up by reverse, strike slip and oblique faults east of the Alpine Fault (Sutherland et al. 2006, Litchfield 2014).

The bedrock of the Wakatipu region consists of the Otago Schist, metamorphosed in the Rangitata Orogeny during the Jurassic and Cretaceous Periods (200-70 Ma) (Mortimer 1993). Schists mostly consist of psammitic and pelitic grey-coloured schists metamorphosed from sandstone and mudstones, or volcanic or volcaniclastic rocks metamorphosed to greenschist. (Mortimer 1993). These also include minor marble, chert, and ultramafic horizons (Craw 1984). The areas to the north and northeast of Lake Wakatipu are dominated by schists of the Rakaia Terrane textural zone IV and IIIB, corresponding to the Aspiring Lithological Association or Aspiring Terrane (Turnbull 2000). West and south of Lake Wakatipu are less metamorphosed schists of the Caples Terrane textural zones II and III (Figure 1.5). The Caples-Rakaia terrane boundary approximately parallels the north-east margin of Lake Wakatipu, and crosses the southern part of the Shotover catchment in the Moke Creek area (Craw 1984, Mortimer 1993) (Figure 1.5).

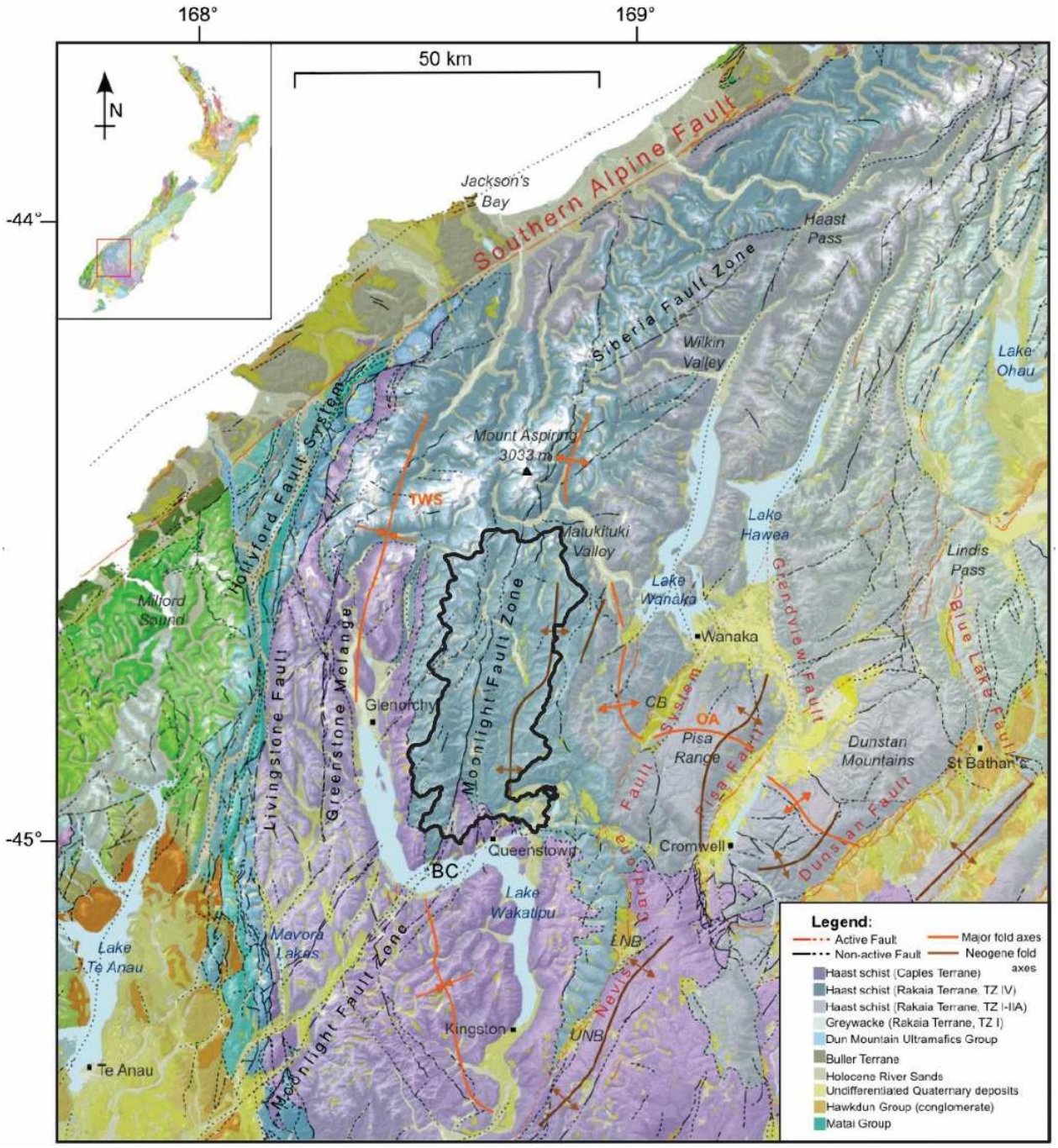

Figure 1.5: *Regional geology and structure of the Wakatipu area, showing major lithological and structural features, the Shotover catchment is outlined (modified from Warren-Smith 2016).*

Shotover Catchment Basement Geology

The Shotover catchment area is included within Turnbull's (2000) 1:250,000 scale geological map of the Wakatipu area, and earlier studies such as Park (1909) and Wood (1962). The composition and structure of the basement

schists are summarised by Craw (1984) and Mortimer (1993). Geological studies of the Shotover catchment were completed as part of the Otago Catchment Board (OCB) soil erosion survey (Brown 1956, OCB 1966), and a Ministry of Works and Development (MWD) sediment sources survey (Turnbull et al. 1975a). More detailed geological studies in the Shotover area have focused on deformation and structural analysis of basement lithologies (Barry 1966), and on the Moonlight Fault and associated fault rock sequences (Hutton 1939, Turnbull et al. 1975b, Alder 2016, Smith et al. 2017).

Pelitic, quartzo-feldspathic, and greenschist types comprise the basement lithologies of the catchment. The majority are part of a range of compositions between pelitic and quartzo-feldspathic end-member schists, with greenschist also making up 5-10% of the basement lithologies. Pelitic and quartzo-feldspathic schists are differentiated based on lamination thickness, mineral composition and hardness, and are interlayered at scales ranging from millimetres to hundreds of metres. The largest and most continuous greenschist is a band up to 500 metres thick lying along the western side of the Moonlight Fault (Barry 1966, Turnbull 1975, Craw 1984) (Figure 1.6). The schist typically has a strong planar foliation and is easily weathered and eroded, a major contributing factor to the high sediment output from the catchment (Barry 1966, Turnbull et al. 1975a, Turnbull 2000). Through most of the Shotover catchment, the schist foliation strikes approximately north, and dips westwards at angles of 20-50°. The largest variation in foliation attitude is on the eastern side of the catchment, where the north-trending Shotover Antiform (Figures 1.4, 1.5) approximately parallels the gorge (Barry 1966). The schist foliation steepens westwards towards the Moonlight Fault, and in the Coronet Peak area dips southwards.

Three major NNE-oriented, steeply west-dipping faults cross the catchment area; the Moonlight, Shotover and Polnoon Faults (Figure 1.6). The Moonlight Fault is the best-known of these, and is a >200 km long reverse fault that originated during the Miocene. It is located on the western side of the catchment, in many locations this fault is marked by discontinuous inliers of late Oligocene marine sediments on the footwall, locally known as the Bob's Cove Beds (Hutton 1939, Barry 1966, Turnbull 1975b, Alder 2016, Smith et al. 2017). The Moonlight Fault was considered inactive by Turnbull (2000), however Wallace et al. (2007) and Stirling et al. (2012) classified the northern fault segment as active. Stahl (2014) found no evidence of late Pleistocene-Holocene activity on the Moonlight Fault, as GPS and Lidar surveys showed consistent elevations of stranded postglacial Lake Wakatipu shorelines, indicating no differential uplift across the fault.

The Shotover Fault (Figure 1.6) was first identified in mining claims near Skippers where it was known as the 'Pug Lode', and has been described as a 'wide shatter zone' (Park 1909, OCB 1966), and as a steeply-dipping and offset kink fold zone (Barry 1966, in Warren-Smith 2016). The fault has been inferred to extend south as far as Queenstown, and north as far as the Shiel Burn confluence (Figure 1.6), giving a total length of approximately 40 km (Brown 1956, OCB 1966). While there is some variation in the interpreted fault location, there is general agreement that it follows the Shotover Gorge from Long Gully as far as Skippers, beyond which it follows the trend of Skippers Creek for at least a further 5 km (Hutton 1939, Brown 1956, OCB 1966, Barry 1966, Turnbull 2000).

The Polnoon Fault follows the line of Polnoon Burn, and has been inferred from a series of broad shatter zones (Figure 1.6). The best defined of these is a 500 m wide zone at the junction of Cabin Creek and Polnoon Burn (Brown 1956). A number of smaller faults have also been noted in the catchment, typically on a similar NNE orientation as the major faults (Figure 1.6). These include the Two Mile Creek Fault (Turnbull, 1975b) and Butchers Creek Fault (OCB 1966) located between the Moonlight and Shotover structures. Warren-Smith (2016) describes the 'Branches Fault' as an inferred active sinistral fault structure on the eastern side of Branches Flat, shown by stream offsets and development of sag ponds. However, these apparent fault-related features may be also due to erosion patterns in schist units of variable weathering susceptibility, in combination with features of the strongly glaciated topography, shown by ice sculpted bedrock, till and moraine deposits (Turnbull et al. 1975a, Turnbull 2000). Prominent joint sets are seen throughout the Shotover gorge, and are often a significant structural control on rockfalls and landslides. These are likely similar to systematic joints described elsewhere in the Otago Schist by Weinberger et al. (2010).

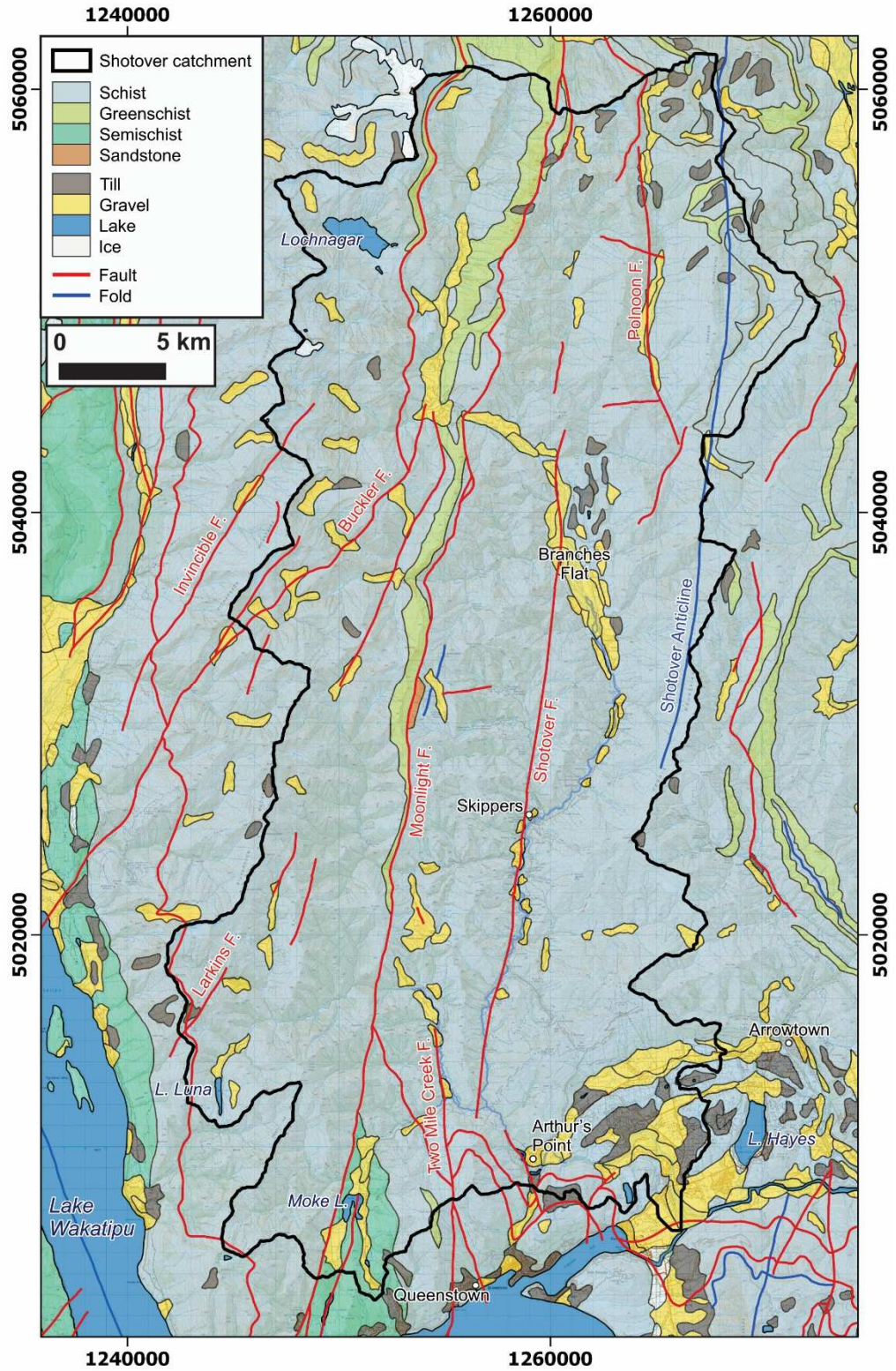

Figure 1.6: *Shotover catchment geology showing the main basement and cover units, and structural features. Lithology and structure obtained from QMAPS compilation (Turnbull 2000), locations and extents of the interpreted Shotover and Polnoon Faults are based on Turnbull et al. (1975) and OCB (1956).*

Shotover Catchment Quaternary Geology

In the Shotover Valley, OCB (Brown 1956, OCB 1966) and MWD (Turnbull et al. 1975a, McSaveney 1978) reports describe aspects of the valley's geomorphology, including the river system, terraces and landsliding. McSaveney's (1978) report investigates the Shotover River's contribution to siltation in Lake Roxburgh. This includes descriptions of the Branches Flat paleolake 'Lake Borrell' and Polnoon Burn landslide dam, discussing their influence on sediment supply and storage. Thompson (1998) discusses formation of the Shotover Valley's glacial, alluvial terrace, and placer gold deposits. Terrace profiles are used to correlate these with equivalent deposits in the Wakatipu Basin and Kawarau Valley and infer ages of glacial advances (Thompson 1998).

The Quaternary geology, geomorphic and glacial history of the Wakatipu Basin are outlined by Bell (1992) and Barrell et al. (1994). These includes glacial extents, mapping of Quaternary deposits, and interpretation of geomorphic history. The Quaternary geology of the area is also discussed in various regional geology studies, including Park (1909), Wood (1962), and Turnbull (2000). Cunningham (1994) carried out a geomorphic and engineering geology study for the Wakatipu Basin and Queenstown areas. Mapping of geomorphology and surficial Quaternary deposits were completed at 1:25,000 scale, including the Shotover River area from the Kawarau confluence to Arthur's Point. Other geomorphic studies in the Wakatipu area have focused on the Kawarau Valley (Stroud 1968, Bell 1992), Rees Valley (Cook et al. 2014) and the Glenorchy district (Kober 1999).

Glacial History

The Wakatipu Valley was glaciated repeatedly throughout the Quaternary with at least 20 Quaternary glacial advances, and 14 in the last 1M years (Table 1.2). Earlier glaciations were larger, with later advances appearing to be successively reduced in extent (Barrell et al. 1994). Extents of the Wakatipu glaciations have been inferred by Bell (1992), Turnbull (2000) and Barrell (2011) based on glacial landforms and deposits. These show ice filling the Wakatipu Valley, scouring out the depression now filled by Lake Wakatipu, and extending south to a main glacier tongue at Kingston. During the Last Glacial Maximum (LGM) a smaller lobe spread northeast towards Arrowtown, with minor ice tongues pushing up the Arrow and Shotover Valleys (Figure 1.7) (Barrell et al. 1994, Barrell 2011).

There is no geochronology to constrain ages of the Shotover Valley's glacial and alluvial deposits. Thompson (1998) interprets seven glacial advances in the Shotover Valley, based on valley morphology, and correlation of terrace levels with equivalent Wakatipu Basin deposits (Figure 1.8). In this interpretation, the oldest events are Waimean Glacial (MIS6) advances into the upper Shotover Gorge, a tentative Skippers Creek advance and an advance to about Sandhill Creek. Three Otiran (MIS2-4) advances are inferred to have reached the Branches Flat area, named the Ironstone, Stockyard (tentative) and Flood Burn advances. A moraine at Seventeen Mile Creek is attributed to a late glacial advance (McSaveney 1978, Thompson 1998). The best-defined advances are the Flood Burn and Sandhill Advances (Figure 1.8). The Flood Burn Advance is defined by widespread moraine deposits in the middle Branches Flat area, and the Sandhill Advance by till and ice-contact sediments (McSaveney 1978, Thompson 1998). Both McSaveney (1978) and Thompson (1998) correlated each main Shotover terrace level with a corresponding glacial advance, interpreting terraces as forming during the Branches Flat and Sixteen Mile Creek advances.

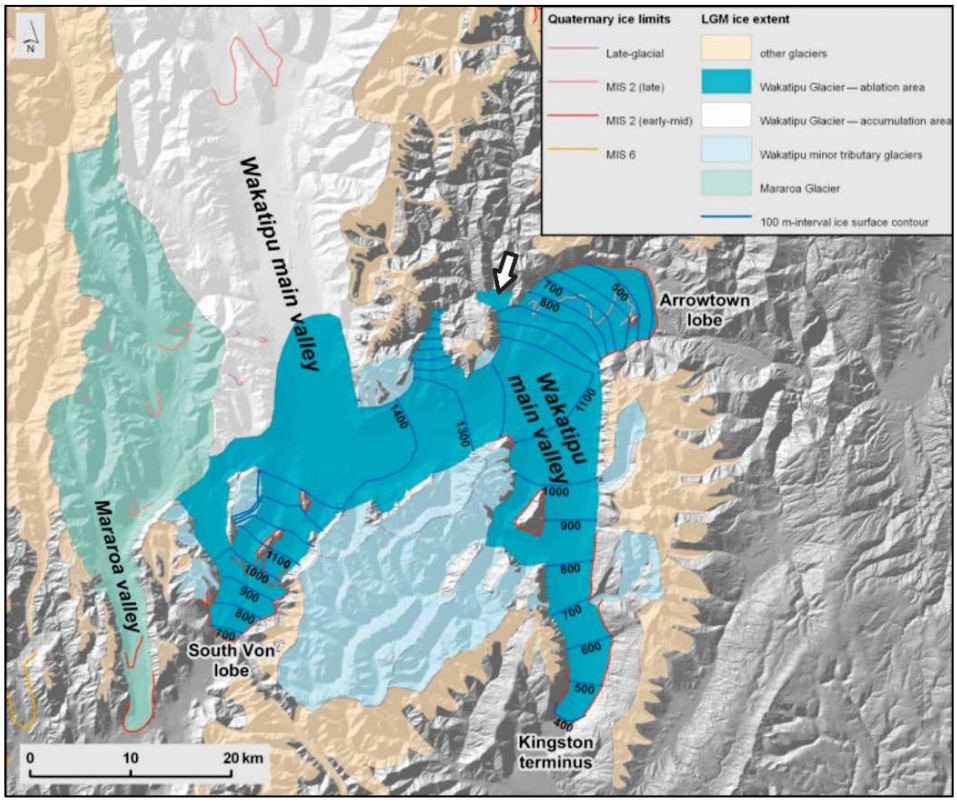

Figure 1.7: *LGM glacial extent in the Lake Wakatipu area, showing a terminus at Kingston, and a northeastern lobe filling the Wakatipu Basin with the Shotover lobe indicated by arrow (Barrell 2011).*

Table 1.1: *Summary of New Zealand Glacial Stages (Barrell 2011), showing glaciation names, approximate ages, and correlation with MIS Stages.*

New Zealand Names for Glaciations and Interglaciations (Suggate, 1990; Suggate and Waight, 1999)

MIS Stage	Glaciation	Interglaciation	Approximate Age (cal. ka)
1		Aranui	0–11.5 (by definition, Aranui includes LGIT, and Spans 0–18)
2	'Last Glacial/Interglacial transition—LGIT' (including 'Late-glacial' events – e.g. Antarctic Cold Reversal (ACR))		11.5–18
	Late Otira		18–30
3	Mid-Otira		30–50
4	Early Otira		~65
5		Kaihinu	Little direct age control in NZ—refer to published MIS stage boundaries
6	Waimea		
7		Karoro	
8	Waimaunga		
9		(Not named)	
10	Nemona		
11		(Not named)	
12	Kawhaka		
(Preceding glaciations and interglaciations not assigned formal names)			
	Porika		> 1.8 Ma, ?<2.6 Ma
	Ross		?<2.6 Ma

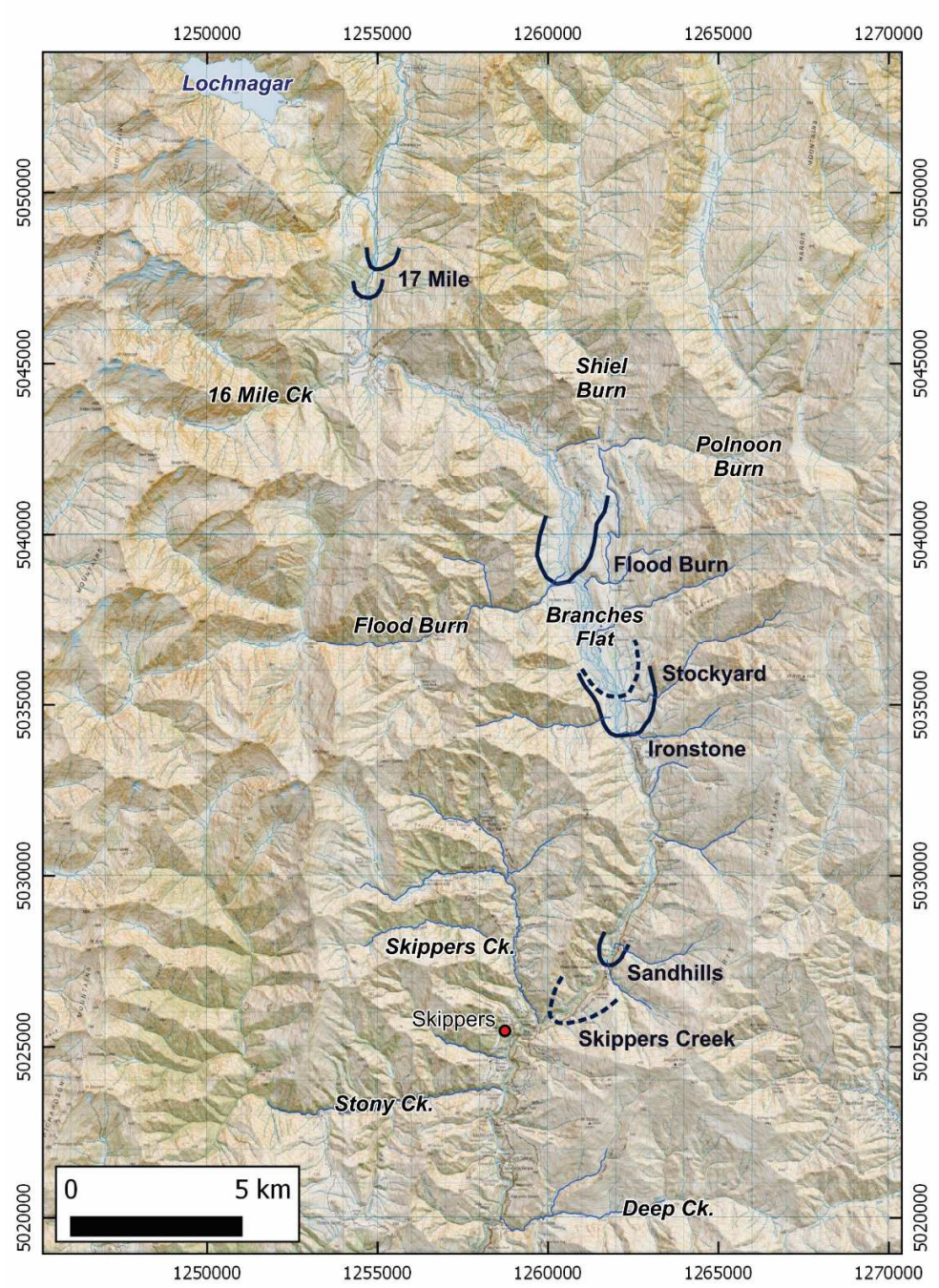

Figure 1.8: *Thompson's (1998) interpreted glacial advances in the Shotover Valley to the upper Shotover Gorge and Branches Flat area. Those dashed are tentatively identified only.*

Landslides and Landslide Dams

Landsliding and erosion in the Shotover catchment has been investigated by several studies. Gibbs et al.'s (1945) soil erosion survey of the high country of the South Island included much of the catchment. The Otago Catchment Board carried out high country resources surveys of the upper and lower Shotover catchment (Gillies 1956, OCB 1966).

These included surveys of geology, soils, hydrology, vegetation, sedimentation, erosion and soil conservation. These reports identified sediment sources, and were followed up by more detailed landuse capability mapping, and erosion surveys over individual farms.

The most comprehensive investigation has been the sediment sources study carried out by the Ministry of Works and Development (MWD 1975), assisted by the NZ Geological Survey, Otago Catchment Board, NZ Forest Service, and Department of Lands and Survey, prompted by concerns about sediment buildup in the lake behind the Roxburgh hydroelectric dam. The report gives a substantial catchment overview including soils, vegetation, climate, landuse and erosion, with appendices covering the catchment's geology and hydrology. The erosion component of the project included classification and evaluation of all mass movement and erosional sources identified within the catchment.

Large landslides at Arthur's Point and Coronet Peak, and the smaller Devil's Creek and Dirty Four Creek landslides were investigated by Willetts (2000). The study described these slides and carried out geotechnical analyses. Several smaller landslides in or near the gorge have been investigated where they impacted on roadways or river usage. Bryant (2011) summarised several rockfalls which impacted the Shotover River, causing temporary blockages and minor lake formation, the largest of these was the 7-8,000 m^3 Criterion Creek rockfall (1993). In 2008, reactivation of a landslide at Moonlight Track threatened to deposit debris into the Shotover River. This resulted in a precautionary closure of the river to rafting activities, and closure of the walking track by the Department of Conservation (DoC) (Dellow et al. 2009, Bryant 2011). A 2012 landslide at Devil's Elbow severely damaged the Skippers Road, which was intermittently closed over the following month while remedial earthworks were undertaken. The landslide debris partially blocked the river channel, forming a small rapid (Downer 2013).

Shotover Landslide Dams

Perrin and Hancox (1992), Korup (2006), and Bryant and Goldsmith (2013) reviewed regional-scale landslide dam occurrences, including the Shotover area. In the upper Shotover landslide dams have been noted during geological investigations by the OCB (Brown 1956), MWD (1975), and McSaveney (1978). Only the Lochnagar and Polnoon Burn dams have been investigated in any detail. Sweeney et al. (2013) interpreted the failure mode and structural controls of the Lochnagar landslide, and carried out ^{10}Be exposure dating of landslide material, with resulting ages ranging from 6,300 ± 300 to 8,900 ± 300 years. The Polnoon Burn landslide dam has been described by Korup (2006) and Korup et al. (2006) and dated to 5,301 ± 78 cal. years BP (3,273-3,429 BCE) (Hancox and Salt 1990, in Hancox et al. 2013).

Several previous landslide dam hazard assessments have been undertaken for the Shotover Gorge. Thompson (1996) investigated the potential for landslide dam formation in the upper Kawarau and lower Shotover Gorges to affect the level of Lake Wakatipu. Bryant's (2011, 2017) reports were prepared for the subdivision approval process for land adjacent to the Shotover River and Delta. Davies (2017) also prepared a submission for ORC in relation to proposed Shotover River developments.

Evolution of Lake Wakatipu and the Shotover River

Lake Wakatipu is the third largest lake in New Zealand (291 km^2) and has a catchment area of 3,067 km^2. It is fed mainly by the Rees and Dart Rivers, which flow into the northern end of Lake Wakatipu where they merge to form the Rees-Dart delta. Lake Wakatipu has a single outlet draining into the Kawarau River at Frankton Arm, then flowing through the Kawarau Gorge to join the Clutha River at Cromwell.

Formation of the postglacial Shotover Delta and evolution of Lake Wakatipu are discussed by Barrell et al. (1994) and Thompson (1996b). The postglacial history of Lake Wakatipu was further refined by Stahl (2014) based on measurement and dating of stranded lake shorelines. The lake is interpreted as forming in a glacially deepened

depression following glacial retreat by approximately 17 ka (Stahl 2014). The lake's initial level may have been as high as ~400 m (Barrell 1994), and then had an extended stillstand at ~355 m (Figure 1.9) shown by shoreline deposits, rock-cut benches, and lacustrine and deltaic deposits (Park 1909, Barrell 1994, Thompson 1996b, Stahl 2014). This lake had a larger extent continuous with Lake Hayes, covering the Frankton Flats area, with an outflow at Kingston into the Mataura River. The lake level gradually lowered as the Kingston outlet incised, then at some stage drainage switched to the Kawarau River. The drainage capture process is not known but a possible scenario is outlined by Thompson (1996b). This involves Kawarau River tributaries downcutting and migrating westwards, and as these incise into Shotover Delta deposits they allow Lake Wakatipu to link with Kawarau River. As the new Kawarau outlet is incised, the lake level continues to lower. From 2.2 ka lowering of lake level accelerates, with a rapid drop to 305 m, approximately 5 m below current lake level (Figure 1.9). The raising of the lake up to its current level of approximately 310 m could have been caused by a landslide into the Kawarau River partially blocking the lake outlet (Thompson 1996b, Stahl 2014).

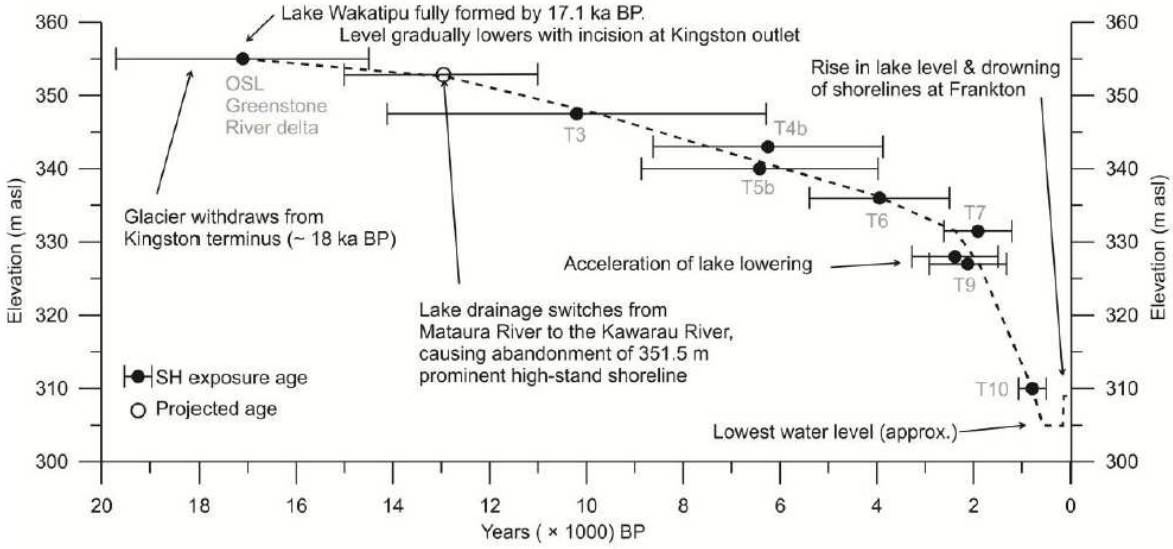

Figure 1.9: *One interpretation of the development of the postglacial Lake Wakatipu, showing lowering to present level, reconstruction by Stahl 2014.*

Bell (1992) envisaged a pre-glacial drainage pattern where the eastern and western arms of Lake Wakatipu are separated by a low divide, with the ancestral Arrow and Shotover drainages flowing along the line of the eastern arm and into the Mataura catchment. During the Waimaungan Glacial (MIS8, 245-303 ka) the ancestral Shotover River flowed to the north of Coronet Peak, leaving the current Shotover channel along the path of Deep Creek, then flowing into the Arrow catchment where it followed the path of Eight Mile Creek. Alluvial sediments 150 m thick are deposited at the Deep Creek-Eight Mile Creek Saddle (Bell 1992). By the late Otiran Glacial at 25-15 ka, the Shotover River followed its current route through the lower gorge to Arthur's Point, but then flowed along the base of Coronet Peak to join the Arrow River. By the early interglacial period (15 ka) the Shotover River was flowing into Lake Wakatipu at about its current path (Bell 1992).

From ~15 ka, the Shotover River flowed into the then-larger Lake Wakatipu at a level of 355 m, forming a large fan-delta estimated to contain 900M m^3 of sediment (Thompson 1985, in ORC 1997). This delta had a head located near Tucker Beach at an elevation of ~357 m. A slightly-inclined delta-plain aggradation surface formed, extending to the foot of the Remarkables Range, and cutting off Lake Wakatipu from Lake Hayes. Remnants of the delta surface are

preserved as the Frankton, Ladies Mile, and Domain Road Flats (Cunningham 1994, Barrell et al. 1994) (Figure 1.10). These deltaic deposits form part of a complex of fluvio-deltaic-lacustrine sediments deposited as the delta prograded into the lake. As the lake lowered to its current level, the lower Shotover River channel degraded in response, incising by 30-40 m into the older delta deposits, and attained its current form by 1000-3000 years ago (Thompson 1996, Stahl 2014). The terrace sequence east of the current delta shows a westwards channel migration during this period of downcutting.

Figure 1.10: *The Shotover delta viewed from the Remarkables Range, the active channel width is 200-350 m, and the delta is about 2 km in length. The river is incised within older post-glacial delta surfaces at Frankton (left) and Ladies Mile (right). The hill in the middle distance (Ferry Hill) is interpreted as a roche moutonee (Cunningham 1994). The Shotover Country development can be seen in progress located to the right (east) of the Shotover Delta (photo taken in November 2017).*

1.5 Community Setting, Ownership and Access

The largest population centre in the Wakatipu area is Queenstown with a permanent population of ~15,000, and a large number of tourist visitors, with a total of over 3.5M guest nights spent in Queenstown annually (May 2017-April 2018, MBIE 2018). Located near the lower Shotover River are the smaller settlements of Arthur's Point, Dalefield, Lower Shotover and Ladies Mile (Figure 1.1). In recent years, population growth and resulting pressures have led to significant residential expansion in these areas, in particular in areas between Lake Hayes and the Shotover River (e.g. the Lake Hayes Estate and Shotover Country residential developments). Of most significance to this study is Shotover Country, located on a low terrace adjacent to the Shotover Delta (Figure 1.10), the consenting process for which led to many of the previous Shotover Delta flooding and landslide dam assessments.

Much of Queenstown's tourist industry is based around adventure tourism activities, some of which utilise the Shotover River, gorge and surrounding areas. The river is used for commercial rafting and jet boat tours, and the gorge for canyon swing and zipline operations. Other tourism activities in the Shotover area include 4WD tours and guided hikes to experience the high country, gorge, and historic sites. In addition to these commercial activities, there is also a network of hiking tracks administered by the Department of Conservation (DOC).

In 2013, tourism activities on the Shotover River were estimated to have total annual value of $37M, or ~$100,000 per day (Bryant and Goldsmith 2013). At this daily rate, even minor landslide events may have significant economic consequences through disruption of commercial tourism activities, as occurred during suspension of river-based activities due to the 2008 Moonlight Track landslide (Bryant 2011), or the 2012 Devil's Elbow landslide limiting access on Skippers Road (Downer 2013). Bryant and Goldsmith (2013) note that the main concern in landslide dam formation is not just the dam or lake magnitude, but also its location and possible threat relative to tourism activities or vulnerable communities.

The Shotover Gorge study area is accessed by the unsealed Skippers Road (Figure 1.1). This road climbs the slopes of Coronet Peak from Arthurs Point, descends along Deep Creek and then follows the true left bank of the Shotover River. The historic Skippers suspension bridge provides access to the terraces on the western side of the valley. From Skippers, the Branches Road continues for ~15 km to Branches Station (Figure 1.1). The Moonlight Valley is accessible as far as Sheepyard Terrace by an unsealed road starting near Moke Lake. Several walking tracks provide access to the true left side of the lower gorge from Skippers Road, including the Devils Creek, Shotover Canyon and Atleys Tracks. The Moonlight Track runs from Arthurs Point to the Moke Lake Road, providing access to the true right side of the lower Shotover Gorge and Moonlight Creek. Footbridges at Campbells Saddle and Wire Rope Terrace cross the Shotover River, and another crosses Moonlight Creek shortly below the Moke Creek confluence.

The majority of the study area comprises high country pastoral leases of Coronet Peak, Branches, Ben Lomond and Mount Creighton Stations. Mount Aurum Station is now conservation land administered as the Mount Aurum Recreation Reserve.

Chapter Two: Geomorphology and Quaternary Geology

2.1 Introduction

This chapter summarises the main geomorphic features and Quaternary geological units of the Shotover Gorge and lower Branches Flat. The new mapping, stratigraphic logging, surveying, and optically-stimulated luminescence (OSL) dating provide geological context for subsequent chapters, are used in identifying and interpreting key events in the valley's recent geological history (Chapter Three), and provide a guide to the nature of possible future landslide events (Chapter Six). The main components of this chapter include

1. Reconnaissance scale (1:20k) mapping of the study areas main Quaternary geological and geomorphic features, including glacial and lacustrine sediments, alluvial terraces, and mass movement features (full size map available in Appendix 1).
2. Mapping and surveying of terrace levels, which has been used to compile long-profiles (Figures 2.6, 2.7) and sketch cross-sections (Figure 2.5) showing the distribution, elevations and correlations of terrace surfaces.
3. Investigation of glacial deposits in the upper Shotover Gorge, with completion of outcrop sketches at Smiths Terrace (Figure 2.19), Sandhill Cut (Figure 2.21), and an outcrop sketch (Figure 2.24) and stratigraphic section (Figure 2.25) at a Sandhill Creek outcrop.
4. Investigation of lacustrine sediments in the upper Shotover Gorge and lower Branches Flat, with completion of stratigraphic sections at Strohles Flat (Figure 2.12) and the Ironstone Creek delta (Figure 2.17).
5. Description of landslides in the Shotover Gorge, noting characteristics of location, size and type. Creeping schist landslides have been mapped in Figure 2.29, other Shotover Gorge landslides are mapped in Chapter Six (Figure 6.11).

2.2 Study Area

This study covers the Shotover Valley from Arthurs Point to Branches Flat, and also includes the lower ~7 km of Moonlight Creek, and a small area of Moke Creek (Figure 1.1). A surficial geology map (Appendix 1) has been compiled for the valley floor and adjacent slopes of the Shotover Valley, mostly limited to areas covered in field reconnaissance. Creeping schist landslides are much larger features, extending from river to ridge crest over distances of up to 2-3 km. These have a distinctive appearance in aerial imagery and have been mapped from photographs over a larger area, which includes the Skippers Creek catchment, and parts of larger tributary catchments such as Moonlight and Stony Creeks (Figure 2.29). Mapped features include

1. **Quaternary geology:** alluvial terrace and fan gravels, lacustrine silt-sands, and glacial sediments.
2. **Geomorphic features:** bedrock and alluvial terrace edges, landslide scarps, and areas of slope deformation.
3. **Historic modifications:** hydraulic sluicing excavations.

2.3 Methods

A combination of remote-sensing and field techniques was used to map the field area. A preliminary map was completed from GIS-based analysis using the datasets noted in Appendix 1. The methodology for GIS-based mapping followed that used in similar studies, for example geomorphic mapping in the Rees Valley (Cook et al. 2014), and landslide mapping in the Southern Alps and Fiordland (Hovius et al. 1997, Hancox et al. 2003, Korup 2005b). Data visualisation and analysis was completed in QGIS and ArcGIS, complemented by use of Google Earth imagery. Field mapping in accessible parts of the Shotover and Moonlight Valleys was recorded on a series of seven 1:20,000 scale basemaps. Geomorphic features were then digitised in ESRI shapefile format.

Terrace long-profiles were surveyed using handheld Trimble GPS (models GeoXH and Geo7x), with a vertical accuracy of ± 0.5 m. Surveyed features included terrace and fan surfaces and river elevations. Survey data were acquired at over 30 individual terrace and fan locations in the Shotover, Moonlight and Moke Creek catchments (Figure 3.4). Mapping and survey data are included as digital files in Appendix 1. Stratigraphic sections have been logged according to Evans and Benn (2004). Logging codes and the coordinates of section locations are shown in Table 2.1.

2.4 Fluvial Landforms

Multiple terrace levels in the Shotover Valley and Moonlight Creek reflect the operation of an active fluvial environment over a long duration. This section summarises the terrace and alluvial deposits, and provides results of terrace surveys. The modern Shotover River varies from a braided alluvial riverbed hundreds of metres in width, to a narrow and deeply incised bedrock channel. From Branches Flat to the Kawarau confluence, the river can be divided into five geomorphically distinct reaches. The locations of these reaches are shown in Figure 2.2, and examples of each are shown in Figure 2.1.

1. **Branches Flat (Shiel Burn to Ironstone Creek):** Braided alluvial flats ~8 km in length and up to 600 m in width, with alluvial fans developed from tributary streams, such as at Flood Burn, Ironstone Creek and Stockyard Creek.
2. **Upper Shotover Gorge (Ironstone Creek to Sandhill Cut):** A valley floor up to 150-200 m wide with large beaches and floodplain sections, such as Sloans Flat, Ashworths Flat and Strohles Flat.
3. **Middle Shotover Gorge (Sandhill Cut to Deep Creek):** An incised bedrock gorge mostly <70 m in width, common high bedrock and alluvial terraces, mostly on the true right.
4. **Lower Shotover Gorge (Deep Creek to Arthurs Point):** A deeply incised gorge with few beach sections, the narrow channel is typically 20-60 m in width.
5. **Lower Shotover River (Arthurs Point to Shotover Delta):** Several large beaches up to ~600 metres in width (Big Beach and Tucker Beach) separated by narrow sections incised into schist or older delta deposits. The Shotover fan-delta extends for ~2 km to its confluence with the Kawarau River, where it is >1 km in width (Figure 1.10).

Active alluvial gravel riverbeds occur throughout the study area. The largest of these are the braided riverbed and alluvial fans at Branches Flat, the beach sections of Big Beach and Tucker Beach, and the Shotover Delta. Alluvial fans are formed by several tributary streams in lower part of Branches Flat, e.g. Ironstone and Stockyard Creeks (Figure 2.1A), and Maori Gully. During alluvial mining operations within the gorge, Braithwaite (1989) reported that alluvial gravels ranged in depth from 0.8 m to greater than 8 m. The deepest gravels were found where rockfalls had blocked the channel, locally raising the base level. At Branches Flat, Price and Brooks (1983) and Nugold (1990) reported

gravels to depths of up to six metres. These alluvial gravels overlie lacustrine sediments, but the depth to the underlying schist bedrock is not known.

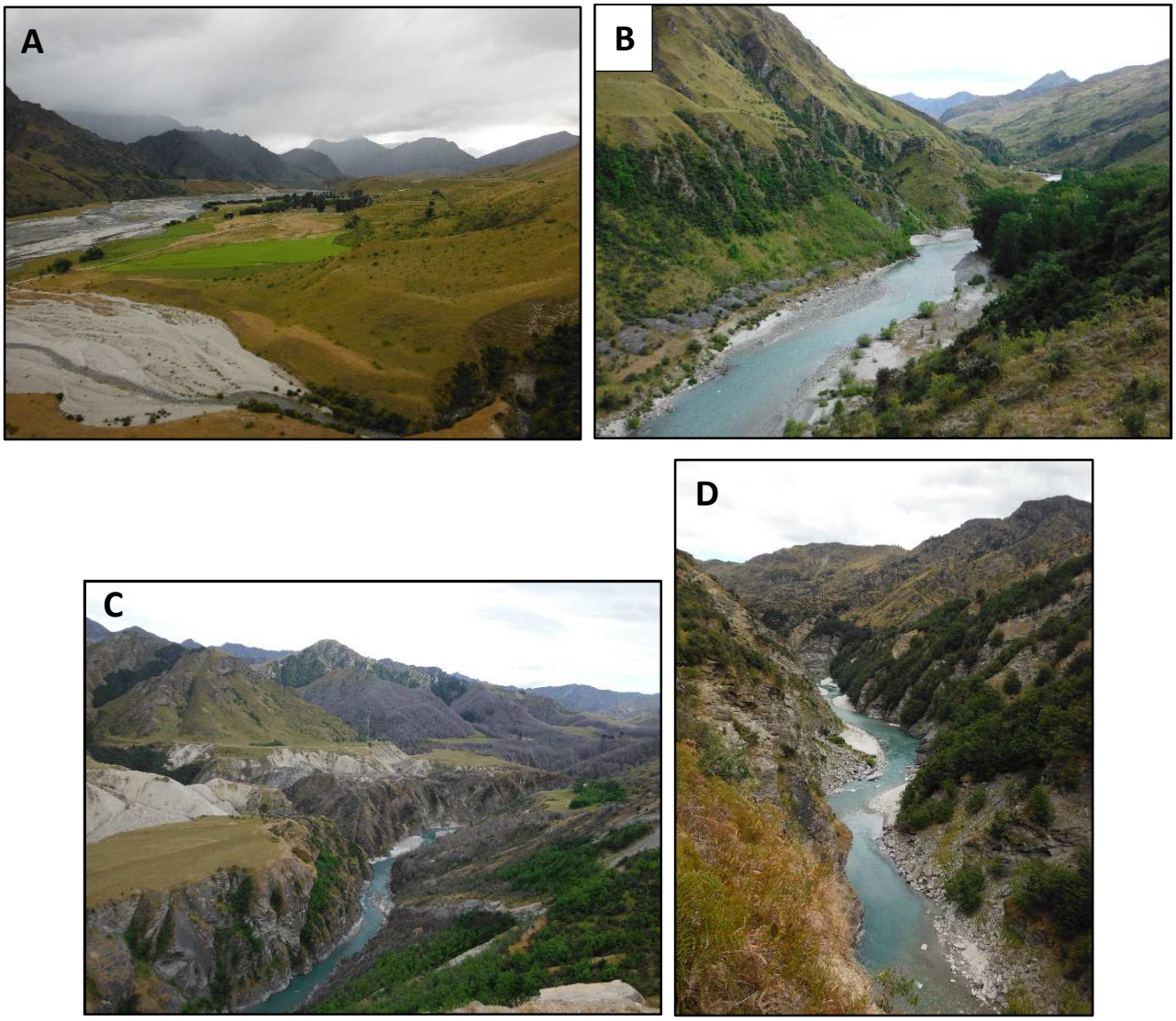

Figure 2.1: *Examples of variable Shotover River planform: A. Braided alluvial Shotover River channel (500-600 m width) and floodplain looking upriver at Branches Flat, with the Stockyard Creek alluvial fan in foreground. B. Valley floor and beaches (~120 m width) in the upper Shotover Gorge, looking upriver to Sloan's Flat. C: Middle Shotover Gorge looking upstream towards Stony Creek and Pleasant Creek terraces, showing channel of 30-40 m width incised 90-95 m below bedrock terraces, with thick alluvial gravels and sluiced excavations on high terraces. D. The lower Shotover Gorge looking downriver at about Siphon Gully, channel is 50-60 m width, debris fan in middle distance at left is remains of the 1993 Criterion Creek rockfall (compare Figure 2.33A).*

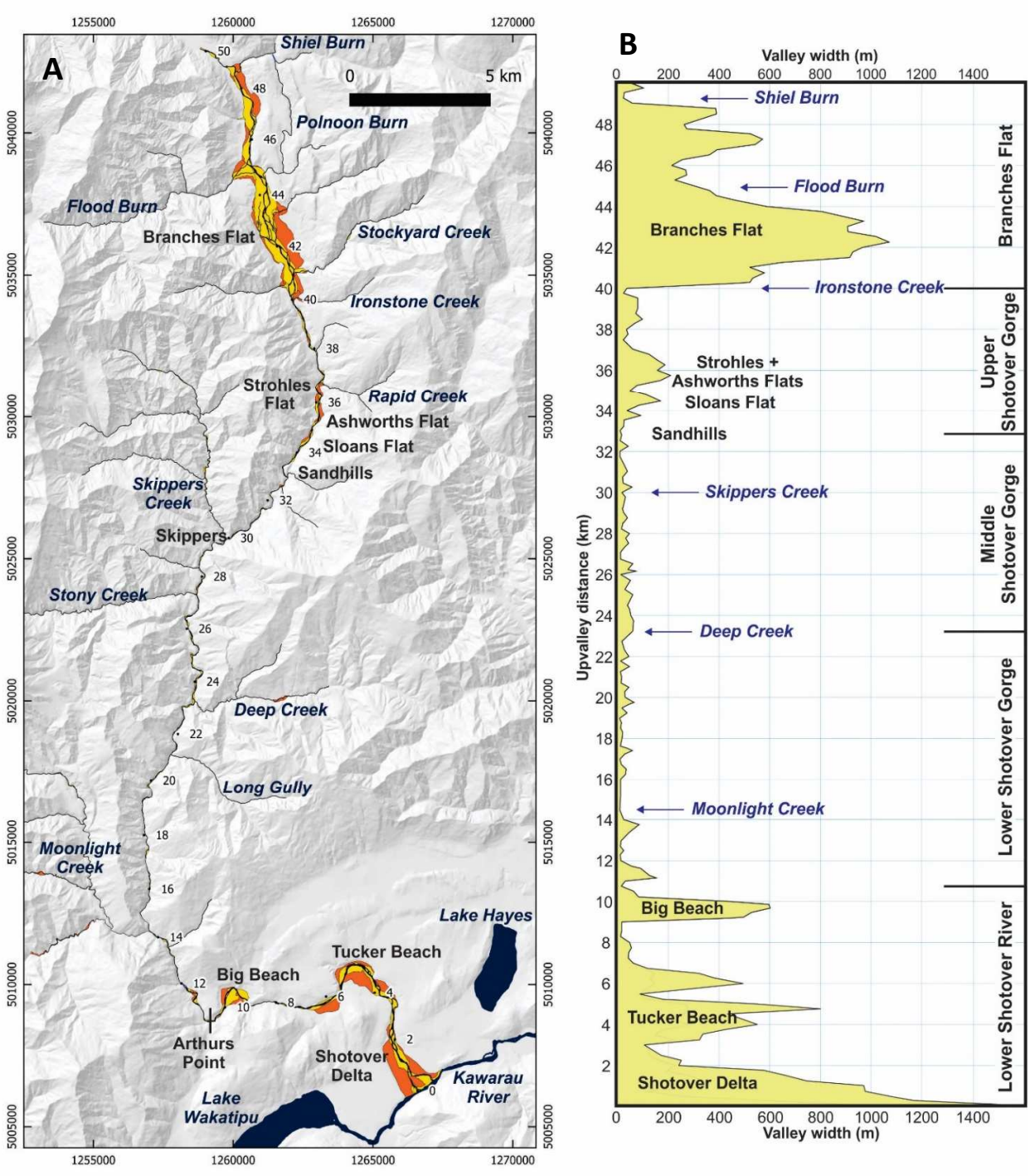

Figure 2.2: *A. Overview of the Shotover Valley and tributary streams, showing alluvial riverbeds (yellow) and floodplains (orange). B. Plot shows the valley floor width, measured as the combined width of the active riverbed plus the adjacent floodplain, this is plotted against the upvalley distance (km) from the Kawarau confluence. This illustrates the broad beach sections in the lower Shotover River and at Branches Flat, and a minor increase in valley width in the upper Shotover Gorge.*

Moonlight Creek runs in a narrow gorge for ~1.5 km upstream from its confluence with the Shotover, it has little alluvial gravel and is incising into bedrock (Figure 2.3). For the next 5-6 km upstream the creek flows in an incised gorge with common beach sections, below large bedrock and alluvial terraces, similar to the Shotover River in the Skippers area.

Figure 2.3: *Lower Moonlight Creek looking upstream towards the Moonlight-Moke Creek confluence (behind footbridge), with Moke Creek entering from the upper left of image. This shows the Moonlight channel incising into bedrock and contrasts with the often alluvium-filled Shotover riverbed. Footbridge is 15-20 metres in length.*

Terraces and Alluvial Deposits

Numerous bedrock and alluvial terraces, and alluvial fan or fan-delta surfaces are found in the study area. The largest area and most continuous terraces are adjacent to the Shotover River and in Moonlight Creek (Figure 2.4). These terraces and fans were investigated through surveying (Figure 2.4), mapping and geological descriptions. Note that not every large terrace surface was surveyed, for example the less accessible terraces on the western side of the upper Shotover Gorge, and some of those in the middle Shotover Gorge. At many of the surveyed terraces, large quantities of alluvial gravels have been removed by hydraulic sluicing and much of the original terrace sequence is no longer present (Figure 2.11).

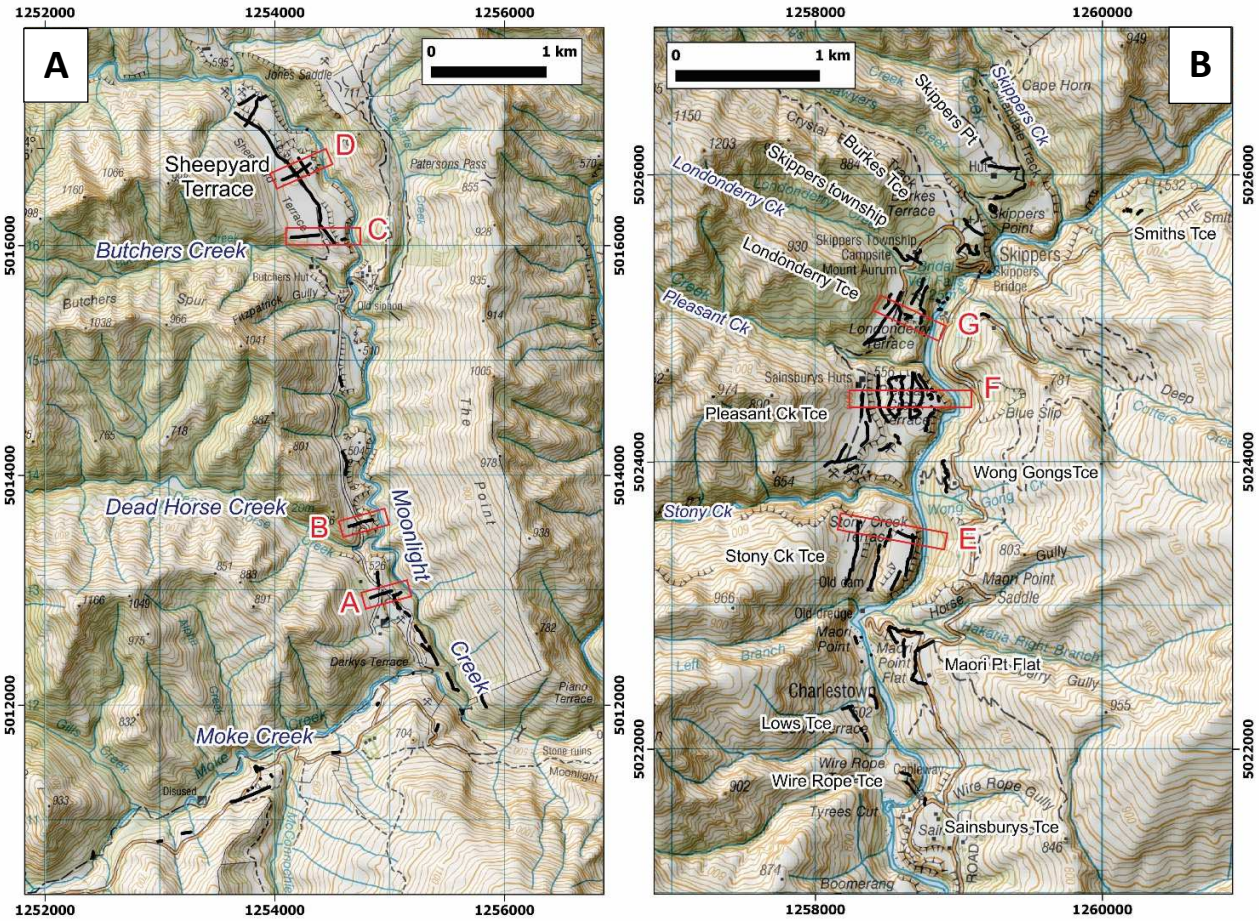
A
B
0
1 km
Sheepyard Terrace
Butchers Creek
Dead Horse Creek
Moonlight Creek
Moke Creek
Darkys Terrace
Piano Terrace
Stone ruins
Moonlight
Patersons Pass
Jones Saddle
Butchers Hut
Old station
Disused
McConnochie
Skippers Pt
Skippers Ck
Cape Horn
Skippers township
Burkes Tce
Burkes Terrace
Londonderry Ck
Londonderry Tce
Skippers Township Campsite
Mount Aurum
Skippers Point
Skippers
Skippers Bridge
Smiths Tce
Pleasant Ck
Londonderry Terrace
Salnsburys Huts
Pleasant Ck Tce
Blue Slip
Wong GongsTce
Stony Ck
Stony Creek Terrace
Stony Ck Tce
Old dam
Old dredge
Maori Point
Maori Point Saddle
Maori Pt Flat
Charlestown
Lows Tce
Wire Rope
Wire Rope Tce
Tyrees Cut
Sainsburys Tce
Boomerang
ROAD
1252000
1254000
1256000
1258000
1260000
5016000
5014000
5012000
5026000
5024000
5022000

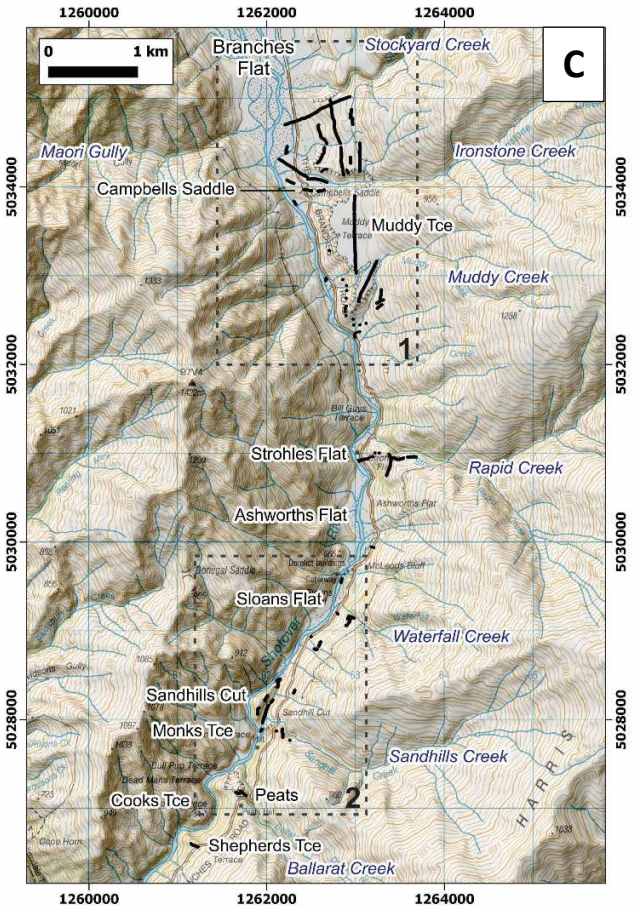

Figure 2.4: *Overview maps showing the main locations referenced in text, survey locations, and cross section locations (red labels A-G), for A. Moonlight and Moke Creek, B. Skippers area of the Shotover River, and C. the upper Shotover Gorge and Branches Flat. Dashed outlines show locations of Figure 2.14 (1) and Figure 2.20 (2).*

Terrace surveys are summarised in cross-profiles (Figure 2.5) and long-profiles (Figure 2.6, 2.7) showing the main terrace and fan levels. Based on the valley long profiles, terraces and fan surfaces have been correlated for the Skippers section of the Shotover Valley and for Moonlight Creek. These show two main terrace levels, named as bedrock terraces (S1, ML1), and the upper alluvial terraces (S3, ML3). In addition to these first-order correlations, there are a number of discontinuous intermediate terrace levels between these main levels; these are not widely correlated and have been collectively named the S2 and ML2 intermediate levels.

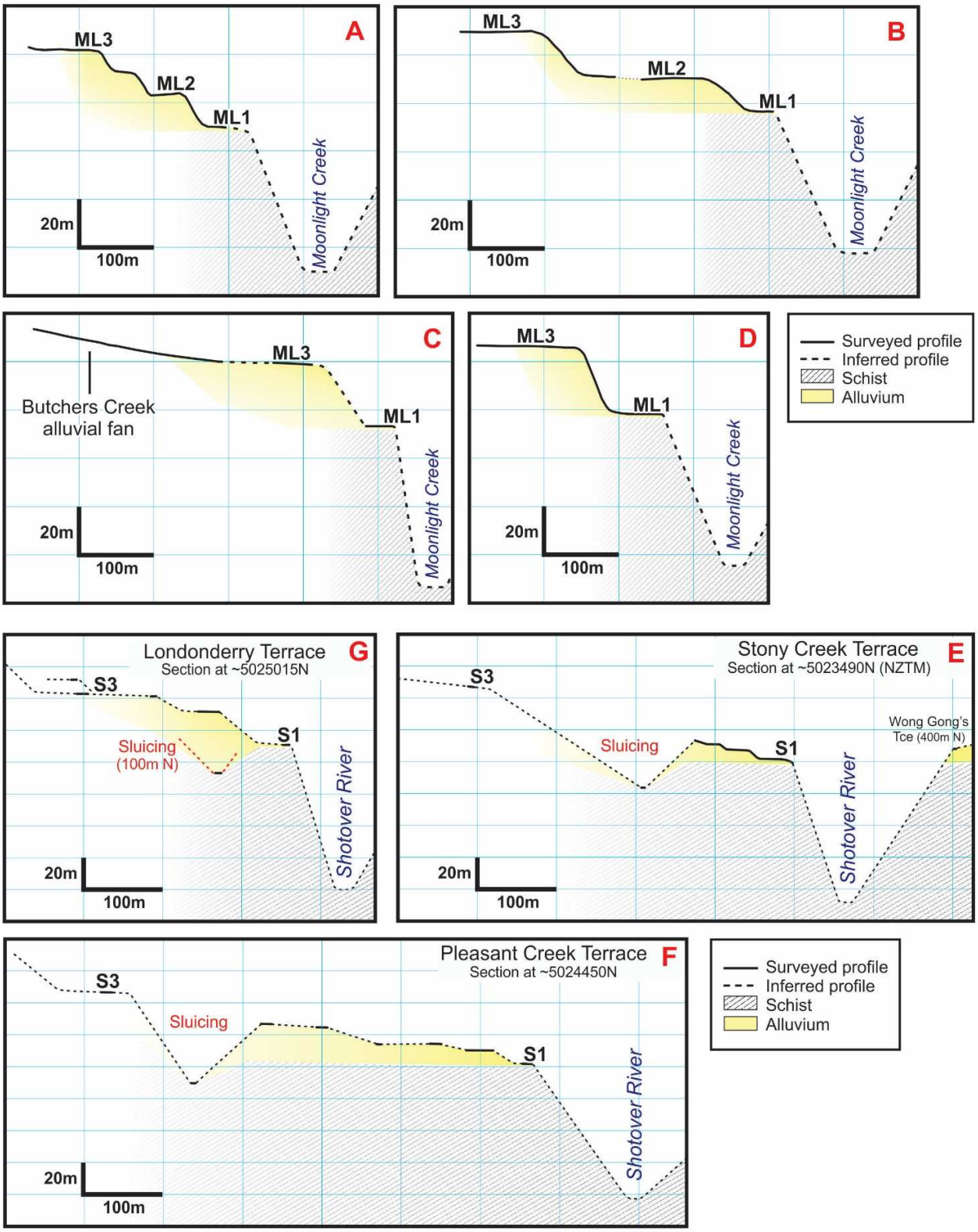

Figure 2.5: *Sketch profiles of Moonlight Creek (A-D) and Shotover River (E-G) terraces based on surveyed elevations, locations of these cross-sections are shown in Figure 2.4A, B and Figure 2.7.*

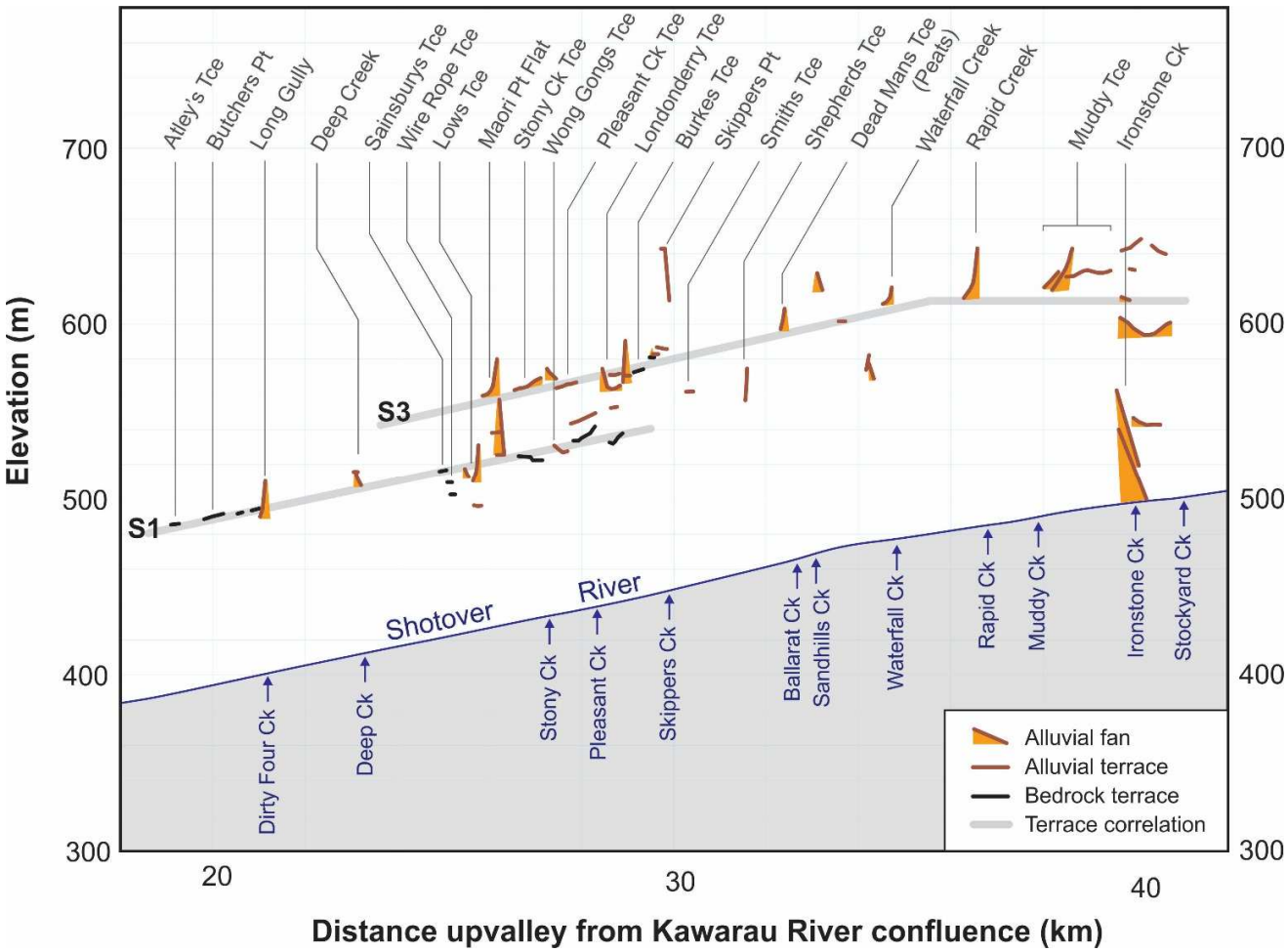

Figure 2.6: *Shotover River terrace long profile showing the elevations of surveyed terraces and alluvial fans, and interpreted correlations (S1, S3).*

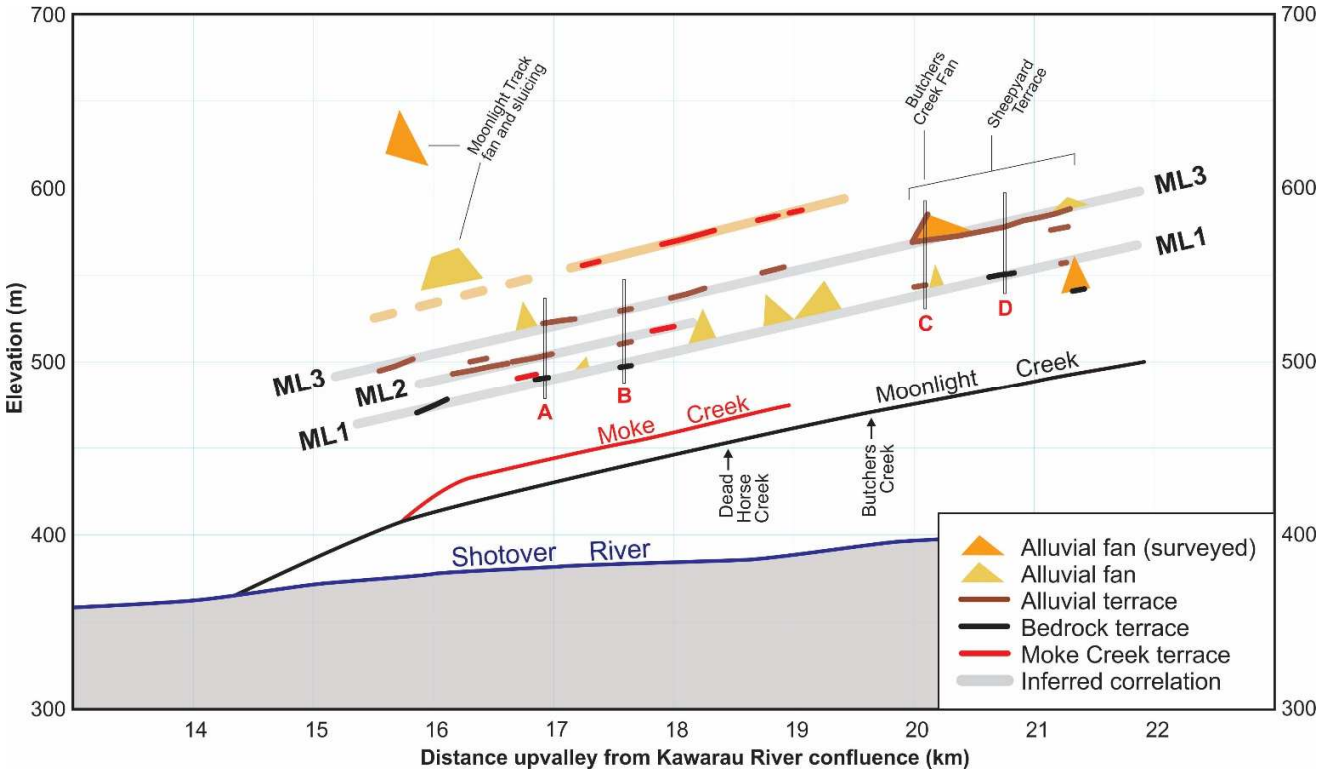

Figure 2.7: *Moonlight and Moke Creek terrace long profiles showing the elevations of surveyed terraces and alluvial fans, and interpreted terrace correlations (ML1-ML3). The locations of terrace cross sections are labelled (A-D).*

Bedrock Terraces (S1, ML1)

Bedrock terraces are found in the Shotover Gorge (S1) and at Moonlight Creek (ML1). In the Shotover catchment the S1 terrace level occurs at 90-95 m above the current river channel (Figures 2.5E-G, 2.7, 2.8), extending from about Atleys Terrace in the lower gorge, for ~10 km upstream to Skippers Point. The high terrace underlying the Arthurs Point settlement is at a level of 80-85 m above the current river channel and may correlate with the Shotover Gorge bedrock terraces. In both the Shotover and Moonlight catchments these bedrock terraces are often covered by up to 30-40 m of alluvial gravel deposits forming the S3 and ML3 terrace surfaces. Where these overlying gravels have been eroded, terraces have a remaining veneer of 1-2 m of alluvial gravels. On several terraces at this level, bedrock paleochannels have been exposed through sluicing, for example at Stony Creek and Londonderry Terraces.

There are also bedrock terraces in the upper Shotover Gorge, but these do not show the large extents or consistent elevation trends of those seen in the Skippers area. Several of the upper gorge bedrock terraces appear to be at a lower level relative to the modern river channel, for example at Monks and Cooks Terraces (Figure 2.4C).

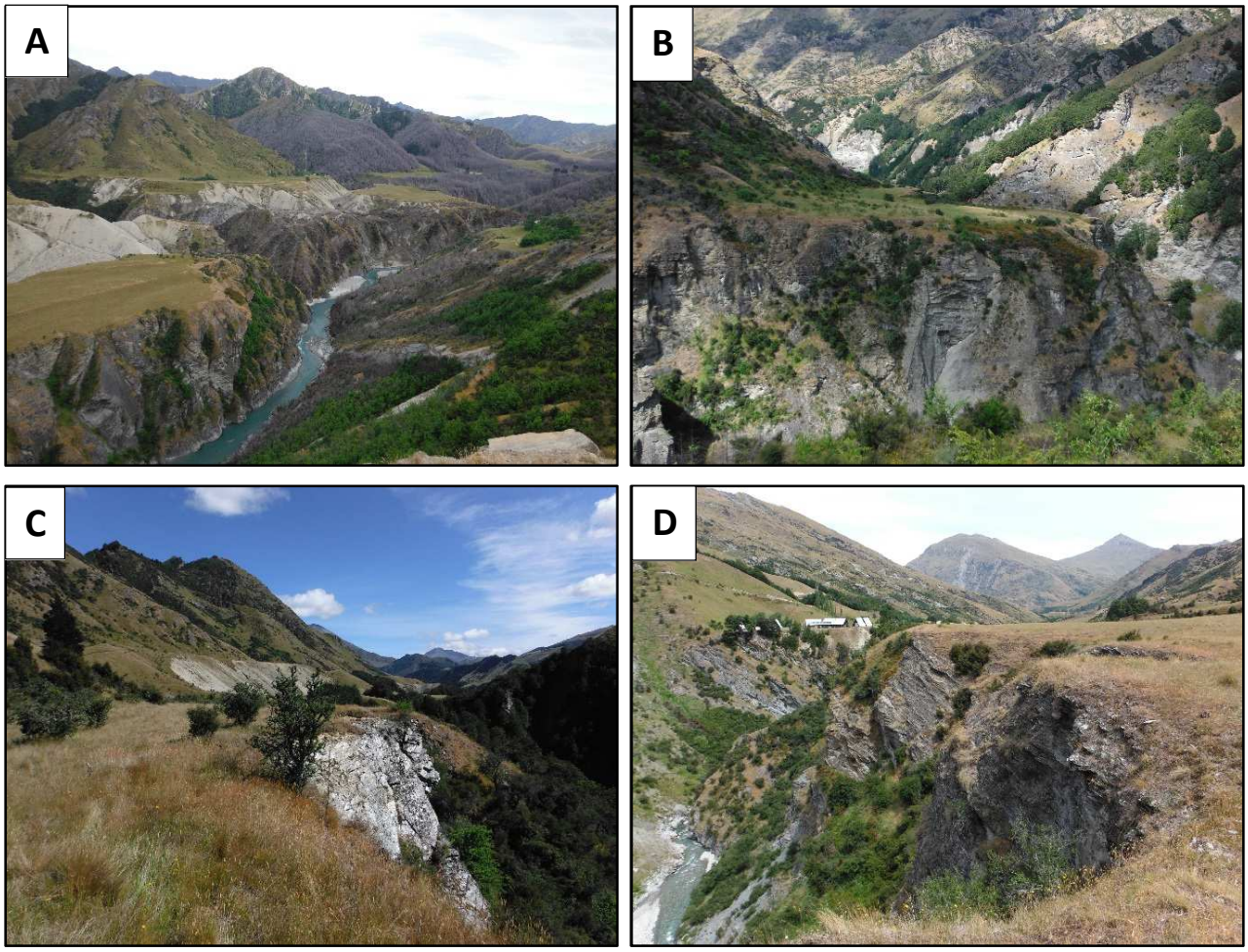

Figure 2.8: *Examples of bedrock terraces in the Shotover River; A. View upstream from about Maori Point, showing Stony Creek and Pleasant Creek terraces with sluiced excavations in higher S3 terrace gravels, and B. view downvalley at the Long Gully confluence. In the Moonlight Creek area, C. shows bedrock terrace level, and ML3 alluvial terraces in background at ~30 m higher elevation, and D. is view downstream at Sheepyard Terrace showing the sloping surface of the Butchers Creek alluvial fan grading to the bedrock level.*

Alluvial Gravel Deposits

Alluvial gravel deposits in the main drainages of the study area (Shotover River and Moonlight Creek) comprise both recent deposits in the active river channels, and older terrace, alluvial fan, and fan-delta gravel deposits preserved on the valley margins. Terrace deposits consist of coarsely-bedded alluvial gravels, with minor crossbedding and sandy-silty lenses. Gravels are predominantly the pelitic and quartzo-feldspathic schists abundant in the Shotover catchment, but also include greenschist, quartz vein material, and other less common lithologies, for example sedimentary clasts sourced from Bob's Cove Beds and lamprophyres (Park 1909, OCB 1956). Most outcrops of these gravels are seen as scree slopes of collapsed alluvium (e.g. Figure 2.9), but sedimentary textures are well exposed in outcrops such as at Smiths Terrace (Figure 2.19), Peats Terrace (Figure 2.10B), and at Ironstone Creek. The main alluvial terrace levels identified are described below.

Aggradational Terraces (S3, ML3)

These terraces are the most extensive and continuous in the study area, with the largest terrace remnants all at this elevation above the present riverbed. The main Shotover S3 terraces extend for 4-5 km upstream from Blue Jacket Terrace to about Skippers Point (Figure 2.4). This surface is located at an elevation of ~130 m above, and approximately parallel to, the modern Shotover River channel (Figures 2.5E-G, 2.6). In the Skippers area and at Moonlight Creek they overlie bedrock terrace surfaces. The Moonlight ML3 terraces are all on the western side of the valley, and extend from about the Moke Creek confluence to Sheepyard Terrace (Figures 2.4A, 2.7). These are at an elevation of ~90 m above, and oriented parallel to, the modern riverbed.

Figure 2.9: *View to south through Pleasant Creek sluicing excavation showing >30 m thickness of alluvial gravels. Sluiced cut is 40-50 metres deep, and 150-180 metres wide. Schist outcrops near base of cut (left) mark approximate base of alluvium and location of interpreted bedrock paleochannel.*

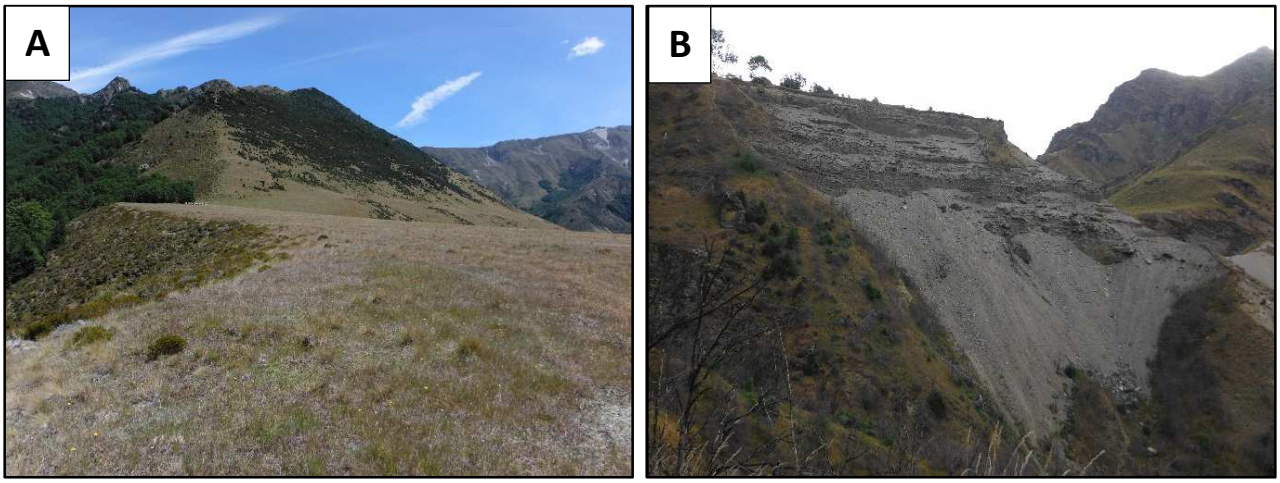

Figure 2.10: *A. Surface of Butchers Creek fan on Sheepyard Terrace (Moonlight Creek) and B. View downvalley of the thick sequence of inclined alluvial fan gravels at Peats Terrace/Ballarat Creek in the upper Shotover Gorge.*

Intermediate Alluvial Terraces

Several intermediate terrace levels are located below the extensive S3 and ML3 alluvial terrace level, and above the S1 and ML1 bedrock terrace level. These are best seen in historical images of the Skippers terraces prior to sluicing, showing a series of up to seven terrace levels at Pleasant Creek Terrace (Figure 2.11). In some locations these can be correlated with reasonable confidence, for example to an intermediate-level Moonlight Creek terrace which can be traced for several kilometres (Figure 2.7). In the Skippers area there are several large intermediate terrace levels, notably at Stony Creek and Pleasant Creek Terraces. While some of these terrace surfaces appear to be topographically correlated along the gorge, these cannot be confidently interpreted as isochronous due to the discontinuous nature of these terrace remnants.

Figure 2.11: *Historical (probably pre-1900s) view of Skippers terraces, prior to* cre*ation of the largest sluiced excavations (compare Figure 3.1C). From left-right, terraces shown are Pleasant Creek (PC), Londonderry (L), and Burkes (B) Terraces. Wong Gongs (WG) terrace is on the east side of valley. The Skippers schoolhouse and homestead is located at S. Note the occurrence of at least 6-7 distinct terraces at Pleasant Creek Terrace (Historic Wakatipu archive).*

High Alluvial and Terrace Remnants

Remnants of a small number of alluvial surfaces are found at higher levels than the S3, ML3 aggradation surface (Figure 2.7). These represent remnants of older aggradation surfaces abandoned by fluvial downcutting and are completely removed from most of the catchment.

1. An alluvial terrace or fan surface above Skippers Point at ~642 m (Figure 2.6). This is ~200 m higher than the modern Shotover River, and 70 m above the S3 terrace.

2. Alluvial fan remnants and sluicings near the Moonlight track at 620 m and about 560 m elevations. These are 60-120 m higher than Moonlight Creek ML3 terraces. At this point Moonlight Creek is at an elevation of about 400 m. The lower of these two areas appear to correlate with the level of the main Moke Creek terrace (Figure 2.7).
3. The large alluvial terrace surface on the southern side of Moke Creek is 30-35 m higher in elevation than the Moonlight ML3 terraces, and does not appear to have an equivalent terrace level alongside Moonlight Creek (Figure 2.7).

2.5 Lacustrine Deposits

A thick sequence of lacustrine sediment outcrops in the upper Shotover Gorge and at Branches Flat. The main exposures are at Strohles Flat and Muddy Terrace, and as fan-delta deposits from three tributaries: Muddy Creek, Ironstone Creek and Stockyard Creek (Figure 2.14). These deposits were noted by Turnbull et al. (1975a) who interpreted their formation in depressions vacated by retreating ice. McSaveney (1978) interpreted the extent of this paleolake, naming it 'Lake Borrell', after a former owner of Branches Station. Finer sediments include schist-derived clays, silts and sands, ranging from laminated clays-silts formed in very low-energy environments (Figure 2.15), to coarser sands and interbedded gravels showing features associated with higher-energy locations. These finer silt-sand dominated units are overlain by fan-delta gravel deposits sourced from tributary streams, with the upper contact of finer sand-silt sediments with the overlying gravels noted at maximum elevations of ~574 m (Strohles Flat) and 570 m (Muddy Terrace).

The total thickness of these lacustrine sand-silts is interpreted to be at least 80-90 m, based on maximum observed elevations of 570-574 m, and the assumption that these extend to the base of the modern river channel and underlie Branches Flat at elevations of ~490 m. The upper Shotover gorge and Branches Flat may be overdeepened through glacial erosion and the true thickness of these lacustrine sediments may be significantly greater. Lake sediments have been documented to underlie the alluvial gravels of the upper Shotover Gorge and Branches Flat. Miners reported the Branches Flat and upper gorge gravel riverbed was underlain by a 'false bottom' or 'bluebottom' of fine blue sand (Price and Brooks 1983, McSaveney 1978), and trenches and boreholes at Branches Flat showed alluvial gravels were underlain by lake sediments (Price and Brooks 1983, Nugold 1990). Several interpreted shorelines can be seen on the eastern side of Branches Flat between Ironstone and Stockyard Creeks (Figure 2.14), the two clearest of which are at elevations of 595 and 614 metres.

Lacustrine sediment outcrops at Strohles Flat and the Campbells Saddle-Ironstone Creek areas are described below. There are two main outcrops in the Strohles Flat area: a north-facing outcrop overlooking Rapid Creek (Figure 2.13A,) and a series of west-facing outcrops overlooking Strohles Flat (Figure 2.12). The north-facing outcrop at Rapid Creek comprises of a sequence of interbedded sands and gravels, with rare silt beds. Large-scale deformation (Figure 2.13A) is interpreted as soft sediment deformation. Cross-bedding is seen in several outcrops at Strohles Flat (e.g. Figure 2.13B); this was not seen in the logged section, but occurs in exposures on either side of this location.

The main west-facing lacustrine sediment outcrop is about 50 m in width, with an upper elevation of about 570 m, overlain by a ~50 m thickness of fan gravels deposited by Rapid Creek. A stratigraphic log was completed for the centre of this exposure (Figure 2.12), which extended to the top of main sand units at about 574 m, but did not include the overlying gravels which continue to an elevation of about 620 m. Sediments consist of planar bedded sands, commonly with flame structures. Minor silts and gravels occur in the upper parts of the section. This is interpreted as a remnant of a lacustrine fan-delta deposit, similar to those observed at Ironstone and Stockyard Creeks (Chapter 3).

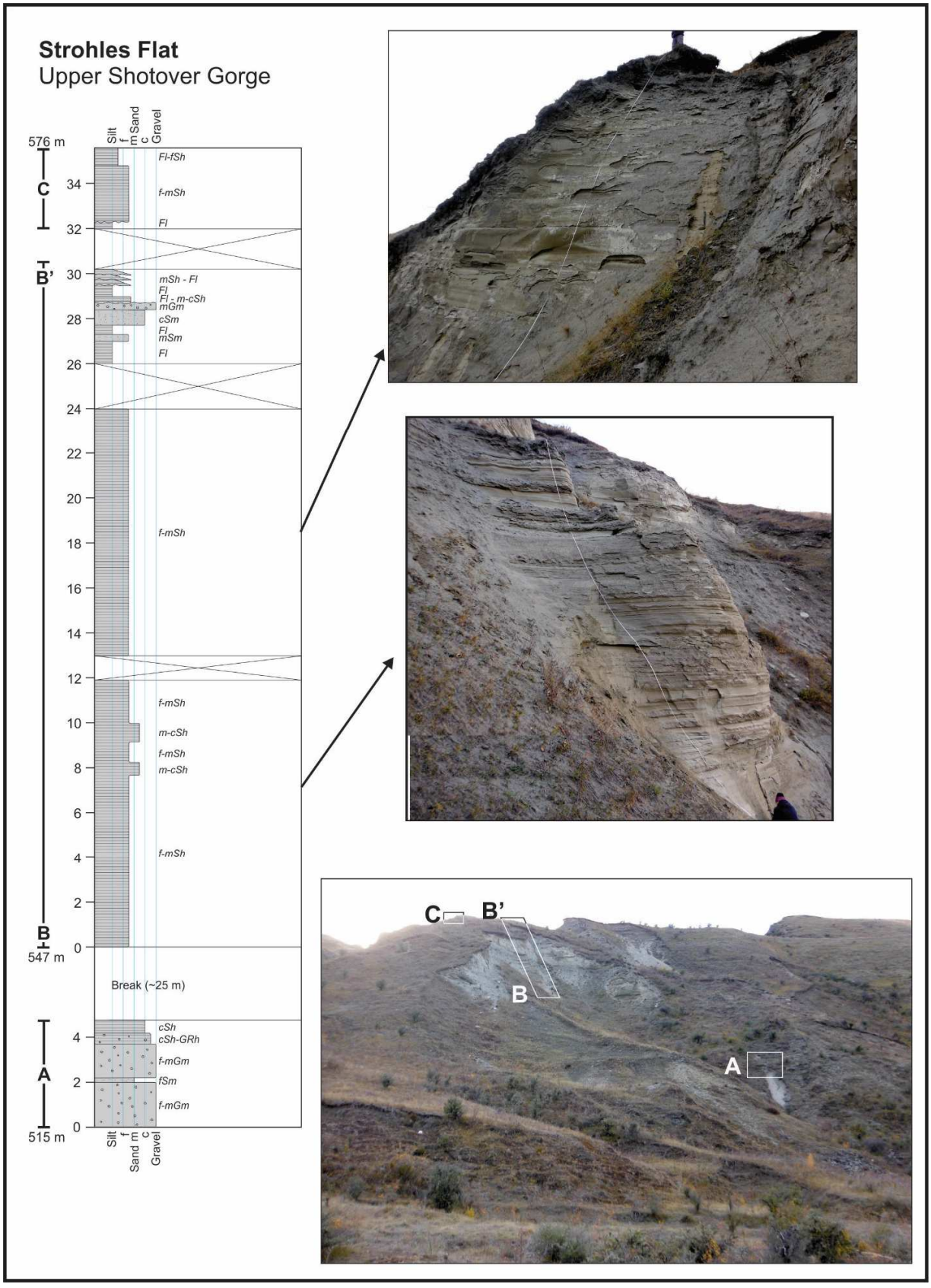
Strohles Flat
Upper Shotover Gorge
576 m
Silt
f
m Sand
c
Gravel
C
B'
B
A
547 m
515 m
Fl-fSh
f-mSh
Fl
mSh - Fl
Fl
Fl - m-cSh
mGm
cSm
Fl
mSm
Fl
f-mSh
f-mSh
m-cSh
f-mSh
m-cSh
f-mSh
Break (~25 m)
cSh
cSh-GRh
f-mGm
fSm
f-mGm
C
B'
B
A

Figure 2.12: *Strohles Flat stratigraphic section. The two upper inset photos show examples of well-bedded sand units. Lower inset photo shows the section location. Logging codes and location coordinates are shown in Table 2.1.*

Table 2.1: *Stratigraphic logging codes and locations of logged sections.*

LOGGING CODES (EVANS AND BENN 2004)

Boulders	
B	Boulders
Gravels	
Gms	Matrix-supported, massive
Gm	Clast-supported, massive
Gsi	Matrix-supported, imbricated
Gmi	Clast-supported, massive (imbricated)
Gfo	Deltaic foresets
Sands	
Scr	Climbing ripples
Sh	V fine-v coarse & horizontally/plane bedded, or low angle cross lamination
Sfo	Deltaic foresets
Suf	Upwards fining
Sm	Massive
Sd	Deformed
Silts and clays	
Fl	Fine lamination, often with minor fine sand & v small ripples
fine	f
medium	m
coarse	c

STRATIGRAPHIC SECTION LOCATIONS

		Easting, Northing (NZTM)
Sandhill Creek	Base of section	1262040, 5028034
	Top of section	1262080, 5028033 (approx)
Strohles Flat	Small lower section	1263198, 5030942
	Base of main section	1263242, 5030992
	Top of section	1263276, 5031011
Ironstone Delta (W)	Base of section	1263560, 5034190
	Top of section	1262591, 5034223
Ironstone Delta (E)	Base of section	1262621, 5034173
	Top of section	1262642, 5034203

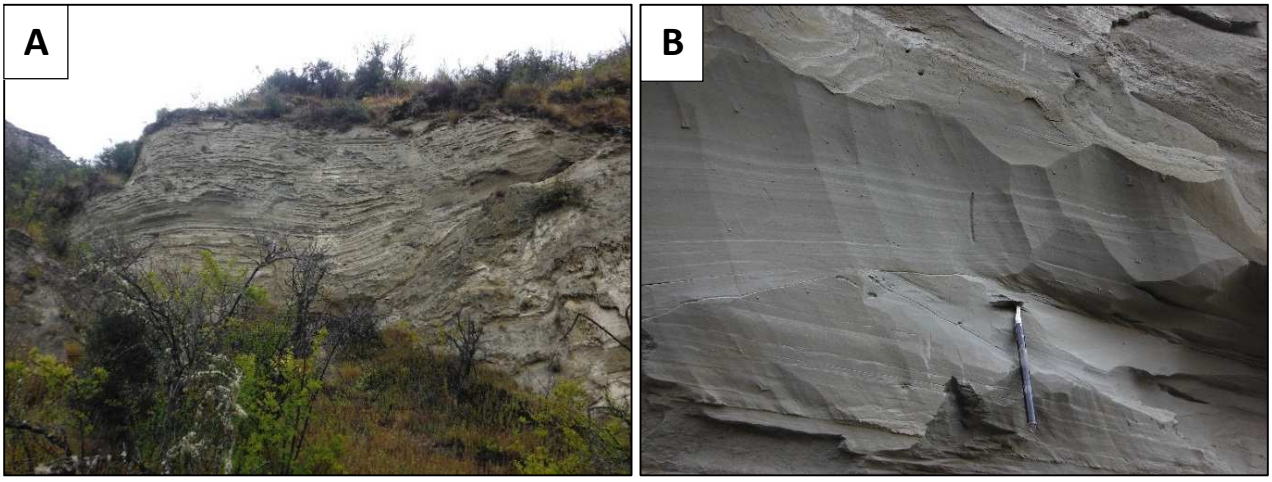

Figure 2.13: *A. Bedded sands at Rapid Creek outcrop, photo width is 15-20 metres. B. Cross-bedded sands at a Strohles Flat outcrop.*

Campbell's Saddle and Ironstone Creek

There are several outcrops of lacustrine and fan sediments in the Campbells Saddle and Ironstone Creek area at the lower end of Branches Flat (Figure 2.14), the largest of which is a deltaic deposit exposed on the northern side of Ironstone Creek (Figure 2.16). In this area, investigations included observations of sediment distribution and characteristics, and stratigraphic logging of two sections at the Ironstone Delta (Figure 2.17).

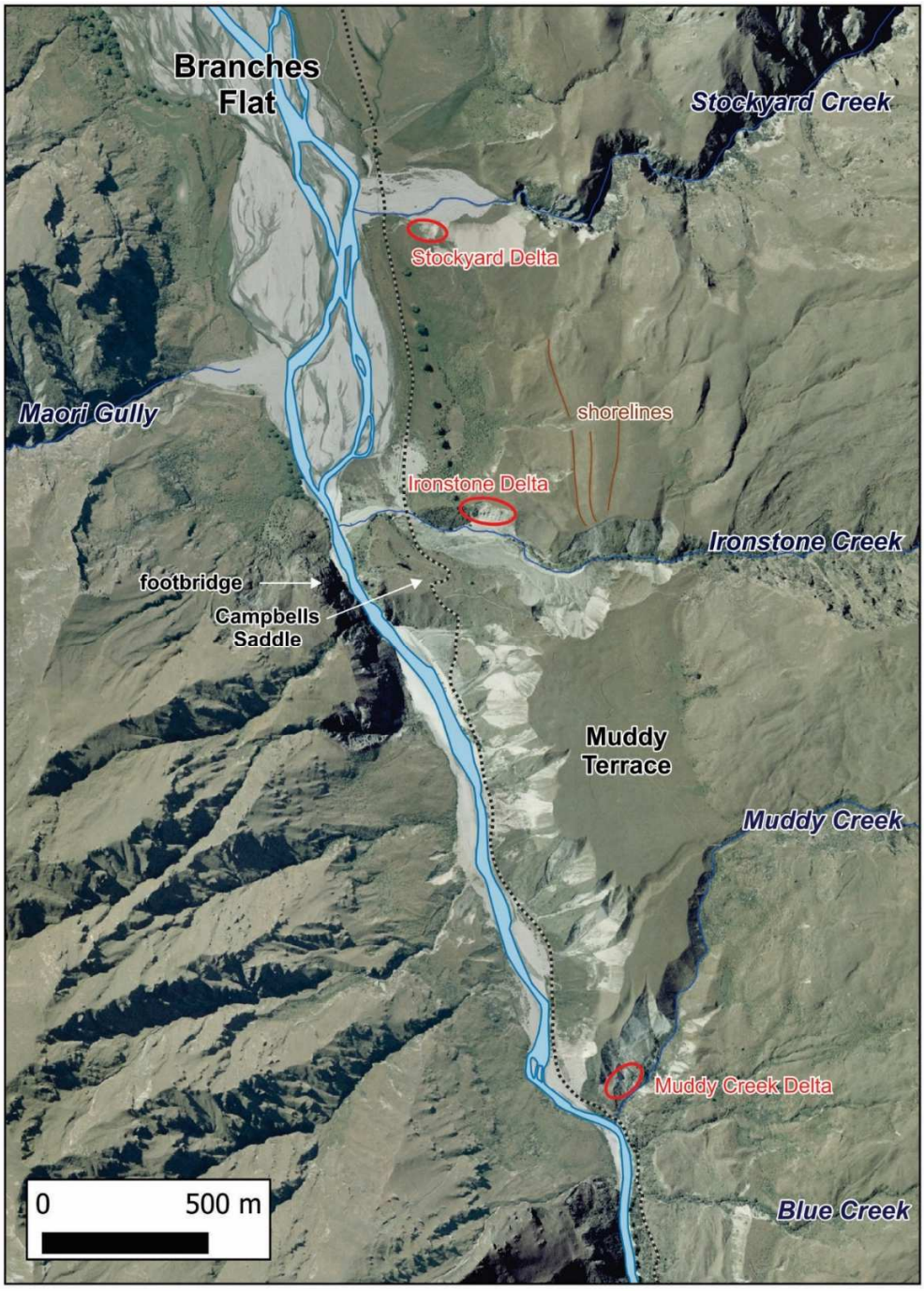

Figure 2.14: *Overview of the Muddy Terrace and lower Branches Flat area, locations of the three delta outcrops are circled. Dashed black line is the Branches Road. The location of this image is shown on Figure 2.4C.*

At the Campbell's Saddle footbridge (Figure 2.14) is an outcrop of, subhorizontally bedded lake sediments. These are finely laminated fine-medium sands and clay-silt (Figure 2.15) and contain flame structures and contorted bedding.

Figure 2.15: *Example of mm-cm scale laminar bedded clay-silt and fine sands from outcrop at the Campbell's Saddle footbridge.*

The Ironstone Delta outcrop (Figure 2.16) shows a transition from inclined, imbricated, gravel-dominant units nearer the valley margin (east), to interbedded silts-sands on the western side. Stratigraphic sections were logged on lower (west) and upper (eastern) parts of delta (Figures 2.16, 2.17). Sediments in the western section are dominantly subhorizontal, interbedded silt-sands (Figure 2.17 inset), with minor gravel units. These are interpreted as fine grained facies of delta deposits. The eastern delta section is composed of inclined (18-22°), cm-scale bedded gravels deposited as progradational foreset beds (Figure 2.17 inset). These are overlain by a 10-15 m thickness of shallower lying bottomset silts/sands/gravels.

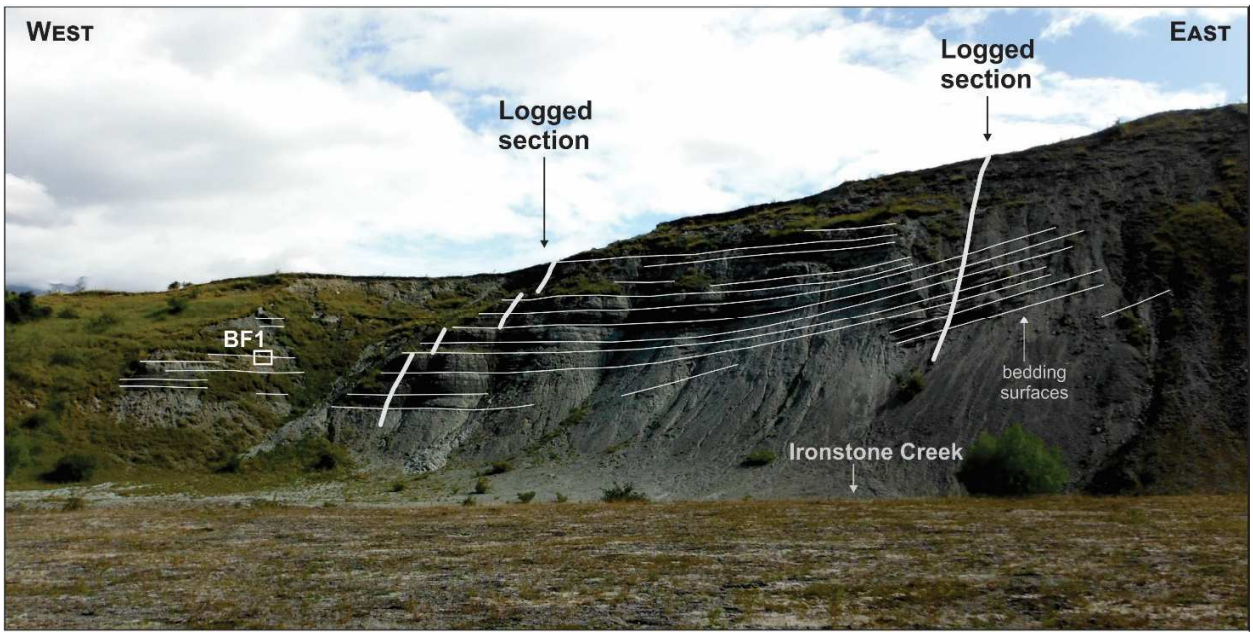

Figure 2.16: *Ironstone Creek delta showing steeper foreset gravel units to the east (right), and shallower bottomset silt-sands to the west (left). The locations of logged sections (Figure 2.17) and OSL sample BF1 (Figure 3.6) are indicated.*

Ironstone Delta
Lower Branches Flat

West Section

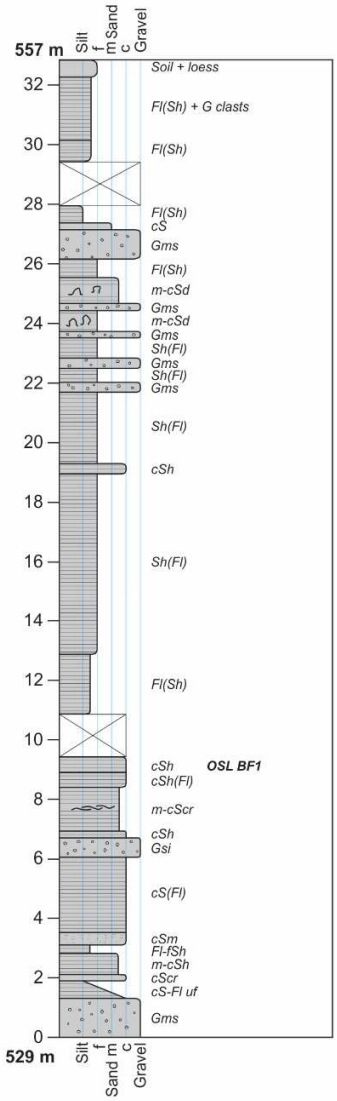

East Section

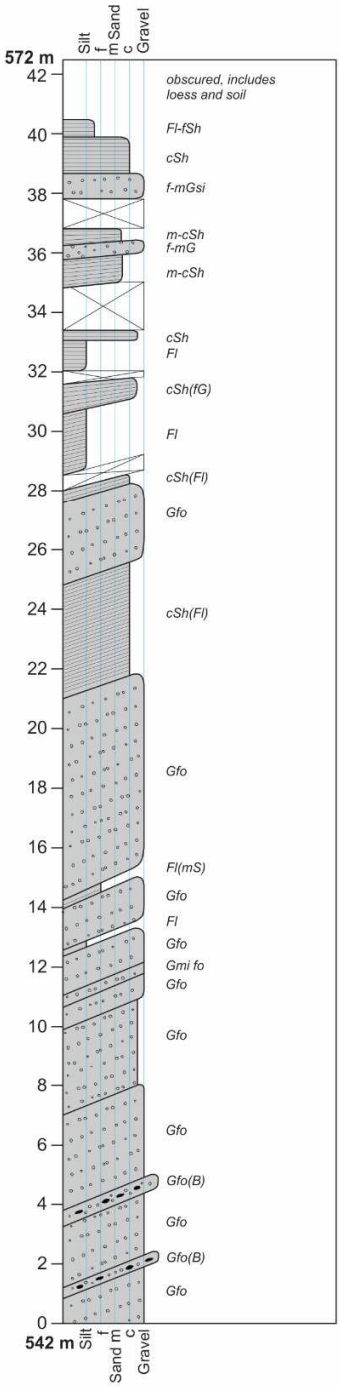

Figure 2.17: *Ironstone Delta stratigraphic sections, logged at the locations shown in Figure 2.16. The two upper inset photos show examples of interbedded silt-sand units in the western section. Lower inset photo shows inclined foreset gravels in the eastern section. Logging codes are shown in Table 2.1.*

2.6 Glacial Deposits

Paraglacial sediments are found over about 4 km in the upper Shotover Gorge, from Smiths Terrace upvalley to near Sloans Flat. These are best exposed at Smiths Terrace (Figure 2.19), in the Sandhill area (Figures 2.20-2.24), and in a large roadside outcrop near Sloans Flat (Figure 2.18). These sediments have been previously noted and described as fluvioglacial sediments, ice-contact sediments, and tills (McSaveney 1978, Thompson 1998). The deposits at Smiths Terrace and the Sandhill area are summarised below.

Figure 2.18: *Examples of highly deformed glacial sediments at Sloan's Flat roadside outcrop.*

At Smiths Terrace, the outcrop extends from the terrace surface at 560-561 metres elevation down to bedrock (and possible paleochannel) at ~500 m, about 50 m above the modern river. The terrace surface is mantled by a cover of loess and soil, which overlies a ~25-30 m thickness of coarsely-bedded gravels. Gravels overlie a 20-25 m sequence of bedded sands, interbedded with gravel lenses. These have an erosional contact with the gravels above, and are deformed, with folding and minor faulting (Figure 2.19).

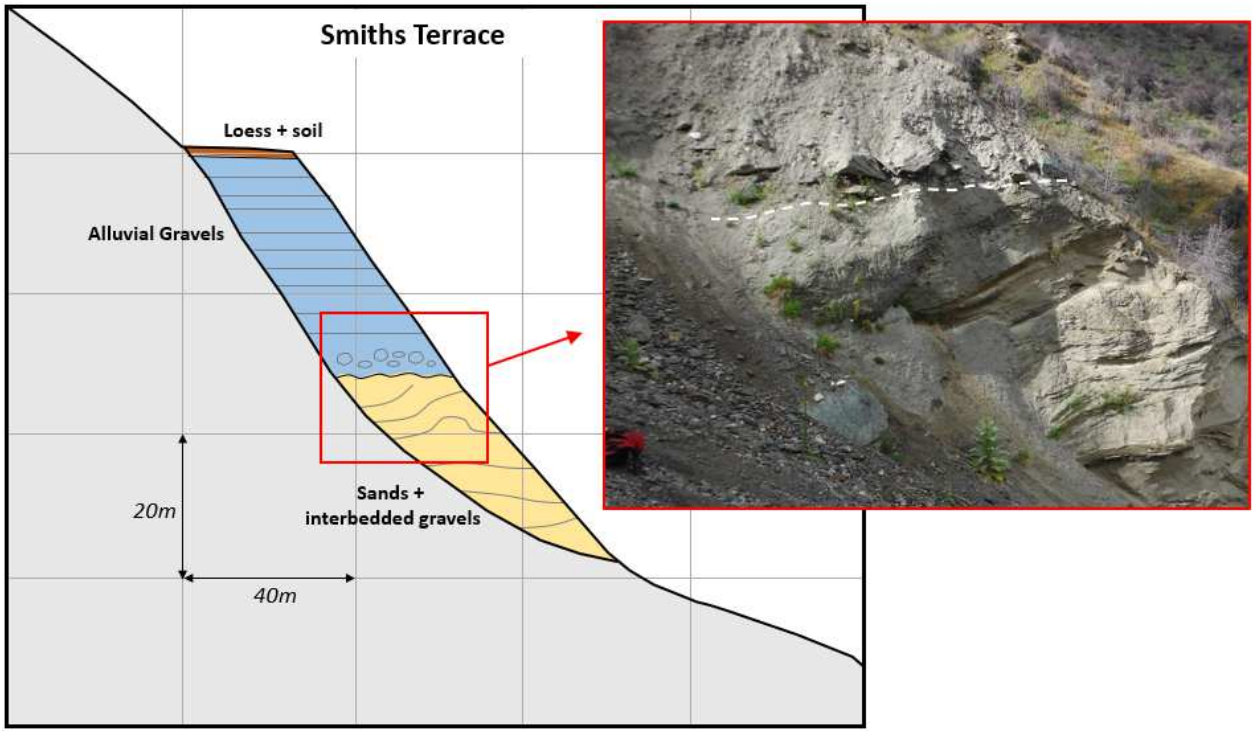

Figure 2.19: *Smiths Terrace outcrop sketch and photo, showing deformed glacial sediments, and overlying fluvial gravels. The coarse clasts near the base of alluvial gravels are interpreted as locally sourced colluvial boulders.*

The Sandhill Cut area has multiple outcrops of glacial sediments over a distance of ~1.5 km (Figure 2.20). Glacial sediments are exposed over a vertical range of about 100 m, from near the base of sluice cut (470 m), to an outcrop above the Branches Road at 570 m (Figure 2.23). Above this, gravels interpreted as alluvial fan deposits extend up to an elevation of about 620 m, such as alluvial fan deposits and minor sluicing at a high terrace immediately to the south of Sandhill Creek.

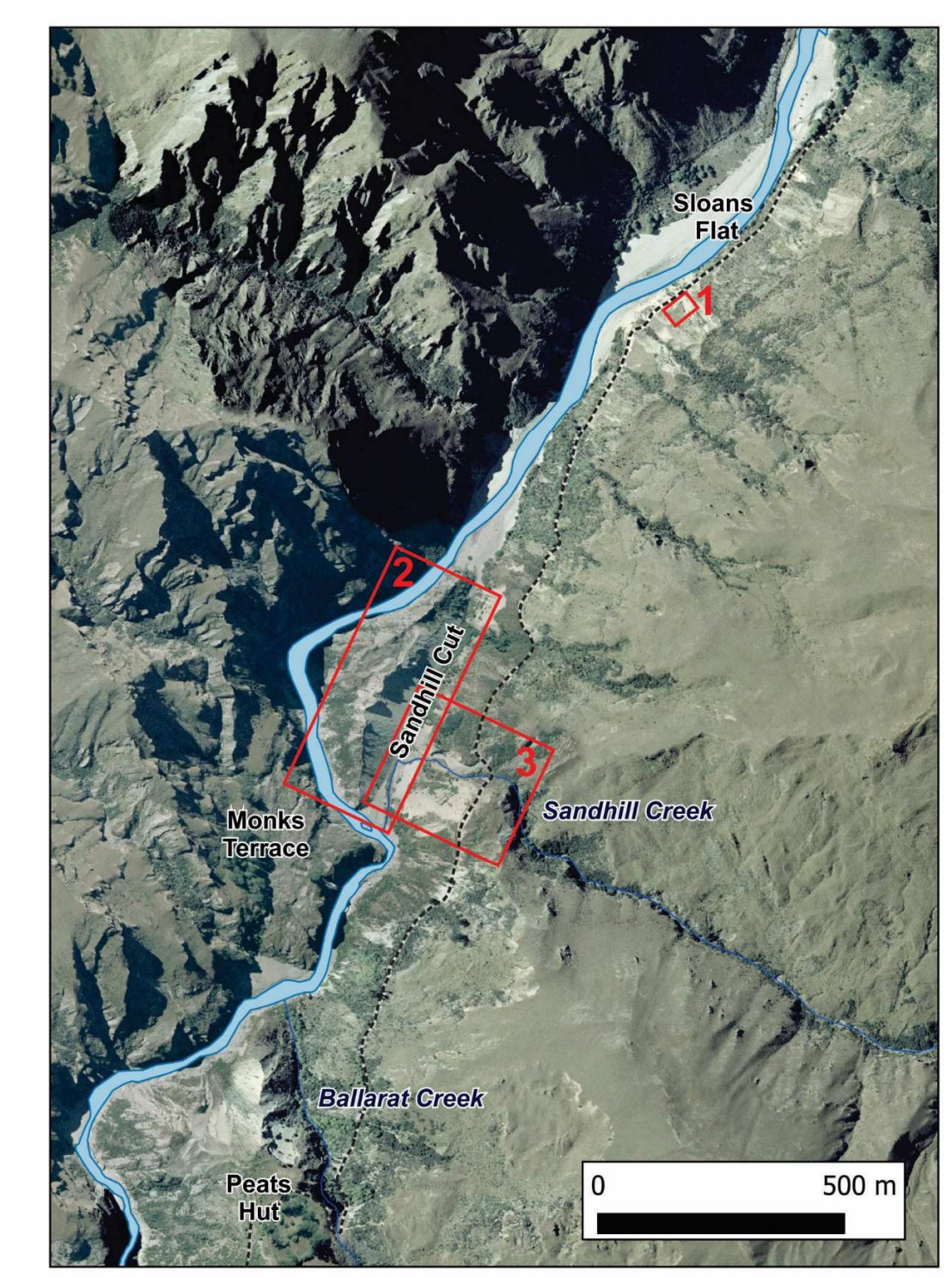

Figure 2.20: *Overview of the Sandhill area. Dashed black line is the Branches Road. The location of this figure is shown in Figure 2.4C. Red outlines show locations of Figure 2.18 (1), Figure 2.21(2) and Figure 2.23 (3).*

Sandhill Cut is a large sluiced excavation ~600 m in length and up to 65 m in depth, created by hydraulic sluicing during the mining era (Figure 2.20, 2.21). The large bluffs in the centre of the cut are coarse-medium bedded fine-medium grained gravels with a thickness of about 20 m exposed in outcrop. These include discontinuous silty lenses with laminar or rippled bedding (Figure 2.22A, B). Much of the Sandhill Cut outcrop comprises or is mantled by coarse (to 2 m), angular schist debris (Figure 2.21).

At mid-level in centre of the cut are several outcrops of well-cemented diamicton, interpreted as a basal till (Figures 2.21, 2.22C, D). This ranges from well-rounded gravel (<50 mm), to coarser sections with clasts up to 500 mm in size. Near the highest ridgeline of the cut is a thin unit of very well-rounded boulder fluvial gravels, which is then overlain by minor loess cover. Basement schist outcrops at the northern and southern ends of the cut, and at several northern outcrops the schists are glacially-smoothed.

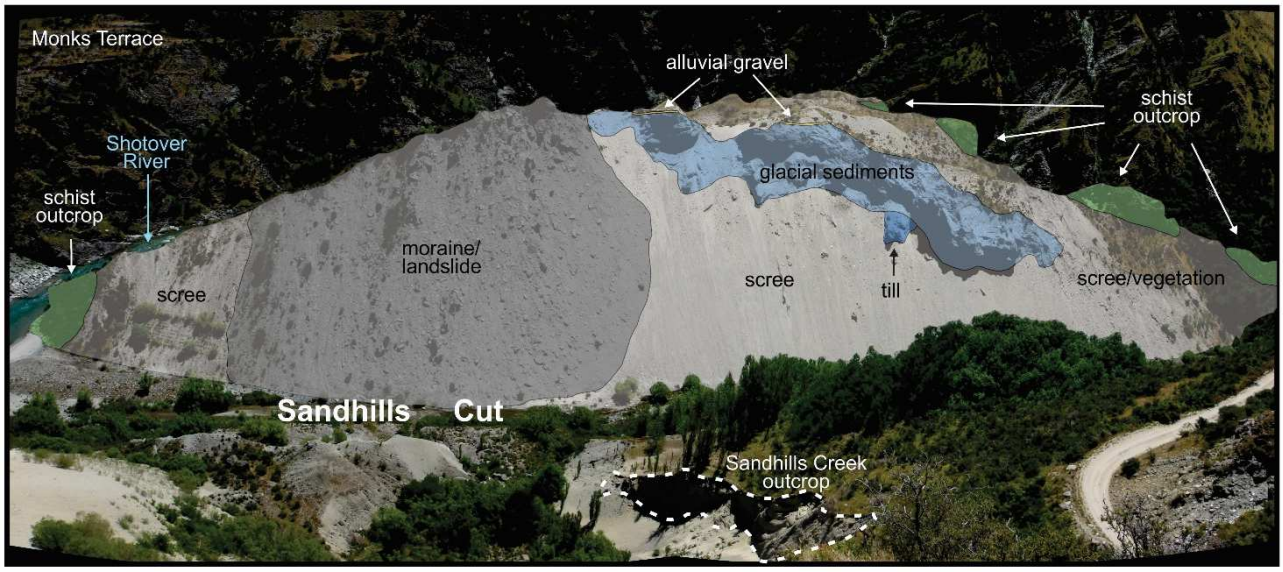

Figure 2.21: *Sketch of Sandhill Cut outcrop, showing distribution of the main geological features. View is towards the west, and outcrop is approximately 500 m in length and 60 m in height.*

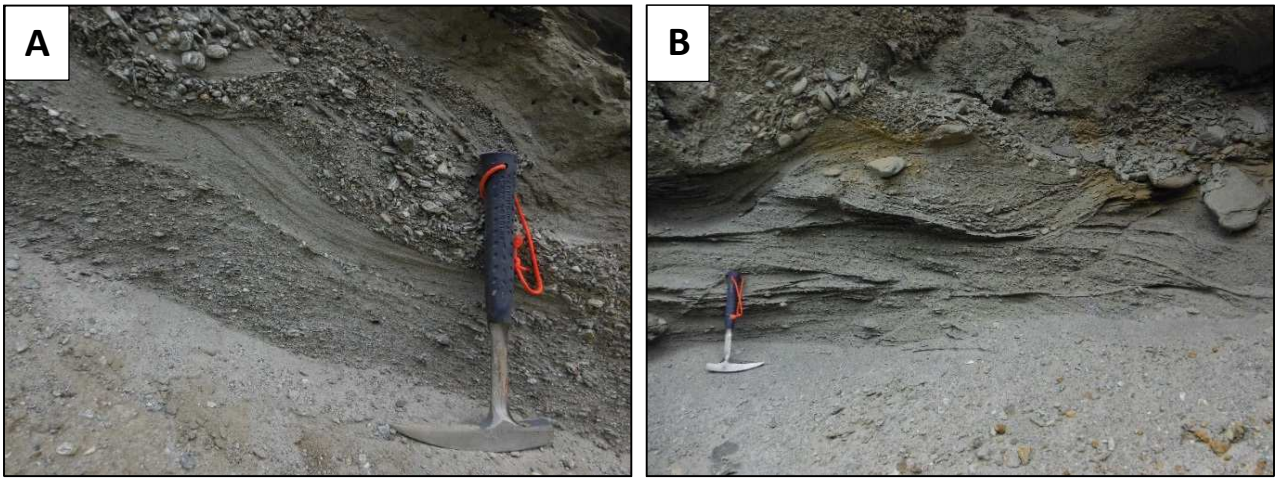

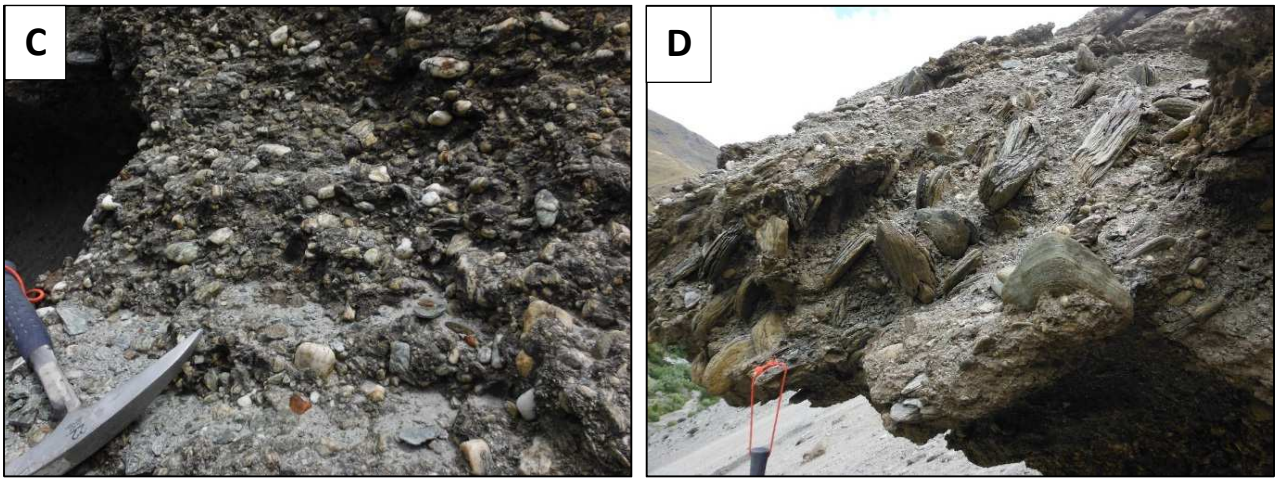

Figure 2.22: *Examples of sands and fine gravels (A, B) showing irregular sand lenses and ripples, and (C, D) a chaotically-bedded diamicton interpreted as basal till.*

At Sandhill Creek, interpreted glacial sediments are exposed as large outcrops to both north and south of the creek, then continuing above the Branches Road to ~570 m elevation (Figure 2.23). The schist bluffs above the Branches road are overlain by fan gravels at ~620 m elevation. The northern outcrop is shown in Figure 2.24 and the stratigraphic section in Figure 2.25. The Sandhill Creek outcrop is a folded sediment sequence including sands, interbedded sand-gravels and gravel-dominant units. There are three sand-dominated units, the largest of which is >10 m thick (Figures 2.24, 2.25). At the eastern side of the outcrop is a remnant of an underlying sediment sequence, with an erosional contact to the overlying sediments. Between the sediment sequences and outcropping schist at the eastern end of the outcrop is a zone of sheared schist debris interpreted as lateral moraine (Figure 2.24).

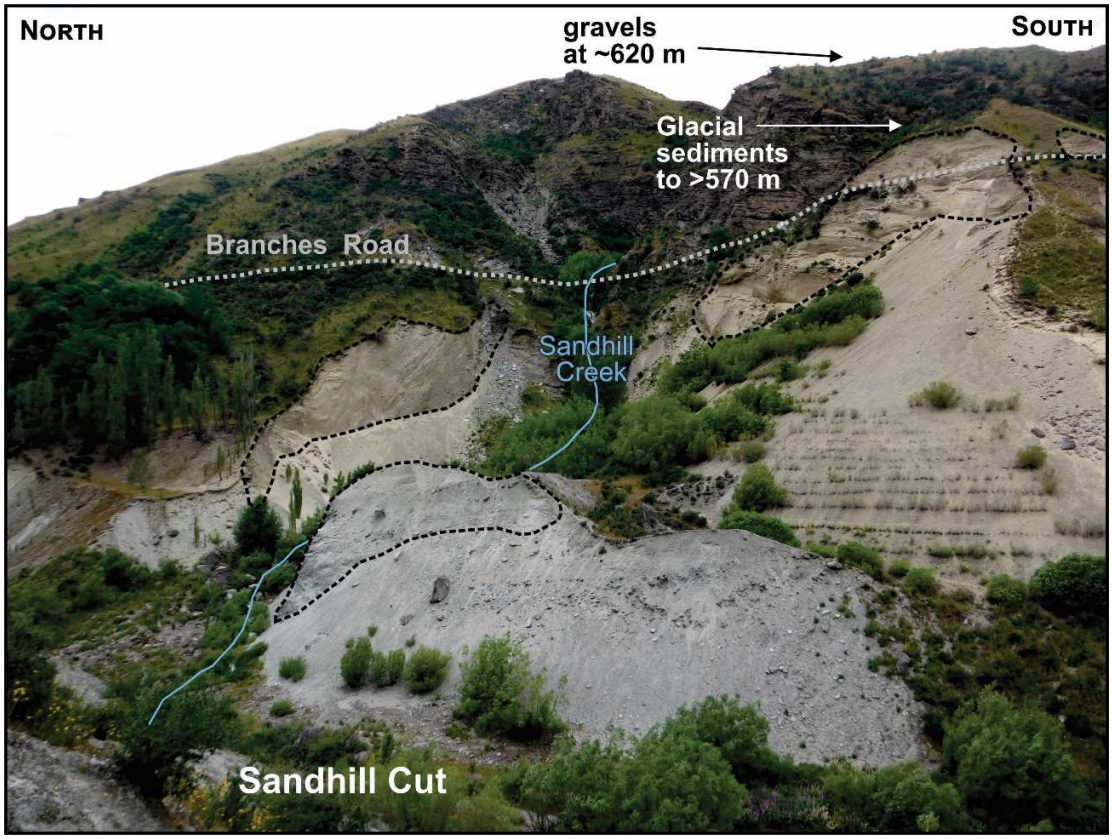

Figure 2.23: *View to east up Sandhill Creek, showing large outcrops of glacial sediments (dashed outlines) on both sides of the creek, and extending to above the Branches Road. Above the glacial sediments are alluvial gravels at elevation of ~620 m. The outcrop to the north (left) of Sandhill Creek is that shown in Figure 2.24.*

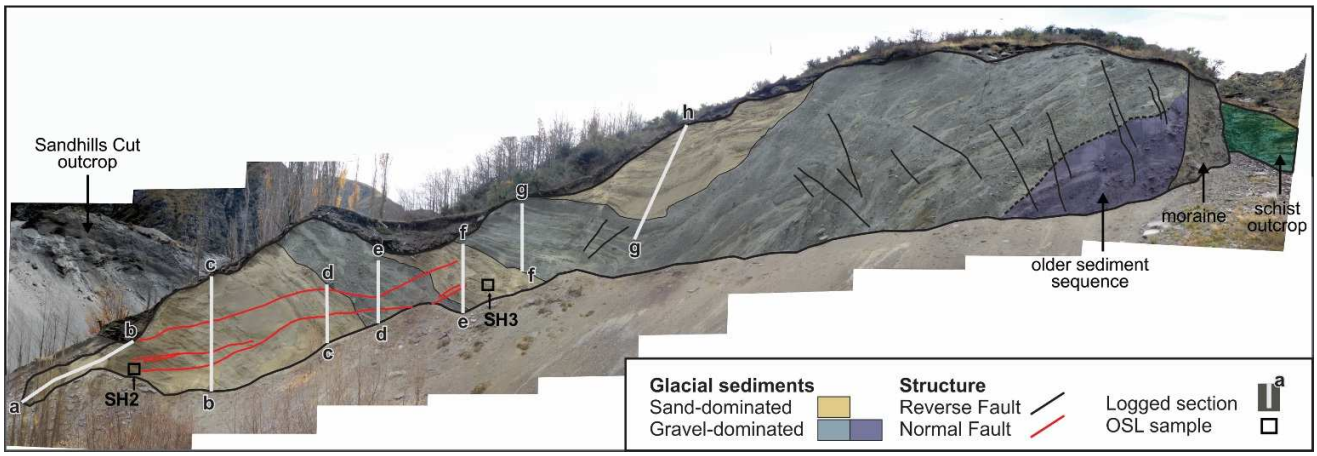

Figure 2.24: *Sandhill Creek outcrop sketch showing main geological units and structural features, and locations of stratigraphic log (Figure 2.25) and OSL sampling (Figure 3.2). Outcrop has a total width of about 80 m.*

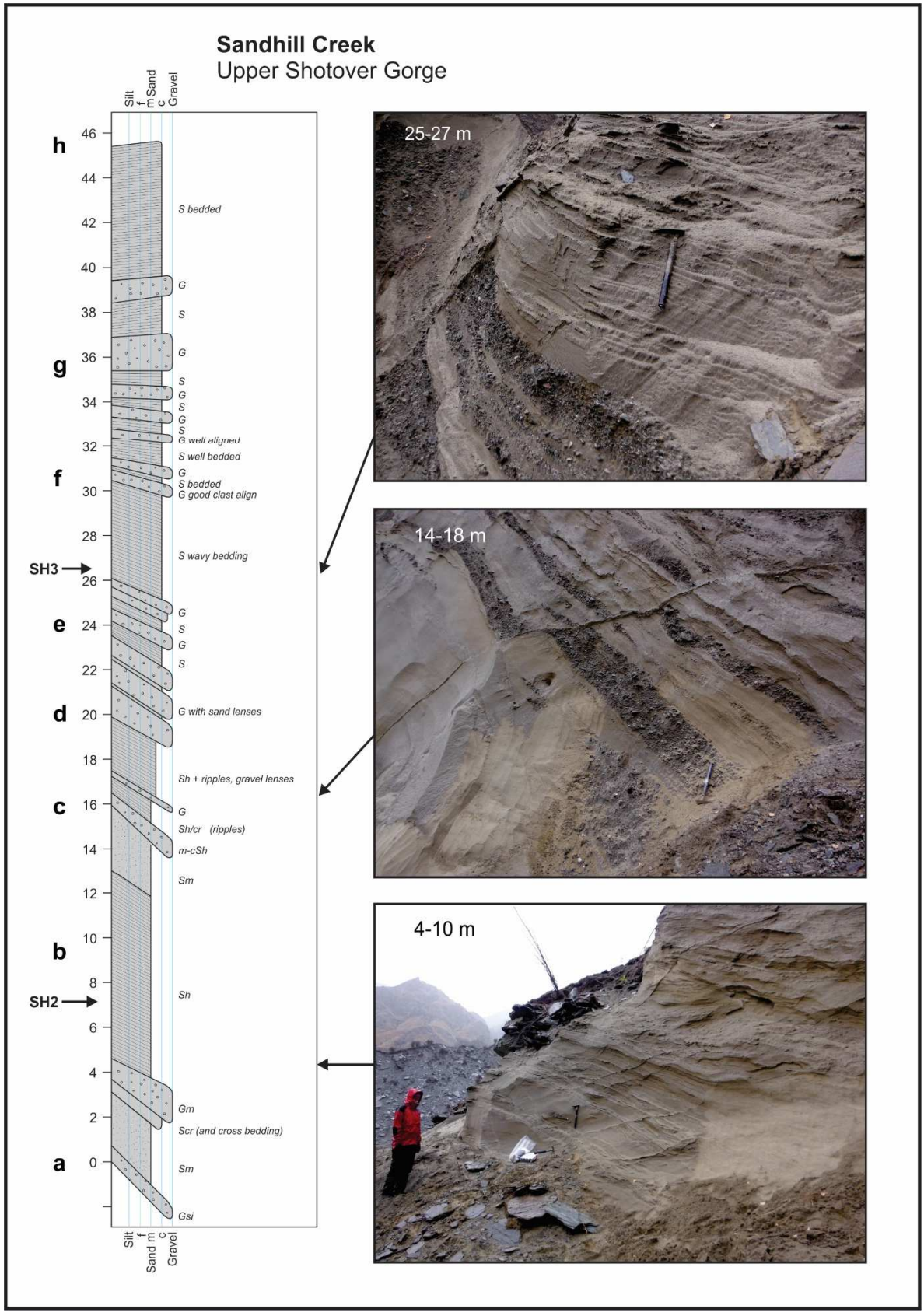
Sandhill Creek
Upper Shotover Gorge
Silt
f
m
Sand
c
Gravel
h
g
f
e
d
c
b
a
SH3
SH2
46
44
42
40
38
36
34
32
30
28
26
24
22
20
18
16
14
12
10
8
6
4
2
0
S bedded
G
S
G
S
G
S
G
S
G well aligned
S well bedded
G
S bedded
G good clast align
S wavy bedding
G
S
G
S
G with sand lenses
Sh + ripples, gravel lenses
G
Sh/cr (ripples)
m-cSh
Sm
Sh
Gm
Scr (and cross bedding)
Sm
Gsi
25-27 m
14-18 m
4-10 m

Figure 2.25: *Sandhill Creek stratigraphic section, logged at the location shown in Figure 2.24. Logging codes are shown in Table 2.1.*

Sediments at Sandhill Creek and Smiths Terrace are commonly deformed, with 10^0-10^1 m scale folding, as seen at Sandhill Creek (Figure 2.24), and smaller-scale folding and faulting with offsets up to several tens of centimetres (Figure 2.26). Deformation includes evidence of both compressional (folding and reverse faulting), and extensional (normal faulting) movement. This is characteristic of glacial deformation patterns and is discussed further in the following chapter.

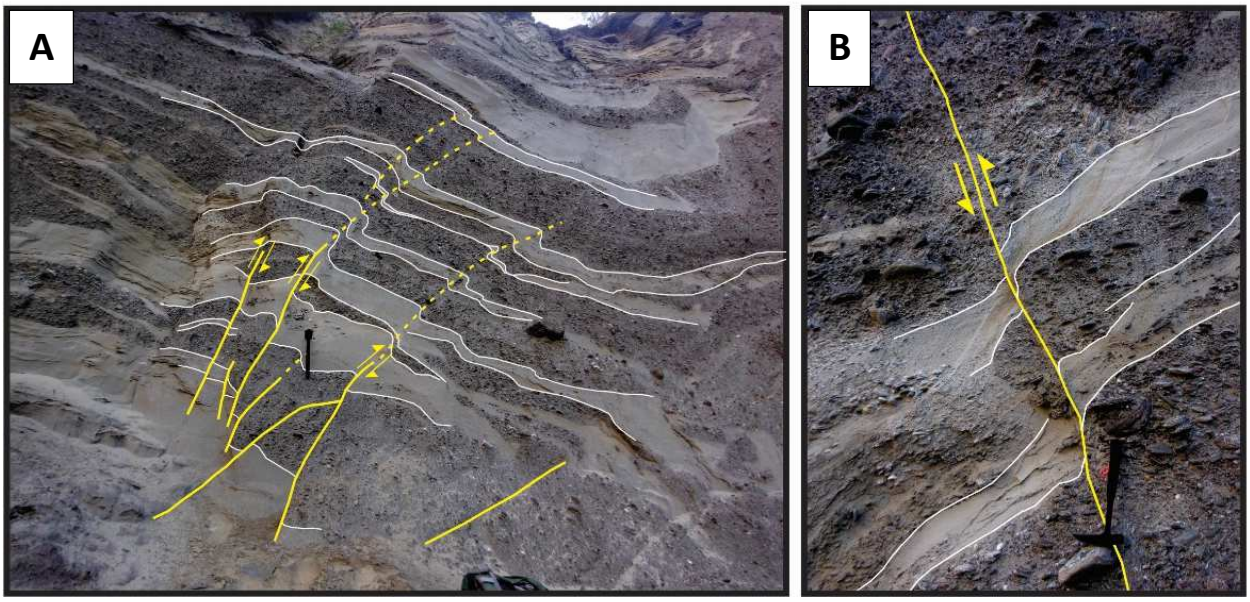

Figure 2.26: *Reverse faulting and deformation of interbedded sand-gravel units at Sandhill Creek.*

Loess

Accumulations of wind-deposited silts are common throughout study area and found on all terrace levels. These units are up to 1 m thick, but more typically 40-50 cm. Loess deposits are found on all terrace levels, with good examples at Smiths and Londonderry Terraces, Strohles Flat and Branches Flat (Figure 2.27).

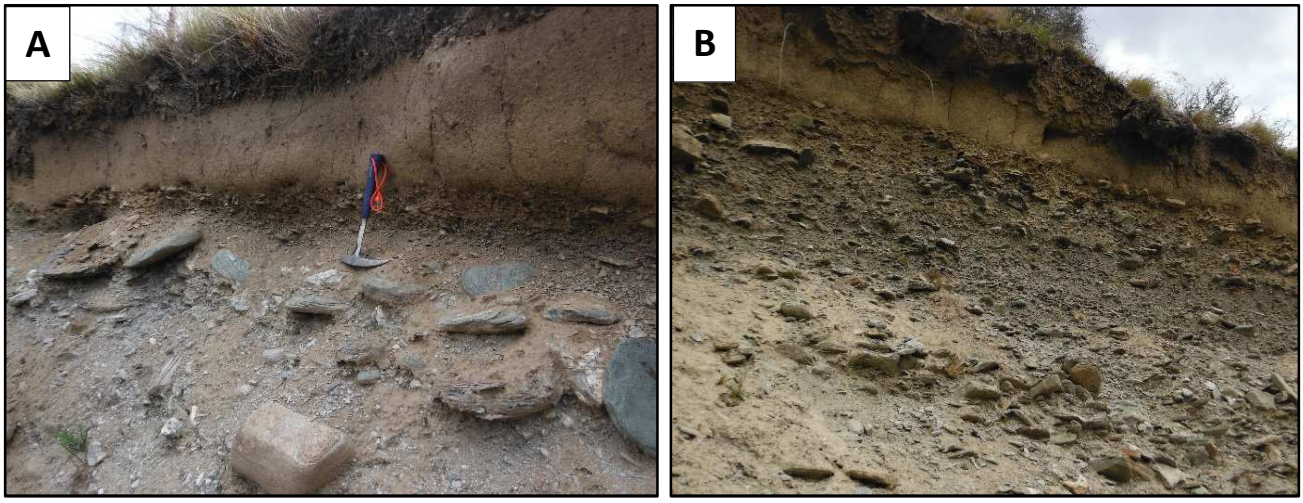

Figure 2.27: *Example of loess cover about 50cm in thickness overlying alluvial gravels at A. Londonderry Terrace and B. Strohles Flat.*

2.7 Mass Movement

The influence of schist foliation is apparent in the Shotover Valley's form, resulting in development of asymmetrical valley profiles with shallower dip slopes and steeper opposite slopes. The majority of the dip-slopes show deformation caused by the development of creeping schist landslides (Figure 2.29), while landslides and rockfalls are widespread throughout the steeper slopes in the Shotover Gorge. The main types of mass movement seen in the study area are summarised below.

Creeping schist landslides are the most widespread type of mass movement in the study area, found on most slopes with moderate steepness (15-30°) that parallel the foliation of the underlying schist bedrock. These slides often cover large portions of slopes, and are distinguished by characteristic ground deformation related 'ripple' or hummocky textures (Figure 2.28A, B). In the study area to the east of the Shotover River over 50% of slope area is affected by creeping schist landslides (Figure 2.29). The largest landslide of this type in the study area is the Coronet Peak landslide, covering an area of >23 km^2 (Willetts 2000). While these landslides typically move through gradual movement and deformation, smaller portions may fail catastrophically where destabilised by fluvial incision at the toe of the slopes. For example at Maori Point and Pinchers Bluff (Figure 2.30), where scarps show failures of up to about 300 m in width.

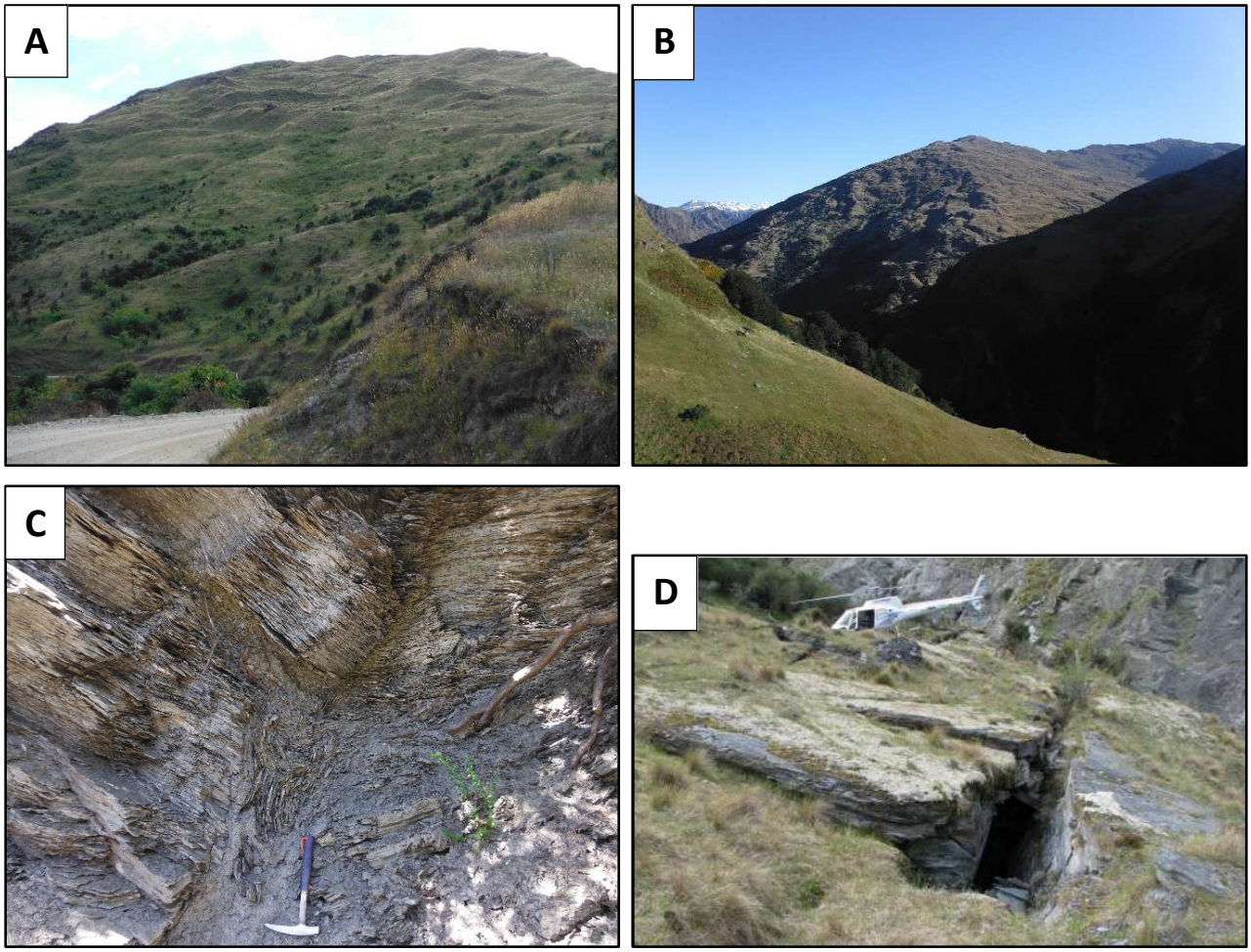

Figure 2.28: *A. Hummocky landslide terrain located NE of the Skippers Road near Long Gully, and B. near Devils Creek, viewed across the Shotover Gorge from the Moonlight Track. C. Internal structure of creeping schist landslide in the lower Shotover Gorge near Siphon Gully, showing gouge material developed between large rotated schist blocks, and D. Example of extensional cracking developed in surface of a Shotover Gorge creeping landslide (ORC 2008).*

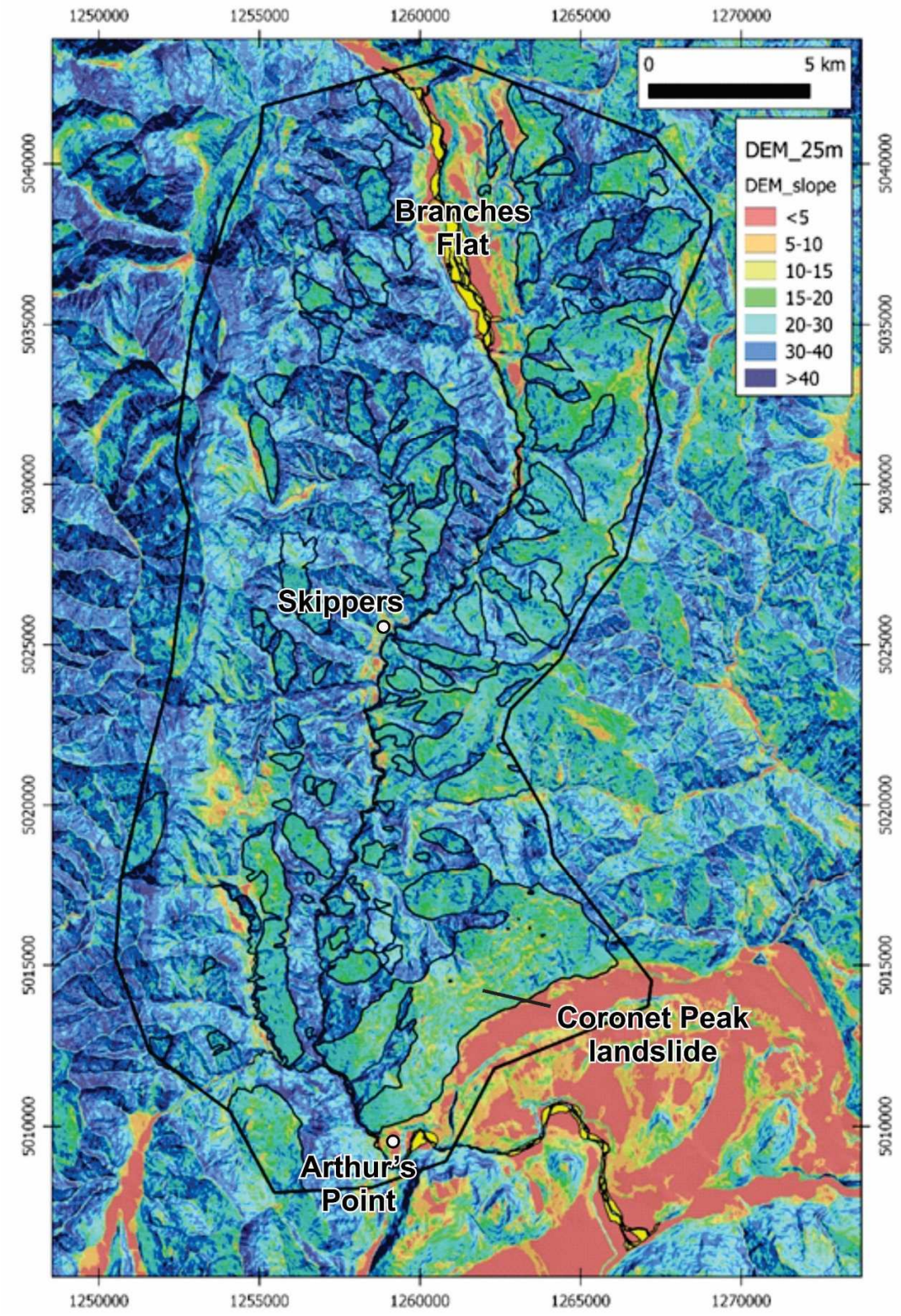

Figure 2.29: *Mapped extents of creeping schist landslides, shown outlined on a slope angle raster image. This shows their presence typically on west-facing slopes with slope angles of 10-30 degrees.*

Figure 2.30: *An example of a creeping landslide with typical rippled deformation, a section of which has progressed to form a rapid failure. This is in the lower Shotover Gorge at Pinchers Bluff, with the rapid failure scarp ~250 m in width outlined (Google Earth 2010).*

Landslides and Rockfalls

The largest landslide from the eastern slopes in the study area is the 40M m^3 Arthur's Point landslide from the western slopes at the exit of the gorge. This was studied by Willetts (2000), and identified as a wedge failure, the failure plane being the intersection of two joint sets. The landslide is now creeping in response to removal of debris at toe by the Shotover River (Willetts 2000). Within the Shotover Gorge, one of the largest landslides is from the western slopes at about McCarron's Beach-Pinchers Bluff (Figure 2.31). This has a scarp width of ~500 metres, and an estimated volume of 15-18M m^3. The scarp is up to 150-200 m in height, with a thick deposit of landslide debris seen within the scarp area. There are common rockfalls from the scarp area of this slide, forming extensive rockfall deposits on the shallower slopes below. Shotover Gorge landslide scarps are shown in more detail in Chapter Six (Figure 6.11) and used in development of a landslide magnitude-frequency distribution.

Landslides and rockfalls are predominantly wedge failures, controlled by planes of weakness such as jointing, shear zones, faulting and schist foliation, based on field observations and descriptions of the Arthurs Point landslide (Willetts 2000), and smaller events such as the 30-40,000 m^3 2008 Moonlight Track landslide (Dellow et al. 2009). Rockfalls and smaller landslides are most common in the gorge where slopes are deeply incised and very steep, and occur from both the eastern and western slopes. Examples include those seen at Maori Point and Cooks Terrace

(Figure 2.32) and the 1993 Criterion Creek rockfall (Figure 2.33A. Most of these failures have heights of <100 m, with their height limited by the size of bluffs alongside the river.

Figure 2.31: *Large landslide scarp in lower Shotover Gorge, this is located at about McCarrons Beach and has a scarp width of about 500 m.*

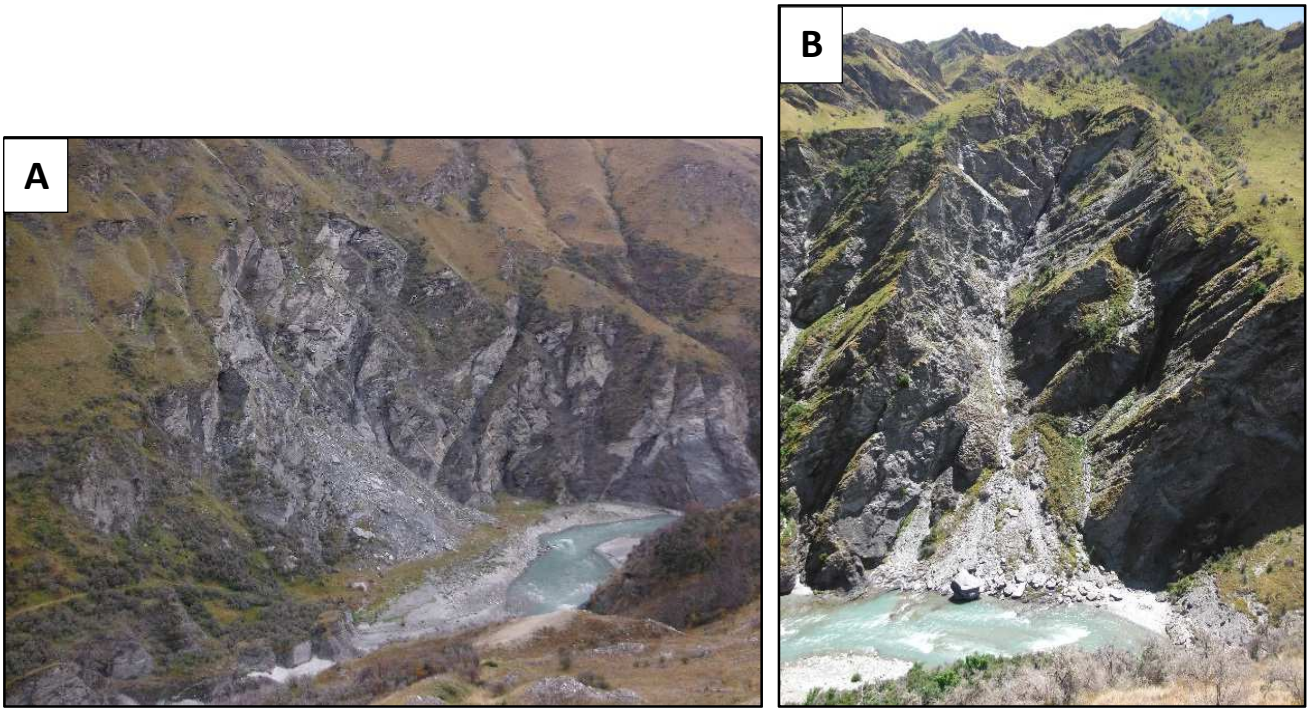

Figure 2.32: *Large rockfalls at A. Maori Point looking northwest across the Shotover River, and B. in the upper Shotover Gorge at about Cooks Terrace.*

2.8 Landslide Dams

There is no preserved evidence for large (>1M m^3) modern or prehistoric landslide dams within the Shotover Gorge, however several smaller-scale blockages have been documented over the last c. 150 years. Within the last few decades, there have been several small rockfall dams formed in the Shotover Gorge, causing partial channel blockages and minor upstream flooding. These include rockfall dams formed in 1993 at Mother Rapids (1993) and 1997 at Criterion Creek (Figure 2.33A) (Bryant 2011, Bryant and Goldsmith 2013), and a 2012 landslide at Devil's Elbow (Downer 2013). A historic Shotover Gorge landslide dam occurred in September 1871 in the Sutherlands Beach-Butchers Point area. This event blocked the Shotover River's flow for several hours (ODT, 12 September 1871). Historical accounts of this event are included in Appendix 4.

A possible Shotover Gorge landslide dam remnant is located at about Sutherlands Beach (Figure 2.33B), but is not thought to be the 1871 landslide dam noted above. This landslide has a width of 200 m and height of ~160 m; the deposit emplaced within the gorge forces the river to the far side of channel and may have formed a dam with a height of several tens of metres. At Sandhill Cut (Figure 2.21), a deposit of coarse schist debris may represent a rock avalanche deposit, and this may have contributed to damming of the valley and formation of the upper Shotover Gorge paleolake.

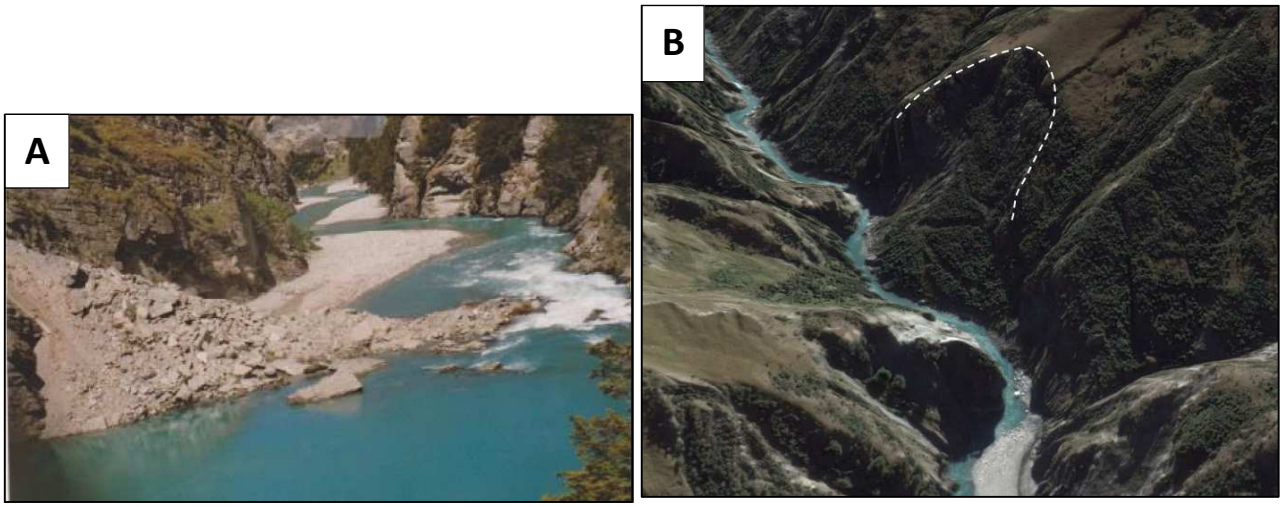

Figure 2.33: *A. The 1993 Criterion Creek rockfall dam, showing a small rapid formed and a lake impounded behind debris (Bryant 2017), Figure 3.1D shows a recent (2017) view of this deposit. B. shows a possible dam-forming landslide in the Shotover Gorge, outlined scarp is about 200 m in width. View looking upriver in the Shotover Gorge at about Sutherlands Beach (Google Earth).*

2.9 Summary of Quaternary Geological and Geomorphological Mapping

The main Quaternary geological units of the Shotover Valley are terrace and fan gravels, lacustrine sediments, and glacial sediments. These have been noted in previous studies, for example Turnbull et al. (1975a), McSaveney (1978), and Thompson (1998). This study has investigated the distribution and features of those deposits in further detail. In conjunction with OSL dating, these observations will be used in the following chapter to interpret the formation and timing of the main events in the valley's recent evolution.

Terrace surveys (Figure 2.4) have enabled construction of terrace correlations (Figures 2.5, 2.6, 2.7) in greater detail than previous studies (McSaveney 1978, Thompson 1998). This has identified two main terrace elevations; a bedrock terrace level (S1, ML1) at ~90 m, and a higher alluvial terrace level at ~130 m above the modern river channel.

Lacustrine and deltaic sediments have been identified at several locations in the upper Shotover Gorge and lower parts of Branches Flat. Bedded sands-silts have a thickness of at least 80-90 metres, and are overlain by gravels interpreted as fan-delta deposits sourced from tributary streams. Stratigraphic sections were completed through this sequence at Strohles Flat and Ironstone Delta (Figures 2.12, 2.16).

Glacial and paraglacial sediments were noted at a number of locations in the upper Shotover Gorge, with the best exposures in the Sandhill area (Figures 2.21, 2.23). A stratigraphic section (Figure 2.25) was logged at a Sandhill Creek outcrop, through a sequence of sands and gravels, deformed by folding and faulting.

Landslide mapping shows extensive landslide activity in the study area. This includes large areas of creeping dip-slope landsliding characterised by rippled ground deformation (Figure 2.29), and many rapid landslide and rockfall failures have occurred from steeper slopes. The observations of landslide distribution, size and style discussed here will be revisited in Chapter Six, to assist with inferring the size and location of future dam-forming landslides in the Shotover Gorge. While there was no evidence identified for any large landslide dams (>1M m^3) in the gorge, there are records of smaller events such as the 1993 Criterion Creek landslide dam (Figure 2.33A) and another in September 1871 (Appendix 4). At Sutherlands Beach, a landslide deposit is interpreted as a remnant of a landslide dam which may have been several tens of metres in height (Figure 2.33B).

Chapter Three: Geological Interpretation

3.1 Introduction

This chapter reviews the formation and timing of the Shotover Valley deposits and landforms described in the previous chapter, including bedrock and alluvial terraces, glacial and lacustrine sediments, and landslide deposits (Figure 3.1). Two of the sedimentary units present in the upper Shotover Gorge have been dated using Optically Stimulated Luminescence (OSL): glacial sediments from the Sandhill Creek area (Figure 3.2), and lacustrine sediments from the Ironstone Delta at lower Branches Flat (Figure 3.6). Field observations and OSL dating have been used to interpret a history of key events in the valley's geological history (Figure 3.8, Table 3.2):

- Last Glacial Maximum (LGM) Shotover Glacier advance.
- Formation of an aggradation surface (S3, ML3 terrace level).
- Glacial retreat and proglacial lake formation.
- Post-glacial degradation of valley fill.
- Bedrock incision forming the modern Shotover Gorge.

3.2 Methods

Three samples were submitted for OSL dating and analysed at Victoria University, Wellington. Two samples were taken from glacial sediments at a Sandhill Creek outcrop (Figure 3.2), and one from deltaic bottomset sediments at Ironstone Creek (Figure 3.6). Samples were prepared using a coarse grain quartz technique, UV luminescence was measured during blue stimulation, and luminescence ages determined by the Single Aliquot Regenerative Dose method (SAR). Results are shown in Table 3.1, and further details of sample location and collection, analysis methods and results are included as Appendix 2.

Table 3.1: *OSL dating results for Shotover samples.*

Location	Sample name	Age (ka)
Sandhill Creek	SH2	26.6 ± 3.4
Sandhill Creek	SH3	33.1 ± 4.6
Ironstone Creek	BF1	24.7 ± 4.7

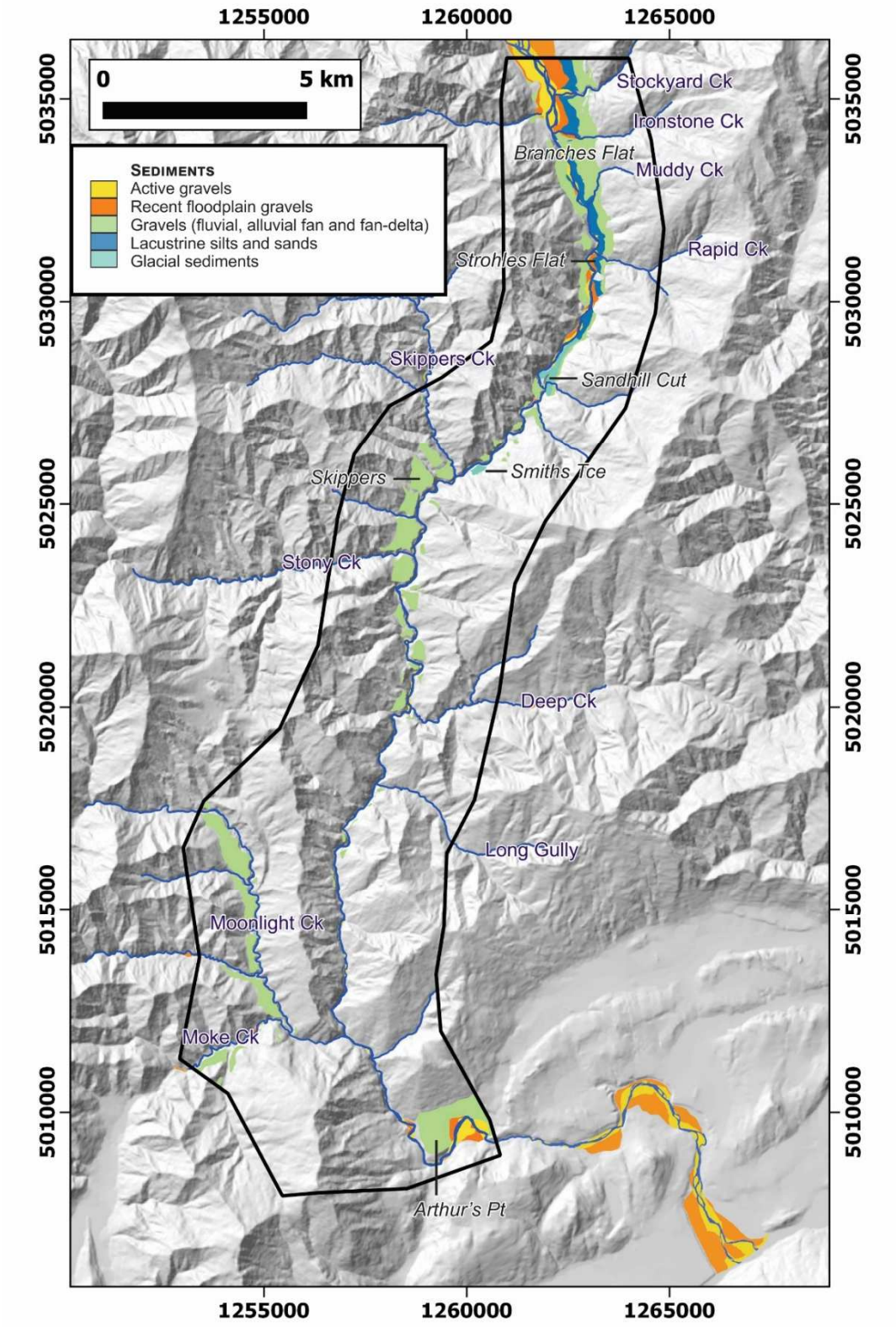

Figure 3.1: *Overview of the Shotover Gorge mapping area, summarising the main geological units discussed in this chapter. A complete geological map is included in Appendix 1.*

3.3 Interpretations

Glacial Advance

The most extensive glacial deposits in the upper Shotover Gorge are sand and interbedded sand-gravel units (e.g. Figures 2.18, 2.22A, B, 2.26). Evidence for fluvial deposition includes the presence of imbricated gravels, climbing ripples and cross bedding, and eroded scour channels. These deposits are interpreted as being dominantly fluvial deposits formed in proglacial ice-contact fan and outwash head/fan environments, and may also include ice-marginal fluvial or ponding deposits. Evidence for a glacier at this location includes valley-side contact with moraine formation (Figure 2.24), and trimlines seen on the western slopes of Branches Flat and in the upper Shotover Gorge.

Deformation observed in glacial sediments at Smiths Terrace and in the Sandhill area contains juxtaposed reverse-sense deformation and extensional normal faulting, this is typical of that seen in other glacial sediment sequences, such as in the Rakaia Gorge (Hyatt et al. 2012), and at Lake Pukaki (Evans et al. 2013). Compressional deformation is interpreted as being glacitectonic, caused by the thrusting of advancing ice into and over sediment complexes (Evans and Benn 2004). Reverse faulting and 10^0-10^1 m scale folding are seen at Sandhill Creek (Figure 2.21, 3.2), with both brittle and plastic deformation styles (e.g. in fault propagation folds) (Figure 2.26). Normal faulting (Figure 2.21, 3.2) is interpreted as being caused by slumping following ice retreat or the meltout of a supporting ice buttress (Evans and Benn 2004).

The upper Shotover Gorge glacial deposits are interpreted as being deposited by a Shotover Glacier advance to about the Sandhill area (Figure 3.1). This has been termed the 'Sandhill Advance', after Thompson (1998). Trimlines on the western slopes of Branches Flat and in the upper Shotover Gorge are at 650-700 m elevation, indicating an ice height of at least 150-200 metres above the modern valley floor. The total ice thickness is unknown as the valley floor is partially infilled by sediments and the depth to bedrock is not known. Figure 3.8A shows an interpretation of the Shotover Glacier's Sandhill Advance, based on a terminus at about Sandhill Creek and using trimlines interpreted from aerial imagery (Google Earth).

Two samples of bedded sand units from the Sandhill Creek outcrop (Figure 3.2) were dated using OSL. The samples are not in stratigraphic order: the stratigraphically lower sample (BF2) having a younger age than the upper sample (BF3). The results of these samples overlap within a 2-sigma uncertainty and can be treated as one age, having a weighted mean age of 29.4 ± 3.9 ka. The age indicates this event was an LGM glacial advance, occurring in late MIS3 or early MIS2. This date is significantly younger than previous speculations on the age of the Sandhill Advance, which was estimated as Waimean (MIS6; 140 ka) in age by Thompson (1998). The OSL age here corresponds with the local New Zealand LGM advance at shortly before 28 ka (Rother et al. 2014), and has been interpreted as being the time of New Zealand's maximum LGM ice extent (Rother et al. 2014, Shulmeister 2017). These are interpreted as the largest of the last glacial (Otiran) advances, with examples including those in Canterbury at 26-29 ka, and in Otago and Fiordland at 31-33 ka (Shulmeister 2017). Other documented glacial advances of this age include the Wanaka Advance 3 at 32.1 ± 5.7 ka (Evans 2015), Clearwater and Heron lobes in Rangitata Valley at shortly before 28ka (Rother et al. 2014), and Lake Ohau moraines at 32.52 ± 0.97ka (Putnam et al. 2013).

Potential issues in the use of optical dating methods in glacial environments include incomplete zeroing, weathering, relatively recent erosion from bedrock, and potentially short proglacial transport paths (Almond et al. 2001, Shulmeister et al. 2010, Rother 2006). Sampled sites were selected to improve likelihood of light exposure and zeroing prior to burial, with bedded sandy facies indicating aqueous sediment transport paths and relatively energetic deposition. If these samples have been subject to only partial bleaching then the resulting date may represent a maximum age for this advance.

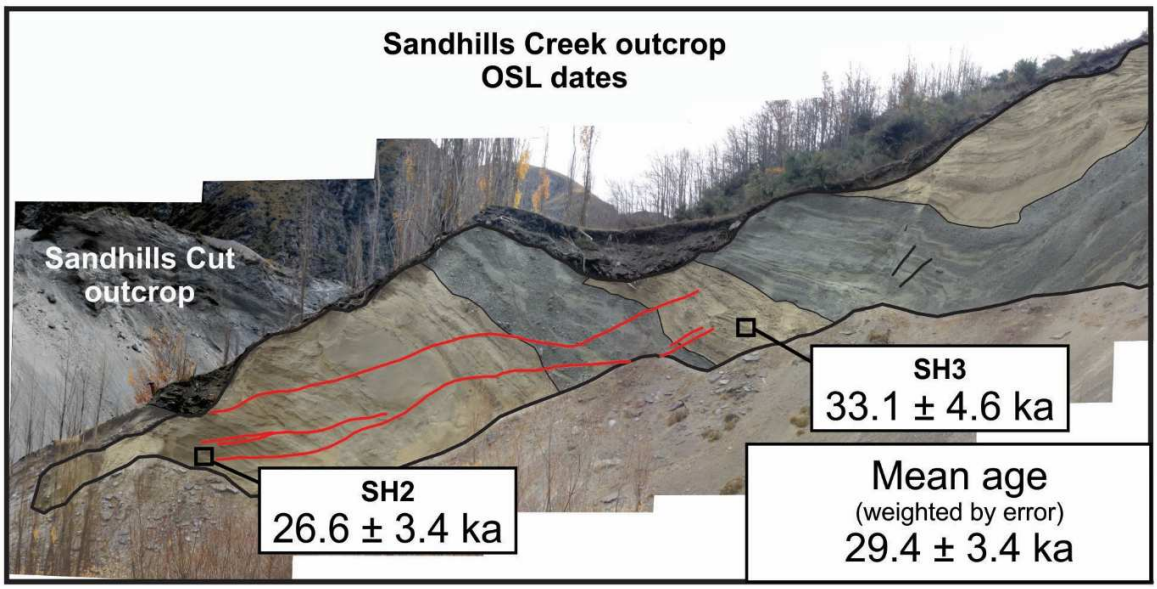

Figure 3.2: *Sketch of the western part of the Sandhill Creek outcrop, showing the location and dating results of OSL samples.*

Aggradation

New Zealand glaciers can be classified as coupled ice-margin glacier systems (Benn et al. 2003, Hyatt 2009). These systems are present in valleys with high relief and precipitation, where plentiful meltwater and a high sediment supply result in rapid sediment transport from the glacier into proglacial environments. These are characteristic of low elevation glaciers in humid environments, such as in Alaska, Patagonia and New Zealand. As large volumes of sediment are transported from the glacier and into the valley, outwash heads and fans are created as the dominant landforms (Shulmeister 2017). As meltwater rivers migrate across the glacier front, moraines are eroded and typically have low preservation potential.

The Shotover Valley alluvial terrace gravels have previously been interpreted as forming during periods of increased sediment production during glacial advances (Turnbull et al. 1975a, McSaveney 1978, Thompson 1998). For example, Turnbull et al. (1975a, p5) notes, 'as the ice advanced, streams were loaded with excess sediment and they aggraded, depositing outwash gravel'. Another explanation for widespread aggradation is a substantial rise in the downstream base level. These two causes of aggradation can be distinguished based on the initial and final riverbed gradients, assuming river flow rates were similar during the glacial advance and the interglacial period. Aggradation surfaces formed under an increased sediment supply will have a steeper gradient than those formed under the previous supply rate. As sediment supply exceeds the transport ability of the river, the riverbed aggrades in response, becoming steeper and thus increasing the river's ability to transport sediment (Figure 3.3). An example of this is seen in the Rakaia Valley, where glacial outwash terrace surfaces are noticeably steeper than the modern river channel (Hyatt 2009). In contrast, aggradation due to a rise in base level will form an aggradation surface with the same gradient, as the sediment supply rate is unchanged.

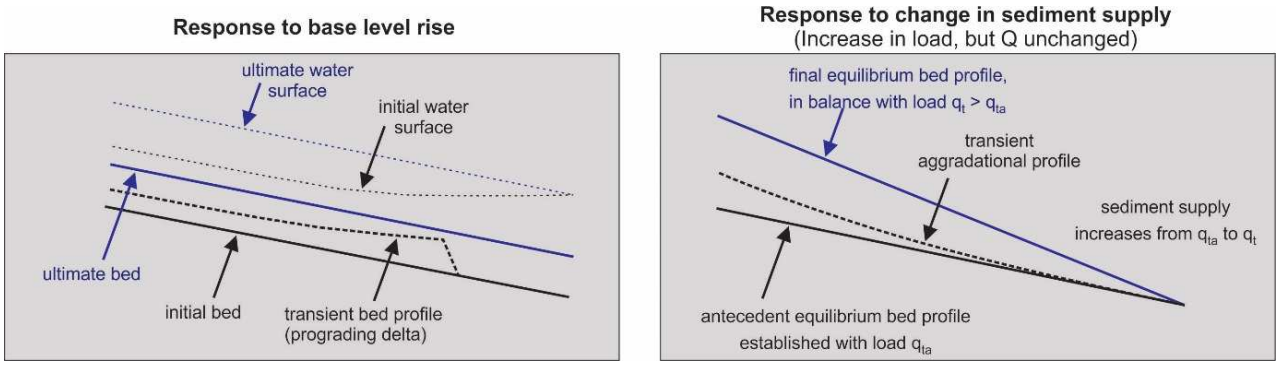

Figure 3.3: *Sketch showing aggradation responses to base level rise and sediment supply increase. This shows base level rise producing an aggradation surface parallel to the initial riverbed, while an increased sediment supply causes a steeper gradient (Parker n.d.).*

The Shotover Gorge aggradation terrace level (S3) is at an elevation of ~130 m above the current Shotover River. A long profile compiled from terrace surveys (Figure 2.5) demonstrates that the gradient of this S3 surface is about parallel to the present-day riverbed. Based on the comparable gradients of the alluvial terrace and the modern riverbed, it is interpreted that these terraces represent an aggradation surface formed largely as a consequence of a significant base level rise, rather than a glacially-induced increase in sediment supply. The height of this S3 alluvial terrace level above the modern Shotover Valley floor is not representative of the aggradation thickness as the gorge has continued to incise in the postglacial period, while the aggradation terrace level has been tectonically uplifted. These gravels have a thickness of about 40 m above the bedrock terrace level (S1), and are locally thicker where gravels fill paleochannels incised into this bedrock surface (Figures 2.5, 2.6).

Shotover Valley aggradation is inferred to have been caused by a significant rise in the valley's base level, controlled by events in the Wakatipu Basin. A glacial reconstruction for the LGM Wakatipu Glacier by Barrell (2011) (Figure 1.6), shows ice infilling the Wakatipu Valley, with a northeastern lobe filling the Wakatipu Basin into the present-day Arrowtown, Lake Hayes and Arthurs Point areas. From this, a smaller Shotover lobe is interpreted as extending up the Shotover Valley as far as about the Moonlight Creek confluence (Barrell 2011). This rise in base level is interpreted as being due to the blocking of the valley outlet by ice of the Wakatipu Glacier, and the associated rise in the water table, which may be within 40 m of the ice surface (Fountain and Walder 1998) (Figure 3.4). The resulting aggradation infilled the Shotover Valley and tributary valleys with alluvial gravels, forming the S3 and ML3 terrace surfaces (Figures 2.1C, 2.9). The timing of the Wakatipu Glacier's LGM advance is not well defined, interpreted by Barrell (2011) as early-mid MIS2 in age.

The Shotover Valley acts as a local base level for tributary streams, and these correspondingly aggrade or degrade in response to changes in the channel bed level in the Shotover Valley. These streams form alluvial fan surfaces grading to the aggradation level, for example those seen at Ballarat Creek (Figure 2.10), and inclined fan surfaces from tributaries in the Skippers area. Figure 3.8A is an interpretation of the Shotover Valley during the time of the maximum LGM ice extent. This shows a lobe of the Wakatipu Glacier extending into the lower Shotover Gorge, and an aggradation surface filling the Shotover Gorge and the main tributaries such as Moonlight Creek, Stony Creek and Skippers Creek.

A number of higher alluvial surfaces are seen at locations of >30 metres higher than the main aggradation surface. These are interpreted as being formed by an earlier aggradation episode and are of unknown age; they may be formed by an earlier Otiran glacial advance(s) or during an earlier glacial cycle.

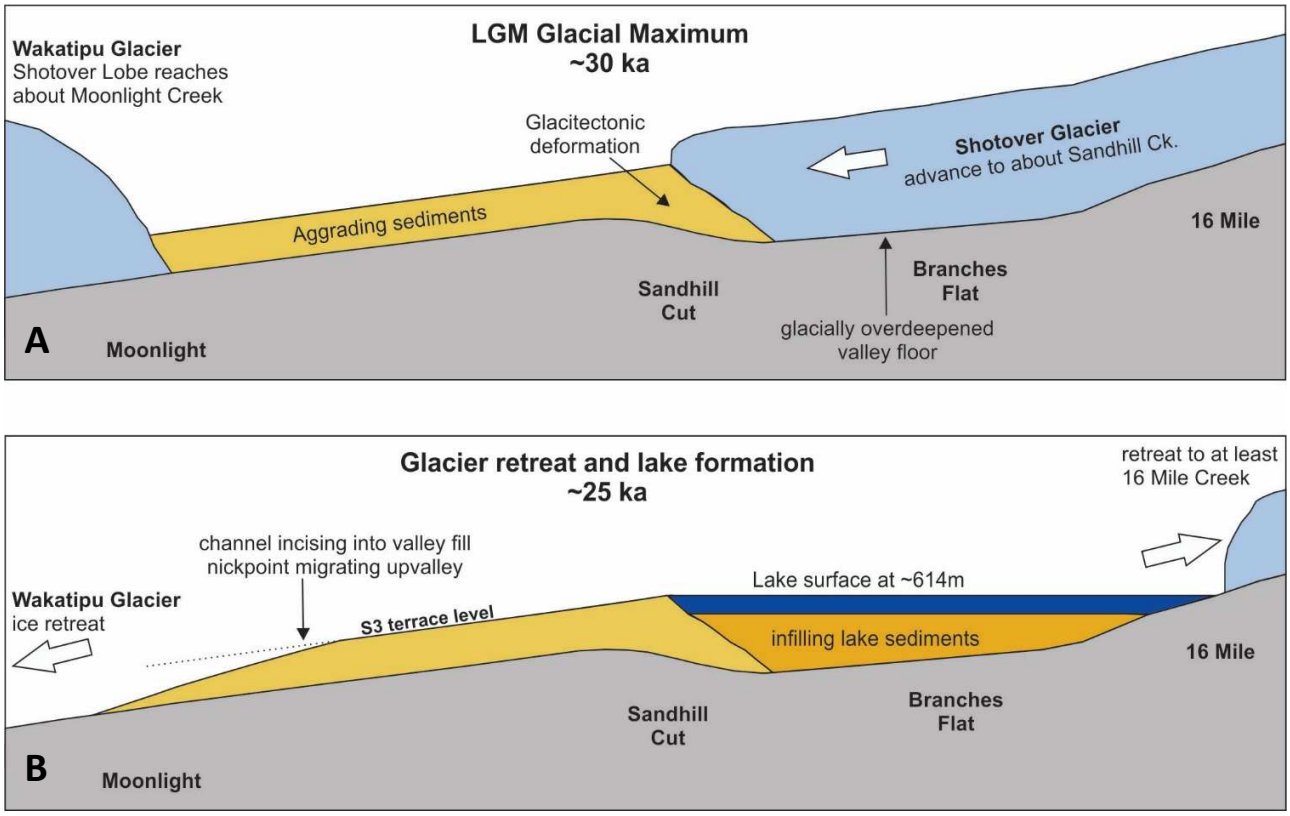

Figure 3.4: *Sketch profiles of the Shotover Valley during (A) Shotover Glacier LGM advance, showing aggradation as a result of the Wakatipu Glacier blocking the lower Shotover Gorge, and (B) following ice retreat, showing lake formation behind a barrier of aggraded outwash sediments.*

Glacial Retreat and Lake Formation

Lacustrine sediments are found in the upper Shotover Gorge and at Branches Flat, with the largest exposures at Strohles Flat (Figure 2.12), Muddy Terrace, and the Ironstone Creek delta (Figure 2.16, 2.17, 3.6). Sediments range from laminated clay-silts (e.g. Campbell Saddle footbridge, Figure 2.15) in low-energy locations in the valley centre, to sands with ripple and crossbedding textures in higher energy locations (e.g. Figure 2.13B). Deltaic deposits have been formed by the main tributary streams entering this lake, within the study area these include; Muddy Creek, Ironstone Creek, and Stockyard Creek (Figure 3.1), with the Rapid Creek outcrop also inferred to be deltaic. These delta deposits show bottomset sands-silts with thicknesses of >50 metres and inclined foreset gravels located towards the valley margins. The extensive gravel fan surfaces overlying finer sand-silts (e.g. at Muddy Terrace) are interpreted as fan-delta gravels.

This was a large lake, with an interpreted maximum water depth of >100 metres, and total length of >20 km (Figure 3.5). Inferred lake shorelines at Branches Flat (Figure 2.14) indicate water levels of at least 614 and 595 metres in two different highstands, a possible shoreline at 631 m may also indicate a higher water level. Observations at Muddy Terrace, Ironstone Delta and Strohles Flat indicate the lake infilled with sediment to an elevation of at least 575 metres. Sediment infilling to a thickness of at least 80-90 m indicates a long-lived lake, McSaveney (1978) estimated this lake persisted for about 3,500 years, filling with 2.6 $x10^9$ tons of sediment. As the depth to the bedrock valley floor is not known in the upper Shotover Gorge or at Branches Flat, the true thickness and volume of these lacustrine deposits may in fact be much greater, and the lake may have persisted for a longer duration than this estimate.

Further upvalley from the study area, deltaic sediments have also been identified at the Flood Burn confluence (Carryer 1984), and as a gravel-dominated delta at Sixteen Mile Creek (McSaveney 1978). Trenches and boreholes in the upper part of Branches Flat show lacustrine sediments underlying the alluvial gravels (e.g. Nugold 1990). An interpreted lake outline based on the highest well-defined shoreline (614 m) is shown in Figure 3.5. This extends upvalley to a point between Lake Creek and Sixteen Mile Creek, and is of similar extent to the lake interpretation of McSaveney (1978).

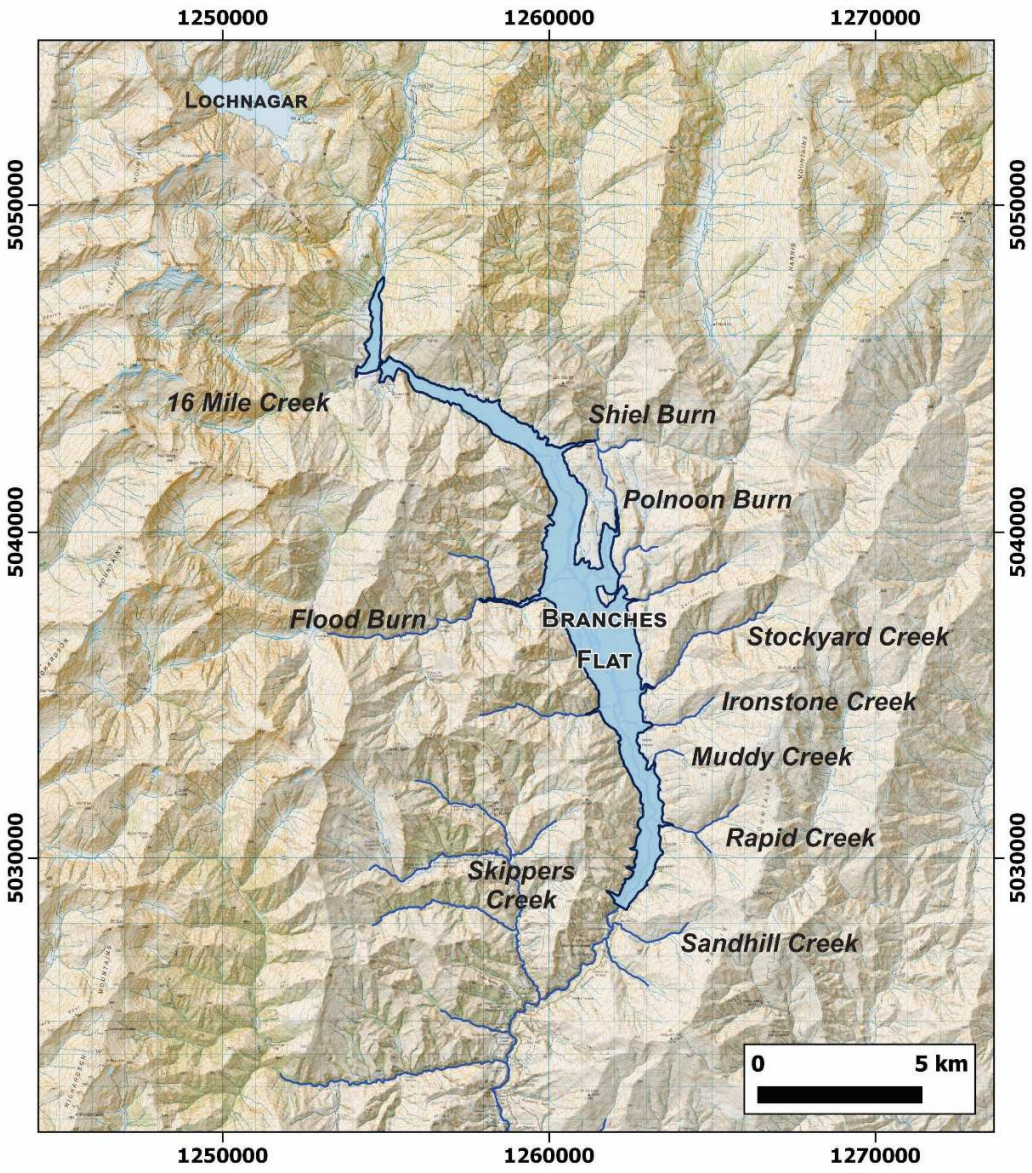

Figure 3.5: *Map showing interpreted extent of the Shotover Valley paleolake, based on a 614 m shoreline.*

This paleolake is interpreted to be a proglacial lake formed following Shotover Glacier ice retreat from the Sandhill Advance. The lake was impounded by a barrier comprising outwash head and ice-contact fan deposits, and the extensive downvalley aggradation sediments (Figure 3.4). Rock avalanche material seen at Sandhill Cut may have also

contributed to the height and/or longevity of this barrier. Shulmeister (2017) notes that proglacial lakes impounded by outwash deposits are a distinctive morphological feature of New Zealand glaciations. Proglacial lakes persist in many valley systems, and evidence of their formation is seen in many other glaciated valley locations. Examples of proglacial lakes partially impounded by outwash sediments include, the modern Tasman Glacier lake (Purdie et al. 2016), and other high country lakes in New Zealand, such as the Lakes Pukaki, Tekapo and Ohau (Shulmeister et al. 2010).

There were no sedimentary features identified that would definitively characterise these lacustrine sediments as being deposited in a proglacial lake, such as ice rafted deposits or dropstones. However, this could be due to a rapid ice retreat leaving the downvalley parts of the lake removed from any influence of glacial processes. As noted by Carrivick and Tweed (2013), distal parts of proglacial lakes are physically separated from the glacier margin and have no moraine or ice-rafted debris, and decreased sediment load and clast sizes compared to ice-contact lakes. They characterise distal glacilacustrine sediments as having rhythmically bedded sand, silt and clay bottom sediments, and deltaic sediments comprising fine-grained, prograding, shallow-dipping foresets, consistent with field observations of Shotover Valley sediments.

Lacustrine and deltaic sediments have an age of 24.7 ± 4.7 ka, based on an OSL sample (BF1) analysed from the Ironstone Delta (BF1, Figure 3.6). This is consistent with interpretation as a proglacial lake formed as ice retreated from an upper Shotover Gorge terminus. These dates indicate significant and rapid ice retreat following the Sandhill Advance. Based on the extent of lacustrine sediments, it is inferred that ice retreated for at least 20 km upvalley to a point beyond Sixteen Mile Creek. As a small volume glacier, with a relatively small, low elevation accumulation area, the Shotover Valley glacier would have been more sensitive to climatic changes than much larger glaciers like the Wakatipu Glacier.

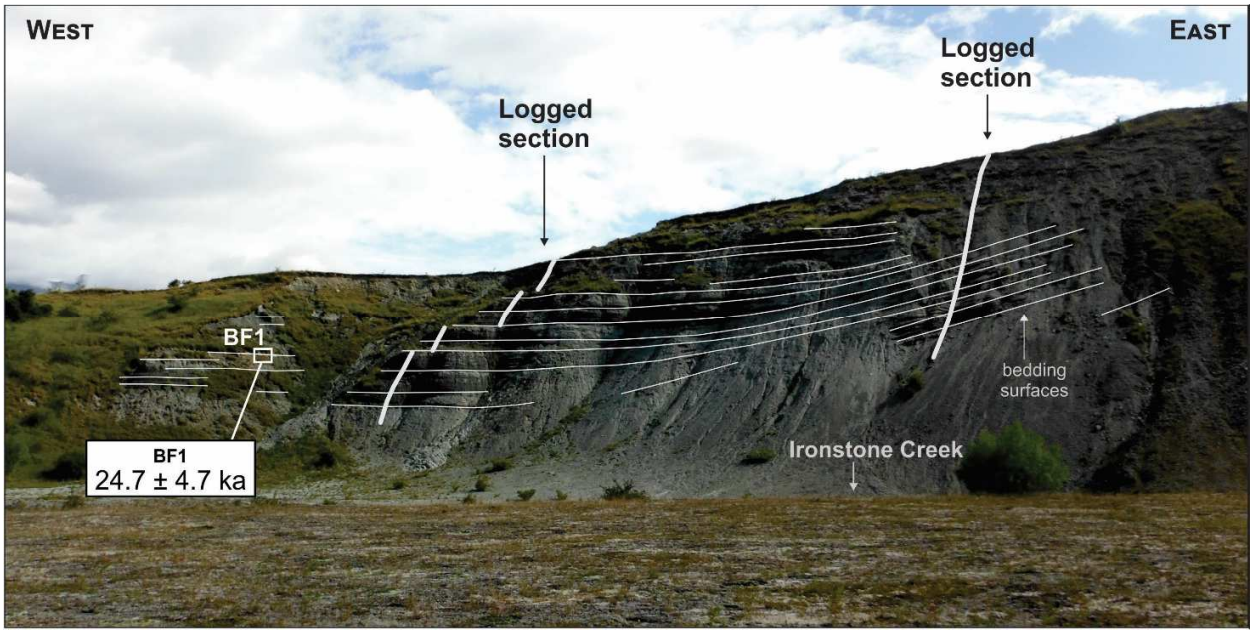

Figure 3.6: *Ironstone Delta, showing OSL dating results, and location of logged sections (Figure 2.17).*

Shotover Glacier ice retreat may be linked to a period of local warming, possibly correlating with a 'warmer and more variable phase' at 27-21 ka (Alloway et al. 2007), or interpreted interstadial periods at 25.4 -24.5 and 22.6-21.7 ka (Barrell et al. 2013). However, temperature is only one factor affecting glacier behaviour, which is also strongly

influenced by factors such as wind regime precipitation rates, debris cover, and proglacial lake formation (Shulmeister 2017). Formation of a proglacial lake may have a strong influence on ice-loss dynamics, and can lead to the rate of glacial retreat becoming decoupled from climatic controls (Shulmeister et al. 2010, Carrivick and Tweed 2013, Rother et al. 2014, Shulmeister 2017). Formation of large, deep proglacial lakes may lead to rapid rates of ice retreat, as ice loss is enhanced through heat advection and wave action impacts (Rother et al. 2014), and positive feedbacks between lake and ice dynamics may cause accelerated ice retreat (Carrivick and Tweed 2013). Glaciers may retreat upvalley until they cease to terminate in a lake (Shulmeister 2017), this appears to have been the case in the Shotover Valley, and explains the large and relatively rapid retreat following the Sandhill Advance.

Figure 3.8B shows an interpretation of the valley following glacial retreat and lake formation. This shows the Shotover Glacier retreating to upvalley of Sixteen Mile Creek, and a lake forming behind a barrier in the upper Shotover Gorge at about Sandhill Creek. Sediments sourced from tributary streams are forming deltaic deposits where they enter the lake, and lacustrine sediments are infilling the lakebed. The Wakatipu Glacier has partially retreated from the Wakatipu Basin, and the Shotover River may be flowing eastwards to join the Arrow River. The Shotover River's base level lowers as Wakatipu ice retreats, and aggraded sediments begin to degrade leaving the aggradation surface as large paired terraces.

In the middle part of Branches Flat are a series of moraine deposits located east of the Shotover River (Figure 3.7). These are outside the study area and have not been field checked, but have been noted by McSaveney (1978) and Thompson (1998). Newly-acquired dates for the Sandhill Advance provides a maximum age for these moraines, and these are therefore interpreted as younger than ~30 ka. Preservation of lake sediments at Sixteen Mile Creek (McSaveney 1978) and upper Branches Flat (Nugold 1990) demonstrates there was no significant ice re-advance following lake formation by 25 ka. These moraines are assumed to be recessional moraines formed during glacial retreat from the Sandhill Advance, deposited in the period 30-25 ka.

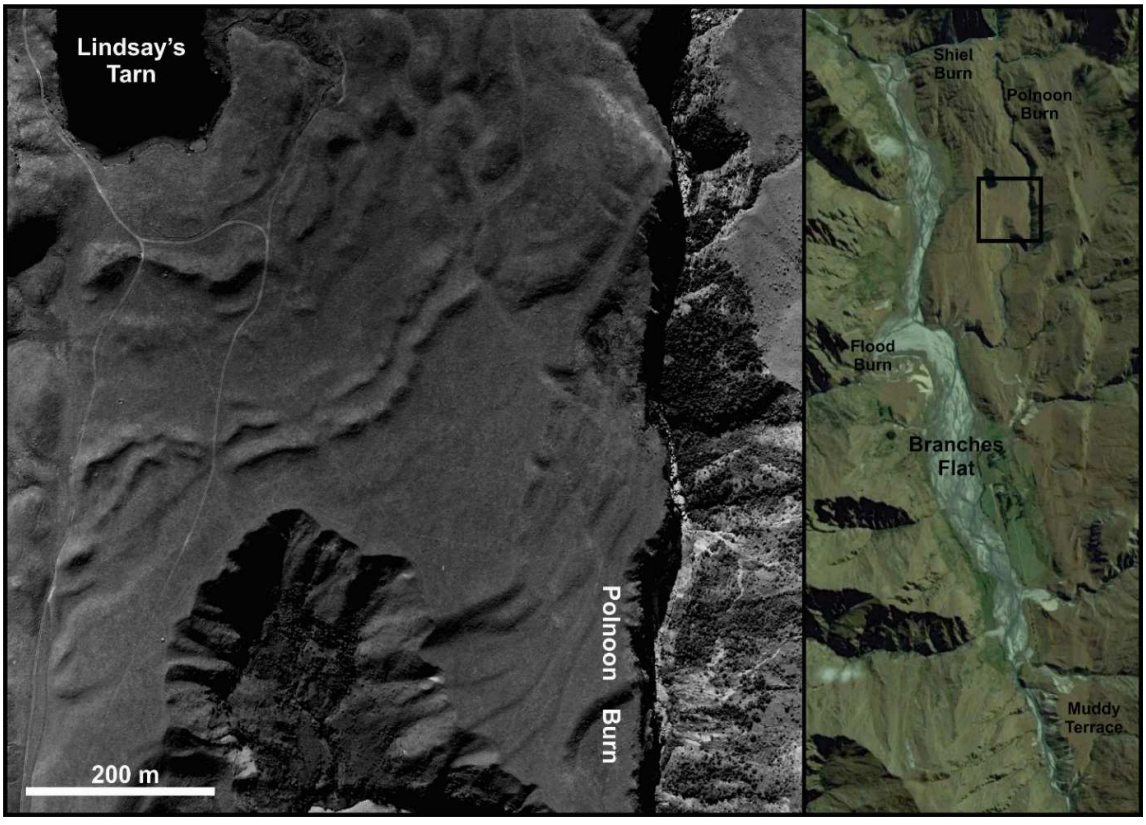

Figure 3.7: *Aerial view of Branches Flat moraines in the Linsay's Tarn-Polnoon Burn area (photo by Kevin Jones, DoC). The right hand image shows location on eastern side of Branches Flat upstream of the Flood Burn confluence, and the black box indicates location of detail image.*

Postglacial Incision

The deglaciation behaviour of the Wakatipu Glacier is uncertain, but meltout has been assumed to be rapid (e.g. Thompson 1996b). The postglacial Shotover River may have flowed eastwards into the Arrow catchment, confined by remnant ice to a path along the base of Coronet Peak (Bell 1992). Ice continued to retreat from the Wakatipu Valley, and the 'greater Lake Wakatipu' formed, with a stable level of about 355 m (Stahl 2014). At this height, the Shotover River flowed into the lake, forming an extensive delta with a head at about Tucker Beach (Barrell et al. 1994). From a stillstand at this level, the lake level continued to fall, firstly due to incision at the Kingston outlet, and later after switching to the Kawarau River outlet (Figure 1.8).

As the Wakatipu Glacier retreated, the base level of the Shotover Valley progressively lowered, and the valley-filling sediments begin to degrade in response. The Shotover River incised into the aggradation surface, leaving remnants of this level as paired terraces. As the channel continued to incise into these sediments intermediate terrace levels are formed through lateral channel migration (Figure 2.11). Eventually incision reaches the pre-glaciation bedrock valley floor and begins to erode into the basement schists in the Shotover gorge. It is not known when the upper Shotover Gorge paleolake drained, but at some stage the barrier impounding the lake would have been breached as the sediments filling the gorge were incised.

Figure 3.8C shows an interpretation of the Shotover Valley in the postglacial period. The Shotover paleolake has been drained and some lacustrine and deltaic sediments are being incised. In the Shotover Gorge, alluvial gravels have been incised to leave remnants of the aggradation surface and forming intermediate level terraces. Bedrock incision has commenced as the river has eroded to the base of gravels, and the incised Shotover Gorge is beginning to form. In the Wakatipu Basin, Lake Wakatipu is at a level of ~355 m and has an outlet at Kingston, and at this time the Shotover River is forming a large fan-delta surface into Lake Wakatipu, which eventually cuts off the modern Lake Hayes from the rest of the lake.

Figure 3.8D shows a summary of the main features of the modern Shotover Valley and Wakatipu Basin. In the middle and lower Shotover Gorge, fluvial incision driven by uplift has formed a deep schist gorge, and remnants of alluvial, glacial, lacustrine and deltaic sediments are preserved at the valley margins. In the Wakatipu Basin, Lake Wakatipu has lowered to its modern level of ~310 m and has an outlet at Frankton into the Kawarau Valley. The lower Shotover River has incised into the larger postglacial delta surface to form the modern fan-delta at the Kawarau River confluence.

Shotover Gorge Incision

The bedrock terrace level (S1) in the Shotover Gorge is found ~90-95 m above the modern river channel (Figure 2.5, 2.6). These terraces are common in the middle Shotover Gorge from Deep Creek to about Skippers (Figure 2.1C, 2.8A, B, 2.11), and in the lower parts of Moonlight Creek (Figure 2.8C, D). This level represents a former valley floor surface, formed prior to downcutting of the Shotover River and tributary streams. This valley floor is interpreted as being formed primarily due to fluvial erosion, shown by the bedrock paleochannels in the Skippers area, and the presence of water-smoothed bedrock surfaces, such as those seen at Pleasant Creek Terrace.

This has been previously interpreted as a glaciated surface; 'a broader, ice-shaped valley floor' by Thompson (1998, p21), although there is no definitive evidence that would prove a glacial origin for this feature, for example bedrock striations which would indicate ice-contact or subglacial channel. However, this section of valley may have been overrun by older, more extensive glacial advances, and the paleochannels could also have been formed as subglacial

channels. For example Barrell (2011) shows older (MIS 4-8) glacial extents beyond the LGM ice limits, and the equivalent Shotover Valley glacier may have reached farther downvalley than the LGM Sandhill Advance.

Prior to the LGM Sandhill Advance in the Shotover Gorge, this surface (S1) had been fluvially incised to form a bedrock river channel about 20 m in depth. This is shown the presence of paleochannels buried by aggradation gravels (Figure 2.5), many of which are marked by sluiced excavations as mining targeted placer gold accumulations at/near the base of the these channels (Park 1909). As the valley incised in the postglacial period, the river may have exhumed and reoccupied the incised pre-glacial channel, or incised a new bedrock channel, leaving the former channel buried by aggradation fill.

The Wakatipu region is being tectonically uplifted at a rate of ~3 mm/year (Upton et al. 2009), with the incising Shotover River maintaining a constant position through fluvial incision. Over the postglacial period, this has formed the modern Shotover Gorge, potentially incising by about 60 m (20,000 years at 3 mm/year). As bedrock incision formed the modern gorge, older valley floor surfaces such as the aggradation surface (S3) and former valley floor (S1) have been uplifted and are now much higher than the modern riverbed level.

In the upper Shotover Gorge and at Branches Flat, the valley is interpreted as having been significantly widened (Figure 2.2) and deepened by erosion during cycles of glacial activity. A clear knickpoint is seen in the Shotover Gorge long profile at about Sandhill Creek (Figure 2.6). Above this point the valley has a lower gradient, and is wider and sediment filled (Figure 2.1A, B). In contrast, the Shotover Gorge below this point has a slightly steeper gradient with exposed bedrock and is actively incising. This is a similar profile to that seen in the Waiau Valley, where Rother (2006) describes a wider, U-shaped, fill-dominated, glaciated upper valley, and a V-shaped lower non-glaciated valley morphology. Both the Sandhill area glacial sediments, and upper Shotover Gorge and Branches Flat lacustrine sediments are deposited to the level of the modern valley floor. The thickness of these deposits above the bedrock valley floor is unknown but may be significant.

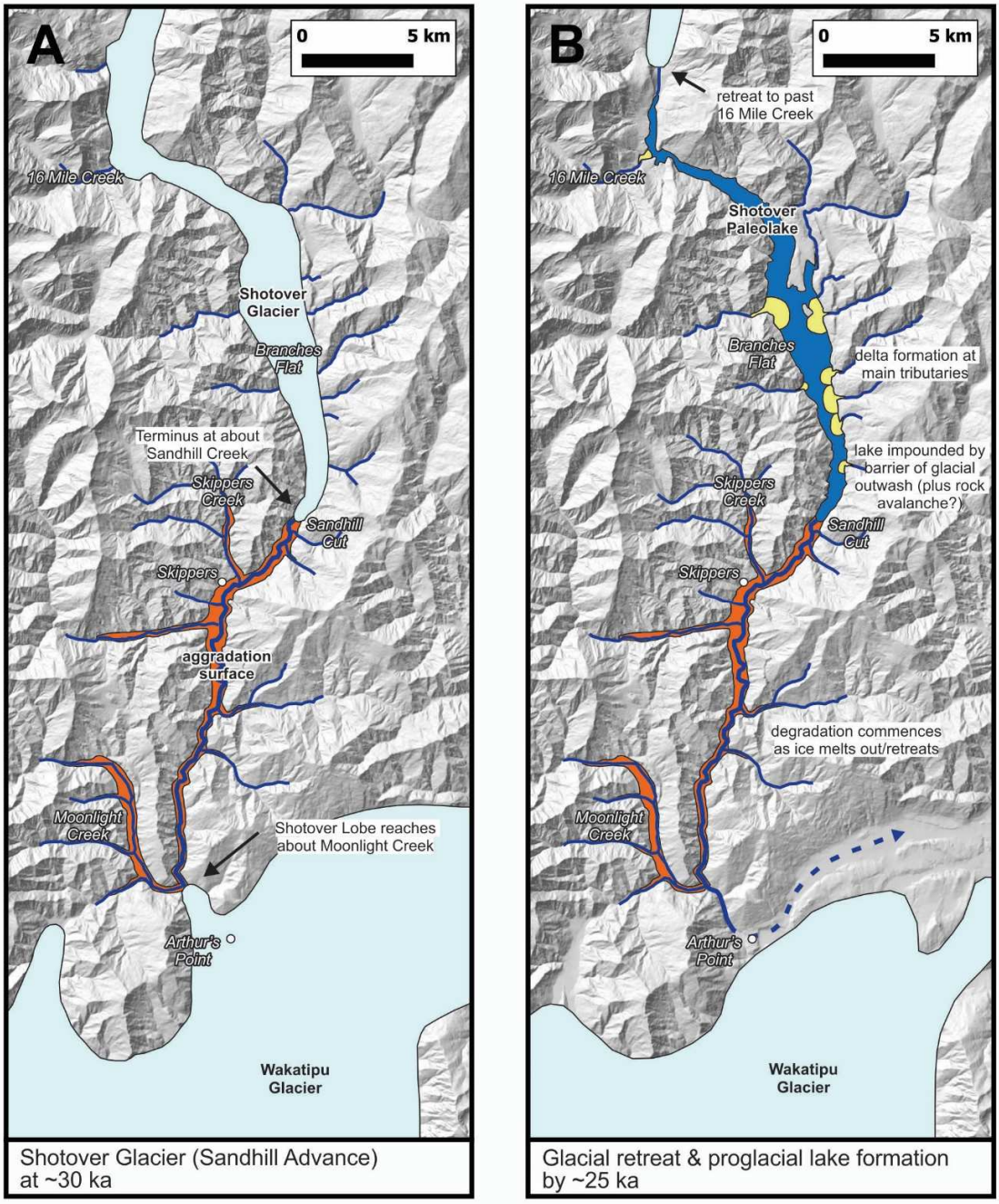

Figure 3.8 A, B: *Sketches showing the main stages of the Shotover Valley's LGM and postglacial development;*

A. Maximum extent of the LGM Shotover (Sandhill Advance) and Wakatipu Glaciers, with Shotover Valley aggradation caused by blocking of the valley by Wakatipu Glacier ice. (Wakatipu Glacier extent based on Barrell (2011). Shotover Valley Glacier is shown, but does not show the likely contribution from others sources such as Polnoon and Shiel Burn.

B. The Shotover Glacier has retreated upvalley to beyond Sixteen Mile Creek and a large proglacial lake has formed. The Wakatipu Glacier has partially withdrawn from the Wakatipu Basin and the lower Shotover River may be flowing eastwards to join the Arrow catchment. Degradation of valley-filling sediments commences as the base level lowers. (Wakatipu Glacier extent based on Barrell 2011).

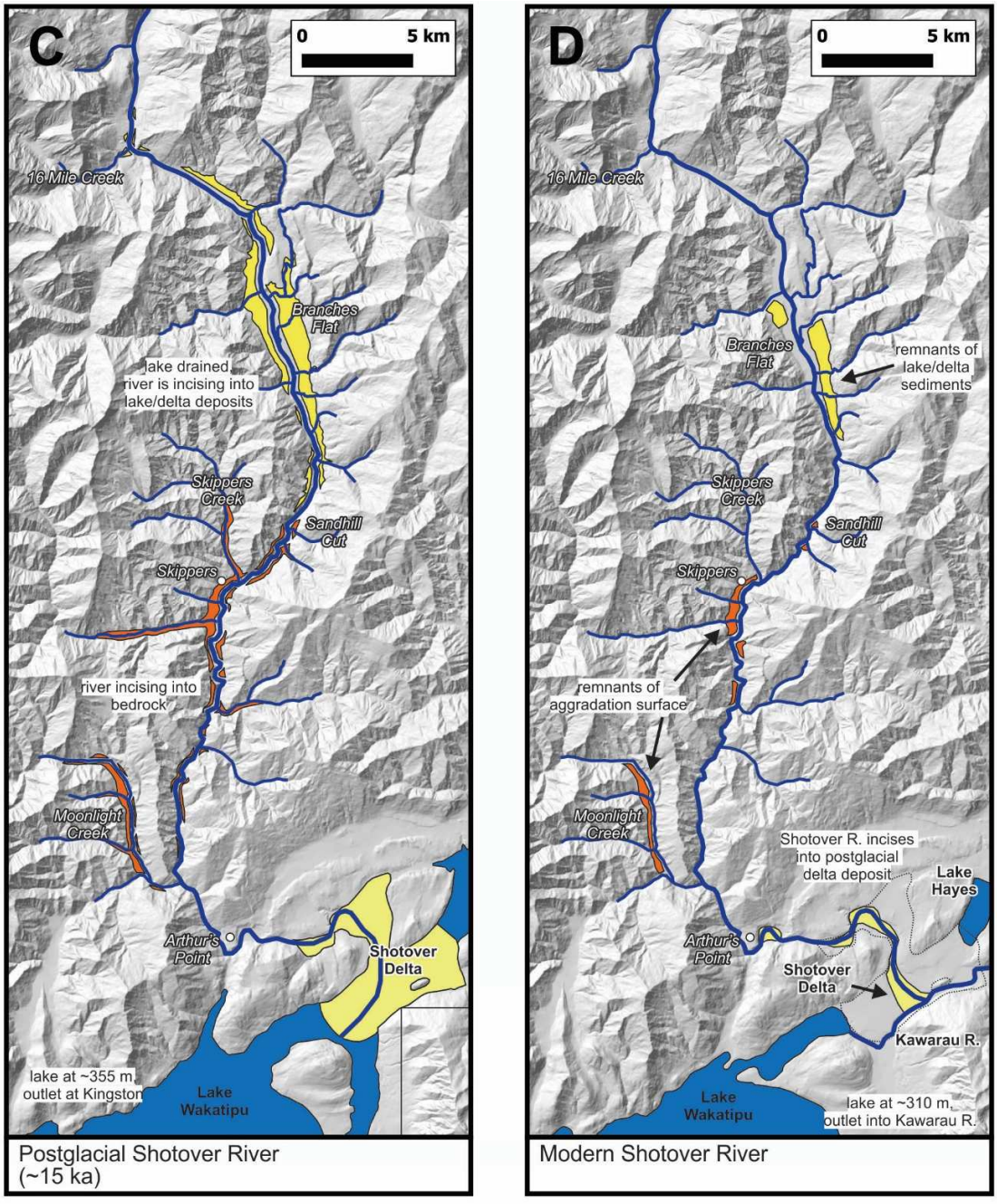

Figure 3.8 C, D: *Sketches showing the main stages of the Shotover Valley's LGM and postglacial development;*

C. The Wakatipu Glacier has retreated and the postglacial 'greater Lake Wakatipu' has formed, the Shotover River is forming an extensive fan-delta surface into the lake. Degradation has continued in the Shotover Gorge, incising into bedrock and forming the S1 terrace level, and the upper Shotover Gorge lake has been drained as the barrier is incised. (postglacial Shotover Delta extent from Barrell et al. (1994).

D. The Shotover River has incised to leave only remnants of Shotover Gorge and Moonlight Creek sediments. As Lake Wakatipu has lowered to its current level, the Shotover River has incised into the postglacial delta surface.

Mass Movement

The extents of large creeping dipslope landslides mapped in this study are similar to those of Turnbull (2000), but have been mapped to a higher resolution (Figure 2.29). These landslides appear similar to those described by other studies in nearby areas, such as the Wakatipu Basin (Willetts 2000), Rees Valley (Cox et al. 2014), Kawarau Gorge (Bell 1976 1992), Roxburgh Gorge (Moon 1997), and alongside the Clyde Dam reservoir (McFarlane 2009). Based on comparison with these other examples, these landslides may be moving at rates of 10-50 millimetres annually, and the largest failures may be up to several hundred metres deep. On average, the rate of rockfall at the toe of the gorge slopes will match the rate of creep, maintaining the gorge at about its current position.

The age of the large landslides in the valley is not known, but are likely to have been initiated by similar processes to other large schist landslides. In the Wakatipu Basin, Kawarau Gorge, and alongside the Clyde Dam reservoir, landslide initiation is thought to have been initiated by glacial deepening and/or removal of ice support, with estimated ages ranging from 50-250 ka (Willetts 2000, McFarlane 2009). Creeping landslides in the Shotover and Moonlight Valleys are interpreted to have been initiated by glacial and/or fluvial erosion leading to a removal of slope toe support. The timing of landslide initiation in the Shotover Gorge is not known, and may have been as early as during or following the Waimean Glacial, and possibly the result of an early glacial advance extending the full length of the Shotover Valley.

In several locations, there are examples of creeping landslides progressing to rapid failure (e.g. Figure 2.30), through destabilisation of toe slopes by gorge incision. This appears similar to examples elsewhere of creeping landslides becoming destabilised and progressing to sudden failure as a rockslide or rock avalanche, for example in Italy (Sacchini et al. 2016, Gori et al. 2014), and the Czech Republic (Panek et al. 2009). The largest landslides in the Shotover Gorge have scarp widths of up to about 500 m, and volumes estimated at >10M m^3. These occur from both sides of the valley and are typically wedge failures controlled by structural features such as jointing, faulting and foliation.

Landslide Dams

A landslide deposit at Sutherlands Beach (Figure 2.33) is interpreted as a former landslide dam deposit, which may have been several tens of metres in height. A deposit of coarse angular schist debris seen at Sandhill Cut (Figure 2.21) is characteristic of rock avalanche deposits (McColl and Davies 2011). This may have been deposited directly from a slope failure at this location, or sourced from a failure located further upvalley and transported to this point as supraglacial debris. Whether this is in-situ or transported debris, it may have contributed to the height and/or longevity of barrier impounding the upper gorge lake.

There are no deposits indicating the presence of large (>1M m^3) former landslide dams in the Shotover Gorge, despite the presence of a number of large landslide scarps adjacent to the gorge channel (map in Appendix 1, Figure 6.11). This shows that any Shotover Gorge landslide dams of this magnitude were formed sufficiently long ago that subsequent erosion has completely removed remains of dam-forming debris, and there is no longer any knickpoint in the river profile.

3.4 Chronology of Key Events

Based on the interpretations above, a summary of the main events in the valley's geological history has been compiled, showing the main events with an interpretation of their formation age (Table 3.2). Figure 3.9 shows Shotover Valley OSL dates relative to the New Zealand climate phases of the last 30,000 years, as defined by the NZ-INTIMATE project (Barrell et al. 2013).

Table 3.2: *Interpretation of the main events in the Shotover Valley's recent geological history.*

Event	Timing	Comments
Creeping landslide initiation	Unknown – maybe during or following MIS6?	Based on inferred ages of landslides elsewhere in Otago (Willetts 2000, McFarlane 2009)
Aggradation during an early glacial advance(s) forms high alluvial deposits above main terrace levels	Unknown – during MI6-4 glaciation(s)?	
Bedrock terrace (S1) level formed as a fluvially eroded valley floor	By ~30 ka	Formed by fluvial downcutting prior to aggradation during LGM glaciation
Shotover Glacier Advance (Sandhill Advance) Shotover lobe of Wakatipu Glacier blocks valley, base level rise causes aggradation, forming S3 terrace level.	At ~30 ka Early LGM (late MIS3/early MIS2)	Based on OSL dating of glacial sediments at Sandhill Creek (Figure 3.2). Summarised in Figure 3.8A
Shotover Glacier retreats to about Sixteen Mile Creek, formation of recessional moraines at middle Branches Flat.	30-25 ka	After Sandhill Advance (~30 ka), and by time of Ironstone Delta formation at ~25 ka.
Proglacial lake formation, sediment infilling and delta formation. Final lake extent reaches to about Sixteen Mile Creek	By ~25 ka	Based on OSL dating of deltaic sediments at Ironstone Creek (Figure 3.6). Summarised in Figure 3.8B
Wakatipu Glacier retreats from the Wakatipu Basin. Degradation of valley fill deposits, and formation of intermediate terraces. Gorge degrades through alluvial deposits, commences bedrock incision and formation of Shotover Gorge. Large postglacial Shotover Delta forms into the 355 m Lake Wakatipu	From late-glacial (20-18 ka), continuing into postglacial period	Based in interpretation of partial retreat of Wakatipu Glacier by late MIS2 (Barrell 2011) Extent of postglacial Shotover Delta shown by Barrell et al. (2004) Summarised in Figure 3.8C
Loess deposition	From/during LGM or late-glacial, continuing into postglacial period	Based on loess occurrence on all Shotover terrace levels, and timing of regional deposition of loess (Alloway et al. 2007)
River continues to incise into bedrock (lower-middle Shotover Gorge), and sediments (upper Shotover Gorge and Branches Flat). Lake Wakatipu lowers to modern level, and switches outlet from Kingston to Kawarau River. Lower Shotover River incises into the postglacial delta surface.	Postglacial (from ~18 ka-present)	
Shotover River attains modern channel form.	Within last 1,000 years	Based on Lake Wakatipu reconstructions (Stahl 2014) Summarised in Figure 3.8D

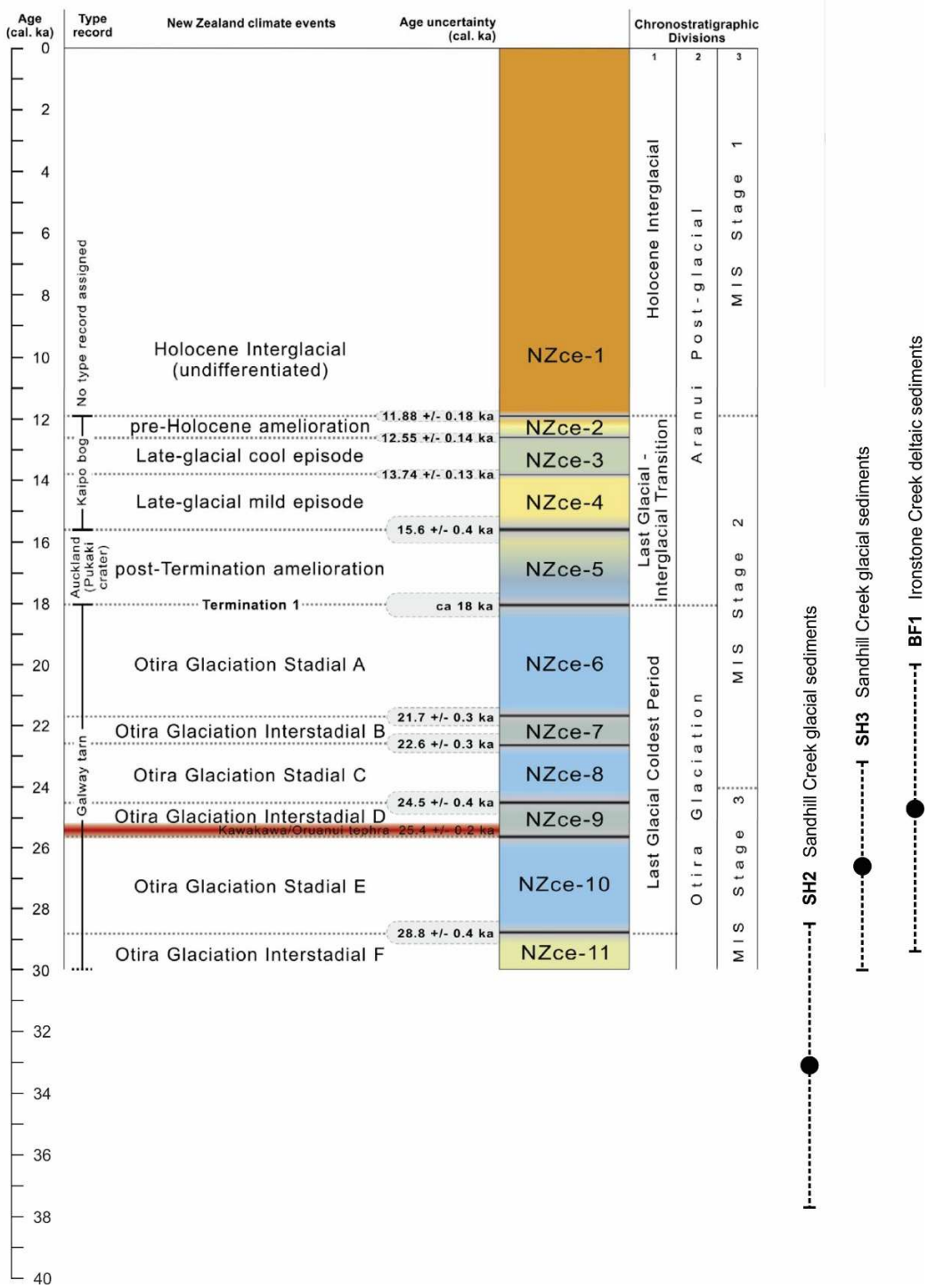

Figure 3.9: *New Zealand climate event phases of the last 30,000 years, based on the NZ-INTIMATE project (Barrell et al. 2013). Shotover Valley OSL dates are shown to right: two samples (SH2, SH3) from Sandhill Creek glacial sediments, and one sample (BF1) of deltaic sediments from Ironstone Creek.*

3.5 Limitations and Possible Further Investigations

This work has identified a number of features of interest, and allowed for a preliminary revision of the valley's recent geological history. However, there is opportunity for further investigations to build on this study and develop more robust interpretations of the valley's recent geological evolution.

The main limitation of this interpreted chronology is that OSL samples were only obtained from two locations, and there are large uncertainties associated with the results (Figure 3.9). If samples have been only partially bleached the ages may represent maximum ages for these deposits. Upper Shotover Gorge glacial interpretations are mainly based on investigations of the northern Sandhill Creek outcrop, and the timing of the Sandhill Advance is based on only two dated samples (Figure 3.2, 3.9). Other outcrops of glacial sediments in this area have been the focus of only brief observations, including Smiths Terrace (Figure 2.19), south of Sandhill Creek (Figure 2.23), at Sandhill Cut (Figure 2.21) and alongside Branches Road (Figure 2.18). These relatively understudied exposures will allow for more detailed future study to characterise these deposits and define this glacial event. This could include detailed glacial sedimentology (clast roundness, ripple geometry, clast fabric) and structural analysis of glacitectonic deformation, as was carried out by Hyatt (2009) in the Rakaia Gorge, and Evans et al. (2013) at Lake Pukaki. Glacial features have also been reported from several Shotover Valley locations outside this project's study area, such as moraines at Branches Flat (Figure 3.7) and Seventeen Mile Creek (McSaveney 1978, Thompson 1998), and these may provide further information to build the valley's glacial history.

Dating of deltaic sediments used to constrain interpretations of glacial retreat and lake formation is based on a single sample with analytical uncertainty of ± 4.7 ka (Figures 3.6, 3.9). Additional dating of sediments from low and high stratigraphic positions within lacustrine or deltaic sequences could help define the maximum age of lake formation, and lake longevity. Outside of the study area, investigation of the Flood Burn (Carryer 1984) and Seventeen Mile deltaic deposits (McSaveney 1978, Thompson 1998) may assist with defining the characteristics of this paleolake.

Shotover Gorge and Moonlight Creek aggradation gravels are interpreted as being deposited during the Shotover Glacier's LGM advance but are undated. Loess is found at many locations within the valley (e.g. Figure 2.27) and dating of this material may better constrain late-glacial and postglacial events. For example at Branches Flat this could be used to identify the date by which the paleolake has been drained, and on lower terrace levels in the Skippers area to show the timing of degradation.

3.6 Summary and Conclusions

This chapter provides an interpretation of the recent geological history of the Shotover Gorge, based on geological and geomorphic observations and mapping summarised in Chapter Two, and OSL dating of glacial and deltaic sediments. There were no previous dates to constrain the Shotover Valley's development so this has allowed for a revision of the valley's LGM and postglacial chronology. This is summarised as a series of sketches interpreting main stages in the valleys development (Figure 3.8), and Table 3.2, which outlines the key events and their interpreted timing.

The Shotover Glacier's maximum LGM extent is interpreted as reaching to about Sandhill Creek in the upper Shotover Gorge (Figure 3.8A). In this area glacial sediments are interpreted as being deposited dominantly in proglacial fluvial ice-contact environments and commonly show evidence for glacitectonic deformation. These sediments have been dated to late MIS3/early MIS2 (29.4 ± 3.4 ka) (Figures 3.2, 3.9), which is similar to the timing of other South Island LGM advances (Rother et al. 2014, Shulmeister 2017).

The extensive terrace gravels in the Skippers area and Moonlight Creek are interpreted as representing an aggradation surface formed in response to a rise in the valley's base level. This is thought to have been due to the Wakatipu Glacier intruding into the lower Shotover Gorge (Figure 3.8A). The Shotover Valley acts as a local base level

for its tributary streams and they also aggraded in response, for example forming the large alluvial terrace surface seen in Moonlight Creek.

Following the Sandhill Advance, the Shotover Glacier retreated and a large proglacial lake formed in the upper Shotover Gorge and Branches Flat (Figure 3.5, 3.8B), impounded by valley-filling glacial and aggradation sediments in the upper Shotover Gorge. The maximum lake level is interpreted as ~614 m based on an inferred shoreline located north of Ironstone Creek, and the lake had an upvalley extent of >20 km (Figure 3.5). The lake infilled with sediments to a thickness of at least 80-90 metres, and formed deltaic deposits at most tributary streams (e.g. Figure 3.6). Dating of deltaic sediments at Ironstone Creek (Figure 3.6, 3.9), shows glacial retreat and partial lake infill by ~25 ka. This interpretation is consistent with observations elsewhere of proglacial lakes impounded by outwash deposits being a common feature of New Zealand valley glacier systems (Shulmeister 2017).

As Wakatipu Glacier ice retreated the Shotover Valley's base level lowered and aggradation deposits in the Shotover Gorge began to degrade, leaving remnants of the aggradation surface as terrace surfaces, and forming intermediate terraces at lower elevations.

These interpretations show that the main influences on the valley's geological development have been glacial cycles and base level changes. Glacial advances have shaped the upper Shotover Gorge and Branches Flat, deepening and widening this part of the valley (Figure 2.2), which still contains an unknown thickness of infilling glacial and lacustrine sediments. The valley's large paleolake was formed as a proglacial lake during glacial retreat, and impounded by sediments deposited during the final glacial advance. Events in the Wakatipu Basin are interpreted as a control on the Shotover Valley base level, and thus an influence on events within the valley. Advance of the Wakatipu Glacier is interpreted to have caused aggradation as a result of raising the Shotover base level, and then later degradation has been controlled by lowering of base level as ice retreated from the Wakatipu Basin and later as the level of Lake Wakatipu lowered. The modern Shotover Gorge has formed as the river has incised in response to tectonic uplift, while older surfaces have been uplifted and are now located high above the valley floor.

Evidence for a large paleolake in the Shotover Gorge demonstrates potential for blocking of this valley and lake development, as could also occur as a result of landslide dam formation. However, outwash fan heads form extensive and durable valley-blocking obstructions (Shulmeister 2017), and in contrast a landslide dam blockage is expected to be an unstable and short-lived landscape feature (Section 7.4).

The geological and geomorphic observations and interpretations of Chapter Two and this chapter provide a geological context to the landslide dam hazard assessment completed in the remainder of this thesis.

Chapter Four:
Historic Shotover River Geomorphic Changes

4.1 Introduction

Understanding the Shotover River's geomorphic response to the historic anthropogenic sediment input during the gold-mining operations of the late 19th and early 20th centuries assists with evaluating the river's possible future response to another episode of increased sediment loading, such as would follow a large landslide dambreak event.

Hydraulic sluicing of alluvial terrace gravels during gold mining operations in the Shotover Valley greatly increased the sediment supply to the lower Shotover River and delta, forming a sediment pulse with significant geomorphic impacts on the river system. These impacts were noted in many reports from throughout the historic mining era, for example;

> *"The river has been worked for the greater part, and is silted up by the enormous quantities of tailings"* (ODT 28 Feb 1891).
>
> *"The miners turned their attention to sluicing away the terraces, material being sluiced into the river. The natural result was that this enormous quantity of debris, and, in addition, the vast amount of material washed in by climatic influences, in time raised the bed of the river and smothered the auriferous gravels"* (Galvin 1906).
>
> *"With each successive year the cover of wash is becoming deeper and deeper, through the large amount of gravel sluiced into the river at and near Skippers Point"* (Park 1909).
>
> *"Owing to the operation of terrace claims, many thousands of tons of debris has been deposited in the river bed"* (Lake Wakatip Mail 15 March 1932).

This chapter investigates and summarises the Shotover River's geomorphic response to this mining-induced sediment pulse. Sluicing locations are identified (Figure 4.2) and the volume of sluicing-derived sediments are estimated (Table 4.1). Changes in river morphology in the Shotover Gorge, lower Shotover River (Figures 4.9, 4.10), and the Shotover Delta are summarised (Figures 4.12, 4.13). Aggradation thickness (Figure 4.14) and changes to the river width (Figure 4.15) are estimated.

Interpretations of geomorphic changes to the river have been based on data compiled from a variety of sources, the main records used were historical photographs and newspaper reports, aerial imagery, and river gauging and survey data. The sources used are summarised in Appendix 1.

4.2 Sluicing and Sediment Inputs

Gold mining activities in the Shotover Valley commenced following the first gold discoveries in 1862, initially at a small scale in the riverbed and terrace alluvial deposits. The earliest terrace mining was carried out through tunnelling in order to access the richest units found near the base of terrace gravels (Park 1909). Sluicing was first carried out by ground sluicing methods, where low pressure water is used to sluice away gravels by running down the terrace face, or to undercut terraces. High-pressure hydraulic sluicing was developed in California and introduced in Otago in the late 1870s or 1880s (Galvin 1906, Hamel 2001), and allowed for the excavation and processing of much

larger volumes of alluvial material. In this method, water was collected by systems of water races and siphons into high-level reservoirs, from where it was piped to a hydraulic nozzle used to direct a high-pressure water jet onto the mining face. Sluiced debris was then run through a tail race into sluice boxes to capture gold, with tailings discharged into the stream channel (Galvin 1906, OCB 1956, Hamel 2001, Jones 2009).

At several locations (e.g. Skippers Point, Pleasant Creek Terrace, Londonderry Terrace), tunnels were excavated in the underlying schist for use in disposal of tailings into the river. Larger boulders and cobbles were often piled or stacked on terraces, and are still visible in many locations. Many of the Shotover terraces show remains of dams used for sluicing on their upper terrace surfaces; these dams were used to collect water overnight, before being used for sluicing the following day (Jones 2008). The largest Shotover area dam has an estimated capacity of >10,000 m^3 (Jones 2008).

In the Shotover Valley hydraulic sluicing continued intensively until the turn of the century, then at reduced levels until 1914. Further sluicing took place during the 1930s depression, with renewed optimism due to increases in gold price and government subsidies, and continued into the 1950's (MWD 1975, Hamel 2001, Chandler n.d.). By the time of the 1956 OCB catchment survey, it was reported that 'little active sluicing being carried on nowadays', but small scale operations were carried out into the 1970s when the last miner retired.

The largest sluiced areas are located on the western side of the Shotover River below Skippers Creek (Figures 4.1, 4.2). From north to south along a two kilometre distance, these are Skippers Point, Burkes, Londonderry, Pleasant Creek, and Stony Creek Terraces (Hamel 2001). The area covered by sluicing on these terraces reaches >20 hectares, and the gravel thicknesses are up to 50 m (Park 1909, Chapter 2). Numerous smaller sluicing claims were located at many terraces elsewhere in the Shotover catchment: Polnoon Burn and Branches Flat in the north, in tributaries such as Moonlight, Moke and Skippers Creeks, and at locations alongside the lower Shotover River (Park 1909, Hamel 2001). At Sandhill Cut a large sluiced cut was excavated from 1926-1931 in an attempt to divert the flow and expose a section of riverbed for mining. The cut is 580 m long, 60 m deep, and involved removal of >1M m^3 of sediment (Figures 2.20, 2.21).

The magnitude of sluiced operations can be approximated by the volume of sluicing dams used to store water used in sluicing operations. The Figure 4.2 inset map shows location and size of the main Shotover River sluicing dams estimated by Jones (2009), this shows the largest dams located in the Skippers area, and the occurrence of numerous smaller dams elsewhere in the catchment. Dams outside of the Shotover River are not shown, for example in the Moonlight, and Skippers Creeks (Figure 4.2).

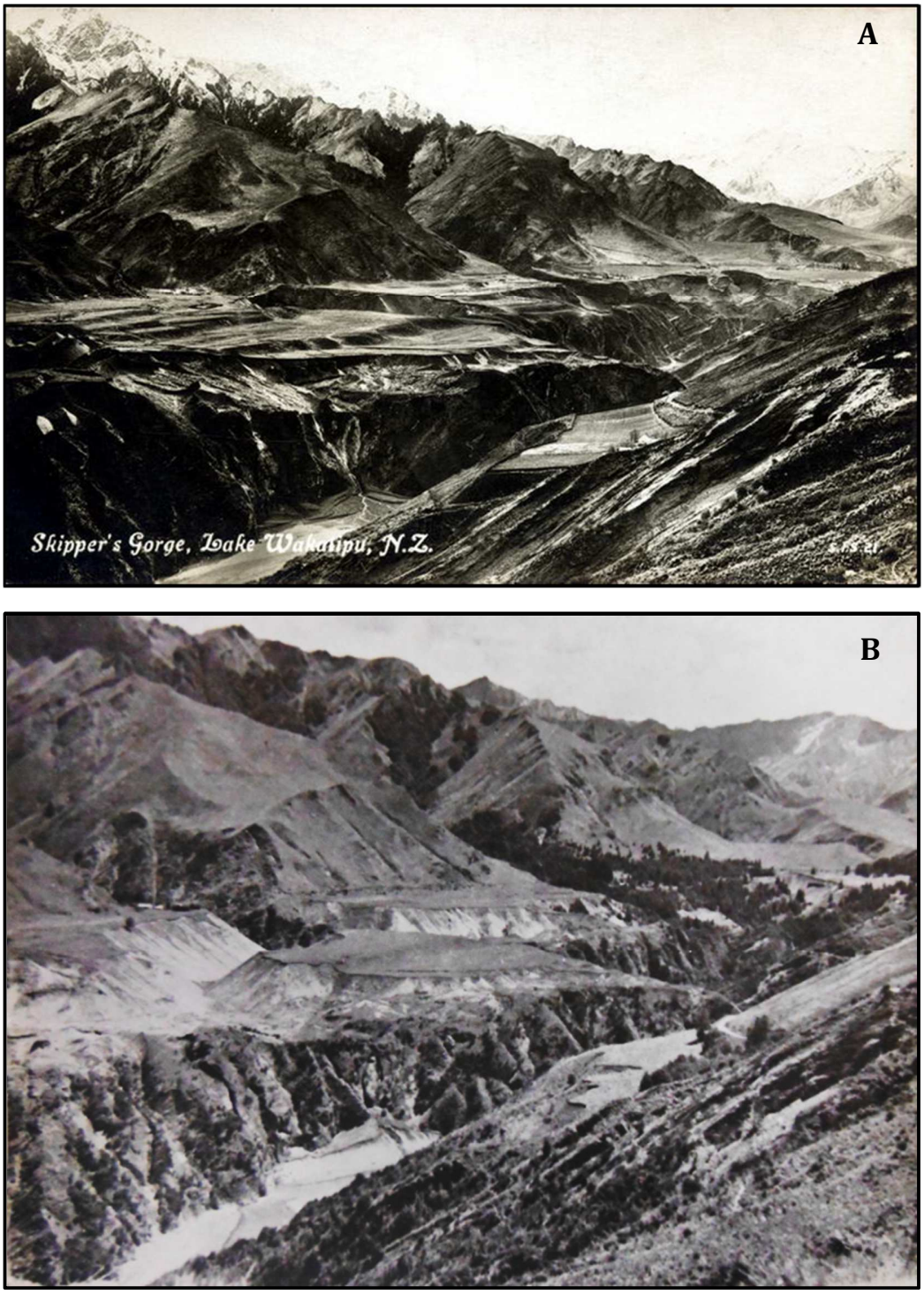

Figure 4.1: *Views of the Pleasant Creek and Londonderry Terraces in the Skippers area. A. is taken prior to any significant sluicing, probably mid-late 1880s and shows the many terrace levels present in this area (Historic Wakatipu), and B. is taken after completion of sluicing operations, showing the large sluiced excavations. Note the remains of a large fan of sluicing debris in the Shotover River below Pleasant Creek terrace (Williams 1965). These images are looking towards the northwest from about Maori Point. Figure 2.1C shows a 2018 view of this same location.*

There are no known estimates of the total volumes of terrace gravels sluiced during the historical mining period, and an initial attempt has been made to estimate the excavated volumes. Historical records of mining are invariably incomplete, and the volumes of sediment excavated are not directly reported. Nelson (2017) discusses various methods of estimating the volumes of sediments mobilised through historic placer mining. These include; estimations from records of water usage, direct surveys of mining areas, estimation based on sediment accumulations in debris dams, calculations based on historically reported gold yields and average pay values, development of regression equations linking areas mined with excavation volumes, and more complex methods involving multiple records such as gold yields, gold concentrations, and mining assumptions (e.g. mining efficiency, days worked, wages paid).

In the Shotover Valley, sluiced areas have been mapped based on aerial photography and field observations (Figure 4.2). Sluicing is often indicated by the presence of water races and dams in the vicinity. In the field, stacked boulders are characteristic of sluiced excavations, remaining behind after removal of the finer gravels. Shotover mining locations are summarised by several sources, such as Jones' (2008) map of sluicing dams, the Park (1909), Chandler (1957) and Williams (1965, 1974) maps of mining claims, and historic reports of mining activities (e.g. Galvin 1906). Mapping includes only those clearly identifiable sluiced areas, many others will now be revegetated and not obvious in aerial imagery. For example, Jones (2008) (Figure 4.2 inset) shows a number of dams located in areas where no sluicing is clearly visible any longer, such as the lower Polnoon Burn area.

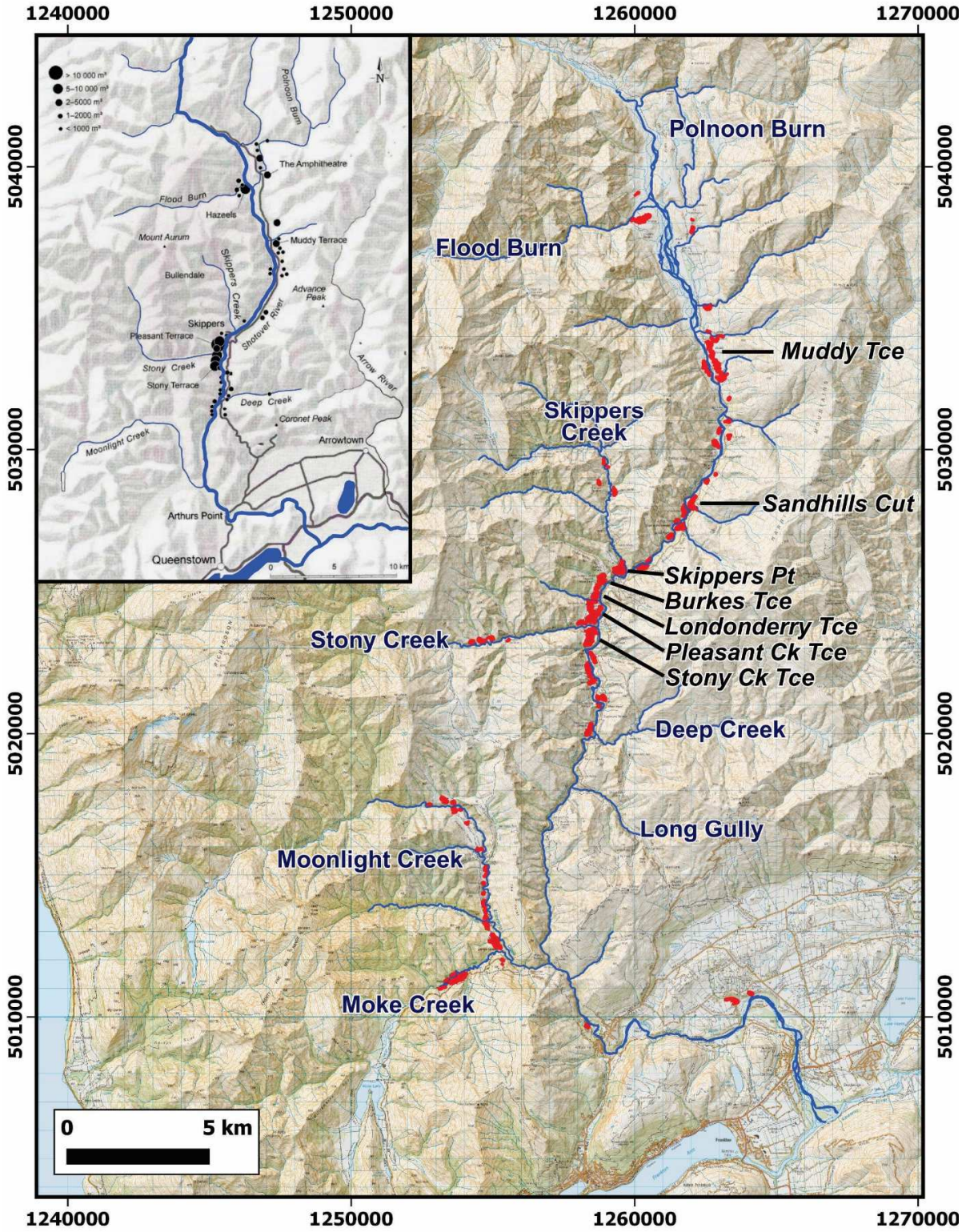

Figure 4.2: *Location of mapped sluicing excavations in the Shotover catchment, showing locations adjacent to the Shotover River, and in a number of tributary streams. The largest sluiced excavations are labelled. Inset figure shows location and relative sizes of historic sluicing dams (Jones 2008).*

Sluiced volumes were approximated from mapped areas and applying an estimated mean depth to each area. The largest and best defined sluicings in the Skippers area and the Sandhill Cut have been assumed to have a mean depth of 10-20 metres, based on field observations and surveys, and reported heights of working faces in sluicing claims (Park 1909). The depths of smaller sluicing areas are not easy to estimate, and have been approximated based on size of the mining area. Those with area of >10 ha are assumed excavated to mean depth of 5-10 m, areas of 1-10 ha (2-5 m depth), and <1 ha (1-2 m depth). Assumed thicknesses are only approximate, and likely underestimate the volumes of some excavations. Any sediment contribution by tailings and waste rock originating from underground quartz-mining is assumed negligible, and dredging is assumed to recycle riverbed sediments, but cause no net sediment addition. These estimates provide an indication of the order of magnitude of sluicing volumes, but are only approximate values and could be refined through further investigation.

Table 4.1: *Estimated hydraulic sluicing sediment volumes for the Shotover River.*

Sluicing Location	Total sluiced area (ha)	Estimated sluicing volume (Mm^3)	
		Low	*High*
Middle Shotover			
Pleasant Ck Tce	34.9	3.5	7.0
Stony Tce	23.3	2.3	4.7
Skippers Pt	16.3	1.6	3.3
Londonderry total	11.3	1.1	2.3
Burkes Tce	9.7	1.0	1.9
Lows Tce	9.3	0.2	0.5
Blue Jacket Tce	8.2	0.2	0.4
Sainsburys Tce	6.7	0.1	0.3
Maori Pt Flat	6.2	0.1	0.3
Wire Rope Tce	5.1	0.1	0.3
Boomerang Tce	1.6	0.03	0.1
Other Shotover			
Muddy Tce-Branches Flat	61.4	2.2	4.6
Sandhills Cut	11.7	1.2	2.3
Upper Shotover Gorge (excl Sandhills)	47.7	0.9	2.3
Lower Shotover	11.1	0.2	0.6
Tributary Creeks			
Skippers Creek	7.8	0.2	0.4
Stony Creek	10.7	0.2	0.5
Moonlight Creek	52.1	1.5	3.4
Moke Creek	19.1	0.8	1.7
TOTAL		**17.5**	**36.7**

This sediment input is thought to have been largely during the period 1880-1915 (Galvin 1906, Park 1909, MWD 1975, Hamel 2001), although some significant excavations are known to have been undertaken later, for example the Sandhill Cut from 1926-1931. It is therefore estimated there may have been an additional 0.5-1M m^3 sediment

entering the river system annually during this time. With the modern Shotover River sediment supply estimated as being 1.6-2M m^3 annually (MWD 1975, Hicks et al. 2000), this is an estimated increase of 25-50% as a result of hydraulic sluicing activity.

The majority of the Shotover River's increased sediment loading in the historic mining period is attributed to alluvial mining activities, and sluicing in particular. However, development of the valley for farming may have also contributed to increased erosion and sediment inputs through deforestation, burning, grazing, and introduction of pest animals (OCB 1966, MWD 1975). Beech forest was burnt to open up land for grazing, and use of timber for construction, mining purposes and firewood, is also assumed to have contributed to significant deforestation. Tussock country was burnt to reduce rank tussock growth and clear scrubland. The link between repeated burning of tussock and increasing soil erosion became known, and from 1955 burning permits were required, with restrictions specifying areas to be burnt. Even with these restrictions in place, from 1955-1974 an average of about 20 km^2 was burnt annually in authorised burns (MWD 1975). Overgrazing by livestock, and introduction of pest animals (e.g. rabbits, hares, goats, deer, chamois, possums) also contributed to reduced vegetation cover and increased soil erosion (MWD 1975).

4.3 Shotover River Geomorphic Changes

Shotover Gorge

The large volumes of gravels sluiced into the river caused significant aggradation of the river bed within the gorge, as illustrated by the following reports;

- An article entitled 'Rise of the bed of the Shotover and lateral streams by tailings' states that sluicing had raised the river bed 35 feet (10 m) by the late 1880s, and it was even higher by the time of the article. The riverbed is described as having a '*general inclined plane from about the bridge across the Shotover to Long Gully*', a distance of about eight kilometres (Lake Wakatip Mail, 9 October 1896). This is interpreted as referring to the first bridge in the Skippers area, located shortly below the present suspension bridge.
- A bridge over Stony Creek was constructed at about 18 feet (5.5 m) above the riverbed, which after some time was filled with gravel nearly up to the bridge level (Lake Wakatip Mail, 23 October 1896).
- In 1881, tailings from Aspinall's sluicing claim at Skippers Point completely blocked the Shotover River's flow, and the riverbed was dry for a mile below the bridge (Lake Wakatip Mail, 2 September 1881, p3).
- Discussing dredging potential of a riverbed claim at Maori Point, a report notes that; "*these terrace claims discharged their tailings into the Shotover, and so prevented the successful working of the Shotover River bed. A modern dredge should have no difficulty dealing with these tailings, which average a depth of about 20 feet* (6m)" (Lake Wakatip Mail 6 Dec 1932, p5).
- MWD (1975) refers to a miner, Joe Scheib, discovering an old flume and other mining remains undisturbed under 3-4 m of gravels in the gorge. He also reported that the river bed in the gorge had been slowly degrading during his time working in the gorge, retiring in 1977.

While these are anecdotal reports and the accuracy of estimated aggradation thicknesses are uncertain, these indicate many metres of tailings accumulated as a result of sluicing. Surveys of alluvial floodplain terraces inferred as the mining–era aggradation surface confirm the thickness of aggradation noted in these reports. At Maori Point these were at ~6 m, and at Deep Creek were ~7 m above current river levels.

Lower Shotover River

The lower Shotover River is interpreted to have been subject to significant aggradation as a result of mining sediment inputs. This section summarises the changes seen at the three largest beach sections; Big Beach, Tucker Beach and the Shotover Delta (Figure 4.3).

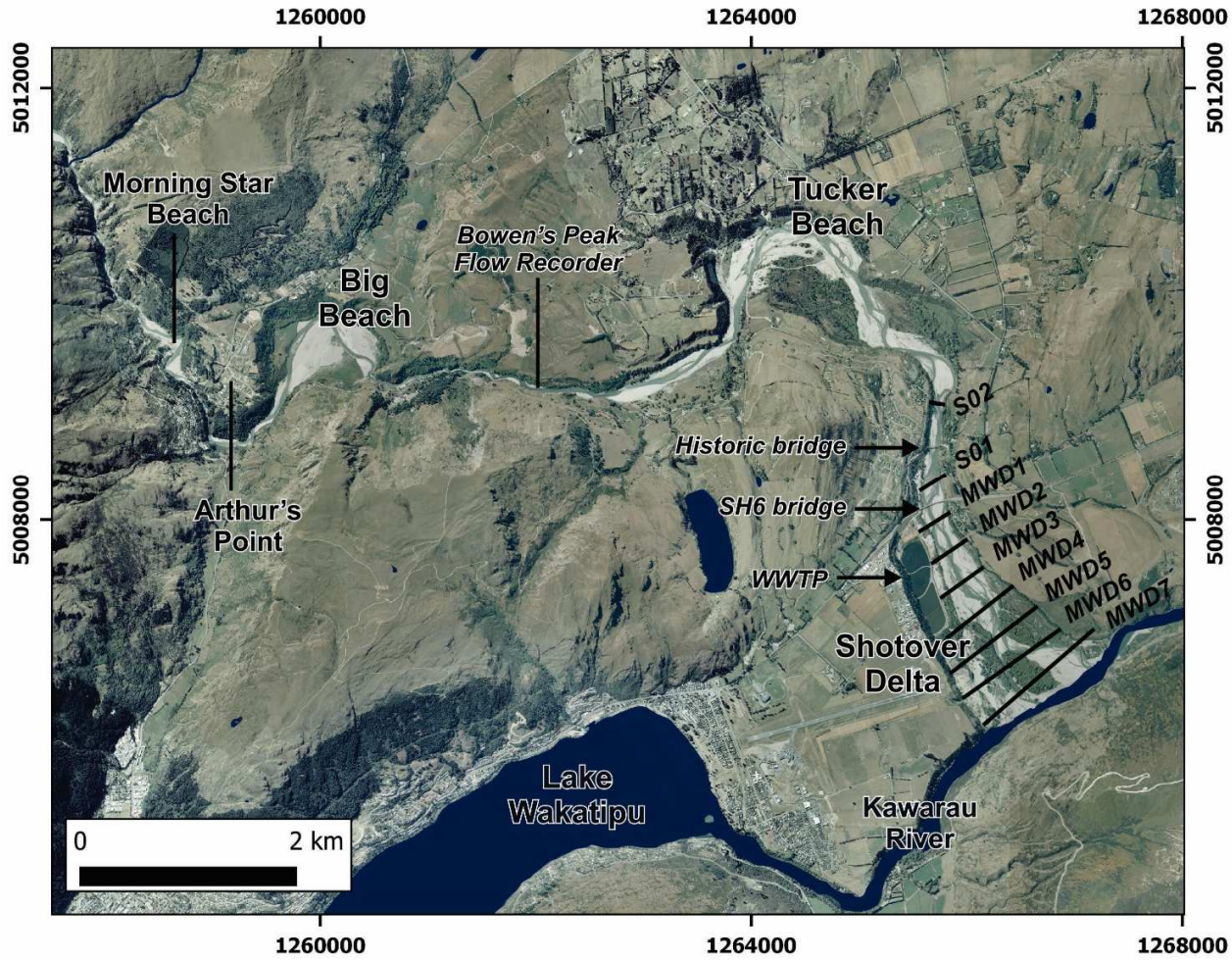

Figure 4.3: *Overview of the lower Shotover River and delta area, showing the main beach sections, the location of the Bowen's Peak flow gauging station, and Shotover Delta cross section locations.*

Prior to large-scale mining in the Shotover Valley, the lower Shotover River and delta are interpreted as having a narrower active riverbed and a deeper incised channel. The first lower Shotover Bridge was located about 200-250 m downstream of the current State Highway Bridge, in about the location of survey lines MWD1-2 (Figure 4.3). The earliest photograph of this area (pre-1893, possibly late 1870s or 1880s) shows the western half of the delta vegetated, with a braided riverbed to the east (Figure 4.4). Later images (1890s-1912) show significant aggradation, with active alluvium extending the full width of the channel (Figure 4.5). Embankments were built above the eastern end of this first bridge bridge in an attempt to prevent water flowing around its eastern end, and remnants of these can be seen in aerial images from the 1950s-1970s prior to construction of the WWTP (wastewater treatment ponds) (Figure 4.13).

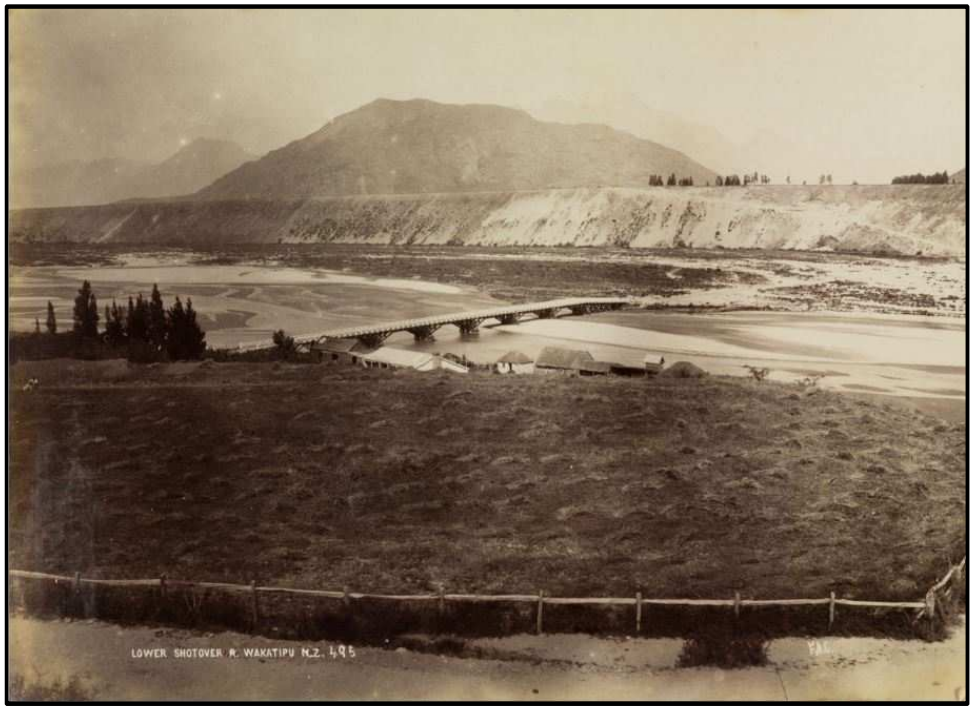

Figure 4.4: *The first lower Shotover Bridge, showing upper Shotover Delta prior to peak aggradation levels. View is looking southwest towards what is now the location of the WWTP (Hocken Library).*

Figure 4.5: *A later image (1890s-1912) shows active alluvium and river channels across entire width of the upper Shotover delta and covering of all vegetation seen in earlier photo. View is looking northeast towards Slope Hill (Shotover Country website).*

A series of three cross-sections compiled by the MWD (1975) shows surveys taken at the site of this first bridge. In 1868 the river was flowing in an incised channel of 1.5-2 metres in depth, and by 1906 this channel had been infilled and the riverbed raised by over 2.5 metres (MWD 1975, Lake Wakatip Mail 16 October 1906 p4). This demonstrates rapid aggradation, with a rate of about 50 mm/year in the period 1868-1906 (Thompson 1976, in ORC 1997).

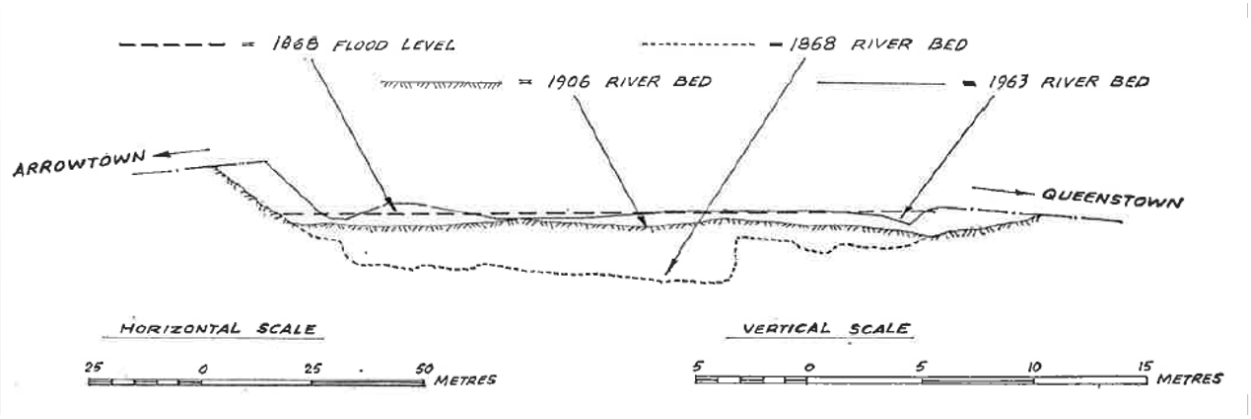

Figure 4.6: *Cross section at first bridge location, from surveys in 1868, 1906, and 1963, showing aggradation of >2.5 metres from the earliest survey by 1906 (MWD 1975).*

Big Beach and Tucker Beach

Big Beach is the first major beach section downstream of the Shotover Gorge, and due to the large increase in width was the site of significant deposition and aggradation. The earliest images of the beach are from the mid-1890s and show a broad, braided channel with three gold-dredges operating (Figure 4.7). The pre-mining form of the river is not known, but have had a deeper incised channel similar to that seen for the 1860s Shotover Delta in Figure 4.6.

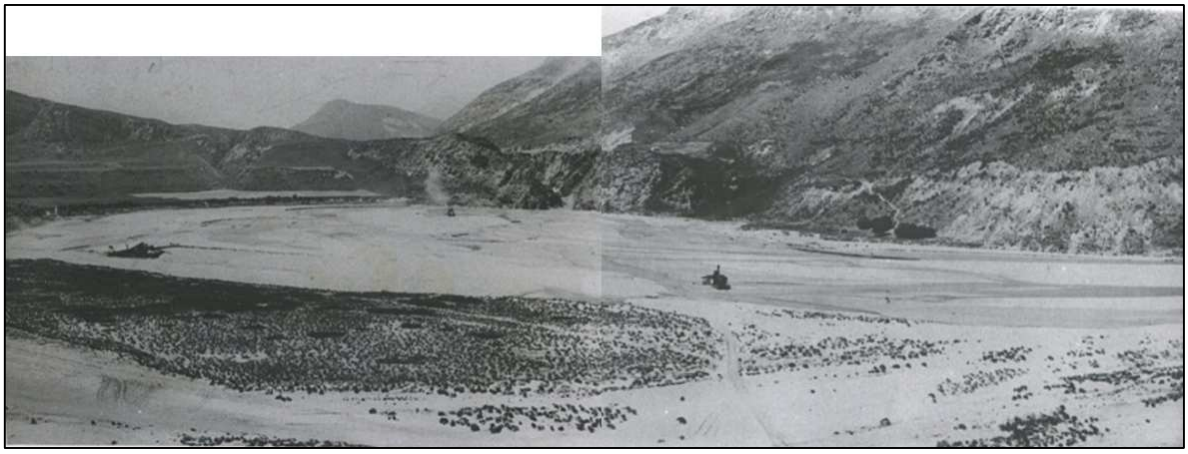

Figure 4.7: *Big Beach looking downstream, with three gold dredges operating, date is at least the mid-1890s. It is not known if the low vegetated surface in the left foreground was later covered by aggradation gravels. View is looking southeast (Hocken Library).*

By the time of the earliest aerial photographs of Big Beach (1956, 1959), significant degradation has already occurred, with the active gravels seen in Figure 4.7 above having become revegetated and forming a wide grassed terrace on the northern side of beach. Surveys by MWD (1975) show the river channel had degraded to about two metres below this terrace level by 1954, then lowered a further metre by 1975. During this period the river migrated across the entire width of the beach (~500 m), eroding most of the grassy terrace seen in Figure 4.8A. This is estimated to have resulted in removal of 156,000 m^3 of material in the nine year period 1966-1975 (MWD 1975). Lidar data shows that the current river is at a level of 4-6 m below the remnants of this terrace, indicating that a further 2-3 metres of channel degradation have occurred since this 1975 survey.

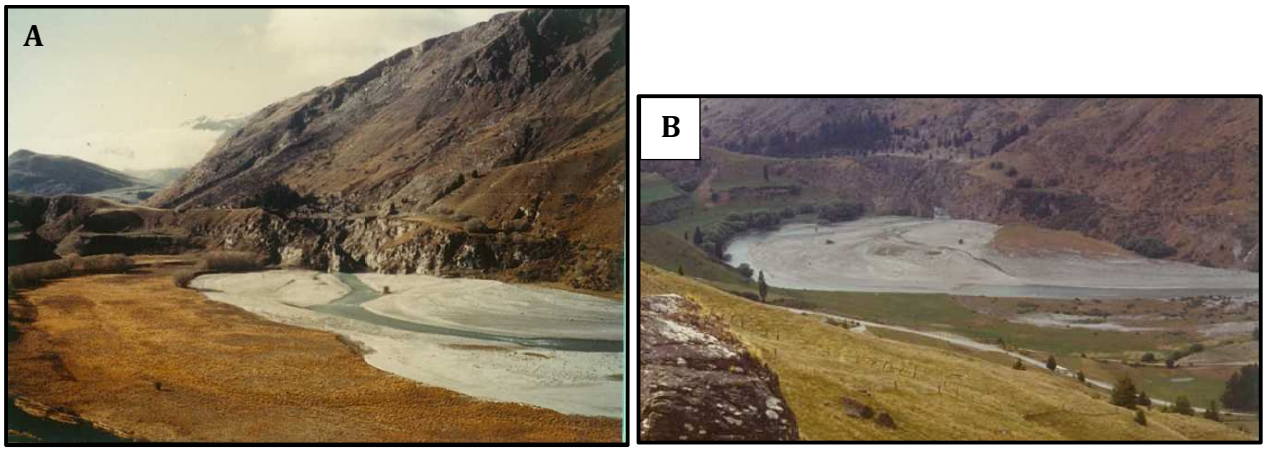

Figure 4.8: *Big Beach in (A) 1961 and (B) 1974, showing rapid erosion of grassy terrace on northern (true left) side of the river, and vegetation becoming established on opposite bank (MWD 1975).*

A sequence of vertical aerial images shows changes to the Big Beach area from 1956 to the present day (Figure 4.9). The main channel has not significantly changed position since migrating to the northern side of the beach by 1973, willows and other vegetation have now become well established on the inside of bend and on the western terrace remnant.

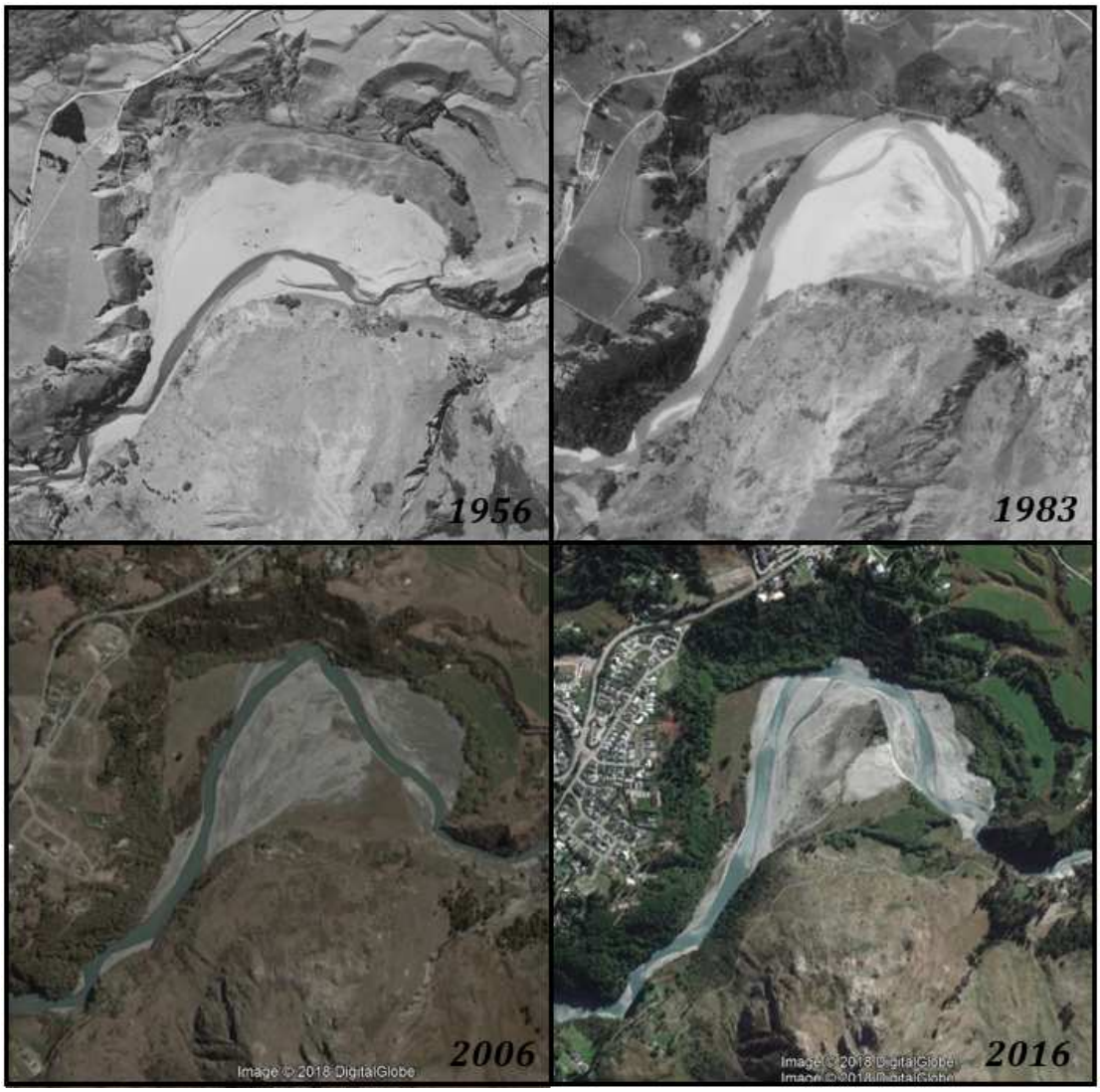

Figure 4.9: *Big Beach aerial images (1956-2016) showing changes to Shotover River planform. Each image is about 1800 m in width (Retrolens, Google Earth).*

Tucker Beach appears to have been impacted by aggradation to a similar extent as Big Beach, with historic reports noting aggradation of fifteen to twenty feet (4.5-6 m). The current channel has degraded by 2-4 metres below remnant terraces marking the aggradation surface (Figure 4.14). The active riverbed has narrowed to less than half of its former width, with the margins becoming well vegetated (Figure 4.10).

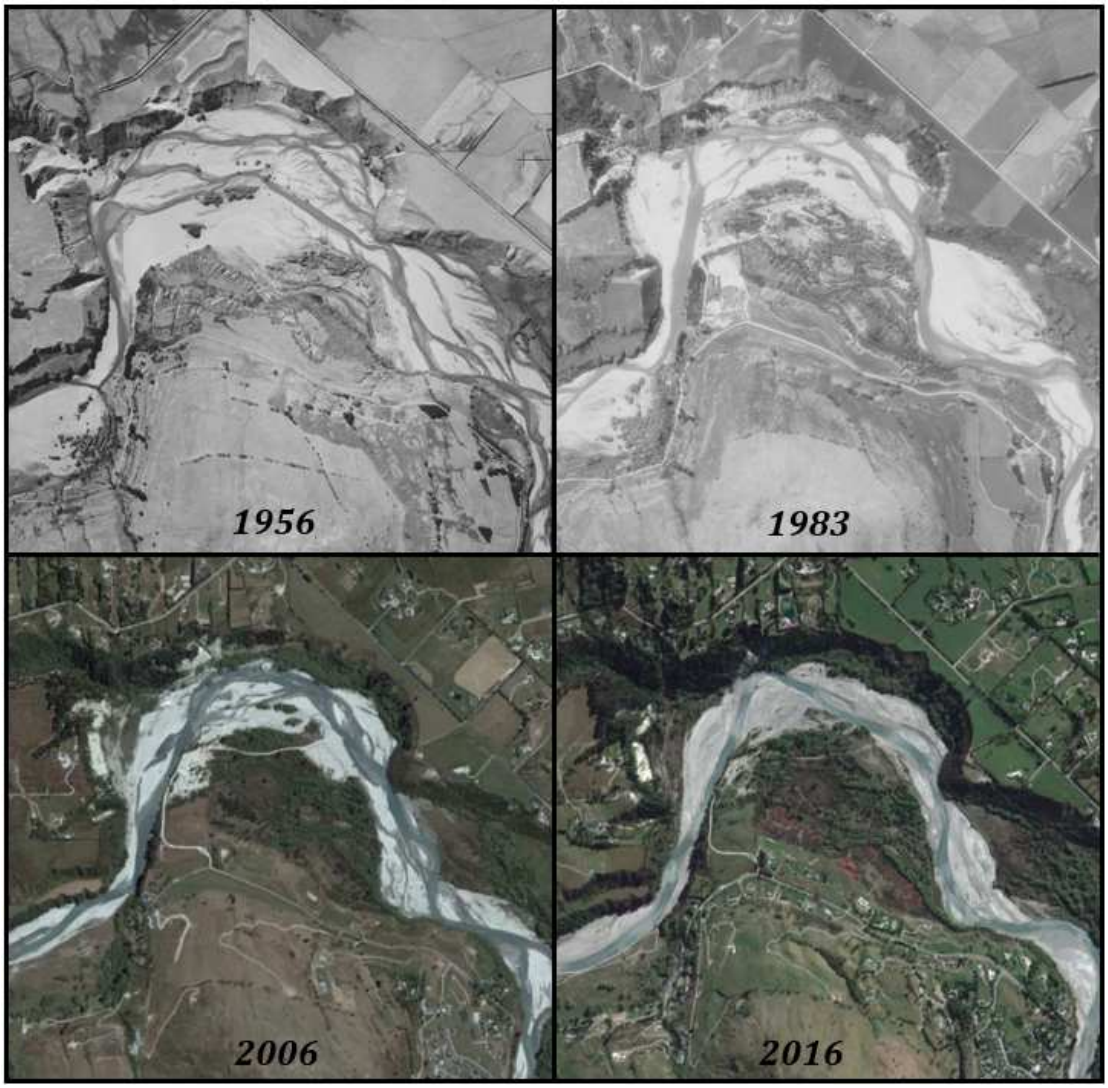

Figure 4.10: *Tucker Beach aerial images: (1956-2016) showing changes to Shotover River planform, notably narrowing of the active channel and revegetation of the inside of the channel. Each image is about 2500 m in width (Retrolens, Google Earth).*

Shotover River Gauging Records

The Bowens Peak gauging station, located in the narrow gorge section between Big Beach and Tucker Beach (Figure 4.3), has been in operation since 1968. Mean water level is used to approximate the riverbed level, with records shown in Figure 4.11. Records show relatively stable levels in the period 1967-1980, then a steady decrease of about 2.5 metres until 2013, when the recorder was relocated to a more stable location (Damwatch 2017).

The relatively stable trend prior to the early 1980s may reflect a higher sediment supply due to erosion from upstream locations, for example seen at Big Beach in Figures 4.8 and 4.9 where the channel migrated to the outside of the bend by the late 1970s, eroding a large volume from the floodplain terraces. As the Big beach channel stabilised, it is inferred that the sediment supply to the Bowens Peak gauging station decreased, and this reach began to degrade.

Minor variations in bed level within the larger trend are thought to be due to erosion and sediment remobilisation by significant flooding events (ORC 2002a). For example, the large floods in January 1994 and November 1999 are followed by rises in bed level of up to about 0.5 metres. Surveyed cross-sections between the Shotover Delta and the Bowens Peak gauging station also show a general degradation trend over time, with an average degradation of ~0.2 m over the 8 year period to 2014 (Barnett and MacMurray 2017).

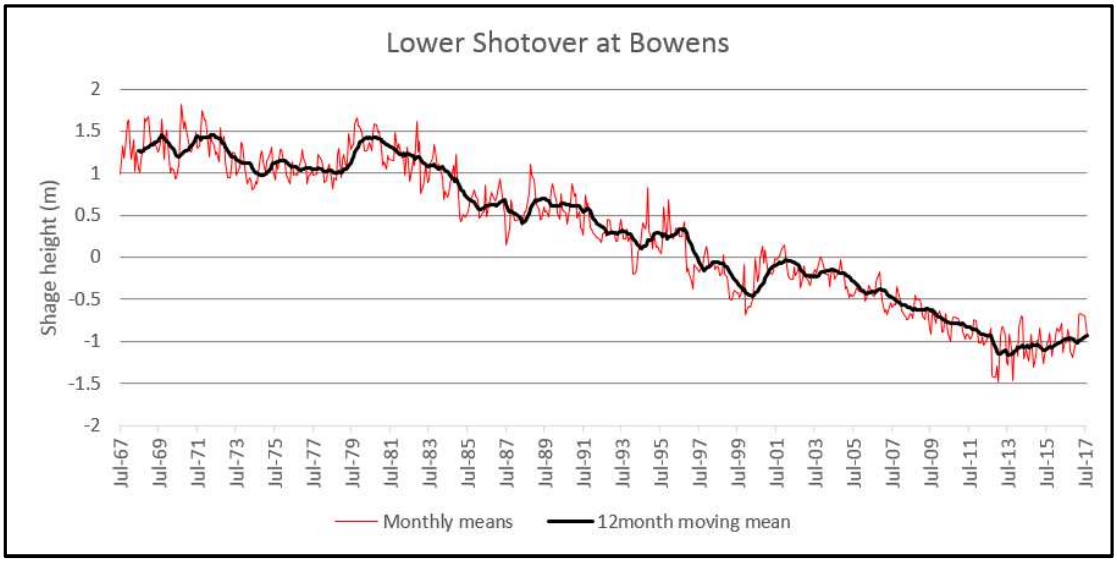

Figure 4.11: *Mean monthly water levels at Bowens Peak gauging station, showing a decrease of ~2.5 metres from 1980 to 2013. The gauge was relocated in 2013 and the minor rise seen after this time may be due to this change.*

Shotover Delta

Riverbed changes at the Shotover Delta are significant due to the strong influence the delta morphology has on Kawarau River outflows and flooding of Lake Wakatipu. As with the rest of the lower Shotover River, the delta aggraded during the historic mining period, as was noted by many reports and seen in surveys (Figure 4.6) and photographs (Figure 4.5) of the delta and lower Shotover bridges.

> *"The river has been worked for the greater part, and is silted up by the enormous quantities of tailings, … as below and above the Lower Shotover Bridge, … dredging will scarcely prove very remunerative …"* (ODT 28 Feb 1891).

Degradation has been ongoing since the sediment supply decreased, and can be seen by erosion around the bridge piers in the lower Shotover River (Damwatch 2017). Lidar data show a drop of 2-3 m from remnant terrace surfaces to the east of the delta down to the current channel levels (Figure 4.14). Cross-section surveys have been taken across the Shotover Delta at regular intervals since 1980 and used to estimate changes in mean bed level, and gravel loss or accumulation rates (ORC 1997 2002a, Hamilton and Associates 2010). Surveys since 1980 show (Figure 4.12);

- Consistent degradation of mid and upper delta by ~1 m (sections S01, S02, and MWD1, 2, 3).
- Little change in the mid-delta reach (section MWD5) until 2012-2014, when it lowers due to gravel extraction.
- Minor aggradation of ~0.5 m at the lowest sections (MWD6, 7) from 1981-2010, then degradation to below 1981 levels by 2016.

The relatively consistent degradation trend observed in the upper parts of the delta appears similar to that seen at the Bowen's Peak gauging station (Figure 4.11) and is interpreted as being part of the river's multi-decadal degradation trend. In the middle and lower parts of the delta, the sediment accumulation pattern is more complex than simply aggradation or degradation over the entire delta surface, and is influenced by factors such as the interaction with the Kawarau River at the delta toe, and the river management/gravel extraction works undertaken. Recent changes to the Shotover Delta morphology are summarised below and in Figure 4.13.

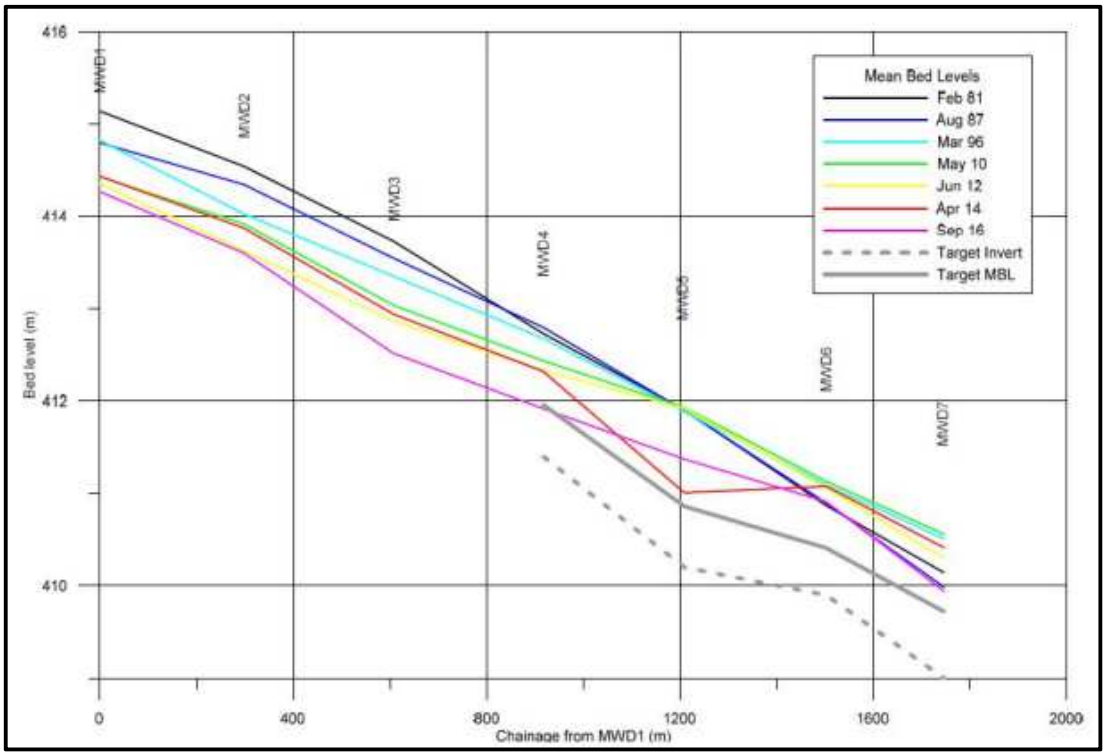

Figure 4.12: *Shotover Delta long profiles showing net degradation of >1 metre from 1981-2016 (Barnett and MacMurray 2017, in Damwatch 2017). The locations of the named sections are shown in Figure 4.3.*

The first major change at the delta was in 1974 when WWTP (wastewater treatment ponds) construction commenced. Two ponds were constructed in 1974-1976, then a lower pond added in 1987. With a width of 200-250 m, these narrowed the upper delta's available channel width by approximately one third. Construction of the WWTP ponds has been interpreted to have contributed to degradation in the adjacent section of delta, due to the ponds restricting channel width and thus increasing flow velocity through this section (ORC 2002a). However, during the same period similar degradation is also observed in other locations (e.g. Figure 4.11) so it seems more likely related to the larger-scale degradation trend, rather than a local effect of WWTP construction.

Introduced crack willow (*Salix Fragilis*) became established on the delta, with small areas seen in 1950s images (Figure 4.13), and these spread aggressively. Willows encourage island formation and expansion, restricting channel development and reducing the active delta area available for gravel deposition and storage. Several large areas of willows have been removed since in an effort to combat the channel restriction caused by their establishment (Figure 4.13).

Gravel has been extracted for aggregate from the upper-mid delta. In the period 1993-2002 this was at relatively minor levels, with a maximum annual extraction of 58,000 m^3 (ORC 2002a). More recently, a consent was granted for extraction of a 2M m^3 volume over a 5 year period (Damwatch 2017). Gravel extraction has been targeted in an attempt to maintain a stable bed profile over time, and prevent further degradation at the State Highway Bridge (Barnett and MacMurray, in Damwatch 2017)

The training wall is a rock wall constructed across the eastern part of the delta toe in 2012. It is designed to force the main channel eastwards to ensure it enters the Kawarau as far downstream as possible, and provides for sediment storage. When the wall was constructed, the river had a minor channel entering the Kawarau midway along the delta toe. This channel has been blocked by the wall, and has been the site of gravel infilling behind this area.

Changes to the Shotover Delta morphology are summarised in Figure 4.13, a series of aerial photographs covering about the last 60 years. The key features and changes seen in these images are noted below;

1959: The active riverbed extends across full width of the delta, and there are only small areas of willow growth on the lower delta. The main river channel is located on the eastern (true left) side of the delta.

1976: The main channel has moved to the western side of delta, WWTP ponds are under construction on the upper delta, and willow islands are slowly expanding.

1996: The active riverbed still extends across entire width of the delta, and three large willow islands are now well established. The third WWTP has now been constructed (in 1987).

2010: Willow islands are coalescing on the western side of delta, and nearly all river flow is through eastern side of delta. Willows on eastern side of main channel have been cleared.

2013: The training wall has been completed (2012), and willows have been cleared from both sides of the main channel. River flow is now constricted to the eastern side of the delta.

2016: Gravel extraction has widened channel on the lower delta, which is now well constrained to an outlet at the eastern side of the delta.

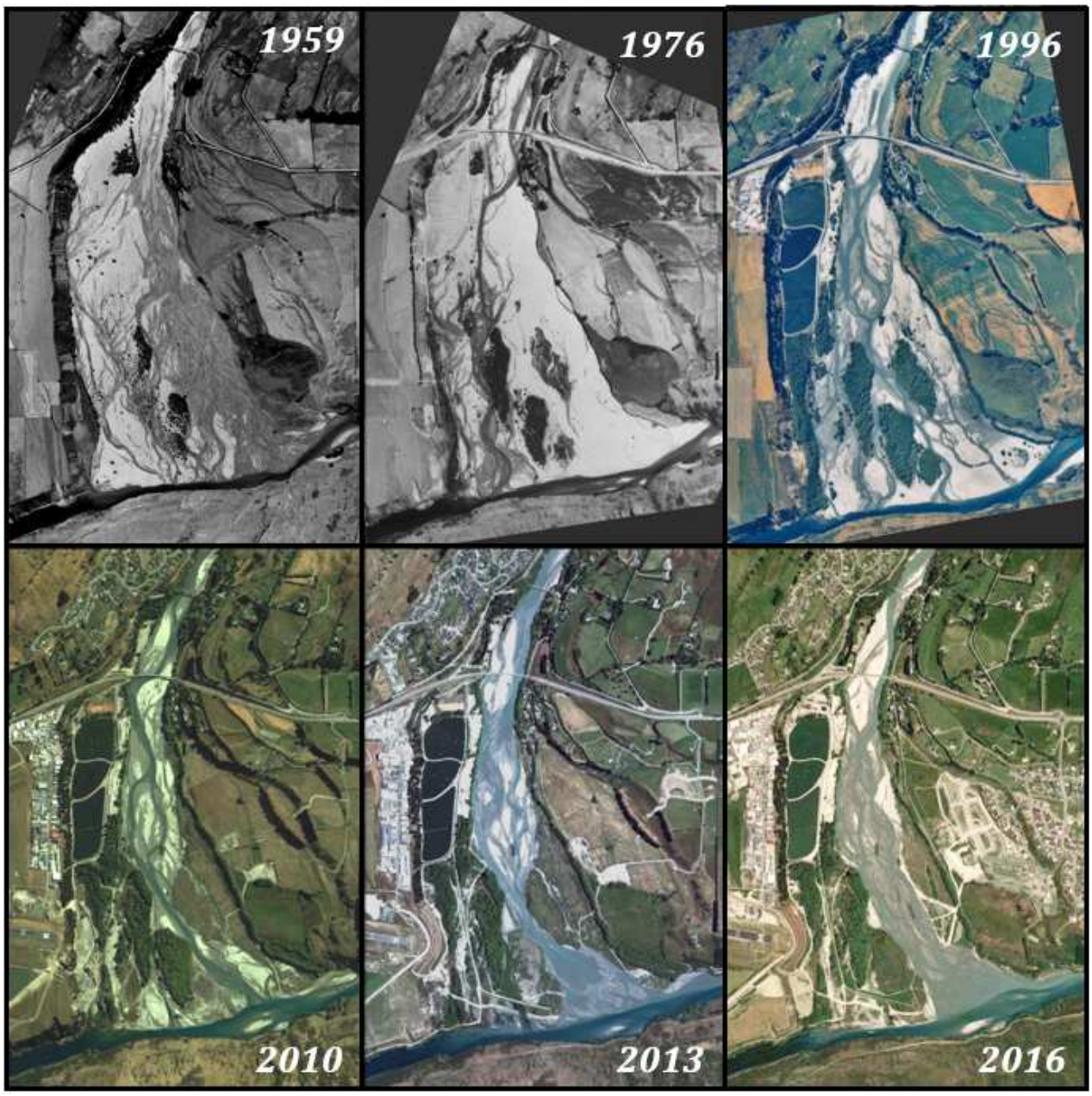

Figure 4.13: *Shotover Delta aerial images: (1959-2016) showing changes in river planform, and changes such as construction of WWTP, growth and later removal of willow islands, and construction of the training wall. Also note recent residential expansion in the area east of the Shotover Delta, where the Shotover Country development is in progress. Each image is about 2 km in width by 3 km in height (ORC, Google Earth).*

4.4 Aggradation Summary

Hydraulic sluicing of alluvial gravel deposits during the historic mining period resulted in a large increase in the supply of sediment entering the river. Additional sediments were sourced from sluicing locations throughout the Shotover catchment, but the largest and most extensively worked deposits were those in the Skippers area (Figure 4.2), where the largest sluice cuts each contributed >1M m^3 of sediment into the river. With an estimated total volume of several tens of millions of cubic metres (Table 4.1), this caused a significant increase in sediment supply for a period of several decades, the river responded to excess sediment by aggrading over all of its downstream length. The maximum aggradation thickness may have been as much as 10 metres in Shotover Gorge proximal to the main sediment sources.

In the lower Shotover River the extent and level of the aggradation surface has been interpreted from Lidar data and historic photos. The approximate aggradation thickness has been estimated from Lidar data, assuming the river channel has now degraded to about the pre-mining level. The terrace surface interpreted as the mining-era aggradation surface is shown relative to the current river level in Figure 4.14. This shows the terrace level to be at 5-7 m above the current river level at Morning Star and Big Beach, reducing to 2-3 m at Tucker Beach and the Shotover Delta. Figure 4.15 shows the interpreted active channel width during peak aggradation, and the current channel width following degradation and narrowing of the active riverbed.

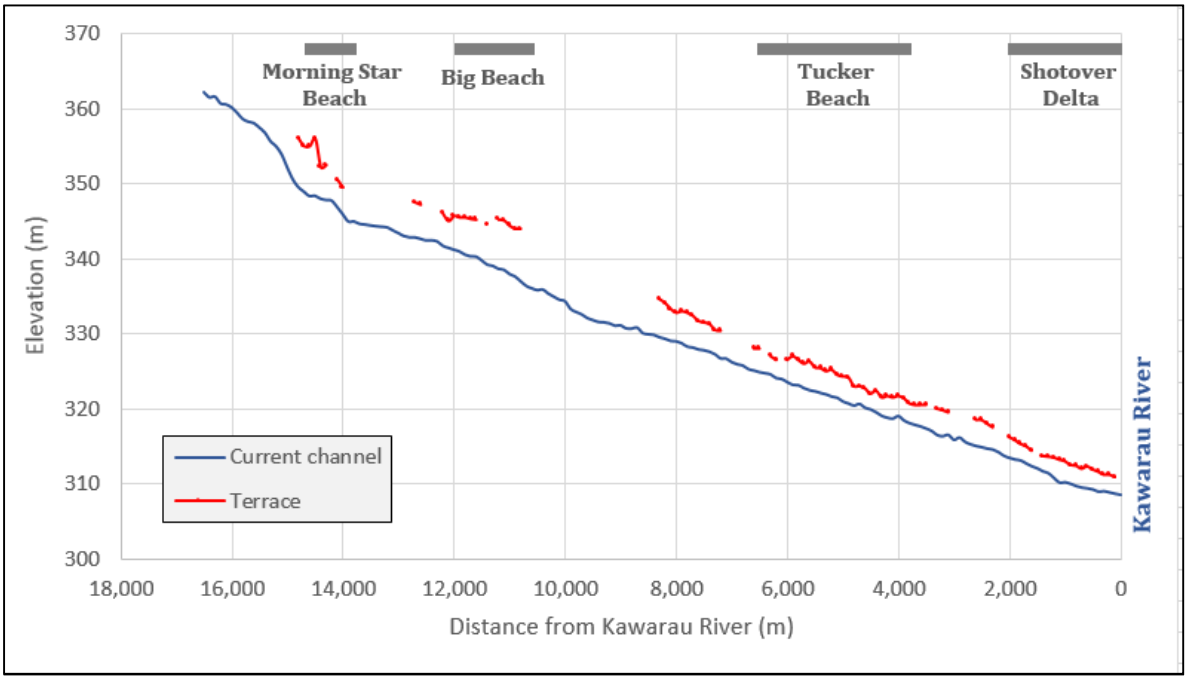

Figure 4.14: *Lower Shotover River long profile showing current river channel and interpreted peak aggradation levels. Channel elevation and terrace elevations from Lidar. The locations of the named beach sections are shown in Figure 4.3.*

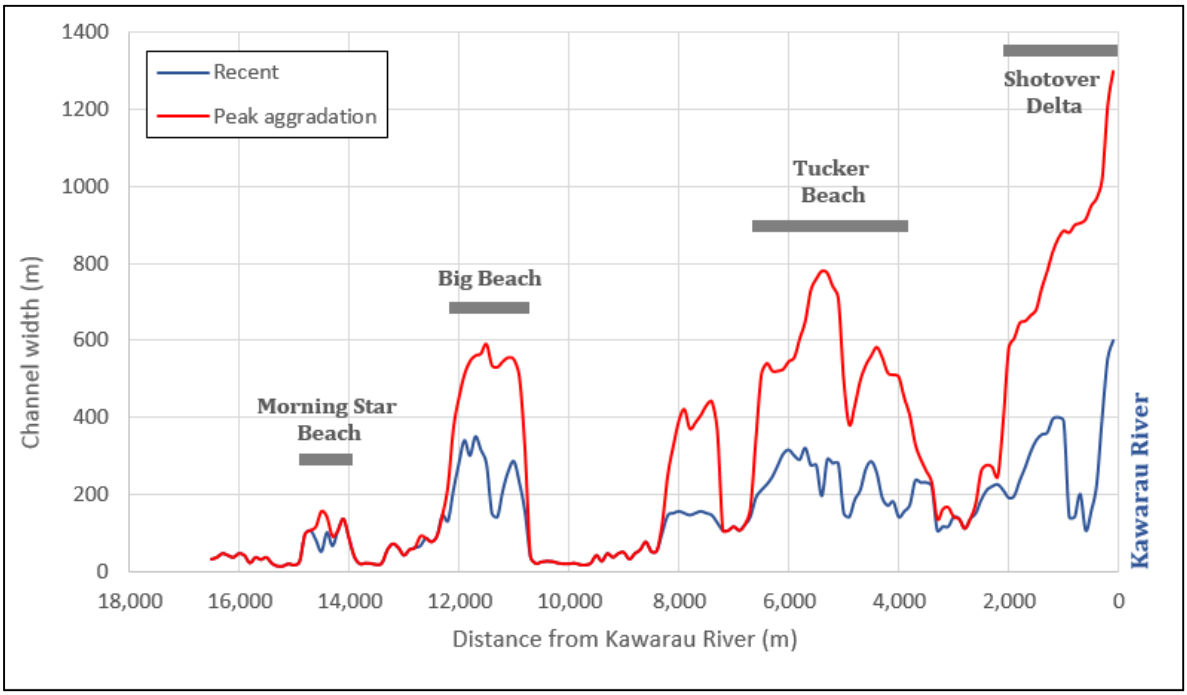

Figure 4.15: *Lower Shotover River channel width plot, showing interpreted peak aggradation channel and recent channel width based on 2006 aerial imagery (LINZ). The locations of the named beach sections are shown in Figure 4.3.*

Peak sluicing activity occurred from the 1880s until ~1915, although sluicing continued at a lesser scale for several decades following this peak. One of the final large excavations was the 1M m³ Sandhill Cut completed in 1926-1931. Degradation of the riverbed would have commenced as sediment supply decreased, but is not known when this began, it may have been as early as the 1920s or 30s. There was noticeable degradation in the lower Shotover River by the late 1940s, as seen in photographs at Big Beach and Tucker Beach showing development of a single, incised river channel.

The river channel may now have reached (or be near to) a thalweg level equivalent to its pre-mining level, but this does not mean all sediment associated with this sediment pulse has moved through the river system. Large volumes of sediment remain stored in lower Shotover River terraces, and will remain until eroded and mobilised in high flows. The influence and duration of the sediment pulse formed by these mining sediments has not always been recognised, for example the degradation trend seen at the Bowen's Peak gauging station (Figure 4.11) was attributed by Damwatch (2017) to variations in flood frequency and magnitude, rather than to a longer-term trend.

4.5 Sediment Pulses Caused by Alluvial Mining

Historic gold mining resulted in large increases in sediment supply in catchments in Otago, Golden Bay and Coromandel (Clement et al. 2017). Clement et al. also note that there have been 'no quantitative measures on the change in sedimentation rates in response to mining activities in New Zealand'. Previous studies on mining-induced sedimentation have mostly focused on geochemical contamination of tailings from hard-rock gold mining, for example at the Shag River (Black et al. 2004, ORC n.d.), and the Ohinemuri and Waihou Rivers (Clement et al. 2017). Harding et al. (2000), and Harding and Boothroyd (2004) discuss the impacts of mining on New Zealand rivers resulting from sluicing and dredging of alluvial deposits, as well as tailings from hard-rock mining, but these mainly refer to

environmental impacts on riverbed ecosystems and water chemistry, rather than geomorphic changes to river systems.

Alluvial mining by hydraulic sluicing was widely used in the Otago goldfields, first introduced in the 1880's and continuing until into the 20th century. This must have had dramatic impacts on Otago river systems, for example reports that by the late 1800s the site of the original Gabriel's Gully township had been covered with 50-100 feet (17-30 m) of tailings (Pyke 1887, Galvin 1906). Aggradation impacts are mainly known by anecdotal reports, and there appears to have been little detailed study of these effects.

The Clutha River has been investigated by the Rivers Commission (1920), and more recently by ORC (2008, 2017). The Rivers Commission (1920) report was prompted by concerns about flooding and loss of navigability in the lower Clutha River, with sedimentation attributed to tussock burning, deforestation, and mining. Deposition of 10 feet [3 m] thick was reported in the upper reaches, and 3 feet [0.9 m] in lower parts. Based on analysis of early bridge and ferry cross sections, ORC (2008) thought that aggradation may actually have been greater than estimated by the Rivers Commission, being as much as five metres at the Roxburgh and Beaumont Bridges. The dramatic change in river character as it aggraded is described by the Rivers Commission (1920);

> *"Before mining became an important factor, the river was a deep clear running stream ... It is now ... full of shingle bars, always muddy, and generally very much shallower than it was, say, in 1860".*

The mining sediment discharge to 1920 was estimated at 300M cubic yards [~230M m^3] and an average rate of 5M cubic yards [3.8M m^3] per annum. Of this, around one-third was thought to have not yet reached the main river, 20% was in the main river channel, and the remainder had been swept out to sea. This report recognised than even though mining was currently not very active (in 1920), the influence of stored sediment would continue for many years. It was estimated that approximately two-thirds of this sediment supply (~150M m^3) was sourced from locations upstream of the Roxburgh Dam site (Rivers Commission, in ORC 2008), but there is no breakdown given of mining sediment inputs by area, which includes Wakatipu basin catchments such as the Shotover, Arrow and Kawarau Rivers.

Alluvial mining by hydraulic sluicing was widely used at many locations globally, and several studies have been made of historic geomorphic responses to excess sediment inputs derived from alluvial mining, for example;

- Sierra Nevada, California (Gilbert 1917, James 1991 1999 2006 2015, Ghoshal et al. 2010)
- Fraser River, British Columbia (Nelson and Church 2012, Ferguson et al. 2015)
- Ringarooma River, Tasmania (Knighton 1989 1991, Bartley and Rutherford 2005)
- Victorian Goldfields, Australia (Lawrence et al. 2016)

The Sierra Nevada and Ringarooma River examples are most comparable to the Shotover Valley, in these cases aggradation reached thicknesses of greater than 5 metres and has had effects lasting for >100 years. These are summarised below, and are two of the best-studied examples of long-duration sediment waves resulting from mining activity.

In the Northern Sierra Nevada, hydraulic sluicing during gold mining from 1853-1884 and 1893-1953 released around $1x10^9$ m^3 of sediment. Aggradation was rapid and widespread, mainly affecting the Bear and Yuba River systems but also several others. Due to destruction of agricultural land downstream, mining was stopped by legal injunction in the 1880's, but resumed from 1893-1953 with addition of a further 24M m^3 of sediment (James 1999). Gilbert (1917) reported up to 5 m of channel aggradation as well as extensive deposition on floodplains. River bed levels plotted from low-water stage levels show rise of bed levels by up to 5 metres during aggradation from ~1860, until the 1890s or early 1900s (James 2006 2010). Floodplain sediment removal is ongoing; observed changes show removal of large volumes of riverbank sediments with little change in thalweg elevation.

In the Ringarooma River, alluvial tin mining began in about 1875, peaked in 1900-1920, and was mostly finished by 1982. Hydraulic sluicing was the most widely used mining method, and introduced a total of 40M m^3 of additional sediment from sources distributed over a 75 km length of the river. Aggradation was most rapid and thickest near to sediment supply points, occurring later and at lower magnitudes at downstream locations. As the riverbed aggraded, this caused development of braided pattern channel and up to 300% increases in channel width. During the post-mining period, the riverbed has incised at rates of up to 50 cm/year, commencing upstream and progressing downriver (Knighton 1989 1991).

Compared to the Sierra Nevada and Ringarooma River sediment pulse events, the Shotover River sediment pulse had a similar magnitude of aggradation thickness, estimated to reach a maximum of >10 metres in parts of the Shotover Gorge, and ranging from 2-7 m in the lower Shotover River (Figure 4.14). Inferred width changes of up to >200% in sections of the lower Shotover River (Figure 4.15) are of a similar magnitude to those reported in the Ringarooma River (Knighton 1989)

4.6 Summary and Conclusions

The mining-induced sediment pulse was a major event in the Shotover River's recent geomorphic history. The locations of hydraulic sluicing have been identified and volumes of excavated sediments estimated (Figure 4.2, Table 4.1). It is estimated that additional sediment inputs due to mining activity are in the order of 20-40M m^3 of excess sediment, and may have increased the river's sediment supply by 25-50% over a period of >30 years.

During the aggradation phase of this sediment pulse, the riverbed rose and expanded in width, for example seen in photographs (Figures 4.4, 4.5) and surveys (Figure 4.6) at the Shotover Delta. As the sediment supply subsequently decreased, a degradation phase commenced, with incision and narrowing of the active riverbed, and revegetation of former aggradation surface (e.g. Figures 4.9, 4.10). Degradation may still be ongoing, with the lower Shotover River still incising as recently as 2012-2014, seen in survey data at the Bowen's peak flow gauging station (Figure 4.11), and cross sections at the Shotover Delta (Figure 4.12). The incising channel level may now have attained or be near to the pre-mining channel, however a large volume of the excess sediment remains stored as floodplain terrace deposits and continues to be eroded and mobilised by flood events, forming minor pulses in riverbed level (e.g. Figure 4.11). The large volume of stored sediments means there is now less vacant storage volume than prior to mining, and so the next major sediment input will cause more rapid and higher aggradation.

The river bed changes at the Shotover Delta behaviour are more complex than those upstream, being influenced by the sediment supply rate from upstream, but also by changes to delta morphology such as gravel extraction, willow removal and training wall construction. With a total duration of >150 years, and an estimated excess sediment volume of >>10M m^3, the Shotover River sediment pulse described in this chapter is a major event in the river's recent geomorphic history. James (2010) outlines several systems of sediment wave classifications; attributes of the Shotover River sediment pulse are classified on this basis in Table 4.2.

Table 4.2: *Classification of the Shotover River sediment pulse, based on classifications in James (2010).*

Spatial scale of bed wave:	Basin-scale valley-floor adjustment (Gilbert wave, secular waves or ADE (aggradation-degradation event), superslug).
Temporal scale of wave persistence:	Catastrophic sedimentation (100-1000 years).
Sediment source:	Exogenous waves from catchment sources (allopulses, exoslugs)
Sediment storage processes:	Overbank deposition with long-term floodplain storage.
Sediment character:	Grain size of wave material similar to bed.
Wave propagation process:	Dispersion-dominant.

With a volume of several tens of millions of cubic metres, this large-volume sediment input provides an example of the Shotover River's geomorphic response to a major long-term sediment input. In Chapter Ten, this sediment pulse is used to inform discussion of the river's possible response to failure of a very large landslide dam. There are a number of differences between a widely dispersed alluvial mining input over a period of decades, and dambreak sediments sourced from a single instantaneous input, however the geomorphic changes documented downstream provide a guide to possible future behaviour.

Chapter Five: Landslide Dam Review

5.1 Introduction

This chapter gives an overview of the characteristics and formation of landslide dams, and the processes and hazards of landslide dam failures (Sections 5.2-5.5). The scope and results of previous Shotover Gorge landslide dam hazard assessments are summarised in Section 5.6. Examples of landslide dam hazard assessments completed for other locations are reviewed in Section 5.7 and are used in developing a methodology for this assessment of the Shotover Gorge landslide dam hazard (Figure 5.10). This background information is used in the following chapters to develop landslide dam scenarios (Chapters Six and Seven), assess dambreak flooding and develop dambreak flood hazard events scenarios (Chapters Eight and Nine), and assess longer-term post-dambreak aggradation impacts (Chapter Ten).

5.2 Landslide Dam Formation

A landslide dam is a natural blockage of a river channel caused by slope movements (Costa and Schuster 1988, Casagli and Ermini 1999); this can result in a number of possible hazards, both short term/local and longer term/further afield. In general, most landslide dams form when a narrow valley is blocked by a rapidly emplaced large landslide. Locations most favourable for landslide dam formation are where there is both a relatively deep narrow valley, and conditions suitable for landslide formation. These conditions include relief and slope gradient, lithology, weathering properties, and the presence of structural weaknesses, soil moisture and groundwater conditions, and the presence of potential triggers such as seismic activity or high rainfall. The global distribution of landslide dams (Figure 5.1a) shows the influence of these factors, and their correlation with active tectonic plate margins undergoing rapid uplift. For example, landslide dams are common in the Himalaya, the Western United States and Canada, Japan, New Zealand and Italy (Ermini and Casagli 2003).

New Zealand landslide dams have been the focus of several national or regional-scale studies, including those of Adams (1981), Whitehouse (1983), Perrin and Hancox (1992), and Korup (2002, 2004). Korup's (2004) compilation of data for 232 known New Zealand landslide dams shows a clustering of landslide dam occurrence, with the largest concentrations found in the mountain ranges of Fiordland, the Southern Alps, Northwest Nelson and northern Westland (Figure 5.1b). Since publication of Korup's study, a number of new landslide dams have formed, including the September 2007 Young River landslide dam (ORC 2007a), and dams triggered by the November 2016 M_w7.8 Kaikoura earthquake (Dellow et al. 2017, Massey et al. 2018).

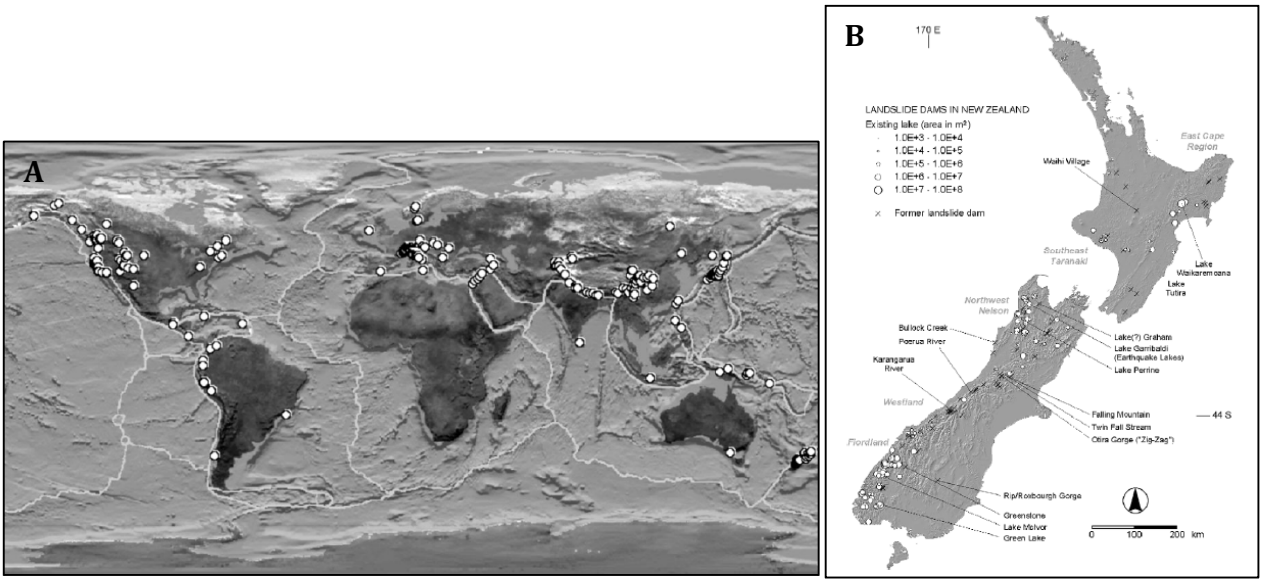

Figure 5.1: *A. Global landslide dam distribution (n=350) compiled by Ermini and Casagli (2003), and B. New Zealand landslide dam distribution by Korup (2004a).*

Landslide dams are most commonly classified using the schemes of Swanson et al. (1986) or Costa and Schuster (1988), which define six classes (I-VI) based on the type of landslide-valley interaction. The most common are Type II blockages of the entire valley width (Figure 5.2). Hermanns et al. (2011) presents an expanded classification scheme (Figure 5.2), with various subtypes and additional classification stages based on a landslide dam's cross-valley and along-valley profiles relative to the buried pre-existing topography. This classification depends on factors such as the channel geometry (width, channel gradient), and properties of the landslide (volume, velocity, type).

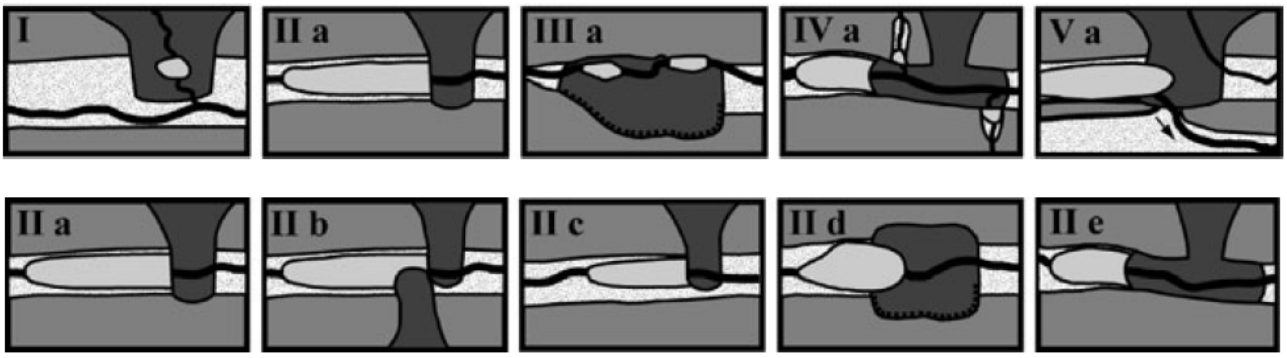

Figure 5.2: *Landslide dam classification of Hermanns et al. (2011), showing the main landslide dam types (I-V) and Type II subtypes a-e.*

A generalised landslide dam morphology is shown in Figure 5.3 below, this is a Type IIa dam, with a single landslide blocking a valley from one side, and a lake impounded behind this blockage. An example of this landslide dam morphology is the 1999 Mount Adams rock avalanche and the resulting Poerua River landslide dam, shown in Figure 5.5. Costa and Schuster (1988) and Ermini and Casagli (2003) found that most landslide dams were formed by rock avalanches, slumps, slides and flows, with the largest contributor being translational slides. Korup's (2004) study of

New Zealand dams also found these to be the dominant types of landslide dam-causing mass movements, but found the largest proportion formed by rock avalanches (27%).

The size and length of a landslide-dammed lake depends on height of the dam, cross-valley profile and upriver channel gradient. Filling time depends on inflow rates (size of the upstream catchment and precipitation rates), and the reservoir volume, a small dam with high inflows may fill in a period of minutes-hours, while very large dams may take months or several years. Some dams may lose water by seepage and may never fill completely, or may only overtop during high flow events.

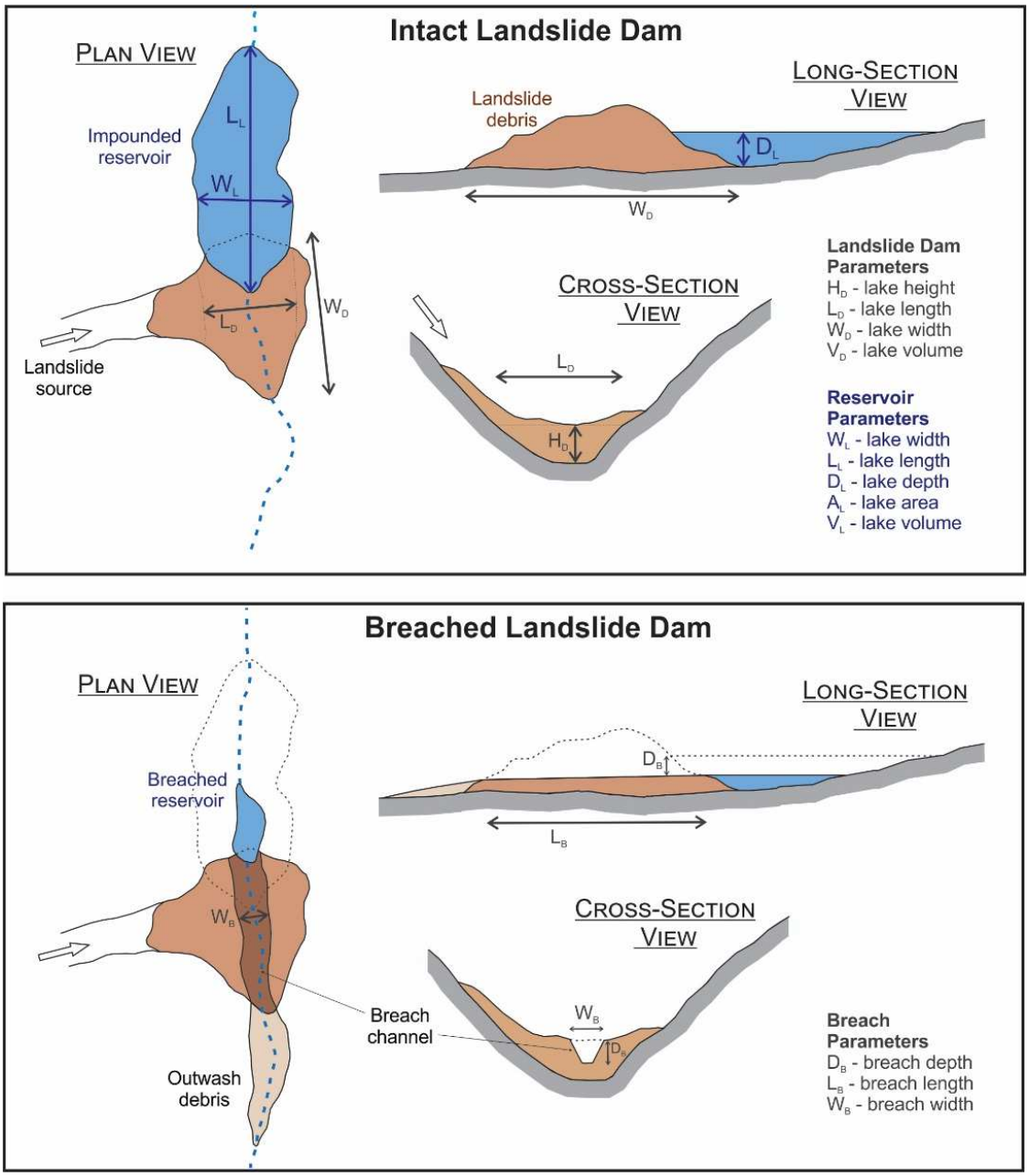

Figure 5.3: *Schematic view of typical landslide dam morphology, showing intact and breached dams, and the main descriptive parameters used to define dam and lake dimensions (redrawn from Nash 2003).*

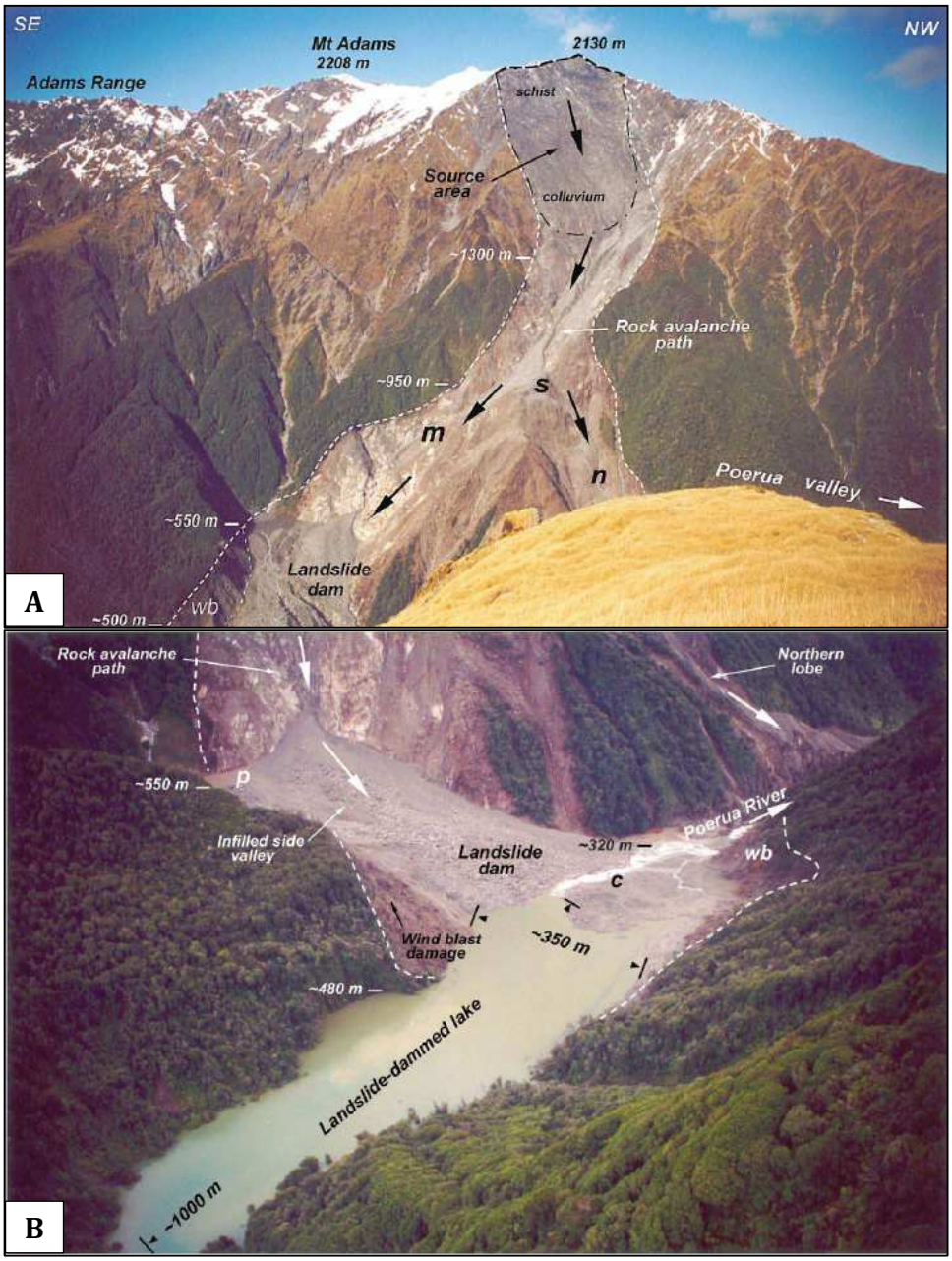

Figure 5.4: *An example of a Type II landslide dam. A. the November 1999 Mount Adams landslide showing rock avalanche source area and path, and B. the resulting Poerua River landslide dam and lake after overtopping but prior to failure (Hancox et al. 2005).*

Many studies note the dominant triggering mechanisms for landslide dam formation as being earthquakes and rainfall. The global datasets of Costa and Schuster (1988), Schuster (1993), and Ermini and Casagli (2003) attributed formation of 80-90% of landslide dams to these triggers. Similarly, a study of 300 landslide dams in Italy attributed >85% of landslide dams to earthquakes or heavy rainfall (Stefanelli et al. 2016). Significant landsliding generally only occurs at earthquakes with M_w6 or greater, in general MM6 shaking is required to cause coseismic landslides in New Zealand, but

formation of larger, deep-seated slides or rock avalanches requires stronger shaking of ≥MM7 (Hancox et al. 1997). The local slope angle and topography are important factors in coseismic landslide susceptibility, with topographic amplification leading to increased landsliding on steep slopes at cliffs and gorges, as well as narrow spurs and ridgelines (Hancox et al. 1997). Widespread coseismic landsliding may form large numbers of landslide dams from a single earthquake event, for example the 2008 M_w8.0 Wenchuan earthquake formed >500 landslide dams (Fan et al. 2012, 2014). At least five historical New Zealand earthquakes are known to have formed multiple or large landslide dams (Robinson and Davies 2013, Dellow et al. 2017), these are;

1. Wairarapa 1855, M_w8.0-8.2.
2. Murchison (Buller) 1929, M_w7.3.
3. Arthurs Pass 1929, M_w7.0-7.1.
4. Inangahua 1968, M_w7.1.
5. Kaikoura 2016, M_w7.8.

5.3 Landslide Dam Failure

Landslide dams may remain intact forming a relatively stable landslide-dammed lake. However, this is only a relative stability, and lakes may fail decades or even hundreds-thousands of years after formation. For example, the Ram Creek landslide dam failed after 12 years (Nash et al. 2008), and the Polnoon Burn landslide dam is thought to have remained intact for ~2000 years prior to failure (Korup 2006). Stable dams may remain intact and drain inflows through infiltration, seepage, evaporation, overtopping, or may eventually completely infill with sediment. For example the Lochnagar landslide dam drains through the dam material, and the lake is maintained at a level below the dam crest.

Failed landslide dams may be identified by remnants of a breached dam, an altered valley profile with a flat area upstream of a gorge, and possibly lacustrine and shoreline deposits from longer-lived lakes. Anomalously steep terraces may have been formed by dambreak deposits formed below a former dam. An example of a breached landslide dam is the Polnoon Burn landslide in the upper Shotover catchment. At this location, a 1.7 km-long gorge is incised into landslide debris of the breached dam, and the former lake is identified by lacustrine sediments and shoreline terraces. A prominent step of >100 m in the river profile marks the former dam location, indicating that even ~2000 years after failure, the channel has not recovered to its former profile (Korup 2006).

There is a very wide range in landslide dam longevity, with examples of dams lasting for periods ranging from minutes-hours, to tens of millennia. Some large dams have remained intact for thousands of years, for example the Lochnagar, Tutira and Waikaremoana landslide-dammed lakes (Korup 2002). Datasets of previous landslide dam failures have been used to provide statistical indications regarding likely dam longevity. The widely referenced study of Costa and Schuster (1988) showed that most dams fail relatively soon after formation; over a quarter fail within a day, half within ten days, and only 15% survive for longer than one year. Similar results are shown by Ermini and Casagli (2003) and Korup and Wang (2015) for larger datasets of >200 landslide dams (Figure 5.5).

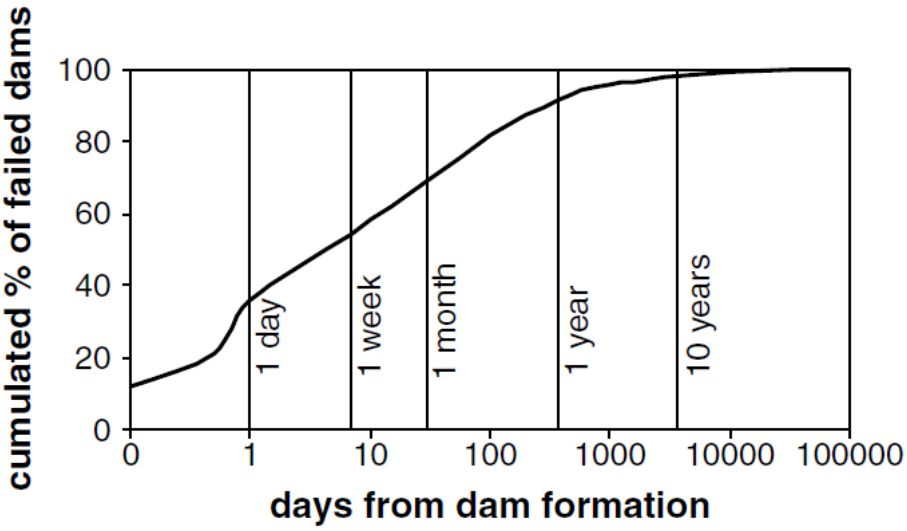

Figure 5.5: *Landslide dam longevity plot, based on a dataset of 205 landslide dam case histories (Ermini and Casagli 2003).*

As well as completely intact or completely failed dams, there are cases of more complex landslide dam development or failure. One type is partial or repeated dam failures where a dam partially fails but retains a lake, for example the landslide dam on the Passirio River, Italy. This dam had six partial failures following formation in 1404, before a complete and final failure in 1774 (Ermini and Casagli 2003). An example of later dam enlargement by landslide reactivation or secondary landsliding is the Lake Matiri landslide dam which formed ~300 years ago, then further landsliding caused by the 1929 Murchison earthquake raised the lake level (Nash 2003). Ollett (2001) and Peng and Zhang (2012) compiled data of dam height and breach depth for breached landslide dams, showing that few dams completely failed to their full height (Figure 5.6). Breach depths ranged from partial breaches of <30% of the initial dam height, to near-complete breaches of >90%, with the mean breach depth about 70% of the dam's initial height.

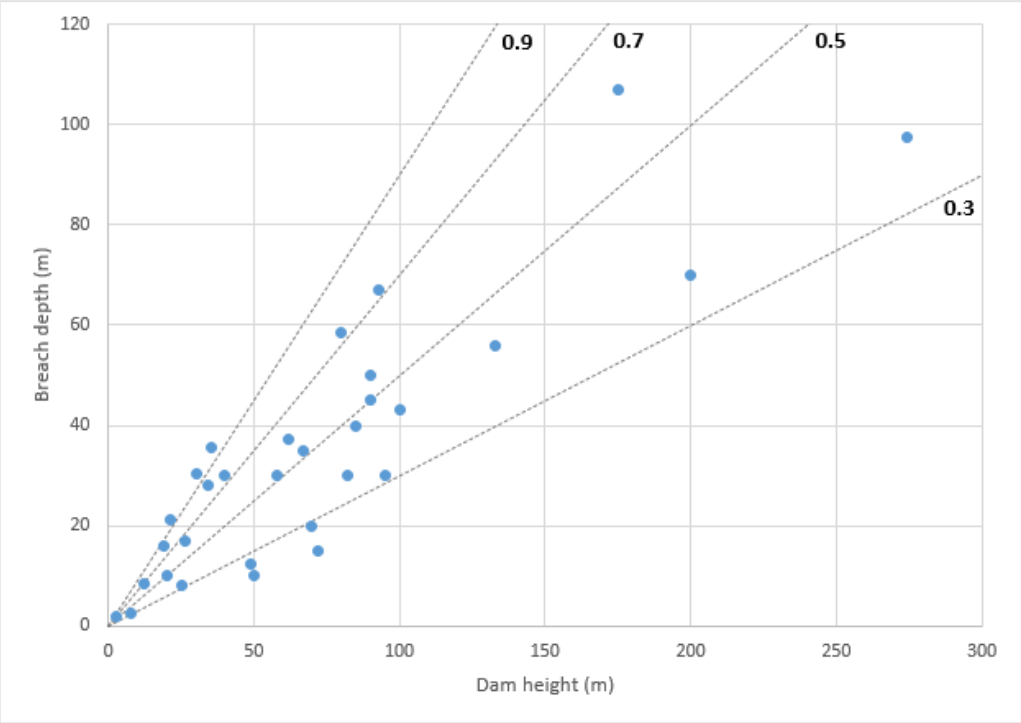

Figure 5.6: *Plot of landslide dam breaching depths, based on 31 landslide dam height and breach depths compiled by Ollett (2001) and Peng and Zhang (2012). Trend lines show breach depth as a proportion of dam height.*

A landslide dam's longevity depends primarily on its resistance to erosion, which is influenced by the dam's geometry, its geotechnical properties, and the erosive power of the dammed river. The most common cause of landslide dam failures is through overtopping, as shown by global (Costa and Schuster 1988), New Zealand (Korup 2004a), and other international datasets (Xu et al. 2009). Overtopping failure is caused by water flowing over the dam crest leading to erosion of a breach channel on downstream face of dam; this creates a positive feedback loop as increasing erosion of the dam crest allows more flow, which in turn further increases the erosive power. Other possible failure mechanisms are though piping, where internal erosion removes fine material leading to failure, and through heave, where the water pressure gradient and seepage contributes to failure, or a secondary slope failure of the dam material (Ermini and Casagli 2003).

Ermini and Casagli (2003) note 40% of dam collapses occur within one day of dam formation, and assume this failure coincides with the dam's first overtopping. Other dams may fail in the first large rainfall event following their formation, for example the 1999 Poerua River landslide dam (Hancox et al. 2005), and the many Kaikoura landslide dams which failed during heavy rainfall from ex-Tropical Cyclone Debbie on 5 April 2017, over 4 months after formation (Dellow and Massey 2017). Some dams may remain intact for many years, but eventual failure is also rainfall-triggered, for example the Ram Creek landslide dam had a stable lake level well below dam crest, but overtopped and failed due to a very heavy rainfall event (Nash et al. 2008). Less common triggers for landslide dam failure are landsliding into the lake displacing water over the dam, or cascading failures triggered by dambreak flood surge from an upstream landslide dam (e.g. Tangjiashan, Xu et al. 2009). Seismic shaking may also destabilise landslide dams; for example the Dadu River landslide dam was formed by coseismic landsliding, and then failed ten days later, triggered by an aftershock (Dai et al. 2005).

Landslide dams with steeper or higher downstream dam faces are more easily eroded, as these have high velocity and erosive power of the overtopping flow (Costa and Schuster 1988, Ermini and Casagli 2003). Geotechnical properties such as grain size distribution, texture and strength have a strong influence on the erodibility of material through overtopping or piping, and the stability of dam slopes. Dams comprising matrix-supported, finer or softer material are more susceptible to erosion through piping or overtopping, and do not typically form stable dams. Dams composed of coarse grained, clast supported material have increased strength and permeability, making them more resistant to overtopping and internal or crest erosion (Nash 2003). Rock avalanche deposits often form a coarse grained, angular, clast-supported carapace that is initially more resistant to erosion, however erosion can proceed rapidly once flow reaches the intensely-fragmented dam interior (Wishart 2007). Landslide dams formed in the Kaikoura earthquake illustrate the effect of dam formation by materials of different lithologies. Dams formed of strong greywacke debris were coarse-grained, blocky and relatively permeable, draining mainly through dam material and only overtopping under flood flows. In contrast, weaker Neogene sedimentary rocks formed large slumps and block slides, and dams were relatively impervious (Dellow et al. 2017).

5.4 Landslide Dam Hazards

Landslide dam formation may initiate a cascade of interlinked hazard events and processes, as illustrated in Figures 5.7 and 5.8 (Korup 2005a). These include immediate and longer-term hazards, located both up and downstream of the dam location. The main upstream hazard is backwater lake formation, causing inundation of the upstream valley floor. Landslide-dammed lakes may extend for tens of kilometres upvalley and submerge housing and infrastructure, as occurred after the 2008 Wenchuan earthquake (Korup and Wang 2015), including inundation of an upstream hydropower station (Chen et al. 2010). Rising lake waters may precipitate further landsliding, as at Mantaro, Peru (Lee and Duncan 1975). A stable landslide-dammed lake will act as a sediment trap, causing upstream aggradation and formation of a prograding delta at the lake inlet.

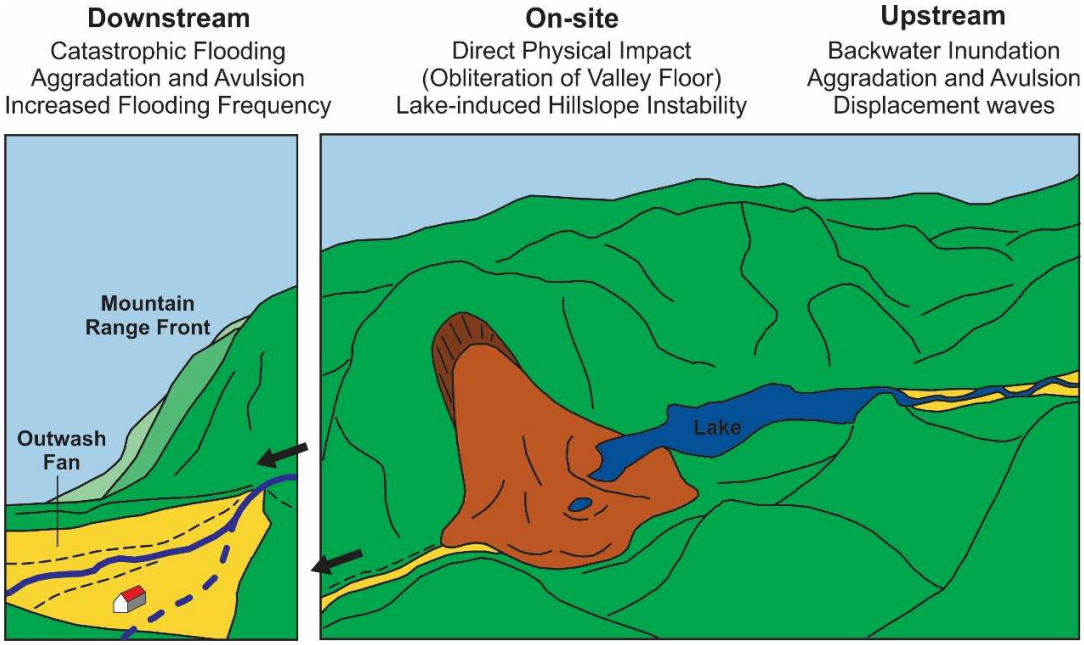

Figure 5.7: *Sketch of geomorphic hazards which may result from formation and failure of a landslide dam in a mountain-foreland system (redrawn from Korup 2005a).*

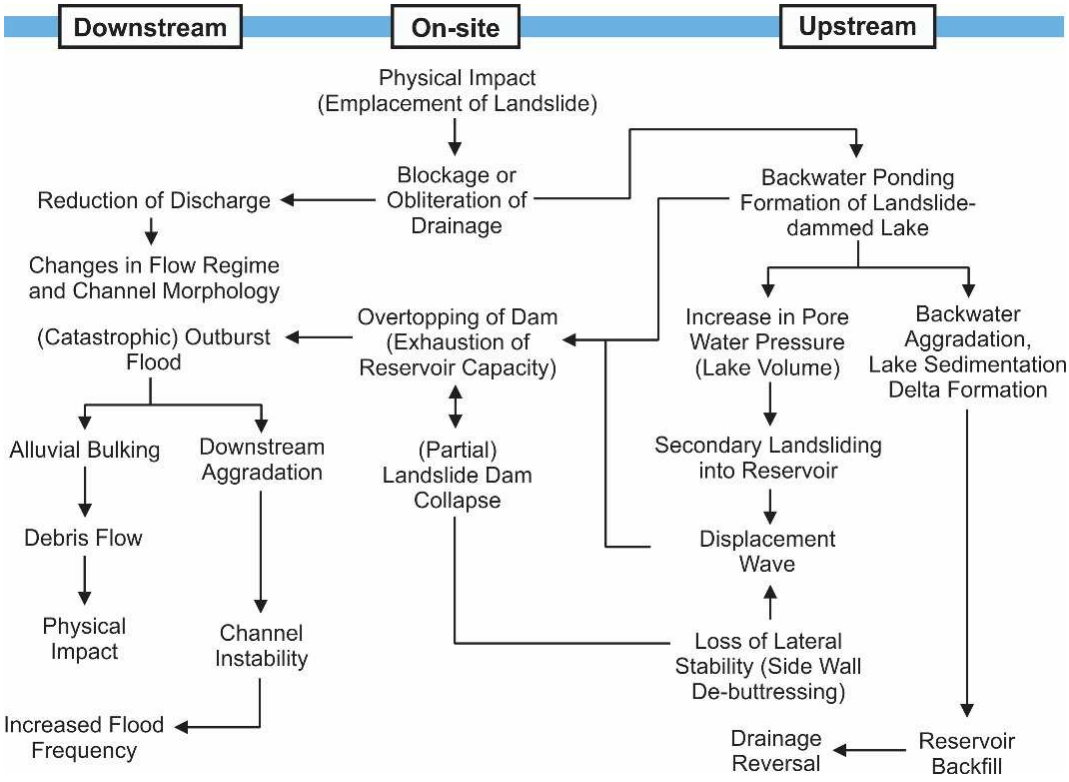

Figure 5.8: *Summary of the geomorphic processes and hazards which may result from landslide dam formation and failure, showing the complex, cascading nature of these relationships (Korup 2005a).*

A Shotover Gorge landslide dam is not expected to be stable long-term, based on fact that only a small number of landslide dams remain stable for long durations (Figure 5.5), so this study focuses on the consequent hazards of a catastrophic dam failure; outburst flooding and aggradation hazards. A dambreak flood results from sudden dam failure, releasing a flood wave of water as the reservoir rapidly drains. These events have also been termed outburst floods or landslide lake-burst floods. Korup and Tweed (2007) preferred the term outburst flow, a term which recognises the fact that dambreak floods often entrain large amounts of sediment to form hyperconcentrated flows or debris flows. Dambreak flood surges may be many times greater than known rainfall-induced flood events, often up to two orders of magnitude larger (Korup and Tweed 2007). Compared to typical meteorological flood events, a dambreak flood is a very short duration flood wave, resulting in a strongly peaked hydrograph (Figure 5.9A). An example of a damaging dambreak flood is the 1974 dambreak on the Mantaro River, Peru. This 170 m dam failed, releasing a flood wave with a peak discharge of about 10,000 m^3/s, eight times larger than the largest meteorological flood on record. There was no loss of life as all inhabitants had been evacuated, but the flood wave destroyed roads, bridges, townships and farmland (Lee and Duncan 1975). Dambreak flood waves attenuate as they propagate downstream, with the hydrograph becoming stretched and flattened (Figure 5.9B). There is minimal flow attenuation in steep, straight or narrow gorges, while highest attenuation rates are in valleys with rapid decrease in gradient, or a rapid increase in width (Manville 2001, Ollett 2001).

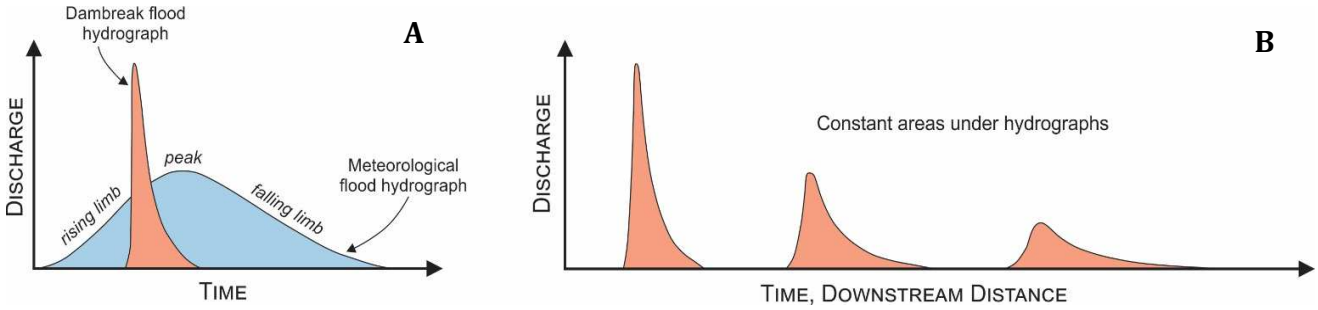

Figure 5.9: *A. Sketch comparing generalised meteorological and dambreak flood hydrographs showing the high peak, short duration character of dambreak floods, and B. illustration of hydrograph attenuation as flood wave propagates downstream (after Manville 2001).*

Many dambreak floods are sediment-laden due to incorporation of eroded dam material into the floodwaters, and erosion and entrainment of pre-existing downstream sediments. Entrained sediments may bulk flows by up to 30-50%, forming a highly erosive hyperconcentrated flow or debris flow (Ermini and Casagli 2003, Korup and Tweed 2007). As the flood wave travels downriver, it may erode and entrain existing sediments, and also deposit entrained material. A flow with a high sediment content may become increasingly fluid as entrained sediment is deposited (Korup and Tweed 2007). In forested catchments dambreak floods may also entrain large volumes of woody debris.

At dam failure, there is immediate transport of large volumes of sediment downriver by the outburst flood, then over the following years or decades there is continued erosion, remobilisation and storage of landslide debris downriver. This sediment influx forms a sediment pulse, which works its way through the river system over timeframes ranging from years to millennia. The resulting aggradation can cause large increases in channel width and channel avulsions, as the river system is overwhelmed by the sediment supply, and floodplains and fans may aggrade by metres or tens of metres in thickness (Korup and Wang 2015). This may result in destruction of farmland, as occurred following the Poerua River dambreak (Hancox et al. 2005), or destruction of infrastructure and residential areas, as in the Tachia River Basin (Chen 2008), and Beichuan County, China (Chen et al. 2011). Riverbed aggradation also reduces channel capacity, increasing the frequency and severity of floods. Sediment pulse literature and the geomorphic impacts of landslide dam failures are reviewed in more detail in Section 10.2.

In cases where a dam poses a dambreak flood threat, the dam may be modified in an attempt to manage the hazard. A common approach is to reduce the reservoir volume, reducing possible dambreak flood magnitude, and minimising or preventing overtopping and dam erosion. This can be achieved by pumping, diverting flow through tunnels or piping, or lowering of the dam crest through excavation of channel construction, for example at the Spanish Fork River, Utah (Schuster 1985) and Mt Zandlia, Italy (Ermini and Casagli 2003). Dams may be modified by construction of a spillway designed to minimise erosion or scour of the dam face, this can maintain a stable lake and reduce the probability of sudden failure. For example, spillways were constructed at Madison Canyon landslide, Montana (Costa and Schuster 1988), Paute, Ecuador (Plaza-Nieto and Zevallos 1994) and the Kii Peninsula, Japan (Korup and Wang 2015). After the 2008 Wenchuan earthquake, 32 landslide dams were artificially breached to reduce risk of catastrophic dambreak floods. At the Tangjiashan landslide dam, a spillway was excavated to avoid an uncontrolled overtopping, which lowered lake level by ~30 m, and reduced the impounded volume by two-thirds (Xu et al. 2009). Release of water from this dam triggered the failure of a series of seven downstream landslide dams. Many New Zealand landslide dams are located in rugged, inaccessible terrain and have generally not been artificially modified, but there are several exceptions. The Matakitaki No.2 landslide dam formed in the 1929 Murchison Earthquake. This dam survived for about ten years but was gradually removed as blasting was used to increase the dam's natural erosion (Nash 2003).

5.5 Shotover Gorge Landslide Dam Studies

Several previous investigation have considered the potential landslide dam hazards within the Shotover Gorge, and these studies are summarised below.

Thompson's (1996a) report to the Otago Regional Council (ORC) investigated the potential for landslide dam formation in the upper Kawarau or lower Shotover Gorges to affect the level of Lake Wakatipu. Five scenario sites were identified in the lower Shotover Gorge, with an area of interest extending to just beyond the Moonlight Creek confluence. Evaluated scenarios were three existing landslides and two possible first time landslide failures. The report concluded there is a relatively high potential for Shotover River blockages to occur, but dams were likely to be small in volume and not prone to rapid failure. No evidence was identified to suggest formation of large landslide dams in the recent past. The dambreak flood hazard was not considered significant due to flow attenuation as a result of the broad river channel in the lower Shotover River. Aggradation resulting from landslide dam failure was considered to be of a similar magnitude to that caused by modern flood events.

Bryant's (2011, 2017) reports were prepared for the subdivision approval process for the Shotover Country development, on land adjacent to the Shotover River and delta. Bryant (2011) used topographic maps, and satellite and aerial imagery, along with helicopter observations to identify active/recent landsliding and possible future landslide dam locations. About 12 active landslides were noted in the lower gorge as far upstream as Long Gully, most of which are dip-slope slides from the eastern slopes. First-time slope failures were considered to be more likely to form a landslide dam, due to the more rapid debris emplacement compared to reactivation of existing slides. Lake volumes were estimated for dams in four sections of river between the Oxenbridge Tunnel and Long Gully, and for four dam heights (5, 10, 20, 50 m). The largest lake volume calculated was ~44M m^3 for a 50 m high dam located near Butchers Point. Peak flood discharges from dam scenarios were estimated using a Costa and Schuster (1988) regression equation, and had values of 500-950 m^3/s for 20 m high dams, and 2700-4600 m^3/s for 50 m high dams.

Bryant (2017) did not identify specific landslide scenario locations, but thought the most likely locations for landslide dam formation to be between Arthurs Point and Long Gully, and to be first-time slope failures. Any first-time failure landslide dam was considered to be relatively stable, and lasting for >12 months. The post-failure distribution of landslide dam debris is discussed, and assumes only 20-25% of landslide dam material is removed by erosion of a breach channel. Of this eroded material, it is assumed over 80% is transported as suspended sediment to the Kawarau River. Based on these assumptions, a 10^7 m^3 landslide dam is estimated to cause aggradation of 380-770 mm in the lower Shotover River, with most deposition at Big Beach and Tucker Beach.

Davies (2017) also prepared a submission for ORC in relation to proposed Shotover Country development, and discusses general impacts of landslide dam formation and failure with reference to the Poerua River and North Young River examples. Davies outlines two landslide dam hazard scenarios with potential to impact developments east of the Shotover Delta. These are, (i) a dambreak flood wave resulting from sudden dam failure, and (ii) delta aggradation following large sediment inputs from landslide or landslide dam debris. Davies (2017) considers future landslides comparable in size to the 10M m^3 Poerua and North Young examples to be possible in the Shotover Gorge, and estimates landslide dam impacts based on this dam size.

Davies (2017) disputes Bryant's (2017) assumptions regarding dam longevity, countering these with the example of the failure of the Poerua landslide dam after only a few days, and data from Costa and Schuster (1988) showing a large proportion (~90%) of landslide dams fail within one year of formation. A dambreak flood of 10,000 m^3/s is estimated from failure of a 100 m high dam, extrapolating from Bryant's (2017) calculations. However, due to a dam of this size taking >1 day to fill, the dams presence would have been recognised and any dambreak event would not be without

warning. Metre-scale aggradation at the Shotover Delta is suggested based on the magnitude of aggradation in the Poerua Valley immediately below a narrow gorge. Like the Thompson and Bryant reports, Davies concludes there is currently insufficient evidence to make a credible estimate of landslide probabilities, or dambreak flood and aggradation magnitudes.

5.6 Landslide Dam Hazard Assessment

The majority of landslide dam literature is descriptive and site-specific, and most landslide dam hazard studies are focused on the stability and possible dambreak flood magnitudes of existing landslide dams (Korup 2005a). There are fewer studies providing examples of methodologies for hazard assessment of future landslide dam events, with studies into future landslide dam hazards described as scarce and 'largely unaddressed' (Braun et al. 2018, Korup 2002 2005a). Large landslide dams are infrequent events, and there is only a short historic record in New Zealand. As a result, there is typically no historic precedent for evaluating possible future landslide dams, and many assumptions are required in assessing the magnitude and character of landslide dams (Korup 2005a). Several studies have noted or investigated aspects of future landslide dam and dambreak hazard from specific catchments or rivers in New Zealand, these include;

- Shotover Gorge: Thompson (1996a), Bryant (2011, 2017), and Davies (2017).
- Callery Gorge: Davies and Scott (1997), Ollett (2001), and Davies (2002).
- Waimakariri Gorge: Yetton and Davies (2002), Yetton and McMorran (2004).
- Roxburgh Gorge: Moon (1997), McFarlane and Roberts (2001).
- Poerua River: Arshad et al. (2004).
- South Westland: Korup (2005a).

Some of these studies were basic assessments, while others involved more detailed investigation. In developing an assessment methodology for this Shotover Gorge study the most useful examples have been those of Ollett (2001) and Korup (2005a). Stages in Ollett's Callery Gorge assessment included;

1. Identification and characterisation of possible landslide dam locations based on aerial photographs.
2. Numerical modelling of landslide volumes.
3. Use of a small-scale physical model to estimate dam dimensions and investigate sensitivity to landslide volume, bed slope and channel angles. Results of this modelling were used to estimate scenario parameters, including dam volume, dam height, and reservoir volume.
4. Peak dambreak flows at the breach were estimated using four methods; empirical regressions (Costa 1985), a parametric model (Mike11), and two erosion-based mathematical models (Mike11, BREACH).
5. Results of Mike11 and BREACH models were used to develop triangular dambreak flood hydrographs, this flow was routed downstream using hydraulic modelling software (Mike11) and used to estimate the attenuation in peak flow as the flood wave travelled downstream.
6. Estimation of sediment volumes eroded during breach formation, and the transport of this material into and through the river.

7. Evacuation time was calculated as the time for the reservoir to fill, under flood (Q_{100}) and mean flow conditions, plus the travel time for the flood wave to reach downstream locations.

Korup (2005a) investigated potential landslide dams in four South Westland test catchments; the Callery, Poerua, Karangarua and Cascade Rivers. A GIS-based approach identified landslide dam scenario locations, based on factors such as slope angles, vertical drop heights and locations beneath dip-slope faces. Landslide dam and lake parameters were extracted for hypothetical dams and used in several analyses:

1. Estimation of peak dambreak flood discharge using Costa's (1985) regression equation. Peak flows were normalised against the 100-year flood discharge to provide an 'outburst flood ratio'.

2. Estimation of filling times for several landslide dam heights and sized catchment areas, at input flows of mean annual flood, and a 100-year flood (Q_{100}).

3. Use of empirical stability indices to assess probability of catastrophic dam failure and an outburst flood.

A number of investigations of dambreak flood magnitudes are widely referenced in Chapter Eight herein. Manville (2001) investigated techniques for estimating dambreak flood magnitudes, making use of empirical, dimensionless, parametric, and physically-based methods. This reference includes spreadsheets which partially automate many modelling processes and are an invaluable resource. Manville (2001) and Davies et al. (2007) apply these techniques to retrospective modelling of the 1999 Poerua River dambreak flood event. Ollett (2001) modelled future Callery Gorge dambreak floods, and Wishart (2007) applied these modelling techniques to breaching of hypothetical rock avalanche dams. Otago Regional Council's (ORC) investigations of the 2007 North Young River landslide dam have included application of stability indices (ORC 2012), estimation of peak dambreak flows using empirical regressions (ORC 2007b), and use of a hydraulic model (Mike11) to investigate flow attenuation and flood wave travel time (ORC 2007b).

The methodology for the present Shotover Gorge study is summarised in Figure 5.10, showing the assessments completed and the relationship between stages of this study. This has been developed based around the cascade of hazard events likely to result from emplacement of a large landslide into the Shotover Gorge (e.g. Figures 5.7 and 5.8), and uses analysis methods compiled from the landslide dam hazard studies noted above. Assessments are grouped into four sections, organised by the main landslide dam events and hazards; landsliding (Chapter Six), landslide dam formation (Chapter Seven), dambreak flooding (Chapter Eight), and the longer-term sedimentary impacts (Chapter Ten).

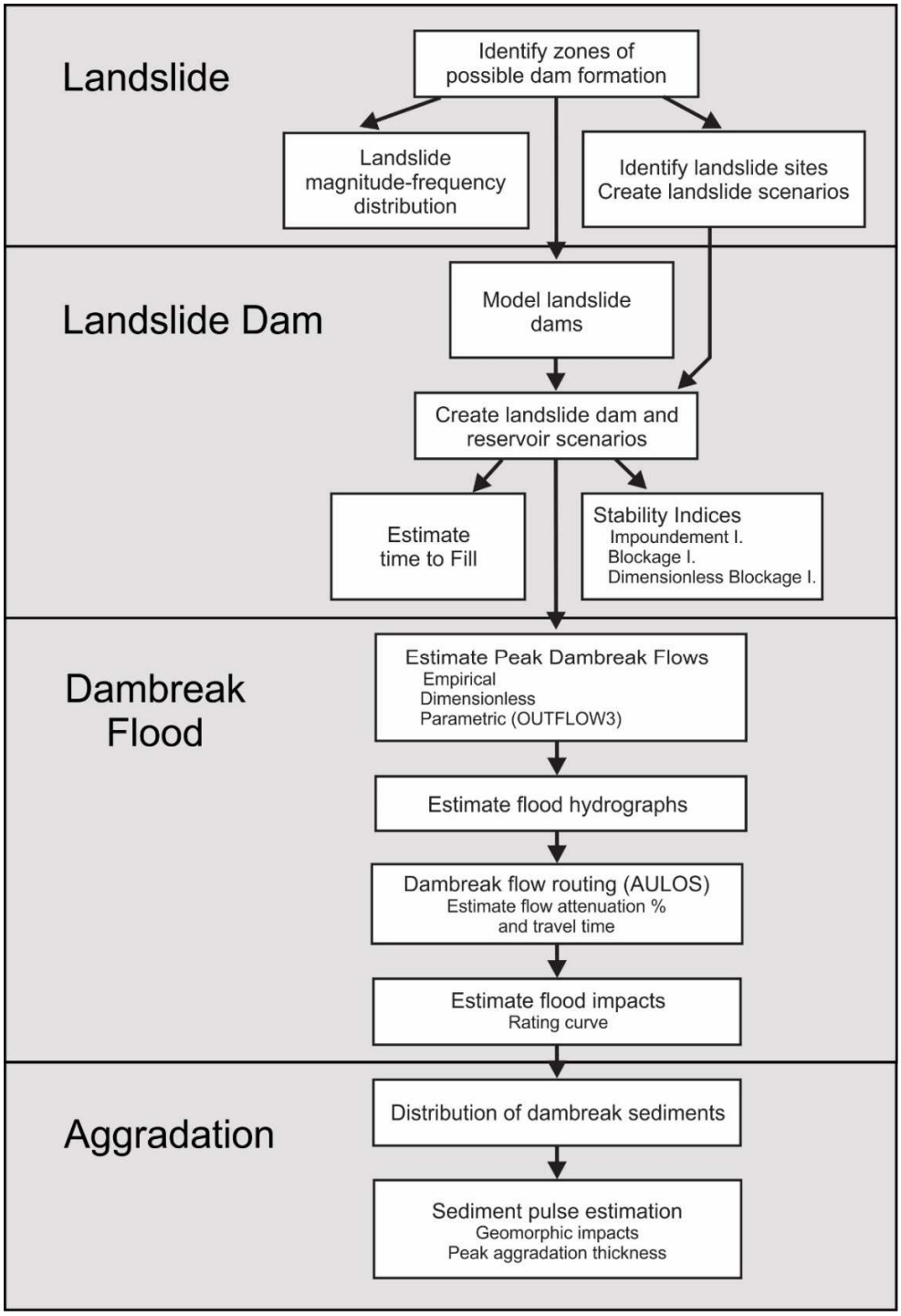

Figure 5.10: *Flow chart summarising the landslide dam hazard investigation methods used in this Shotover Gorge assessment.*

Chapter Six: Landslide Assessment

5.1 Introduction

This chapter investigates aspects of landsliding in the Shotover Gorge, including the location, likelihood, and landslide style, and these are used to guide assessment of the potential for occurrence of a future dam-forming landslide. The chapter identifies zones in the Shotover Gorge and Moonlight Creek where landslide dam formation is considered to have potential to occur (Figure 6.3 and 6.4). Within those zones a number of possible landslide scenarios are identified, landslide parameters are estimated for these scenarios (Table 6.1) and are used in landslide dam modelling (Chapter Seven).

Landslide dam likelihood is difficult to estimate, with no record of large landslide dams in the Shotover Gorge. A magnitude-frequency relationship has been developed for Shotover Gorge landslides on slopes adjacent to the gorge (Figure 6.12). Assuming that many of these landslides are in locations where debris may have impacted on the river channel, this can be used to approximate landslide dam frequency and magnitude.

Landslide dams occurring elsewhere in the Shotover catchment can be used as examples to characterise a future Shotover Gorge landslide dam. These have been compiled from a literature search, and several others newly identified from aerial imagery. These show widespread landslide dam formation in the Shotover catchment (Figure 6.13), and are summarised in Appendix 3.

6.2 Landslide Scenarios

The possible locations and likely characteristics of large landslides capable of forming a landslide dam in the Shotover Gorge can be inferred based on factors required for dam formation. These include;

1. Slope dimensions and structural conditions allowing for formation of a large volume landslide.

2. A landslide sourced from a location where proximity to channel means debris can reach channel.

3. A high-mobility landslide style, with sufficient debris runout that much of the debris reaches the river channel.

4. Debris emplacement in a location where the valley has a relatively narrow width and can be completely blocked.

Many of the Shotover Gorge slopes are steep (>30°), with high slopes adjacent to the river channel, containing many past slope failures (Figure 6.11), and evidence for ongoing slope instability (e.g. Figure 6.5). Incision of the modern Shotover River channel has resulted in significant oversteepening at the toe of most slopes (e.g. Figure 6.6). This fluvial slope undercutting and the resulting slope relaxation/dilation is expected to be the main destabilising factor preconditioning slopes for landsliding. It is likely that any large landslide location will exhibit significant slope weakening and deformation prior to an eventual catastrophic failure. For example extensional cracking was noted at the site of the 2008 Moonlight Track landslide for about 20 years prior to slope failure. (Dellow et al. 2009). While progressive slope relaxation is likely to be the main contributor to failure, the final slope failure event may also be triggered by heavy rainfall or coseismic shaking.

The distribution of existing Shotover Gorge landslide scarps (Figure 6.11) shows the potential for future large landslides to occur from both the western or eastern sides of the gorge, and these are thought to be possible as either a first-time landsliding event, or a reactivation of an existing slide. Based on observations of existing landslides during field

investigations, and documentation for existing landslides (Willetts 2000, Dellow et al. 2009), the most probable landslide type is a wedge failure controlled by jointing, faulting, shear zones, and schist foliation.

The Shotover Gorge typically has a valley-floor width of <100 metres in the lower and middle gorge, becoming wider in the upper gorge upstream of about Sandhill Cut (Figures 2.1B, 2.2). Landslide dam formation is still possible in these wider sections of the gorge, but a much lower dam would form for any given landslide volume, compared to narrower locations elsewhere in the lower and middle gorge. Landslide dam formation is also possible in the larger tributary streams (e.g. Moonlight Creek, Stony Creek, Skippers Creek), many of which show evidence of past landslide dam formation (Figure 6.13, Appendix 3). Of those tributaries, only the lower section of Moonlight Creek was assessed in this study. As narrower, steeper gradient valleys, these side streams have less potential for impoundment of large volume lakes, and the threat of a damaging outburst flood is considered to be less significant.

Korup's (2006) study of Southern Alps landslide dams noted two types of valley-damming slope failures; (1) rock-slope failures, often catastrophic, with clearly detached deposits, and (2) deep seated, low displacement, sackung-type failures causing river occlusion or diversion. Observations of landslide dams occurring elsewhere in the Shotover catchment also show occurrence of dams formed by these distinct failure types (Figures 6.1, 6.2, Appendix 3).

The most hazardous dam-forming landslide type are highly mobile, catastrophic failures as a rock slide or rock avalanche. In this event the total landslide volume rapidly moves in a single event, and can form a high dam impounding a significant volume reservoir. Recent examples of dam-forming landslides of this style are the rock avalanches forming the 1999 Poerua River landslide dam (Hancox et al. 2005), and the 2007 North Young River landslide dam (Massey et al. 2013). In the Shotover catchment, examples of landslide dams formed by rock slides or rock avalanches include the very large Lochnagar and Polnoon Burn landslide dams (Appendix 3). Smaller examples include those found in Stony Creek (Figure 6.1A), and in the Shotover River at Saddle Creek (Figure 6.1B), which have landslide widths of 300-350 m and estimated landslide volumes of 2-4 M m^3. These landslide dams may be of a comparable magnitude to those which could plausibly form in the Shotover Gorge.

It is also possible that a dam-forming landslide of the second, low-displacement, type could also occur in the Shotover Gorge, most likely from the eastern dip slopes. This more gradual slope movement can constrict the river if the rate of debris emplacement exceeds the rate of fluvial erosion of debris. This can block a valley and cause minor upstream aggradation (e.g. Figure 6.2), but in contrast to the more highly mobile landslide types, only a smaller portion of landslide debris is transported to the river channel and contributes to dam formation.

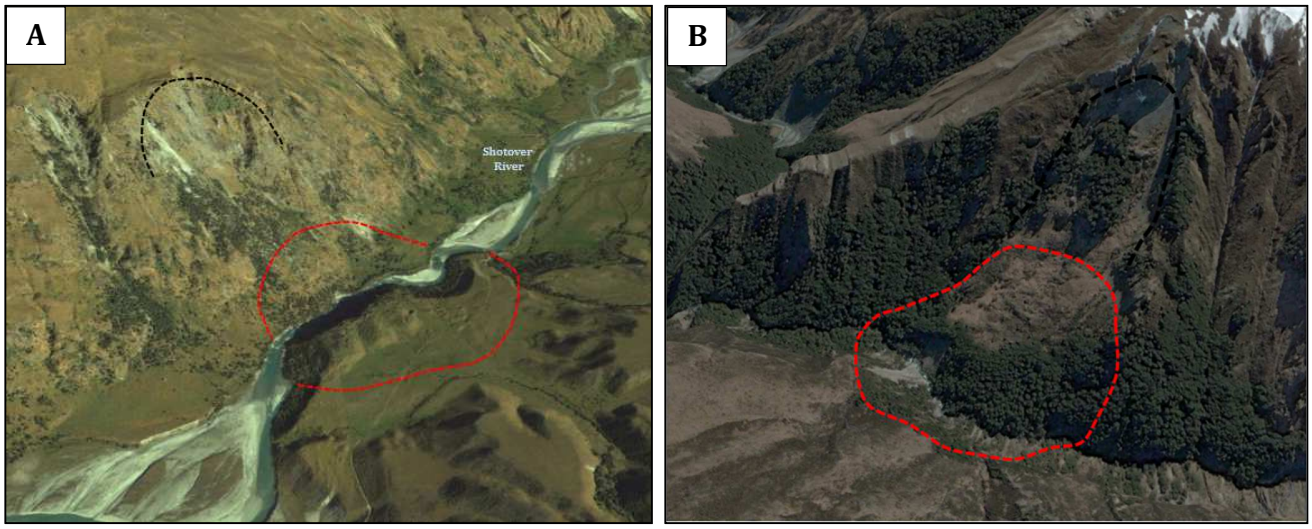

Figure 6. 1 *Examples of Shotover catchment landslide dams; A. in the Shotover River at Saddle Creek (Google Earth 2010), and B. in Stony Creek (Google Earth 2004), numbered as 8 and 9 respectively in Figure 6.13. These landslides have estimated volumes of 2-4M m³. Figures show interpreted outline of landslide scarp (black dashed line) and the resulting deposit (red).*

Figure 6. 2 *Example of a low-displacement type landslide dam, located in the Upper Moonlight Creek, labelled as 18 in Figure 6.13. This landslide is about 280 metres in width and may have a volume of >5M m³. Constriction of the valley has formed a broad alluvial flat upstream of this dam (lower centre). Figure shows interpreted outline of landslide scarp (black dashed line) and the resulting deposit (red). (Google Earth 2010).*

Shotover Gorge Landslide Scenarios

Using the criteria discussed above, five zones have been identified in the study area where large landslide dam formation is thought most likely (Figure 6.3). These zones are;

Shotover Gorge

- Lower Shotover Gorge: Shady Creek to Moonlight Creek (Zone A)
- Lower Shotover Gorge: Moonlight Creek to Criterion Creek (Zone B)
- Middle Shotover Gorge: Criterion Creek to Devil's Elbow (Zone C)
- Upper Shotover Gorge: Skippers Bridge to Sandhill Cut (Zone D)

Moonlight Creek

- Lower Moonlight Creek: Shotover confluence to Moke Creek (Zone M)

Within these zones a number of landslide scenarios have been developed. These are shown in Figures 6.3 and 6.4, and Table 6.1 outlines landslide parameters of these scenarios. These are considered realistic scenarios for larger dam-forming failures based on dimensions of existing slope failures, and observations of ongoing slope instability. These are not the largest landslides possible in these locations, as shown by presence of some larger existing landslide scarps within the gorge (Figure 6.11, Table 6.2). Based on the landslide magnitude-frequency distribution developed for the study area (Figure 6.12), these larger landslides are relatively infrequent, and so the scenarios developed here are for smaller and more frequent landslide magnitudes.

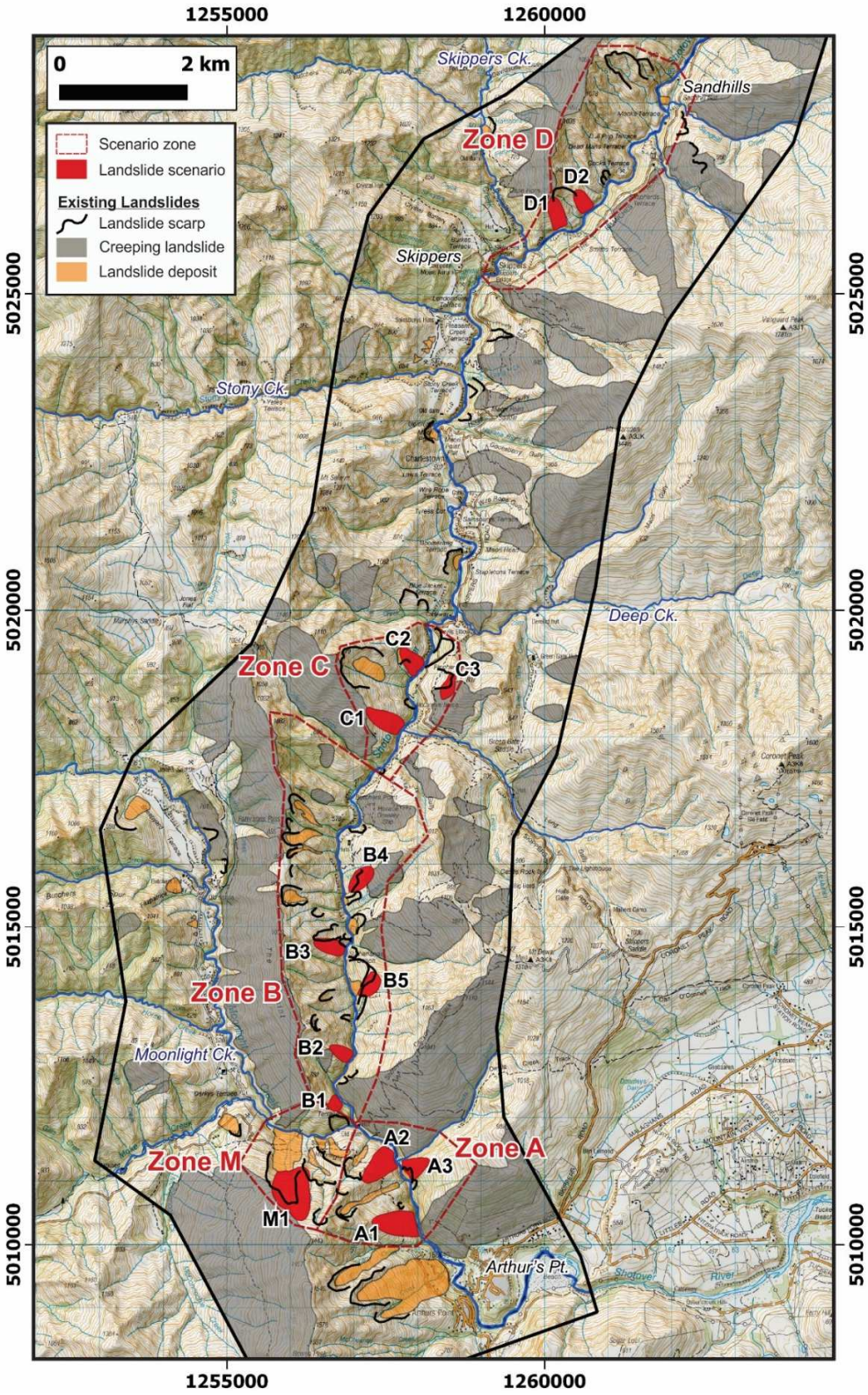

Figure 6. 3 *Shotover Gorge landslide dam zones and scenarios, and selected existing landslide features. Scenario parameters are shown in in Table 6.1.*

Table 6.1: *Shotover Gorge landslide scenarios, landslide parameters, and estimated volumes.*

Location	Max elevation (m)	Channel elevation (m)	Max Fall height (m)	Plan distance (m)	Slope angle (deg)	Landslide source area (m^2)	Volume[1] (Mm^3)	Mean thickness (m)
A1	870	350	520	700	36.6	220,000	5.2	23
A2	800	360	440	630	34.9	181,000	3.9	21
A3	660	355	305	440	34.7	97,000	1.5	16
M1	1330	375	955	1390	34.5	376,000	11.5	31
B1	620	370	250	220	48.7	39,000	0.4	10
B2	690	375	315	355	41.6	64,000	0.8	13
B3	780	380	400	490	39.2	96,000	1.5	15
B4	710	385	325	610	28.0	102,000	1.6	16
B5	690	380	310	485	32.6	85,000	1.2	15
C1	840	400	440	620	35.4	146,000	2.8	19
C2	690	415	275	445	31.7	100,000	1.6	16
C3	800	405	395	530	36.7	63,000	0.8	13
D1	800	445	355	440	38.9	104,000	1.7	16
D2	720	450	270	370	36.1	75,000	1.0	14

1. Estimated using Hovius et al (1997) equation

Most scenarios are in locations where the slopes are steep, and undercut by river incision (e.g. Figure 6.6). These scenarios are mostly sites which have not previously failed, but are located in areas where the presence of nearby large landslides indicate geological conditions favourable for formation of large slope failures. Ground cracking and deformation is seen at many scenario locations, for example at Moonlight Creek (Figure 6.5A), and the middle Shotover Gorge (Zone C, Figure 6.5B), indicative of continuing slope instability which may progress to sudden failure. Eastern dip-slope scenarios are from locations where the toes of large creeping landslides have been undercut by river incision, and adjacent to slopes which appear to have previously failed, shown by the presence of existing landslides/rockfalls.

All Shotover Gorge landslide scenarios are located adjacent to the gorge and it is expected the majority of landslide debris would be transported into the river channel to form blockages. The Moonlight Creek landslide scenario originates near the top of slope and debris would need to run out for >500 m to reach the creek channel (Figure 6.5A). The lower slopes below this source area are relatively gentle and mantled by extensive landslide and rockfall deposits, so for modelling purposes it has been assumed only 20% of landslide debris reaches the channel and contributes to landslide dam formation.

Smaller rockfalls and rockslides are common from the deeply incised gorge slopes (e.g. Figure 2.32); the magnitudes of these failures are limited by the height of the steep bluffs adjacent to the river. These failures are typically <120 m in height, and may have volumes reaching 30-40,000 m^3. Any slope failure of this type is likely to have impacts comparable to the 1993 Criterion Creek rockfall (Bryant 2011), or the 1871 Sutherland's Beach landslide dam (Appendix 4). These are expected to form a minor or partial channel blockage and to be relatively ephemeral, impounding a small lake and forming a minor rapid in the riverbed.

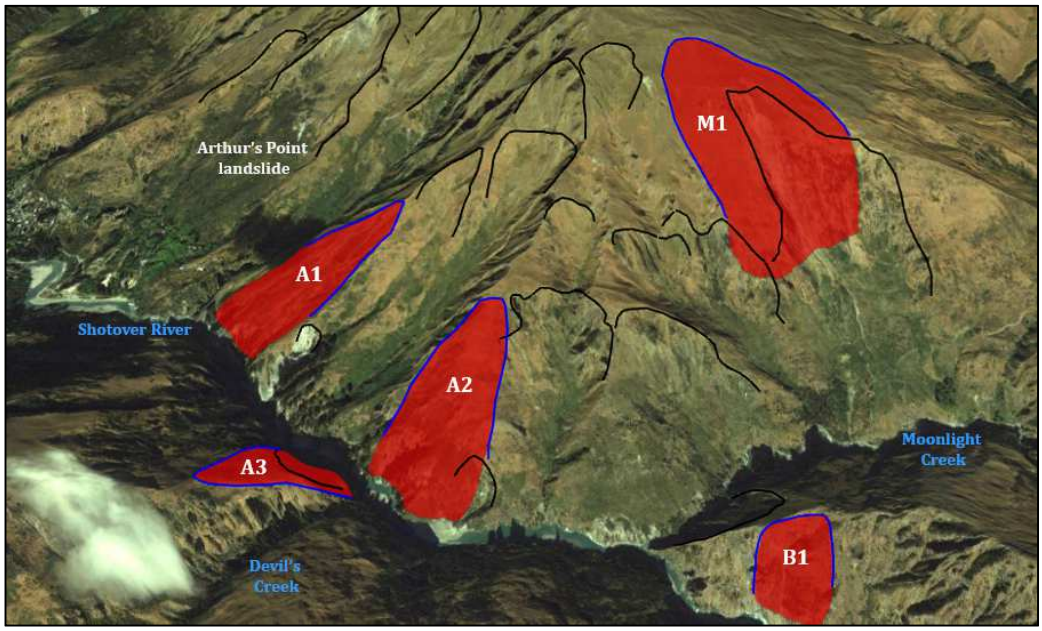

Figure 6. 4A *Oblique view of lower Shotover Gorge (Zone A) and Moonlight Creek (Zone M) landslide scenarios. View is towards the southwest. Black outlines indicate existing landslide scarps. (Google Earth 2010).*

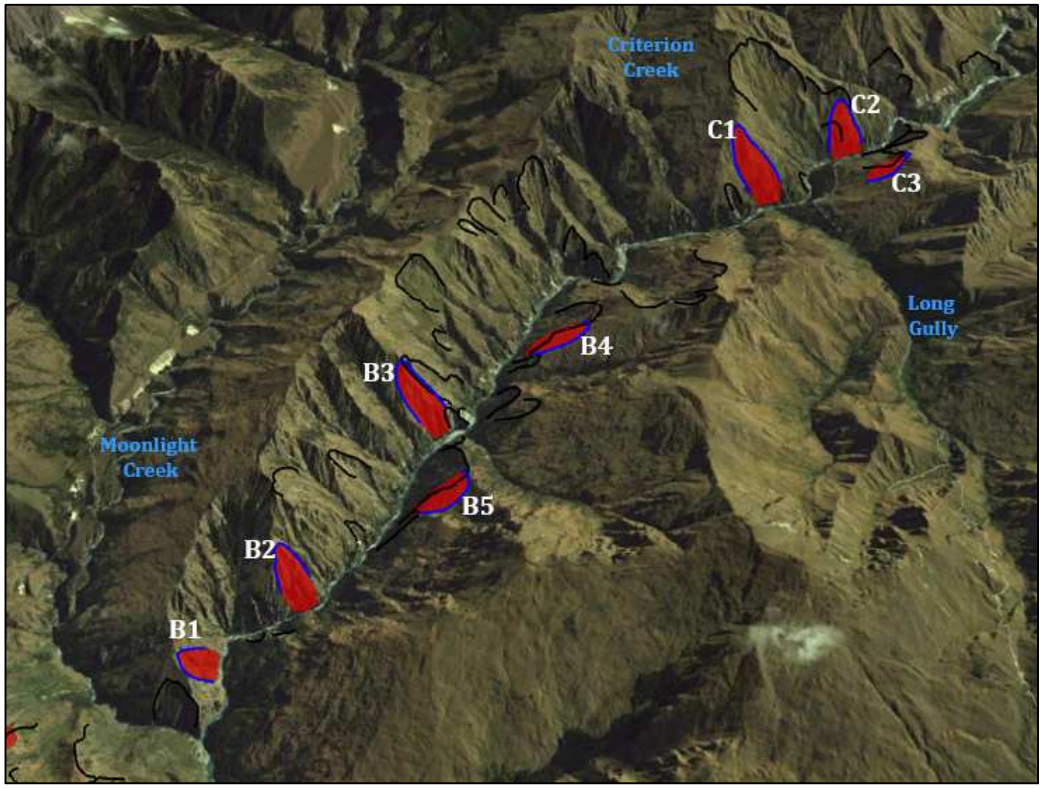

Figure 6. 4B *Oblique view of lower (Zone B) and middle (Zone C) Shotover Gorge landslide scenarios. View is towards the north-northwest. Black outlines indicate existing landslide scarps. (Google Earth 2010).*

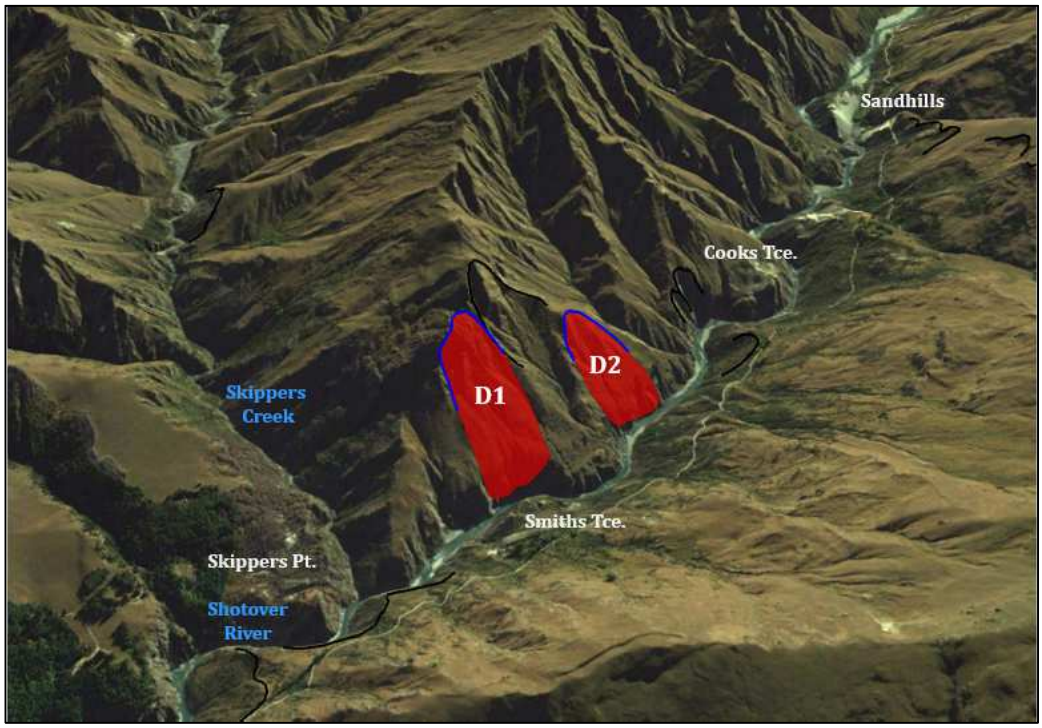

Figure 6. 4C *Oblique view of upper Shotover Gorge (Zone D) landslide scenarios. View is towards the northwest. Black outlines indicate existing landslide scarps. (Google Earth 2010).*

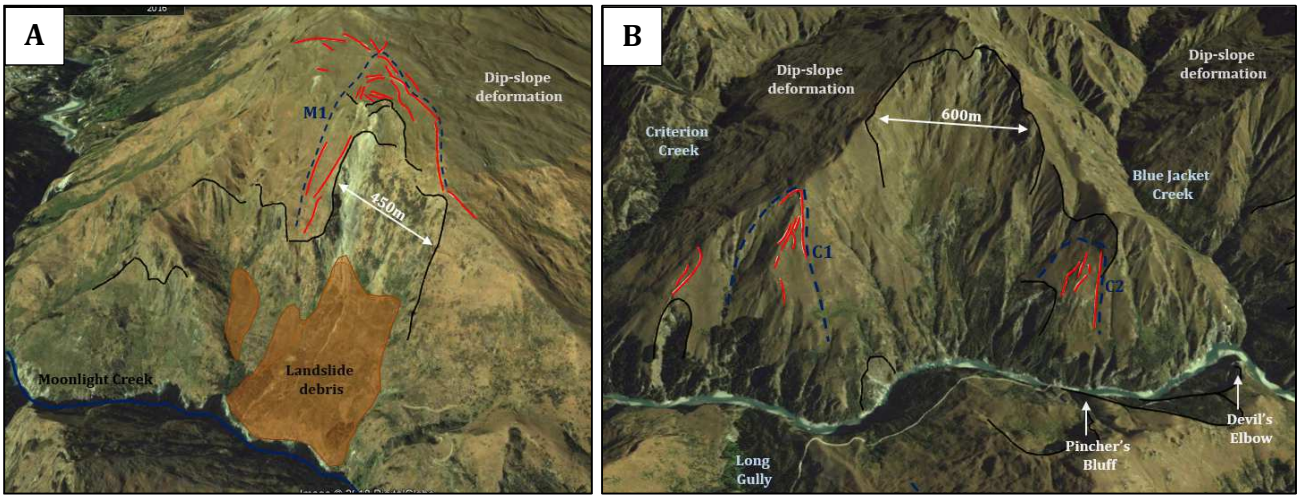

Figure 6. 5 *A. Detail of Moonlight (Zone M) and B. Zone C landslide scenarios (C1, C2), showing large existing landslide scarps (black lines), and cracking and ground deformation (red lines) indicating ongoing slope instability. (Google Earth 2010).*

Figure 6. 6 *Example of slope undercutting in the upper Shotover Gorge at about the location of scenario D1. The steep cliffs are 80-90 m in height and are interpreted to have formed by fluvial incision during the postglacial period.*

Landslide Volume Estimation

A simple method of estimating landslide volume is the use of an empirical relationship defined from landslide inventory data (Guzzetti 2009). These are typically power-law relationships with the form $V = \alpha A^{\gamma}$: Where V is landslide volume in m^3, A is landslide planform area in m^2, α is a dimensional coefficient, and γ is a scaling exponent. Four of these relationships have been assessed for suitability to use in Shotover Gorge estimations, these are;

1. $\boldsymbol{V = 0.05\ A^{1.5}}$ Hovius et al. (1997): based on a study of nearly 5000 rainfall-triggered landslides in the western Southern Alps.
2. $\boldsymbol{V = 0.146\ A^{1.332}}$ Larsen et al. (2010): based on >4000 global landslides.
3. $\boldsymbol{V = 0.074\ A^{1.450}}$ Guzzetti et al. (2009): based on 677 globally distributed landslides (excludes soil/debris slides and flows).
4. $\boldsymbol{V = 0.769\ A^{1.250}}$ Guzzetti et al. (2009): using data from Whitehouse (1983) for rock avalanches in greywacke in the eastern Southern Alps, with areas of 5×10^4 to 3.86×10^6 m^2.

The suitability of these equations has been assessed by comparing results of these equations with modelled volumes of a number of existing Shotover Gorge landslides (Figure 6.7). Volume estimates have been made for six of the better-defined Shotover Gorge landslide scarps by GIS modelling. A triangulated (TIN) surface was created for an approximate pre-failure slope surface and volume estimates obtained by a difference calculation from current topography. These slides cover a wide magnitude range, and include one small, four moderate sized landslides (0.6-1.7 M m^3) and two larger landslides (approximately 10-20M m^3). The smallest landslide is the 2008 Moonlight Track rockfall, which is plotted using the landslide volume estimated by GNS (2008). Based on the fit with modelled Shotover landslide points, the most appropriate equation for use in the Shotover area appears to be the Hovius et al. (1997) relationship, while

Guzetti et al. (2009) would also give satisfactory results. The relationship developed by Hovius et al. (1997) was based on rainfall-triggered landslide events in the western Southern Alps. The Shotover Gorge study area may differ from that Southern Alps study area in some climatic and geological factors, and earthquake-triggered landslides are also possible, but the relationship appears to provide a suitable approximation for estimation of landslide volume.

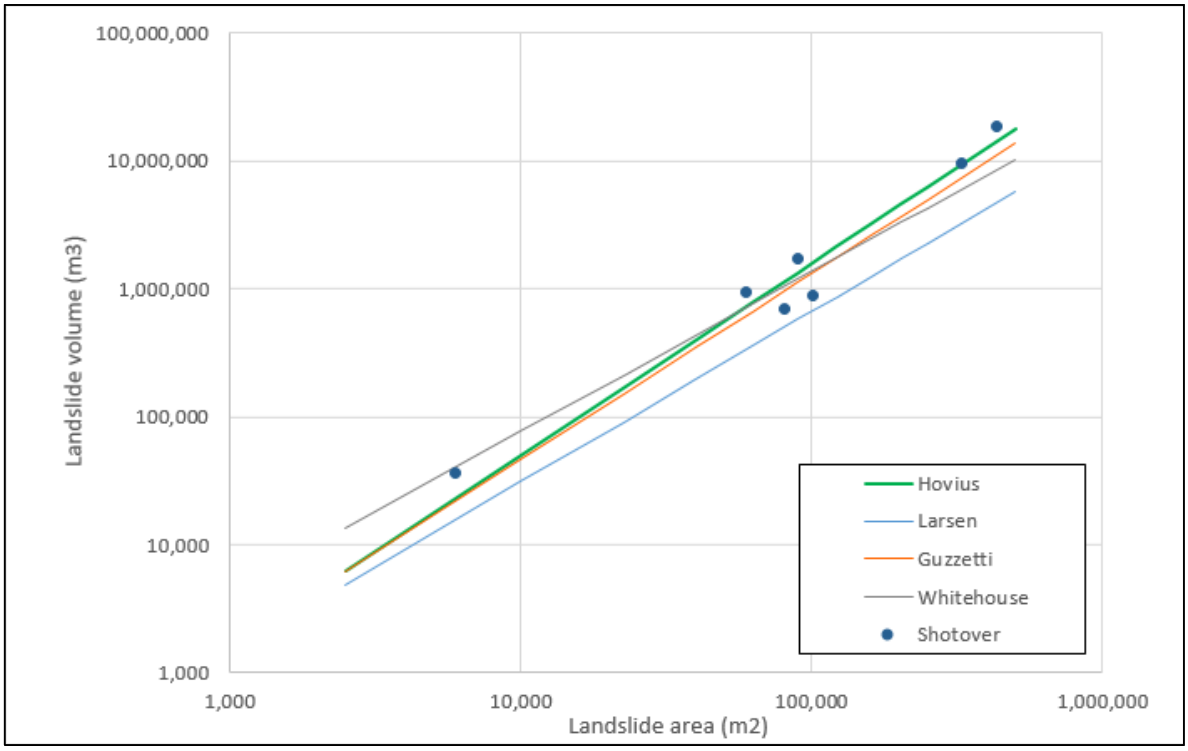

Figure 6. 7 *Examples of empirical landslide area-volume relationships, and comparison with modelled volumes for selected Shotover Gorge landslides.*

6.3 Landslide Frequency

Prediction of the size or frequency of future large landslide or landslide-damming events is difficult, as these are infrequent events, with few occurring within the relatively short period of historical records. The record of prehistoric landslide or landslide dam events is of limited usefulness (Korup 2005a, Moon et al. 2005), being incomplete due to erosion, obscuring of evidence by vegetation, and undersampling of events in remote locations. Even the identified landslides typically have unknown formation dates, and may not include evidence of extreme rare events. Korup (2005a) concluded it was not possible to use frequency distributions to determine return periods for a landslide dam or lake of a given volume, due to issues of erosional censoring, undersampling, and a lack of landslide dams with known formation dates.

Despite these limitations, it is possible to develop magnitude-frequency relationships for landslide events, based on the fact that landslides and other natural hazard events typically follow a well-defined size-frequency relationship (e.g. Malamud et al. 2004). This landslide frequency relationship may be able to be used as a guide to frequency of potentially dam-forming landslides. This section gives an overview of landslide power-law distributions (e.g. Figure 6.8), and an example of development of this relationship from an incomplete landslide inventory dataset (Figures 6.9 and 6.10). A

dataset of Shotover Gorge landslides has been compiled (Figure 6.11), and is used to develop a magnitude-frequency plot (Figure 6.12). Assuming many of the landslides are located near enough to the river channel to have had significant channel interaction, this distribution can be used to approximate the frequency of landslide dam formation in the gorge.

Landslide Power-Law Distributions

Many potentially hazardous natural events have nonlinear size-frequency relationships, often characterised as an inverse power-law. The best-known of these is the Gutenberg-Richter relationship between earthquake magnitude and frequency. Such distributions have also been identified for events such as landslides, landslide or moraine dammed lakes, wildfires, windstorms, landslide and fault grain-size distributions, turbulence (e.g. Turcotte et al. 2005, Korup and Clague 2009).

For landslides, this magnitude-frequency relationship has a characteristic form (Figure 6.8), where magnitude is reported as either landslide area or volume (Hovius et al. 1997, Stark and Hovius 2001, Malamud et al. 2004, Catani et al. 2016). For medium to large landslides, the frequency-area distribution decays as an inverse power of the landslide size, while at smaller sizes, this distribution has an exponential 'rollover' showing under-representation of events at smaller magnitudes. This apparent undersampling of smaller events may be a censoring effect caused by evidence of smaller events being more rapidly removed or obscured, or a mapping artefact due to the scale of images used in identification (Stark and Hovius 2001). Alternatively, this rollover is interpreted as a real feature of the distribution, and only partially an artefact of inventory data (Malamud et al. 2004).

This relationship can represent the distribution of landslides resulting from a single triggering event, such as an earthquake, snowmelt or storm. If the landslide probability distribution resulting from a single event follows this power-law behaviour, then the sum of landslide distributions from multiple events will also follow the same distribution. An inventory of historic landslides resulting from multiple events and of unknown age can therefore be assumed to also satisfy power-law behaviour (Malamud et al. 2004). Rockfalls form a different distribution with a power-law but no lower end rollover (Malamud et al. 2004).

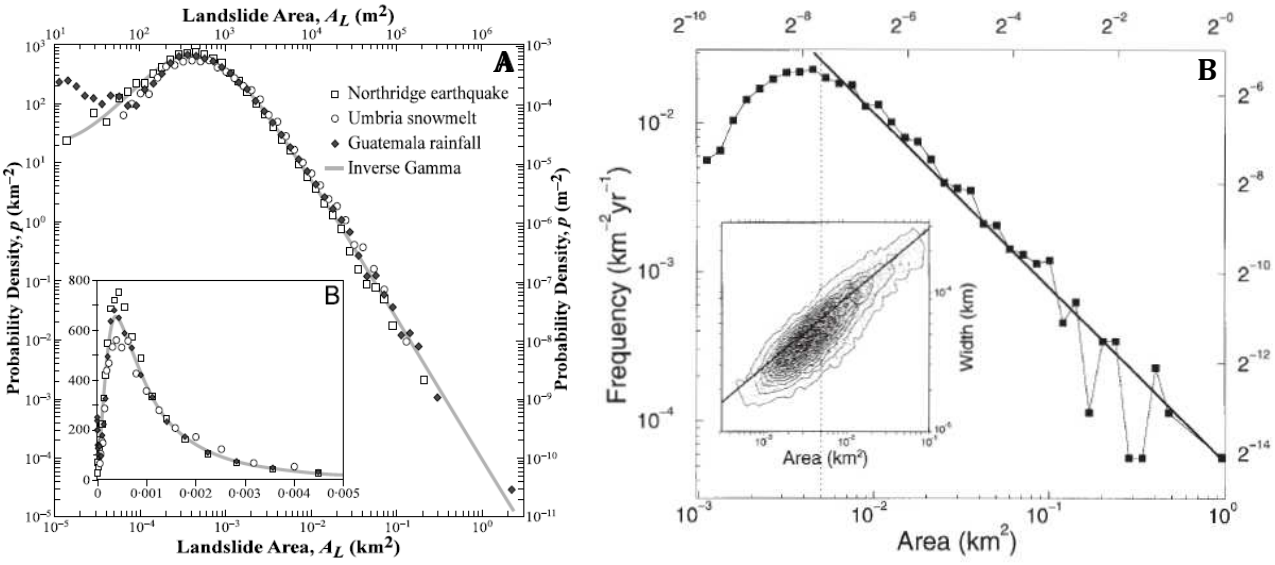

Figure 6. 8 *Examples of landslide magnitude-frequency distribution plots from A. Malamud et al. (2004), and B. Hovius et al. (1997).*

Ideally, an accurate hazard estimation requires a largely complete event inventory of events with known ages. Moon et al. (2005) discuss the development of a landslide distribution from an incomplete record and use of this distribution for hazard assessment (Figure 6.9). Landslide inventory datasets typically have better evidence at the lower and higher ends of the size range. Smaller, more frequent events are well represented as these are either observed or their evidence has not yet been removed from the landscape. Evidence for larger, infrequent events persists in the landscape for longer periods and is also more easily documented. For hazard assessment, there are two key size parameters to consider (Moon et al. 2005);

1. Critical landslide size: This is the size below which landslides are unlikely to cause a significant hazard, based on an evaluation of the elements or locations at risk.
2. Maximum credible landslide size: A function of the slope's geometry and dimensions, geology and failure mechanisms.

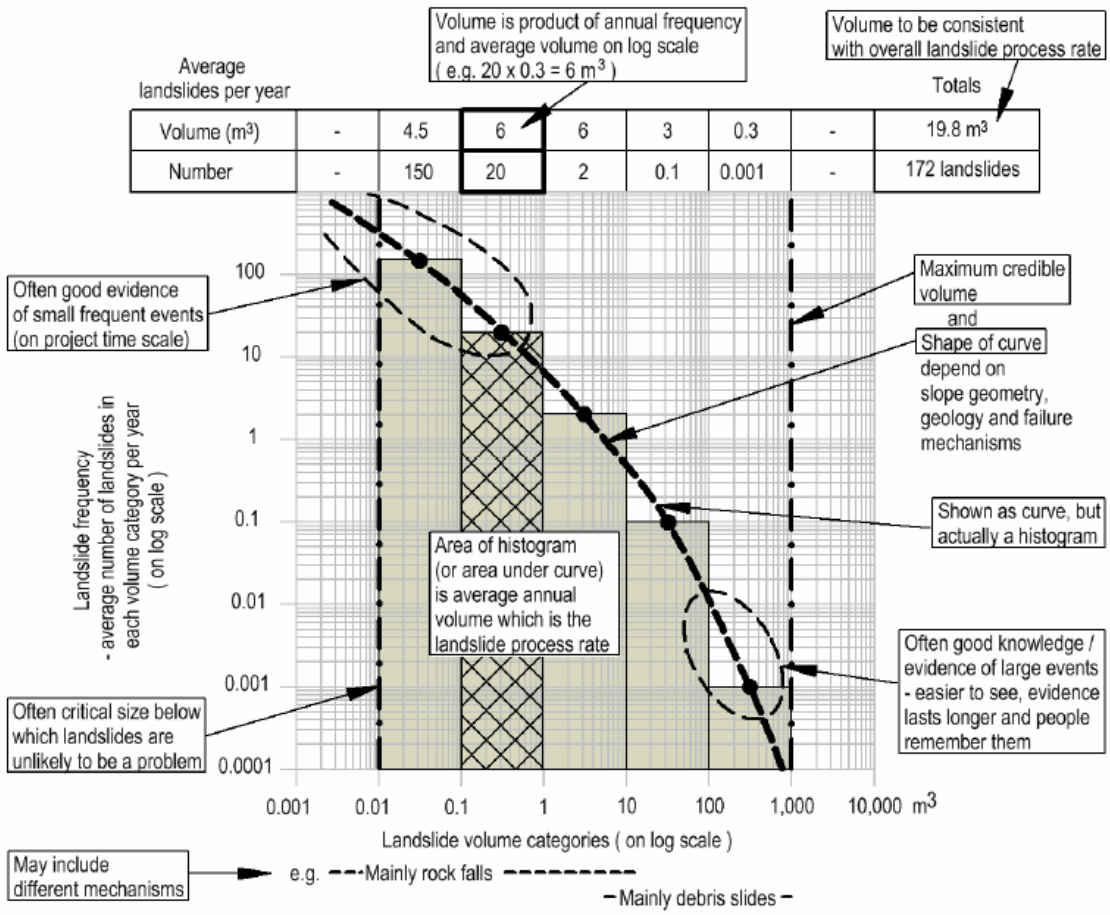

Figure 6. 9 *An example of development of a hypothetical landslide frequency distribution, showing critical size and maximum credible landslide size thresholds. The frequency curve is estimated from the plotted histogram (Moon et al. 2005).*

An example of the development of a landslide probability distribution is the study of Moon (1997) at the Roxburgh Gorge, assessing rapid landslides with potential to form a landslide dam (Figure 6.10). This was used as a guide to methodology for this study and is briefly summarised below. This Roxburgh study evaluated a 56 km section of lake

frontage, of which 35 km contains existing landslide activity. The largest landslide in this dataset is the 6M m^3 Rip Rockslide, which may be a failed landslide dam (McFarlane and Roberts 2001). An estimated average rate of slope movement (2 mm/year), was used to estimate the annual rate of volume loss from rapid landslide failures, most of which was assumed to result from small failures. The oldest landslides are assumed to be up to 400,000 years old, based on regional landslide studies (e.g. McSaveney et al. 1991). The critical size landslide was estimated at 0.3M m^3, thought sufficient to form a landslide dam with a height of about 10 metres, and the maximum credible landslide volume was estimated to within an order of magnitude (10-100M m^3). Results of the Roxburgh study are summarised in Figure 6.10 (Moon 1997). The landslide frequency envelopes in Figure 6.10 were used to estimate the probability of landslide dam formation. For landslides greater than the estimated critical landslide volume, it was thought that 70% of landslides would be emplaced rapidly enough to form a landslide dam. It was assumed that any larger (>1M m^3) landslide would form a landslide dam, while smaller (0.1-1M m^3) landslides were estimated to have a 50% probability of a landslide dam resulting. Estimated probabilities of landslide dam formation for the Roxburgh Gorge ranged from one in 3000-60,000 years, with a best estimate of 1 in 12,000 years.

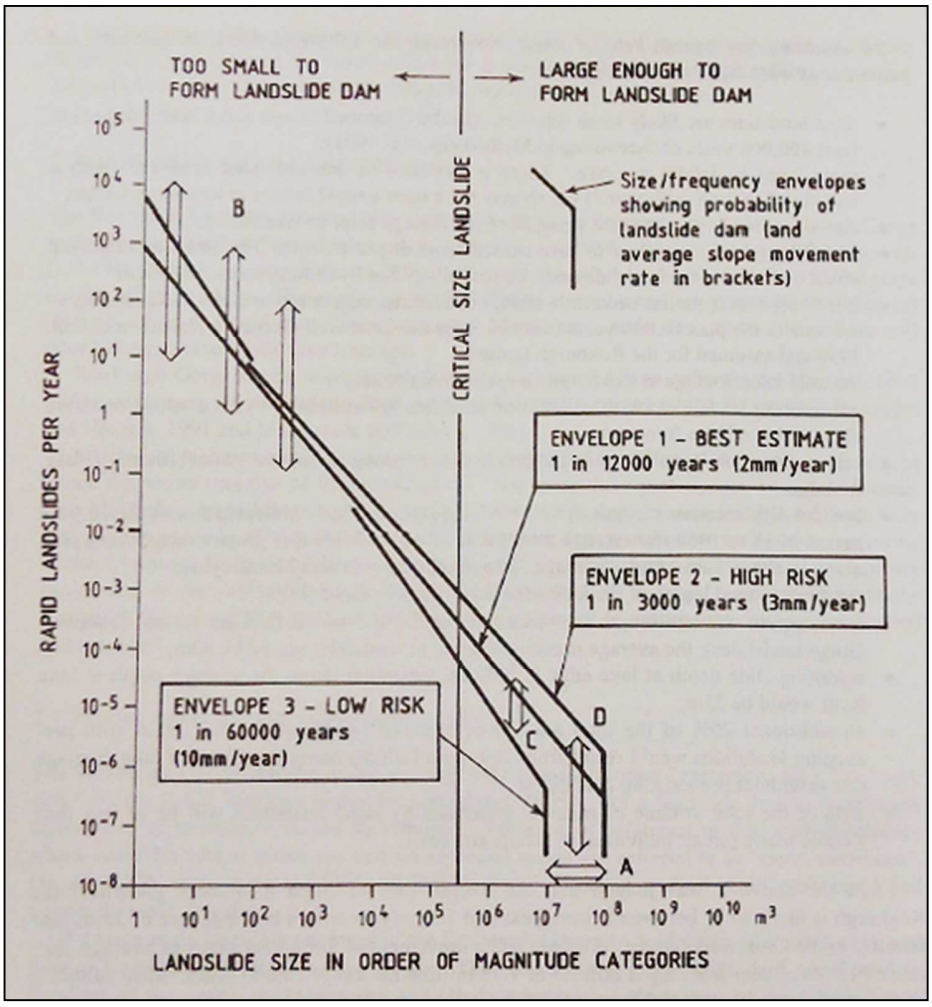

Figure 6. 10 *Roxburgh Gorge landslide frequency distribution and landslide dam hazard assessment by Moon (1997). 'Critical landslide' magnitude is indicated, and 'maximum credible' landslide volume is shown by Arrow A with an order of magnitude uncertainty. Arrow C indicates frequency range for 1-10M m^3 landslides, Arrow B indicates the considerable uncertainty (three orders of magnitude) in the estimated frequency rate of small landslides (<1000 m^3).*

Shotover Gorge Magnitude-Frequency Relationship

For the Shotover Gorge study area, a landslide magnitude-frequency distribution has been created (Figure 6.12), and used as a guide to the frequency of potentially dam-forming landslides. This has been based on a dataset of digitised landslide scarps adjacent to the Shotover Gorge from Arthurs Point to about Sandhill Cut, and including the lower Moonlight Creek as far upstream as Sheepyard Terrace (Figure 6.11, Table 6.2). The dataset (n=127) includes all well-defined scarps on slopes adjacent to the gorge, where landslide debris is considered to have potentially impacted the river channel. In order to assess landslide frequency, assumptions have been made regarding landslide age, with mapped landslide scarps grouped into three age categories;

1. **Recent:** Four smaller landslides of known age; 1993 Criterion Creek (Bryant 2011), 2008 Moonlight Track (Bryant 2011), 2009-2010 Moonlight Creek (Google Earth) and 2012 Devil's Elbow (Downer 2013). Another dam-forming landslide has been historically recorded (an 1871 event noted in Appendix 4), but its location and size are not known, so it cannot be included.
2. **Postglacial:** Assumed formation within the last 10,000–20,000 years; landslides assumed to have been formed since degradation of the valley's LGM sediment infill and incision of the modern gorge. Most are located within the incised gorge, some forming minor landslide deposits at the channel margins.
3. **Older/unknown:** Assumed formation within last 100-200,000 years; landslides of unknown age, mostly those larger scarps located higher on the valley slopes. Assumed ages are based on inferred initiation of creeping landslide activity elsewhere in the Otago region (Willetts 2000, McFarlane 2009).

Table 6.2: *Summary of landslide dataset (n=127), classified by landslide area and inferred age.*

	Historic	**Postglacial**	**Unknown**
Assumed maximum age (Years)	25-50	10-20k	100-200k
Landslide Area (m^2)	**Count**		
<10k	3	13	2
10-31.6k	1	25	20
31.6-100k	0	13	21
100k-316k	0	1	23
316k-1M	0	0	4
1M-3.16M	0	0	1

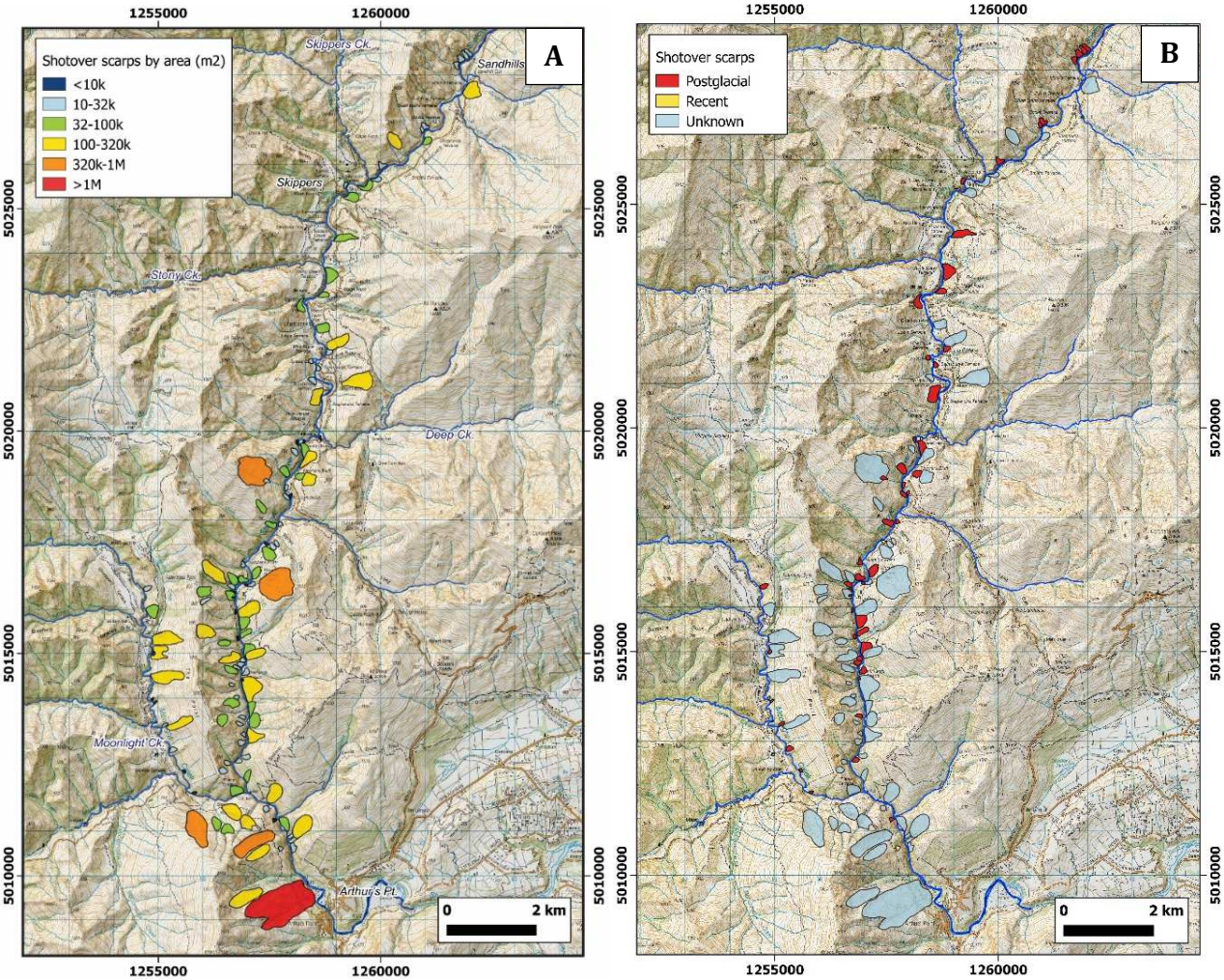

Figure 6. 11 *Shotover Gorge landslide dataset, showing landslides classified by area (A) and assumed age (B).*

A landslide frequency plot was developed based on the examples of Moon (1997) and Moon et al. (2005), shown as Figure 6.12. Landslides were classified in logarithmic bins based on landslide source area, then landslide counts converted to frequencies based on estimates of the assumed maximum age of that age class. Landslide frequencies of age classes were summed and plotted as a histograms, then used to create the frequency envelope as shown in landslide magnitude-frequency plot (Figure 6.12).

Critical landslide size is the landslide volume below which the hazard is unlikely to be a problem, this was estimated assuming the most significant hazard is a damaging dambreak flood affecting the lower Shotover River. Based on modelling in chapters seven and eight, this is estimated to be a landslide dam of about 40 m in height (Table 7.3) , capable of generating a dambreak flood wave equivalent to a 100-year flood at the lower Shotover Gorge exit. Modelled 40 m height dams (Zones A, B, C) have volumes of 270-500,000 m^3, equivalent to a critical landslide area of 30-46,000 m^2, estimated using the landslide area-volume equation of Hovius et al. (1997).

The upper Shotover catchment contains two very large landslide dams, formed by the Lochnagar (690M m^3) and Polnoon Burn (140M m^3) landslides, classified as 'giant' landslides (>100M m^3) by Hancox and Perrin (2009). In the Shotover Gorge study area, slope lengths and possible fall heights are less than at the sites of these deposits, so events

of this magnitude are not thought possible. However, there is evidence for larger landslide events in the gorge area, for example the 40M m³ Arthurs Point landslide (Willetts 2000), and several Shotover Gorge and Moonlight Creek landslides estimated as 10-20M m³ in volume (Figure 6.7). The maximum credible landslide volume in the Shotover Gorge is estimated at 30-60M m³, equivalent to a landslide source area of 0.7-1.1M m² (Figure 6.12).

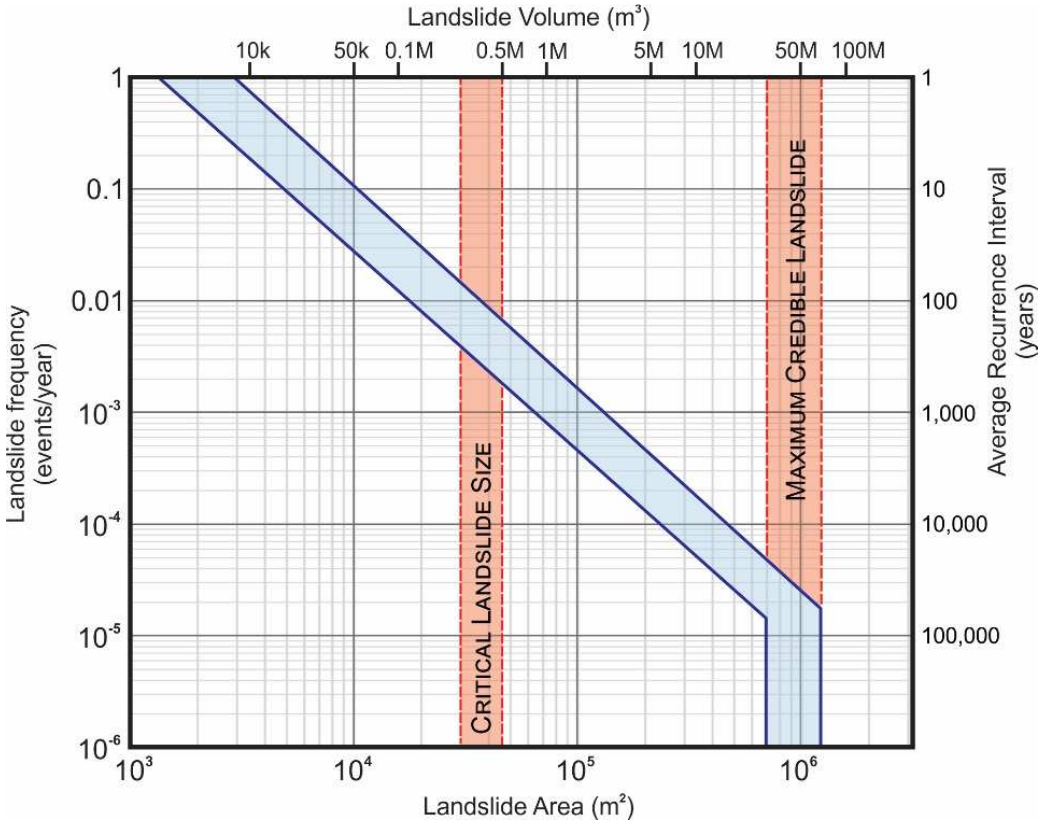

Figure 6. 12 *Shotover Gorge landslide magnitude-frequency plot, developed based on landslides shown in Figures 6.11 and Table 6.2.*

Table 6.3: *Shotover Gorge landslide frequency, estimated from Figure 6.12.*

Landslide Volume (m^3)	**Frequency** (events/year)	**RI** (years)
Critical landslide (270-500k m^3)	10^{-2} - 10^{-3}	100-1,000
1M m^3	$2x10^{-3}$ - $4x10^{-4}$	500-2,500
5M m^3	$4x10^{-4}$ - 10^{-4}	2,500-10k
10M m^3	$2x10^{-4}$ - $5x10^{-5}$	50-20k

Shotover Gorge landslide frequency estimates have been compared to two other landslide frequency distributions (Table 6.4); Hovius et al. (1997) in the central Southern Alps, and Moon's (1997) study in the Roxburgh Gorge area. The Hovius et al. study was based on mapped landslide occurrences from aerial photographs over the period 1948-1986.

For comparison with Southern Alps data, Shotover landslide frequency rates have been converted to a per area rate, based on a 70 km^2 Shotover Gorge study area. Compared with Hovius et al.'s (1997) estimated landslide frequency rates for the Southern Alps (Figure 6.8B, Table 6.4), Shotover Gorge landslides are estimated to occur an order-of-magnitude less frequently. Compared to Moon's (1997) Roxburgh Gorge assessment (Figure 6.10), Shotover Gorge landslides are estimated to occur an order-of-magnitude more frequently. These values are presented as events/year, but are over comparable size areas; the Roxburgh Gorge study of ~35 km of lake frontage with existing landslides, and this study of ~25-30 km total length of the Shotover and Moonlight valleys.

Table 6.4: *Comparison of Shotover Gorge landslide frequency with the South Island studies of Hovius et al. (1997) in the Central Southern Alps, and Moon (1997) for the Roxburgh Gorge.*

Landslide Area	**Landslide Frequency** Events/km^2/year	
	Central Sth. Alps Hovius et al (1997)	Shotover Gorge
10^4 m^2	$1x10^{-2}$	$1x10^{-3}$ to $4x10^{-4}$
10^5 m^2	$8\ x10^{-4}$	$3x10^{-5}$ to $6x10^{-6}$
10^6 m^2	$5\ x10^{-5}$	$7x10^{-7}$ to $1x10^{-7}$

Landslide Area	**Landslide Frequency** Events/year	
	Roxburgh Gorge Moon (1997)	Shotover Gorge
10^4 m^2 (~50k m^3)	10^{-2} to 10^{-3}	10^{-1} to 10^{-2}
10^5 m^2 (~2M m^3)	10^{-4} to 10^{-5}	10^{-3} to 10^{-4}
10^6 m^2 (~50M m^3)	10^{-5} to 10^{-6}	10^{-4} to 10^{-5}

The large differences in estimated landslide occurrence rates between these Southern Alps, Shotover and Roxburgh studies may in part be due to differences in study methodologies, but likely indicate real differences in landslide frequency rate between these areas, related to the relative uplift and erosion rates. Erosion rates are very high in the rapidly uplifting (up to 10 mm/year), high rainfall (to 14 m/year), steep topography of the Southern Alps (Hovius et al. 1997, Korup et al. 2004), compared to the less tectonically active, arid Central Otago landscape at Roxburgh. Estimation of a Shotover Gorge landslide frequency rate between the Southern Alps and Roxburgh studies indicates results are within a reasonable order of magnitude, as the Shotover Gorge is located in an intermediate location in terms of uplift (2-4 mm/year, Upton et al. 2009) and rainfall rates.

The estimation of landslide frequency is difficult when based on an incomplete landslide inventory containing landslides of unknown age, and requiring estimation of uncertain parameters. Due to these significant errors and approximations, results are thought accurate only to within an order of magnitude. However, as a first approximation of landslide frequency in the Shotover Gorge, these results appear to be reasonable when compared to other studies. This indicates that landslides of sufficient volume to cause a significant landslide dam hazard may occur on average at intervals of a few thousand years. A landslide of 1M m^3 volume has an estimated return period of 500-2500 years, or an annual probability in the order of ~0.1%.

6.4 Shotover Catchment Landslide Dams

A review of landslide dam occurrences in the Shotover catchment has identified about twenty large landslide dams, most with landslide volumes estimated at >1M m^3 (Figure 6.13). These have been compiled from a literature review and a search of aerial imagery, and are summarised in Appendix 3. Landslide dam locations are reasonably well distributed throughout the catchment, although a larger number are found in the upper parts of the catchment, upstream of Branches Flat. The largest recorded landslide dams are the Lochnagar and Polnoon Burn dams (>100M m^3), but another six are estimated to have landslide volumes of >10M m^3.

Notably there are no large (>1M m^3) landslide dam deposits identified in the Shotover Gorge area, despite the presence of several of large landslide scarps with estimated volumes of >10M m^3 located adjacent to the river channel (Figure 6.11). This is interpreted as being due to fluvial censoring of the Shotover Gorge landslide dam record, rather than the absence of landslide dam formation in this area. Most of the Shotover catchment landslide dams identified are located in tributary streams and/or headwaters locations. In these locations, streams have lesser flows, contributing to increased preservation of the former landslide dam. Most of these preserved landslide dams are in locations thought to have been glaciated during the LGM, so can be assumed postglacial in age.

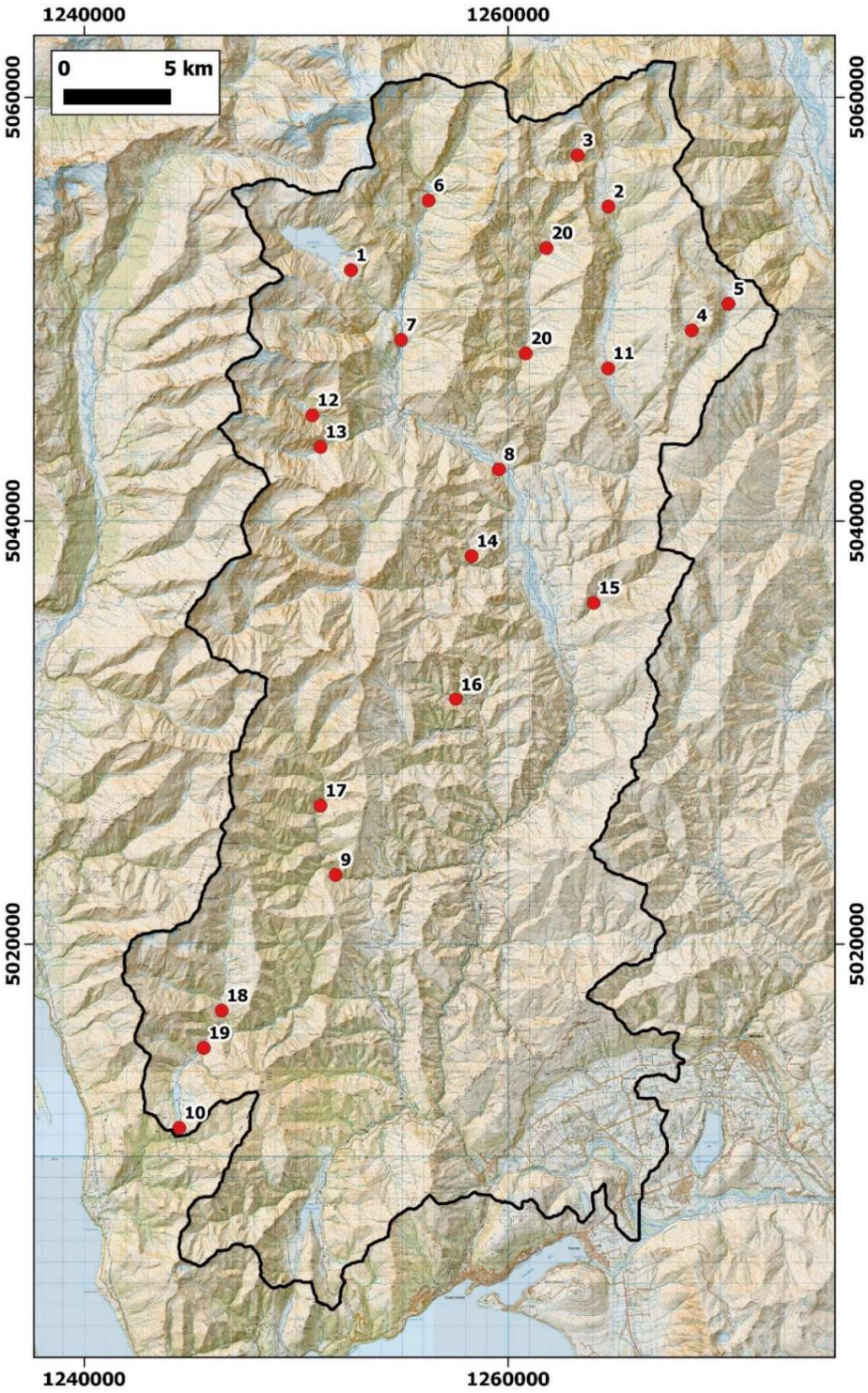

Figure 6. 13 *Large landslide dam occurrences in the Shotover catchment, identified from literature and a search of aerial imagery. The largest landslide dams are the Lochnagar (1) and Polnoon Burn (2) landslide dams. Black outline shows the Shotover catchment. Landslide dams shown as examples within the text are the Shotover River at Saddle Creek (8, Figure 6.1A), Stony Creek (9, Figure 6.1B), Moonlight Creek (18, Figure 6.2), and Stockyard Creek (15, Figure 9.8). Brief descriptions of all of these dams are given in Appendix 3.*

6.5 Summary and Conclusions

The Shotover Gorge is considered susceptible to landslide dam formation, with steep slopes adjacent to a narrow river channel and evidence for many past slope failures and ongoing instability. While there is no evidence preserved for large (>1M m^3) landslide dam events in the Shotover Gorge, these have occurred in many locations elsewhere in the Shotover catchment (Figure 6.13, Appendix 3). The presence of landslide scarps of comparable dimensions in the Shotover Gorge (Figure 6.3) suggests geological and structural conditions suitable for occurrence of a dam-forming landslide of this magnitude. Formation of landslide dams in the Shotover Gorge is demonstrated by smaller historical occurrences, such as the 1993 Criterion Creek (Figure 2.33A) and a historically reported 1871 landslide dam in the Sutherlands Beach area (Appendix 4). While relatively small, these were of sufficient size to temporarily block the Shotover River's flow for several hours.

Zones of possible landslide dam formation have been identified in the Shotover Gorge and at Moonlight Creek, and landslide scenarios are developed within these zones (Figures 6.3, 6.4). It is estimated that dam-forming landslides of >1M m^3 volume are possible in all Shotover Gorge zones, with the largest landslides estimated in the lower Shotover Gorge and Moonlight Creek where slope lengths are greater (Table 6.1).

These landslide scenarios are estimated as reasonable values for future landslides originating within these zones and have been used in landslide dam modelling (Chapter Seven) and dambreak flood estimations (Chapter Eight). A landslide magnitude-frequency distribution for the Shotover Gorge shows that landslides of ~1M m^3 may have an annual likelihood in the order of 0.1% (Figure 6.12), and this may approximate the rate of landslide dam formation for events of this size.

The largest existing landslide scarps in the Shotover Gorge have volumes estimated at 10-40M m^3, so future magnitudes of this magnitude are thought possible. These are less frequent, having an annual probability in the order of 0.01-0.001% (Figure 6.12), but would be expected to form a very large landslide dam.

Chapter Seven: Landslide Dam Modelling

7.1 Introduction

This chapter outlines the development of landslide dam scenarios for the Shotover Gorge. Landslide dam models have been created for each of the zones identified in the previous chapter, with model results used to investigate the relationships between dam and lake parameters (Figures 7.4 and 7.5). Based on modelled landslide dams and the landslide volumes estimated for scenarios in Chapter Six (Table 6.1), landslide dam scenarios have been created to represent possible landslide dam events. The geomorphic dam and reservoir parameters estimated for these landslide dam scenarios have been used to analyse several aspects of the landslide dam hazard, these are;

1. An assessment of landslide dam stability using empirical stability indices (Figure 7.7).
2. Estimation of the time to fill for modelled reservoirs (Table 7.5, Figure 7.9), as an approximation of the minimum warning time for a sudden dambreak event.
3. Estimation of breach characteristics and modelling of dambreak flood magnitudes (Chapter Eight).

7.2 Modelling Details

Landslide dam models were created for representative locations within each of the zones identified in the previous chapter (Figures 6.3 and 7.2). Within Zone C the gorge is narrow in the Criterion Creek-Long Gully area, becoming slightly wider upstream of this point, and two models (C, C2) were created to account for this variation (Figure 7.2B). Triangulated dam surface (TIN) models were created in ArcGIS for a range of five dam magnitudes (20, 40, 60, 100, and 150 metre dam heights) at each location, shown in Figure 7.2. Modelling assumptions are discussed below, including the landslide bulking factor and dam slope angles. Dam volumes were calculated using a difference calculation from a triangulated topographic surface, and other dam parameters were measured in GIS.

Landslide Bulking and Dam Volume

The volume of a landslide dam may be lower or higher than the volume of the initial landslide, depending on substrate entrainment, fragmentation and bulking effects, and material remaining on slopes above the dam location, but in general, the dam volume is approximately equal to landslide volume (Kumar 2018). Landslide debris may significantly expand in volume when converted from an in-situ rock mass to transported debris, this volume increase is termed the 'bulking factor'. Hungr and Evans (2004) note the unreliability of many estimates of the bulking factor, as an accurate calculation requires measurement of both source and deposit volumes. They compiled published volume increase estimates ranging from 7-26%, using a value of 25% (bulking factor 1.25) in their study of rock avalanche deposits. However, if the rock mass is already dilated prior to failure, this value may be significantly less than 25%. Other landslide dam investigations have used bulking factor values of 1.2-1.4 (Yetton and McMorran 2004), and 1.33 (Arshad et al. 2004).

The volume increase due to landslide bulking is approximately balanced by the fact that not all landslide debris contributes to dam formation, with landslide debris deposited above the level of the lowest point on the dam crest not contributing to damming. Ermini and Casagli's (2003) plot of landslide and dam volumes shows a wide variation in proportion of landslide volume involved in dam formation, ranging from near to 100% to less than 1% (Figure 7.1). Arshad et al. (2004) assumes 66% of landslide material contributes to dam formation, based on example of Poerua River landslide dam. In a high-relief area such as the Shotover Valley, there is little storage capacity for landslide debris

on steep slopes, so the majority of debris is expected to be transported to the river channel. For modelling purposes it is assumed 70-80% of landslide debris contributes to dam formation, and the in-situ landslide volume can be approximated as equivalent to dam volume.

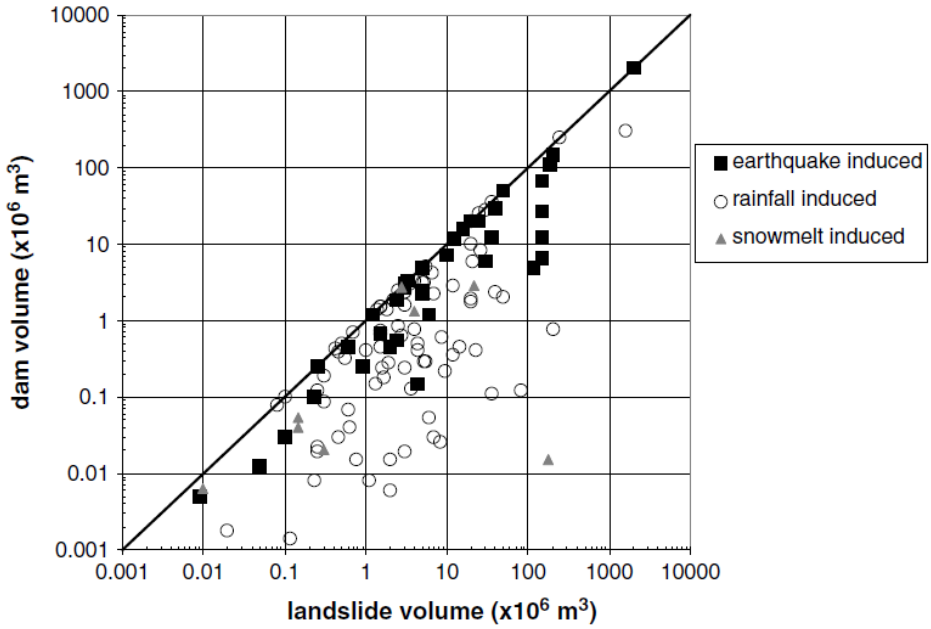

Figure 7.1: *Plot of landslide dam volume vs landslide volume for a dataset of 143 landslide dam case studies (Ermini and Casagli 2003). The solid 1:1 line shows where landslide dam and landslide volumes are equal, i.e. the total landslide volume contributes to dam formation.*

Landslide Dam Slope Angles

There is a wide variation in recorded slope angles for landslide dams, with dam geometry being influenced by valley morphology, speed and mobility of landslide emplacement, and the physical properties of the landslide debris. Murchison and Inangahua landslide dams have slope angles averaging 8-10°, although these may have been modified during dam failure and subsequent erosion (Nash 2003). Ollett (2001) modelled landslide dams in the Callery Gorge with slope angles of 7-20° upstream and 15-22° downstream, based on results of small-scale modelling, and calibrated against three case study dams. The 1999 Poerua River landslide dam had slope angles of 12° (upstream), and 24° (downstream) (Hancox et al. 2005). As the Poerua River dam was formed in a narrow schist gorge similar to the Shotover Gorge study area, these values will be used in landslide dam modelling.

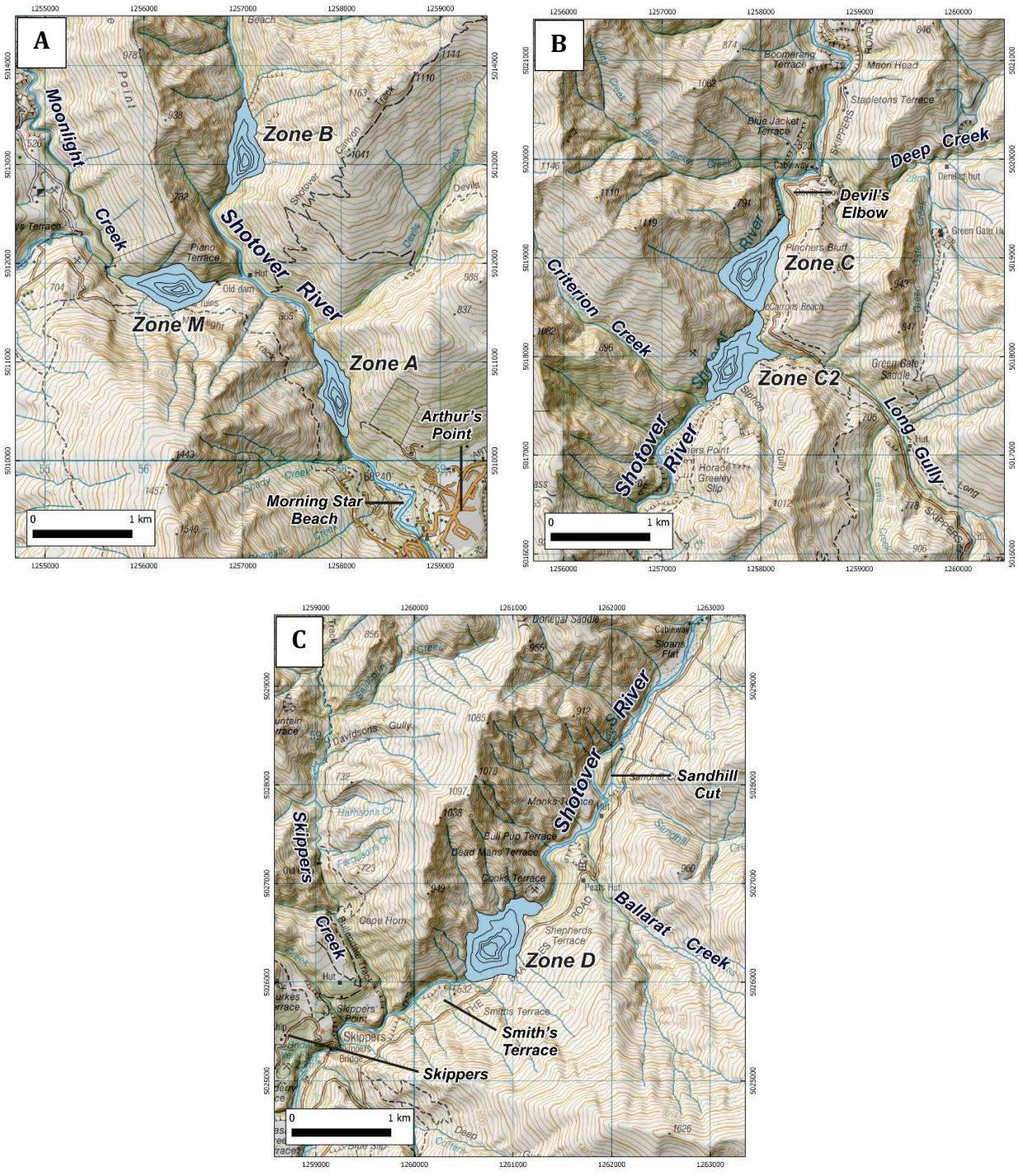

Figure 7.2: *Outlines of modelled landslide dams in; A. lower Shotover Gorge and Moonlight Creek, B. middle Shotover Gorge, and C. the upper Shotover Gorge. Outlines show dam footprints for modelled dam heights of 20, 40, 60, 100 and 150 metres.*

Landslide Dam Lake Modelling

Reservoir modelling assumes the lake has been completely filled to the height of the dam crest, and forms a straight dam crest across the valley. This method implies a vertical dam wall, and overestimates the lake volume, as the upstream dam volume within the lake area is not taken into account (Korup 2005a). Korup (2005a) addressed the issue of overestimation of lake volume by developing an empirical 'dam displacement factor' based on New Zealand landslide dam case studies and hypothetical modelled dams, this negative correlation coefficient was applied to provide a corrected lake volume.

In this study, modelled lake volumes have been corrected to account for the upstream dam volume. This correction was calculated by modelling and subtracting the upstream portion of the dam from the lake volume to provide a corrected volume. Modelled upstream dam volumes (Zones A, C, D and M) varied from 52-72% of the total dam volume, with a mean value of ~62%. This value was used to estimate corrected lake volumes for the remaining models (Zones B, C2), where;

*corrected lake volume = uncorrected lake volume – (dam volume*0.62)*

For the Shotover Gorge landslide dam models, lake volumes are relatively large compared to dam volumes and the impact of this correction is minor, with the subtracted dam volumes mostly <2.0% of the uncorrected lake volume. In the Moonlight Creek dam models, the dam volume was relatively larger compared to the lake volume and this correction factor was correspondingly larger (4-9%).

Examples of modelled reservoirs are shown in Figure 7.3, demonstrating the influence of valley width on lake geometry and volume. Lower Shotover Gorge dam models result in lakes confined within the narrow gorge (Figure 7.3A), while middle and upper gorge lake models extend into the broad Branches Flat basin and have much larger volumes (Figures 7.3B, C).

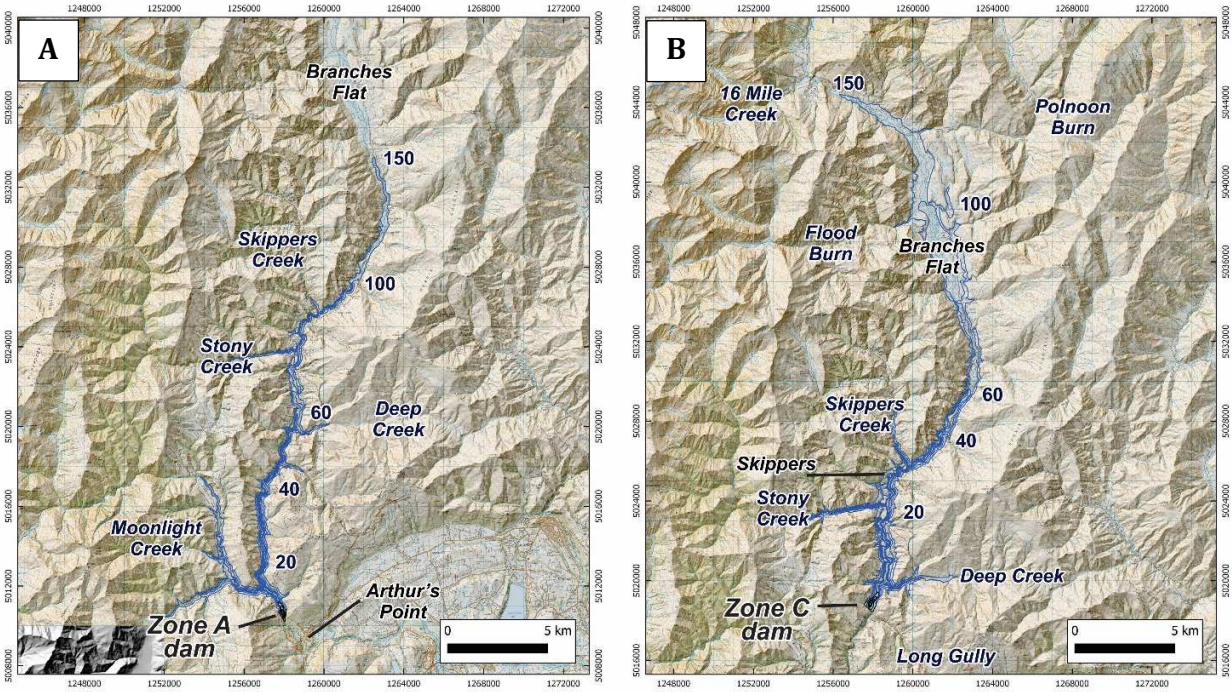

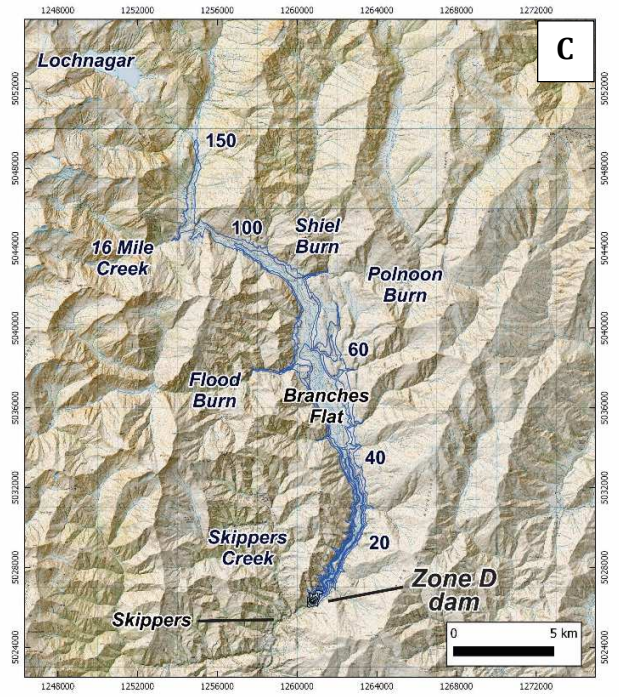

Figure 7.3: *Modelled landslide dammed lakes for; A. lower Shotover gorge (Zone A), B. mid Shotover Gorge (Zone C), and C. the upper Shotover Gorge locations (Zone D), showing lake extents for dams with heights of 20-150 m.*

7.3 Landslide Dam Scenarios

The main geomorphic parameters used to describe landslide dams and landslide-dammed reservoirs are shown in Table 7.1 and Figure 5.3. For each landslide dam and reservoir model, these parameters were estimated, with results summarised in Table 7.2. Model results are summarised below as plots showing the relationship between landslide dam height and dam volume (Figure 7.4), and reservoir volume (Figure 7.5).

Model results illustrate the influence of valley morphology on the dam geometry, showing that a single dam height-volume relationship cannot be applied to all locations (Figure 7.4). In locations with a narrow valley such as at Moonlight Creek and lower Shotover Gorge (Zones A, B, M) a smaller volume of landslide debris is required in order to block the valley. Where the valley is wider (e.g. Zone D) a larger landslide volume is required to form a blockage of the same height. For example, in the lower Shotover Gorge (Zone A) a landslide volume of 1M m^3 will form a dam of about 65 m height, while in the upper Shotover Gorge (Zone D) it requires a volume of >2M m^3 to form a dam of the same height (Figure 7.4).

Table 7.1: *The main geomorphic parameters used to describe landslide dam and lake models, these parameters are also shown schematically in Figure 5.3.*

Landslide Dam

Height	H_D	Maximum crest height
Length	L_D	Maximum across-valley dam length
Width	W_D	Maximum along-valley dam width
Volume	V_D	Landslide dam volume

Landslide-Dammed Lake

Length	L_L	Maximum lake length
Width	W_L	Maximum lake width
Area	A_L	Lake area
Volume	V_L	Estimated lake volume

Upstream Catchment

Area	A_C	Catchment area upstream of dam location

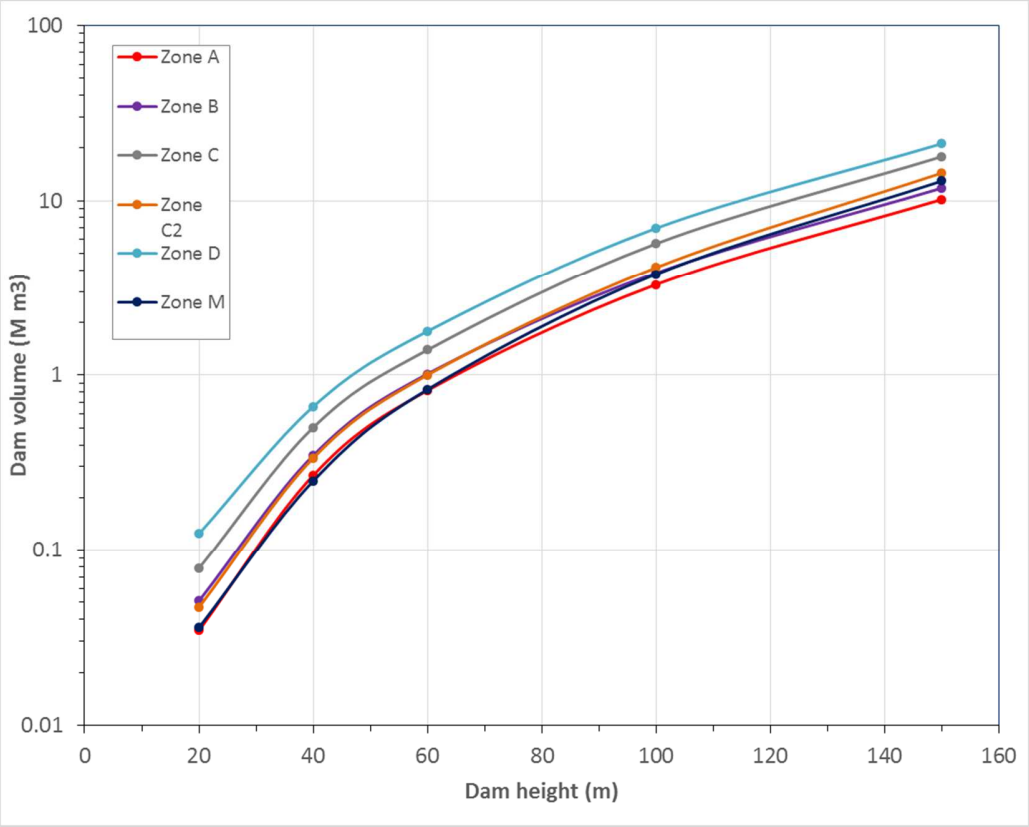

Figure 7.4: *Semi-log plot of dam height vs dam volume for modelled landslide dams. This plot shows the highest dams for a given dam volume formed in Zones A, B, C2 and M, while in Zones C and D the equivalent dam volume forms significantly lower dams.*

Lake volumes are dependent on the dam height, valley width and channel gradient. Figure 7.5 shows a plot of modelled lake volumes for each modelled scenario. Of these modelled landslide-dammed lakes, the larger volume lakes are those which fill the wider upper gorge, and especially those which extend to Branches Flat (Zones C, D) (Figure 7.5). Moonlight Creek has a steeper gradient than the Shotover River, forming lakes with a reduced length and volume in comparison to Shotover Gorge scenarios. Korup (2005a) notes the poor correlation between dam volumes and reservoir volumes, with up to three orders of magnitude variance in lake volume for a given dam volume. These hypothetical dams show a similarly poor correlation, with greater than one order of magnitude variance in lake volumes between modelled zones for a similar dam height.

The landslide scenario volumes estimated in Chapter Five (Table 6.1) and the relationships in Figure 7.4 have been used to estimate the dam heights in landslide dam scenarios for each model zone (Table 7.2). These dam heights are then used with Figure 7.5 to estimate reservoir volumes for model scenarios in each zone (Table 7.2).

The highest landslide dam scenario is located in the lower Shotover Gorge below the Moonlight Creek confluence (Zone A). This is due to the larger slope lengths and estimated landslide volumes in this area, and a narrow gorge resulting in formation of a relatively tall dam for this landslide volume. In the lower Shotover Gorge above Moonlight Creek (Zone B), and the middle Shotover Gorge (Zone C) landslide scenarios have smaller volumes, and landslide dam scenarios have resulting dam heights of ~80 metres (Table 7.2). In the upper Shotover Gorge (Zones D) slope lengths and estimated landslide volumes are smaller, and landslide dam scenario has an upper dam height of about 60 metres. Moonlight Creek (Zone M) is the largest volume landslide scenario, but it is assumed much of this material will be deposited on the valley slopes and will not contribute to dam formation. Assuming only 20% of landslide volume forms a landslide dam, the dam height is estimated at ~90 m.

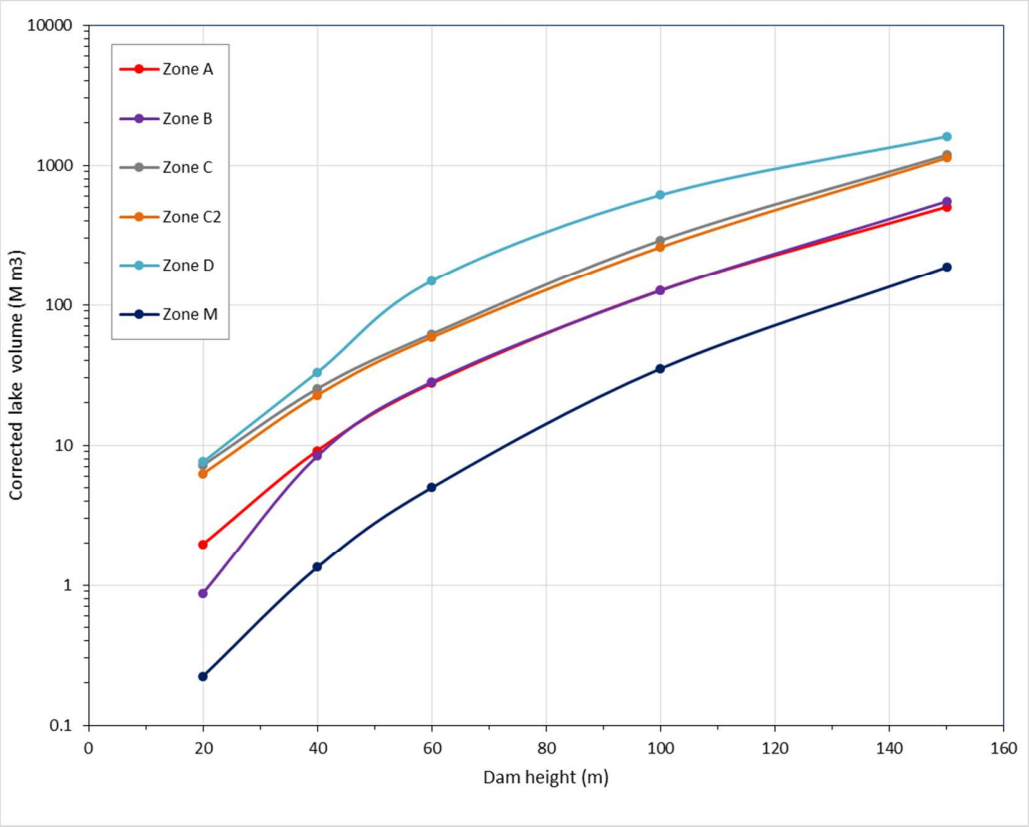

Figure 7.5: *Semi-log plot of dam height vs corrected lake volume for modelled landslide dams. This shows a variation of greater than an order of magnitude in lake volume for lakes formed by modelled dams with any given dam height.*

Shotover Gorge and Moonlight Creek landslide dam scenarios are plotted in Figure 7.6 and compared to global case studies reported by Korup (2004a). Compared to these case studies, modelled Shotover Gorge and Moonlight Creek landslide dam scenarios have relatively large dam heights for their dam volume, plotting near to an approximate dam height-landslide volume envelope curve (Figure 7.6). This is due to dam formation within a narrow gorge, and modelling of dams with relatively narrow crest widths and steep dam slopes. While these scenario parameters are within the realistic range, their location near the upper end of this envelope may indicate that some assumptions used in model construction have led to an overestimation of dam height. These models should be considered to approximate the maximum landslide dam height formed by a given landslide volume.

Table 7.3 compares parameters of selected Shotover Gorge and Moonlight landslide dam scenarios (60-100 m) with those documented for four recent South Island landslide dams of comparable magnitude. Modelled dam scenarios have relatively low dam volumes compared to these case studies. In the Shotover Gorge these landslide-dammed lake scenarios have relatively high lake volumes compared to those formed in steeper gradient mountain streams such as the Poerua River, Ram Creek or North Young River examples (Table 7.3).

Table 7.2: *Estimated dam and lake parameters for landslide dam scenarios.*

	Dam height	Dam volume	Lake Area	Lake volume	Catchment Area
	m	M m^3	km^2	M m^3	km^2
Zone A	20	0.03	0.21	2.0	1048
	40	0.27	0.64	9.2	
	60	0.82	1.37	28	
	80	1.8	2.50	63	
	100	3.3	4.21	127	
	125	6.6	7.97	294	
Zone B	20	0.05	0.21	0.9	845
	40	0.35	0.69	8.4	
	60	1.0	1.45	28	
	80	2.2	2.44	50	
Zone C	20	0.06	0.59	6.8	815
	40	0.42	1.37	24	
	60	1.2	2.67	60	
	80	2.6	6.70	128	
Zone D	20	0.12	0.66	7.6	599
	40	0.66	1.77	33	
	60	1.8	7.60	148	
Zone M	20	0.04	0.03	0.2	193
	40	0.25	0.11	1.3	
	60	0.83	0.31	5.0	
	80	2.0	0.74	11	
	90	2.8	1.01	20	

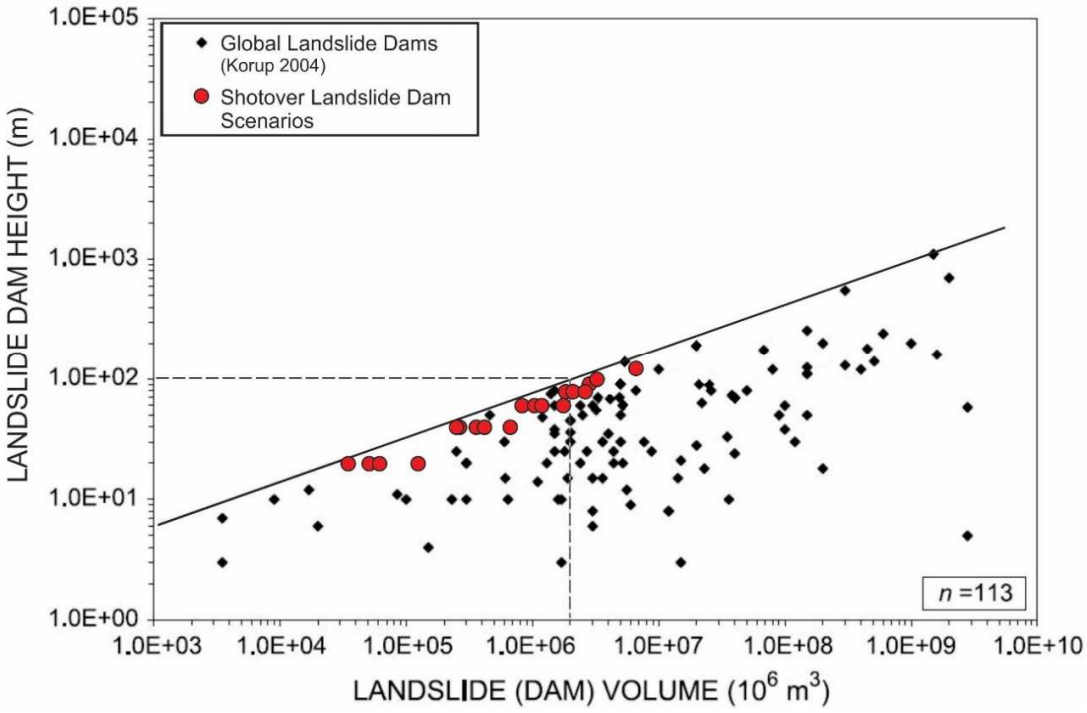

Figure 7.6: *Landslide dam height-volume plot for Shotover and Moonlight Creek landslide dam scenarios, compared to a dataset of 113 global landslide dams (modified from Korup 2004a).*

Table 7.3: *Comparison of New Zealand case studies with selected Shotover and Moonlight Creek landslide dam scenarios.*

	Dam Height	Dam Volume	Lake Volume	Catchment Area	Reference
	m	M m3	M m3	km2	
Poerua River	80-100	10-15	5-7	50	Hancox et al 2005, Korup 2006
North Young River	74	11	23	38	ORC 2012, Massey et al 2013
Ram Creek	40	2.8	1.1	4.5	Nash et al 2008
Hapuku	100	12	-	-	Dellow et al 2017
Shotover Scenario					
A60	60	0.82	28	1048	
A80	80	1.8	63	1048	
A100	100	3.3	127	1048	
C60	60	1.2	60	815	
C80	80	2.6	128	815	
Moonlight Scenario					
M60	60	0.8	5	193	
M80	80	2.0	11	193	
M90	90	2.8	20	193	

7.4 Landslide Dam Stability Analysis

Several approaches can be used to assess stability and hazard of landslide dams, the simplest of these being the use of an empirical relationship based on combinations of geomorphic variables, such as dam height or volume, lake volume or upstream catchment area. These indices show the balance between 'resisting' and 'disturbing' forces acting on the dam. Resisting forces are represented by the magnitude of valley blockage (dam height or volume), and removing forces by some proxy for stream power, often catchment area (Ermini and Casagli 2003, Korup 2004a).

These empirical relationships are based on datasets of documented landslide dams, with stability thresholds based on occurrence of intact and failed dams (e.g. Figure 7.7). Stability thresholds are specific to characteristics of dams from a particular area, and are not necessarily applicable to dams in a different region. Three commonly used indices are the Blockage Index, Impoundment Index (Casagli and Ermini 1999), and the Dimensionless Blockage Index (Ermini and Casagli 2003), referred to as the Dimensionless Impoundment Index by Korup (2004a). Figures 7.7A-C show these indices for a dataset of New Zealand landslide dams and the stability thresholds interpreted for these dams (Korup (2004a). Shotover Gorge and Moonlight Creek landslide dam scenarios (Table 7.2) are overlain on these stability plots (Figure 7.7), showing all modelled dam scenarios to be well below the stability thresholds in all of these indices.

In the Blockage Index (Figure 7.7C) and Dimensionless Impoundment Index (Figure 7.7B) the main factor influencing dam instability is the large upstream catchment area; 500-1000 km² for Shotover Gorge landslide dam scenarios, and nearly 200 km² for Moonlight Creek (Table 7.2). This results in high river power, and thus high erosive forces acting on dam. The relatively shallow gradient channel in the Shotover Gorge allows for formation of large volume landslide-dammed lakes, relative to the dam dimensions, which influences the expected instability in the Impoundment Index plot (Figure 7.7). Due to these factors, and illustrated by empirical stability plots, any landslide dams formed in these Shotover Gorge and Moonlight Creek locations have a high likelihood of failure and are expected to be unstable and relatively short-lived.

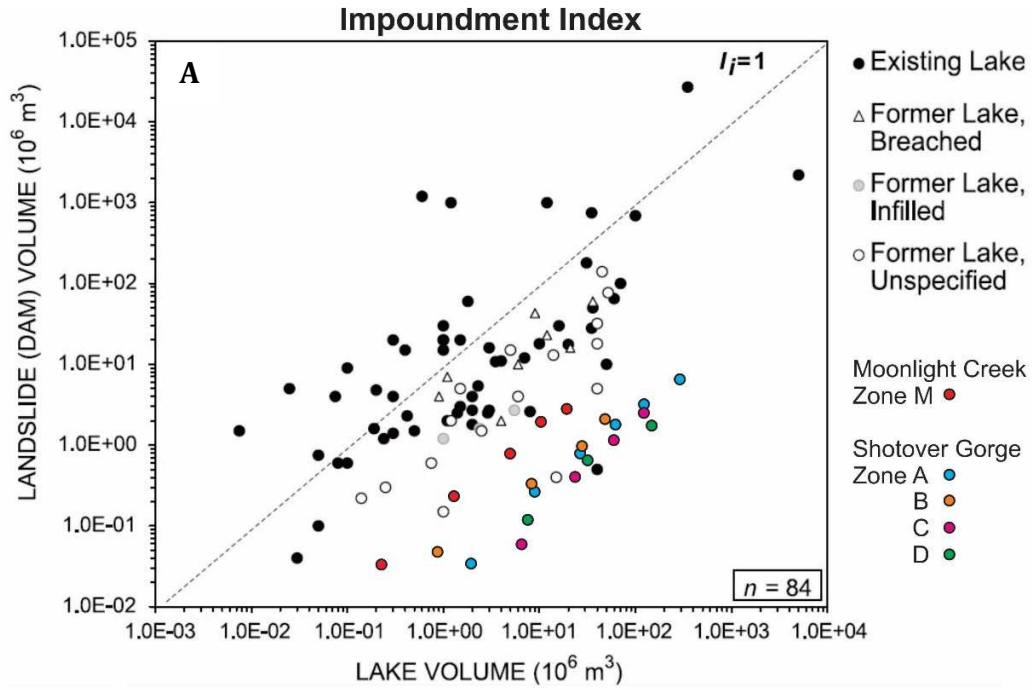

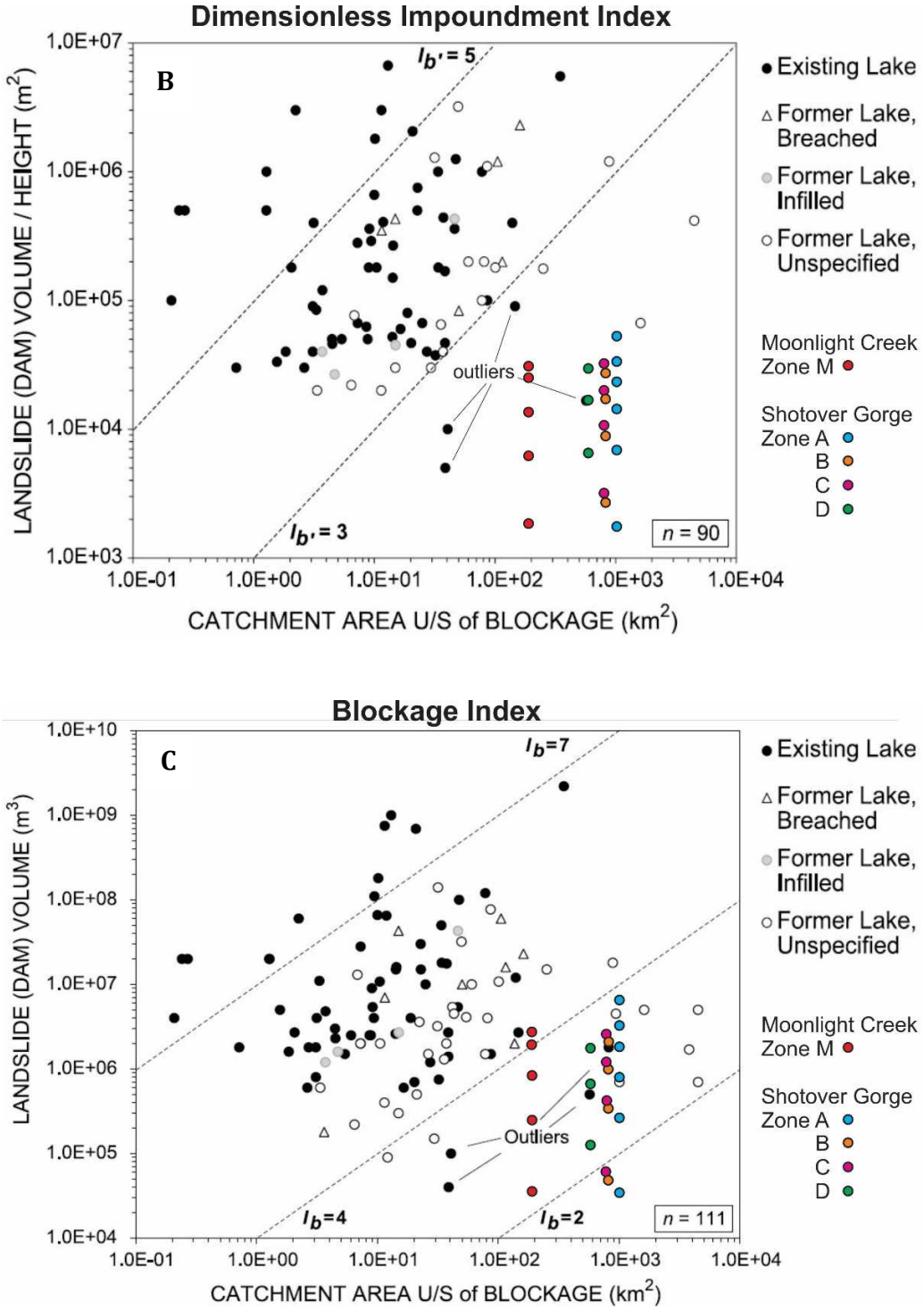

Figure 7.7: *Stability Indices for modelled Shotover Gorge and Moonlight Creek landslide dam scenarios (Table 7.2) compared to a dataset of New Zealand landslide dams compiled by Korup (2004a). Indices shown are A. Impoundment Index, B. Dimensionless Impoundment Index, and C. Blockage Index. (plots modified from Korup 2004a).*

7.5 Reservoir Time to Fill

The duration of filling of the landslide-dammed reservoir is an important factor in landslide dam hazard assessment. As many dams fail at their first overtopping, this duration gives an estimate of the minimum warning time which may be available for decision-making (Korup 2005a). Becker et al. (2007, p41) note, "the worst case scenario is a landslide dam caused by heavy rain on a saturated catchment at night. The dam may overtop before dawn, before anyone realises the river flow is anomalously low".

A Shotover Gorge landslide dam forming during daylight hours is expected to be identified by a dramatic decrease in the Shotover River's flow, because parts of the lower river are visible to commercial river users, residents and road users in the Arthur's Point and Shotover Delta areas. Even relatively small Shotover River blockages have been seen as downstream disturbances in river flow. The 1871 landslide dam reduced river flow for several hours, with the downstream flow noted as 'almost completely dry' and 'little more than ankle deep' (see historic accounts in Appendix 4). The 1993 Criterion Creek landslide dam caused a halving of river flow for a period of several hours (Bryant 2017).

The calculated time to fill these modelled reservoir volumes assumes all incoming river flow is retained behind the dam, and there is no loss due to seepage or evaporation. The simplest option for estimating inflows at each scenario location is to assume a river flow proportional to the total Shotover catchment area. However, analysis of one year of recorded flows from the Bowens Peak and Peats Hut flow recorders shows that the upper parts of the catchment contribute higher portion of flows relative to area (Figure 7.8). At the Peats recorder in the upper Shotover Gorge, the Shotover River captures runoff from 55% of the total catchment area, but flows range from 60-80% of the total catchment outflow measured at Bowens Peak (Figure 7.8). This is due to precipitation rates varying throughout the catchment, with a gradient strongly influenced by elevation (Figure 1.2).

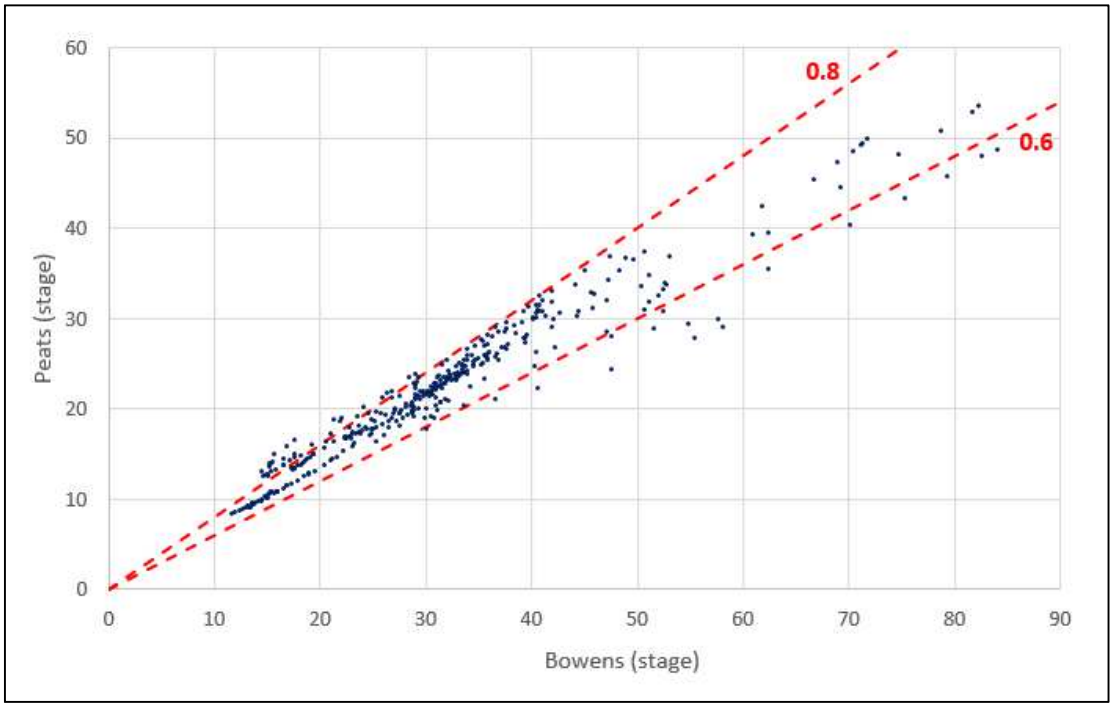

Figure 7.8: *Scatterplot of Shotover River stage heights at Bowens Peak and Peats Hut recorders. Trend lines are at 60% and 80% of the Bowens Peak flow (Data from August 2017-August 2018, 7-day rolling-mean, data provided by ORC).*

Table 7.4: *Estimated inflows used in 'time to fill' calculations for landslide dam reservoirs.*

	Catchment area (km^2)	% of Shotover catchment	Mean flow (m^3/s)	Mean annual flood (m^3/s)	50-year flood (m^3/s)
Zone A	1,048	96	41	420	1,046
Zone B	845	78	35	357	889
Zone C	822	76	35	357	889
Zone D	599	55	29	294	732
Zone M	193	18	6	63	157

Filling times are shown in Table 7.5 and Figure 7.9 for landslide dam reservoirs scenarios at mean annual flow, mean annual flood, and 50-year flood inflows. For dams with the same height, there is an order of magnitude variation in filling time between lower Shotover Gorge (Zone A, B) and upper Shotover Gorge (Zone D), mostly due to the large increase in lake volumes seen upstream as the valley becomes wider, but also due to reduced flows at locations further upstream. Filling times for Moonlight Creek dams are approximately the same as those in the lower Shotover Gorge (Zones A, B); the Moonlight Creek dams impound smaller volume lakes, but have correspondingly smaller inflows and thus similar filling times. Time to fill estimates during flood flows are clearly unrealistic for some of the largest volume reservoirs, as the duration of the flood peak will not last for longer than several days.

Based on these estimations (Table 7.5, Figure 7.9), at 50-year flood inflows, a dam of <50-60 m height could potentially form undetected, fill to capacity, and catastrophically fail within an overnight period (10-12 hours). Modeled dams of greater than 80 m height will likely take longer than 12 hours to fill, even at large flood inflows, and any dam of this magnitude is not expected to overtop and fail without its formation being identified.

Table 7.5: *Time to fill landslide dam reservoir scenarios under inflows of mean flow, mean annual flood, and 50-year flood flows.*

	Dam height (m)	Reservoir volume (M m3)	Time to fill reservoir (Hours)		
			Mean Flow	*Mean Annual Flood*	*50-year Flood*
Zone A	20	2.0	13	1.3	0.5
	40	9.2	62	6.1	2.4
	60	28	187	18	7.3
	80	63	424	41	17
	100	127	860	84	34
	125	294	1992	194	78
Zone B	20	0.9	7.0	0.7	0.3
	40	8.4	67	6.5	2.6
	60	28	225	22	8.8
	80	50	399	39	16

Zone C	20	6.8	54	5.3	2.1
	40	24	192	19	7.5
	60	60	480	47	19
	80	128	1020	100	40
Zone D	20	7.6	74	7.2	2.9
	40	33	320	31	13
	60	148	1435	140	56
Zone M	20	0.2	10	1.0	0.4
	40	1.3	61	5.9	2.4
	60	5.0	226	22	8.8
	80	11	479	47	19
	90	20	885	86	35

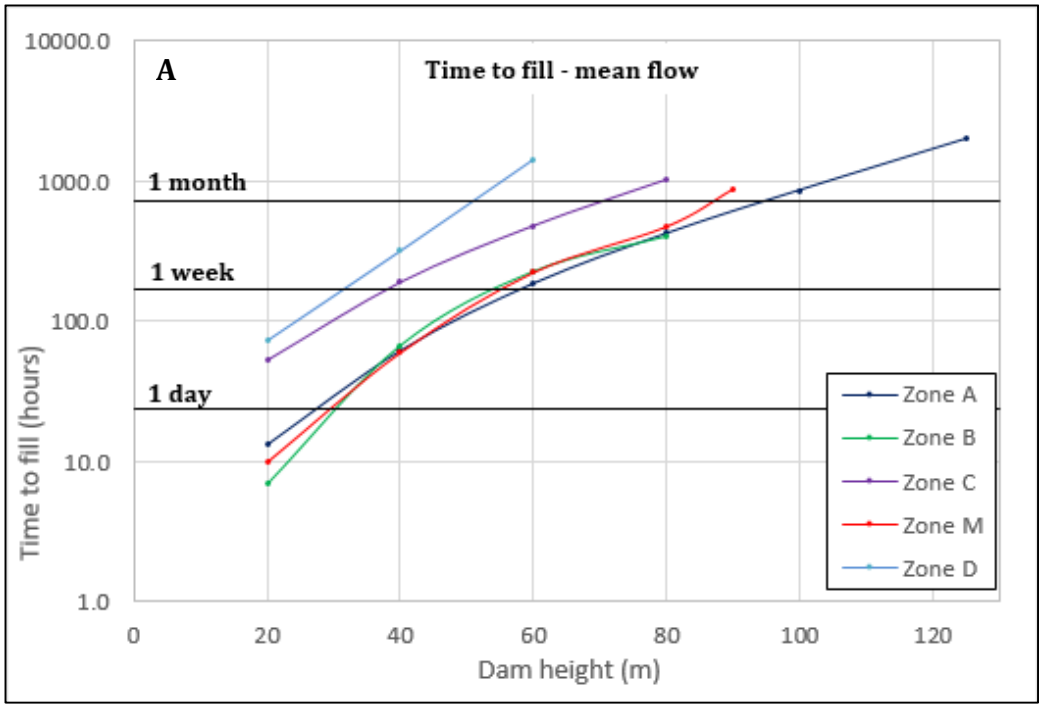

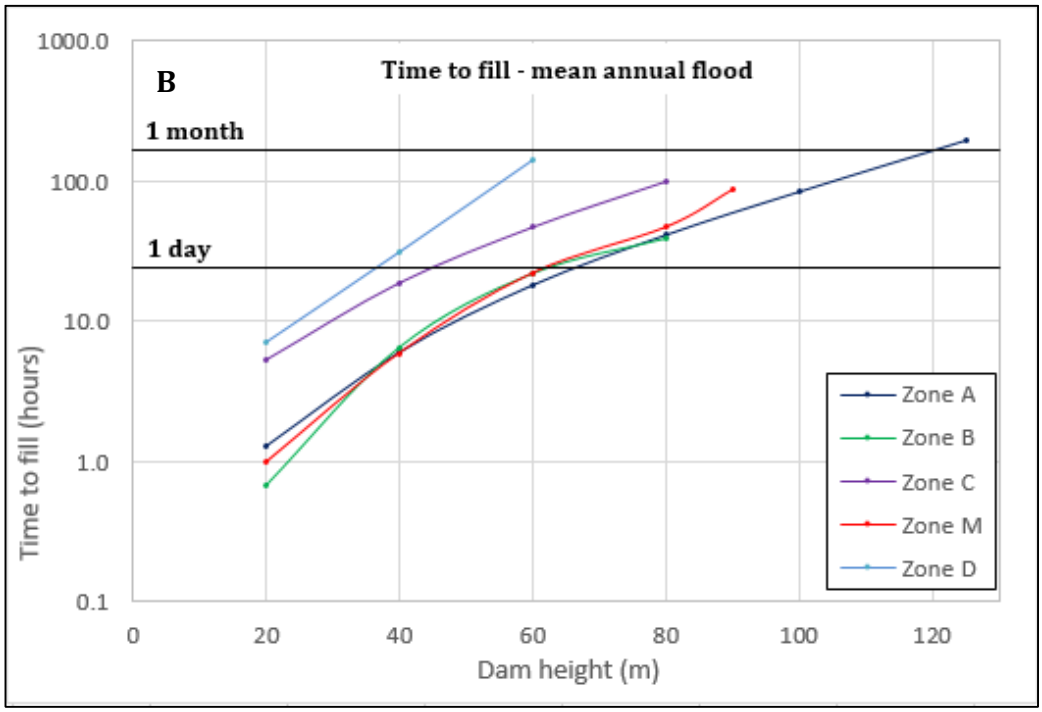

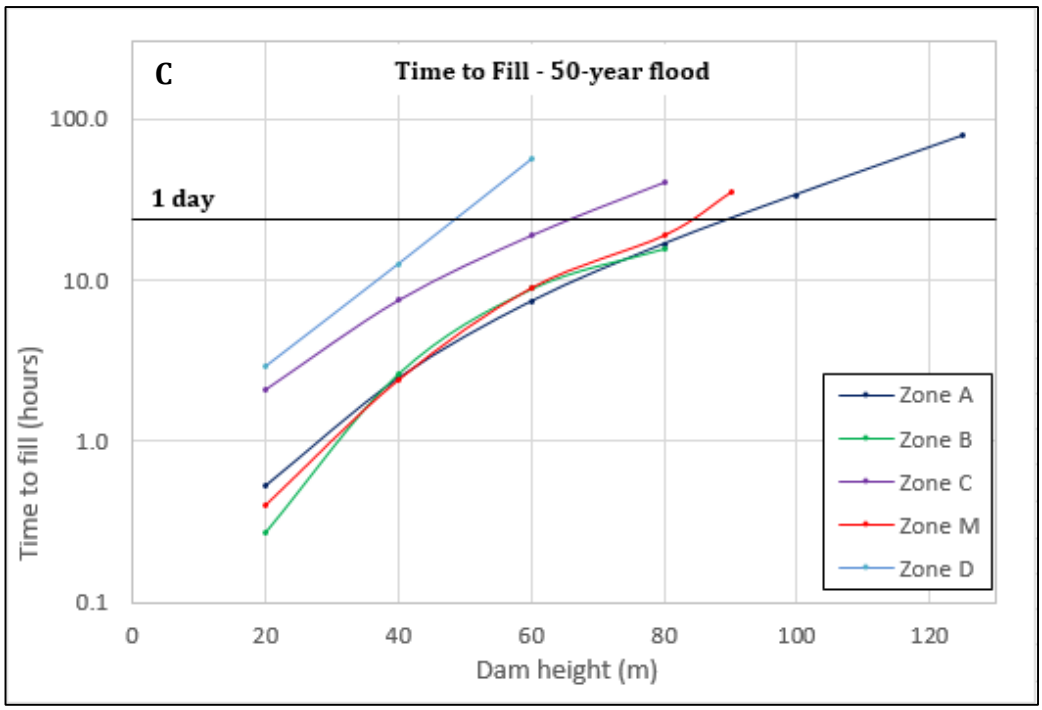

Figure 7.9: *Plots showing time to fill landslide dam scenario reservoirs under inflows of A. mean flow, B. mean annual flood, and C. 50-year flood flows.*

7.6 Summary and Conclusions

This chapter has developed landslide dam scenarios for locations in the Shotover Gorge and Moonlight Creek. These are based on GIS modelling of hypothetical landslide dams, used to investigate the relationships between the geomorphic landslide dam and reservoir parameters (Figures 7.4, 7.5), and landslide volumes estimated for landslide scenarios in the previous chapter (Table 6.1).

The influence of valley morphology on landslide dam dimensions can be seen in Figure 7.4, with the tallest dams relative to landslide volume formed in narrower valley locations such as the lower Shotover Gorge and Moonlight Creek. Compared to database of global landslide dams (Figure 7.6), and South Island landslide dam case studies (Table 7.3) these scenarios have relatively high dams compared to the landslide dam volumes involved. These are plausible scenarios but may represent about the maximum dam heights possible for a given dam volume. Reservoir volume is also strongly influenced by valley floor morphology, with the largest volumes formed for dam locations in the upper parts of the Shotover Gorge, where these lakes extend into the broad Branches Flat basin (Figure 7.5).

Landslide dam modelling has assumed a catastrophic slope failure, with the majority of the high mobility debris emplaced into the river channel, however, there are a number of possible alternative outcomes in the landslide and dam formation and geometry. For example a progressive or more gradual slope failure, or formation in a location where a larger proportion of landslide debris remains stored on the slopes. If the pre-failure landslide material has dilated and expanded through slope relaxation there may be significantly less bulking of landslide debris than assumed in modelling. Landslide dam geometry may also differ from the simplified morphology used in modelling, potentially with a broader dam crest or shallower slope angles which would result in a dam of lower height.

Stability indices (Figure 7.7) show an expected instability for all landslide dam scenarios, influenced by the large upstream catchment areas, and relatively large reservoir volumes. These dams are predicted to be unstable, likely failing either at their first overtopping, or during the next high flow event (as occurred at the Poerua River landslide dam in 1999). While these indices are only a guide to dam stability, being based on datasets with a large magnitude variation, and including dams located in a variety of different geomorphic and geological settings, the indication that dams in the Shotover Gorge are likely to fail is strong.

Time to fill calculations (Table 7.5, Figure 7.9) show that small-moderate sized dams of 50-60 m height could potentially fill within an overnight period during flood flows. This would result in a dambreak flood occurring with no prior warning for the downstream community. Any dam higher than this will take longer to fill, maybe days or weeks depending on infill rates. These larger dams may be capable of generating larger dambreak flows but are not expected to fail without being identified, thus allowing time for monitoring, warning, and possible evacuation.

Chapter Eight: Dambreak Flood Modelling

8.1 Introduction

Dambreak flooding is a major hazard associated with landslide dam formation, with potential for damaging impacts many tens of kilometres distant from the dam location, and generation of flood discharges many times greater than any known meteorological flood events at that location. Estimation of possible dambreak flood magnitudes is a common component of hazard assessments undertaken following formation of a landslide dam, for example at the Poerua River (Hancox et al. 2005, Becker et al. 2007) and North Young River (ORC 2007a) landslide dams. The same estimation methods have been used to assess dambreak flooding resulting from failure of a hypothetical future landslide dam, for example at the Callery Gorge (Davies and Scott 1997, Ollett 2001), Shotover Gorge (Bryant 2011), and in South Westland (Korup 2005).

This chapter estimates dambreak flows at the Shotover Delta, resulting from catastrophic failure of the Shotover Gorge and Moonlight Creek landslide dam scenarios developed in the previous chapters (Table 7.2). This is achieved through;

1. Estimation of peak outflows at breach location using empirical, dimensionless and parametric models (Table 8.3, Figure 8.8).
2. Estimation of breach characteristics such as breach depth, width and breach development time (Table 8.2).
3. Estimation of dambreak flood hydrographs at breach, based on estimates of peak flows and timings (Figure 8.10).
4. Use of a hydraulic routing model (AULOS) to simulate passage of this flood flow downvalley from dam location, and investigate attenuation of flood peak and travel time of flood wave (Figures 8.14 - 8.17).

The possible impacts of a dambreak flood at the Shotover Delta are assessed using a rating curve created by Hamilton (2017), shown as Figure 8.18.

8.2 Modelling Methods

There are four main methods for landslide dambreak flood estimation and modelling (Manville 2001, Davies et al. 2007); empirical regressions, parametric models, dimensionless models, and physically-based models. These methods vary in speed, usability and precision, with each having its own strengths and weaknesses (Manville 2001). It is difficult to choose a 'best' method, but a consensus approach is the most suitable, combining multiple methods, and using comparison with case studies and knowledge of the scenario location to judge how realistic inputs and results are. The approach recommended by Manville (2001) (Figure 8.1) and Davies et al. (2007) is to;

1. Use empirical equations to obtain initial approximations of peak discharge, comparing results to check consistency.
2. Carry out breach characteristics analysis to estimate breach width and breach development time.
3. Use dimensionless or parametric models to investigate sensitivities to breach development time and breach width, and to refine peak flow estimates.
4. Then if time permits, use physically-based models to further fine-tune predictions of outflow hydrographs.

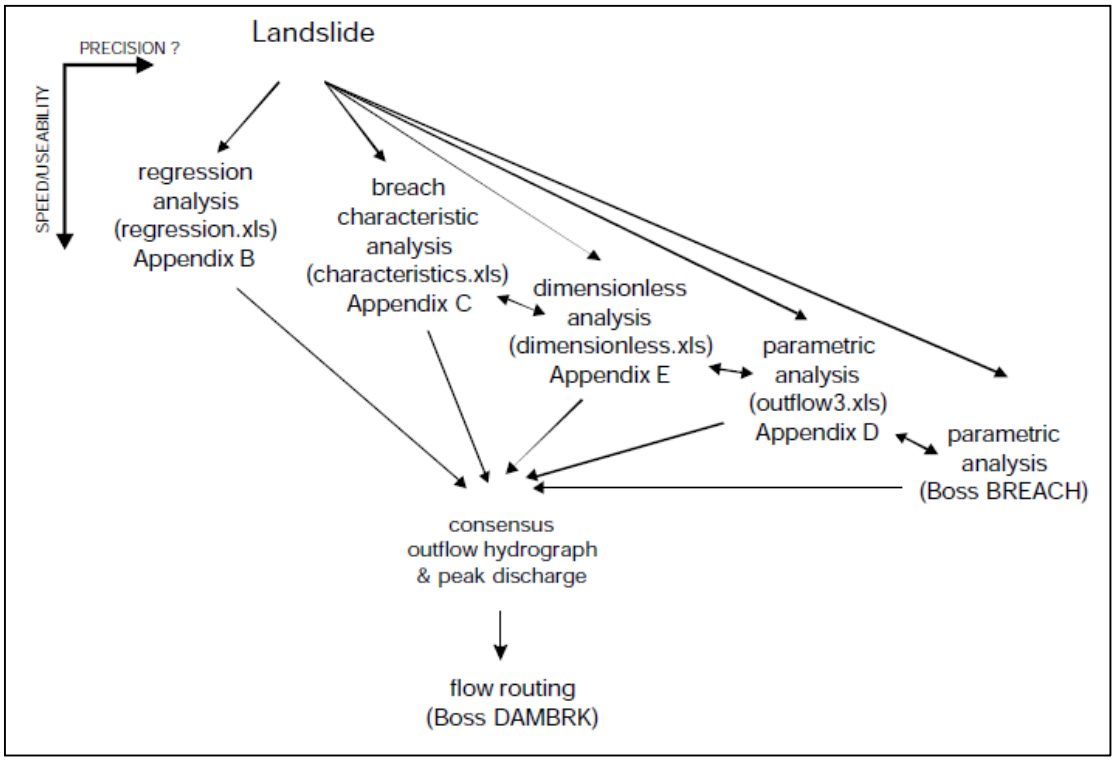

Figure 8.1: *Flow chart of dambreak flood analysis methods, this indicates increasing precision (left to right), and an increasing time requirement and model complexity (top to bottom) (Manville 2001).*

This Shotover study utilises empirical regression equations, breach characteristics analysis, dimensionless analysis and a parametric model (OUTFLOW3). These analysis methods and the required input parameters are summarised below.

Empirical regression equations have been developed from datasets of observed dambreak events in natural and constructed earth dams. Most are power-law relationships of the form $Q_c = aX^b$; where Q_c is the peak flow, a and b are coefficients and X is a parameter representing dam and/or lake magnitudes (dam height or lake depth, and lake area or volume). Peak discharge at the breach is not a simple function controlled only by lake volume or breach depth (Manville 2001), but also by shape of the breach, reservoir and dam, and rate of breach development. More complex equations attempt to include these factors, including parameters for dam width, bed gradient and inflow discharge, or breach parameters such as dam erodibility, breach width or shape (Peng and Zhang 2012, Dang et al. 2014, Cui et al. 2012).

There is a large variance in observed dambreak discharges, and for a given dam height or lake volume these peak flows vary by greater than an order of magnitude (e.g. Figure 8.9). These observed values are often uncertain, due to extrapolation of observed down-valley flows to estimate peak value at breach, and to sediment bulking effects (Manville 2001) and bed aggradation. Use of these equations is known to be only moderately reliable, and different equations often show an order of magnitude scatter between predicted values (Korup and Tweed 2007). This method is applicable only to water or hyperconcentrated flows, but not debris flows (Korup and Tweed 2007). Despite these limitations, empirical equations are commonly used to provide easily-calculated estimates of peak dambreak flows based on limited input data. A number of empirical regression equations have been used to estimate peak dambreak flows for Shotover landslide dam scenarios. These are the seven landslide dambreak peak flow regressions compiled by Manville (2001) (Table 8.1), sourced from Costa (1985), Costa and Schuster (1988) and Walder and O'Connor (1997). In addition, two

more recently developed equations by Dang et al. (2014) were used (Table 8.1). These equations require inputs of lake volume and/or dam height or lake depth.

Table 8.1: *Dambreak peak flow regression equations used. V_0 is initial lake volume (m^3), H_d is dam height (m), and E_p is potential energy (joules).*

Reference	n	r^2	Equation
Costa & Schuster 1988	12	0.81	$Q_p = 0.0158E_p^{0.41}$
Costa 1985 (1)	10	0.73	$Q_p = 672(V_0/10^6)^{0.56}$
Costa 1985 (2)	10	0.74	$Q_p = 6.3d^{1.59}$
Costa 1985 (3)	10	0.76	$Q_p = 181(dV_o/10^6)^{0.43}$
Walder & O'Connor 1997 (1)	19	0.6	$Q_p = 1.6V_0^{0.46}$
Walder & O'Connor 1997 (2)	19	0.82	$Q_p = 6.7d^{1.73}$
Walder & O'Connor 1997 (3)	19	0.7	$Q_p = 0.99dV_o^{0.40}$
Dang et al 2014 (1)	21	0.75	$Q_p = 0.2(V_0H_d)^{0.47}$
Dang et al 2014 (1)	21	0.72	$Q_p = 0.19V_0^{0.58}$

Figure 8.2 shows examples of these nine equations applied to Shotover Gorge (Zone A) and Moonlight Creek (Zone M) dambreak scenarios. Most results are relatively well-clustered, with the Walder and O'Connor (2) equation a clear outlier in most scenarios, returning discharge values significantly greater than those of the other equations. Excluding the Walder and O'Connor (2) outlier value, the mean of the remaining eight equations have been taken as the best empirical peak flow estimate.

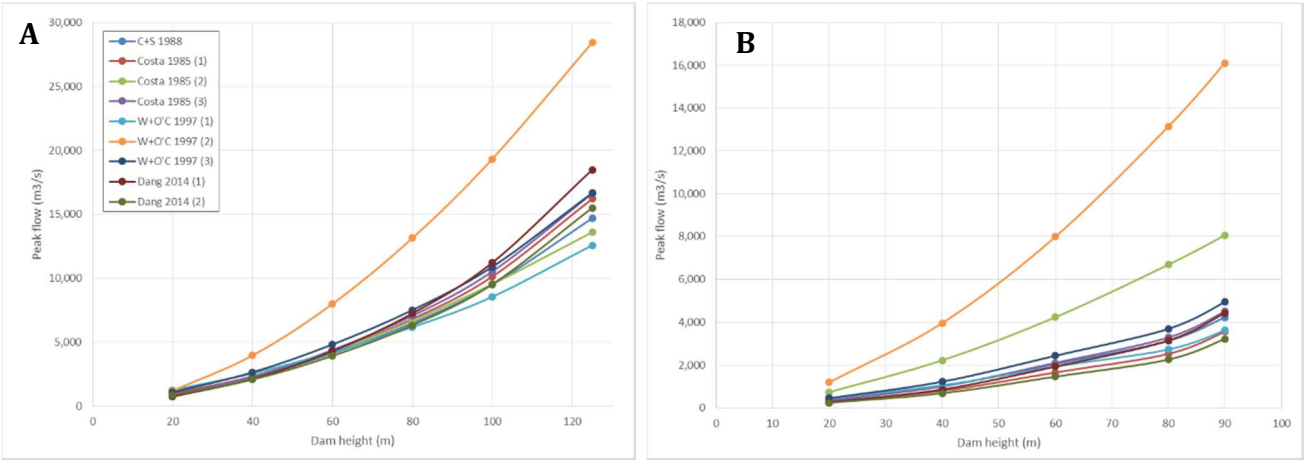

Figure 8.2: *Comparison of empirical peak flow estimation equations for A. lower Shotover gorge (Zone A) and B. Moonlight Creek (Zone M) landslide dam scenarios. The nine equations used are those shown in Table 8.1. The upper outlier in both plots is the Walder and O'Connor (2) equation.*

Dimensionless models investigate the relative importance of the breaching factors; breach growth rate, lake shape and volume, on the peak dambreak flood discharge, assuming that physical processes involved in dam failure are scale-invariant (Walder and O'Connor 1997). These models are simple to use, requiring only four input parameters; lake volume, dam height and breach depth, and breach development time. This model type is sensitive to the breach width-depth ratio (Manville 2001, Davies et al. 2007) and is limited by lack of inclusion of breach width as a parameter (Manville 2001). Dimensionless model results can be equally well obtained using parametric modelling methods (Manville 2001). Shotover Gorge landslide dam scenarios have been modelled using the spreadsheet *dimensionless.xls* of Manville (2001), which partially automates the dimensionless analysis developed by Walder and O'Connor (1997). The required input parameters are; dam height, breach depth (assumed 70% of dam height), water volume released (assumed 96% of total reservoir volume), and breach development time (estimated using the empirical equation of Ollett (2001)).

Parametric models estimate discharges through a trapezoidal breach using broad-crested weir hydraulic flow equations. These equations can be used to calculate an instantaneous peak dambreak discharge, this is the theoretical outflow resulting from instantaneous formation of a breach at its final dimensions, while the lake was at its initial level. This method defines the maximum upper limit on peak dambreak discharge, and the actual peak discharge will be lower due to lake surface drawdown prior to formation of the final breach dimensions (Manville 2001). This study uses the instantaneous parametric equation of Manville (2001) in the spreadsheet *characteristics.xls*. This makes use of equations developed by Fread (1981) and Wetmore and Fread (1984), which have been converted to metric units by Manville (2001).

$$Q_e = 3.1\,\overline{width}\left[\frac{C}{t_b + \frac{C}{(h_d)^{0.5}}}\right]^3$$

Where: $C = 23.4\frac{As}{width}$, A_s is reservoir surface area (km^2), *width* is mean breach width (m), and H_d is the breach depth (m).

A parametric time-stepping model can be used to estimate peak dambreak flows, time to peak flow and model flood hydrographs. This model recalculates flows in a series of steps, taking into account the enlarging breach, reservoir drawdown and reduction in hydraulic head, These models and can be useful for rapidly assessing sensitivity to variation in parameters, such as between model locations, dam heights, breach width and breach formation time. Shotover dambreak modelling uses Manville's (2001) OUTFLOW3 spreadsheet-based parametric model. This makes use of three alternative equations for flows through trapezoidal breaches in broad-crested weirs;

1. $Q_b = 0.296[(0.4\ B_w) + (0.6T_w)]g^{0.5}H_b^{1.5}$
2. $Q_b = 1.7\ B_w\ (H_b)^{1.5} + 1.35\ z\ (H_b)^{2.5}$
3. $Q_b = 0.591\ C_d\ H_b^{1.5}\ (5\ B_w + 4\ z\ H_b)$

where T_w and B_w are the final width at top and base of breach (m), H_b is the head over the weir (m), and C_d is a discharge coefficient, with a value of 0.57 for a trapezoidal breach. This model assumes the breach erodes down to a specified level (B_d), and the breach shape remains constant throughout (same width-depth ratio and sidewall angles). Breach outflow starts at zero and level pool routing is assumed (no velocity drawdown of the lake surface). The three weir equations used in the OUTFLOW3 model give a range of peak flow and timing results. The second and third equations are in close agreement, while the first equation gives significantly lower (~20%) peak flows, and longer times to peak

flow. The flow values given for parametric modelling in Table 8.3 are the mean of equations 1 and 3. Parametric methods typically overestimate flows as they do not take into account frictional or turbulent flow resistance at the outlet channel, neglect backwater effects, and assume level-pool routing in the lake (Manville 2001).

The main input parameters for instantaneous and time-stepping parametric models are outlined below;

Lake parameters: The OUTFLOW3 model uses parameters of the lake's surface area at maximum elevation, and at minimum level (base of breach) to calculate the volume of a hypothetical funnel-shaped lake. Based on dam height-lake area plots, the final lake area for a 70% breach has been approximated as 5% of the initial lake surface area. Where lake volumes automatically calculated in OUTFLOW3 are significantly different from those estimated in landslide dam modelling, the lake area inputs were adjusted to make volumes consistent with modelled reservoir volumes.

Walder and O'Connor (1997) describe three idealised reservoir shapes, each with a characteristic hypsometric function (Figure 8.3). Any reservoir confined within the V-shaped Shotover Valley will be of the third type (shape factor m=3), and contain the majority of its capacity in the upper portions of the lake. Based on modelled landslide-dammed lake volumes, about half of the lake's volume is contained within its upper 20-30% by height. A breach to 30-40% of the total dam height will release 60-80% of the reservoir volume, and a breach to ≥80% of the dam height is essentially a complete draining of the reservoir (97-100%).

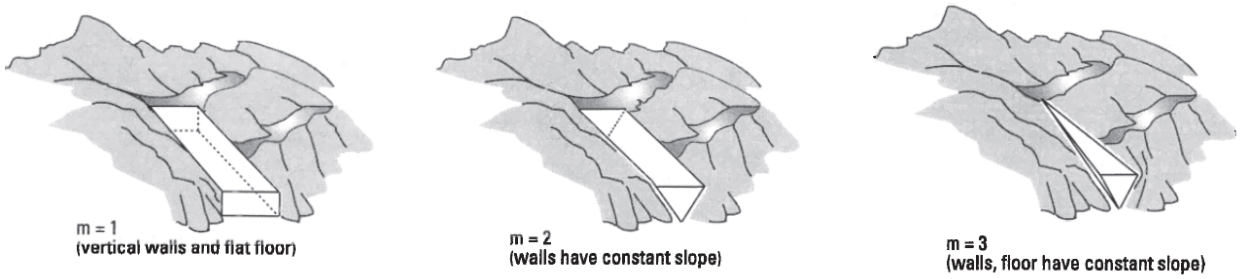

Figure 8.3: *Idealised reservoir shapes and lake shape factors, from Walder and O'Connor (1997). Shotover Gorge landslide dammed lakes can be approximated as the third type (m=3).*

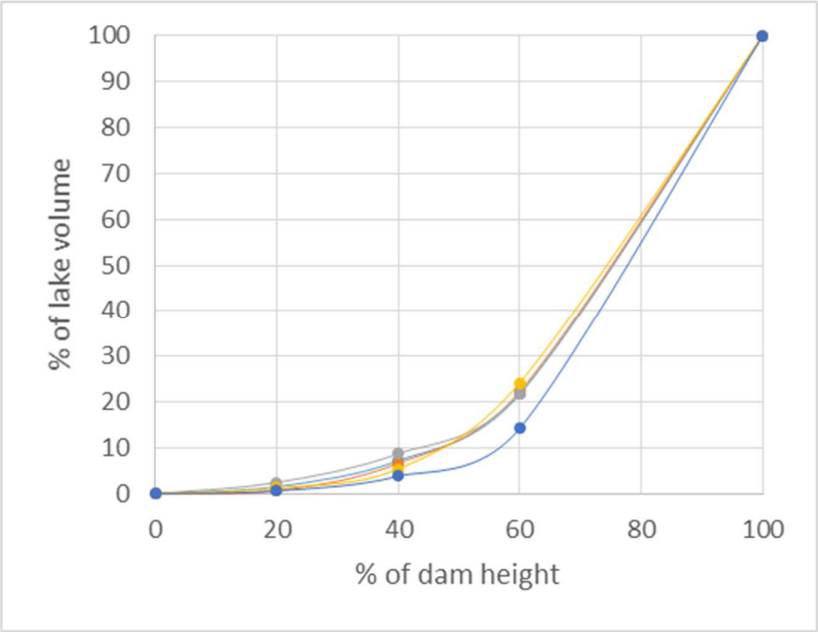

Figure 8.4: *Plot showing percentage of lake volume released by breaching of 100 m scenario dams, showing the large proportion of lake capacity stored in the upper parts of the reservoir.*

Breach depth: Landslide dam breach channels typically start as a narrow V-shaped channel, then develop into a trapezoidal shape. The breach is usually assumed to retain the same shape throughout development, growing equally on both sides. The extent of breach development varies with both dam height and reservoir volume, and breach width-breach depth ratios vary widely, with reported value ranges of 1-5 (Manville 2001). A breach channel is typically not eroded to the full depth of the dam (Figure 4.5), this is due to the dam thickness increasing with depth eroded, whereas the lake volume rapidly decreases. In the initial stages of breach development there is a large volume of water to erode the narrow dam crest, but as the breach develops there a decreasing volume of water available to erode the broad base of the dam. In addition, deposition of eroded dam material at the downstream margin of the dam may provide a buffer against further erosion (Ollett 2001). Based on mean breach depths and the modelled lake characteristics in Figure 8.4, Shotover landslide dam breaching scenarios are approximated as a breach to 70% of the total dam height, releasing ~96% of the total lake volume.

Breach width: Mean breach width has been estimated using an empirical equation developed by Froehlich (1995);

$$Width = 9.5k_0(V_r H_d)^{0.25}$$

where k_0 is a constant, set at 1.4 for overtopping failures, and V_r and H_d are the volume released (m^3) and breach depth (m) respectively. Mean breach widths are used to estimate dimensions of three alternative breach geometries, these are; a trapezoidal breach with 1:1 (45°) side slopes, a trapezoidal breach with 35° side slopes (~angle of repose), and a triangular breach (Figure 8.5). Top and base widths have been calculated using equations from Manville (2001). In several Shotover Gorge scenarios, the top breach width estimated using empirical equations exceeds the modelled across-valley dam length modelled at that location (Table 8.2). In these cases, the estimated breach width has been corrected to the value obtained during dam modelling (Chapter Seven).

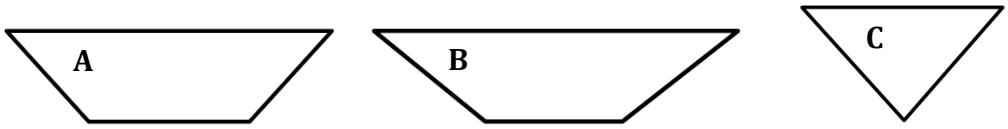

Figure 8.5: *Examples of alternative breach geometries; A. trapezoidal with 45° side slopes, B. trapezoidal with 35° side slopes, and C. triangular.*

Breach formation time: The duration of breach formation is controlled by factors such as the rate of breach incision, dam height and lake volume. There are two different cases of breach development depending on the relative magnitudes of dam and reservoir volumes (Davies et al. 2007). If the dam volume is of similar magnitude to lake volume, then lake drainage takes about as long as breach development. Peak flow occurs before the breach is fully developed, and the breach continues growing even as flow decreases. This is termed a 'small reservoir/slow erosion' case by Walder and O'Connor (1997) and Wahl (2004). If the dam volume is small relative to lake volume, peak flow occurs when breach development is complete, and before any significant reservoir drawdown. These have been termed 'large reservoir/fast erosion' cases by Walder and O'Connor (1997) and Wahl (2010). In 'large reservoir/fast erosion' cases, the rate of breach development is typically in the range of 50-100 m/h.

A number of empirical equations have been developed for estimation of breach development time, most of which are based on failures of constructed earthfill and rockfill dams (e.g. MacDonald and Langridge-Monopolis 1984, Froehlich (1987, 1995). These are based on factors of water volume and dam height or breach depth, for example the Froehlich (1995) equation:

$$t_f = 0.00254\ V_w^{0.53} h_b^{-0.9}$$

Although based on constructed dams, these equations have been applied to estimation of breach development time for natural dams (e.g. Manville 2001, Wishart 2007). Ollett (2001) applied the Froehlich (1995) equation to six landslide dambreak case studies, and found it significantly underestimated breach formation duration, with resulting values <25% of actual times, and therefore significantly overestimated peak discharges. The breaching duration of landslide dams is typically longer than of constructed dams with similar dam heights or lake volumes, due to differences in their material and internal structure. Peng and Zhang (2012) also note this as being due to landslide dams having larger dam volumes and widths, and gentler downstream slopes. Ollett (2001) developed an empirical failure time equation based only on landslide dam failures:

$$t_f = 5.51\ V^{0.45} H^{-0.56}$$

The empirical breach formation equations of Froehlich (1995) and Ollett (2001) have been applied to Shotover landslide dam scenarios (Table 7.2). Breach formation times estimated using the Froehlich (1995) equation result in unrealistically high peak outflow rates when used as inputs in instantaneous peak flow equations or parametric models. The Ollett (2001) equation gives significantly longer failure times than those estimated using Froehlich (1995) equation, and these longer times give more realistic peak flow results when used as a model input.

8.3 Breach Characteristics and Parametric Model Results

Estimated landslide dam breach widths and breach development times for Shotover landslide dam scenarios are shown in Table 8.2. Most breach widths take a large portion of the valley width, and for larger dams in lower-middle Shotover Gorge (Zones A, B, C) the estimated top breach width exceeds the landslide dam's cross-valley width found in landslide dam modelling. Top breach width is required as an input in parametric models, and where estimated values exceed actual dam width they have been reduced to match the actual value. Breach width-depth ratios (Table 8.2) are all within

ranges reported for landslide dam case studies (Manville 2001). For Shotover River dams this ratio ranges from 2.3-5.0, while Moonlight Creek dams have narrower modelled breaches, all with a ratio of 1.5-2.0.

Parametric modeling in OUTFLOW3 shows peak outflows occurring prior to final breach development, a similar result to Manville's (2001) modelling of the Poerua River dambreak. This indicates that the duration of the hydrograph's rising limb may underestimate the actual duration of breach development. The sensitivity of the OUTFLOW3 parametric model has been assessed by varying key input parameters to determine the impact of these changes on peak outflows and the time to peak outflow (Figures 8.6, 8.7). This shows that the model is highly sensitive to changes in failure time, while there is little response to variations in breach width on peak flows or the time to peak flows.

Table 8.2: *Breaching parameters and parametric model (OUTFLOW3) results for Shotover Gorge and Moonlight Creek dambreak scenarios.*

Zone	Dam Height	Breach Depth	Failure time (hr)		Mean breach width	Top breach width	Total dam width	Top width/ breach depth	Time to peak flow	Time to peak flow/ failure time	Lake level at peak flow	Lake level/ final breach height
			Froehlich 1995	Ollett 2001	Froehlich 1995	1:1 sides			OUTFLOW3		OUTFLOW3 (m below initial level)	
	(m)	(m)	(hr)	(hr)	(m)	(m)	(m)	ratio	(hr)	(%)		(%)
A	20	14	0.50	1.68	43	57	58	3.0	1.30	77	9	67
	40	28	0.61	2.27	79	107	88	2.8	1.58	69	22	77
	60	42	0.75	2.97	122	164	138	2.9	1.94	66	34	81
	80	56	0.90	3.65	167	223	173	3.0	2.32	63	47	85
	100	70	1.07	4.43	219	289	212	3.1	2.77	63	60	86
	125	88	1.37	5.71	299	386	279	3.4	3.51	61	76	87
B	20	14	0.33	1.16	33	47	73	2.3	0.84	72	10	71
	40	28	0.58	2.18	77	105	108	2.8	1.46	67	22	79
	60	42	0.76	3.00	123	165	152	2.9	1.92	64	34	82
	80	56	0.80	3.30	156	212	193	2.8	2.01	61	48	86
C	20	14	0.96	2.91	63	77	88	4.5	2.42	83	9	62
	40	28	1.01	3.50	108	136	121	3.9	2.57	73	21	75
	60	42	1.14	4.22	156	198	175	3.7	2.87	68	33	79
	80	56	1.31	5.04	210	266	253	3.8	3.25	64	46	82
D	20	14	1.03	3.08	65	79	149	4.7	2.59	84	8	60
	40	28	1.20	4.04	120	148	226	4.3	3.14	78	19	67
	60	42	1.84	6.33	209	251	277	5.0	4.50	71	32	76
M	20	14	0.16	0.63	21	35	65	1.5	0.43	68	10	71
	40	28	0.22	0.96	43	71	114	1.5	0.56	59	22	80
	60	42	0.31	1.38	71	113	170	1.7	0.77	56	37	87
	80	56	0.35	1.64	95	151	233	1.7	0.89	54	50	89
	90	63	0.44	2.03	118	181	265	1.9	1.09	54	56	89

Time to peak and lake level values are mean of values from equations 1 and 3 in OUTFLOW3 model (Manville 2001). 'Total dam width' is the across-valley dam width found in landslide dam modelling (Chapter Six), note that in several cases this is exceeded by the estimated breach width.

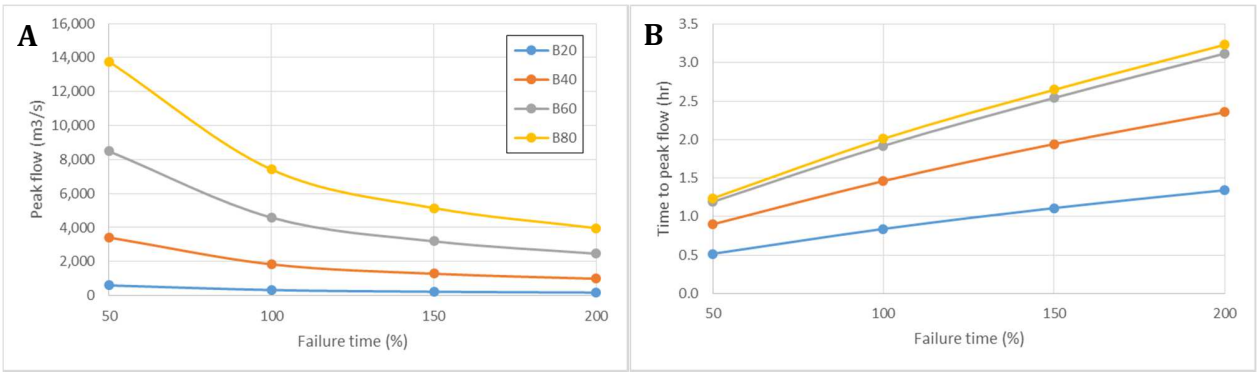

Figure 8.6: *Parametric model (OUTFLOW3) sensitivity to breach formation time. Showing impact on A. peak flows and B. time to peak flow for Zone B models at dam heights of 20-80 m. Failure times are relative to a 100% value estimated using Ollett's (1995) equation.*

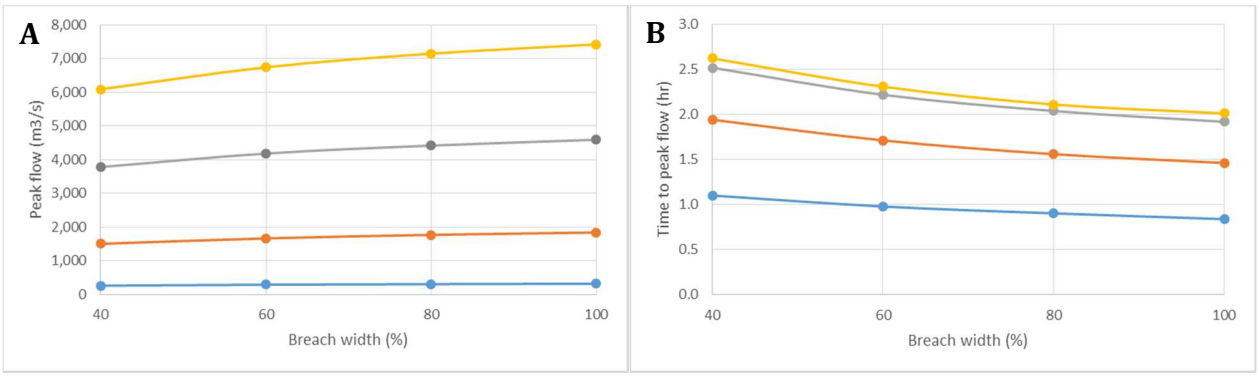

Figure 8.7: *Parametric model (OUTFLOW3) sensitivity to breach width. Showing impact on A. peak flows and B. time to peak flow for Zone B models at dam heights of 20-80 m. Failure times are relative to a 100% value estimated using Ollett's (1995) equation.*

8.4 Peak Flow Estimation Results

Estimated peak dambreak flows for Shotover landslide dam scenarios are summarised in Table 8.3 and Figure 8.8 comparing results of the various estimation methods used. There is reasonable agreement between estimation methods at dam heights of ≤60 m, with increasing variance between methods for larger dams. Estimation of peak flows shows moderate-large (≥40 m dam height) Shotover Gorge landslide dambreak scenarios are capable of generating flows exceeding a 100-year flood event (1500 m^3/s). Larger dams are capable of generating floods with a peak discharge many times larger than that caused by a meteorological event, potentially greater than 10,000 m^3/s.

Table 8.3: *Estimates of peak dambreak flows for the Shotover Gorge and Moonlight Creek landslide dam scenarios, using empirical, dimensionless, instantaneous parametric, and time-stepping parametric (OUTFLOW3) models.*

Zone	Location	Dam height (m)	*Empirical Regression* Peak Flow (m^3/s) ± 1 Std Dev	*Dimensionless* Peak Flow (m^3/s)	*Instantaneous parametric equation* Peak Flow (m^3/s)	*Parametric (OUTFLOW3)* Peak Flow (m^3/s) ± 1 Std Dev
A	**Shotover River** Arthur's Point to Moonlight Creek	20	928 ± 176	531	318	551 ± 63
		40	2,306 ± 198	1,893	1,251	1,918 ± 229
		60	4,289 ± 255	4,388	2,726	4,529 ± 536
		80	6,786 ± 462	8,146	5,019	8,363 ± 1,020
		100	9,981 ± 875	13,651	8,267	14,278 ± 1,788
		125	15,542 ± 1,882	24,537	14,645	25,880 ± 3,299
B	**Shotover River** Moonlight Creek to Criterion Creek	20	663 ± 123	350	591	323 ± 33
		40	2,224 ± 194	1,805	1,572	1,838 ± 201
		60	4,331 ± 256	4,440	2,943	4,590 ± 526
		80	6,189 ± 501	7,261	6,203	7,419 ± 839
C	**Shotover River** Criterion Creek to Devils Elbow	20	1,589 ± 447	1,008	533	1,024 ± 127
		40	3,474 ± 576	3,110	1,740	3,274 ± 408
		60	5,969 ± 767	6,578	3,927	6,763 ± 834
		80	9,179 ± 1,177	11,816	13,839	12,482 ± 1,499
D	**Shotover River** Skippers Creek to Sandhills	20	1,676 ± 488	1,070	570	1,130 ± 141
		40	3,998 ± 801	3,666	1,973	4,442 ± 544
		60	8,883 ± 2,068	10,473	9,686	11,123 ± 1,384
M	**Moonlight Creek** Shotover River to Moke Creek	20	395 ± 160	169	94	115 ± 8
		40	1,106 ± 481	704	384	617 ± 45
		60	2,223 ± 863	1,808	1,122	1,725 ± 141
		80	3,431 ± 1,392	3,248	3,738	3,109 ± 255
		90	4,572 ± 1,523	4,827	4,001	4,704 ± 420

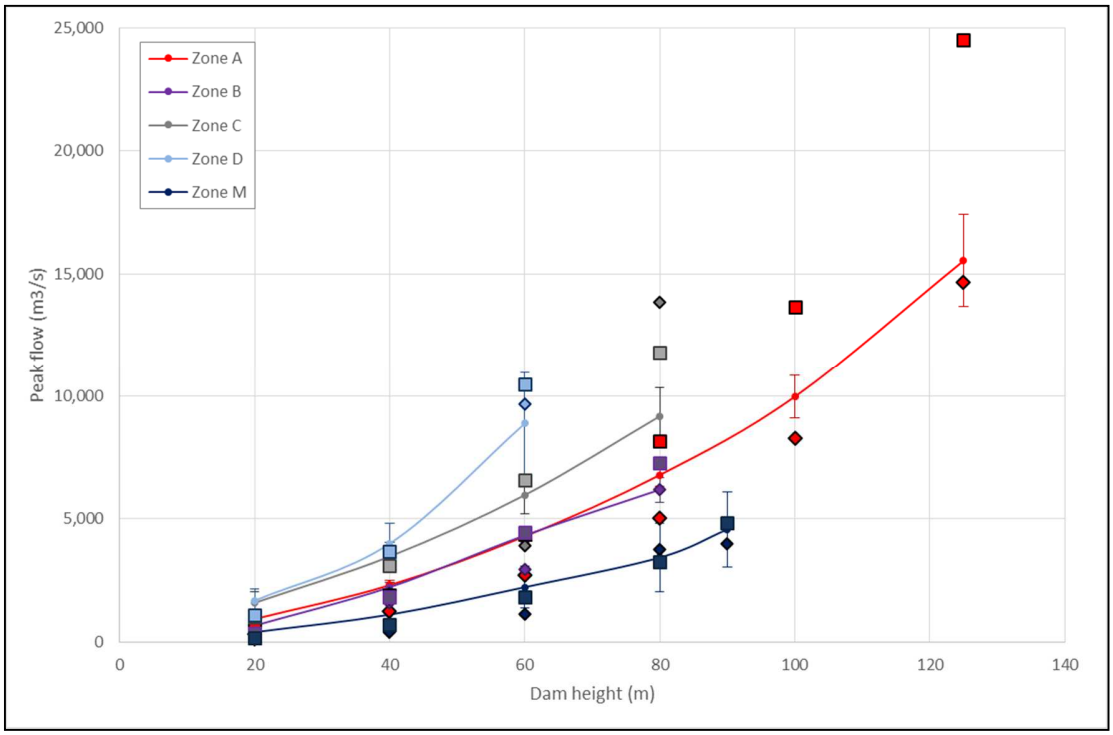

Figure 8.8: *Peak flow vs dam height plot for Shotover and Moonlight landslide dam scenarios. Empirical estimates shown with trend lines, error bars are ±1 standard deviation. Parametric estimates shown as diamond symbols, dimensionless estimates as squares, using same colour scheme as lines.*

Compared to a global dataset of documented dambreak floods (Figure 8.9), these estimated values are within the range of case study events. It may appear uncertain how realistic the largest peak flow estimates (15-26,000 m^3/s) are for failure of a 125 metre dam in the lower Shotover Gorge. However, there are documented dambreak flows of similar magnitudes for failure of dams with comparable dam heights and reservoir volumes to this largest scenario, so these are assumed to be realistic if such a dam height occurs. For example (Peng and Zhang 2012);

- La Josefina, Ecuador, March 1993: A 100 m height dam, impounding a 200M m^3 reservoir, resulting in a peak dambreak flow of 10,000 m^3/s.
- Mantaro River, Peru, August 1945: A 133 metre height dam, impounding a 300M m^3 reservoir, resulting in a peak dambreak flow of 35,400 m^3/s.

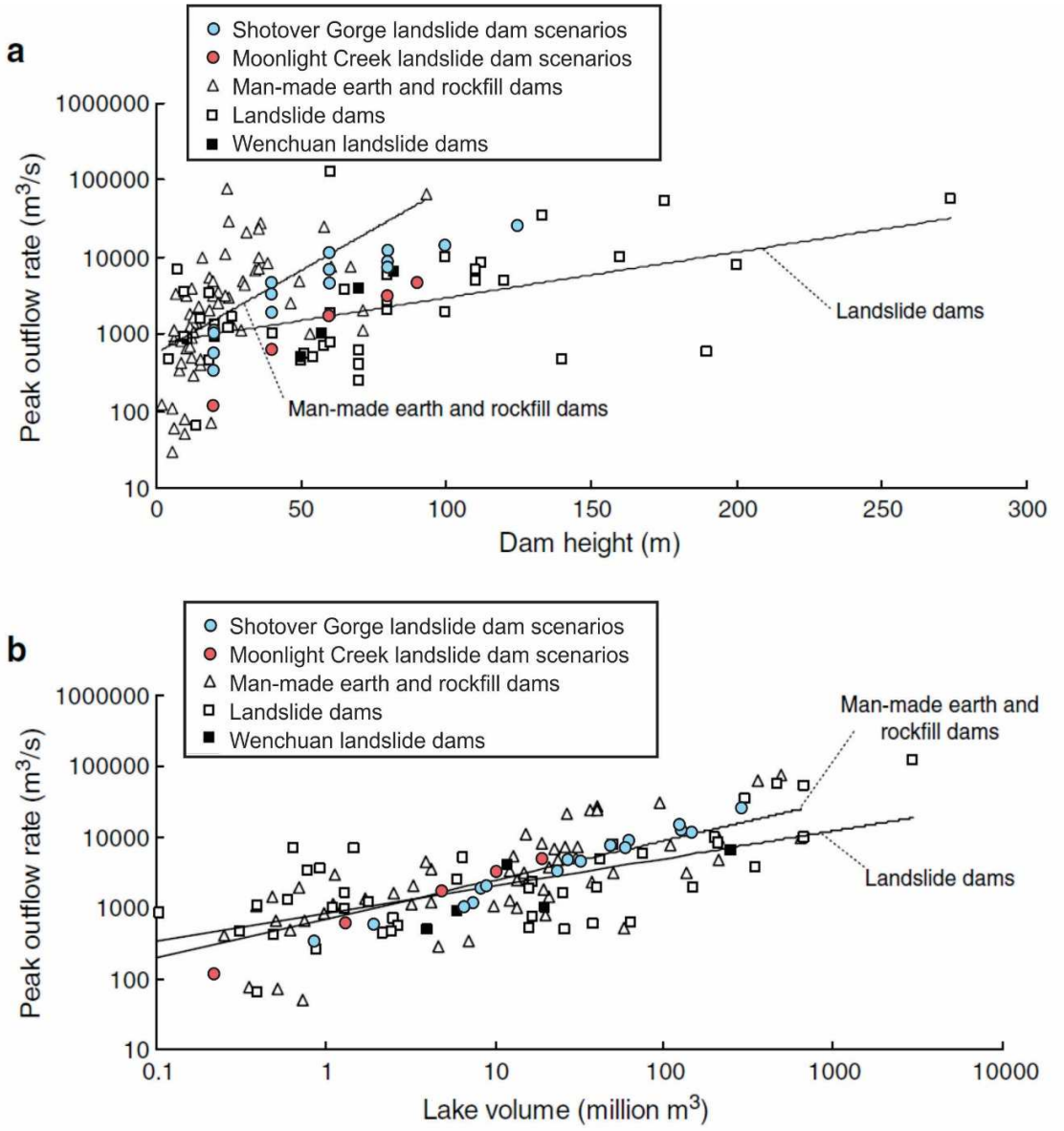

Figure 8.9: *Peak flow estimates (parametric model) for Shotover Gorge and Moonlight Creek dambreak scenarios, plotted against A. landslide dam height, and B. Reservoir volume. Scenarios shown on dataset of dambreak flood case histories from landslide and man-made dams compiled by Peng and Zhang (2012).*

The magnitudes of these dambreak flood scenarios appear realistic based on comparison with case studies (Figure 8.9). However, these estimations of flood discharges contain significant assumptions and uncertainty in estimation of input parameters and peak flows. Estimates of peak dambreak flows by empirical regression equations are only moderately accurate, while parametric models place some physical constraints on discharges, but still rely on estimated input parameters. Parametric OUTFLOW3 modelling used empirical estimates of breach development time (Ollett 2001) and breach width (Froehlich 1995), which are based on limited datasets with substantial scatter. Wahl (2004) found the best predictions of breach time have uncertainties of ± 2/3 order of magnitude, and those for breach width prediction

have uncertainty of ± 1/3 order of magnitude (Wahl 2004). Nevertheless, Figure 7.9 indicates that the estimated Shotover peak flows are realistic.

The total uncertainty in estimated discharges may be substantial, but these still provide a guide to the nature of a possible future dambreak event. This Shotover Gorge study has found a similar magnitude of variation in peak flow values as those found in other dambreak modelling studies investigating estimates made by several methods (e.g. Manville 2001, Ollett 2001, Davies et al. 2007, Wishart 2007). For example, Manville (2001) applied empirical, parametric (OUTFLOW3), dimensionless and a physically-based breach erosion model (Boss BREACH) to the Poerua River landslide dambreak, finding variations of ±50% between various methods. Ollett (2001) tested modelling methods against the documented Mantaro dambreak event, with the errors in estimates of peak discharge ranging from underestimates by 70%, to overestimates by 65-76%.

At best, these Shotover Gorge dambreak flood estimates can be considered to be no more accurate than ±50%, and at worst, may only be accurate to within the correct order of magnitude. Despite these uncertainties, these are the best available methods for a basic estimation of dambreak flows, and results are sufficient for use in initial dambreak hazard assessments. Modelling has assumed the worst-case scenario of a rapid, catastrophic dam failure, with a near-complete draining of the impounded reservoir. A slower breach development, or a partial dam failure would be expected to result in lower peak flows than the modelled scenarios. The magnitude of peak flows potentially generated by failure of larger dams are significant discharges and justify further investigation of the downstream flood. This was achieved through simulation of Shotover Gorge dambreak flood events using a hydraulic flood routing model.

8.5 Dambreak Hydrograph Estimation

Dambreak floods can be approximated as a triangular hydrograph (Walder and O'Connor 1997, O'Connor et al. 2002, Wahl 2010), with these used as inputs for flood routing models, for example Ollett (2001) for the Callery Gorge, and ORC (2007b) for the Young River landslide dam. A triangular hydrograph assumes that discharge increases steadily from zero at breach initiation, to a peak outflow Q_p, then decreases linearly to zero at a termination point T_d set such that total area equals water volume released ($V = 0.5\ Q_p * T_d$). This equation can be solved for the total flood duration ($T_d = 2V/Q_p$), where peak flow (Q_p) and total flood volume (V) have been previously estimated. Triangular dambreak hydrographs have been estimated for Shotover Gorge and Moonlight Creek dambreak scenarios, based on estimations of peak flow, time to peak flow, and total duration (Figure 8.10).

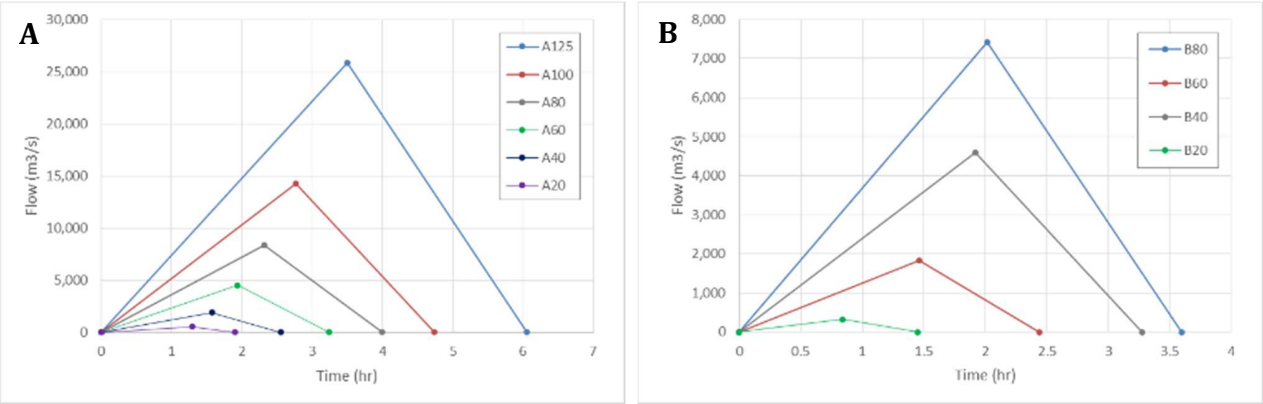

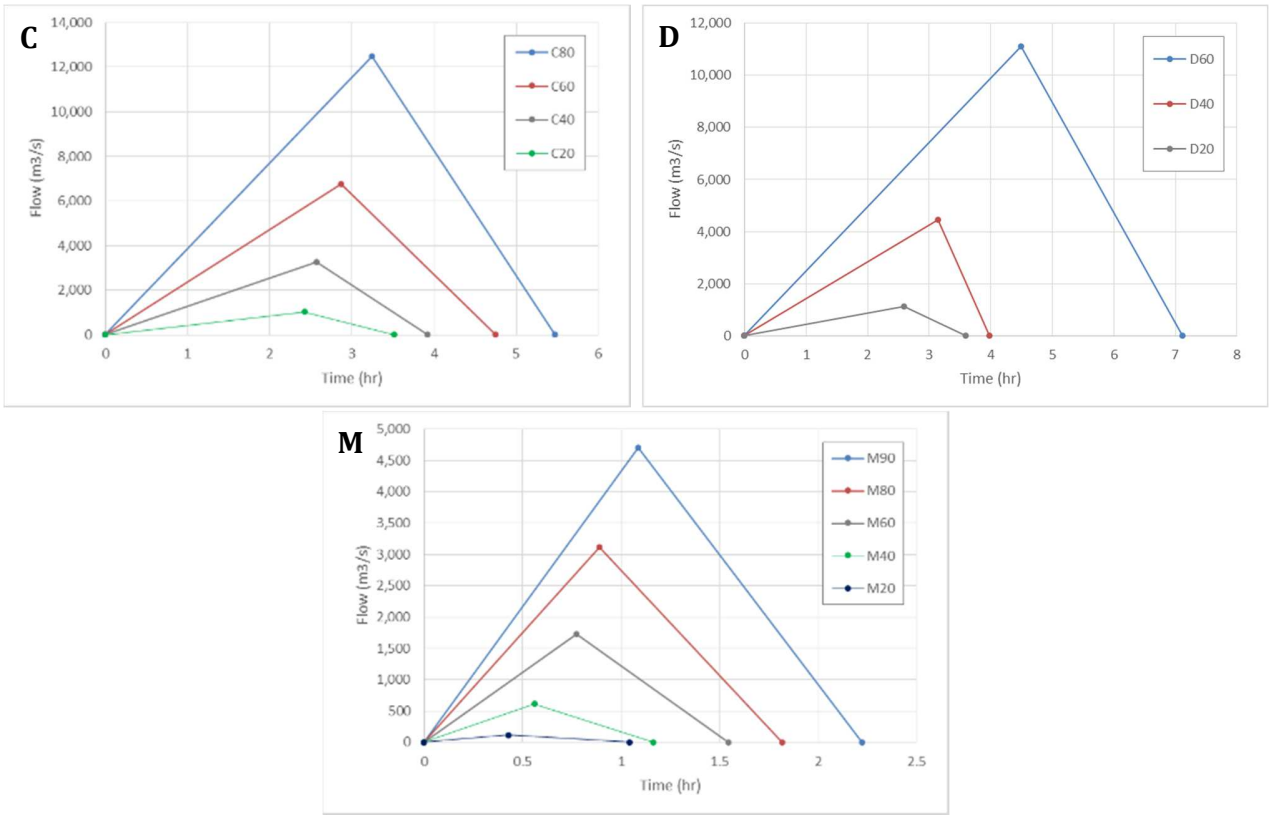

Figure 8.10: *Estimated dambreak hydrographs for the Shotover Gorge (Zones A, B, C, D) and Moonlight Creek (Zone M).*

8.6 Dambreak Flood Routing

Peak discharges (Figure 8.8, Table 8.3), breach characteristics (Table 8.2) and dambreak hydrographs (Figure 8.10) have been estimated as an initial step in evaluation of the dambreak flood hazard. These estimations have shown potential for landslide dam failures to create dambreak flood discharges of much greater than the largest recorded flooding events in the Shotover River. In order to better assess the dambreak flood hazard in the lower Shotover River and delta, a hydraulic model has been created to simulate the propagation and attenuation of the flood wave downvalley.

Shotover dambreak flood routing has been completed using AULOS, a hydraulic modelling software developed by Hydra Software Limited, Hamilton, NZ (Barnett et al. 2008). AULOS routes water through a network, using flow equations based on conservation of momentum or energy. This is a 1D model with a channel network of branches and reaches defined by a series of cross sections.

Model Description and Parameter Selection:

Dambreak floods were modelled as originating from a lower Shotover Gorge landslide dam scenario (Zone A), and the model extends downstream to the Kawarau River confluence (Figure 8.12). Flow inputs at the upstream end of the model are defined as a discharge time series, with models run at combinations of flood magnitudes and baseflows. Input flood hydrographs (Figure 8.11) are based on those estimated for Zone A during dambreak modelling (Figures 8.9), these are;

1. Low flood peak: 2000 m^3/s, resulting from failure of a ~40 m height dam
2. High flood peak: 4500 m^3/s, resulting from failure of a ~60 m height dam
3. Very high flood peak: 10,000 m^3/s, resulting from failure of a ~80-100 m height dam

These dambreak hydrographs were superimposed on low (50 m^3/s) or high (400 m^3/s) constant baseflows to give model input time series (Figure 8.11). These baseflows were modelled for a 14 hour period prior to dambreak initiation, to provide stable initial model conditions, defined as a 'hot start' file.

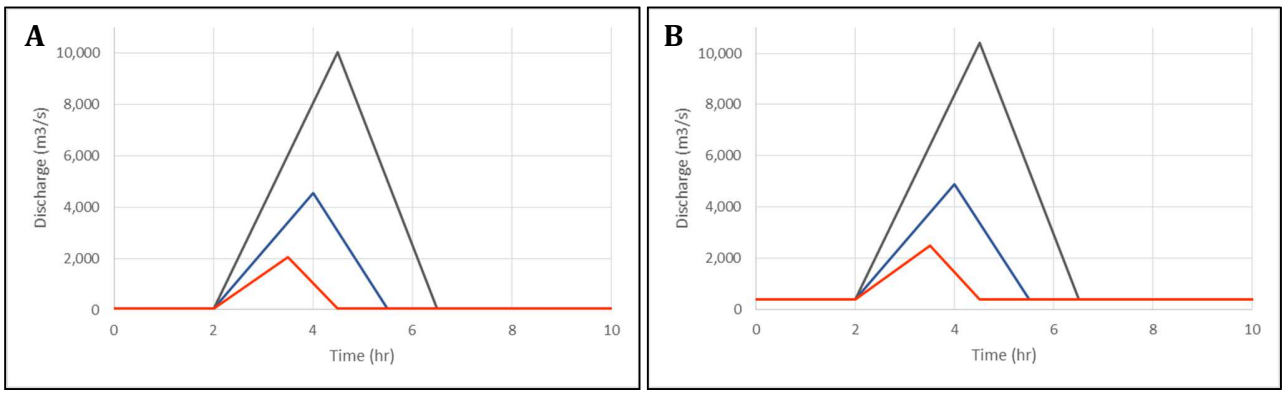

Figure 8.11: *Input dambreak hydrographs used in AULOS modelling, for A. low and B. high baseflow conditions.*

The model comprises a single channel, extending from a starting point in the lower Shotover Gorge, downriver to the Shotover Delta. This channel is defined by a series of 17 cross-sections, spaced at 0.5-1.6 km distances along the river at significant changes in channel width (Figure 8.12). The model was extended to an endpoint at a 'dummy' section ~1 km beyond the modelled Shotover Delta (km 26.0). A constant water level time series at this point acts as an infinite reservoir, this causes drawdown of the upstream water surface, but does not influence results within the true model extent.

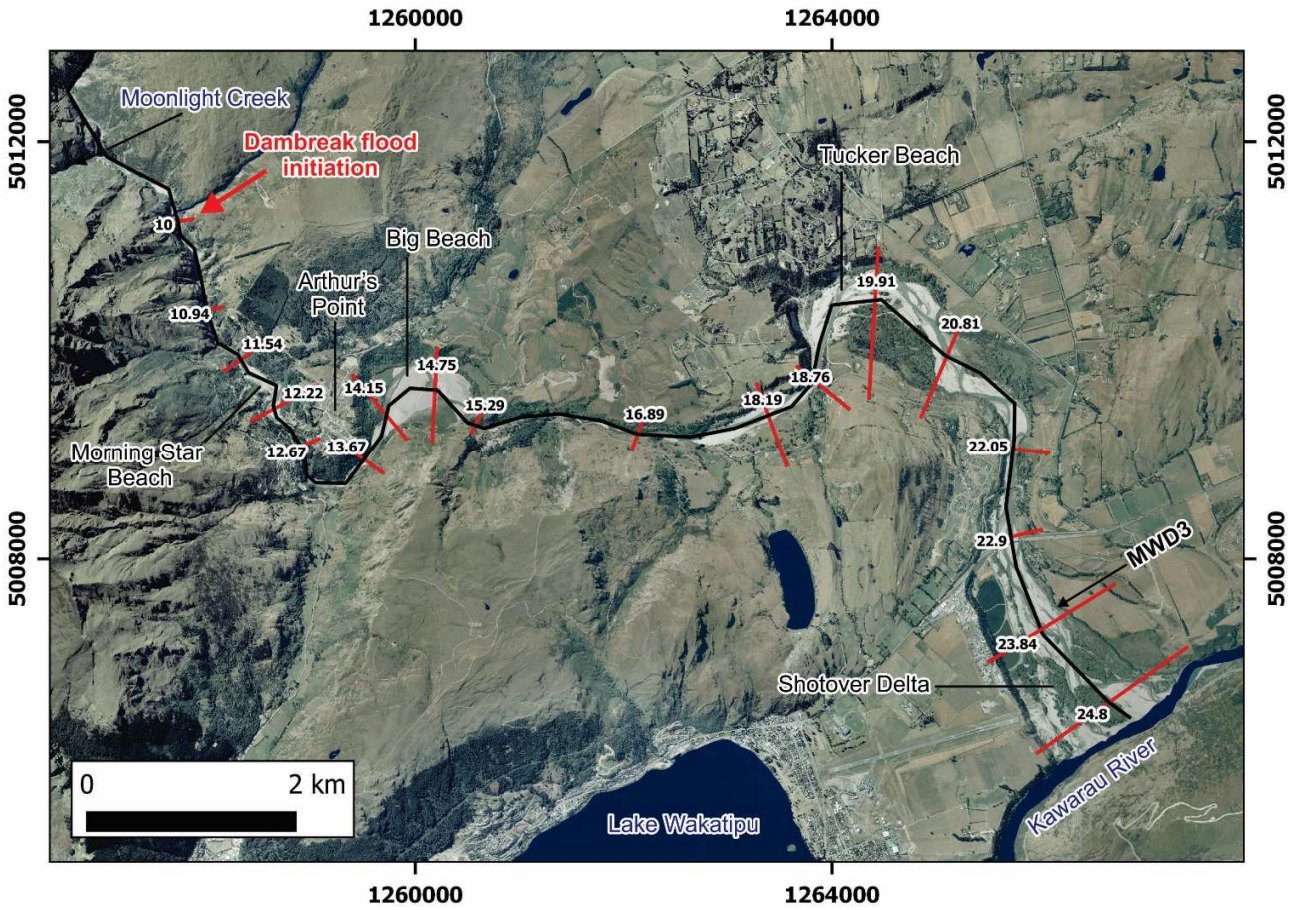

Figure 8.12: *Overview of AULOS dambreak flood model, showing flood initiation in the lower Shotover Gorge, and model extending to the Kawarau River confluence. Cross-sections used in defining the model channel are shown in red, and labelled with distance downriver (km) from a first section labelled as '10 km'. The location of the mid-Shotover Delta rating curve shown in Figure 8.18 is labelled MWD3.*

For the Shotover Gorge, Manning's roughness coefficient has been estimated as 0.04, as for a 'normal mountain stream floored with gravels, cobbles and boulders, and vegetated banks submerged at high flows' (Chow 1959, in Manville 2001), and applied to the Poerua River by Manville (2001) and Davies et al. (2007). Previous hydraulic models at the Shotover Delta have used Manning's values of 0.03-0.035 (ORC 2002b), and 0.025-0.04 with a best match at 0.03 (Hamilton 2010). This modelling has used 0.035 as a global value across the whole model, however the model could be refined by use of different values for different model reaches, for example with a value of 0.04 in gorge sections and 0.03 for the lower river. Model sensitivity to variations in Manning's number has been tested by comparison of models with Manning's values of 0.03, 0.035 and 0.04 (Figure 8.13), demonstrating that this parameter has little impact on peak flows or other hydrograph characteristics.

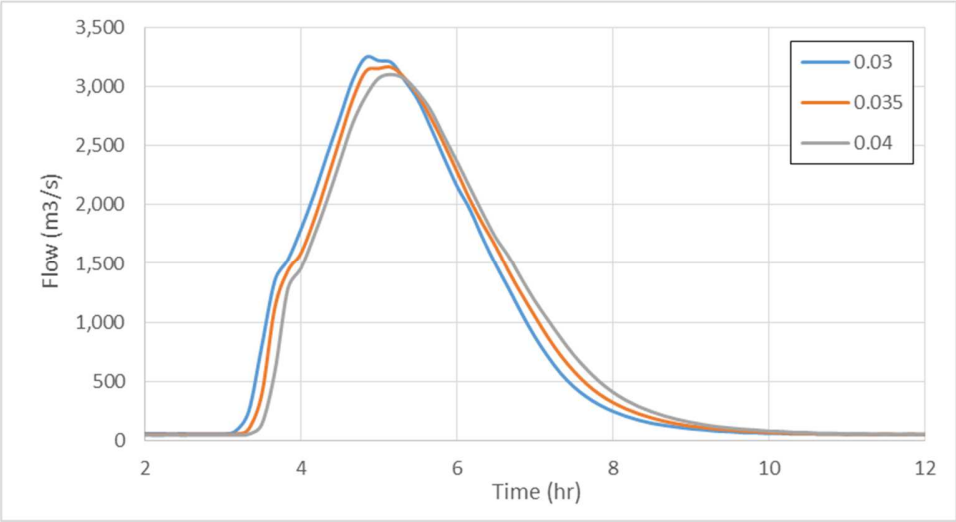

Figure 8.13: *Routed hydrographs for dambreak flows at the Shotover Delta, modelled at a range of values for Manning's number, showing little sensitivity to variation in this parameter (low baseflow scenario, initial peak discharge 4500 m^3/s).*

Flood Routing Results

Table 8.4 shows initial dambreak and routed Shotover Delta discharge and depth values for the combinations of baseflow and dambreak magnitudes modelled. Figure 8.14 shows results for low baseflow scenarios, showing initial hydrographs at the dam breach and the routed hydrographs at selected downstream locations.

Table 8.4: *Flow attenuation and maximum flow depths at the Shotover Delta.*

	Maximum Discharge		Flow attenuation	Maximum depth
	At breach (m^3/s)	At delta (m^3/s)	%	(m)
Low baseflow	2,050	1,267	38.2	1.8
	4,550	3,166	30.4	2.7
	10,050	7,730	23.1	4.1
High baseflow	2,400	1,547	35.5	2.0
	4,900	3,516	28.2	2.9
	10,400	8,079	22.3	4.2

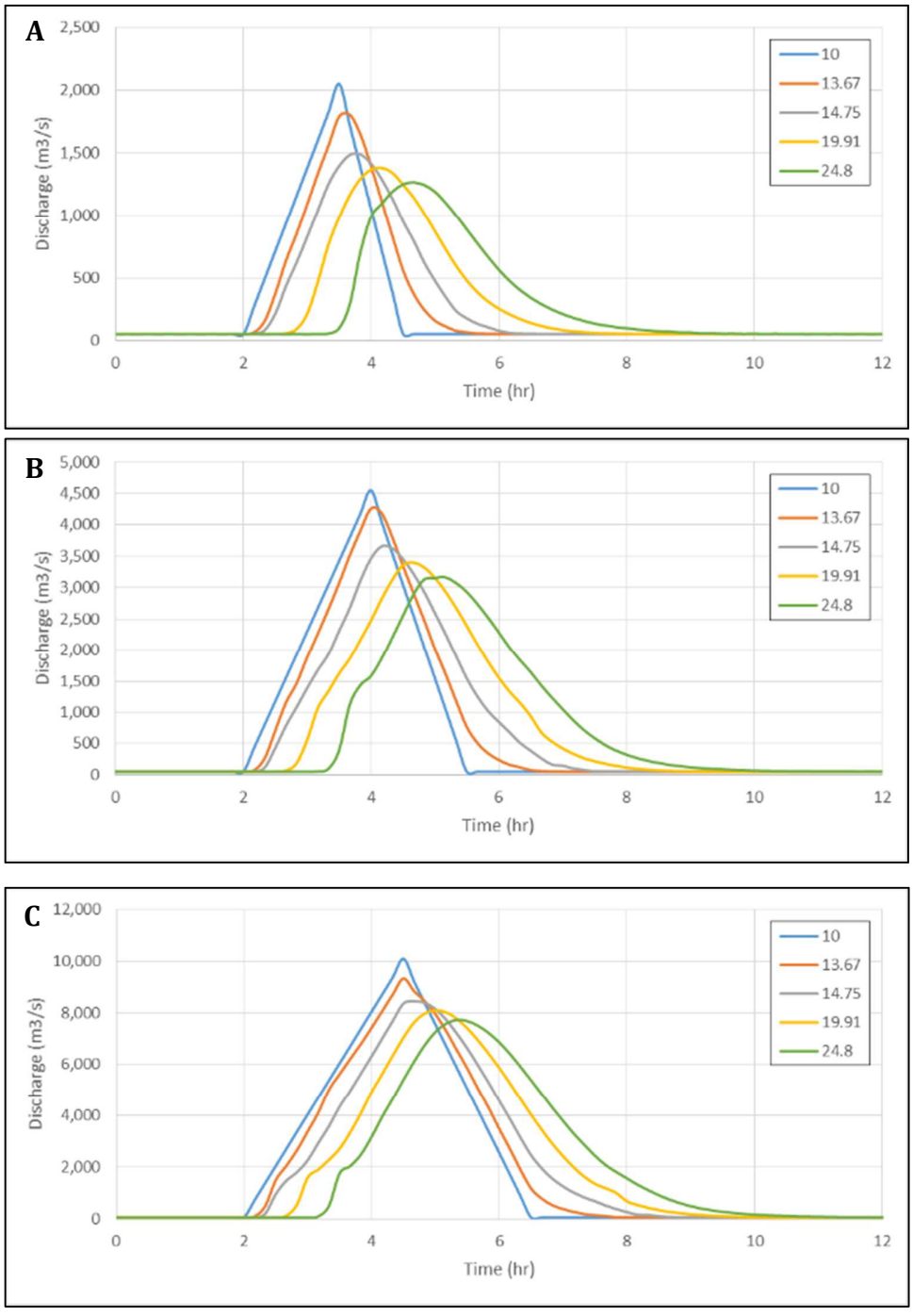

Figure 8.14: *Hydrographs for low baseflow scenarios, showing initial triangular hydrograph (10 km) and routed hydrographs at downstream locations; Arthurs Point (13.67), Big Beach (14.75), Tucker Beach (19.91), and the Shotover Delta (24.8).*

Peak flow attenuation for the modelled scenarios are in the range of 20-40%, with decreasing attenuation for higher flow scenarios (Table 8.4, Figure 8.15). There is minor attenuation of modelled flows within the gorge section, decreasing on reaching the slightly wider Morning Star Beach section at about 2 km from the dam location, then a rapid

decrease in peak flow at about Big Beach. At Big Beach, the peak flow is modelled as decreasing by ~15% within the space of two kilometers, and continues to decrease gradually over the remainder of river downstream to the Kawarau confluence (Figure 8.15).

The influence of sediment bulking on peak flows, or sediment entrainment on the physical properties of the flow are not thought to be significant. Modelled Shotover Gorge landslide dam volumes are all <6% (most <3%) of the estimated volume of the impounded lake (Table 7.2). With erosion of the breach channel likely to only erode less than half of the total dam volume, it can be seen that any sediment bulking impacts will be inconsequential. Moonlight Creek scenarios have relatively higher dam volumes, where the total dam volume is modelled as 14-20% of the lake volume, and any bulking effect is expected to be much less than 10%.

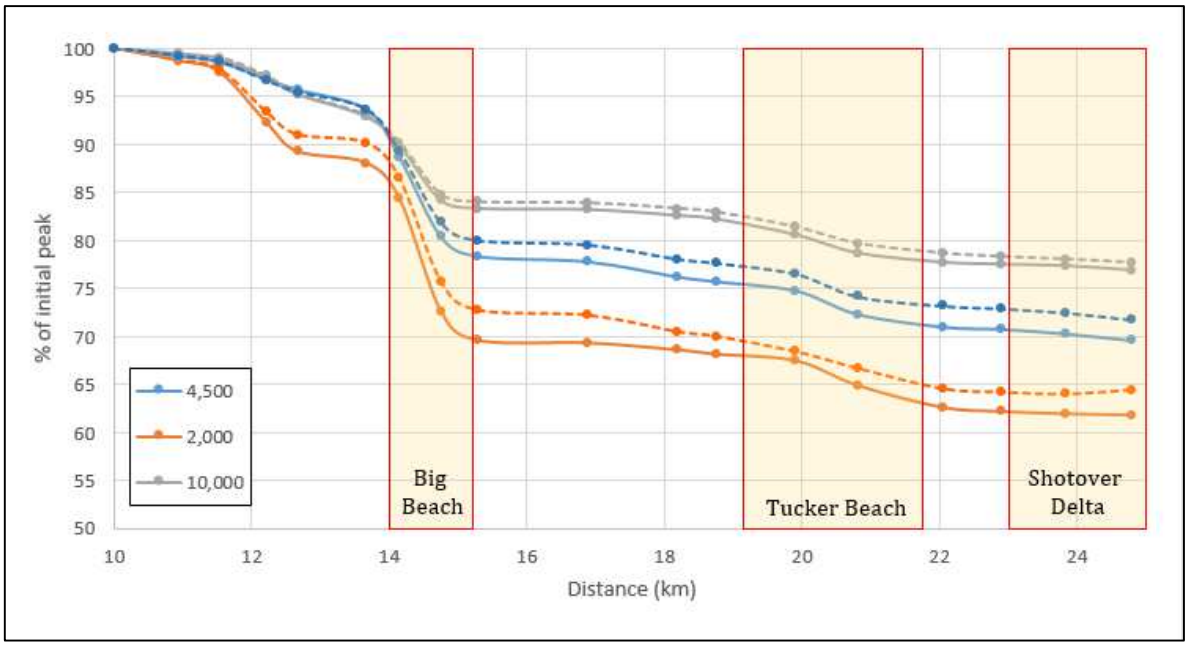

Figure 8.15: *Flow attenuation for dambreak flood scenarios, where 100% represents the peak flow at the breach location. Solid lines are low baseflow scenarios, dashed are high baseflow. This shows minor flow attenuation within the Shotover Gorge (10-14 km), then a significant decrease in peak flows on exiting the Shotover Gorge at Big Beach, and a gradual decrease over the remainder of the lower Shotover River.*

Maximum inundation depths during dambreak flood events are estimated to occur in the Shotover Gorge and at Big Beach, the water depths then decreasing dramatically between Big Beach and Tucker Beach, followed by a more gradual decrease to the Shotover Delta (Figure 8.16). The large decrease in flow depth below Big Beach is due to a corresponding increase in channel width from the narrow channel downstream of Big Beach (about 25 m wide at section 15.29), widening to >100 m by section 18.15, and then to about 500 m width at section 18.76 (Figure 8.12). With a large available storage area and a narrow outflow channel, Big Beach is interpreted to act as a detention basin, storing and slowly releasing floodwaters, contributing to attenuation of peak flows and a decrease in flood depth downstream.

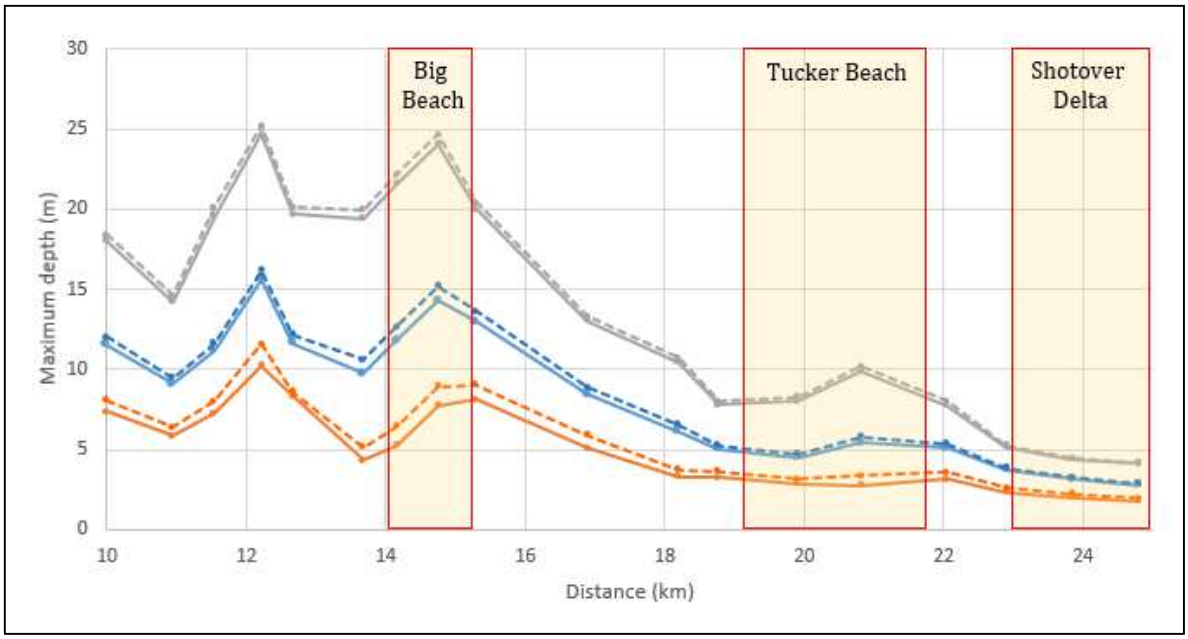

Figure 8.16: *Maximum inundation depth for dambreak flood scenarios. This shows maximum depths within the Shotover Gorge and at Big Beach, before rapidly decreasing in depth before reaching the Shotover Delta. Solid lines represent low baseflow scenarios, dashed are high baseflow.*

Figure 8.17 illustrates travel times of the dambreak flood wave, showing hydrographs at the breach and those routed to the Shotover Delta. From start of breaching, the time for the start of the modelled flood wave to reach the Shotover Delta ranges from 1-1.5 hours, and the total time from start of breaching to attain peak flow at the Shotover Delta is 2.7-3.3 hours.

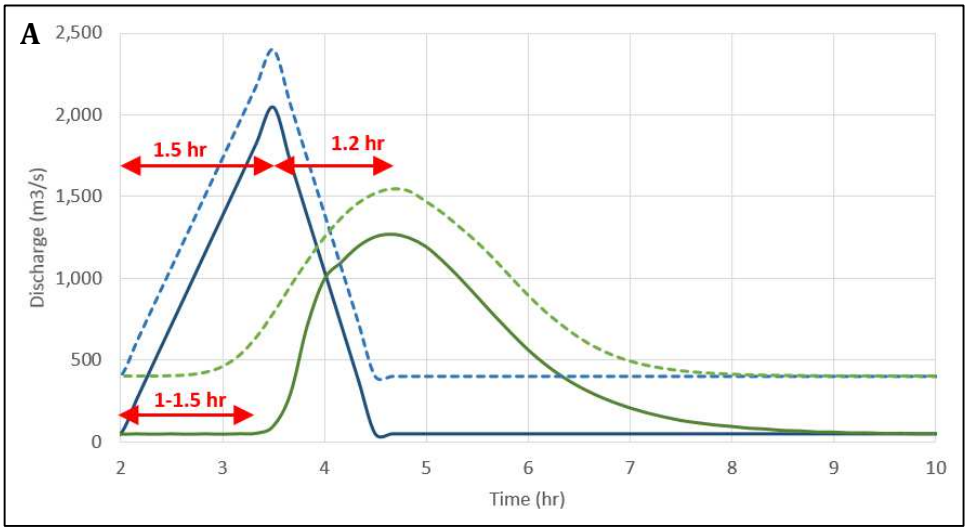

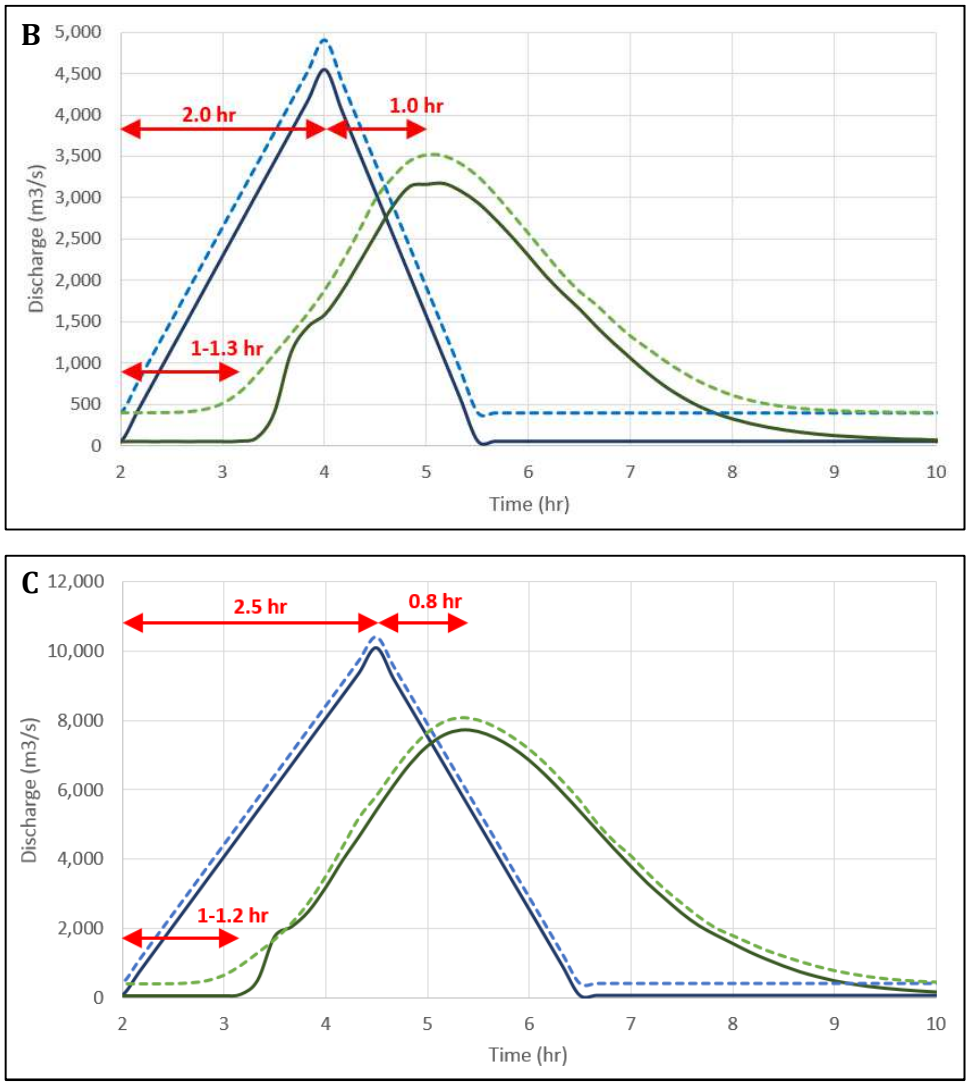

Figure 8.17: *Travel time results for A. low, B. high and C. very high flood peak scenarios, showing hydrographs at the breach (blue lines), and at the Shotover Delta (green), where solid lines are low baseflow scenarios, and dashed lines are high baseflow scenarios. Labels show duration of rising limb at breach, the time for start of flood wave to reach Shotover Delta, and travel time for peak flow to reach delta.*

At the Shotover Delta, the possible impact of a dambreak flood on the housing areas adjacent to the Shotover Delta can be assessed using a rating curve developed by Hamilton (2017), for the middle reaches of the Shotover Delta at cross-section MWD3 (Figure 8.18). This rating curve was based on hydraulic modelling in HEC-RAS, created for the surveyed 2016 riverbed level, and for a projected 2110 bed level assuming 0.8 m of future aggradation at this point on the delta. Extrapolating from Hamilton's rating curve, it is estimated to require a flood peak at the delta of >8,000 m^3/s in order to overtop the Shotover Country dwelling level (Figure 8.18). Assuming 20% attenuation in flood peak from the dam breach location to the Shotover Delta, generation of a flood peak of this magnitude would require a dambreak flood with a peak discharge at the breach of 10,000 m^3/s. Based on the peak dambreak flow estimations in Figure 8.8, this is likely to require failure of a lower Shotover Gorge dam with a height of at least 100 metres.

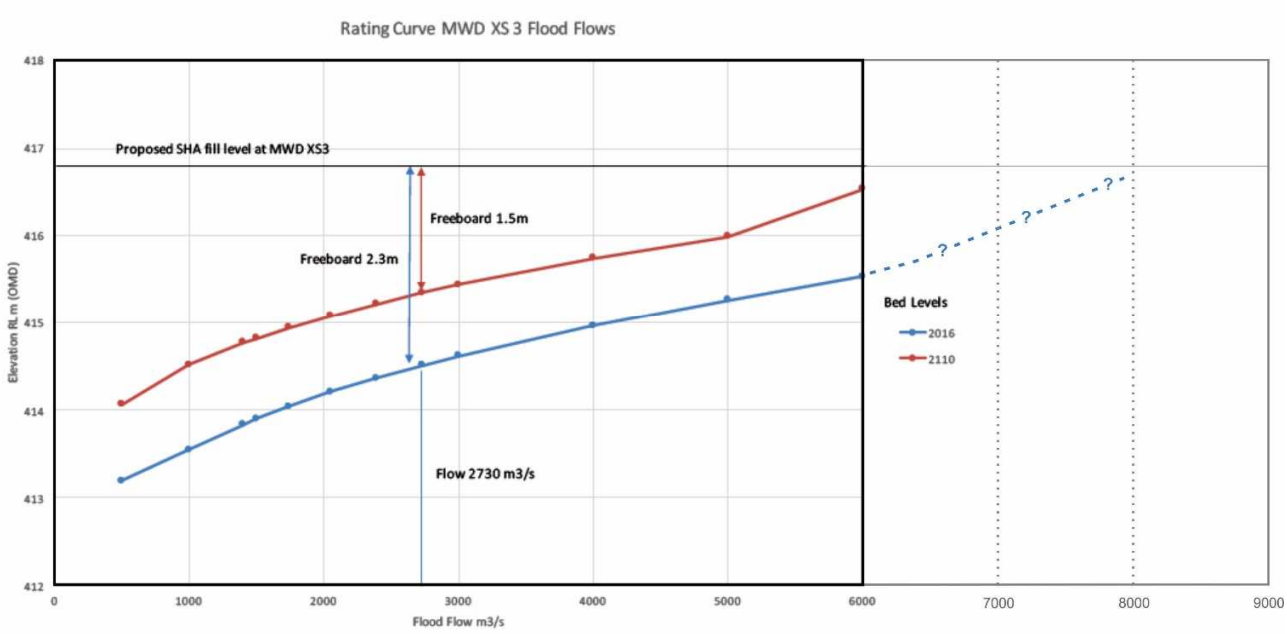

Figure 8.18: *Hamilton's (2017) Shotover Delta rating curve at cross section MWD3 (black outline), and an extrapolated curve for higher flows of 6000-9000 m^3/s. Water levels are shown for the surveyed January 2016 riverbed level (blue) and a projected bed level for the year 2110 (red). Elevation is in Otago Metric Datum (OMD), 100 metres above the true RL.*

Model Limitations

This model represents only a small number of possible dam breaching scenarios, and other failure scenarios could result in significant variations in breach dimensions and formation times, and thus significantly different peak outflows and flood durations. This model is a basic approximation of the dambreak flood progression, and is inferred to underestimate flow attenuation, resulting in conservative values for peak flows and flood depths at the Shotover Delta. The main approximations and limitations of this modelling are;

1. A simplified channel geometry is assumed and interpolated from a limited number of cross sections. The model could be improved through inclusion of more detailed and more closely spaced cross sections, or use of a 2D model.
2. Dambreak floods were modelled from only a single initiation point, in the lower Shotover Gorge. Dambreak floods originating from mid/upper Shotover Gorge dam failures or in tributary streams have not been modelled and may attenuate to a greater extent before reaching the lower Shotover River and the delta, however the potential for flow attenuation is limited within the narrow gorge.
3. This model does not model the interaction of the dambreak flood wave with the Kawarau River confluence, which would be expected to cause a damming/backwater effect on the Kawarau River, as is observed during large meteorological flood events (Webby and Waugh 2006). The downstream model boundary was a fixed level at a dummy cross section ~1 km beyond the true model extent. This model boundary acts as an infinite reservoir, and does not account for potential flow restriction caused by the hydraulic interactions at this point.

Flood Routing Results Discussion

These model results appear to be comparable to those from dambreak models in similar settings, such as the North Young River (ORC 2007b) and Callery Gorge (Ollett 2001) dambreak studies. Both the Shotover and Callery Gorge models show little peak flow attenuation within gorge sections (<15%). North Young River dambreak flood modelling shows similar peak flow attenuation results to Shotover models, with both having attenuations of 20-40% over distances of 10-15 km (Figure 8.19). Much of the flow attenuation in the Young River model occurs at Ram Flat, a wide flat with a constricted outlet which acts as a detention basin, with ORC estimating that almost half of the total outflow volume is temporarily stored in this area. This is similar to characteristics of Big Beach, which also appears to act as a detention basin due to its large storage area and narrow outlet.

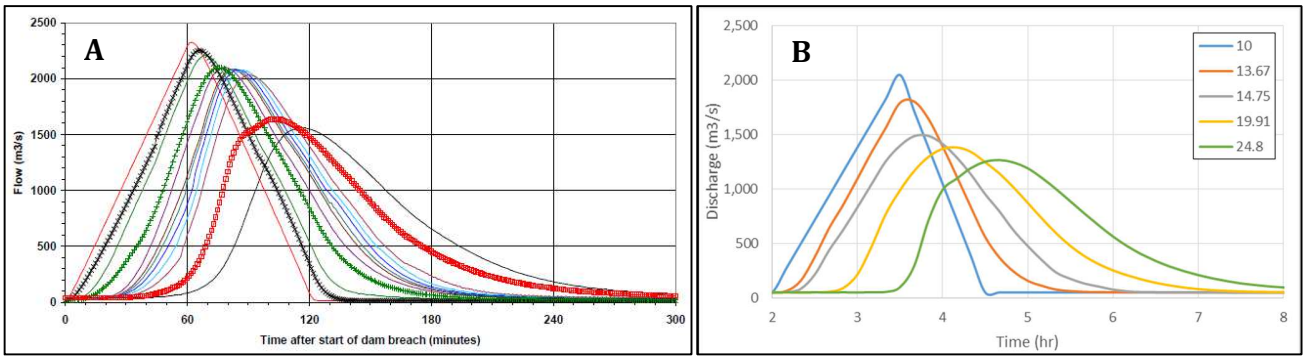

Figure 8.19: *Comparison of routed flood hydrographs modelled for A. failure of the North Young River landslide dam (ORC 2007b), and B. for a Shotover Gorge dambreak flood of similar magnitude (2000 m³/s discharge, 50 m³/s baseflow).*

8.7 Summary and Conclusions

This chapter has investigated dambreak flooding resulting from catastrophic failure of the landslide dam scenarios developed in Chapter Seven. This has included estimation of peak discharges (Figure 8.8, Table 8.3), breach characteristics (Table 8.2), and dambreak hydrographs (Figure 8.10). A flood routing model was used to simulate the downvalley progression of the flood wave and estimate flow attenuation (Figure 8.15, Table 8.4), inundation depths (Figure 8.16) and the flood wave's travel time (Figure 8.17).

Estimation of dambreak discharges show the potential for a large dambreak flood event to originate in the Shotover Gorge. A 100 m lower Shotover Gorge landslide dam scenario resulting in estimated discharges of ~10,000 m³/s, and a larger 125 m high scenario resulting in an estimated discharge of 15-25,000 m³/s Table 8.3). In the upper Shotover Gorge relatively larger volume lakes are able to form as these fill the wider upper gorge and Branches Flat (Figure 7.3C). As the result these landslide dams result in large estimated discharges despite a lower modelled dam height, for example an estimated peak discharge of ~10,000 m³/s from a 60 m high dam scenario.

Modelling of flow attenuation shows that the peak discharge will attenuate as the flood wave travels downriver, with much of the attenuation occurring at Big Beach, the first broad riverbed section below the gorge exit. Flow attenuation is estimated at 20% between the lower Shotover Gorge and the Shotover Delta for the largest modelled scenario, although this may be underestimated due to simplification of the channel geometry. The flood routing model does not include modelling of the hydraulic interaction at the Shotover-Kawarau confluence, which is beyond the scope of this project, and this may lead to an underestimation of the flood level at the lower-mid Shotover Delta.

There are large uncertainties in the estimation of peak flows, model parameters and the magnitude of attenuation, but modelling indicates a dambreak event could be capable of generating flows of much greater magnitude than meteorological flood events. A dambreak flood could potentially impact the Shotover Country residential area, based on a rating curve at the Shotover Delta (Figure 8.18) this is estimated to require a flood discharge at the delta of >8,000 m^3/s. Generation of a flood of this magnitude is estimated to require catastrophic failure of a large landslide dam (>100 m height). A flood generated the largest lower Shotover Gorge landslide dam scenario (125 m high) has a significantly higher peak discharge estimated at 15-25,000 m^3/s and would be likely to be of a damaging magnitude at the delta, potentially with severe impacts on the residential area.

The largest potential flood magnitudes at the delta are likely to be generated by rapid, near-complete dam failures, from locations in the lower Shotover Gorge. Peak flows are expected to be lower if development of dam breach is slower, or for partial breaching of the dam. Although these estimations and modelling contain considerable uncertainty, they demonstrate the potential magnitude of possible future dambreak flood events, and assist the understanding of these hazard events in the Shotover River.

The landslide scenarios used as a basis for landslide dam and dambreak flood scenarios are not the largest landslide events possible in the Shotover Gorge, and thus larger dams and dambreak flood magnitudes are possible. A lower Shotover Gorge landslide dam of ~100 m height is modelled as having a volume of 3-4M m^3 (Table 7.2), and this is an order of magnitude smaller than the estimated volumes of the largest existing landslides, for example a landslide in the middle Shotover Gorge has a scarp width of ~500 m and an estimated volume of 15-20M m^3 (Figure 2.31). This shows the potential for formation of landslide dams very much larger than the modelled scenarios, and these would be expected to generate extremely large and damaging dambreak floods at failure.

Chapter Nine: Dambreak Events Scenario

9.1 Introduction

A statistical approach to quantitative risk assessment is of limited use for investigation of large, infrequent hazard events. Using a probabilistic approach, the low likelihood reduces the apparent threat of low frequency, high consequence events, and these tend to be dismissed (Davies et al. 2015, Tonkin and Taylor 2016). Another approach to hazard assessment is through the development of event and effects scenarios (Davies et al. 2015). These scenarios show understanding of the hazard processes and potential adverse effects, and are a useful method of presenting and communicating what future events could look like (Tonkin and Taylor 2016). A hazard scenario should be "realistic and defensible" (Yetton and McMorran 2004, p38), and will ideally have the following characteristics (Porter et al. 2011);

1. Be scientifically realistic,
2. Large enough to generate significant consequences,
3. Likely enough not to be dismissed as rare or extreme, and
4. Consisting of a single, specific scenario rather than probabilistic ranges.

Two hazard events scenarios for the Shotover Gorge have been developed based on the assessments and modelling carried out in Chapters Six-Eight, landslide dam case studies (e.g. Hancox et al. 2005, ORC 2007a) and other landslide dam hazard assessments such as at the Callery Gorge (Ollett 2001). A possible civil defence response is outlined, based on documented responses to other landslide dam events. These include the Tunawaea (Parkin 1993), Poerua River (Hancox et al. 2005, Becker et al. 2007), North Young River (ORC 2007a), and Kaikoura (Dellow et al. 2017) landslide dams. Possible impacts on residents and tourism are based on the impacts of smaller Shotover Valley events such as the Moonlight Track landslide (Bryant 2011), and the Devil's Elbow landslide road closure (Downer 2013). Disruption caused by the threat of dambreak is shown by examples such as the North Young River landslide dam, where the downstream walking track was closed as a precaution (ORC 2007a).

The scenarios describe possible sequences of events for formation and failure of a large (80-100 m height) landslide dam in the lower Shotover Gorge. This provides an example of the hazards cascade resulting from landslide emplacement in a narrow river channel (Figures 5.7, 5.8), including dam formation, dam failure and dambreak flooding. The longer-term sedimentary impacts are addressed in Chapter Ten.

Two scenarios have been developed to illustrate differences in the landslide dam hazard events at different river flow levels. The first scenario while the Shotover River is at a low flow (40-50 m^3/s), and the second a rainfall-triggered landslide occurring while the river is in flood (100-year flood event with a peak of ~1500 m^3/s).

The Shotover Gorge landslide dam described in these scenarios is of a comparable magnitude to several recent South Island landslide dam events, for example the 80-100 m Poerua River (Hancox et al. 2005), the 74 m North Young River (ORC 2007a), and 100 m Hapuku River (Dellow et al. 2017) landslide dams. However, there are several differences between the Shotover Gorge and the setting of those case studies. Located in the lower reaches of a large catchment (~1000 km^2) a Shotover Gorge landslide dam has much larger river flows, and is expected to be less stable than the still-intact Young River landslide dam. The Shotover Gorge has a lower gradient than the steeper Poerua Gorge at the Poerua River dam. This allows for formation of a larger volume reservoir in the Shotover, potentially resulting in a much larger dambreak flood magnitude.

9.2 Landslide Dam Hazard Scenario (Low Flow)

Slope Failure

In the early morning during a late November period of settled weather, a large rapid landslide or rock avalanche occurs in the lower Shotover Gorge. This landslide has a volume of about 3M m^3 and occurs at a location between Arthurs Point and Moonlight Creek (Figure 9.1). The landslide is from an area of steep terrain (>35°), destabilised by incision of the Shotover River (e.g. Figure 6.6). The failure site had been exhibiting signs of extensional deformation such as tension cracks for many years or decades prior to failure, and there was no obvious trigger for the final catastrophic failure (e.g. Poerua River and North Young River landslide dams).

The landslide is a wedge failure controlled by the many structural weaknesses present in the schists of the valley, including, jointing faulting, and the schist foliation. The rock mass increases in volume as the landslide debris fragments, bulking by ~20% in volume during deposit emplacement. Due to the steep slopes and a highly mobile landslide, little landslide debris is stored on the slopes and the majority of this material is transported into the river channel.

The landslide is noted from a distance as a large dust cloud, and reduced and discoloured river flows are observed at Arthur's Point and the Shotover Delta. These effects are widely visible and are reported by a number of observers, including walkers on the Moonlight Track or at Morning Star Reserve, helicopter flights into the valley, and rafting/jet boat operators.

Landslide Dam Formation and Lake Filling

Landslide debris is rapidly emplaced into the Shotover Gorge, forming a dam with a height of 80-100 metres (Figure 9.1), this obstructs all river flow downvalley and a landslide-dammed lake forms and begins to fill. Shotover River inflows are relatively low (<50 m^3/s) at the time of the landslide and the new landslide-dammed lake slowly fills within ~3 weeks, to contain a volume estimated at ~100M m^3. The final lake extends upvalley for about 15 km, inundating the Skippers Road at the Deep Creek Bridge and preventing road access into the Shotover Valley (Figure 9.2). Once the lake infills, the overtopping flow forms a narrow outlet channel in the dam crest. Finer material is eroded to leave the channel armoured by larger clasts and stable under lower flow rates, as at the presently-stable North Young River landslide dam (ORC 2012, Massey et al. 2013).

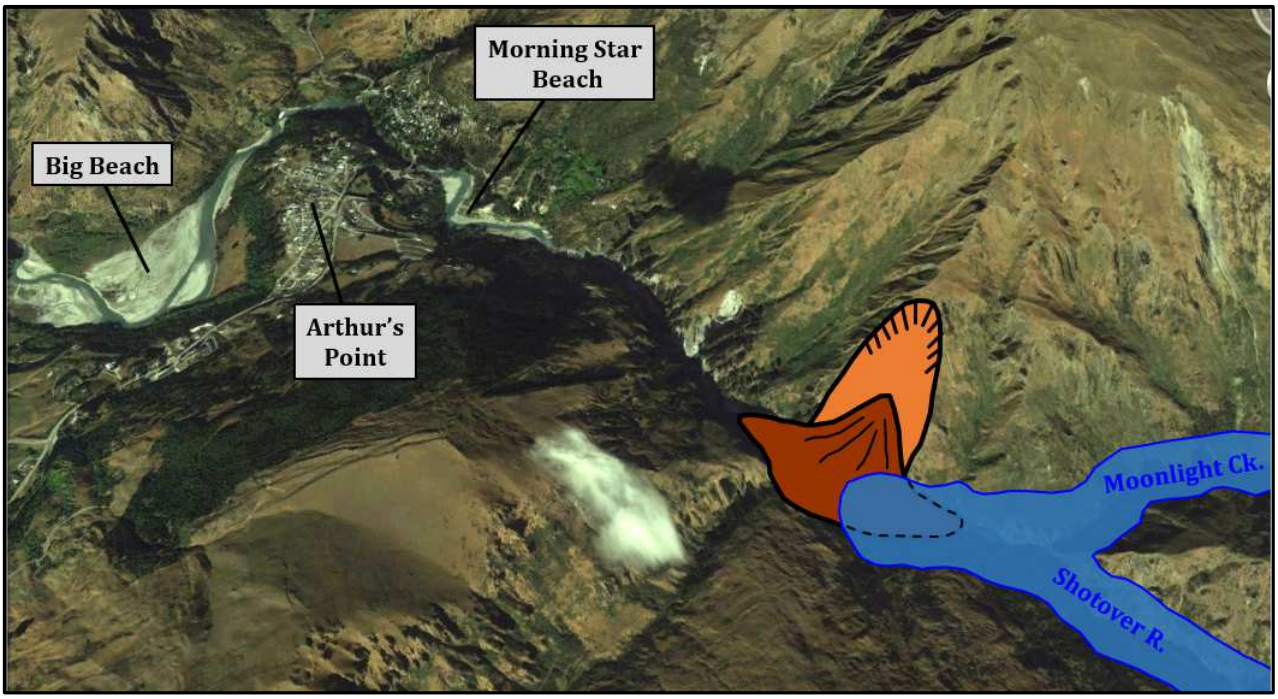

Figure 9.1: *Sketch of a possible lower Shotover Gorge landslide dam scenario. View is looking south towards Arthur's Point and the lower Shotover River (Google Earth 2010).*

Figure 9.2: *Extent of a landslide-dammed lake, formed by a lower Shotover Gorge landslide dam scenario. View is looking upvalley from about the Wakatipu Basin (Google Earth).*

Landslide Dam Response

Once the landslide dam formation has been reported by the public, a multiagency response is initiated. This team includes regional and district government representatives (ORC, QLDC, CDEM), supported by geological expertise (GNS, universities, and/or geological consultants), and police and community representatives. A visual inspection of landslide and dam location is undertaken, with preliminary geomorphic mapping of the landslide and dam, and initial estimates made of the landside volume, dam height, reservoir filling rate, and apparent dam stability. Dam and lake parameters are used in empirical equations for initial assessments of dam stability (e.g. Figure 6.7) and estimation of possible dambreak flood magnitude (e.g. Figure 7.2). These indicate the Shotover Gorge dam is unlikely to be stable in the long-term, and to be capable of generating a dambreak flood flow of 6-11,000 m^3/s. Initial assessments are completed within several days, concluding; "the integrity of the dam cannot be assured, therefore planning must cater for a rapid, significant dam breach occurring with little warning" (ORC 2007a, p1).

There is significant concern that the dam will fail at its first overtopping, and given the magnitude of possible dambreak flood flows, a precautionary evacuation is undertaken for residents in the lower elevation parts of the Shotover Country residential area as the dam approaches capacity. Several walking tracks alongside the lower Shotover River at Morning Star Beach, Tucker Beach Reserve, and the Shotover Delta are also closed due to threat of dambreak flooding. The dam finally overtops several weeks after formation, and does not immediately fail. After inspection, the dam is interpreted to be temporarily stable at the current flow rates, and the evacuation order is lifted.

As the dam does not fail immediately on overtopping, a telemetered monitoring system is installed to provide warning of dambreak flooding. This simple system comprises a series of VHF radio transmitters located in the riverbed downstream of the landslide dam and designed to transmit intermittently, with the successive loss of these signals indicating destruction due to dambreak flooding (ORC 2007a). If time and resources permit, more advanced monitoring systems can be installed, such as downriver water level float switches or pressure sensors (ORC 2007a) or a water level monitor in the landslide-dammed lake, where a sudden drop in lake level will indicate breaching (ORC 2007a). Remote cameras or webcams may be used to provide visual assessment of dam conditions.

Several weeks after the dam's first overtopping, heavy rainfalls are forecast to result from an approaching weather system. A precautionary evacuation of residents is again undertaken from residential areas adjacent to the Shotover Delta. The dam is closely monitored, both remotely and by regular field inspections.

Dam Failure and Dambreak Flooding

The heavy rainfall event increases river flows to greater than mean annual flood levels (500 m^3/s), and these larger and more erosive overtopping flows increase the erosion rate of dam material. Erosion of the downstream dam face rapidly migrates headwards, progressively weakening the dam, and eventually inducing a catastrophic failure. The breach channel erodes to a depth of 50-70% of dam height over a period of ~4 hours, rapidly releasing the majority (>90%) of the reservoir volume. From the start of breaching, flood discharge rapidly increases, reaching a peak of 9-10,000 m^3/s after about 2.5 hours.

The first sign of the flood wave is observed at the Shotover Delta about an hour after the start of breaching, peaking after another two hours (Figure 7.17C). The flood wave has been stretched and flattened through downstream travel over the wide beach sections, attenuating to a peak flow of 7-8,000 m^3/s. At its peak discharge, the flow reaches the lowest parts of the Shotover Country housing area, although is not deep enough to cause significant damage. The flow remains greater than 50-year flood levels (~1,050 m^3/s) for a total period of around four hours, hydraulically damming the Kawarau River and causing some reverse flow 'upstream' towards Lake Wakatipu.

Following the dam breach a much smaller remnant lake is still present at the dam location, this has a depth of only about 20 metres and no longer presents any significant threat of sudden dam failure or dambreak flooding. All access restrictions to riverbank areas are lifted, and rafting and jet boat operations can recommence although operations are

limited by the presence of the remnant dam. Eroded landslide material is transported by the flood and deposited in the gorge and sections of the lower Shotover River. Over the following years the remnant landslide dam continues to erode and significant aggradation occurs as this excess sediment is mobilised through the river system.

9.3 Landslide Dam Hazard Scenario (High Flows)

Slope Failure

There have been a series of heavy rainfall events throughout November, the Shotover River level has fallen from its most recent flood peak but still has a relatively high base flow of ~200 m^3/s. Another large weather system causes sustained, heavy rainfall in the Shotover Gorge and throughout much of the catchment. Falling on already saturated ground, runoff is rapid and the river rises to a high flow of >1,000 m^3/s.

In the early morning, a large rapid landslide or rock avalanche with a volume of about 3M m^3 occurs in the lower Shotover Gorge, at a location between Arthurs Point and Moonlight Creek (Figure 9.1). The landslide is from an area of steep terrain (>35°), destabilised by incision of the Shotover River (e.g. Figure 6.6). The failure site had been exhibiting signs of extensional deformation such as tension cracks for many years or decades prior to failure, and the extremely heavy rain event triggers the final slope failure.

The landslide is a wedge failure controlled by the many structural weaknesses present in the schists of the valley, including, jointing faulting, and the schist foliation. The rock mass increases in volume as the landslide debris fragments, bulking by ~20% in volume during deposit emplacement. Due to the steep slopes and a highly mobile landslide, little landslide debris is stored on the slopes and the majority of this material is transported into the river channel.

Landslide Dam Formation and Lake Filling

Landslide debris is rapidly emplaced into the Shotover Gorge, forming a dam with a height of 80-100 metres (Figure 9.1), this obstructs all river flow downvalley and a landslide-dammed lake forms and begins to fill. At Arthur's Point and the Shotover Delta the river is observed to rapidly fall from its previously high flood levels. These effects are reported by a number of observers, although due to storm conditions there were no helicopters operating at the time, and rafting and jet boat operations had suspended activities due to the very high river flows.

Shotover River inflows are relatively high (~1,000 m^3/s) at the time of the landslide and increase throughout the day as rainfall continues at a high intensity, with the new landslide-dammed lake rapidly filling,

Landslide Dam Response

The reduced river flows are reported by observers and a small emergency management group is quickly assembled to assess the situation. Formation of a landslide dam has been assumed, but its location or size are not yet known. With heavy rain continuing, by the time a weather window allows for a helicopter-based inspection of the dam it is past midday. The landslide dam is quickly identified in the lower Shotover Gorge, and observed to be large and the lake to be filling rapidly, already nearing a level approximated at half of the dam height.

Based on these observations, the dam is expected to overtop within 1 day, and the dam dimensions are such that a large magnitude dambreak flood is thought probable. This is of major concern, and the decision is made to evacuate all low-lying areas alongside the Shotover Delta. A full evacuation is undertaken as soon as possible, with all residents evacuated by nightfall. A final inspection of the dam in the evening confirms the lake to still rapidly filling, and plans are made for another inspection as early as possible the following morning.

Dam Failure and Dambreak Flooding

River flows continue to stay very high from time of dam formation, increasing to a peak of ~1,500 m^3/s. About 20-24 hours after formation the lake reaches capacity and the dam overtops, the incoming river flows are still near their peak and these large flows begin to rapidly erode the downstream face of the dam. An initial breach channel is formed by the first overtopping flows and this rapidly incises. The enlarging breach allows for greater flows and erosion of the dam material accelerates, resulting in catastrophic dam failure. The breach channel erodes to a depth of 50-70% of dam height over a period of ~4 hours, rapidly releasing the majority (>90%) of the reservoir volume.

From the start of breaching, flood discharge rapidly increases, reaching a peak of 10-12,000 m^3/s which is made larger by the contribution of the high inflows from the flooded Shotover River. The first sign of the flood wave reaches the Shotover Delta about an hour after the start of breaching, with the flood discharge building steadily and reaching a peak after another 2.5 hours. The flood wave has been stretched and flattened through downstream travel over the wide beach sections below the exit of the gorge, but still reaches a peak flow of 9-10,000 m^3/s at the Shotover Delta. At its peak discharge the flood wave inundates the lower parts of the Shotover Country housing area at the Shotover Delta and causes major damage to those structures exposed to the deepest and highest velocity flows. The flow remains greater than 50-year flood levels (~1050 m^3/s) for a total period of around six hours, hydraulically damming the Kawarau River and causing some reverse flow 'upstream' towards Lake Wakatipu.

Following the dam breach a much smaller remnant lake is still present at the dam location, this has a depth of only about 20 metres and no longer presents any significant threat of sudden dam failure or dambreak flooding. All access restrictions to riverbanks areas are lifted, and rafting and jet boat operations can recommence although operations are limited by the presence of the remnant dam. Eroded landslide material is transported by the flood and deposited in the gorge and sections of the lower Shotover River. Over the following years the remnant landslide dam continues to erode and significant aggradation occurs as this excess sediment is mobilised through the river system. These longer-term sedimentary impacts are discussed in Chapter Ten.

9.4 Conclusions

These scenarios illustrate a potential sequence of events for the formation and failure of an 80-100 m Shotover Gorge landslide dam. There is no historic precedent for a landslide dam of this magnitude in the Shotover Gorge, and this scenario has been based on the interpretations and modelling in the previous chapters (6-8), and with reference to documented landslide dam and dambreak events. Illustrating possible sequences of events and relative timings, these scenarios can serve as a focus for inter-stakeholder discussion regarding management and decision making for a future landslide dam event.

The scenarios demonstrate the influence of river flows on the timing of events, potential dambreak flood magnitudes, and response style. At lower river flows the landslide-dammed lake fills relatively slowly, and allowing time for an in-depth response, involving monitoring of the lake and evaluations of possible event magnitudes and impacts. With the river already at high flood flows the lake fills very rapidly and the dam may overtop within 24 hours. A rapid assessment and response is required, with decisions quickly made based on the limited information available.

These are considered to be a realistic series of landslide and dambreak events, however these are only two possible scenarios, and there are many other plausible events sequences. Events will in reality differ from this scenario, with possible variations in landslide size, trigger, style or location. Landslide volumes may be smaller or greater than those in this scenario, and there may be significant variation in the portion of landslide volume contributing to dam formation, amount of bulking of landslide debris, and in dam morphology.

A landslide dam could also be formed at a location in the middle or upper Shotover Gorge, or in a tributary catchment such as Moonlight or Skippers Creek. Variations in valley morphology will influence the dam height formed for a given landslide volume, the reservoir volume able to be impounded, and thus the possible magnitude of dambreak flooding. Breaching may occur at the dam's first overtopping or during a later high flow event. The depth and duration of breach formation will strongly influence the peak dambreak discharge, with a slower breach development resulting in a longer duration flood wave with a lower peak. Reservoir filling times and peak dambreak flows are influenced by Shotover River inflows, these may be as low as several tens of cumecs, or as high as flood flows of 420 m^3/s (mean annual flood) or 1000-1500 m^3/s (50-100 year floods).

Chapter Ten: Aggradation Impacts

10.1 Introduction

Failure of a large landslide dam in the Shotover Gorge will add several million cubic metres of additional sediment into the river, and the downstream mobilisation of this material may cause significant geomorphic changes to the river system. These changes would include the rapid deposition of dambreak flood deposits, then continued erosion of remaining landslide dam material and reworking of flood deposits over the following years.

This influx of sediment will form a sediment pulse, with an initial aggradation/expansion phase in response to increased sediment supply, followed by degradation/incision as the sediment supply decreases to pre-event levels – probably over decades. In the lower Shotover River, this aggradation may contribute to increasing the flood hazard in two ways; (1) raising of riverbed levels will cause flood flows to be superimposed on a higher base and so reach higher levels, and (2) progradation of the Shotover Delta toe may impede Lake Wakatipu outflows, thus increasing flood hazard to Queenstown.

This chapter builds on the landslide dam scenarios developed in the previous chapters, investigating the geomorphic changes expected to result from the sediment influx following a large landslide dam failure. The chapter starts with a review of sediment pulse literature, then includes three analysis sections;

1. A sediment pulse scenario, describing geomorphic changes through time resulting from a large dambreak in the lower Shotover gorge.
2. Estimates of thickness distribution of dambreak flood deposit and maximum aggradation thickness for moderate and large volume dam failures.
3. A river morphodynamics model is used to simulate effects of increased sediment supply on the Shotover River.

10.2 Sediment Pulses Review

Any large input of additional sediment into a river system will form a sediment pulse as this excess material progresses downstream. Sediment pulses may be caused by a wide range of events, both anthropogenic and geological in nature (Kondolf et al. 2002, James 1999 2006, Ferguson et al. 2015). Anthropogenic sedimentation is often due to widespread landuse changes such as deforestation, agriculture, road building, fire or urbanisation, but can also be caused by localised events like dam removal or the input of mining wastes. Geological events causing sediment pulses include sediments resulting from large landslides, landslide dambreak floods and volcanic eruptions.

A sediment pulse may be caused by debris from a single isolated landslide or landslide dambreak, or multiple widespread events, for example large numbers of landslides triggered by earthquake shaking or a heavy rainfall event. Many studies document the sedimentary impacts of geological events, with examples including:

- Landslide dam failure: Poerua River 1999 (Hancox et al. 2005), Ram Creek (Nash et al. 2008, Harrison et al. 2015), Tunawaea 1992 (Riley et al. 1993).
- Landslide/rock avalanche (with no dam formed): Falling Mountain 1929 (coseismic triggered) (Korup et al. 2006)
- Chronic mass movements: Gaunt Creek/Waitangitaona River (Korup et al. 2004, Korup 2004b, Nelson 2012).
- Coseismic landsliding: Murchison 1929 (Pearce and Watson 1986, Korup and Wang 2015), Chi-Chi, Taiwan 1999 (Chen 2008), Wenchuan 2008 (Korup and Wang 2015, Wang et al. 2015)

- Meteorologically-triggered landsliding: Storm-triggered debris flows, Gate Creek, Oregon 1996 (Miller and Benda 2000), Typhoon Talas landsliding, Japan 2011 (Korup and Wang 2015).

In mountainous terrain, sediment supply has an episodic behaviour, where a large portion of material may be due to a single event and can dominate all other sources (Cui et al. 2003). Many catchments are thought to never attain an 'equilibrium' state, as they are subjected to intermittent, catastrophic sediment influxes, which are not completely cleared from the catchment before occurrence of another similar event (Davies and Korup 2007). For example, Pearce and Watson (1986), thought it unlikely that all earthquake-generated debris from the 1929 Murchison earthquake would be removed from the river system before the occurrence of the next major earthquake.

Conceptual Models of Sediment Movement

A number of models describe the influence of landsliding on fluvial systems, geomorphic landforms, and valley evolution. Hewitt (2006) and Bainbridge (2017) outline conceptual models showing typical effects of formation and failure of a large dam-forming landslide on development of mountain river valleys, termed the 'landslide interruption epicycle' by Hewitt. The main phases in these models are summarised in Table 10.1, and the Bainbridge model is shown in Figure 10.1. Korup et al. (2010) discuss the influence of landslides on mountain range evolution, including their role as sediment sources, and resulting impacts on valley floor morphology, and sediment delivery and storage. Sediment cascade concepts integrate catchment-scale interactions and processes of sediment generation, transport, deposition, and storage (e.g. Davies and Korup 2010, Trimble 2010, Fuller 2014). Davies and Korup (2007) developed a conceptual model for the response of rangefront alluvial fans to infrequent, catastrophic sedimentation caused by episodic delivery of landslide-generated sediments.

Table 10.1: *Conceptual models of landslide impacts on a valley system.*

Hewitt (2006)	Bainbridge (2017)
	a. The pre-landslide system
1. Landslide complex – landslide emplacement	**b. Landslide emplacement** – upstream delta formation, downstream sediment starvation
2. Impoundment complex – aggradational landforms upstream of barrier, downstream erosion and/or sedimentation	
3. Degrading interruption complex – trenching and removal of impoundment complex, downstream sedimentation	**c. Dam breach flood** - alluvial fan development and overbank flows
	d. Post-flood system - stabilised dam breach, deposition of reworked landslide material, downstream avulsion
	e. Material burial - progradation of sediment pulse, avulsion channels abandoned
4. Superimposed interruption complex – exhumation of buried valley fill, incision into pre-landslide valley floor	**f. River incision** - exhausted sediment pulse, river incises into alluvial deposits
5. 'Shadow' interruption complex – minor, persistent legacies of interruption	

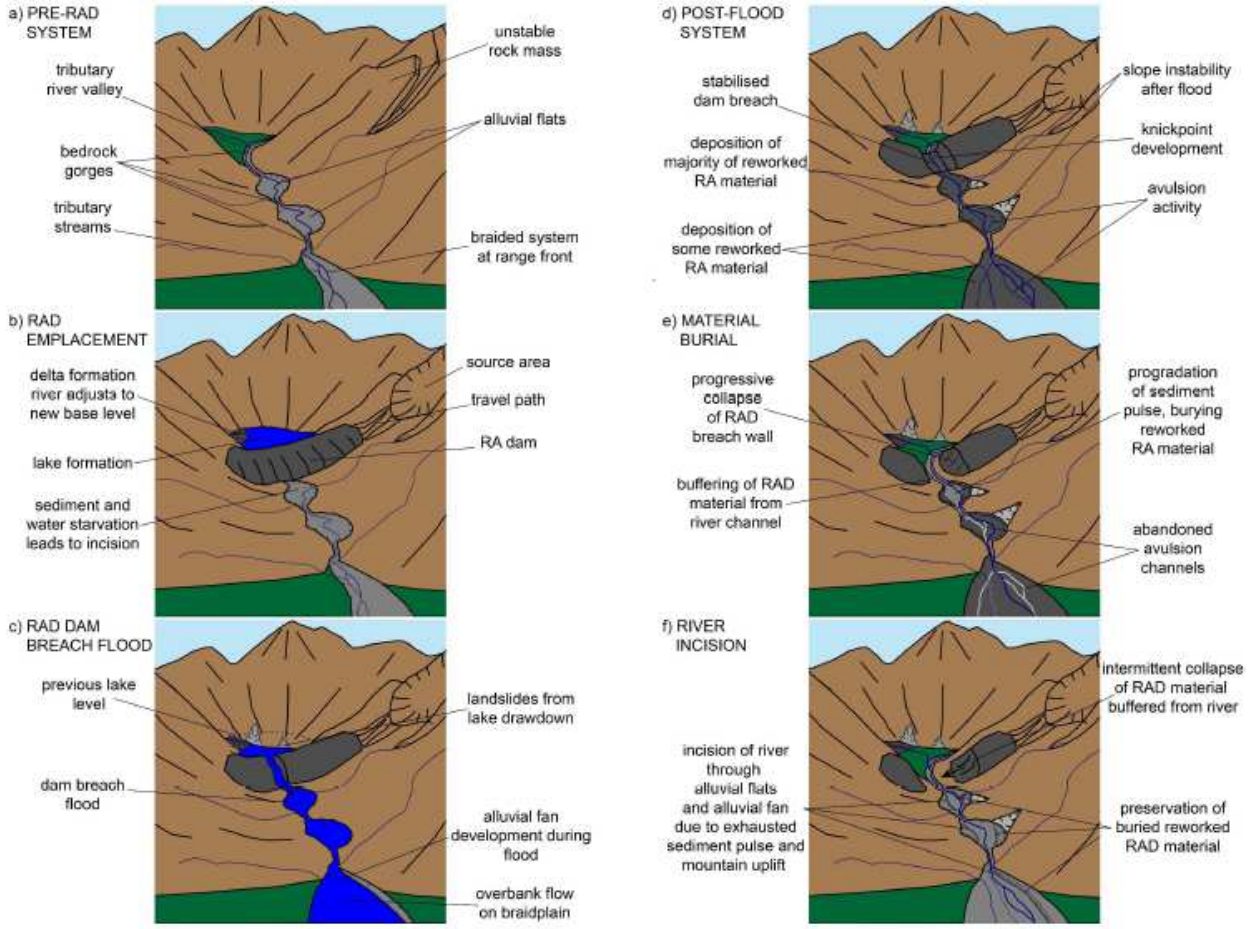

Figure 10.1: *Model for river evolution following emplacement of rock avalanche debris into a river system (Bainbridge 2017).*

Generalised sediment pulse models describe movement of any pulse of sediment through a river system, and are not specific to landslide-derived sediments. One of the first reports to document sediment wave behaviour was Gilbert's (1917) study of changes to the Sacramento Valley in response to the addition of mining sediments. Since then, this behaviour has been referred to a sediment wave, sediment slug, or sediment pulse (Gran and Czuba 2017, James 2010, Cui et al. 2003).

Many studies have used the term 'sediment wave' due to the wave-like behaviour seen in rise and fall of channel bed elevations as excess debris is transported downstream, others preferred the term 'slug' or 'pulse' as it is often difficult to identify coherent waveforms, and these terms do not infer wavelike behaviour. Sediment pulse or wave is probably the best term, and many studies use these interchangeably. A sediment pulse has been defined as;

> "The influx and movement of a volume of excess sediment in a fluvial system" (Gran and Czuba 2017)
>
> "A propagating disturbance in bed elevation and sediment properties that might translate and/or disperse" (Sutherland et al. 2002).
>
> "A transient sediment flux that includes but is not necessarily identical to a 'channel bed wave' that represents the rise and fall of the bed in response to sedimentation" (James 2010). This more detailed definition takes into account

two distinct processes, both of which have been described as 'sediment waves'; bed waves (changes in channel-bed elevations), and sediment flux (timing of passage of sediment).

Sediment wave models are based around sediment movement through processes of translation and dispersion (Figure 10.2A). Many early models assumed that sediment waves were largely translated downstream, based on observations of bed levels rising and later falling as debris progressed downstream (James 2006, 2010). Later studies recognised that a similar pattern of bed rise-and-fall at a point can also be created by dispersion processes (Figure 10.2B) and this is now recognised as the predominant process, with the influence of translation often 'weak or questionable' (James 2010, Sutherland et al. 2002, Gran and Czuba 2017, Cui et al. 2003).

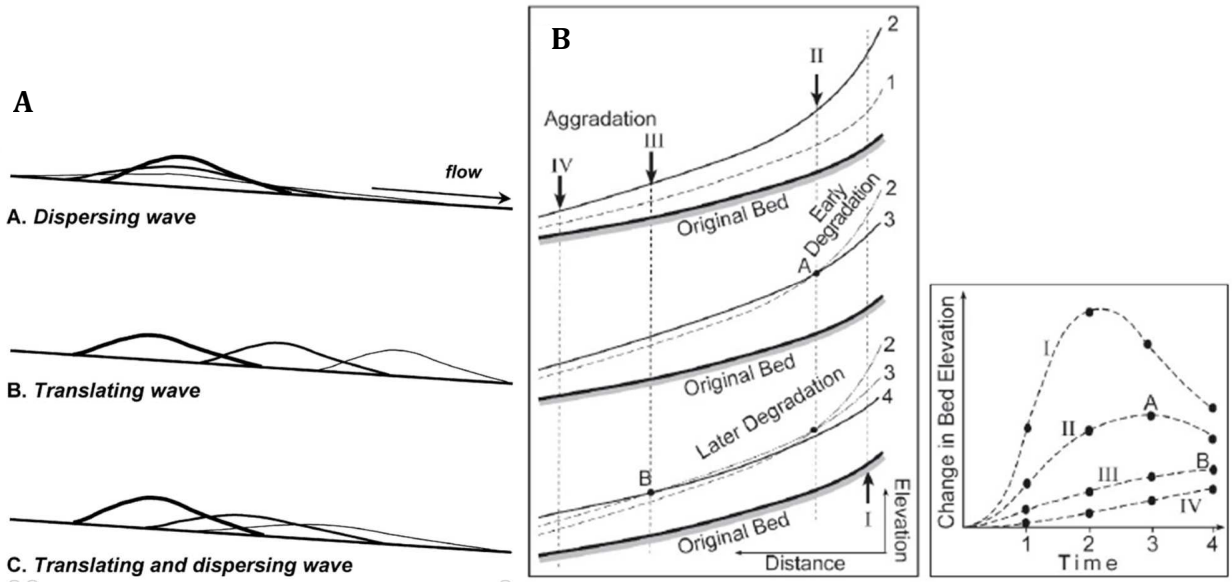

Figure 10.2: *A. Sketch of idealised dispersing and translating processes of sediment transport (Sutherland et al. 2002), and B. a sketch demonstrating apparent translation in 'at-a-point' elevation changes, due to progression of sediment downstream through dispersion (James 2006).*

A conceptual model for sediment wave evolution by James (2006, 2010) is summarised below;

1. High sediment inputs lead to aggradation in main channel, and substantial sediment storage as floodplain deposits.
2. Degradation occurs in response to lowered sediment input, and the channel incises to the pre-disturbance level, leaving deposits on floodplain or as bars
3. Stored floodplain sediment is slowly released through lateral channel migration.

The slow-release of stored sediment outside the main channel leads to formation of a skewed sediment wave, with an episodic behaviour linked to larger sediment producing/transporting events (Figure 10.3). As sediment is remobilised from outside the main channel it may require successively larger flood events to initiate remobilisation. As the flood discharge able to initiate sediment transport becomes larger and hence less frequent this may lead to the perception that the system has recovered. (James 1999).

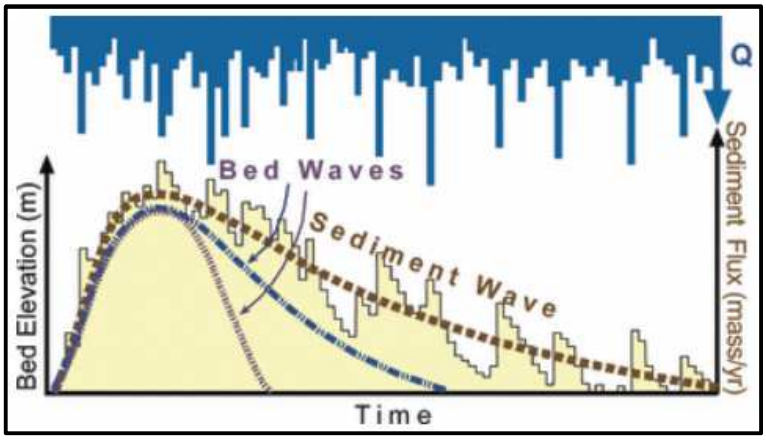

Figure 10.3: *Model of bed wave and sediment flux, showing the episodic release of sediment over time. (James 2010).*

Geomorphic Impacts From Landslide Dam Failures

The geomorphic impacts of sediment pulses caused by landslide dam failures include; development of a long-profile knickpoint, changes to valley floor morphology, and storage and release of sediment (Korup, 2005, Korup et al. 2010). Following a landslide dam failure, a long-profile knickpoint forms as the dam remnants and aggraded riverbed displace the fluvial profile upwards, forming a convex step in the channel profile. Upstream of the landslide dam aggradation will occur to form a low-gradient flat. From the dam downstream, the channel is locally steepened by the dam remnants and dambreak flood and aggradation deposits. Steepening of the channel increases stream power and erosive potential, causing channel adjustment of the profile downwards towards the pre-event profile.

Valley floor morphology changes observed following landslide dam failures is typical of behaviour of braided gravel-bed rivers under a changing sediment supply (Piegay et al. 2009). First, an expansion phase occurs under increased sediment supply, the channel aggrades and becomes braided, widening to progressively occupy more of valley bottom. This is followed by a contraction phase as the sediment supply decreases, the river incises and narrows, forming a sinuous single thread channel and formerly active braided surfaces become inactive and revegetated.

Case studies of the Poerua River and Ram Creek landslide dam failures and their sedimentary impacts are reviewed below, with these and other examples used to guide interpretation and assessment of possible impacts of a Shotover Gorge landslide dam.

The 1999 Poerua River landslide dam and its geomorphic impacts are well-documented (Korup 2004b 2005, Korup et al. 2004, Hancox et al. 2005, Davies et al. 2005, Nelson 2012, Croissant et al. 2017). A series of surveyed cross sections (June 2000 to May 2008) across alluvial fan and floodplain deposits (Figure 10.4) have allowed measurement of changes in mean bed level, and estimation of sediment flux.

The dam (100-120 m height, 10-15 M m^3 volume) was formed in the Poerua River by a rock avalanche from Mount Adams (Figure 5.4). This breached to a depth of 40-50 m in October 1999, releasing a dambreak flood with peak flows of 2000-3000 m^3/s at the breach, including bulking of 15% due to entrainment of dam debris (Hancox et al. 2005). An estimated total of ~5.5M m^3 of material was deposited during the dambreak flood; erosion of the dam continued and by 2005 about 75% of the dam material had been eroded. Dambreak deposits filled the gorge and intramontane flats (~3.8 km in length), and deposited gravel, sand and silts on an alluvial fan extending for several kilometres at the gorge exit. These deposits reached depths of 10-20 m in the gorge, and rapidly decreased from a peak of about 4 m at the alluvial fanhead.

By 2003 erosion of the dam material had slowed and degradation in the gorge had commenced, with gorge deposits downcut by 10-15 metres. Aggradation continued at the alluvial fan until about 2005, with a total of 1.0-1.5 M m^3 of sediment transported to Poerua alluvial fan over this period (Davies et al. 2005). This caused the width of the active channel to greatly increase, and formation of an avulsion channel which was intermittently occupied up to 2005, and reactivated as recently as 2013 (Bainbridge 2017). Alluvial fan aggradation rapidly decreased in thickness downstream; at 2.5 km from the gorge exit it reached a maximum thickness of about 1 m, and by 4.5 km did not exceed 0.5 m. Degradation commenced at the fanhead in 2005, but was still aggrading lower on the alluvial fan (Nelson 2012). By 8-15 years after the dambreak, total degradation at fanhead locations of 3.5-4 m was noted by Nelson (2012), and Bainbridge (2017). By 2008 the riverbed was degrading at most locations, with localised patterns of aggradation and degradation seen in survey data.

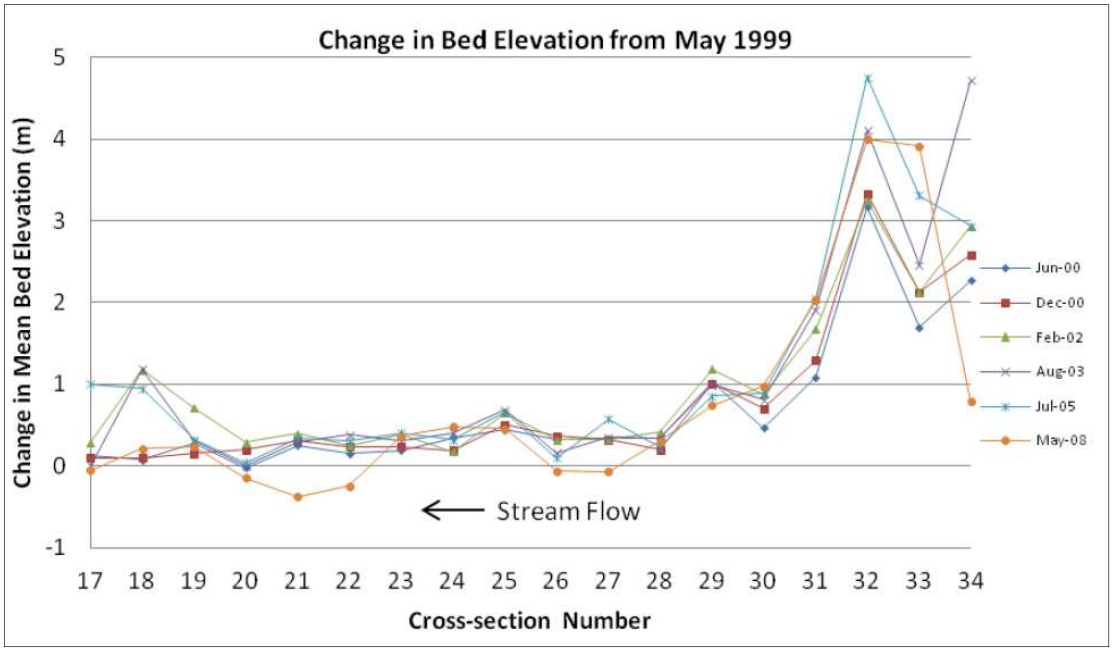

Figure 10.4: *Riverbed surveys at the Poerua River (2000-2008) showing aggradation resulting from the November 1999 dambreak event. These showing aggradation thickness rapidly decreasing with distance from rangefront (Nelson et al. 2012).*

The failure and consequences of the Ram Creek landslide dam have been described by various studies; Nash (2003), Nash et al., (2008), Harrison et al. (2015) and Bainbridge (2017). The landslide dam was formed by a 4.4M m^3 rock avalanche triggered by the 1968 Inangahua earthquake. The dam had a volume of 2.8M m^3, and failed catastrophically in April 1981, eroding a 40 m deep breach channel, and draining the entire lake volume. The flood entrained landslide dam material and lake sediments, to form a hyperconcentrated flow or debris flow, travelling down the 5.5 km incised gorge, before exiting onto river flats below.

1M m^3 of debris was deposited in the gorge, most of it immediately downstream of the dam location. On the river flats ~25 ha of land was covered by up to 2 m depth of debris. The gorge and river flats sediments show evidence for localised aggradation, reworking and channel switching, but there has been little fluvial incision into the deposits. Infilling of the gorge has caused abundant lateral erosion into the relatively soft fluvial sandstones and mudstones of the gorge walls, preferentially eroding these rather than the more resistant granitic rock avalanche debris armouring the valley floor.

Twenty-eight years since dam failure, 3.4M m^3 (>75%) of the original rock avalanche deposits still remained in place (Harrison et al. 2015). The abundance of sediment has caused a transport-limited channel with insufficient flow to erode and remove material in subsequent floods, and this system may never regain its pre-dambreak equilibrium form due to the limited erosional power of this creek.

Other dambreak examples referred to for this Shotover gorge assessment include;

- Tunawaea Stream, 1992 (Riley et al. 1993, Parkin et al. 1993, Jennings et al. 1993).
- Navarro River, California 1995 (Sutherland et al. 2002, Lisle et al. 2001, Cui et al. 2005).
- Partnach River, Bavarian Alps, 2005 (Morche et al. 2007, Morche and Laute 2009, Morche and Schmidt 2014).
- Nostetuko Valley, British Columbia 1997 (failure of a moraine-dammed lake; Kershaw et al. 2009).

All case studies show a maximum aggradation thickness immediately downstream of the dam location. The Poerua River dambreak is the most comparable example event to a future Shotover Gorge dambreak, but aspects of these other examples are also useful for evaluating possible effects, for example; sediment wave dispersion (Navarro River), changes to bedload and suspended sediment loads (Partnach River), grain size changes (Partnach River), patterns of downstream erosion and deposition (Nostetuko River).

The Poerua River landslide dam was of a comparable magnitude to the largest modelled Shotover Gorge landslide dams (100-125 m height), and is in a similar geomorphic setting, being located within a narrow gorge which opens out onto alluvial flats several kilometres downstream. However, there are also several important differences between the Poerua River and the Shotover Gorge settings. With a lower channel gradient than the Poerua Gorge, any Shotover gorge landslide dams will be capable of impounding relatively larger volume reservoirs, and thus creating larger magnitude dambreak flows. Compared to the Poerua River gorge, the Shotover Gorge contains less area available for sediment storage, with the only significant sized beach in the gorge being at Morning Star Beach at the gorge exit. Combined with potentially larger dambreak flows, this may result in a larger portion of sediment being transported beyond gorge onto the beach sections.

10.3 Sediment Modelling

Sediment Pulse Scenario

The sediment pulse and geomorphic changes expected following failure of a large Shotover Gorge landslide dam are summarised in a scenario outlining a possible sequence of events over the years following the dambreak. The scenario is*:* catastrophic failure of a large landslide dam 80-125 m in height, with a volume of 1.8-6.5M m^3, located in the lower 5-6 km of the Shotover Gorge. This sediment pulse scenario is discussed in four key periods;

1. Dam failure and formation of dambreak flood deposits.
2. An aggradation phase as dam remnants erode and sediment supply remains high.
3. Incision commences, aggradation continues downriver as eroded sediment is transported.
4. Degradation phase as channel level returns to pre-event level.

This scenario is summarised in Figure 10.9, a series of images showing the expected geomorphic changes following a lower gorge dambreak. Figure 10.10 shows sketch long-profiles showing possible sediment distributions and aggradation changes for the same periods.

1. Dambreak Flood Deposits

The landslide dam breaches, releasing a flood wave with a peak discharge of at least 7000 m^3/s. Over a period of 3-5 hours this flow erodes a breach channel to at least 50-70% of the dam's initial height, removing 30-50% of total landslide dam volume. A smaller lake of 20-30 m depth remains behind the failed dam, extending upriver for 2.5-5 kilometres (e.g. Figure 10.5A).

The flood wave erodes and remobilises existing colluvial and alluvial riverbank deposits from downriver locations. There is little material available for erosion within the Shotover Gorge, but the flood erodes riverbank terrace alluvium from locations in the lower Shotover River. Most of this erosion will occur at constrictions in channel width, such as the downstream parts of Morning Star Beach, Big Beach and Tucker Beach. Entrained sediments are transported and deposited downstream by dambreak floodwaters. Gravel deposits fill the gorge (Figure 10.5B), with thickest deposits in dam-proximal locations, and extend downstream where they also fill wider beach area at Morning Star Beach.

A debris fan forms immediately below the dam breach, with a surface grading to the aggraded gorge riverbed. Episodic downcutting during the dambreak flood may form terraces in this debris, as seen at Ram Creek (Nash 2003, Harrison et al. 2005) and Poerua River (Figure 10.5A, Davies and Korup 2007).

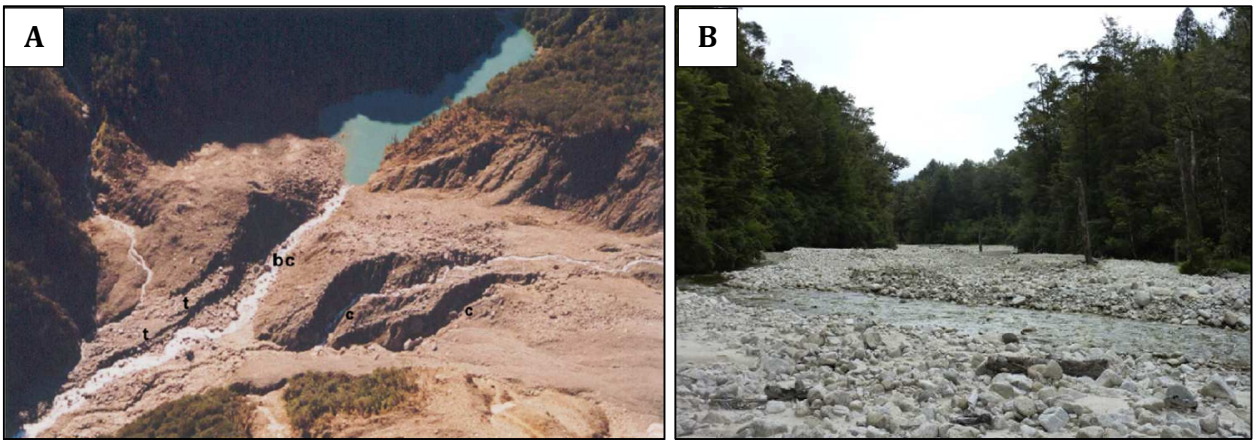

Figure 10.5: *A. Example of a recently breached landslide dam; the Poerua River dam showing remnant lake, breach channel (bc), and terraces of reworked landslide debris (t) (Davies and Korup 2007). B shows an example of valley-filling gravel deposits downstream of Ram Creek landslide dam (Harrison et al. 2015).*

The dambreak flood wave then passes through narrower section at Arthur's Point Bridge and enters the much broader Big Beach area, up to about 600 m in width. There will be a rapid reduction in velocity as the floodwaters spread over wide this floodplain area and outgoing flow is impeded by the narrow downstream outlet. With a rapid reduction in the floodwater's transport capacity, the bulk of the remaining transported sediment is deposited within this area.

The depositing sediments rapidly fill and overwhelm the existing channel, forming an alluvial fan with a fanhead at start of Big Beach, and deposits cover most of floodplain but rapidly thin downriver and to fan margins. Fan deposits comprise gravels and finer sand and silt sized material (Figure 10.6A). The flood wave is of sufficient volume to inundate floodplain terraces at Tucker Beach and the Shotover Delta, depositing minor sand and silt overbank deposits (Figure 10.6B). Any fine sediments remaining in suspension are transported to the Kawarau River.

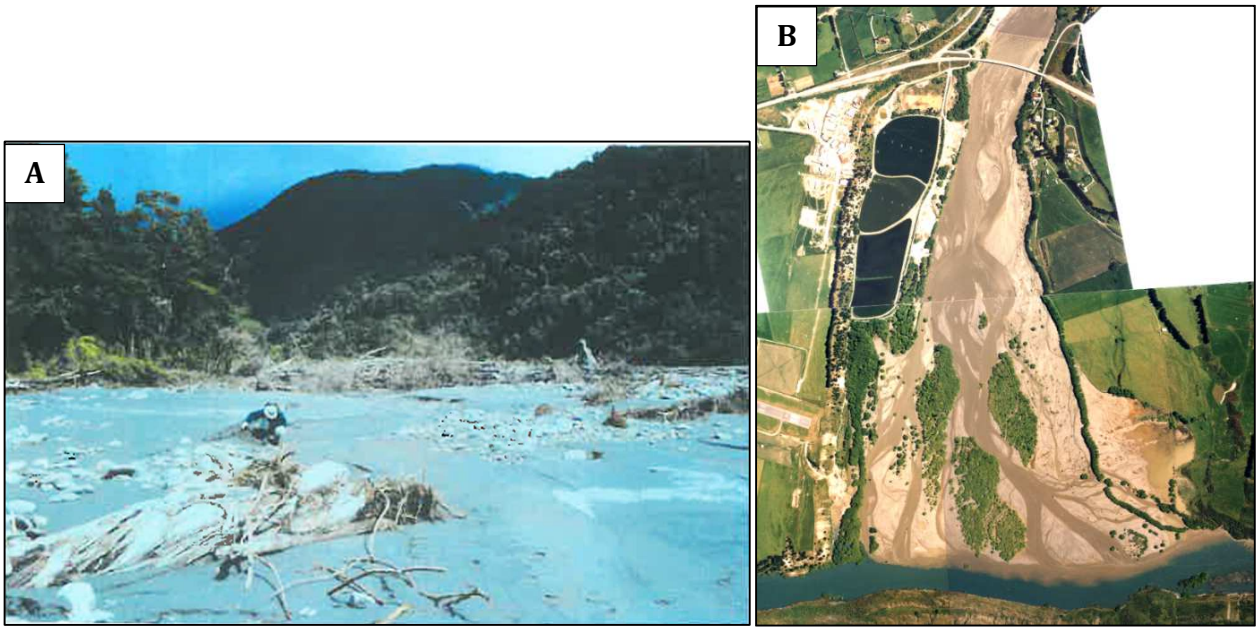

Figure 10.6: *A. Example of sandy dambreak flood deposits at Poerua River alluvial fan (Davies et al. 2005). B. Example of flood-deposited silt deposits covering riverbed and lowest terrace level at the Shotover Delta, this example is from the November 1999 flood (ORC).*

2. Post-flood Aggradation (for 4-6 years post dambreak)

The remnant lake remains behind the failed dam, lasting either until lake drains through further downcutting of the breach channel, or until it is completely infilled with sediment deposited from upstream inflows. With a reservoir volume of 1-2M m^3, the remaining lake could infill within about 1 year, assuming it captures most of inflowing sediments. As it infills it forms a fan/delta at upstream end of lake, which rapidly progrades as lake infills with sediments.

Over the following years removal of landslide dam material continues through fluvial erosion, widening and deepening the breach channel. Most erosion occurs during flooding events, which also rework the gorge-filling alluvium causing small-scale sediment pulses downvalley and onto the alluvial fan. As erosion of dam continues the sediment supply remains high, and aggradation continues in the gorge. Continued aggradation at the Big Beach alluvial fan causes expansion in channel width until recent deposits may take up nearly all the available floodplain width. The sediment pulse continues to disperse downriver as further sediments are delivered to the Big Beach alluvial fan and deposits are reworked by flood events. This causes aggradation of the river channel at downstream locations such as Tucker Beach, and possibly as far as the Shotover Delta.

Older alluvial terrace gravels at Big Beach may be eroded as aggradation allows lateral erosion into these deposits, as occurred on banks of the Waipa River due to aggradation caused by the Tunawaea landslide dam (Hoyle et al.), and on the Poerua River floodplain (Hancox et al. 2005). As aggradation occurs, sediments may overwhelm and bury currently vegetated areas at such as at Big Beach. Buried soils and vegetation may be preserved, marking the pre-aggradation surface, as is seen at several West Coast alluvial fans (Davies et al. 2005, Davies and Korup 2007). Sediment deposition around willows and other vegetation on the floodplain may cause aggradation-induced die-back, similar to that noted at locations in South Westland and Fiordland by Korup (2004b).

3. Incision Commences (from 4-5 years post-dambreak).

By this time erosion of landslide dam material has slowed, although minor downcutting of the dambreach channel still takes place during flood events, sediment supply in the gorge has essentially returned to pre-event background levels. The remnant dam still has a height of >10 m, forming a prominent knickpoint in the channel long-profile, with a shallow gradient reach upstream marking location of the infilled lake. The breach channel and debris fan below have become relatively stable and armoured with coarse boulder material impeding further erosion (Figure 10.7A).

The waning sediment supply causes degradation and incision to commence, initially in gorge reaches below the dam, possibly as soon as 2-3 years after the dambreak event. As valley-filling sediments are eroded and remobilised downstream during flood events, sediment pulse progresses downstream and aggradation continues at the Big Beach alluvial fan.

After several years, degradation progresses to the lower Shotover River where the fanhead begins to incise, becoming entrenched and leaving aggradation sediments stored as terrace deposits (Davies and Korup 2007)(Figure 10.7B). Degradation and reworking of alluvial fan material continues to provide an increased sediment supply to lower parts of the river system. As sediments are remobilised and dispersed downstream aggradation occurs at lower locations such as Tucker Beach and the Shotover Delta, but with a much reduced amplitude compared to the deposits of the gorge and alluvial fan.

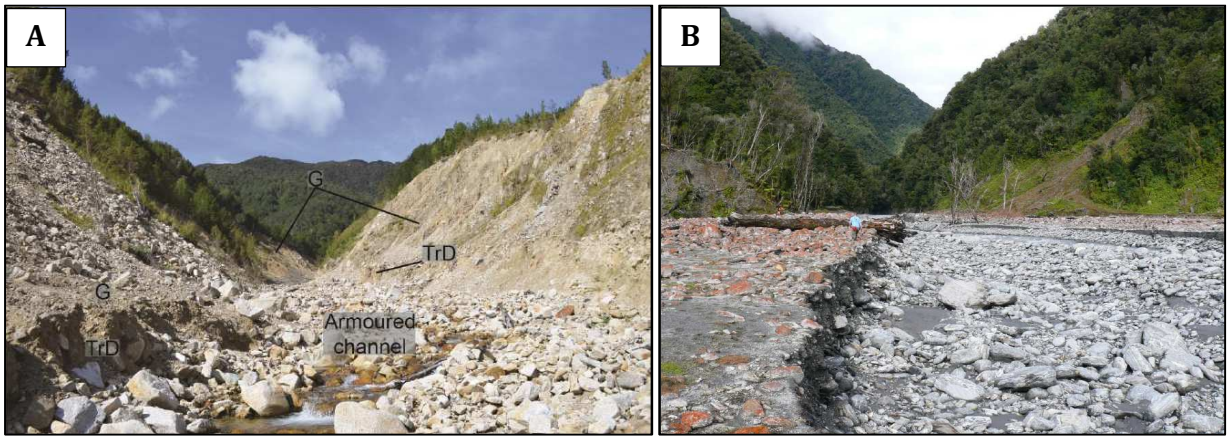

Figure 10.7: *A. The Ram Creek landslide dam breach channel, showing channel armoured by coarse material, and revegetation on side slopes (Bainbridge 2017). B. The Poerua River alluvial fan in 2008, ~9 years after dambreak, showing degradation to several metres below the aggradation fan surface at left (Nelson 2012).*

4. Degradation phase (from 8-10 years post-dambreak)

Sediment supply has been stable at about the pre-event rate for several years, and the lower Shotover River channel is actively degrading to at least Tucker Beach, narrowing and developing a single entrenched channel as it becomes incision-dominant. In the gorge and lower Shotover River, the channel thalweg incises to near its pre-event level, and the now-inactive aggradation surfaces are starting to becoming revegetated as grass and willows re-establish.

Flood events rework sediments from within the gorge, and erode terrace deposits at the Big Beach alluvial fan, and other beaches. These eroded sediments are remobilised through the lower river, forming short-duration (2-3 year) sediment pulses. These cause riverbed aggradation of up to 1 m, and are of similar magnitude to those seen in records from the Bowens Peak gauging station (Figure 4.11). Geomorphic changes during this degradation phase are similar to those observed in the lower Shotover River as it degraded from effects of historic aggradation over the last 80-90 years.

As described in Chapter Four, the channel incises and narrows, with the aggradation surface becoming inactive and revegetated (e.g. Figure 4.10).

At the landslide dam location, debris is gradually eroded during high flow events, and the dam's form becomes less distinct over decades or hundreds of years as it becomes more topographically subdued and vegetated. As the dam remnants become less recognisable, the former dam location can still be identified as a diagnostic knickpoint in the channel profile. Such features commonly comprise a steeper boulder-armoured rapid in the channel, with shallow gradient alluvial flats upstream. Examples of former landslide morphology elsewhere in the Shotover Catchment are seen in Appendix 3. These include sites with well-defined landslide scarps, remnant dams, and alluvial flats upstream, such as the Stockyard Creek landslide dam (Figure 10.8). In other locations the landslide scarp and dam-forming deposits are unclear or obscured, but can be interpreted from the stream morphology.

Figure 10.8: *Example of landslide dam morphology at Stockyard Creek, showing the landslide scarp and deposit, with a small alluvial flat developed from upstream aggradation. This landslide scarp is about 270 m in width, and located approximately 2.4 km upstream from Branches Flat.*

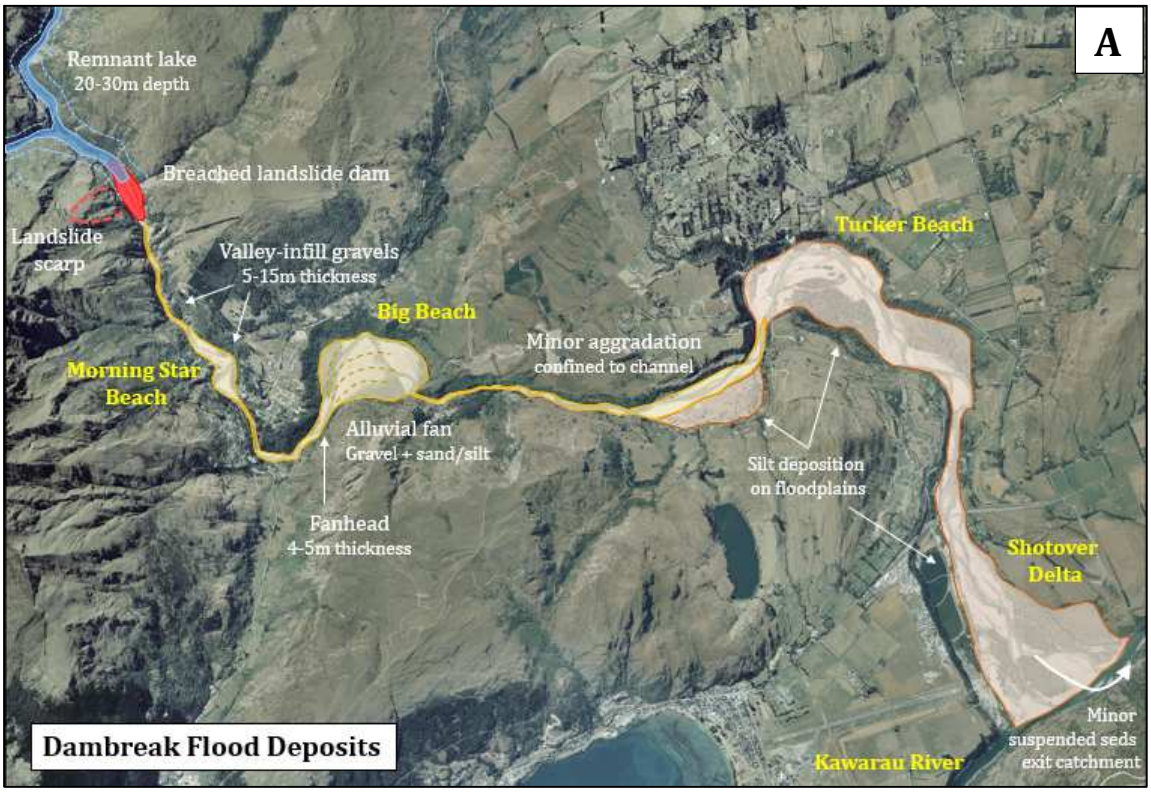
A
Remnant lake
20-30m depth
Breached landslide dam
Landslide
scarp
Valley-infill gravels
5-15m thickness
Big Beach
Tucker Beach
Minor aggradation
confined to channel
Morning Star
Beach
Alluvial fan
Gravel + sand/silt
Silt deposition
on floodplains
Fanhead
4-5m thickness
Shotover
Delta
Minor
suspended seds
exit catchment
Dambreak Flood Deposits
Kawarau River


B
Former lake now
sediment-infilled
Low rates of erosion
of dam material
Tucker Beach
Gorge deposits
degrading from 2-3
years post-dambreak
Aggradation pulse progrades
as sediments reworked
Maximum thickness ~1m
Big Beach
Morning Star
Beach
Alluvial fan at
peak aggradation levels
Shotover
Delta
4-5 Years Post-dambreak
Kawarau River

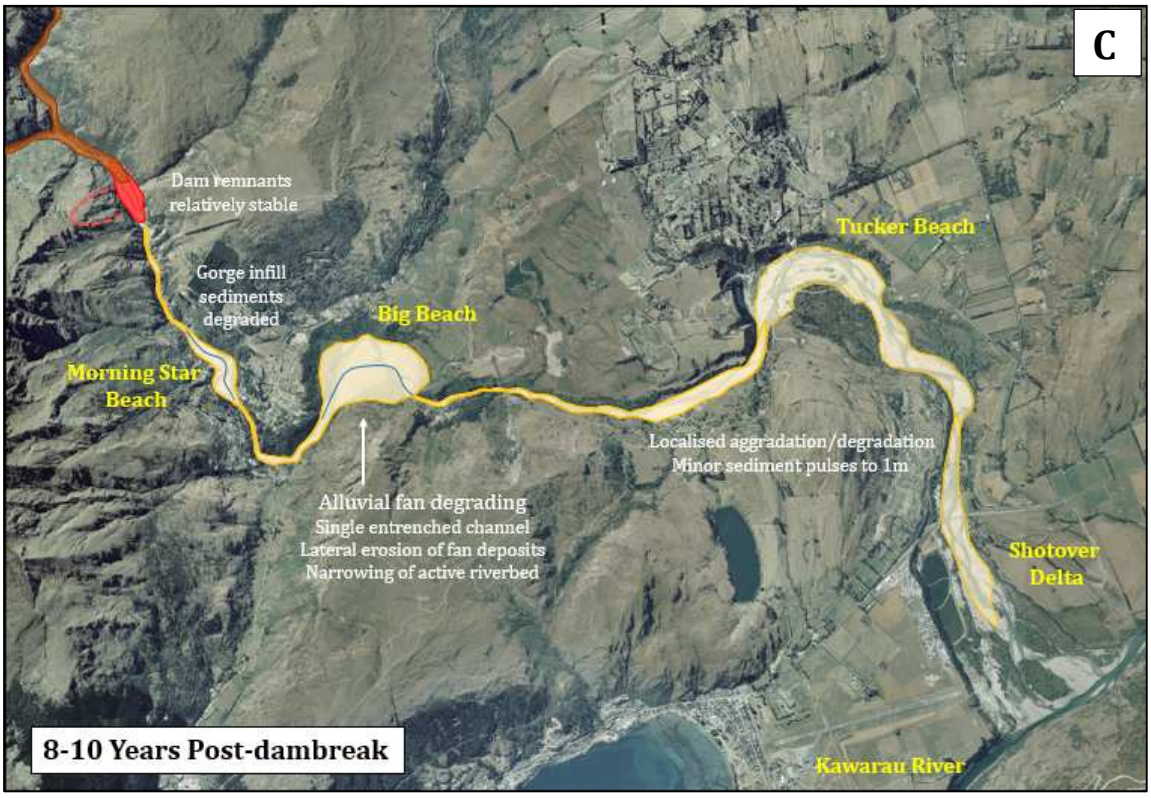

Figure 10.9: *Aggradation scenario showing geomorphic impacts in the lower Shotover River. These are; A. Immediately after dam breaching showing the distribution of dambreak deposits, B. 4-5 years after the dambreak showing extensive aggradation, and C. 8-10 years after the dambreak, showing widespread degradation in most locations.*

Sediment Transport Estimations

This section attempts to estimate the volumes of sediment eroded and transported during dam breaching and subsequent dam erosion over the next 5-6 years. Estimates of sediment volumes and aggradation thickness are made for two lower Shotover Gorge landslide dam scenarios (Table 10.2);

- Moderate: 2M m^3 landslide dam volume, dam of ~80 m height,
- Large: 6.5M m^3 landslide dam volume: dam of ~125 m height.

Estimations are based on the aggradation scenario outlined above (Figure 10.9), and characteristics of case studies such as the Poerua River dambreak (Hancox et al 2005, Nelson 2012) and others. Results are shown in Table 10.2 and summarised in Figure 10.10.

Dambreak Deposit (Table 10.2A)

The volume of dam material eroded during breach formation is estimated as 30-50% of total dam volume, but does not include any additional material added through erosion and entrainment of existing downvalley sediments. The majority of dambreak flood deposits will be deposited proximal to the dam location, forming a thick valley-filling aggradation surface extending through the gorge and including Morning Star Beach. This is estimated to contain 75% of the total dambreak flood deposit, with the remaining 25% transported into the lower Shotover River.

Dambreak deposit thicknesses are estimated assuming all of lower Shotover River dambreak deposit is deposited in the Big Beach area, with negligible volumes transported further downstream or removed as suspended sediments. This overestimates aggradation thickness at Big Beach, as in reality, at least some of the dambreak deposits will be deposited further downstream, and some will be removed from the catchment immediately as suspended sediments. For the largest volume scenario, it is estimated that the gorge-filling dambreak deposit (e.g. Figure 10.5B) may have a mean thickness of >10 metres, with Big Beach (~600,000 m^2) being covered by a large alluvial fan deposit with a mean thickness of >1 metre.

Aggradation Deposits (Table 10.2B)

Assuming rapid erosion of the remaining landslide dam material over the years following dambreak, the volume of landslide dam material eroded by the time of peak aggradation is estimated as 60-80% of total dam volume. The possible deposit thickness has also been estimated for Big Beach at the peak aggradation levels. This assumes a maximum of 25-40% of the eroded volume has been transported through the Shotover Gorge and deposited in the lower river, and the majority of this is deposited at Big Beach. These estimates show that at peak aggradation levels, the mean thickness of aggradation deposits at Big Beach may reach a maximum of >3 metres (Table 10.2B).

Table 10.2: *Estimates of sediment distribution in the Shotover Gorge and lower Shotover River. A. Following dam breaching, and B. At the peak aggradation levels.*

A. Dambreak deposits

		Scenario	
		Moderate	Large
		Volume ($M m^3$)	
Total dam volume		2.0	6.5
Dambreak volume eroded	30-50% of total	0.6-1.0	2.0-3.3
Dambreak deposit distribution	Gorge (75%)	0.4-1.7	1.4-2.3
	Lower river (25%)	0.15-0.3	0.5-0.8
Dambreak deposit thickness	**Storage area (m^2)**	**Mean deposit thickness (m)**	
Shotover Gorge	200,000	2.1-3.5	6.8-11.3
Big Beach	600,000	0.3-0.4	0.8-1.4

B. Aggradation deposits

		Scenario	
		Moderate	Large
Dam vol eroded after		Volume ($M m^3$)	
5-6 years	60-80%	1.2-1.6	3.9-5.2
Vol deposited at Big Beach	25%	0.3-0.4	1.0-1.3
	40%	0.5-0.6	1.6-2.1
Aggradation depth at Big Beach	**Storage area (m^2)**	**Mean deposit thickness (m)**	
	600,000	0.5-0.7	1.7-2.2
		0.8-1	2.7-3.5

Bedload sediment supply rates have been estimated for first 6 years post-dambreak for a large landslide dam scenario. This scenario is a 6.5M m^3 dam volume, of which ~5M m^3 is eroded over the first six years (Table 10.3). The sediment

supply rate (e.g. Poerua, Nelson 2012), and bedload content (e.g. Morche and Schmidt 2012) are assumed to rapidly decrease over the years following the dambreak event. This landslide dam-derived sediment supply is compared to the compared to the 'background' rate of bedload sediment supply.

This shows that in the first few years post dambreak, the sediment supply may greatly exceed the background sediment supply. The sediment volumes transported during the dambreak event and the first year following are estimated to be equivalent to ~18 years of the catchments background sediment supply rate. There are several simplifications in this evaluation, for example, it does not include the possible erosion and entrainment of downstream sediments, increasing the total volume of sediment transported during the during dambreak flood. Additionally, the remnant landslide dam lake will capture bedload and all/some of suspended sediment content from upstream until this lake has been infilled.

Table 10.3: *Estimation of sediment transport over the years immediately following a large landslide dambreak in the lower Shotover Gorge.*

	% of eroded volume	Eroded dam volume (M m3)	% transported as bedload	Additional bedload rate (M m3/year)	Equivalent years of background supply	Background bedload rate (M m3/year)	Total bedload rate (background + additional)
Year 1	60	3.12	90	2.81	18.72	0.15	2.96
Year 2	20	1.04	60	0.62	4.16	0.15	0.77
Year 3	10	0.52	40	0.21	1.4	0.15	0.36
Year 4	5	0.26	10	0.03	0.17	0.15	0.18
Year 5	2	0.104	10	0.01	0.07	0.15	0.16
Year 6	1	0.052	10	0.005	0.03	0.15	0.16
			Mean	0.61	4.09	0.15	0.76

Aggradation thickness and geomorphic changes are summarised in Figure 10.10, a series of schematic long-profiles of the lower Shotover Gorge and extending to the Shotover Delta. These profiles are based on the estimated thicknesses estimated in Table 10.2 and the geomorphic changes summarised in Figure 10.10. These three sketches show the same three time periods as Figure 10.9, and illustrate stages of sediment pulse movement through the river.

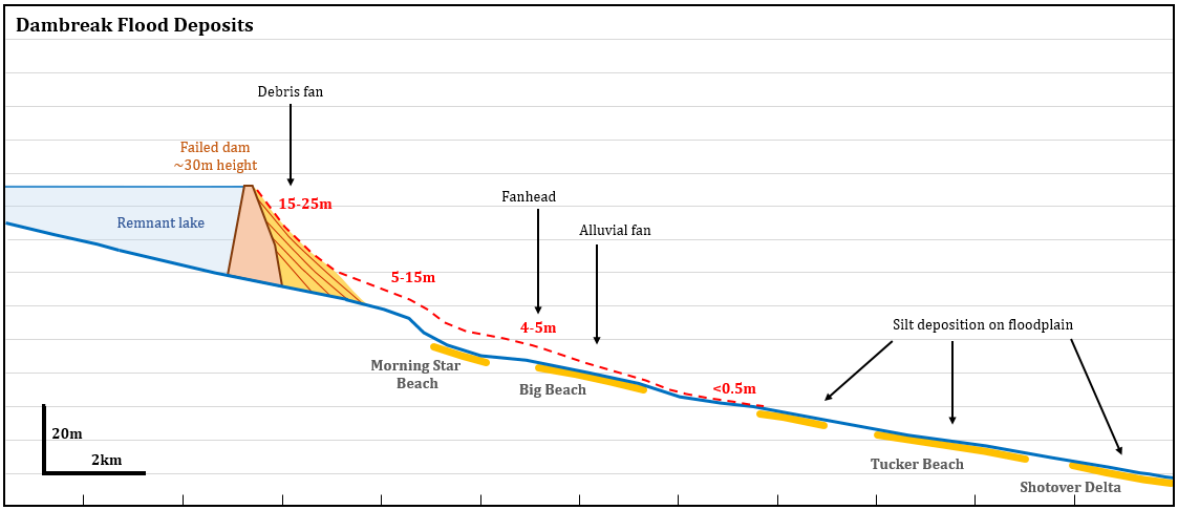

Figure 10.10A: *Distribution of post-dambreak sediment deposit. This shows the remnant dam, with a debris fan below, and the bulk of aggradation within the lower Shotover Gorge and at Morning Star and Big Beaches.*

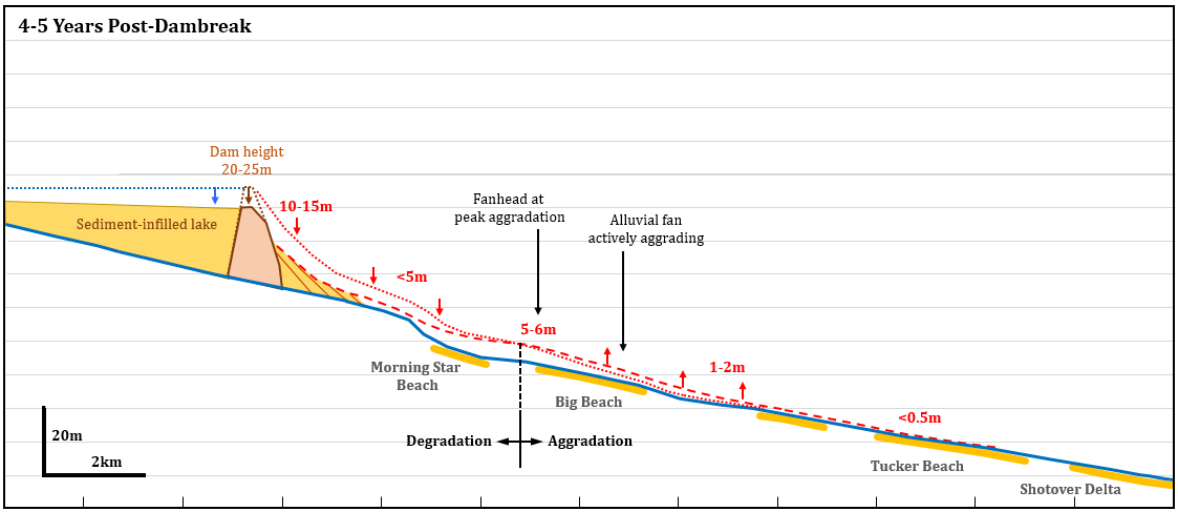

Figure 10.10B: *By the time of 4-5 years post-dambreak, the remnant dam has been infilled with sediments and erosion has lowered the dam crest. Shotover Gorge deposits have begun to degrade, with remobilisation of this sediment causing ongoing aggradation at Big Beach and locations further downstream.*

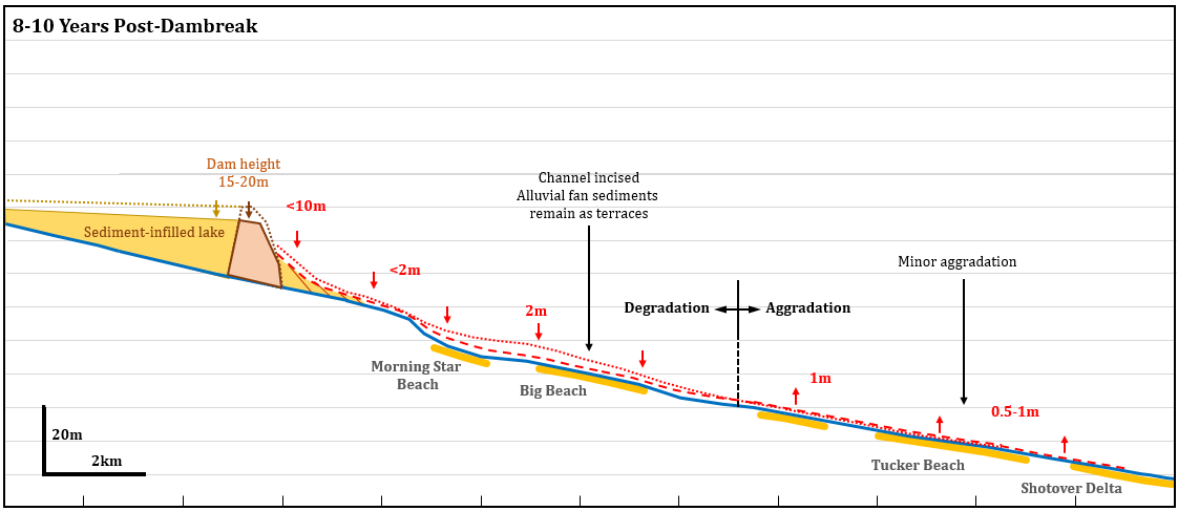

Figure 10.10C: *By 8-10 years post-dambreak the majority of the river is degrading, with localised aggradation and degradation occurring in the lowest parts of the Shotover River (Tucker Beach and Shotover Delta).*

Aggradation Modelling

Dambreak aggradation was modelled using a one-dimensional sediment transport model developed by Gary Parker, University of Illinois. This spreadsheet-based morphodynamics model can be used to show the response of a river reach to a changed sediment input rate. Modelling was completed using Parker's spreadsheet (*RTe-bookAgDegNormal.xls*)

named '1D aggradation and degradation of rivers: normal flow assumption'. Model theory, development and examples are detailed in Chapter 14 of Parker's accompanying e-book (Parker, n.d.).

The model calculates a background bedload transport capacity of channel (tons/year), based on input parameters of flood discharge and frequency, channel width and gradient, grain size, bed roughness and porosity. Initial conditions are Q_{ta} (ambient sediment supply) and a starting equilibrium bed profile. At t=0, sediment supply changes to Q_t (modified sediment supply), and model shows response as either degradation if $Q_t<Q_{ta}$, or aggradation if $Q_t>Q_{ta}$. If the modified sediment input continued indefinitely, eventually a final equilibrium profile would be attained, where the gradient balances the increase in sediment supply (Figure 10.11).

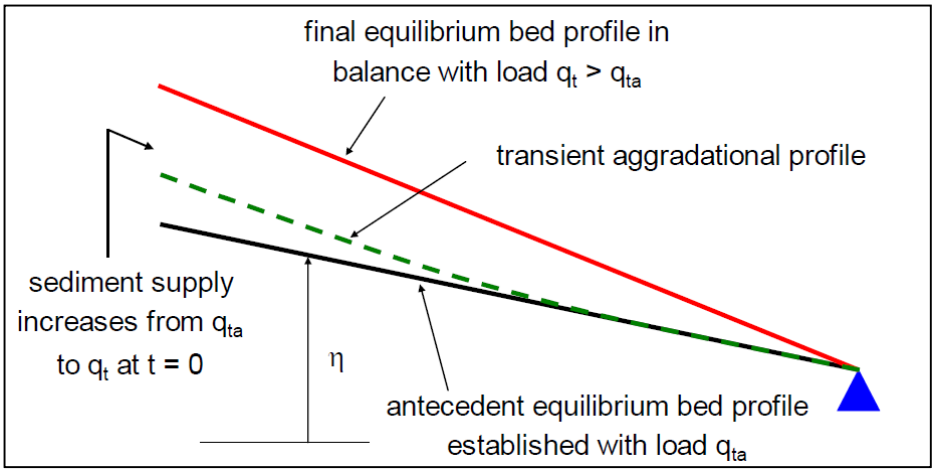

Figure 10.11: *Sketch showing a conceptual aggrading bed profile approximated by Parker's morphodynamics model (Parker ebook, Ch14).*

This is a 1D model designed to investigate changes over a single reach, and assumes a constant channel gradient and width, and a fixed increase/decrease in sediment supply rate. Many input factors are simplified to a constant value, where inputs from a landslide dam failure will actually have significant spatial and temporal variations, for example;

- Sediment supply rate varies with time, as does the proportion of bedload content.
- Channel width and gradient will vary with distance downstream.
- Channel width may increase with time due to aggradation, although will remain relatively constant in gorge sections where confined by the bedrock channel.
- Grain size decreases downstream due to progressive deposition of larger material, and abrasion of sediment.
- Model assumes sediment is transported by episodic high flow events, but does not take into account the very large discharge of the dambreak flood.

Model Scenarios

Three scenarios have been modelled, the largest is based on the scenario estimated in Table 10.3, for erosion of a large dam with a volume of 6.5M m^3. It is assumed that ~5M m^3 of additional sediment is input over a 6 year period. Averaged over this period, the modified bedload sediment supply is increased to about five times the pre-event background rate.

Models were also completed at lesser sediment increases, at rates of 2 and 3 times the background rate (Figure 10.12). The model is a narrow channel of 10 km in length, a channel width of 50 m, and a gradient of 3.5 m/km.

Results

The changing bed levels as the riverbed aggrades are shown in Figure 10.12 for the first six kilometres below the sediment input, and Figure 10.13 shows aggradation increases over time following the initial dambreak event. The mean aggradation thickness in the first few kilometres below the sediment input point may give a reasonable approximation of the peak aggradation thickness within gorge. These values are of comparable magnitude (within 50%) of thicknesses estimated for the gorge based on the distribution of deposits (Table 10.2B). Figure 10.12 shows the concave-up form of the aggrading riverbed, with aggradation thickness rapidly decreasing downstream. The delayed downstream impacts are seen in Figure 10.13. Aggradation impacts are seen immediately proximal to the sediment source (Figure 10.13A), while at a location 5 km downstream, there is little response until about 2 years.

This type of sediment transport model may be better suited to modelling longer-term increases in sediment supply, where sediment is supplied at a more constant rate, rather than a short duration sediment pulse with a very large initial input at the dambreak event and then decaying supply rate after. However, it appears to approximate aggradation thicknesses and shows relative changes in aggradation thickness for differing input rates, and with distance downstream from dambreak location.

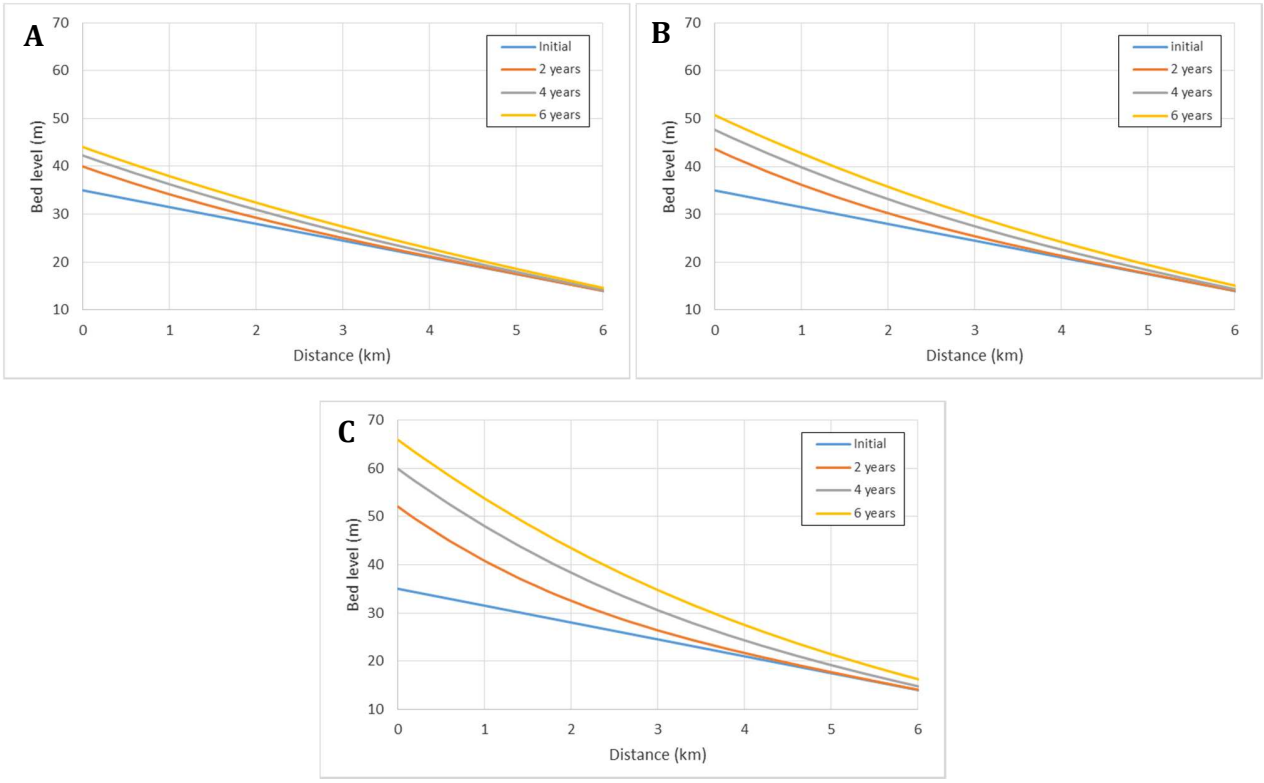

Figure 10.12: *Modelled changes to riverbed levels for the 6 km from sediment source, at increases of 2 (A), 3 (B) and 5 (C) times background bedload supply.*

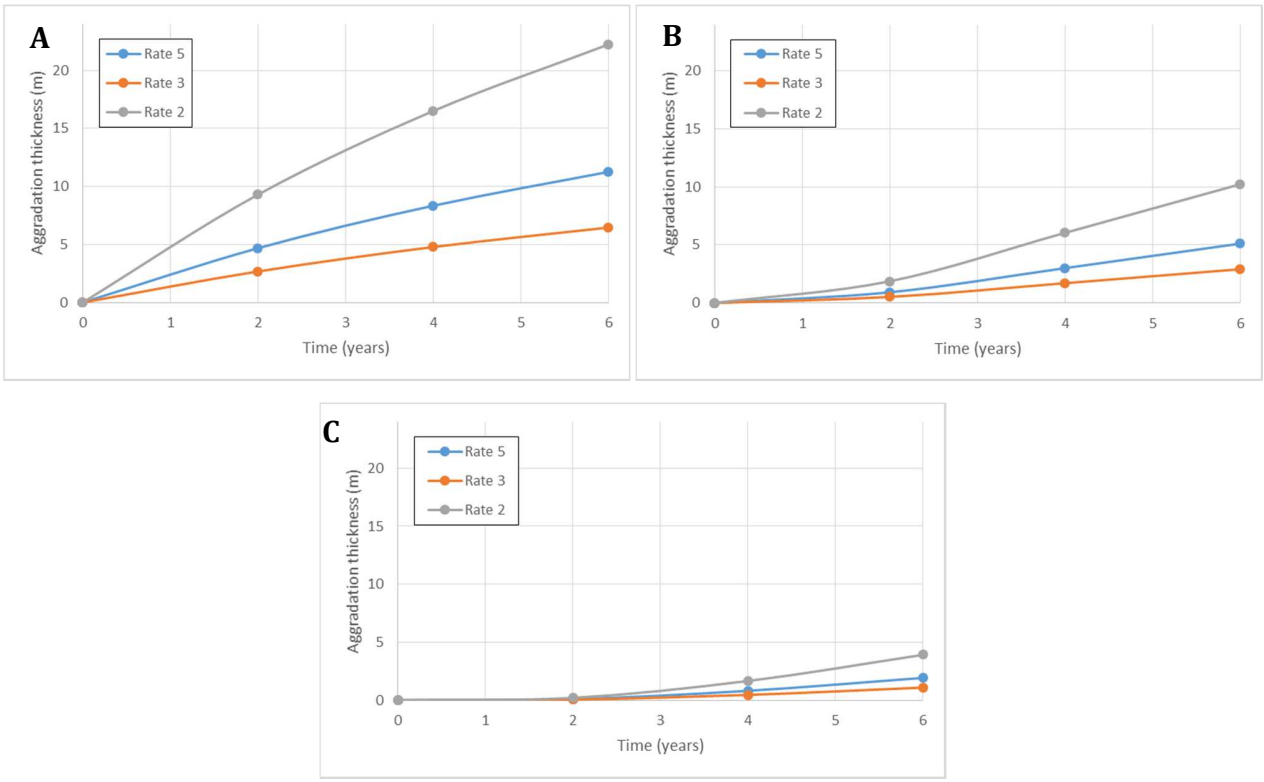

Figure 10.13: *Modelled aggradation thickness over time, for an increased sediment supply (2, 3 and 5 times background rate). Plots are for locations at 1 (A), 3 (B) and 5 (C) kilometres downstream from dam location.*

10.4 Summary and Conclusions

This chapter has evaluated the expected geomorphic changes and the magnitude of aggradation expected following dambreak events in the Shotover Gorge. The maximum sediment thickness will be proximal to the dam location, in the largest landslide dam scenario considered (125 m height dam, dam volume of ~6.5M m^3) the mean thickness of aggradation gravels within the gorge may be as much as 10 metres. A large alluvial fan is expected to form at Big Beach, as the channel rapidly widens to about 600 m. The fanhead would be located at about Arthur's Point, with deposit thickness rapidly decreasing downstream. Further downstream in the Shotover River, at Tucker Beach and the Shotover Delta, the maximum aggradation thickness is not expected to exceed a depth of 1-2 metres.

Within-gorge deposition and alluvial fan aggradation will account for the majority of the excess sediment released by the dambreak flood and erosion of dam remnants, limiting aggradation impacts in locations further downstream. These temporarily stored sediments will buffer the downstream aggradation response, delaying sediment transport and muting the downstream aggradation magnitude. Remobilisation of this stored sediment further downstream will be gradual, as in the asymmetrical rate of sediment loss shown by James (2006)(Figure 10.3), and the 'fast in, slow out' principle of Trimble (2010), where deposition occurs over much more rapid timescales than erosion.

The raised riverbed due to aggradation will reduce the available river freeboard, consequently increasing the flood hazard. At current riverbed levels, flood levels are well below the level of the developments adjacent to the delta, as shown in a rating curve developed by Hamilton (2017) (Figure 7.18). Due to the delta predominantly degrading over the last few decades, aggradation of 1 m would return the delta riverbed to about the previous 1981-1987 riverbed levels as shown in Figure 4.12). Even with 2 m of aggradation at the Shotover Delta a 100-year flood (1500 m^3/s) is

unlikely to impact the Shotover housing area. However, at this bed level the freeboard is significantly reduced for larger magnitude floods, and with climatic changes predicted to increase flood magnitude and frequency (Jones 2017), future aggradation of this scale would be of concern.

Larger Sediment Inputs

The geomorphic response of the Shotover River to larger events can be approximated by the characteristics of the historic mining-induced sediment pulse, summarised in Chapter Four. This was a major sediment input (>20M m^3) into the Shotover River, from a number of locations within the catchment (Figure 4.2), and spread over a duration of >30 years. The resulting aggradation is estimated as >10 m in the Shotover Gorge, 5-7 m at Big Beach, and 2-3 m at the Shotover Delta (Figure 4.14). A landslide dambreak sediment input differs from this in several ways, being sourced from a single location, with a large portion emplaced rapidly in a very high discharge dambreak event. However, this historical event can be used to guide interpretation of the impacts of a very large sediment input. A large volume of the mining-era aggradation sediments remain stored as floodplain deposits in the lower Shotover River, and the reduction in vacant storage capacity may lead to more rapid and higher aggradation from a future large volume sediment input.

The largest landslide dam scenario modelled in this chapter had a landslide volume of 6.5M m^3 and an annual probability of 0.1-0.01%, but there is potential for larger landslide events in the Shotover Gorge. A landslide event with a volume of several tens of millions of cubic metres may have geomorphic impacts comparable with, or even exceeding, those of the mining-induced aggradation episode summarised in Chapter Four. The potential for landslide events of this magnitude is demonstrated by the presence of larger landslide scarps at locations in the Shotover Gorge (Figure 6.11), and the formation of a number of large landslide dams at locations elsewhere in the catchment (Appendix 3). A large sediment input could also be formed by multiple landslide events with a large combined volume. These could be triggered by the same event, such as an earthquake or high intensity rainfall (Korup and Wang 2015). Based on the landslide magnitude-frequency distribution developed in Chapter Six (Figure 6.12), a very large landslide of 20-40M m^3 has an estimated annual probability in the order of 0.01-0.001%. A future large Shotover Gorge sediment input of this magnitude would be expected to have significant geomorphic consequences, and these would impact on the flood hazard at the Shotover Delta and for Lake Wakatipu.

Comparison with Previous Studies

A number of previous landslide dam assessments discuss aspects of sedimentary impacts on the Shotover River (e.g. Thompson 1996a, Hamilton and Associates 2010, Bryant 2011 2017, Davies 2017). This section compares this studies modelling with those results, and reviews assumptions made by previous assessments.

Bryant (2017) and Hamilton (2017) assume ~80% of Shotover sediments move in suspension and will be flushed into the Kawarau River, based on sediment budget studies such as Hicks et al. (2000). This assumption leads to interpretation of insignificant aggradation magnitudes as most sediment is transported into the Kawarau River. Evidence from several case studies suggests that the bedload content during a dambreak flood is significantly higher than during a typical meteorological flood. For example, the deposition of abundant fine material within dambreak aggradation deposits following the Poerua River dambreak (Hancox et al 2005), and case studies noting that a large portion (~75%) of the dambreak deposit is carried as bedload and deposited (e.g. Partnach River, Moche and Schmidt 2012; Nostetuko Valley, Kershaw et al. 2009). It appears reasonable to assume the majority of the dambreak material will be deposited rather than being removed as suspended sediment load. However, the high bedload rates will rapidly decrease, likely returning to about background rates within several years.

Bryant (2017) comments that only 20-50% of the landslide dam material is mobilised by breach channel. This is a correct assumption, however the dam material will continue to be eroded over the following few years, with up to 75% of landslide dam volume potentially being removed within a period of 6-8 years. In addition to landslide dam material,

other sediments may also contribute to aggradation. For example, the dambreak flood may erode and entrain debris further downriver, or aggradation may allow for significant lateral erosion of existing alluvial deposits, as happened at Tunawaea and the Poerua River. In the lower Shotover River this could result in significant erosion of the abundant stored terrace sediment from Big Beach and Tucker Beach, further increasing the downstream sediment supply.

Bryant (2017) calculates aggradation thicknesses from failure of hypothetical landslide dams from 0.1-10 M m^3 in volume, assuming 25-50% of the dam is eroded during breaching, and the bulk of this is removed as suspended sediment. Bryant estimates mean aggradation thicknesses of 40-80 mm for a 1M m^3 dam, and 0.4-0.8 m for a 10M m^3 dam. Hamilton and Associates (2010) evaluates sediment overload resulting from a coseismic landslide or landslides. Show potential sediment storage areas in lower Shotover River, noting that it would require a sediment volume of 4.7M m^3 to aggrade the potential storage areas between Kawarau River and Big Beach by 1 metre depth.

Bryant and Hamilton's basic estimates assume a constant aggradation thickness over the entire lower Shotover River storage area, while this study takes into account the rapid decrease in deposit thickness downstream. Based on examples such as the Poerua River landslide dam (Figure 10.4), it is estimated that the bulk of initial aggradation will occur within the Shotover Gorge, and at the first wide, unconfined floodplain at Big Beach, from where it will be more gradually reworked into the lower river.

Davies (2017) inferred possible metre-scale aggradation at the Shotover Delta, based on the example of the Poerua River landslide dam where aggradation reaches thicknesses of ~1 m at a distance of 2 km from the gorge exit (Figure 10.4). The Shotover Delta is located at a distance of ~10 km downriver from the gorge exit so this Poerua example may not be directly applicable for locations further downriver, but Figure 10.4 also shows local aggradation peaks of ~1 m at points further from the rangefront.

Shotover Delta Impacts

The impact of future aggradation on the Shotover Delta morphology and the consequential impacts on the Queenstown flood risk are difficult to quantify. Sediment supply and aggradation at the delta toe is only one factor in the Shotover Delta-Kawarau River interactions influencing Lake Wakatipu levels. Even without significant future aggradation at the delta toe, several other factors may lead to increases in the future flood hazard. Over the last few decades the elevation difference between Lake Wakatipu and the Kawarau River below the Kawarau Falls weir has been steadily decreasing (Strong and Davies 2010). This is interpreted as representing a gradual rise in the Kawarau River level below the lake outlet. If this difference continues to decrease it will requires a smaller magnitude damming effect at the delta to cause the same amount of constriction to the Lake Wakatipu outflows.

Estimates of future climatic variation have predicted increases in the Wakatipu area winter and spring precipitation and runoff (e.g. Mojzisek 2006, Poyck et al. 2011, Jones 2017). This may lead to more frequent or larger magnitude flood events in the Shotover River and those catchments contributing to Lake Wakatipu, and thus an increase in the Lake Wakatipu flood hazard.

A landslide dam failure causing an increased sediment supply and significant (>1 m) aggradation at the delta is expected to lead to progradation of the Shotover Delta toe, and the resulting constriction of the Kawarau River channel will impede lake outflows and increase flooding hazard in Lake Wakatipu. Quantifying the possible impacts of these changes is difficult, requiring modelling of the complex hydraulic and sedimentary interactions at the Shotover Delta-Kawarau River confluence, such as was carried out by Barnett and MacMurray et al. (2006)

Chapter Eleven:
Conclusions and Discussion

11.1 Introduction

This chapter summarises the key findings of this thesis, and discusses results and implications of this work. These are discussed in three sections related to the main components of this study;

1. A geological and geomorphic study providing geological context of the Shotover Valley and an interpretation of its geological development (Chapters Two and Three).
2. An investigation of the impacts of a mining-induced sediment pulse on the Shotover River's historic fluvial geomorphology (Chapter Four).
3. Investigation of the landslide dam hazards in the Shotover Gorge; including dam formation, dambreak flooding hazards, and aggradation impacts (Chapters Five-Ten).

11.2 Geology and Geomorphology

The Quaternary geology of the Shotover Valley has received surprisingly little detailed study, with a number of brief descriptions of the recent geology and geomorphology (OCB 1956, 1966, MWD 1975, Turnbull et al. 1975a, McSaveney 1978, Thompson 1998), but little more detailed work. This is despite the long history of alluvial gold mining (from the early 1860s) and geological studies (e.g. Park 1909) in the Shotover Valley, and several more recent erosion and sediment sources studies by the Otago Catchment Board (OCB 1956, 1966) and Ministry of Works (MWD 1975, McSaveney 1978). The best previous geological mapping of Quaternary units is the regional-scale QMAPS compilation (Turnbull 2000) and there has been no dating of any Quaternary units, with only speculation regarding the age of any geological events (e.g. Thompson 1998). The presence of glacial sediments and lacustrine/deltaic sediments in the Shotover Gorge and at Branches Flat were noted in a small number of reports (e.g. Turnbull et al. 1975a, McSaveney 1978, Carryer 1984, Thompson 1998), and interpretations had been made of the paleolake extent (McSaveney 1978) and terrace profiles (Thompson 1998).

This investigation built on those previous observations, identifying and describing the main Quaternary geological units and geomorphic features of the Shotover Gorge and lower Branches Flat study area, and develops a preliminary interpretation and chronology for the valley's LGM and postglacial history.

Key Findings

1. Interpretation of the extent and timing of the Shotover Glacier's Last Glacial Maximum (LGM) advance.

Glacial sediments in the upper Shotover Gorge (e.g. Figures 2.24, 2.25) are interpreted as forming in a proglacial fluvial environment, and reverse-sense glacitectonic deformation indicates formation in an ice-contact location (Figure 2.26). The glacial advance is interpreted to have reached to about Sandhill Creek (Figure 3.8A), and is named the 'Sandhill Advance' after Thompson (1998). Optically Stimulated Luminescence (OSL) dating of two bedded sand units from an outcrop of glacial sediments at Sandhill Creek shows these were deposited at ~29 ka (Figure 3.2). This early-LGM date (late MIS3/early MIS2) (Figure 3.9) is consistent with formation during New Zealand's maximum LGM ice extent.

2. Aggradation is interpreted as a result of base level rise caused by the Wakatipu Glacier.

The extensive terrace gravels in the Shotover Gorge and Moonlight Creek (e.g. Figure 2.9) are interpreted as being remnants of an aggradation deposit. This terrace surface is approximately parallel to the modern channel gradient (Figure 2.26) and is thus interpreted as forming under a comparable sediment supply, and as a result of a significant rise in the valley's base level. This rise in base level is interpreted as being a consequence of the early-LGM Wakatipu Glacier intruding into and blocking the lower Shotover Gorge (Figure 3.8A). A glacially-induced base level rise as an aggradation cause contrasts with many other locations, where outwash aggradation is generally attributed to increases in sediment supply during glacial advance.

3. A large paleolake is identified as a proglacial feature formed during LGM glacial retreat.

An extensive paleolake has been identified in the upper Shotover Gorge and Branches Flat, based on the occurrence of thick sequences of lacustrine and deltaic sediments (e.g. Figures 2.12, 2.16, 2.17). The lake is interpreted to have had an upvalley extent of >20 km (Figure 3.5), and to have persisted for at least several thousand years. The timing of lake formation has been constrained by a single OSL sample from deltaic deposits at Ironstone Creek, dated to ~25 ka (Figure 3.6). Forming relatively soon after the Sandhill Advance, the lake is interpreted to have formed as a proglacial lake during ice retreat, impounded by a barrier comprising outwash material in the upper Shotover Gorge (Figures 3.4, 3.8B). The rapid glacier retreat is interpreted to be due to ice-lake dynamics, as glacier behaviour becomes decoupled from climatic influences as a floating ice-front is formed (Shulmeister 2017). The formation of a large proglacial lake in the Shotover Valley is consistent with the typical behaviour of New Zealand valley glacier systems, where proglacial lakes impounded by outwash fan heads are a characteristic feature (Shulmeister 2017).

4. Formation of the modern Shotover Gorge in response to Wakatipu Basin events and tectonic uplift.

Postglacial incision of aggradation sediments is interpreted to have commenced as the valley's base level lowered on retreat of the Wakatipu Glacier from the lower Shotover Gorge (Figure 3.8B). In response the river began incising into the aggradation surface, leaving remnants of the aggradation surface and forming lower degradational terrace levels. Incision into bedrock has kept pace with tectonic uplift to form the modern gorge, while older surfaces have been uplifted to their present elevations.

Discussion

The Quaternary deposits described in the Shotover Gorge are interpreted as being dominated by the influence of the LGM glacial events. The relationships of glacial, lacustrine and alluvial deposits are typical of those found in New Zealand valley glacier systems, and are a function of a very high, tectonically-controlled sediment supply and high rainfall and dominance of fluvial processes (Shulmeister 2017). These Shotover Valley deposits and formation processes are interpreted to be similar, albeit on a smaller scale, to those found at many South Island locations, such as deposits at Pukaki, Ohau, and Tekapo (Shulmeister et al. 2010) or observations of the modern Tasman Glacier (Purdie et al. 2016), where a proglacial lake has formed behind a glacial outwash head and abundant outwash sediments have formed a downvalley aggradation surface.

A preliminary chronology of the main events in the Shotover Valley's recent geological development (Table 3.1) is the first interpretation constrained by absolute dates. This chronology is limited by the small number of analysed samples, and the wide analytical uncertainty, however it is sufficient to demonstrate that these units were formed by events in the LGM and postglacial period. The date of the Sandhill Advance is consistent with the interpreted timing of New Zealand's maximum LGM ice extent (Rother et al. 2014), and with other dated events in the region. For example at southern Lake Wanaka, located only 30 km to the northeast, Evans (2015) dated a glacial advance to ~32 ka.

As a reconnaissance scale investigation of a large field area, (~30 km of the Shotover Valley, plus ~7 km of Moonlight Creek), more detailed investigations were necessarily limited to a small number of locations (e.g. the Sandhill area, Strohles Flat, Ironstone Delta). There are a number of opportunities to build on these preliminary findings, including;

1. Further investigation of deposits in the upper Shotover Gorge, where many exposures of glacial, lacustrine, deltaic and alluvial sediments were identified but only briefly noted during field work. Further work should be conducted to characterise the sedimentology of these exposures to better define their depositional environments (Chapter 2).
2. Additional geochronology of Quaternary sediments to better constrain the timing of the main geomorphic events identified (Chapter 3).
3. Study of previously reported features of interest outside the Shotover Gorge study area, and incorporation of these observations with those from the Shotover Gorge study area. These include deltaic sediments at Flood Burn and Sixteen Mile Creek, and moraines at middle Branches Flat and Sixteen Mile Creek (Figure 3.7) (McSaveney 1978, Carryer 1984, Thompson 1998).
4. Integration of Shotover Valley interpretations with Wakatipu Basin events. This study has interpreted Shotover Gorge and Wakatipu Basin events to be closely interrelated, for example, the Wakatipu Glacier advance caused aggradation in the Shotover Gorge, and glacial retreat from the Wakatipu Basin then controlled degradation. During the postglacial period reworking of Shotover Valley sediments was the source for the abundant volumes of sediment forming the postglacial Shotover Delta.

11.3 Historic Shotover River Geomorphic Changes

Alluvial gold-mining in the Shotover Valley from the 1860s caused significant modification to the Shotover River as a large volume of sediment was input to the river system, causing widespread aggradation. The largest sediment contribution was from hydraulic sluicing of gravel deposits from high terraces (Figure 4.2), and it is estimated that the volume of additional sediment was on the order of at least 20-40M m^3 (Table 4.1), and may have increased the river's sediment loading by 50% over the period of peak mining activity.

The magnitude and extent of the resulting aggradation has been interpreted based on photographs (e.g. Figure 4.4 and 4.5), surveys (Figure 4.6), and anecdotal reports from this time. Following a reduction of mining activity and decreased sediment supply, the river degraded in response, with changes to the river's form clearly seen in aerial imagery (Figures 4.9, 4.10, 4.13), and monitoring of riverbed levels (Figures 4.11, 4.12).

Key Findings

1. Mining-induced aggradation had a significant geomorphic impact on the Shotover River.

The historic mining-induced sediment pulse in the Shotover River was a significant event in the river's recent geomorphic history. This caused aggradation and expansion of the river channel, changing from a single incised channel to a broad braided riverbed as excess sediments were deposited. Surveys at the upper Shotover Delta showing ~2.5 m of aggradation by the early 1900s (Figure 4.6) and photographs show the active delta greatly increasing in width compared to the pre-mining form (Figures 4.4, 4.5). It is estimated that aggradation reached levels of >10 m in the Shotover Gorge proximal to the larger sluicing locations, and at lower levels at the lower Shotover beaches (~5 m) and the Shotover Delta (2-3 m).

2. Geomorphic impacts of the sediment pulse's degradation phase are interpreted as being ongoing.

It is interpreted that the river's morphology is still undergoing geomorphic changes as the degradation phase of the sediment pulse continues, and the river recovers towards its pre-mining state, even >100 years after cessation of most larger-scale sluicing activity. Geomorphic changes to the river include a transition from a wider braided riverbed to an incised single channel, with narrowing of the active riverbed and revegetation of the former aggradation surface. These changes are clearly seen in photos at locations in the lower Shotover River, including Big Beach (Figures 4.8, 4.9), Tucker Beach (Figure 4.10) and the Shotover Delta (Figure 4.13). Figure 4.14 shows a profile of the current river level compared to the interpreted aggradation surface. Measured changes in mean riverbed level show consistent degradation trends since the 1980s, for example measurements at the Bowen's Peak gauging station (Figure 4.11), and the upper Shotover Delta (Figure 4.12), and these records indicate that the bed level has been consistently decreasing in recent years. If this degradation is caused by recovery from mining-induced aggradation then it may be expected to continue. If it is not related to the mining, however, then it may be the case that under normal conditions the delta can aggrade and degrade by some metres over decadal time-scales. This affects the susceptibility of developments near the river to landslide dam-related hazards

Discussion

The geomorphic impacts of mining-induced sediment pulses have not been well-described in New Zealand, despite the widespread use of hydraulic sluicing in the Otago alluvial goldfields from the 1880s (Hamel 2001). These effects are mainly known from brief descriptions (e.g. aggradation at Gabriels Gully, Galvin 1906), and a few other reports, such as investigations of aggradation in the lower Clutha River (Rivers Commission 1920, ORC 2008). The Arrow River is also noted as aggrading in the mining-era due to hydraulic sluicing (ORC 2015), and recent monitoring (1987-2011) at that river also demonstrates an overall degradation trend similar to that observed at the Shotover, with both attributed to decreasing sediment supply associated with the completion of mining activities. Aspects of this Shotover River sediment pulse are similar to the geomorphic changes seen at other rivers where mining-induced aggradation has had significant impacts, such as Ringarooma River (Knighton 1989), and Yuba River (James 2015).

The mining-induced sediment pulse is interpreted as a significant influence on the lower Shotover River's degradation trend over recent decades, although the long-term and interpreted ongoing degradation impacts of this sediment pulse have not always been well recognised. For example, a recent report attributed degradation trends to variations in the magnitude and frequency of flooding events, and to gravel extraction at the delta (Damwatch 2017).

As noted by James (2015, p47), "managing the river in its altered state requires an understanding of how it evolved to that geomorphic condition." Recognition of the Shotover River as undergoing a long-term degradation trend as a result of the mining-induced sediment pulse, if correct, may assist with inferring possible future river behaviour, and assisting with decision making for river management. Conceptual models of sediment pulse behaviour (e.g. Figure 10.3, James 1999, 2010, 2015) show the process of river system response to a large sediment input. This shows changes in channel elevations 'bed waves' and the movement of sediment through the river system 'sediment waves'. The bed elevation is expected to recover to a stable level much more rapidly than the removal of stored sediments, with the river responding to a lowered sediment supply first through incision, then by widening (James 1999). Removal of excess sediment from the river system is episodic and linked to flood events, and as these stored sediments stabilise 'the discharge required to initiate transport may become larger and less frequent leading to the perception that the system has recovered' (James 1999).

In the Shotover River the effects of the mining-related sediment pulse are expected to continue. The bed level will eventually reach a stable level in equilibrium with present input and processes and cease to degrade. The sedimentary effects will continue, with episodic release of stored sediments currently stored as remnants of aggradation surface (e.g. at Big Beach and Tucker Beach). This behaviour is seen in a plot of the bed level at the Bowens Peak gauging station (Figure 4.11), where episodic flood events have eroded and mobilised sediments and form small magnitude bed waves.

Narrowing of the active river channel and revegetation of the now inactive surfaces has been ongoing for many decades (e.g. Figures 4.10) and is expected to continue.

The Shotover River is a dynamic system, assumed to be still adjusting to a large-scale anthropogenic perturbation in sediment transport regime. The implications for management of the river and delta are that it may prove difficult to maintain a stable river form and further geomorphic changes can be expected. Management of the delta attempts to balance various objectives, including attempting to maintain a stable bed level through gravel extraction, increasing sediment buffering ability of lower delta through removal of willows to limit aggradation at the delta toe, and to limit degradation at the upper delta, where ongoing scour around the piers of the State Highway Bridge is of concern (Damwatch 2017).

11.4 Landslide Dam Hazard Investigation

The Shotover Gorge shows extensive evidence for landslide activity in locations along the narrow, deeply incised gorge, and a future large landslide has potential to form a landslide dam. The threat posed by a possible landslide dam has been identified as a concern in recent decades, with aspects of the landslide dam hazard assessed by Thompson (1996a), Bryant (2011 2017) and Davies (2017). These previous investigations reached little consensus regarding the threat posed by landslide dam events, most concluding that further work was required in order to better evaluate the hazard.

This project aimed to build on those studies through investigation of the potential magnitude and consequences of a landslide dam in the Shotover Gorge, in particular the hazard events caused by catastrophic dam failure and which may impact on downstream locations; dambreak flooding and post-dambreak aggradation. The possible impacts considered included

- Direct impact of dambreak flooding on the Shotover Country residential area located on low-lying land at the Shotover Delta.
- Aggradation of the Shotover Delta riverbed reducing channel capacity and increasing the flood hazard to adjacent areas as freeboard is reduced.
- Aggradation at the Shotover Delta toe reducing capacity of the Kawarau River channel, impeding outflows from Lake Wakatipu and increasing the Queenstown flood hazard.
- Economic impacts through disruption to tourism activities such as commercial rafting and jet boat tours, caused by the threat of landslides or dambreak flooding.

Key Findings

1. Formation of a large landslide dam in the Shotover Gorge is possible.

It is interpreted that large landslide dams have formed in the Shotover Gorge in the past, although the evidence for these events has now been removed by fluvial erosion. This interpretation stems from the many large landslide scarps adjacent to the gorge in locations where landslide debris would be expected to have been deposited into the river channel (Figure 6.11), the largest with estimated volumes of >10M m^3. Elsewhere in the Shotover catchment, evidence for many large landslide dams is preserved, illustrating that these events have occurred locally in the past and showing examples of their characteristics (Figure 6.13, Appendix 3). This demonstrates that local geological conditions and valley geomorphology are suitable for formation of a large landslide dam in the future. The rate of landslide formation was investigated through development of a magnitude-frequency relationship for landslides in the Shotover Gorge (Figure 6.12). Using this as a proxy for the frequency of dam-forming landslides shows that larger landslides (1M m^3) may form on average every few thousand years, having an annual probability in the order of 0.1-0.01%.

2. Any future Shotover Gorge landslide dam is expected to be unstable and short-lived.

The Shotover Gorge is located in the lower part of a large high-rainfall catchment area, and has a moderate gradient valley, which becomes wider in in its upper parts allowing for formation of large volume landslide-dammed lakes. These are important factors contributing to predicted dam instability (Figure 7.7), and all modelled landslide dams are predicted to be unstable in the long term. Shotover Gorge landslide dams are predicted to fail at the time of their first overtopping, or as a result of dam erosion triggered by a subsequent high flow event.

3. Catastrophic failure of a large Shotover Gorge landslide dam is capable of generating significant dambreak discharges, with the ability to potentially impact residential areas at the Shotover Delta.

Modelling of possible dambreak flood events demonstrate the potential for very large dambreak floods with discharges of >10,000 m^3/s to result from catastrophic failure of larger landslide dams (Table 8.3). The largest landslide dam scenario estimated to generate a peak dambreak discharge of 15-25,000 m^3/s. All estimation and modelling methods used involve considerable uncertainty and are only a guide to possible flood magnitudes, however these are shown to be realistic through comparison with documented floods from failure of dams with comparable dimensions (Figure 8.9).

Flood routing was used to simulate the progression of dambreak flood waves, indicating that flows will attenuate with distance downriver, with a large portion of this attenuation occurring at Big Beach (Figure 8.15), the first large floodplain downstream of the narrow gorge section. This is interpreted to act as a detention basin, temporarily storing and slowly releasing floodwaters, and contributing to the degree of flow attenuation. However, even allowing for attenuation, a dambreak flood event generated in the Shotover Gorge could result in a flood event at the Shotover Delta with significantly greater magnitude than any recorded meteorological flood, potentially over an order of magnitude greater than the 100-year flood peak (1500 m^3/s). Failure of small-moderate dams (<50 m) is not thought to be a significant dambreak flood threat. Most scenarios of this magnitude are estimated to generate flood discharges of <4,000 m^3/s (Table 8.3), and are modelled as attenuating by a greater extent than larger flood events, estimated at reducing in peak flows by at least 30% by the Shotover Delta (Figure 8.15).

Dambreak flood impact on residential areas at the Shotover Delta is possible, and is estimated to require a flood event with a peak flow at the delta of >8,000 m^3/s (Figure 8.18). Modelling and routing of dambreak flood events suggests a flood of this magnitude is a likely consequence of catastrophic failure of a 100 m high landslide dam in the lower Shotover Gorge. The largest landslide scenarios (6.5M m^3) considered in developing Shotover Gorge landslide dam and dambreak scenarios are still significantly smaller than a number of larger landslide scarps seen in the Shotover Gorge (Figure 6.3), which have estimated landslide volumes of 20-40M m^3. A landslide of this greater magnitude could form a much larger dam and its failure would generate extremely large flood discharges, which would be expected to impact on the Shotover Delta residential area. While these very large landslide events are less frequent than smaller landslides (Figure 6.12) they are possible in the Shotover Gorge, and could occur at any time. Thus the potential for a very large and damaging landslide dambreak flood in the future cannot be ruled out.

4. A large dambreak flood is not expected to occur without prior warning.

The minimum warning time available for decision making has been assessed. Assuming a dam failure commencing immediately at the dam's first overtopping, the warning time can be approximated by the time to fill the landslide-dammed reservoir (Figure 7.9, Table 7.5), plus the travel time of the dambreak flood wave to progress downriver. Travel time is modelled to be at least 2.5 hours for lower Shotover Gorge scenarios (Figure 8.17) and will be longer from locations further upvalley. There is interpreted to be little risk of a large and potentially damaging dambreak flood

occurring unexpectedly. Any larger dam (>80 m in height) capable of generating a significant dambreak discharge will have a large volume reservoir, and the longer filling time means the dam is expected to be identified prior to overtopping and failure, allowing time for warning and possible evacuation (Figure 7.9). Reservoirs formed by smaller landslide dams could conceivably form unnoticed, fill, overtop, and catastrophically fail to generate a dambreak flood within the hours of darkness (<12 hours)(Figure 7.9). However a dam of this magnitude is not expected to generate a flood discharge sufficient to impact on the residential area (Table 8.3, Figure 8.18).

5. Disruption and economic losses may be significant, even for a landslide dam event with relatively small physical impacts.

While large magnitude landslide dam events with potential to cause significant physical impacts are relatively infrequent, smaller landslide and dam-forming events are much more common in the Shotover Gorge, historically occurring at about every decade on average (e.g. Bryant 2011). Despite their smaller size and expected minor physical impacts, the smaller landslide events may cause significant disruptions. Even a small-moderate sized landslide dam, if it remained temporarily stable following overtopping, could block the passage of water craft and would be sufficient to justify precautionary closures of the lower river to recreational use. Relatively minor landslides or the threat of landslide impact can also cause disruption although no dam is formed, or even if debris does not reach the river channel, as shown by the impacts of the 2008 Moonlight Track landslide (Dellow et al. 2008, Bryant 2011). Additionally, operations including tourism (rafting, jet boats, 4WD tours etc.) and Branches Station are reliant on the single road access into the Shotover Valley, which is vulnerable to landslide damage. An event causing disruption to tourism activities for a period of weeks could potentially have economic impacts of millions of dollars (Bryant and Goldsmith 2013), which would be much more severe if this event occurred during the peak tourism season.

6. Aggradation impact on the Shotover Delta flood hazard could be significant, but would require very large sediment inputs.

Following a Shotover Gorge landslide dam failure, dambreak deposits are expected to fill the gorge and form a large alluvial fan at the Big Beach floodplain section below the gorge exit (Figure 10.9), with aggradation then continuing for a number of years as the remnant dam continues to erode and gorge sediments are remobilised downstream. For a dambreak scenario with a dam volume of ~6M m^3 (~0.1-0.01% annual probability) this is estimated to result in aggradation thicknesses of 5-15 m within the gorge and mean thicknesses of at least several metres at Big Beach (Table 10.2, Figure 10.10).

The aggradation magnitude at the Shotover Delta, >10 km downriver from the exit of the gorge, will be limited by sediment buffering as much of the dam sediment is temporarily stored in the gorge and the beach sections, then eroded and dispersed during the degradation phase of the sediment pulse. At the delta a maximum aggradation of 1-2 m is estimated to result from landslide dambreak events involving up to about 6M m^3 of sediments. Greater aggradation is possible, but requires a very large sediment input such as of comparable magnitude to the historic mining-induced sediment pulse (20-40M m^3). Landslide scarps with estimated volumes of this magnitude are present in the Shotover Gorge and have an annual probability of 0.01-0.001%, demonstrating that events of this size are possible and may have occurred in the past.

The large volume of stored sediments deposited by the historic mining-induced aggradation pulse reduce the vacant storage volume available for future sediment deposition in the lower Shotover River, meaning a major sediment input will cause more rapid and higher aggradation. If the vacant storage volume presently available is significantly lower than was available for sediment deposition prior to the mining-induced aggradation episode, then use of this historic aggradation event to estimate levels of future aggradation may not be accurate. This would result in an underestimation of aggradation levels, and thus underestimates the flood hazard due to future post-dambreak aggradation.

Any Shotover Delta aggradation will influence the flood hazard as this raises the riverbed level and reduces the available freeboard. A rating curve (Figure 8.18, Hamilton 2017) for the middle Shotover Delta shows that even with 2 m of aggradation at the Shotover Delta a 100-year flood (1500 m^3/s) is unlikely to impact the Shotover housing area. However, at this bed level the freeboard is significantly reduced, and potential impacts of larger magnitude floods would be of concern. Future aggradation of a magnitude that flooding impacts the residential area cannot be ruled out, but is estimated to require very large sediment inputs of at least 10-20M m^3.

7. Shotover Delta toe aggradation impacts on the Lake Wakatipu and Queenstown flood hazard are complex.

An increased post-dambreak sediment supply and aggradation at the toe of the Shotover delta may have some effect on the Kawarau River channel and the Lake Wakatipu flood hazard, but quantifying this is difficult. The influence of Shotover Delta toe aggradation on the Kawarau River channel and the Lake Wakatipu flood hazard is complex and is also influenced other factors in addition to sediment supply and aggradation rates, including changes in the Kawarau River channel and activities at the delta such as gravel extraction and willow removal.

Even without any significant future aggradation, the flood hazard to Queenstown is expected to gradually increase as the difference in levels between Lake Wakatipu and the Kawarau River decrease (Strong and Davies 2010). In addition, climatic changes are predicted to cause increases in runoff from the Shotover catchment and those rivers contributing to Lake Wakatipu (Poyck et al 2011). If increased Shotover Delta aggradation becomes a significant influence on flooding hazard at the delta or Lake Wakatipu in future, it may be feasible to manage the hazard through targeted gravel extraction to manage the delta form and maintain an optimum bed profile, as is currently being undertaken in attempts to limit upper delta degradation (Barnett and MacMurray 2017).

Discussion

Assessment methodology

The hazards of future landslide dam formation are relatively understudied, with most landslide dam hazard literature focused on assessment of the hazards from existing landslide dams (Korup 2005a). This study has illustrated the complexities of assessing a sequence of multiple events within a hazards cascade, each with significant uncertainty around their future behaviour. Assessment of this complex cascade of possible future events involves many assumptions, use of empirical relationships with large uncertainties, and often requires an estimation of 'realistic' values. There is no historical precedent for large landslide dam events (>1M m^3 volume), or any evidence preserved for earlier occurrences of this magnitude in the Shotover Gorge, so assessments must be based on comparison with analogue events in other locations. However, these are also infrequent events, and there are few well-documented examples in comparable geological settings (e.g. Poerua River).

The methodology developed and applied in this study of the Shotover Gorge landslide dam hazard is summarised as a flow chart in Figure 5.10. This approach to assessment of future landslide dam hazards and the estimation processes used may be a useful example for future landslide dam investigations in other locations. A number of previous studies were important resources in developing the approach taken in this study (e.g. Ollett 2001, Manville 2001, Korup 2005a), and it is hoped that process and results of this Shotover Gorge investigation will also prove to be a useful resource in future evaluations of landslide dam hazards.

Scenario development

This investigation used an approach aiming to develop an understanding of each of the steps in the landslide dam hazards cascade; landslide emplacement, dam formation, dam failure, dambreak flooding, and post-dambreak

aggradation (Figures 5.7, 5.8). The possible magnitudes, likely behaviour and impacts of these events have been investigated through modelling and estimations used to develop plausible, realistic hazard events scenarios (e.g. Tables 6.1, 7.2, 8.3). A probabilistic risk-based approach to this study was not possible as event likelihoods cannot be reliably quantified, however the approximate likelihood of large landslide formation (Figure 6.12) indicates the threat is sufficient to be considered and investigated in more detail. These scenarios can be evaluated using the ideal hazard scenario characteristics noted by Porter et al. (2011);

Scientifically realistic: Many of the estimations and modelling methods used involve considerable uncertainty, especially those requiring use of empirical equations. Despite this, these are often the best methods available for a simple analysis, and are commonly used to assess future (e.g. Ollett 2001) and existing landslide dam hazards (e.g. ORC 2007b). Modelling results have been compared with case studies and datasets of existing landslide dams and dambreak flood events and lie within realistic ranges (Figures 7.6, 8.9).

Large enough to generate significant consequences: Landslide events described in these scenarios are not the largest possible in the study area, shown by the presence of several much larger scarps in the area, for example the large (40M m^3) Arthurs Point landslide. However, the scenarios used are of sufficient magnitude that possible consequences such as dambreak flooding are significant, being potentially large enough to impact on the residential housing area.

Likely enough to not be dismissed as rare or extreme: The larger landslide dam scenarios developed are of similar magnitude (1-10M m^3) to many landslide dam remnants identified in the Shotover area (Figure 6.13, Appendix 3), and to numerous existing landslide scarps identified in the Shotover Gorge (Figure 6.11). This shows that landslides and landslide dams of this scale have previously occurred in the area and could potentially occur again in the future. Landslide frequencies estimated in Figure 6.12 show the larger landslide scenario events may have annual likelihoods in the order of 0.1-0.001%. The scenario landslide dams are of comparable height to a number of South Island landslide dams formed in the last few decades (Table 7.3), demonstrating that events of this magnitude are not unrealistic.

Dambreak flooding

This assessment demonstrates the importance of considering dambreak flooding as a component of flood hazard assessments for the Shotover Delta, and reinforces that these should be undertaken in other locations where landslide dam formation is thought possible. Landslide dam failures may generate very large peak dambreak flood discharges, potentially up to two orders of magnitude greater than known meteorological flood events in that location (Korup and Tweed 2007). The results of Shotover Gorge dambreak modelling are consistent with these observations (Table 8.3, Figure 8.8), with the largest landslide dam scenarios estimated to generate very large outflows (15-25,000 m^3/s) of about an order of magnitude larger than the largest known flood event (~1500 m^3/s in the November 1999 flood)(Hamilton 2017).

The use of a simple 1D model for flood routing was appropriate for an initial investigation of flow attenuation and flood wave travel time, however there is opportunity to address the limitations of this model in future modelling. For example, the Shotover channel was defined only by a series of widely-spaced cross-sections and did not include the hydraulic interaction with the Kawarau River, so these simplifications could be improved on in future modelling.

Shotover aggradation

The approach taken to estimation of aggradation was based on comparison with sediment deposition and transport patterns from comparable dambreak events, and use of a simple 1D sediment transport model. This is an improvement from the basic estimates of previous studies (e.g. Bryant 2011, Hamilton 2017) but was still relatively subjective and involved many assumptions, which could be refined by more robust assessment using numerical or physical sediment transport modelling.

Previous investigations (e.g. microscale modelling by Davies 2007) were designed to investigate changes at the delta, and increased sediment loads were supplied directly to the delta. There is a ~9 km riverbed section between the exit of the gorge and the head of the Shotover Delta, including several very broad floodplain sections (Big Beach and Tucker Beach)(Figure 10.9), which are interpreted as having a significant sediment buffering impact. Future sediment transport modelling should include the entire lower river in order to account for these impacts, including part of the gorge, beach sections and the delta. The flume experiment of Bainbridge (2017) may provide an example of a model which shows sediment pulse progression through a similar river system. This could attempt to simulate a range of post-dambreak sediment pulse events, and the observed mining-induced aggradation pulse, aiming to confirm interpretation that this level of aggradation would require very large sediment inputs.

Shotover catchment landslide dams

Further study of the known landslide dam deposits elsewhere in the Shotover catchment (Figure 6.13, and summarised in Appendix 3) may be of use in better defining the Shotover Gorge landslide dam hazard. The only two Shotover catchment landslide dams to have received any detailed investigation are the Lochnagar and Polnoon Burn landslide dams, however these are extremely large (>100M m^3) and of limited usefulness as examples when evaluating potential smaller events in the Shotover Gorge. Many of these dams are interpreted to have comparable landslide volumes (1-10M m^3) (e.g. Figure 6.1) to Shotover Gorge landslide scenarios and may be a better guide to possible landsliding behaviour and dam formation. This could include investigation of aspects such as the landslide type, structural controls on failure and possible trigger events.

Shotover catchment landslide dams (Appendix 3) and other Southern Alps dams noted by Korup (2006) are formed by landslides with two distinct styles, of which high mobility, rapid landslides are of much more concern as landslide dam hazards. Identifying factors influencing development of these landslide styles may assist with identifying which of these are more likely to occur in the Shotover Gorge. Estimation of geomorphic parameters for these dams such as dam height, and length may be used to guide modelling of plausible dam dimensions and geometries for future Shotover Gorge landslide dams. Being situated locally to the Shotover Gorge, with similar geological and structural controls (Figure 1.6), these may be more applicable than using examples from elsewhere in New Zealand (e.g. Korup 2004a), or globally (e.g. Figure 7.6).

Identification of any evidence for catastrophic dam failure and generation of dambreak flooding may assist with estimations of the rate of dam failure and possible flood magnitudes from Shotover Gorge landslide dams. Korup et al. (2006) notes the presence of outburst flood debris below the Polnoon Burn landslide dam, and these deposits may also be identifiable in other locations.

References

Adams J, 1981, Earthquake-dammed lakes in New Zealand. Geology 9: 215-219.

Alder S, 2016. Structure and fault rock sequences of the Moonlight Fault Zone, West Otago: constraints on fault reactivation during basin inversion. Master of Science thesis, University of Otago.

Alloway BV, Lowe DJ, Barrell, DJA, Newnham RM, Almond PC, Augustinus PC, Bertler NAN, Carter L, Litchfield NJ, McGlone MS, Shulmeister J, Vandergoes MJ, Williams, PW and NZ-INTIMATE members, 2007. Towards a climate event stratigraphy for New Zealand over the past 30 000 years (NZ-INTIMATE project). Journal of Quaternary Science 22(1): 9–35.

Arshad WA, Doscher C, and Davies TR, 2004. Landslide dambreak hazard analysis in Westland, New Zealand – a GIS approach. In: Liong, Phoon and Babovic (Eds), 6th International Conference on Hydroinformatics, World Scientific Publishing company.

Bainbridge R, 2017. Lost landslides: Rock-avalanche occurrence and fluvial censoring processes on South Island, New Zealand. PhD thesis, Northumbria University.

Barnett AG, MacMurray HL, Hoare RA, Henderson VJ and Wang D, 2008. An introduction to AULOS. Hydra software Ltd, Hamilton.

Barnett and MacMurray Ltd, 2017. Shotover Delta target profiles. Report prepared for Otago Regional Council, Ref. BM1-459, July 2017.

Barnett and MacMurray Ltd., Canterprise Ltd., Lincoln University and Hunziker, Zarn and Partner AG, 2006. Kawarau and Shotover Rivers sedimentation investigation. Report prepared for the Otago Regional Council.

Barrell DJA, 2011. Quaternary glaciers of New Zealand. In: Ehlers J, Gibbard PL and Hughes PD (Eds), Developments in Quaternary science 15, Amsterdam, Netherlands. pp 1047-1064.

Barrell DJA, Riddolls BW, Riddolls PM and Thomson R, 1994. Surficial geology of the Wakatipu Basin. Institute of Geological and Nuclear Sciences Report 94/39.

Barrell DJA, Almond PC, Vandergoes MJ, Lowe DJ, Newnham RM and INTIMATE members, 2013. A composite pollen-based stratotype for inter-regional evaluation of climatic events in New Zealand over the past 30,000 years (NZ-INTIMATE project). Quaternary Science Reviews 74: 4-20.

Barry J, 1966. Structural analysis in the middle Shotover Valley, northwest Otago. Master of Science thesis, University of Otago.

Bartley R and Rutherford I, 2005. Re-evaluation of the wave model as a tool for quantifying the geomorphic recovery potential of streams disturbed by sediment slugs. Geomorphology 64: 221-242.

Becker JS, Johnston DM, Paton D, Hancox GT, Davies TR, McSaveney MJ, and Manville VR, 2007. Response to landslide dam failure emergencies: Issues resulting from the October 1999 Mount Adams landslide and dam-break flood in the Poerua River, Westland, New Zealand. Natural Hazards Review 8(2): 35-42.

Bell DH, 1976. Slope evolution and slope stability, Kawarau Valley, Central Otago, New Zealand, 1976. Bulletin of the International Association of Engineering Geology 14: 5-16.

Bell DH, 1992. Geomorphic evolution of a valley system: The Kawarau Valley, Central Otago. In: Landforms of New Zealand. (Ed. Soons JM and Selby MJ). Longman Paul Ltd, Auckland. pp 456-481.

Benn DI, Kirkbride MP, Owen LA and Brazier V, 2003. Glaciated valley landsystems. In: Evans D (ed), Glacial landsystems. Hodder Arnold, London.

Black A, Craw D, Youngson JH and Karubaba J, 2004. Natural recovery rates of a river system impacted by mine tailing discharge: Shag River, East Otago, New Zealand. Journal of Geochemical Exploration 84: 21–34.

Braithwaite JC, 1989. Gold mining in the Shotover and Kawarau Rivers, Central Otago, New Zealand. In: Kear D (Ed), Mineral deposits of New Zealand. Monograph 13. Australasian Institute of Mining and Metallurgy: 181-188.

Braun A, Cuomo S, Petrosino S, Wang X, and Zhang L, 2018. Numerical SPH analysis of debris flow run-out and related river damming scenarios for a local case study in SW China. Landslides 15: 535–550.

Brown DA, 1956. Report on geology of upper Shotover. In: Otago Catchment Board Bulletin No.1 Shotover River Survey (Upper Catchment).

Brown J, 2017. Statement of evidence of Jeffrey Andrew Brown on behalf of Shotover Country Limited, 14 March 2017. In the matter of the Housing Accords and Special Housing Areas Act 2013 and in the matter of an application by Shotover Country for consent for subdivision and land use within a Special housing Area (SH160139), before the Queenstown Lakes District Council Independent Hearings Panel.

Bryant J, 2011. Lower Shotover River: Flood risk through landslide dam breach. Report prepared for David Hamilton and Associates Ltd.

Bryant J, 2017. Statement of evidence by Jeff Bryant, presented on behalf of Shotover Country Limited. In the matter of the Resource Management Act 1991 and in the matter of Consent Application SH160139 under s25 of the Housing Accords and Special Housing Areas Act 2013 by Shotover Country Ltd, before Queenstown Lakes District Council.

Bryant JM and Goldsmith M, 2013. The incidence and importance of landslide dams in inland Otago. Proc. 19th NZGS Geotechnical Symposium. Ed. CY Chin, Queenstown.

Carrivick JL and Tweed FS, 2013. Proglacial lakes: character, behaviour and geological importance. Quaternary Science Reviews 78: 34-52.

Carryer SJ, 1984. Report on prospecting of Londonderry Terrace, Skippers. Minerals Report MR2391, Aorere Mining Ltd.

Casagli N and Ermini L, 1999. Geomorphic analysis of landslide dams in the Northern Apennine. Transactions of the Japanese Geomophological Union 20(3): 219-249.

Catani F, Tofani V, and Lagomarsino D, 2016. Spatial patterns of landslide dimension: A tool for magnitude mapping. Geomorphology 273: 361–373.

Chandler P, papers held by Hocken Library Archives, Dunedin.

Chandler P, 1957. Map of late 19th and early 20th Century gold-mining along the Shotover and Arrow Rivers. Figure 2 in Schmidt M, 2005. Coronet Peak Pastoral Lease, Conservation Resources Report, February 2005.

Chen CY, 2008. Sedimentary impacts from landslides in the Tachia River Basin, Taiwan. Geomorphology 105(3/4): 355-365.

Chen XQ, Cui P, Li Y, and Zhao WY, 2011. Emergency response to the Tangjiashan landslide-dammed lake resulting from the 2008 Wenchuan Earthquake, China. Landslides 8: 91–98.

Clement AJH, Novakova T, Hudson-Edwards KA, Fuller IC, Macklin MG, Fox EG and Zapico I, 2017. The environmental and geomorphological impacts of historical gold mining in the Ohinemuri and Waihou river catchments, Coromandel, New Zealand. Geomorphology 295: 159-175.

Cook SJ, Quincey DJ, and Brasington J, 2014. Geomorphology of the Rees Valley, Otago, New Zealand. Journal of Maps 10 (1): 136-150.

Costa JE, 1985. Floods from dam failures. USGS open file report: 85-560.

Costa JE and Schuster RL, 1988. The formation and failure of natural dams. US Geological Survey, open file report 87-392.

Cox SC, Barrell DJA, Dellow S, McColl ST, and Horspool N, 2015. Landslides and ground damage during the Mw5.8 Matukituki Earthquake, 4 May 2015, central Otago, New Zealand. GNS Science Report 2015/17.

Craddock FW, 1975. Golden Canyon: the story of Skippers Road and the Shotover Valley. Pegasus, Christchurch.

Craw D, 1984. Lithologic variations in Otago Schist, Mt Aspiring area, northwest Otago, New Zealand. New Zealand Journal of Geology and Geophysics 27(2): 151-166,

Croissant T, Lague D, Steer P and Davy P, 2017. Rapid post-seismic landslide evacuation boosted by dynamic river width. Nature Geoscience 10: 680-684.

Cui Y, Parker G, Lisle TE, Gott J, Hansler-Ball ME, Pizzuto JE, Allmendinger NE and Reed JM, 2003. Sediment pulses in mountain rivers: 1. Experiments. Water Resources Research 39(9): 1-12.

Cui Y, Parker G, Braudrick C, Dietrich WE and Cluer B, 2005. Dam Removal Express Assessment Models (DREAM). Part 1: Model development and validation. Journal of Hydraulic Research.

Cui P, Dang C, Zhuang J, You Y, Chen X and Scott KM, 2012. Landslide-dammed lake at Tangjiashan, Sichuan province, China (triggered by the Wenchuan Earthquake, May 12, 2008): risk assessment, mitigation strategy, and lessons learned. Environ Earth Sci 65: 1055–1065.

Cunningham V, 1994. Land use planning and development suitability in Queenstown, New Zealand. Masters of Engineering Geology thesis, University of Canterbury.

Dai FC, Lee CF, Deng JH, and Tham LG, 2005. The 1786 earthquake-triggered landslide dam and subsequent dam-break flood on the Dadu River, southwestern China. Geomorphology 65: 205–221.

Damwatch Engineering, 2017. Review of gravel extraction on Shotover River Delta and impact on security of SH6 Bridge. Memo from Grant Webby (Damwatch Engineering), to Russel Nicholls (Opus International Consultants Limited, Dunedin), 4 October 2017.

Dang C, Chu N and Ding Yu, 2014. Predictive uncertainty of peak outflow relations for landslides dam breach. Environ Earth Sci 72: 4265–4271.

Davies TR, 2002. Landslide-dambreak floods at Franz Josef Glacier township, Westland, New Zealand: a risk assessment. Journal of Hydrology (NZ) 41 (1): 1-17.

Davies TR, 2007. Shotover River sediment management: Microscale modelling. Final Report to Otago Regional Council.

Davies TR, 2017. Shotover Country resource consent evidence.

Davies TR and Scott BK, 1997. Dambreak flood hazard from the Callery River, Westland, New Zealand. Journal of Hydrology (NZ) 36 (1): 1-13.

Davies TR and Korup O, 2007. Persistent alluvial fanhead trenching resulting from large, infrequent sediment inputs. Earth Surface Processes and Landforms 32: 725-742.

Davies TR and Korup O, 2010. Sediment cascades in active landscapes. In: Burt T and Allison R (eds), Sediment Cascades: An Integrated Approach. John Wiley and Sons.

Davies TR, McSaveney MJ and Doscher C, 2005. Monitoring and effects of landslide-induced aggradation in the Poerua Valley, Westland. Project No. 03/499, final report on research project.

Davies TR, Manville V, Kunz M and Donadini L, 2007. Modelling landslide dambreak flood magnitudes: Case study. Journal of Hydraulic Engineering 133 (7): 713-720.

Davies TR, Beaven S, Conradson D, Densmore A, Gaillard JC, Johnston D, Milledge D, Oven K, Petley D, Rigg J, Robinson T, Rosser N and Wilson T, 2015. Towards disaster resilience: A scenario-based approach to co-producing and integrating hazard and risk knowledge. International Journal of Disaster Risk Reduction 13.

De La Mare AJ, 1993. The Shotover River, the richest river in the world: a history of gold mining on the Shotover River. Lakes District Museum. Arrowtown.

Dellow GD, Allen S, Cox S, Ferris B, Hancox GT, McColl S, Nelis S, Paler N, and Perrin ND, 2009. Landslides in 2008. New Zealand Geomechanics News, Issue 77, June 2009: 57-60.

Dellow S, and Massey C, 2017. Kaikoura Earthquake – Landslide dams: identifying the hazard and managing the risks. New Zealand Geomechanics News, Issue 93, June 2017.

Dellow S, Massey CI, and Cox SC, 2017. Response and initial risk management of landslide dams caused by the 14 November 2016 Kaikoura Earthquake, South Island, New Zealand. Alexander GJ and Chin CY (Eds), Proc. 20th NZGS Geotechnical Symposium. Napier.

Downer, 2013. 'Skippers – Broken at the Elbow' presentation.

Ermini L and Casagli N, 2003. Prediction of the behaviour of landslide dams using a geomorphological dimensionless index. Earth Surface Processes and Landforms 28: 31–47.

Evans DJA and Benn DI, 2004. A practical guide to the study of glacial sediments. Arnold, London.

Evans DJA, Rother H, Hyatt OM and Shulmeister J, 2013. The glacial sedimentology and geomorphological evolution of an outwash head/moraine-dammed lake, South Island, New Zealand. Sedimentary Geology 284-285: 45-75.

Evans LP, 2015. Sedimentological investigation of late glacial (Otiran) exposures along the southern margins of Lake Wanaka, South Island, New Zealand. A thesis submitted for the degree of Master of Philosophy at The University of Queensland.

Fan X, van Westen CJ, Xu Q, Gorum T, and Dai F, 2012. Analysis of landslide dams induced by the 2008 Wenchuan earthquake. Journal of Asian Earth Sciences 57: 25–37.

Fan X, Rossiter DG, van Westen CJ, Xu Q, and Gorum T, 2014. Empirical prediction of coseismic landslide dam formation. Earth Surf. Process. Landforms 39: 1913–1926.

Ferguson RI, Church M, Rennie CD and Venditti JG, 2015. Reconstructing a sediment pulse: Modeling the effect of placer mining on Fraser River, Canada, J. Geophys. Res. Earth Surf., 120: 1436–1454.

Fountain AG and Walder JS, 1988. Water flow through temperate glaciers. Reviews of Geophysics 36(3): 299-328.

Fread DL, 1981. Some limitations of contemporary dam-break flood routing models: Preprint 81-525, Annual Meeting of American Society of Civil Engineers, St. Louis, Missouri, 15 pp.

Froehlich DC, 1987. Embankment-dam breach parameters: Proceedings of the National Conference on Hydraulic Engineering, ASCE, Williamsburg, Virginia, p. 570-575.

Froehlich DC, 1995. Embankment dam break parameters revisited. Water Resources Engineering, Proc. 1995 ASCE Conf. on Water Resources Engineering, New York, 887–891.

Fuller IC, 2014. Towards an understanding of catchment-scale sediment dynamics: cascades & connectivity in steepland systems. International Journal of Erosion Control Engineering 7(1) 1-8.

Gallino GL, and Pierson TC, 1985. Polallie Creek debris flow and subsequent dam-break flood of 1980, East Fork Hood River Basin, Oregon. US Geological Survey Water Supply Paper 2273.

Galvin P (ed), 1906. The New Zealand Mining Handbook. Government Printer, Wellington.

Ghoshal S, James LA, Singer MB and Aalto R, 2010. Channel and floodplain change analysis over a 100-year period: Lower Yuba River, California. Remote Sensing 2(7).

Gibbs HS, Raeside JD, Dixon JK and Metson AJ, 1945. Soil erosion in the high country of the South Island. NZ DSIR Bulletin 92.

Gilbert GK, 1917. Hydraulic-mining debris in the Sierra Nevada. US Geological Survey Professional Paper 105. Washington, DC: Government Printing Office.

Gillies AJ, 1956. Hydrology and sedimentation. In: Otago Catchment Board Bulletin No.1 Shotover River Survey (Upper Catchment).

GNS, 2008. Shotover River landslide response. Geonet landslide response report, at *geonet.org.nz/landslide/reports.*

Gori S, Falcucci E, Dramis F, Galadini F, Galli P, Giaccio B, Messina P, Pizzi A, Sposato A, and Cosentino D, 2014. Deep-seated gravitational slope deformation, large-scale rock failure, and active normal faulting along Mt. Morrone (Sulmona basin, Central Italy): Geomorphological and paleoseismological analyses. Geomorphology 208: 88-101.

Gran KB and Czuba JA, 2017. Sediment pulse evolution and the role of network structure. Geomorphology 277:17-30.

Guzzetti F, Ardizzone F, Cardinali M, Rossi M, and Valigi D, 2009. Landslide volumes and landslide mobilization rates in Umbria, central Italy. Earth and Planetary Science Letters 279: 222–229.

Hamel J, 2001. The archaeology of Otago. Department of Conservation, Wellington.

Hamilton and Associates, 2010. Shotover Country plan change river and flooding risk assessment. Report by David Hamilton & Associates Ltd, Consulting Engineers, Dunedin.

Hamilton DJ, 2017. Statement of Evidence of David John Hamilton. In The Matter of The Resource Management Act 1991 And In The Matter of Consent Application SH160139 Shotover Country SHA By Shotover Country Limited, before Queenstown Lakes District Council.

Hall-Jones J, 2005. Goldfields of Otago: an illustrated history. Craig Printing, Invercargill.

Hancox GT, Perrin ND, and Dellow GD, 1997. Earthquake-induced landsliding in New Zealand and implications for MM intensity and seismic hazard assessment. GNS Client Report 43601B, December 1997.

Hancox GT, Cox S, Turnbull IM, and Crozier MJ, 2003. Reconnaissance studies of landslides and other ground damage caused by the Mw7.2 Fiordland earthquake of 22 August 2003. Institute of Geological and Nuclear Sciences science report 2003/30.

Hancox GT, McSaveney MJ, Manville VR, and Davies TR, 2005. The October 1999 Mt Adams rock avalanche and subsequent landslide dam-break flood and effects in Poerua River, Westland, New Zealand. New Zealand Journal of Geology and Geophysics 48 (4): 683-705.

Harding J and Boothroyd I, 2004. Impacts of mining. In: Harding (ed) Freshwaters of New Zealand. New Zealand Hydrological Society and New Zealand Limnological Society.

Harding JS, Quinn JM and Hickey CW, 2000. Effects of mining and production forestry. Collier KJ and Winterbourn M J (eds), New Zealand stream invertebrates: ecology and implications for management. New Zealand Limnological Society, Christchurch. Pp. 230 - 259.

Harrison LM, Dunning SA, Woodward J and Davies TRH, 2015. Post rock-avalanche dam outburst flood sedimentation in Ram Creek, Southern Alps, New Zealand. Geomorphology 241: 135-144.

Hermanns RL, Hewitt K, Strom A, Evans SG, Dunning SA and Scarascia-Mugnozza G, 2011. The classification of rockslide dams. In: Evans SG, Hermanns RL, Strom A and Scarascia-Mugnozza G (Eds), Natural and Artificial Rockslide Dams. Lecture Notes in Earth Sciences 133. Springer-Verlag Berlin Hiedelberg.

Hewitt K, 2006. Disturbance regime landscapes: mountain drainage systems interrupted by large rockslides. Progress in Physical Geography 30(3): 1–28.

Hicks DM, Walsh JM and Duncan MJ, 2000. Clutha River sediment budget. Report prepared by NIWA for Contact Energy Ltd.

Hovius N, Stark CP, and Allen PA, 1997. Sediment flux from a mountain belt derived by landslide mapping. Geology 25 (3): 231–234

Hoyle JT, Measures RJ, Bind J and Hicks DM, undated. How to track a sediment slug: morphological modelling of the upper Waipa River.

Hungr O and Evans S, 2004. Entrainment of debris in rock avalanches: An analysis of a long run-out mechanism. Geological Society of America Bulletin 116: 1240-1252.

Hutton CO, 1939. The Bob's Cove Tertiary Beds and the Moonlight Thrust Fault. Trans Roy. Soc. N.Z. 69 (1): 73–88

Hyatt OM, 2009. Insights into New Zealand Glacial Processes from studies of glacial geomorphology and sedimentology in Rakaia and other South Island Valleys. A thesis submitted in partial fulfilment of the requirements for the degree of Doctor of Philosophy in Geology, University of Canterbury.

Hyatt OM, Shulmeister J, Evans DJA, Thackray GD, and Rieser U, 2012. Sedimentology of a debris-rich, perhumid valley glacier margin in the Rakaia Valley, South Island, New Zealand. Journal of Quaternary Science 27 (7): 699-712.

James LA, 1991. Incision and morphologic evolution of an alluvial channel recovering from hydraulic mining sediment. Geological Society of America Bulletin 103: 723-736.

James LA, 1999. Time and the persistence of alluvium: River engineering, fluvial geomorphology, and mining sediment in California. Geomorphology 31: 265-290.

James LA, 2006. Bed waves at the basin scale: implications for river management and restoration. Earth Surface Processes and Landforms 31: 1692-1706.

James LA, 2010. Secular sediment waves, channel bed waves, and legacy sediment. Geography Compass 4/6: 576-598.

James LA, 2015. Designing forward with an eye to the past: Morphogenesis of the lower Yuba River. Geomorphology 251: 31-40.

Jennings DN, Webby MG and Parkin DT, 1993. Tunawaea landslide dam: Part 2 – Hazard assessment. Proceedings of IPENZ Annual Conference 1993, Hamilton.

Jones KL, 2008. Goldmining and enclosure on the middle and upper Shotover River, Central Otago, New Zealand. New Zealand Journal of Archaeology 29: 109-144.

Jones KL, 2009. Aerial photographs and the record of agriculture and engineering in Otago, New Zealand. 3rd Australasian Engineering Heritage Conference 2009.

Jones R, 2017. Uncertainty in climate change impacts on Southern Alps river flow: the role of hydrological model complexity. Masters of Science Thesis, University of Otago, Dunedin.

Kershaw JA, Clague JJ and Evans SG, 2005. Geomorphic and sedimentological signature of a two-phase outburst flood from moraine-dammed Queen Bess Lake, British Columbia, Canada. Earth Surface Processes and Landforms 30: 1-25.

Knighton AD, 1989. River adjustment to changes in sediment load: The effects of tin mining on the Ringarooma River, Tasmania, 1975-1984. Earth surface Processes and Landforms 14: 333-359.

Knighton AD, 1991. Channel bed adjustment along mine-affected rivers of northeast Tasmania. Geomorphology 4: 205-219.

Kondolf GM, Piegay H and Landon N, 2002. Channel response to increased and decreased bedload supply from land use change: contrasts between two catchments. Geomorphology 45: 35-51.

Korup O, 2002. Recent research on landslide dams – a literature review with special attention to New Zealand. Progress in Physical Geography 26 (2): 206–235.

Korup O, 2004a. Geomorphometric characteristics of New Zealand landslide dams. Engineering Geology 73: 13–35.

Korup O, 2004b. Landslide-induced river channel avulsions in mountain catchments of southwest New Zealand. Geomorphology 63: 57-80.

Korup O, 2005a. Geomorphic hazard assessment of landslide dams in south Westland, New Zealand: Fundamental problems and approaches. Geomorphology 66: 167-188.

Korup O, 2005b. Distribution of landslides in southwest New Zealand. Landslides 2: 43–51.

Korup O, 2006. Rockslide and rock avalanche dams in the Southern Alps, New Zealand. Italian Journal of Engineering Geology and Environment, Special Issue 1 (2006).

Korup O and Tweed F, 2007. Ice, moraine, and landslide dams in mountainous terrain. Quaternary Science Reviews 26: 3406–3422.

Korup O and Clague JJ, 2009. Natural hazards, extreme events, and mountain topography. Quaternary Science Reviews 28: 977–990.

Korup O, and Wang G, 2015. Multiple Landslide-Damming Episodes. In Davies TR (ed), Landslide Hazards, Risks, and Disasters. Elsevier.

Korup O, McSaveney MJ and Davies TRH, 2004. Sediment generation and delivery from large historic landslides in the Southern Alps, New Zealand. Geomorphology 61: 189-207.

Korup O, Strom AL and Weidinger JT, 2006. Fluvial response to large rock-slope failures: Examples from the Himalayas, the Tien Shan, and the Southern Alps in New Zealand. Geomorphology 78:3-21.

Korup O, Densmore AL and Schunlegger F, 2010. The role of landslides in mountain range evolution. Geomorphology 120: 77-90.

KTCO Ltd, 2017. Cultural Values Report: Arrow River / Wakatipu Basin Aquifers, Cardrona River. Report prepared for the Otago Regional Council.

Kumar V, Gupta V, Jamir I, and Chattoraj SL, 2018. Evaluation of potential landslide damming: Case study of Urni landslide, Kinnaur, Satluj valley, India. Geoscience Frontiers: 1-15.

Larsen IJ, Montgomery DR, and Korup O, 2010. Landslide erosion controlled by hillslope material. Nature Geoscience 3: 247–251.

Lawrence S, Davies P and Turnbull, 2016. The archaeology of Anthropocene rivers: water management and landscape change in 'Gold Rush' Australia. Antiquity 90(373): 1348-1362.

Lee KL and Duncan JM, 1975. Landslide of April 25, 1974 on the Mantaro River, Peru. Report to the Committee on Natural Disasters, Commission on Sociotechnical Systems, National Research Council.

Lee S-P, Chen Y-C, Shieh C-L, and Kuo Y-S, 2014. Using real-time abnormal hydrology observations to identify a river blockage event resulted from a natural dam. Landslides 11: 1007–1017.

McColl ST and Davies TR, 2011. Evidence for a rock-avalanche origin for 'The Hillocks' "moraine", Otago, New Zealand. Geomorphology 127: 216-224.

MacDonald TC and Langridge-Monopolis J, 1984. Breaching characteristics of dam failures: Journal of Hydraulic Engineering 110: 567-586.

Macfarlane D, and Roberts K, 2001. Managing a landslide hazard in the Roxburgh Gorge. In: Engineering and Development in Hazardous Terrain, New Zealand Geotechnical Society 2001 Symposium, Christchurch, August 2001.

Malamud BD, Turcotte DL, Guzzetti F, and Reichenbach P, 2004. Landslide inventories and their statistical properties. Earth Surf. Process. Landforms 29: 687–711.

Manville V, 2001. Techniques for evaluating the size of potential dam-break floods from natural dams. Institute of Geological & Nuclear Sciences science report 2001/28.

Massey C, McSaveney M, and Davies T, 2013. Evolution of an overflow channel across the Young River landslide dam, New Zealand. In Margottini et al. (eds.), Landslide Science and Practice, Vol. 6: 43-49.

Massey et al, 2018. Landslides triggered by the 14 November 2016 Mw 7.8 Kaikōura Earthquake, New Zealand. Bulletin of the Seismological Society of America 108 (3B): 1630–1648.

McFarlane DF, 2009. Observations and predictions of the behaviour of large, slow-moving landslides in schist, Clyde Dam reservoir, New Zealand. Engineering Geology 109: 5-15.

McSaveney MJ, 1978. Shotover River – aspects of its erosion history relating to control of siltation in the Clutha Valley development. Water and soil Unpublished Alpine Processes Report AP9. Ministry of Works and Development, Water and Soil Division, Christchurch.

Miller DJ and Benda LE, 2000. Effects of punctuated sediment supply on valley-floor landforms and sediment transport. GSA Bulletin 112(12):1814-1824.

Ministry of Works and Development (MWD), 1975. Shotover River catchment sediment sources - Feasibility Report.

Mojzisek J, 2006. Precipitation variability in southern New Zealand. PhD Thesis submitted to University of Otago.

Moon A, 1997. Predicting low probability rapid landslides at Roxburgh Gorge, New Zealand. In: Cruden and Fell (Eds), Landslide Risk Assessment. Balkema, Rotterdam.

Moon AT, Wilson RA, and Flentje P, 2005. Developing and using landslide size frequency models. Proceedings of the International Conference on Landslide Risk Management, 18th Annual Vancouver Geotechnical Society Symposium, Vancouver, 31 May - 4 June 2005: p589-598.

Morche D and Laute K. 2009. Investigating channel response to a dambreak flood event in an Alpine river - Downstream trends in stream power and channel bed particle characteristics. Arct Antarct Alp Res 41(1): 69-78.

Morche D and Schmidt K-H, 2012. Sediment transport in an alpine river before and after a dambreak flood event. Earth Surface Processes and Landforms 37(3).

Morche D, Schmidt K-H, Heckmann T and Haas F, 2007. Hydrology and geomorphic effects of a high-magnitude flood in an Alpine River. Geogr. Ann. 89A (1): 5-19.

Mortimer, N. 1993 Geology of the Otago schist and adjacent rocks. Scale 1:500 000 map. Institute of Geological & Nuclear Sciences geological map 7. Institute of Geological & Nuclear Sciences, Lower Hutt.

Nash TR, 2003. Engineering geological assessment of selected landslide dams formed from the 1929 Murchison and 1968 Inangahua earthquakes. Master of Science in Engineering Geology thesis, University of Canterbury, Christchurch.

Nash T, Bell D, Davies T, and Nathan S, 2014. Analysis of the formation and failure of Ram Creek landslide dam, South Island, New Zealand. New Zealand Journal of Geology and Geophysics 51 (3): 187-193.

Nelson AD, 2017. Gold in the documents: Estimating placer mining excavation volumes in the Fraser Basin, British Columbia, using historicals. BC Studies 196, Winter 2017/2018.

Nelson AD and Church C, 2012. Placer mining along the Fraser River, British Columbia: The geomorphic impact. GSA Bulletin 124(7/8): 1212-1228.

Nelson MC, 2012. The impact of landslides on sediment yield, South Westland, New Zealand. Thesis submitted in partial fulfilment of the requirements for the degree of Master of Science. Simon Fraser University, British Columbia, Canada.

Nugold Hills Gold Mines NL, 1990. Final report to Coal and Minerals, Energy and Resources Division, Branches Flat prospect (PL 31-1593), Central Otago. Minerals Report MR2996.

O'Connor JE, Grant GE and Costa JE, 2002. The geology and geography of floods. Ancient floods, modern hazards: principles and applications of paleoflood hydrology. Water Science and Application Volume 5, pages 359-385.

Ollett PP, 2001. Landslide dambreak flooding in the Callery River, Westland. Master of Natural Resources Engineering thesis, Lincoln University.

Otago Catchment Board (OCB), 1956. Bulletin No 1: Shotover River Survey (Upper Catchment).

Otago Catchment Board (OCB), 1966. Bulletin No 2: Shotover River Survey (Lower Catchment).

Otago Regional Council (ORC), 1997. Shotover River delta sedimentation investigation.

Otago Regional Council (ORC), 2002a. Shotover River delta sedimentation.

Otago Regional Council (ORC), 2002b. A theoretical consideration of sediment transport within the Shotover and Kawarau Rivers (Draft V).

Otago Regional Council (ORC), 2007a. Young River landslide dam. Report No 2007/584 to the Engineering & Hazards Committee.

Otago Regional Council (ORC), 2007b. Young River landslide dam flood hazard – Initial assessment. Gavin Palmer, Otago Regional Council, November 2007.

Otago Regional Council (ORC), 2007c. Management of the Shotover Delta. Report No. 2007/267 to Engineering & Hazards Committee.

Otago Regional Council (ORC), 2008. Channel morphology and sedimentation in the Lower Clutha River.

Otago Regional Council (ORC), 2012. Long-term residual risk of the Young River landslide dam. Report No 2010/2465.

Otago Regional Council (ORC), 2015. Flood and erosion hazard in the Arrow River at Arrowtown.

Otago Regional Council and Queenstown Lakes District Council (ORC and QLDC), 2006. Learning to live with flooding: A flood risk management strategy for the communities of Lakes Wakatipu and Wanaka.

Park K, 1909. The geology of the Queenstown Subdivision, Western Otago Division. Geological Survey Bulletin No.7.

Parkin DT, Jennings DN and Webby GM, 1993. Tunawaea landslide dam: Part 1 – Hazard management issues. Proceedings of IPENZ Annual Conference 1993, Hamilton.

Parker G. 1D sediment transport morphodynamics with application to rivers and turbidity currents. Ebook available at Gary Parker's morphodynamics web page, University of Illinois. *(hydrolab.illinois.edu/people/parkerg/).*

Pearce AJ and Watson AJ, 1986. Effects of earthquake-induced landslides on sediment budget and transport over a 50-year period. Geology 14: 52-55.

Peng M and Zhang LM, 2012. Breaching parameters of landslide dams. Landslides 9: 13–31.

Perrin ND and Hancox GT, 1992. Landslide-dammed lakes in New Zealand – preliminary studies on their distribution, causes and effects.Proceedings of the 6th International Symposium on Landslides: 1457-1466. AA Balkema, Roterdam.

Piegay H, Grant G, Nakamara F and Trustam N, 2009. Braided river management: from assessment of river behaviour to improved sustainable development. In: Sambrook Smith et al. (eds), Braided Rivers: Process, Deposits, Ecology and Management (Special Publication 36 of the IAS), edited by John Wiley & Sons.

Plaza-Nieto G and Zevallos O, 1994. The La Josefina rockslide. In: The 1993 La Josefina rockslide and Rio Paute landslide dam, Ecuador. Landslide news 8: 4-6.

Porter K, Jones L, Cox D, Goltz J, Hudnut K, Mileti D, Perry S, Ponti D, Reichle M, Rose AZ, Scawthorn CR, Seligson HA, Shoaf KI, Treiman J and Wein A, 2011. The ShakeOut Scenario: A hypothetical Mw7.8 earthquake on the Southern San Andreas Fault. Earthquake Spectra 27(2): 239–261

Poyck S, Hendrikx J, McMillan H, Hreinsson EO, and Woods, 2011. Combined snow and streamflow modelling to estimate impacts of climate change on water resources in the Clutha River, New Zealand. Journal of Hydrology (NZ) 50(2): 293-312.

Price GD and Brooks PK, 1983. Final report on prospecting licence No 311004: The Branches, Upper Shotover River, Central Otago, New Zealand. Mineral Report MR1830, CRA Exploration Co. Ltd.

Purdie H, Bealing P, Tidey E, Gomez C and Harrison J, 2016. Bathymetric evolution of Tasman Glacier terminal lake, New Zealand, as determined by remote surveying techniques. Global and Planetary Change 147: 1-11.

Putnam AE, Schaefer JM, Denton GH, Barrell DJA, Birkel SD, Andersen BG, Kaplan MR, Finkel RC, Schwartz R and Doughty AM, 2013. The Last Glacial Maximum at 44°S documented by a ^{10}Be moraine chronology at Lake Ohau, Southern Alps of New Zealand. Quaternary Science Reviews 62: 114-141.

Pyke V, 1887. History of the early gold discoveries in Otago. Otago Daily Times and Witness Newspapers Company Ltd, Dunedin.

Riley PB, Meredith AS and Lilley, 1993. Tunawaea landslide dam collapse physical and environmental consequences. Proceedings of IPENZ Annual Conference 1993, Hamilton.

Rivers Commission, 1920. Report of the Rivers Commission on the Clutha River.

Robinson TR and Davies TRH, 2013. Review Article: Potential geomorphic consequences of a future great (Mw = 8.0+) Alpine Fault earthquake, South Island, New Zealand. Nat. Hazards Earth Syst. Sci., 13: 2279–2299.

Rother H, Fink D, Shulmeister J, Mifsud C, Evans M and Pugh J, 2014. The early rise and late demise of New Zealand's last glacial maximum. Proceedings of the National Academy of Sciences of the United States of America 111(32): 11630-11635.

Sacchini A, Faccini F, Ferraris F, Firpo M and Angelini S, 2016. Large-scale landslide and deep-seated gravitational slope deformation of the Upper Scrivia Valley (Northern Apennine, Italy). Journal of Maps 12(2): 344-358.

Shulmeister J, 2017. Blowing on the West Wind. The Most Recent Quaternary Glaciation of New Zealand. In: Shulmeister J (ed), Landscape and Quaternary Environmental Change in New Zealand, Atlantis Advances in Quaternary Science 3.

Shulmeister J, Thackray GD, Rieser U, Hyatt OM, Rother H, Smart CC and Evans DJA, 2010. The stratigraphy, timing and climatic implications of glaciolacustrine deposits in the middle Rakaia Valley, South Island, New Zealand. Quaternary science Reviews 29: 2362-2381.

Smith SAF, Tesei T, Scott JM, and Collettini C, 2011. Reactivation of normal faults as high-angle reverse faults due to low frictional strength: Experimental data from the Moonlight Fault Zone, New Zealand. Journal of Structural Geology 105: 34–43.

Stahl T, 2014. Active tectonics and geomorphology of the central South Island, New Zealand: Earthquake hazards of reverse faults. PhD thesis, University of Canterbury, Christchurch.

Stark CP and Hovius N, 2001. The characterisation of landslide size distributions. Geophysical Research Letters 28 (6): 1091-1094.

Stefanelli CT, Segoni S, Casagli N, and Catani F, 2016. Geomorphological analysis for landslide dams. In: Aversa et al. (Eds), Landslides and Engineered Slopes. Experience, Theory and Practice, Associazione Geotecnica Italiana, Rome, Italy.

Stirling M, and 19 others, 2012. National seismic hazard model for New Zealand: 2010 update. Bulletin of the Seismological Society of America 102(4): 1514–1542.

Strong R and Davies TR, 2010. The influence of the Shotover River on Lake Wakatipu flood hazard. Report prepared for Otago Regional Council.

Sutherland DG, Hansler-Ball M, Hilton SJ and Lisle TE, 2002. Evolution of a landslide-induced sediment wave in the Navarro River, California. GSA Bulletin 114(8): 1036-1048.

Swanson FJ, Oyagi N and Tominaga M, 1986. Landslide dams in Japan. In Schuster RL (ed.), Landslide Dams: Processes, Risk, and Mitigation. American Society of Civil Engineers, New York, NY, pp. 131–145.

Sweeney CG, Brideau MA, Augustinus PC and Fink D, 2013. Lochnagar landslide-dam – Central Otago, New Zealand: geomechanics and timing of the event. In: Chin CY, Proc. 19th NZGS Geotechnical Symposium, Queenstown.

Thompson R, 1985. A discussion of some evidence for a prehistoric natural damming of Lake Wakatipu. NZGS EGI report 85/047.

Thompson R, 1996a. Landslide dam scenarios in the upper and lower reaches of the Kawarau and Shotover rivers respectively. Report prepared for the Otago Regional Council.

Thompson R, 1996b. Prehistoric changes in the level of Lake Wakatipu. Report prepared for the Otago Regional Council.

Thompson R, 1998. Shotover alluvial gold: an evaluation of the genesis and chronology of the host sediments. The Australian Institute of Mining and Metallurgy, Mining and Environment, New Zealand Branch, 31st annual conference, Christchurch.

Tonkin and Taylor, 2016. Risk based approach to natural hazards under the RMA. Report prepared for the Ministry for the Environment.

Trimble SW, 2010. Streams, valleys and floodplains in the sediment cascade. In: Burt T and Allison R (eds), Sediment Cascades: An Integrated Approach. John Wiley and Sons.

Turcotte DL, Malamud BD, Guzzetti F, and Reichenbach P, 2005. A general landslide distribution: further examination. In: Hungr et al. (eds), Landslide Risk Management. Taylor and Francis Group, London: 675-680.

Turnbull IM, Thomson R and Read SAL, 1975a. Shotover River catchment sediment sources - Geological report. Appendix E in: Ministry of Works and Development report, 1975. Shotover River Catchment Sediment Sources

Turnbull IM, Barry JM, Carter RM and Norris RJ, 1975b. The Bobs Cove Beds and their relationship to the Moonlight Fault Zone. Journal of the Royal Society of New Zealand, 5:4, p355-394.

Turnbull IM, 2000. Geology of the Wakatipu Area. Institute of Geological and Nuclear Sciences Limited, Lower Hutt, New Zealand.

Upton P, Koons PO, Craw D, Henderson CM and Enlow R, 2009. Along-strike differences in the Southern Alps of New Zealand: Consequences of inherited variation in rheology. Tectonics 28:

Wahl TL, 2004. Uncertainty of predictions of embankment dam beach parameters of hydraulic engineering 130 (5): 389-397.

Wahl TL, 2010. Dambreach modelling – an overview of analysis methods. 2nd Joint Federal Interagency Conference, Las Vegas, NV, June 27 - July 1, 2010.

Walcott RI, 1998. Modes of oblique compression: Late Cenozoic tectonics of the south island of New Zealand. Reviews of Geophysics 36: 1-26.

Walder JS and O'Connor JE, 1997. Methods for predicting peak discharge of floods caused by failure of natural and constructed earthen dams. Water Resources Research 33(10): 2337-2348.

Wang J, Zhangdong J, Hilton RG, Zhang F, Densmore AL, Li G and West J, 2015. Controls on fluvial evacuation of sediment from earthquake-triggered landslides. Geology 43(2): 115-118.

Warren-Smith E, 2016. Lithospheric deformation in the Southern Lakes, New Zealand. PhD thesis, Victoria University of Wellington.

Webby MG and Waugh JR, 2006. Hydraulic behaviour of the outlet of Lake Wakatipu, Central Otago, New Zealand. Journal of Hydrology (New Zealand) 45: 29 – 40.

Weinberger R, Eyal Y, and Mortimer N, 2010. Formation of systematic joints in metamorphic rocks due to release of residual elastic strain energy, Otago Schist, New Zealand. Journal of Structural Geology 32: 288–305.

Wetmore J N and Fread DL, 1984, The NWS simplified dam break flood forecasting model for desk-top and hand-held microcomputers: Federal Emergency Management Agency, 122 pp.

Whitehouse IE, 1983. Distribution of large rock avalanche deposits in the central Southern Alps, New Zealand. New Zealand Journal of Geology and Geophysics, 26 (3): 271-279.

Willetts AJ, 2010. The geology and geomorphology of the Coronet Peak and Arthur's Point landslide complexes. Masters of Science in Engineering Geology thesis, University of Canterbury.

Williams GJ, 1965. In Kear D (ed), Mineral deposits of New Zealand. Monograph 13, Australasian Institute of Mining and Mineralogy.

Williams GJ, 1974. Economic geology of New Zealand. Monograph 4, Australasian Institute of Mining and Mineralogy.

Wishart JS, 2007. Overtopping breaching of rock-avalanche dams. Master of engineering thesis, University of Canterbury, Christchurch.

Wood BL, 1962. Sheet 22, Wakatipu, Geological Map of New Zealand, 1:250,000. Department of Scientific and Industrial Research, Wellington.

Xu Q, Fan X-M, Huang R-Q, and van Westen C, 2009. Landslide dams triggered by the Wenchuan Earthquake, Sichuan Province, south west China. Bull Eng Geol Environ 68: 373–386.

Yetton M and Davies T, 2002. Preliminary landslide dam hazard assessment – Waimakariri River gorge study. Environment Canterbury report.

Yetton M, and McMorran T, 2004. Landslide dam hazard assessment, Waimakariri River Gorge Study – Part 2a. Report prepared for Environment Canterbury by Geotech Consulting Ltd.

Appendix One: Mapping and Survey Data

GIS Analysis

A preliminary geologic and topographic map was completed from GIS-based analysis using the datasets summarised below.

Aerial Imagery

- LINZ images, sourced through the Koordinates data portal (koordinates.com). Photos are downloaded from the dataset named 'Otago 0.75m Rural Aerial Photos (2004-2011)', and have a 75 cm pixel resolution and spatial accuracy varying between +/-2.5 m & +/- 10 m (@ 90% confidence). Photos used in the Shotover Gorge study area are dated to 2006 and 2007.
- Older images (1950s-1980s) were obtained from the retrolens historical imagery resource (retrolens.nz). In many cases these images provide a better view of features in areas now obscured by recent vegetation growth.
- Kevin Jones (Department of Conservation) provided high-resolution aerial images for selected parts of Skippers terraces, Branches Flat, and Moonlight Creek. These were obtained in 2006 as part of an archaeological study, as described in Jones (2008).
- Google Earth was used extensively for viewing alternate imagery and providing 3D visualisation of features. In most locations in the study area a range of images are available dating from ~2004 to the present.

Topographic and Basemap Data

- A digital elevation model, was obtained from the Koordinates data portal (koordinates.com), and used to derive hillshade, slope and aspect rasters, as well as forhydrological analysis such as watershed definition. These DEM files at 15 m resolution were created by the University of Otago School of Surveying, interpolated from LINZ topographic vector data.
- Various LINZ 50k vector datasets were used in compiling basemaps; including contours, rivers and lakes, roads and tracks.

Geomorphic changes to the Shotover River as a consequence of gold mining were assessed based on a variety of data sources, the main records used are outlined below.

Historical Photographs

- Sourced from online photo archives, primarily the National Library of New Zealand (natlib.govt.nz), Historic Wakatipu (historicwakatipu.co.nz), and the Hocken Library (otago.ac.nz/library/hocken).

Historical Newspaper Reports

- Sourced from historical newspaper archives accessible and searchable online at the Papers Past site (paperspast.natlib.govt.nz).

Aerial Imagery

- 1956-1983 imagery was sourced from Retrolens.nz, ORC provided a series of aerial images of the Shotover Delta from 1959-1998. Google Earth imagery covers the period from 2004-present.

Historical Mapping

- Francis Hawden's 1865 'Topographical sketch of the Shotover district' shows the pre-mining form of the lower Shotover River, this map was provided by Peter Petchey, Southern Archaeology Ltd, Dunedin. Other historical maps available from the National Library of New Zealand (natlib.govt.nz) also show the lower

Shotover River, including 'Map of the Shotover Survey District' drawn by WJ Percival in 1887 and revised in 1923, and the 'Geological Map of the Shotover Survey District' in Park (1909).

Reports

- Sediment sources and erosion reports by the Otago Catchment Board (OCB) and Ministry of Works and Development (MWD), also many Shotover Delta investigations by the ORC and consultants, and resource consent documentation relating to the Shotover Country development.

River Gauging and Survey Data

- ORC provided flow and stage height data for the Peats Hut and Bowens Peak gauging stations, and Lidar data covering the lower Shotover River. Shotover Delta cross sections and long-profiles showing bed level changes are included in various reports by ORC and consultants.

Field Mapping and Surveying

The bulk of field mapping was completed during December 2017, with some details checked and modified during the course of later field work in February and May 2018. Mapping was completed on a series of seven 1:20k scale basemaps and mapped features include

1. **Quaternary geology:** alluvial terrace and fan gravels, lacustrine silt-sands, and glacial sediments.
2. **Geomorphic features:** bedrock and alluvial terrace edges, landslide scarps and deposits, and areas of slope deformation.
3. **Historic modifications:** hydraulic sluicing excavations.

This map (and all others in this thesis) are in the NZTM coordinate system and oriented north. The final map is presented as an A2 sized (55k scale) digital file in PDF format (*Shotover Gorge surficial geology map, Tim van Woerden 2018*). Mapping data is included digitally as the files listed below, these are all in ESRI shapefile format, and the NZTM coordinate system.

Surveying was carried out using handheld Trimble GPS (models GeoXH and Geo7x) during field work in December 2017, with some additional locations surveyed during later field work in February and May 2018. Surveyed features included terrace and fan surfaces, river elevations, and spot heights at geological features and to locate stratigraphic sections. Survey points from these three field campaigns have been combined into a single digital file (CSV format text file), with all coordinates in NZTM coordinate system.

Digital Files

Mapping PDF file

1. Shotover Gorge surficial geology map

Mapping shapefiles

1. Study area polygons (e.g. Figure 1.1).
2. Geology mapping polygons.
3. Geomorphic features - line features such as terrace edges and landslide scarps.
4. Ground deformation due to creeping schist landslides (e.g. Figure 2.29).
5. Landslide scarps used in landslide magnitude frequency plot (Figure 6.11).
6. Sluicing extents (e.g. Figure 4.2)

Surveys

1. All survey locations (e.g. Figure 2.4)

Appendix Two: Optical Dating

Introduction

Optical dating methods such as infrared stimulated luminescence (IRSL) or optically stimulated luminescence (OSL) have successfully been used for the dating of glacial, paraglacial and lacustrine sediments in South Island locations (e.g. Shulmeister et al. 2010, Rother et al. 2010, Hyatt et al. 2012, Evans 2015). Although potential issues have been noted with the use of optical dating methods for glacial environments including incomplete zeroing, weathering, and potentially short proglacial transport paths (Almond et al. 2001, Shulmeister et al. 2010, Rother 2006).

The analysis relies on the sampled sediments having been exposed to light during transport prior to burial, and resetting or 'zeroing' the excess energy stored in the crystal lattice of quartz or feldspar grains. To ensure suitable sample material, sampled sites are selected to improve likelihood of light exposure and zeroing prior to burial. Sample material ideally is that indicating aqueous sediment transport paths and relatively energetic deposition, such as well-sorted, horizontally bedded sand lenses (Evans 2015).

Sample Collection

Samples were taken using standard collection procedures as summarised below.

1. Excavate into outcrop at least 200 mm to expose a fresh face.
2. Prepare stainless steel sample tube by tightly packing end with crushed newspaper to ensure a light-proof seal and eliminate the chance of light contamination.
3. Force sample tube into sediments until flush with surface, cover exposed end with black plastic and securely tape on.
4. Carefully excavate sample tube to avoid sediment mixing, covering other end with black plastic to prevent any light exposure, securely tape and label with sample code.
5. Wrap sample in plastic bag to retain moisture content.
6. Take ~1 kg bulk sample from approximately 1 m^2 of sediments around sampled location.
7. Note sample depth below top of outcrop, lithology of sample, and interpret environment of formation.

Sample Details

Location	**Branches Flat**	**Sandhills Creek**	
Field Code	BF1	SH2	SH3
Lab Code	WLL1323	WLL1324	WLL1325
Easting, Northing (NZTM)	1262544, 5034197	1262040, 5028033	1262060, 5028032
Longitude, Latitude	168° 44' 08.69" E, 44° 45' 57.41" S	168° 43' 31.10" E, 44° 49' 15.769" S	168° 53' 32.01" E, 44° 49' 15.83" S
Altitude (m)	535.4	493.7	500.8
Depth below the surface	90 cm	5.1 metres	80 cm

Branches Flat (Samples BF1)

These samples were taken the lower part of Branches Flat, from within the large outcrop of deltaic sediments to the north of Ironstone Creek (Figure 1). Two samples were taken (BF1, BF2) and were treated as a single sample during analysis.

Sample BF1 comprises coarse-medium sands (Figure 2), and is interpreted as fine grained deltaic sediments. The sample location is about 15 m west from the western stratigraphic section (Figure 2.17), and the sampled unit correlates with that logged at ~9 m on the section.

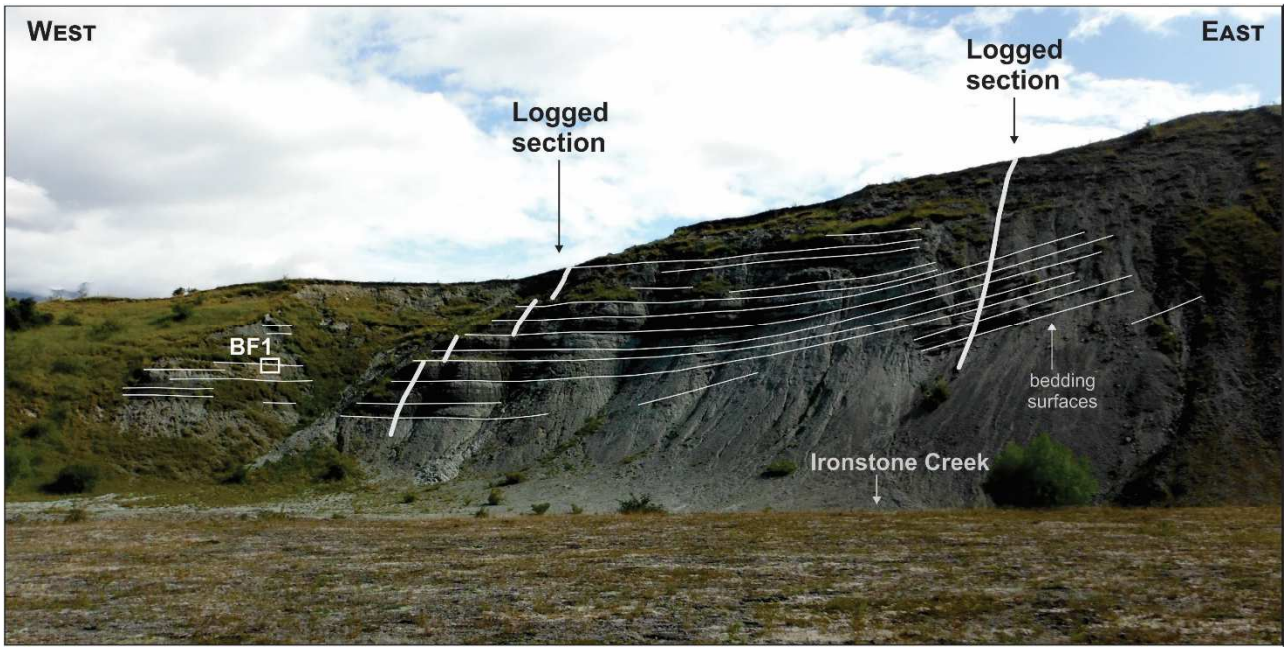

Figure 1: *The Ironstone Creek delta outcrop, showing location of OSL sample BF1.*

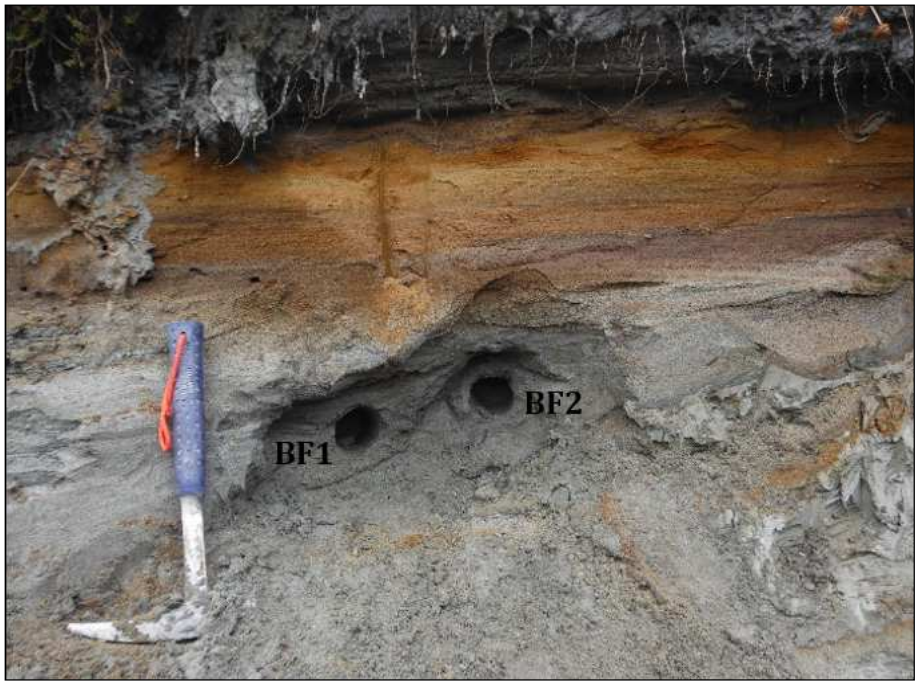

Figure 2: *Detail of the sample location for Ironstone Creek OSL samples, the location of this image is shown in Figure 1 above.*

Sandhill Creek (Samples SH2, SH3)

These samples were taken from the large outcrop on the northern bank of Sandhill Creek (Figure 3). Deposits are interpreted as synglacial in origin, formed in a proglacial meltwater fluvial environment.

Sample SH2 is of bedded coarse sand (Figure 4), from within a sand unit of ~10 m in thickness. This sample is at ~7 m on the Sandhill Creek stratigraphic section (Figure 2.25, Chapter 2).

Sample SH3 is of well-bedded coarse-medium sands (Figure 5), sampled at approximately 45cm from base of a thick (~5 m) sand unit. This sample is at ~26 m on the Sandhill Creek stratigraphic section (Figure 2.25, Chapter 2).

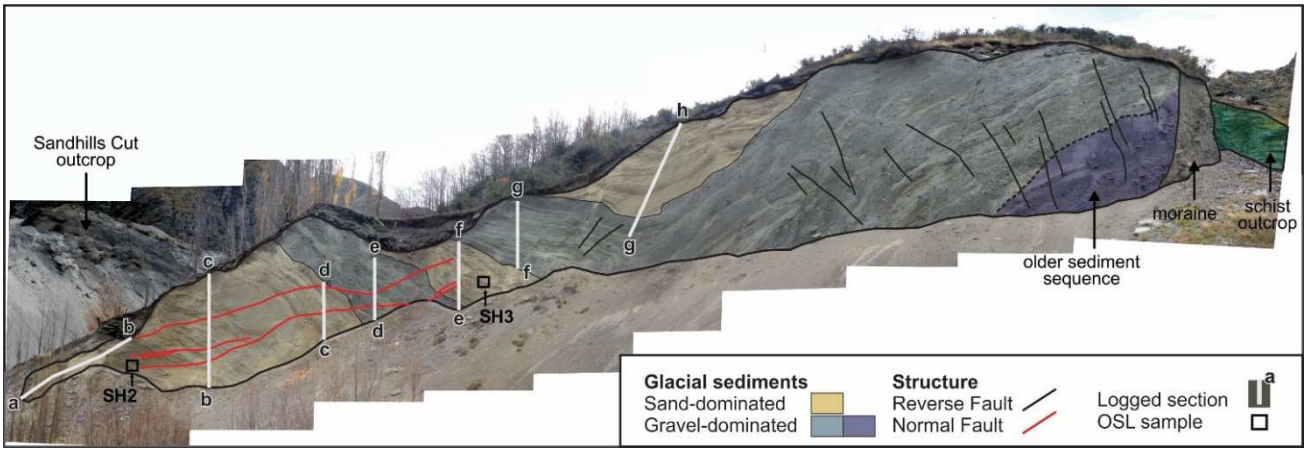

Figure 3: *The Sandhill Creek outcrop, showing location of OSL samples SH2 and SH3.*

Figure 4: *Outcrop location (left), and detail of sampled unit for OSL sample SH2 at Sandhill Creek.*

Figure 5: *Outcrop location (left), and detail of sampled unit for OSL sample SH3 at Sandhill Creek.*

Analysis Details

Samples were analysed at the Luminescence Dating Laboratory, Victoria University of Wellington, by Ms Ningsheng Wang. Samples were prepared using a coarse grain quartz technique, UV luminescence was measured during blue stimulation, and luminescence ages were determined by the Single Aliquot Regenerative Dose method (SAR).

The appended VUW report (Report No. 15/18, September 2018) gives the full technical details of sample preparation, measurements and results.

Report No. 15/18

Luminescence Dating Technical Report

Luminescence Dating Laboratory
School of Geography, Environment and Earth Sciences
Victoria University of Wellington
Wellington
New Zealand

Reported by: Ms. Ningsheng Wang
Date of Issue: 10-09-2018
Contact: Room 414
Cotton Building
Victoria University of Wellington
Ph: (04) 463 6127

CONTENTS

1. SUMMARY

Three samples (Field code: BF1,SH2 and SH3 were submitted for luminescence dating by Tim van Woerden and Tim Stahl , University of Canterbury. The laboratory codes of the samples are WLL1323-WLL1325 respectively.

Due to coarse material, coarse grain (125-200µm) quartz preparation technique was used. The UV luminescence from coarse grain quartz was measured during blue stimulation. The luminescence ages were determined by Single Aliquot Regenerative Dose Method (SAR). The dose rate was determined on the basis of gamma spectrometry measurements.

2. SAMPLE PREPARATION

The sample preparation consisted of two parts:

(i) Preparation for measurement of equivalent dose (equivalent to the paleodose)

(ii) Preparation for measurement of dose rate

Part 1: The Preparation for Measurement of Equivalent Dose (D_e)

1. Chemical Treatment

Samples had their outer surfaces removed. Of this removed outer scrapings, 100g was weighed and dried in an oven in preparation for gamma spectrometer analysis.
A plastic cube was then filled with remaining scrapings in preparation for water content measuring.

"Fresh" sample material, that had outer surfaces removed earlier (unexposed light sample material), was treated in 10% HCl. This was carried out overnight until all carbonate was removed by the reaction. Following this treatment the sample was further reacted overnight with 10% H_2O_2 in order to remove organic matter.

The next step involved 200ml CBD* solution being added to the sample for 12 hours to remove iron oxide coatings. Note, after every chemical treatment procedure distilled water was used to wash the sample several times.

*CBD solution: 71g sodium citrate, 8.5 g sodium bicarbonate, and 2g sodium dithionate per litre of distilled water

2. Coarse Grain Quartz Separation Technique (125-200µm)

After chemical treatment, sample material was dry in an oven. The dry material was sieved to obtain 125-200µm grain size. The next step was extracted coarse grain quartz (125-200µm) by density separation 2.62g/mLLithium heteropolytungstates to separate feldspar from quartz and heavy minerals, then 2.75g/mL Lithium heteropolytungstates to separate quartz from heavy minerals.

The quartz had 10µm of its surface removed by etching it for 45minutes using 48%HF. Following this, 10% HCl for 30 minutes was used to remove fluoride salts. Note, after each chemical treatment, the coarse grain sample was washed carefully with distilled water.

The quartz was dried and then sieved again, discarding grains less than 125µm. Finally it was coated onto a stainless steel disk (1cm diameter) with silicon oil and ready for measurement.

Part 2: The Preparation of Measurement of Dose Rate

The dry, ground and homogenised sample material were weighed and sealed in air tight perspex containers and stored for at least four weeks. This storage time minimizes the loss of the short lived noble gas ^{222} Rn and allows ^{226}Ra to reach equilibrium with its daughters ^{214} Pb and ^{214} Bi.

3. MEASUREMENTS

Luminescence age was determined by two factors: the equivalent dose (D_e) and the dose rate.

Equivalent dose: obtained from the lab equivalents to the paleodose absorbed by samples during the burial time in the natural environment since their last exposure to the light.
Dose rate: amount dose received by the sample each year.

Part 1: Determination of Equivalent Dose (D_e)

D_e was obtained by using SAR.

Single Aliquot Regenerative Method (SAR)

The Single Aliquot Regenerative Method (SAR) was used to determine the equivalent doses. This technique is described by Murray and Wintle (2000).

For the SAR method, a number of aliquots (disks) were subjected to a repetitive cycle of irradiation, preheating and measurement. Firstly, natural shining down curves was measured after preheating. Then shining down curves were measured for the next four or five cycles for different beta doses. Then from the variety of shining down curves, a luminescence growth curve (β induced luminescence versus added dose) was established. This was used to determine the equivalent dose (equivalent to the palaeodose). The measurement for the aliquots resulted in a variety of equivalent doses, spread over the arithmetic mean of the data.

In order to correct potential sensitivity changes from cycle to cycle, the luminescence response to a test dose was measured after preheat between cycles.

The UV luminescence of 24 aliquots of each sample were measured at 125 ^{o}C for 40s using a Riso TL-DA-20 reader with blue diodes that have maximum emission at 470nm used to deliver a stimulated beam. UV luminescence from quartz was then detected by an EMI 9235QA photomultiplier fixed behind one Hoya U-340 filter with 7mm thick. Beta irradiation were done on the Riso TL-DA-20 ^{90}Sr/Y β irradiator, calibrated against Risø National Laboratory, Demark with about 3% uncertainty. Preheat and cut heat temperature was 250 ^{o}C for 10 seconds.

Luminescence growth curve (β induced luminescence intensity versus added dose) was constructed by using the initial 10 channels (1.6 seconds) of the shine down curves and subtracting the average of the last 100 channels which was thought to be a mixture of background and hardly bleachable components. Interpolation of this growth curve to the dose axis was yielded the equivalent dose D_e which was used as a paleodose. The measurements of 24 aliquots obtained 24 D_e's, the D_e's were accepted within 10% recycling ratio 10% recapture. D_e used for the age determination was used the central age model due to data scatter. A dose recovery test and a zero dose were checked no anomalies.

Part 2: Determination of Dose Rate

Dose rate consisted of two parts.
(i) Dose rate from sample's burial environment
(ii) Dose rate from cosmic rays.

(i) ***Dose rate from burial environment***

Dose rate from sample's burial environment was determined by radionuclide contents of ^{238}U, ^{232}Th and ^{40}K, and water content.

Determination of Contents of U, Th and K by Gamma spectrometry

Gamma rays produced from sample material was counted for a minimum time of 24 hours by a high resolution and broad energy gamma spectrometer. The spectra were then analysed using GENIE2000 software. The contents of U, Th and K were obtained by comparison with standard samples. The dose rate calculation was based on the activity concentration of the nuclides ^{40} K, ^{208}TL, ^{212}Pb, ^{228} Ac, ^{214} Bi, ^{214}Pb, ^{226} Ra, using dose rate conversion factors published by Guérin, G., Mercier, N., Adamiec, G. (2011).

Measurement of Water Contents

Water content was measured as weight of water divided by dry weight of the sample taking into account a 25% uncertainty.

(ii) ***Dose rate from cosmic rays***

Dose rate from cosmic rays were determined by the depth of sample below the surface along with its longitude, latitude and altitude, convention formula and factors published by Prescott, J.R. & Hutton, J.T. (1994).

4. RESULTS

Table 1 Cosmic Dose Rates

Table 2 Water Contents, Radionuclide Contents

Table 3 Equivalent Doses, Dose Rates and Luminescence Ages

Table 1: Cosmic Dose Rates

Laboratory Code	Depth Below the Surface(m)	Cosmic Dose Rate (Gy/ka)	Field Code
WLL1323	0.9	0.2029±0.0101	BF1
WLL1324	5.1	0.1171±0.0059	SH2
WLL1325	0.8	0.2043±0.0102	SH3

Table 2: Water Contents, Radionuclide Contents

Laboratory Code	Water Content (%)	U(ppm) from ^{234}Th	U(ppm) from ^{226}Ra, ^{214}Pb, ^{214} Bi	U(ppm) from ^{210}Pb	Th(ppm) From ^{208}Tl ^{212} Pb ^{228} Ac	K(%)	Field Code
WLL1323	13.9	2.01±0.27	1.50±0.13	1.42±0.20	5.78±0.08	0.97±0.02	BF1
WLL1324	8.9	1.58±0.25	1.57±0.13	1.26±0.19	6.05±0.08	0.88±0.02	SH2
WLL1325	12.5	1.11±0.21	1.22±0.11	1.39±0.18	5.13±0.07	1.06±0.02	SH3

Table 3: Equivalent Doses, Dose Rates and Luminescence Ages

Laboratory Code	D_e(Gy)	Dose Rate(Gy/ka)	**Luminescence Age(ka)**	Field Code
WLL1323	42.43±7.88	1.72±0.06	**24.7±4.7**	BF1
WLL1324	44.20±5.67	1.66±0.05	**26.6±3.4**	SH2
WLL1325	56.91±7.70	1.72±0.06	**33.1±4.6**	SH3

5. REFERENCES

Guérin, G., Mercier, N., Adamiec, G. 2011: Dose- rate conversion factors: update. Ancient TL, Vol.29, No.1, 5-8.

Murray, A.S. & Wintle, A.G. 2000: Luminescence dating of quartz using an improved single aliquot regenerative dose protocol. Radiation Measurements 32, 57-73.

Prescott, J.R. & Hutton, J.T. 1994: Cosmic ray contributions to dose rates for luminescence and ESR dating: Large depths and long-term time variations. Radiation Measurements. Vol.23,Nos.2/3, 497-500.

Appendix Three: Shotover Catchment Landslide Dams

This appendix presents a summary of known landslide dams in the Shotover catchment, the locations of these are shown in Figure 1 and Table 1, and each is then briefly described in the following section. This dataset includes twelve landslide dams which have been documented in various sources, but have not previously been compiled in a single document. In addition, a search of aerial imagery has noted a number of previously undocumented landslide dams, identified based on typical landslide dam morphology as summarised by Korup (2004, 2006) and Hermanns et al. (2011a). These are recognised by hummocky or blocky landslide deposits covering the valley floor, or slope deformation with bulging or lobate toe slopes. Channel interaction is shown most clearly by development of a knickpoint in the valley long profile. This is typically seen as a steep-gradient, bouldery rapid formed where the stream channel has incised through landslide debris, and shallow gradient alluvial flats upstream.

Those landslide dams noted here are only the larger or more well-defined dam-forming landslides, most of which are estimated to have volumes of >1M m^3, With a total of ~20 landslide dams noted, this compilation significantly expands the number of large landslide dams known in the Shotover catchment, and demonstrates landslide dam formation is a frequent phenomenon in the Shotover catchment. Several other possible landslide dams have been reported but their locations are uncertain, for example, Willett's (1939) geology report describes the Flood Burn catchments, where streams are described as flowing in *"deep, rugged schist gorges, the entrances to some of which are blocked by large post-glacial slips, over which the streams discharge in rough cascades".*

Two distinctive landslide types were noted in Korup's (2006) study of Southern Alps landslide dams;

1. Rock-slope failures, often catastrophic, with clearly detached deposits.
2. Deep seated, low displacement, sackung-type failures causing river occlusion or diversion.

This distinction is also present in the Shotover catchment, with examples of both rapid failures (e.g. 1, 2, 3, 5, 8,) and low-displacement sackung-type failures (e.g. 4, 14, 18) present. Most of these land slide dams show a characteristic geomorphic landslide dam expression with steep gradient, channel incised through landslide debris, and wider, shallow gradient alluvial flats upstream. The alluvial flats upstream of the Polnoon Burn landslide dam have been described as an infilled lake deposit with lacustrine silts and peat bog deposits. Similar deposits may also be present showing lake formation upstream of some of these other dams, however are not known. The presence of a long-profile channel knickpoints indicate that none of these dams have recovered to their former fluvial grade, even though all are assumed to be at least several thousands of years in age. A variety of landslide dam morphologies are seen, including;

- Intact landslide-dammed lake: Lochnagar (1), possibly also Lake Luna (19).
- Landslide dam with ponding on landslide debris: Polnoon Burn West Branch (3), also Lochnagar (1).
- Breached landslide or rock avalanche dam with deeply incised breach channel: Polnoon Burn (2), Saddle Creek (8), Blue Creek (5), Stony Creek (9).
- Infilled landslide-dammed lake with preserved lake deposits: Polnoon Burn (2).
- Landslide dam at/near drainage divide (Type Vb of Hermanns 2011b): Lake Luna (19).
- Channel blockage by debris flows: Shiel Burn (20).

The ages of only two landslide dams are known; Polnoon Burn and Lochnagar. The upper Shotover River and tributaries (e.g. Polnoon Burn, Blue Creek, Shiel Burn) were interpreted to have been glaciated during an LGM ice advances to the upper Shotover Gorge, so any landslide dams in these areas are assumed to be postglacial in age. Small 'ice streams' from the LGM Wakatipu Glacier are also inferred to have intruded into the Moke Lake and Lake Luna areas (Bell 1992) so landslide dams in these areas may also be postglacial in age. Lower elevation parts of the catchment (e.g. Skippers Creek, Stony Creek) may have not been glaciated during the LGM, and landslide dams in

these locations may be older. Based only on the relatively recent appearance of the landslide scarp and deposit, the Stockyard Creek landslide dam is interpreted as being the most recent of those dams noted here.

Where no previous landslide volume values exist, an estimate has been made of landslide volume using an empirical area-volume relationship (Hovius et al. 1997). This relationship was developed based on a dataset of rainfall-triggered West Coast landslides, and may not be the most appropriate for the landslides noted here, but provides an order-of-magnitude approximation of the landslide volume. Aerial photograph interpretations primarily made use of Google Earth imagery, however interpretations are limited by image resolution, and in some locations are obscured by vegetation, clouds or shadows. Figures 1-20 below show these landslide dams, annotated to show their interpreted landslide scarps (dashed black lines), and interpreted limits of the landslide deposit (dashed red lines). Landslide dam height is difficult to accurately estimate from the resolution of available topographic data, and has not been included. Further work based on these landslide dams could include estimation of geomorphic parameters such as landslide dam height, width, length etc. as in Korup (2004), Hermanns et al. (2011a), and Stefanelli et al. (2018).

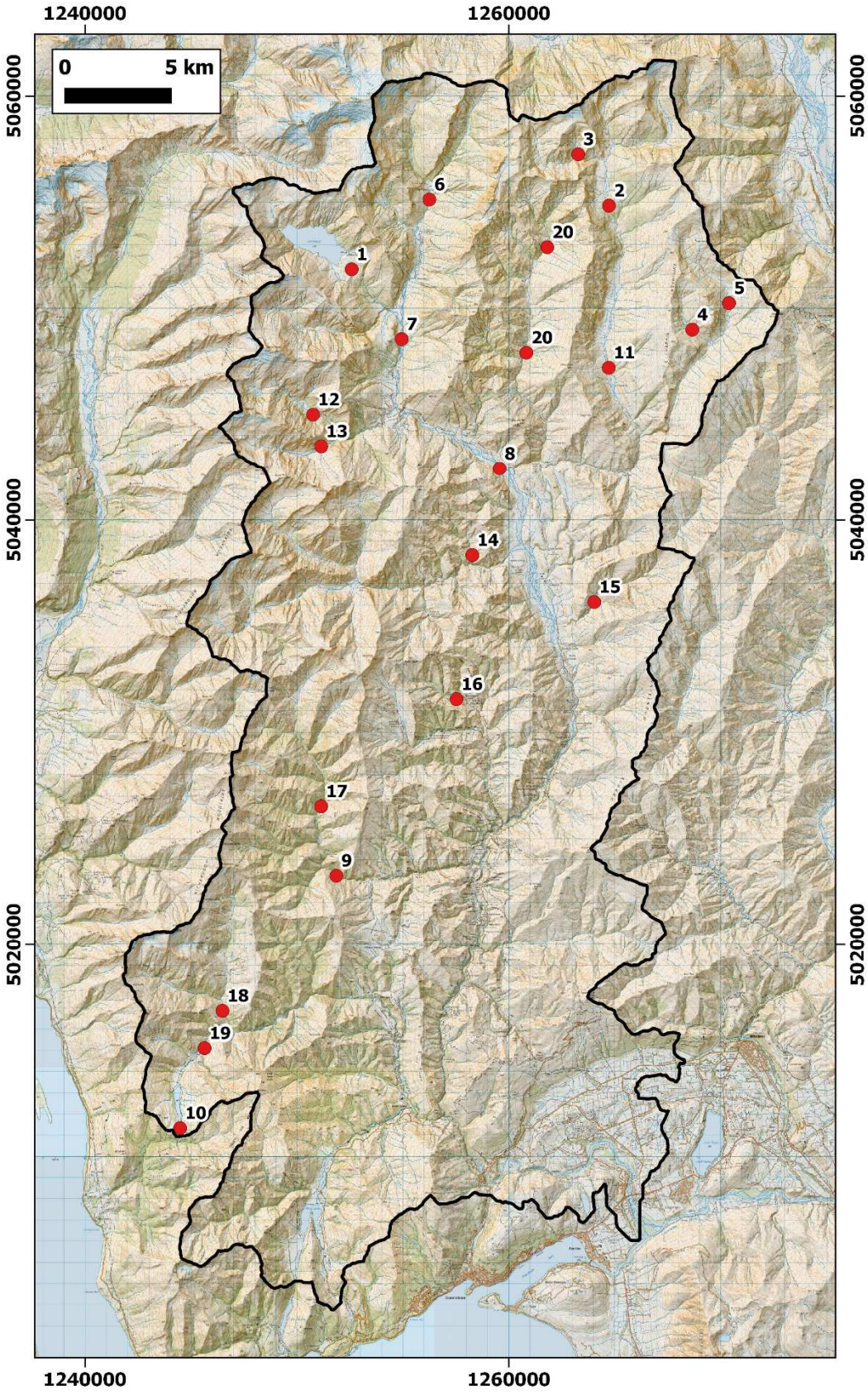

Figure A: *Shotover catchment landslide dams, numbers reference Table 1.*

Table 1: Summary of dam-forming landslides in the Shotover catchment.

#	Location	Latitude	Longitude	Easting (NZTM)	Northing (NZTM)	Elevation (m)	Reference	Landslide Width (m)	Landslide Area (m^2)	Landslide Volume ($M\ m^3$)
1	Lochnagar (Lake Creek)	-44.6005	168.6353	1,252,581	5,051,845	1100	Sweeney et al 2013, Korup 2006, Hancox & Perrin 2008, McSaveney 1978, Brown 1956, MWD 1975	1050	2,500,000	690*
2	Polnoon Burn	-44.5806	168.7802	1,264,724	5,054,846	960	Korup 2006, McSaveney 1978, MWD 1975, Brown 1956	1100	700,000	140*
3	Polnoon Burn West Branch	-44.5603	168.7374	1,263,271	5,057,265	1395	Bryant and Goldsmith 2013	280	60,000	0.7
4	Blue creek tributary	-44.6358	168.8221	1,268,653	5,049,001	1360	Korup 2006	450	300,000	8*
5	Blue Creek headwaters	-44.6250	168.8458	1,270,388	5,050,255	1320	Korup 2006	450	350,000	10
6	Shotover at Forks	-44.5747	168.6695	1,256,246	5,055,133	770	Brown 1956, MWD 1975, McSaveney 1978	700	700,000	29
7	Shotover at 17 Mile	-44.6298	168.6499	1,254,943	5,048,555	610	McSaveney 1978	450	100,000	1.6
8	Shotover at Saddle Creek	-44.6896	168.7047	1,259,564	5,042,439	560	Brown 1956, MWD 1975, McSaveney 1978	350	110,000	1.8
9	Stony Creek	-44.8585	168.5937	1,251,857	5,023,269	640	OCB 1966	300	180,000	3.8
10	Lake Luna	-44.9619	168.4934	1,244,483	5,011,337	820	McSaveney 1978	280	100,000	1.6
11	Lower Polnoon Burn	-44.6658	168.7768	1,264,714	5,047,207	800		500	440,000	15
12	Sixteen Mile Creek	-44.6631	168.595	1,250,761	5,044,998	960	Willett 1939	600	700,000	10-20
13	Robertson Creek	-44.6774	168.5974	1,251,149	5,043,492	1100	Willett 1939	800	>1,000,000	>50?
14	Campbells Creek	-44.7265	168.6848	1,258,276	5,038,348	700		260	250,000	6.3
15	Stockyard Creek	-44.7489	168.7561	1,264,031	5,036,141	700		250	80,000	1.1
16	Skippers Creek North (Caspers Flat)	-44.7872	168.6712	1,257,527	5,031,568	740		400	180,000	3.8
17	Upper Stony Creek	-44.8296	168.5869	1,251,143	5,026,529	760		400	400,000	13
18	Upper Moonlight Creek	-44.9136	168.5213	1,246,484	5,016,867	700		280	240,000	5.9
19	Luna Creek	-44.9289	168.5095	1,245,636	5,015,106	700-750		150-350	60,000 to >200,000	1-6
20	Shiel Burn	-44.5982	168.7231	1,261,811	5,052,887	900		-	-	-
		-44.6421	168.7231	1,260,829	5,047,916	800		-	-	-

* Landslide volumes from Korup (2006)

1. Lochnagar

This extremely large landslide has an area of 2.5 km^2 and a volume of approximately 690M m^3, forming a dam in Lake Creek, a western tributary of the Shotover River (Hancox and Perrin 2009). The landslide dam has a height of about 340 m (may be up to 400 m), and extends both across and along the valley for about 2 km. The impounded lake has an area of about 3.5 km^2, and an estimated volume of about 10^8 m^3. This dam is intact and the lake is at a stable level below the dam crest, with subterranean drainage taking place through the dam material.

Sweeney et al. (2015) investigated the timing and geomechanics of the landslide event, interpreting it to have failed in two separate events, one a wedge failure controlled by a foliation plane and a fault/crush zone, the other failing under gravity with no sign of any controlling structural feature.

Seven schist boulders in the slide mass were dated by ^{10}Be exposure dating, with ages ranging from 6300 ± 300 to 8900 ± 300 years (Sweeney et al. 2013). Hancox and Perrin (2009) infer that the slide may have been triggered by an Alpine Fault earthquake, while Sweeney et al. (2013) attribute failure to a consequence of glacial undercutting and post-LGM retreat of supporting ice.

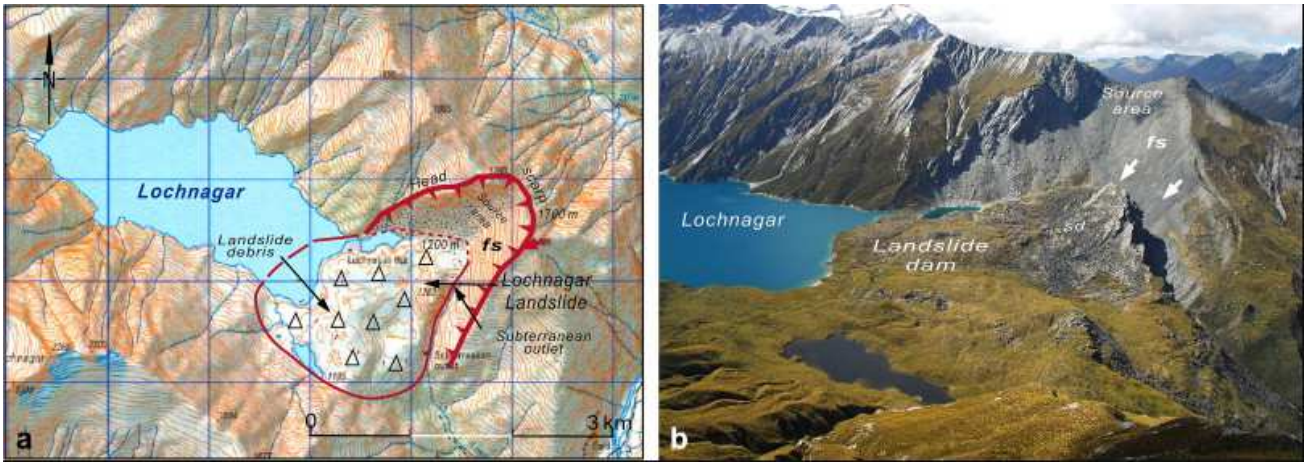

Figure 1: *Lochnagar landslide dam, showing A. landslide scarp and deposit on topomap, and B. photo of landslide source area and dam. Image: Hancox and Perrin (2009).*

2. Polnoon Burn

This large landslide has a scarp >1000 m in width, and volume estimated at 140M m^3 (Korup 2006). This landslide dam extends for >1000 m along the valley, and has a height estimated at 120 m (max height 140 m) (Korup 2006). The creek has incised a deep gorge into the dam material, although Korup shows there is still a prominent knickpoint of ~100 m height in the channel long-profile. Korup et al. (2006) notes outburst debris immediately downstream of the dam.

The dam was thought to have remained intact for ~2000 years before failure, with a lake extending for ~3 km upvalley from dam, shown by strandlines, shoreline terraces and lake deposits (Korup 2006). Korup et al. (2006) estimates 45M m^3 of sediment to have infilled behind dam over ~2000 years, of which 40M m^3 has now eroded. The upstream infill deposits have been noted in several reports. Brown (1956) note 40 foot (12 m) gravel terraces upstream of the dam location, with a cap of peaty material. MWD (1975) describes banks upstream of the dam as comprising varved silts. Massey et al. (2013) also notes that the lake was largely infilled with sediment and became a sphagnum bog persisting for several thousand years.

The landslide has been dated to 5301 ± 78 years BP (3273-3429 BCE). The material dated was peat and twigs in lake sediments from the time of lake formation. (Hancox and Salt 1990, in Hancox et al. 2013).

Figure 2: *Polnoon Burn landslide dam. Showing landslide deposit extending for >1 km along valley, and incised gorge through deposit.*

3. Polnoon Burn West Branch

This dam has been referenced only in Bryant and Goldsmith (2013). The landslide is about 300 m in width, there appears to be recent rockfall activity with minor, relatively fresh debris seen at the at base of the slope. There is another similar sized landslide immediately downstream, and a smaller slide located ~200 m upstream. These may have also caused channel blockages. A 100 m width scarp from the opposite (eastern) slope may have also contributed to dam material. The creek has partially incised through the dam forming a well-defined terrace on east side of creek, and there is a pond of ~40 m in length formed on dam remnants to east of creek. Immediately upstream from dam is a broad section of braided riverbed (600 m length x 100 m width) showing an infilling of the upstream basin.

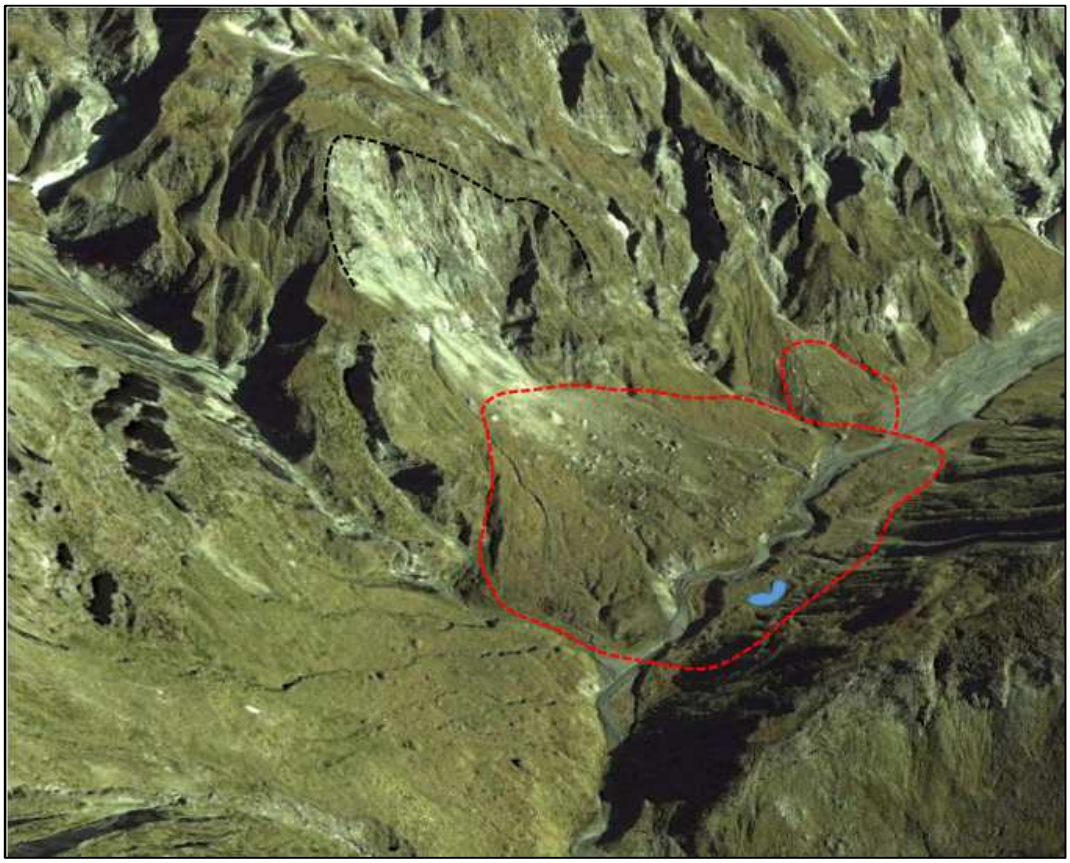

Figure 3: *Upper Polnoon Burn landslide dam, showing incised channel through landslide deposit and small pond developed. A more recent rockfall has deposited minor debris at base of slope.*

4. Blue Creek (1845) eastern tributary, and 5. Blue Creek (1970)

There are two landslide dams in the upper parts of Blue Creek, the main eastern tributary of Polnoon Burn. Located in the Harris Mountains, these dams are referred to as 'Harris (1870)' and 'Harris (1845)' by Korup (2006).

The eastern landslide (from about point '1970') forms a dam in the headwaters of Blue Creek. This landslide appears deeper seated and larger volume, potentially up to ~10M m^3. The dam has a height of many tens of metres, and extends for >900 m along the valley. The valley is relatively wide at this point and the dam may have had a cross-valley width of >500 m. The stream has incised a deep channel ~700 m in length through the dam material. For about 1500 m upstream the creek is strongly meandering and sediment infilled.

The western landslide (from about point '1845') forms a dam in the main western tributary of Blue Creek, with a volume estimated at 8M m^3 (Korup 2006). The dam height has been estimated at 30 m (Korup 2006). Has formed a sediment infilled basin for ~700 m upstream.

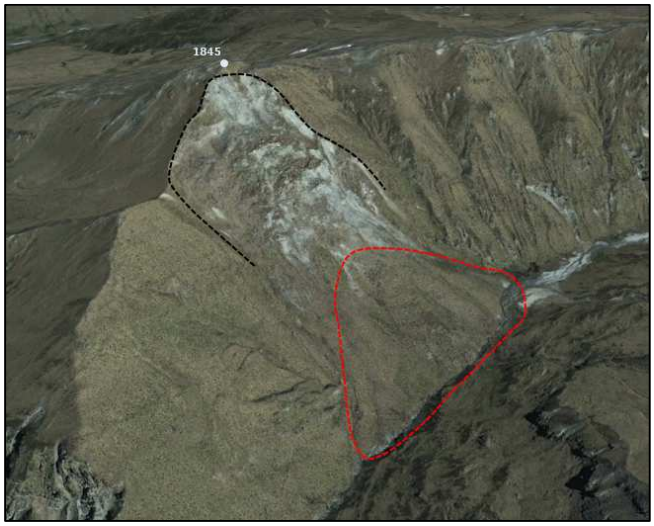

Figure 4 (left): *Blue Creek (1970), showing large landslide dam deposit and incised gorge.*

Figure 5 (right): *Blue Creek (1845) showing large landslide constricting valley, and alluvial flats developed upstream.*

6. Shotover River at the Forks

A large landslide with a width of about 800 m and a volume estimated to be 20-30M m^3. This landslide and the gorge cutting across landslide deposits was noted by both Brown (1956) and MWD (1975) reports. This large dam has an along-valley length of >1000 m. Upstream of the dam, Junction Flat represents a small sediment-infilled lake (MWD 1975). Steep rapids fall through the landslide dam section of creek, with an estimated elevation drop of 60-70 m.

Figure 6. *Shotover River landslide dam at the Forks.*

7. Shotover River at 17 Mile Creek

Located on the Shotover River between 17 Mile Creek and Lake Creeks. Noted in McSaveney (1978, Fig5) where it is shown as two landslides sourced from western slopes. A large landslide scarp about 400 m in width, with a smaller, poorly defined scarp to the north. The main landslide may have a volume of up to about 1.5M m^3. The remains of any landslide dam formed in this location are not obvious. They may have been largely eroded, or obscured by Shotover River alluvial deposits and the large alluvial fan originating from the creek on the opposite (eastern) side of valley.

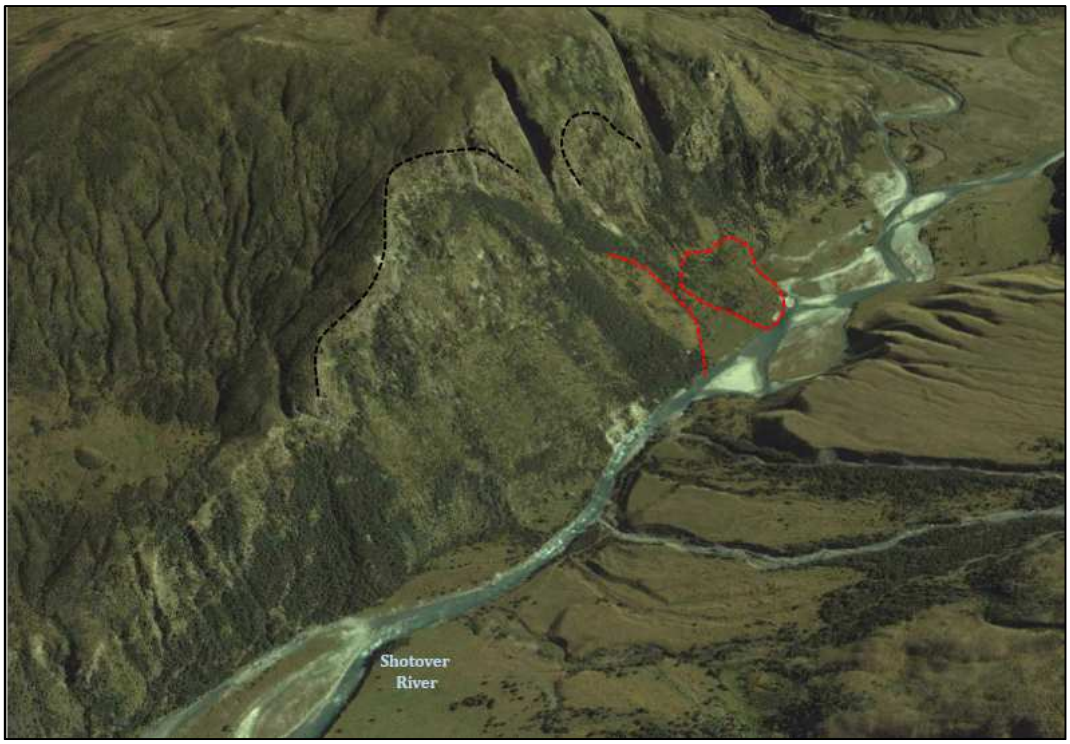

Figure 7: *Possible Shotover River landslide dam between 17 Mile and Lake Creeks. Landslide scarps can be seen but deposits are unclear.*

8. Shotover River at Saddle Creek

This landslide is sourced from a scarp to the west of the Shotover River, shortly upstream from the Shiel Burn confluence. Debris has runout for a distance of about 400 m length from the base of the scarp. The river has incised deeply into landslide debris, forming a narrow gorge about 400 m in length. The river forms rapids through this section, with a surveyed elevation change of about 10 m (McSaveney 1978, Figure 7). There are a number of large alluvial terraces in this area. The landslide deposit may post-date and be emplaced onto alluvial terraces, or these terrace gravels may be younger, and have aggraded around and partially covered this landslide deposit.

Figure 8: *Shotover River landslide dam at Saddle Creek, showing landslide deposit and incised river channel.*

9. Stony Creek

This is interpreted to be the landslide referred to by the OCB (1966) - *"the lower reaches of this creek are deeply entrenched in a gorge which, because of a large debris avalanche in its upper portion, does not provide convenient access to the upper valley."* Although mostly obscured by vegetation, it appears the creek has incised a deep gorge through the landslide debris. The lower portion of the slope shows a hummocky texture with many large boulders up to ~10 m visible.

Figure 9: *Stony Creek landslide dam.*

10. Lake Luna

Interpreted by McSaveney (1978) as a small rock avalanche, blocking the south end of Lake Luna. This landslide may have led to the capture of ~8 km^2 of 25 Mile Creek, which now drains into Luna Creek and the Moonlight catchment (McSaveney 1978).

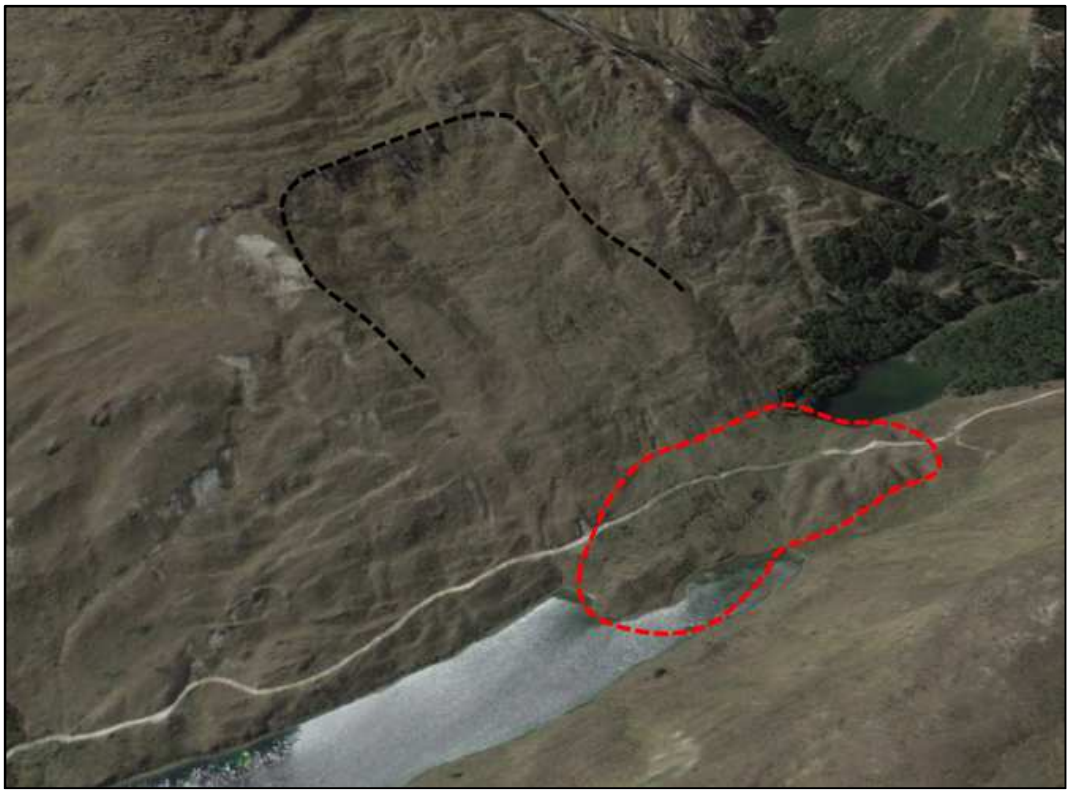

Figure 10: *The interpreted Lake Luna rock avalanche at the southern end of Lake Luna. To the right of the landslide deposit is another small lake – Dukes Tarn.*

11. Lower Polnoon Burn

There are several large landslides in the Polnoon valley downstream of the main Polnoon Burn landslide dam. The slide with the most distinct interaction with the channel is shown below. The riverbed is strongly aggraded for several km upstream from landslide, suggesting a significant blockage. Creek has incised a channel through debris at toe of slide. Common channel margin terraces may show remains of a higher aggradation surface, now incised. A larger landslide shortly upstream appears to have reached the valley floor but not formed a landslide dam.

Figure 11: *Possible landslide dam in the lower Poloon Burn.*

12. Sixteen Mile Creek

Located in the right-hand breach of Sixteen Mile Creek, this landslide was noted by Willett (1939), *"Below the falls [Alexander McKay Falls] the stream meanders along a typical glaciated valley, some two miles long, whose U-shaped cross-section has been somewhat obscured by post-glacial landslides and slips".*

This may be one single large landslide or two adjacent landslides with a combined width of ~600 m, and total volume estimated at 10-20M m^3. The creek forms a rapid where it cuts through the toe of the landslide debris. Upstream the valley is sediment infilled for >1 km, and a large alluvial fan is formed from an unnamed northern tributary.

Between the Sixteen Mile and Robertson Creek landslide dams, and the Lochnagar landslide dam in Lake Creek, there are several other large landslides in Glencairn Creek. It is unclear if these formed landslide dams, the largest of these, from NE at an elevation of about channel 1150 m, appears to have had toe of landslide deposit fluvially eroded and formation of minor alluvial flat base of landslide, but any lake formation would have been insignificant.

Figure 12: *Possible landslide dam in Sixteen Mile Creek.*

13. Robertson Creek

In the left-hand branch of Sixteen Mile Creek (Robertson Creek), a very large landslide blocks the creek around 900 m upstream from the junction of the left and right branches. This is probably that described by Willett (1939): *"Two huge landslides block the mouth of the glacial valley and over them the stream cascades to the junction some 700 ft below".* This landslide is ~800 m in width, and may have a volume of several tens of millions of cubic metres. A smaller landslide deposit from the opposite (northern slopes) also appears to contribute to dam formation.

The alluvial flats upstream are at an elevation of about 1160 m, and landslide debris appears to extend downstream to an elevation of <900 m. This indicates the possible formation of a very large landslide dam, although in a relatively small, steep gradient catchment, there would have been little potential for formation of a significant reservoir.

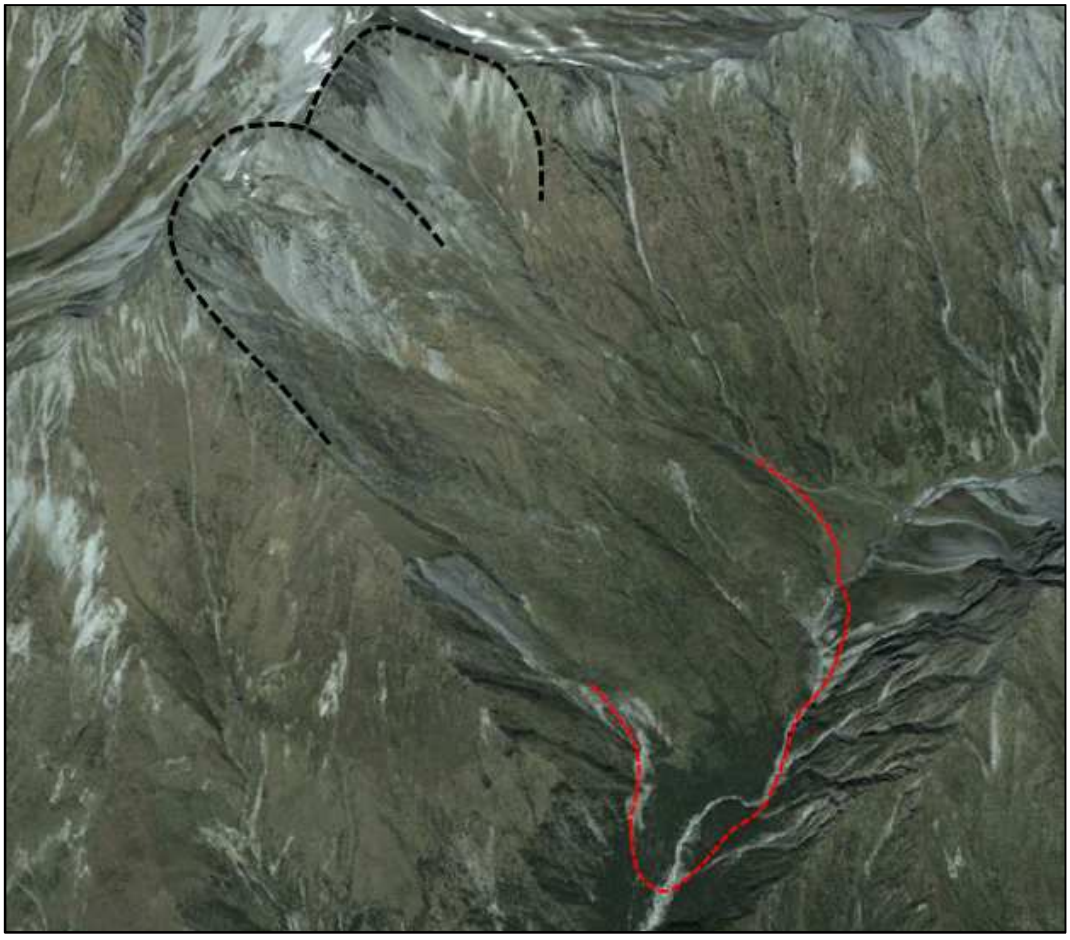

Figure 13: *A very large, and potentially dam-forming landslide in Robertson Creek.*

14. Campbell's Creek

Located in Campbell's Creek, a northern tributary of Flood Burn, this is a relatively minor feature formed by a large dip-slope landslide (260 m W x 940 m L). It is not known if full landslide area involved in landslide dam formation, or only a reactivated portion shown by smaller inset scarps. The upstream portion of landslide dam shows landslide deposit with an incised gorge through debris. Below this any landslide dam is indistinct and was either not formed or has been extensively eroded. Alluvial flats extend upstream for around 500 m from dam location, where another poorly-defined landslide may also constrict the creek channel.

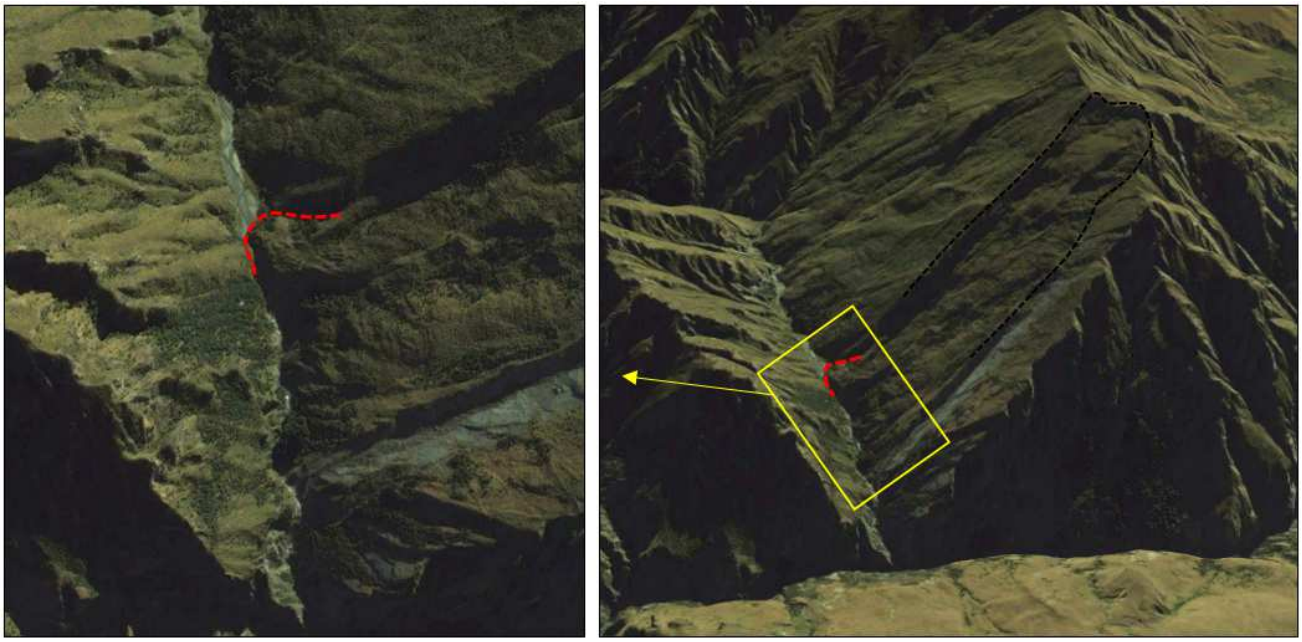

Figure 14: *Campbells Creek landslide dam, minor damming caused by creeping movement or more rapid reactivation on a large dip-slope landslide.*

15. Stockyard Creek

This landslide is located at about 2 km up Stockyard Creek from Branches Flat. The landslide has width of >500 m and estimated volume of ~1M m^3. The creek has been pushed to the far side of the valley by the slide, and forms a section of rapids through this part. For about 400 m upstream of the dam is a broad sediment-infilled channel up to 50 m in width.

Figure 15: *Dam-forming landslide in the lower reaches of Stockyard Creek.*

16. Skippers Creek North (Caspers Flat)

A large landslide up to about 400 m in width, blocking creek and forming the alluvial flat 'Caspers Flat' upstream. The landslide area has a well-defined scarp and hummocky terrain showing landslide deposit, but any landslide dam remnants are indistinct and partially obscured by vegetation on N side of valley.

Figure 16: *Possible landslide dam in Skippers Creek North Branch. The alluvial flat immediately upstream is Caspers Flat.*

17. Upper Stony Creek

A well-defined landslide scarp ~400 m in width, the creek appears to be incised into possible landslide dam debris at toe of slope, although this is indistinct and obscured by vegetation on the opposite side of the channel.

Figure 17: *Upper Stony Creek landslide dam.*

18. Upper Moonlight Creek

A large landslide ~300 m in width, constricting the creek and forming an alluvial flat immediately upstream. Around 1800 m upstream is an even larger, but poorly defined possible landslide(s) from the northern slopes, where the creek has incised into debris and formed alluvial flats.

Figure 18: *Upper Moonlight Creek landslide dam.*

19. Luna Creek.

A cluster of large landslides in Luna Creek, a tributary to Moonlight Creek. At least some of these appear to have impacted the creek channel and may have formed landslide dams. These largest of these landslides have areas of 150-250,000 m^2, with volumes estimated at 3-6M m^3. The creek has incised a channel estimated at several tens of metres depth into landslide debris forming a steep section of rapids. Upstream for a distance of >1 km is a broad, braided riverbed showing the extensive sediment infilling of valley.

Figure 19: *A number of large landslides in Luna Creek, some of which may form landslide dams. The stream visible in the upper right of image is Moonlight Creek.*

20. Shiel Burn

In Shiel Burn are several examples of valley blockages formed by debris flows, with the two most prominent shown below. These both show large debris fans filling the channel at the base of the slope, extending for ~100 m across valley, and >100-200 m along valley. The debris fan deposits have been incised to form a coarse grained boulder section, and shallow gradient alluvial flats are formed upstream.

Figure 20: *Examples of dam-forming debris flows in Shiel Burn.*

References

Bell DH, 1992. Geomorphic evolution of a valley system: The Kawarau Valley, Central Otago. In: Soons JM and Selby MJ (Eds.), Landforms of New Zealand: 456–481. Longman, Auckland.

Brown DA, 1956. Report on geology of Upper Shotover. In: Otago Catchment Board (OCB) Bulletin No.1: Shotover River survey (Upper Catchment).

Bryant JM and Goldsmith M, 2013. The incidence and importance of landslide dams in inland Otago. Proc. 19th NZGS Geotechnical Symposium. Ed. CY Chin, Queenstown.

Hancox GT and Perrin ND, 2009. Green Lake Landslide and other giant and very large postglacial landslides in Fiordland, New Zealand. Quaternary Science Reviews 28: 1020-1036.

Hancox GT, Langridge RM, Perrin ND, Vandergoes M and Archibald G, 2013. Recent mapping and radiocarbon dating of three giant landslides in northern Fiordland, New Zealand. GNS Science Report 2012/45. 52p.

Hermanns RL, Folguera A, Penna I, Fauqué L and Niedermann S, 2011a. Landslide dams in the Central Andes of Argentina (Northern Patagonia and the Argentine Northwest. In: Evans SG, Hermanns RL, Strom A and Scarascia-Mugnozza G (Eds), Natural and Artificial Rockslide Dams. Lecture Notes in Earth Sciences 133. Springer-Verlag Berlin Hiedelberg.

Hermanns RL, Hewitt K, Strom A, Evans SG, Dunning SA and Scarascia-Mugnozza G, 2011b. The classification of rockslide dams. In: Evans SG, Hermanns RL, Strom A and Scarascia-Mugnozza G (Eds), Natural and Artificial Rockslide Dams. Lecture Notes in Earth Sciences 133. Springer-Verlag Berlin Hiedelberg.

Hovius N, Stark CP and Allen PA, 1997. Sediment flux from a mountain belt derived by landslide mapping. Geology 25 (3): 231-234.

Korup O, 2004. Geomorphometric characteristics of New Zealand landslide dams. Engineering Geology 73: 13–35.

Korup O, 2005. Distribution of landslides in southwest New Zealand. Landslides 2: 43-51.

Korup O, 2006. Rockslide and rock-avalanche dams in the Southern Alps, New Zealand. Italian Journal of Engineering Geology and Environment, Special Issue 1: 33-43.

Korup O, Strom AL and Weidinger JT, 2006. Fluvial response to large rock-slope failures: Examples from the Himalayas, the Tien Shan, and the Southern Alps in New Zealand. Geomorphology 78: 3-21.

Massey C, McSaveney M and Davies T, 2013. Evolution of an Overflow Channel Across the Young River Landslide Dam, New Zealand. In: Margottini C et al. (Eds.), Landslide Science and Practice 6. Springer-Verlag Berlin Heidelberg.

McSaveney MJ, 1978. Shotover River – aspects of its erosion history relating to control of siltation in the Clutha Valley development. Water and Soil Unpublished Alpine Processes Report AP9. Ministry of Works and Development, Alpine Processes Group, Christchurch.

Ministry of works and Development (MWD), 1975. Shotover River Catchment – Report on Sediment Sources Survey and Feasibility of Control. Ministry of Works and Development, Water and Soil Technical Publication No.4, 1977.

Otago Catchment Board (OCB), 1966. Bulletin No.2: Shotover River survey (Lower Catchment).

Stefanelli CT, Vilímek V, Emmer A and Catani F, 2018. Morphological analysis and features of the landslide dams in the Cordillera Blanca, Peru. Landslides 15: 507-521.

Sweeney CG, Brideau MA, Augustinius PC and Fink D, 2013. Lochnagar landslide-dam – Central Otago, New Zealand: geomechanics and timing of the event. Proc. 19th NZGS Geotechnical Symposium. Ed. CY Chin, Queenstown.

Willett RW, 1939. Glenorchy Subdivision. In: Department of Scientific and Industrial Research, Thirteenth Annual Report. H-34, Appendix to the Journals of the House of Representatives 1, January 1939.

Appendix Four:
Historic Shotover Landslide Dams

This appendix compiles accounts of landslide dam and other mass movements documented during the mining era (1860s-1930s). These demonstrate the formation of one Shotover Gorge landslide dam during this period, and a number of other dambreaks or debris flows from tributary streams, most of which were associated with flood events. These were identified through a review of newspaper archives, using a keyword search of the Papers Past online newspaper archives (*paperspast.natlib.govt.nz/newspapers*).

Shotover River landslide dam (September 1871).

This is likely the largest Shotover Gorge dam to form in the last 160 years, forming a blockage sufficiently large to completely block the flow of the Shotover River for several hours. There is no report of a sudden flood following this dam overtopping so it is assumed to have failed gradually or the flood peak to have rapidly attenuated. This landslide is noted as being located in the Sutherland's Beach and Atley's Terrace area, but the exact location has not been identified.

> *"The miners in the neighbourhood of Arthur's Point were astounded, last Monday, at seeing the Shotover River fall suddenly, until it was almost completely dry. The cause of this extraordinary occurrence proved to be a very extensive slip of rock and mullock at Campbell's Terrace, some ten miles up. The river was blocked up for nearly a mile and a quarter, the Alabama Claim being swamped out and many other claims were seriously damaged"* (Cromwell Argus, Vol 2, Issue 96, 12 September 1871). [Alabama Beach is immediately upstream from Atleys Terrace (Chandler 1957)].

> *"That the Shotover should be walked over a little more than ankle deep, from side to side, may seem strange to many. Yet such, says the Wakatip Mail, was the fact on the 4th inst., when it could be crossed for a few hours. The causes were gigantic landslips, at or near Sutherland's Beach, which effectually dammed back the waters of this rapid river. … In modern days they are probably the largest slips that have taken place, and it is said that some enormous rocks have been deposited in the bed of the river which will materially affect the river's level at this site, and above it"* (Otago Daily Times, Issue 2995, 12 September 1871).

Stony Creek tributary dambreak flood (1888).

> *"… at a claim on one of the branches of Stoney Creek. It appears that the creek got blocked … and afterward breaking away, is rushed down in body of water fully 100 feet high … sweeping everything into Stoney Creek"* (Lake Wakatip Mail 12 October 1888, p2).

Stony Creek dambreak flood (1894).

> *"Had been sluicing at the mouth of the Stoney Creek, Shotover … The night of the heavy rain a slip came down from the hillside, damming up the creek for a time, but presently the pent-up waters burst through …"* (Lake County Press 26 April 1894, p3; Otago Witness 3 May 1894, p17).

Deposits seen at the Stony Creek (aka Rapid Creek) alluvial fan in the upper Shotover Gorge are interpreted as being that formed by this event. This well-preserved deposit on the alluvial fan intrudes into and constricts the Shotover River channel, and coarse debris can be seen as a train of larger boulders transported downriver from this point. This deposit contains many large boulders up to 4-8 metres in size, both within the inactive vegetated parts of the fan, and within the active stream channel. The bed of this small creek appears to be stripped of vegetation for a distance of >3 km upstream, suggesting formation by a debris flow caused by remobilisation of colluvium from the

upper reaches of this creek. A smaller debris fan deposit is found at an unnamed creek 300-400 metres upriver, and may have been formed by a similar debris flow event.

Aerial view of debris flow deposit at Rapid Creek in the upper Shotover Gorge, this contains many large (>4 m) boulders (examples arrowed), and intrudes into the Shotover River channel, with a train of coarse debris being remobilised downstream.

Debris flow deposit at Rapid Creek. A. Looking upstream from near Branches Road, the boulder in foreground is 4-5 m in size. B. collection of large (>2m boulders) on alluvial fan to the south of the active stream channel.

Note that there are two Shotover tributaries named Stony/Stoney Creek: one in the Skippers area between Stony Creek and Pleasant Creek terraces, the other in the upper Shotover Gorge at about Strohles Flat, and is also known as Rapid Creek. The 1888 event above is interpreted as being from the Skippers area creek, due to it being the only one of these two streams to have any significant sized tributaries (e.g. Elgin Creek, and Murphy's Creek). The 1894 event is interpreted as taking place in the upper gorge at Stony Creek/Rapid Creek, where

there are minor sluiced excavations at Strohles Flat, and the presence of a deposit interpreted as resulting from this dambreak flood or debris flow event.

The 1863 Flood

The severe flood event of 1863 caused widespread landsliding. Runoff from melting of thick snowfalls and a second heavy rain event several weeks later triggered several dambreak events causing multiple fatalities. This flood and the resulting dambreak are well described in many newspaper reports (e.g. Otago Witness 25 September 1875, p16). These events were interpreted as landslide dambreaks by contemporary accounts, however, they are sourced from steep, narrow tributaries, with little room for formation of any significant volume lake. They may in fact have been debris flows resulting from remobilisation of landslide debris, similar to the fatal Cleft Peak debris flow triggered by torrential rainfall in small gullies (McSaveney and Glassey 2002).

A landslide dambreak flood on Ballarat Creek was responsible for the deaths of 13 miners on the 26th July 1863.

> *"The first creek below the Sandhills runs down a steep gully into the river, and is ordinarily a mere rivulet… The ground slipped suddenly on both sides, filling up the bed of the gully entirely; this natural dam gave way at last, under the great force of water, which dashed down in a bore, calculated to have been 30 feet high"* (Otago Witness, Issue 610, 7 August 1863).

> *"It appears that on the occasion of the last flood, about a fortnight previous, a slip had taken place into a gully or watercourse running into the Shotover, damming up the water, which swollen to a great extent by the rain, forced away the earth, and the whole mass gave way, utterly overwhelming the huts and their unfortunate inmates below"* (Hawkes Bay Times, Volume III, Issue 136, 21 August 1863).

On the same date, three sawmillers were killed and one injured when a dambreak flood swept through their camp in the Moke Creek area.

> *"It appeared from an examination of the localities that a landslip has occurred some 1000 feet above the hut in the gully, forming a natural dam to the swollen creek - which rising to the top, suddenly burst through, hurling every obstacle before its impetuous force."* (Otago Daily Times, Issue 505, 3 August 1863).

Within weeks of the July 1863 flooding, a flood wave was observed in the Shotover Gorge near Maori Point. This is interpreted as being caused by failure of a landslide dam in a tributary catchment (probably Stony Creek), as there is no mention of reduced flows in the Shotover River prior to this event.

> *"A sudden sound or roar was heard … Some said it was a slip, while others averred it to thunder; but it was a sudden rush of water through the gorge above Maori Point, which swept down with incredible velocity"* (Lake Wakatip Mail 1 August 1863, p6).

The 1878 Flood

Skippers Creek Right Branch, dambreak flood.

> *A large landslip took place at the base of Mount Aurum, and dammed the waters back as if it were a large reservoir, when again the temporary bank gave way and down it came, roaring and tearing up trees, carrying them in its front … leaving his house buried up to the roof*" (Lake Wakatip Mail, Issue 1079, 10 October 1878, p3).

> *"At Skippers Reefs a heavy slip came down from the flat below Mount Oram [Aurum] carrying away the Phoenix fluming, and covering Southberg's house almost to the eaves …"* (Lake County Press, Volume VII, Issue 386, 3 October 1878).

Observations of creeks appear to describe debris flow formation;

> *"I and a few others were watching the caprice of one of the smallest of those side streams, viz., Londonderry Creek. The rain was pouring down, whilst the thunder and lightning at very short intervals were terrific. All at*

once the water in the creek would stop running, then would be a sound as of a thousand cannons, and a hundred cords of timber in all dimensions came rolling down along with sticks and stones, clearing away everything in their way as if they had been feathers" (Lake Wakatip Mail 10 October 1878, p3).

"Gullies and creeks that had an accumulation of decomposed vegetable matter, together with scrub and timber … have been swept to bare rock" (Otago Witness 26 October 1878, p3).

Reports following this flood event also describe the extensive landslide formation;

"Slips, or disturbed country that to all appearance has not moved for a century, has gone to solid rock, leaving smooth inclined planes of adamant for hundreds of feet in some places. Miles of our mountain roads have been destroyed …" (Otago Witness, Issue 1405, 26 October 1878).

The OCB also describes the extensive landslides caused by the 1863 and 1878 floods;

"More than 15 hours of torrential rain brought the river up 40 feet in the gorge and for miles of its length rocks, sand and gravel slid away from the bed rock and fell into the rapids below" (Miller 1961, in OCB 1966).

References

Chandler P, 1957. Map of late 19th and early 20th Century gold-mining along the Shotover and Arrow Rivers. Figure 2 in Schmidt M, 2005. Coronet Peak Pastoral Lease, Conservation Resources Report, February 2005.

McSaveney MJ and Glassey PJ, 2002. The fatal Cleft Peak debris flow of 3 January 2002, Upper Rees Valley, West Otago Institute of Geological & Nuclear Sciences report 2002/03. 28 p.

Otago Catchment Board (OCB), 1966. Bulletin No.2: Shotover River survey (Lower Catchment).